AN EVALUATION OF GEOMORPHOLOGICAL CONTRIBUTIONS TO MOUNTAIN HIGHWAY DESIGN WITH PARTICULAR REFERENCE TO THE LOWER HIMALAYAS

Gareth J Hearn

A thesis submitted for the degree of Doctor of Philosophy
in the University of London

Department of Geography
London School of Economics
and Political Science

February 1987

CONTAINS

PULLOUTS

ABSTRACT

Mass movement, fluvial erosion, sediment transport and earthworks - induced instability, often pose major problems for highway design and construction in mountain terrain. This thesis examines the contribution that geomorphological techniques can make to the evaluation of these hazards for highway design purposes in the Lower Himalaya.

A review of the consequences of geomorphological hazards to highway stability is illustrated by reference to selected mountain roads in India and Nepal. The design, stability and construction costs of these roads are discussed in respect to their status or function in the road network and, more particularly, the severity of hazards and terrain conditions they encounter. Techniques of hazard and terrain assessment for highway design purposes are examined and tested in the remainder of the thesis.

Techniques of medium-scale (1:10 000-1:50 000) landslide hazard mapping and large-scale (greater than 1:10 000) geomorphological ground survey are discussed and tested in the Dharan-Dhankuta area of Nepal, in terms of their ability to provide useful information for alignment design, road stabilization and protection works. The contribution of geomorphological ground survey to highway design is critically assessed by reference to the Dharan-Dhankuta road, and its stability following a high magnitude storm in 1984.

A proforma method for assessing flooding, erosion and sediment hazards in small mountain channels is developed. Discharge data for the 1984 storm are derived from these proformas and used to test a number of selected ungauged catchment equations, and to develop empirical relationships between peak discharge and catchment variables for purposes of high magnitude runoff prediction from small catchments. In addition, low-cost, low technology methods for monitoring discharge, slope erosion, sediment transport and mass movement are tested in terms of their ability to provide meaningful data in the short-term for design purposes.

Finally, optimum strategies of hazard and terrain assessment for highway design are proposed. The potential for further application of geomorphological techniques and expertise to mountain highway design is discussed.

To Jane

'You can fool all the people some of
the time and some of the people all
the time, but you can not fool all
the people all of the time'.

Abraham Lincoln 8 September 1858

CONTENTS

CONTENTS

CONTENTS

CONTENTS

CONTENTS

CONTENTS

ACKNOWLEDGEMENTS

I am indebted to Mr. D.K.C. Jones (London School of Economics and Political Science) for his encouragement and helpful advice and guidance during the period of my research. I also gratefully acknowledge the advice and comments provided by Dr. R.P. Martin (Geotechnical Control Office, Hong Kong), Mr. D. Thompson (Royal Holloway and Bedford College, London), Dr. J.S. Griffiths (Geomorphological Services Limited), Professors D. Brunsden (Kings College, London), J.B. Thornes (Bristol University), P.G. Fookes (Queen Mary College, London), Mr. C.N.D. Manby (Delft Geotechnics, UK), Mr. W.K. Cross and Mr. L.W. Hinch (Rendel Palmer and Tritton) and Miss H. Scoging (London School of Economics and Political Science).

I am also grateful for the advice given by the Geography Department Drawing Office of the London School of Economics and Political Science with regard to the preparation of some of the diagrams in this thesis, and for the logistical support provided by the Property Services Agency, Rendel Palmer and Tritton, Roughton and Partners, the Nepal Roads Department and the Swiss Association for Technical Assistance (Kathmandu) during my periods of fieldwork in Nepal. The Transport and Road Research Laboratory (Crowthorne) and Land Resource Development Centre (Tolworth) allowed access to their collections of air photographs of Nepal.

Finally, I would like to thank my parents for providing encouragement and financial support for thesis reproduction and Jane Bell for tolerance and understanding during the difficult and demanding years of my research.

The research was undertaken whilst in receipt of a Studentship from the Natural Environmental Research Council.

LIST OF FIGURES

LIST OF TABLES

LIST OF PLATES

CHAPTER 1

INTRODUCTION

1.1 Introduction

In young, fold mountain terrain with monsoonal rainfall regimes, geomorphological hazards of mass movement, flooding and erosion are often both highly active and widespread, and consequently pose considerable problems for road design, construction and maintenance. Successful road construction in this terrain often depends on the extent to which these hazards can be quickly evaluated and properly accommodated in the choice of alignment and construction design. Unfortunately, road construction in remote mountain terrain is often faced with an almost total lack of relevant detailed background data concerning geological and geomorphological conditions and, more particularly, the location, mechanisms and severity of these hazards.

Geotechnical appraisals for road design and construction purposes in the less severe terrain of Great Britain, for example, have conventionally consisted of walk-over engineering geological surveys, followed by detailed ground investigation using boreholes, trial pits and in situ and laboratory testing. However, in unstable and remote mountain terrain, detailed site specific geotechnical investigations are likely to be inappropriate due to constraints of cost, time, access and operational difficulties. Oboni et al (1984, p474) maintain that in mountain regions the "high cost of drilling in difficult topographical conditions oblige to limit the investigation" and that in these areas "where the risks (from landslides) do not seem catastrophic, the social cost of these phenomena does generally not justify an exhaustive study in order to design suitable stabilization work. " Under these conditions, it may be more practical to employ rapid and relatively inexpensive approaches to terrain and hazard evaluation based upon geomorphological techniques (Falkowski and Lozinska - Stepien 1979). This development in engineering geomorphology for highway projects, has been illustrated in publications by Brunsden et al (1975a and b, 1981) and Fookes et al (1985). Indeed, Fookes (1986, p375) has recently suggested that ".... geomorphology probably has more to offer civil engineering than does geology." This contention is probably most appropriate in some of the more geomorphologically active terrains outside Great Britain, such as those found in unstable mountains, where conventional geotechnical methods of ground assessment alone may be insufficient. Useful discussions of the development of applied geomorphology

in the fields of engineering[1], resource and environmental management and planning are given by Jones (1980, 1983), Cooke (1984) and Hart (1986).

1.2 Aims and Scope of the Research

This thesis evaluates and develops geomorphological techniques of hazard assessment for highway design purposes in unstable young fold mountains with sub-tropical climates and monsoonal rainfall regimes. In the Lower Himalaya, geomorphological hazards pose considerable risk to road stability and consequently, this region has been chosen as the fieldwork area. Field research has been concentrated on the Dharan-Dhankuta road in east Nepal, where the geotechnical and geomorphological input to highway design has been considerable. The geomorphological reconnaissance surveys undertaken for this road in 1974 and 1975 are among the first, and probably the most noteworthy, applications of geomorphological expertise and techniques to slope and drainage assessment for highway design purposes and, therefore, the choice of this road as a case study is justified.

The aims of the research are essentially three-fold. First, the observations and recommendations made by the geomorphological reconnaissance surveys for the design of the Dharan-Dhankuta road, together with the techniques used, will be critically assessed with regard to the final design and present stability of the road. The impact of a high magnitude storm, with a locally maximum recurrence interval of 75-80 years, will serve to highlight the efficacy of the geomorphological interpretations and predictions made. Second, this critical hindsight review, along with an assessment of the design and stability of other Lower Himalayan roads and an appraisal of the relevant published literature, will allow the identification of fields where further geomorphological research could lead to the improvement of methods for evaluating geomorphological hazards for highway design purposes. The development and application of these methods will be described and discussed. Finally, a progressive strategy for geomorphological and geotechnical evaluations will be proposed for use from the desk study to the maintenance stages of highway projects in similar terrain.

Although the majority of this thesis is concerned with slope and drainage hazard assessment for highway design and maintenance in the Dharan-

---

1. In this thesis, the term 'engineering' is used synonimously with 'civil engineering'.

Dhankuta area, it is considered that the techniques and recommendations can be equally applied to highway projects throughout the Lower Himalaya of Nepal and India, and to similarly unstable young fold mountain terrain experiencing high intensity precipitation.

As the prime intention of this thesis is to develop a package of geomorphological evaluation techniques for future highway design purposes, each aspect can only be investigated in a relatively superficial manner. Clearly, more detailed research on individual topics should be undertaken at a later date, once the broad framework has been established. Recommendations for further research are made where appropriate.

1.3 Thesis Format

The research undertaken is presented in the following format. Chapter 2 provides a brief description of the geomorphological hazards present in young fold mountain terrain, and illustrates their impact on road stability by reference to examples from the Lower Himalaya of Nepal and India. A critical appraisal of the techniques presently available for evaluating these hazards is also given in this chapter.

In Chapter 3, the most relevant geological and geomorphological features of the Lower Himalaya are described with reference to the Dharan-Dhankuta area. A critical assessment of the contribution made by the geomorphological reconnaissance surveys of 1974 and 1975 to the design of the Dharan-Dhankuta road is given in Chapter 4, along with suggestions for future practice in this terrain.

Chapters 5 to 8 inclusive, are devoted to the development and evaluation of geomorphological techniques of slope and drainage hazard assessment, for use from the feasibility to the maintenance stage of a highway project. Present constraints on, and potential applications for the further use of geomorphological techniques and expertise in highway projects are discussed in Chapter 9, in conjunction with a proposed ideal strategy for the evaluation of mass movement and drainage hazards, for future highway alignment and construction design purposes.

The conclusions to the research are presented in Chapter 10, along with their implications for highway design. Recommendations for further research are made, where necessary.

CHAPTER 2

HIGHWAY DESIGN AND CONSTRUCTION IN YOUNG FOLD MOUNTAINS WITH PARTICULAR REFERENCE TO THE LOWER HIMALAYA

2.1 Introduction

Young fold mountain belts represent the most dynamic of geomorphological systems, where highly fractured bedrocks, continued tectonic activity, high relative relief and often intense precipitation, result in denudation systems characterised by high rates of slope and channel erosion. Hewitt (1972) reports rates of overall land surface denudation in the Alaskan Mountains of 0.6 mm per year, while corresponding rates in the Karakoram Mountains (N. Pakistan) are 0.4 mm per year, locally rising to 2mm per year in the Hunza valley (Goudie et al 1984). Saunders and Young (1983) suggest that denudation rates in mountainous terrain are of the order of ten times greater than those in 'normal' relief. The most rapid rates of geomorphological activity are likely to be found when continued uplift, drainage incision and high intensity rainfall occur in steep terrain underlain by highly weathered rock. These conditions are characteristic of young fold mountains experiencing sub-tropical climatic regimes with a distinct wet season, and are well exemplified by the Lower Himalaya.

Until recently, few attempts have been made to monitor or model surface processes in mountain terrain. Although this is surprising considering the rate at which mass movement and fluvial processes operate in these environments, it may be explained in part by the historic remoteness and inaccessibility of many mountainous areas, and the fact that monitoring, especially during moderate to high magnitude events, is particularly hazardous. Nevertheless, human activities and especially road construction, have been expanding rapidly into mountain regions, and have had to contend increasingly with these geomorphological hazards (Jones et al 1983, Verstappen 1983). In order to avoid ill-conceived engineering design and accelerated erosion, it is essential that these projects are undertaken with full regard to the nature and severity of potential slope and drainage hazards. The need to know more about geomorphological processes in such areas is therefore clear, particularly with respect to their location, mechanisms, magnitude and frequency characteristics, and likely impact on the intended road. The aims of this chapter are therefore to:

i) define the major geomorphological hazards that operate in young sub-tropical fold mountains and discuss their significance for road design and construction with specific reference to the Lower Himalaya,

ii) describe and assess the available geotechnical, including geomorphological, techniques applicable to slope and drainage hazard evaluation in this terrain, and

iii) identify the main areas of research where the evaluation, refinement and development of geomorphological desk study, reconnaissance and observational techniques would improve hazard and ground assessment for highway engineering purposes.

2.2 Geomorphological Hazards in the Lower Himalaya and their Impact on Road Construction

The precise nature and scale of geomorphological processes operating in young fold mountains depends largely on geology, physiography and climate, and in particular, slope inclination, rainfall regime and the susceptibility of slope materials to mass movement and erosion. Fookes et al (1985) have proposed a five-fold classification of mountain terrain (Figure 2.1), based largely on climate, physiography and slope processes. Within zones 2-5 of the model, which refer to morphoclimatic regions outside the glacial and periglacial zones, geomorphological hazards are generally similar in nature, although their causes and severity vary considerably. Essentially, the major hazards operating in these zones are mass movement, flooding, soil erosion, and sediment transport (Plate 2.1) and deposition (Plate 2.2). These hazards are described below under the general headings of mass movement and fluvial processes. The impact of these hazards on road construction and stability in the Lower Himalaya will also be discussed and illustrated by reported cases of road damage or loss (Table 2.1) and by the author's survey of selected mountain roads in India and Nepal (Table 2.2) undertaken in 1983 and 1984. The locations of these surveyed roads are shown on Figure 2.2.

2.2.1 Mass Movement

Mass movements are en-mass downslope displacements of slope material, under the force of gravity. An extensive literature has been established concerning the nature, classification and engineering treatment of mass

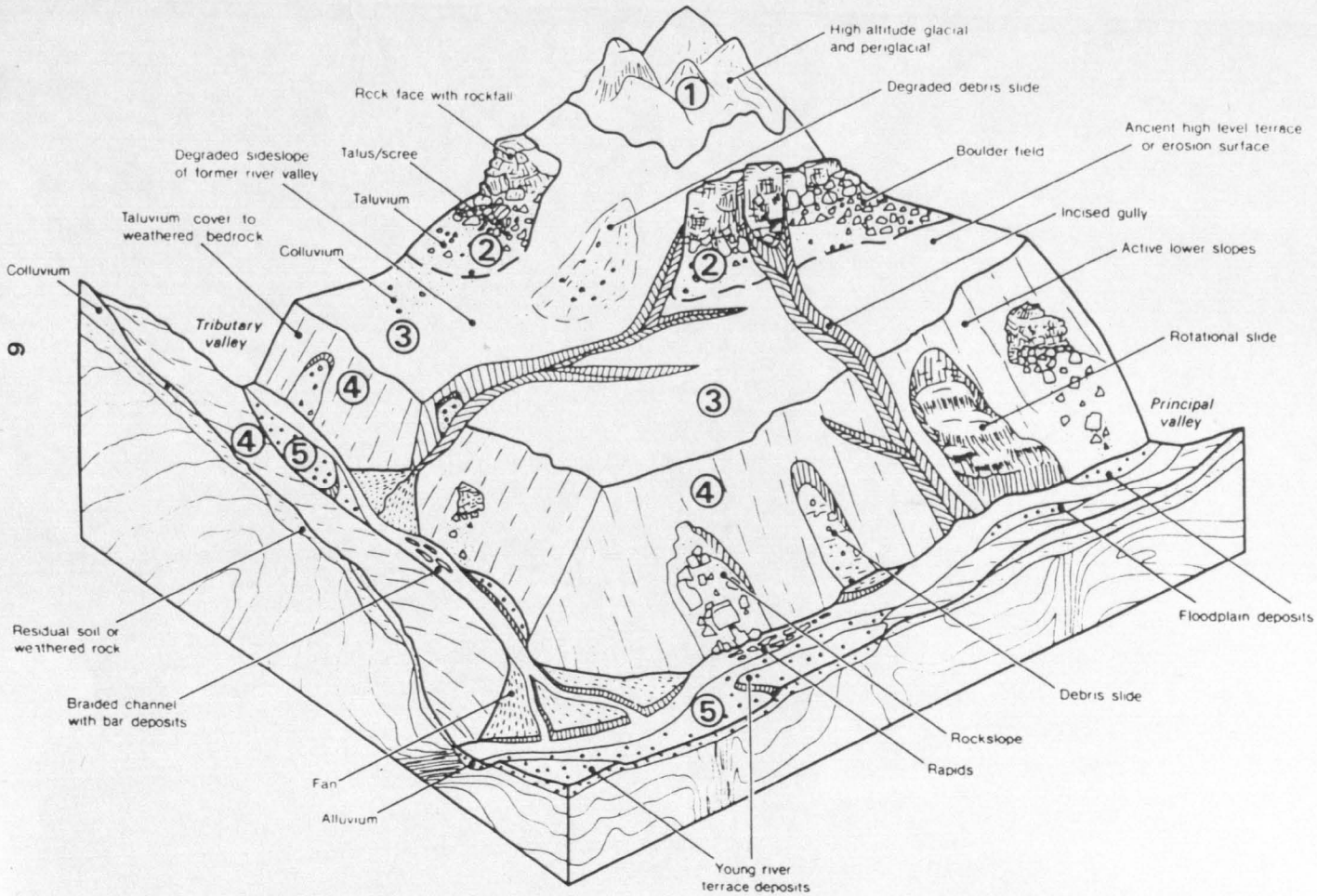

Mountain Zone

1 High altitude glacial and periglacial

2 Free rock face and associated debris slopes

3 Degraded middle slopes and ancient valley floors

4 Active lower slopes

5 Valley floors

FIGURE 2.1 A Model for Mountain Physiography - (After Fookes et al 1985).

PLATE 2.1 Typical Debris Flow in East Nepal.

PLATE 2.2 Debris Fan Below Eroding Gully in East Nepal.

PLATE 2.3 Renewed Instability on Meander Bend Along the Kathmandu-Kodari Road, Reactivated by Road Excavation.

AUTHOR	HIGHWAY	AREA	HAZARD	DATE	RAINFALL	AFFECT ON ROAD
AYYER(1975)	Gangtok-Sherbathang	Sikkim	Debris slide, rock fall	1968		Road displaced 10m vertically by 230m.
CHATTERJEE (1975)	Lungleh-Tuipang	Sikkim	Rock-debris slide	—	140mm in 5 days	150m of road affected.
CHOPRA (1977)	Indian roads in general	Sikkim, Bengal	Rock and debris slides	1968	240mm in 4-5 hours	8kms of road damaged.
DUTTA(1966)	Darjeeling-Tista	Bengal	Rock and debris slides	1950	447mm in 24 hours	Unspecified.
HAIGH(1979)	Mussoorie-Tehri	Garhwal	Rock falls, slides, gullies	1978	4712mm per year	63 slope failures on 20kms of road.
KHAIRE (1975)	Sonauli-Pokhara	W.Nepal	Rock slide	—	—	120m of road lost.
KRISHNASWAMY (1980)	Jammu-Srinagar (Khuni)	Kashmir	Rock slide	—	—	General damage
"	(Painthal)	"	Landslide	—	—	Bridge damaged
"	(Nashri)	"	Mudflow	—	—	General damage
"	Rajourie-Bafliaz	"	Debris flow	—	—	"
"	Chakki-Dalhousie	Himachal Pradesh	Unspecified	—	—	Road subsidence
"	Hardwar-Bodrinath (Kaliasor)	"	Rock slide	—	—	Unspecified
"	(Pakhi)	"	Unspecified	—	—	Road realigned
"	(Belakuchi)	"	Rock slide	—	—	"
"	(Nandprayang)	"	Rotational slide	—	—	Unspecified
"	(Sial)	"	"	—	—	Road realigned
"	Hardwar-Joshi (Helang)	Uttar Pradesh	Debris slide	—	—	Road lost
"	Joshimath-Malari(Dhak)	"	Rotational slide	1970	—	Road realigned
"	Birehi-Bodrinath	"	"	1970	—	Road lost for 3kms.
"	Sonauli-Pokhara	W.Nepal	Block glide	1970	—	Damage to bridge abutment.
KRISHNASWAMY and JAIN (1975)	Jammu-Srinagar	Kashmir	Debris slide	—	—	100m of road affected.
"	Rajouri-Punch	"	Debris slide, debris flow	—	—	Unspecified
"	Chakki-Delhousie	Himachal Pradesh	Debris slide	—	—	70m of road subsided by 1.8-2.1m.
"	Hardwar Badrinath	Uttar Pradesh	Debris slides	1970	—	160, 300 and 300m of road affected by 45m subsidence.

TABLE 2.1 Reported Cases of Slope and Drainage Hazards Affecting Roads in the Lower Himalayas (continued on next page).

AUTHOR	HIGHWAY	AREA	HAZARD	DATE	RAINFALL	AFFECT ON ROAD
NATARAJAN, et al(1980)	Gangtok-Chungthang	Sikkim	Debris slide	1970	4000mm per year	Subsidence of road by 10m for 500m.
"	Gangtok-Siliguri	Sikkim, Bengal	Landslide	1966	—	Subsidence of road by 20m for 200m.
NOSSIN(1967)	Dehra Dun-Mussoorie	Uttar Pradesh	Unstable catchment.	—	1892mm in 3 months	Bridge overtopped
RACKSHIT (1982)	Manebhanjan-Rinibic	Sikkim	Cut slope failure.	—	5000mm per year	390m of road affected.
SOIN(1980)	North Sikkim Highway	Sikkim	Gully erosion, rock fall.	1978	403mm in 3 days	Road subsidence by 4.5m for 3164m.
STARKEL (1972)	Darjeeling-Siliguri	W.Bengal	Debris slides	1958	1091mm in 4 days	More than 200 slides on road.
This thesis	Kathmandu-Kodari	Nepal	Flooding	1981	—	Loss of approx. 20kms of road.
"	"	"	Two deep-seated slides (rotational).	1983	—	Subsidence of road by 3-5m for 1km at each site.
"	"	"	Rock-debris slide.	1983	—	Road blocked for 60m.
"	Kathmandu-Pokhara	"	Cut slope failure.	1983	—	Road blocked for 30m.
"	Dharan-Dhankuta	"	"	1983	70mm in 2.5 hours	Road blocked for 20m.
"	"	"	Rotational slide.	1983	348mm in 3 days	Road lost for 40m.
"	"	"	"	1984	260mm in 24 hours	Road lost for 100m.
"	"	"	Rock-debris slide.	1984	"	Approx. 30m of road deformed.
"	"	"	Flooding	1984	"	Road lost in 8 places; total 70m.

TABLE 2.1 cont/

Road	Date built	Cost (£/km)	Length (km)	Geology/ rock types	Physiography/ topography	Alignment design	Design standard	Severity and nature of hazards	Specific hazards	Km	Effects on road	Stabilization preventative measures
Naubise-Hetauda (Tribhuvan Raj Path) (Indian)	1953-1956	-	107	Slates, phyllites, limestones quartzites granites.	Undulating, shallowly inclined ridge top slopes with incised slopes below.	One hair-pin stack and contour traverse across side-long ground and headwater slopes of incised ravines.	Low-moderate. Occassional gabion and dry-stone slope revetment and erosion protection.	Low-moderate Numerous signs of relic naturally occuring and construction induced slope and drainage instability.	Debris slide	40.5	Shallow cut slope failure.	Debris clearance.
									Debris slide	57	Shallow cut slope failure. Half blocked carriageway.	"
									Eroding gully	57.42	Accumulation of debris onto road.	Gabion wall.
									Rock slide	59.3	Cut slope failure.	Gabion and dry-stone revetment.
									Rock and debris slides and slope erosion.	83	Continual collapse of gabion wall below road.	Repeated reconstruction of revetment.
									Eroding gully.	112.3	Debris fan on road, check-dams overtopped.	Check dams immediately upstream of road.
Dhankuta-Hile (British/ Nepalese)	1981	63.6×10^3	13	Gneiss, schist.	Shallowly inclined ridge-top topography. Slope inclinations up to 30°.	Contoured traverse immediately below ridge top.	As above.	Low. Very little naturally occuring instability. Shallow cut slope failures.	None.			
Hile-Siduwa (British/ Nepalese)	Under construction.	90.9×10^3	13	Gneiss.	Undulating shallowly inclined ridge-top topography.	Contoured traverse immediately below ridge top. Minor detours into shallow ravines.	As above.	Low. Shallow cut slope failures and localised gully erosion. Pipe erosion in cut slopes.	None.			
Bhedetar-Rajarani (Nepalese)	Under construction.	-	22	Quartzites phyllites, schists.	Steeply inclined slopes, often greater than 40° below Sangure Ridge	Contoured alignment below ridge top	Low. Minimal-non existant slope revetment and erosion protection.	Moderate. Extensive cut slope failure and erosion on tip slopes.	None.			

TABLE 2.2A A Summary of the Design and Stability of Selected Mountain Roads in Nepal.

Road	Date built	Cost (£/km)	Length (km)	Geology/ rock types	Physiography topography	Alignment design	Design standard	Severity and nature of hazards	Specific hazards	Km	Effects on road	Stabilization preventative measures
Dharan-Dhankuta (British)	1976-1982	234x 10^3	52	Siwaliks, shales, phyllites, schists, quartzites gneisses. Highly shattered.	Foothills. High relative relief composed of long, steep slopes (locally up to 50°)	Vertical and offset hairpin stacks, contour traverses and flood-plain alignments.	Moderate-high. Extensive cut slope revetment/ retaining structures, area drains and erosion protection.	High. Extensive naturally occuring and construction induced slope instability and erosion, associated with steep slopes and incoherent slope materials.	Two rotational slides on opposite sides of re-entrant.	3.84, 4.20	Approximately 60m and 100m of road lost respectively.	Road reconstruction, area drains, channel protection and slope revetment.
									Debris flow	4.8	Minimal. Scour of channel protection.	Bridge with cascade below.
									Unstable ravine flank.	4.8-5.15	Road blocked for 20m. Extensive cracks in road and hairpin above	Cracks filled with bitumen/ jute.
									Rock and debris slides on terrace flank below road.	5.28	Back scar below road.	Checkdams.
									Debris flow.	8.44	Three road levels on hairpin stack blocked with debris.	Debris clearance. Repair to contour drain and checkdams in gully.
									Scree	8.75	Repeated failure of gabion retaining wall.	Wall reconstructed with area drains.
									Translational rock and debris slides on natural slopes and tip bench below road.	8.9	Road subsidence.	Crib revetment below road.
									Rock slide.	15.28	Cut slope failure.	Debris clearance.
									Rock slide.	15.97	Debris fan on road.	"
									Debris slide/ flow with gully erosion.	23.44	Pipe culvert and road destroyed.	Road rebuilt on gabion embankment with extensive erosion protection.
									Rock and debris slides.	24.56-24.87	Extensive cut slope failure.	Debris clearance, cut slope revetment and area drains.

TABLE 2.2A Continued.

Road	Date built	Cost (£/km)	Length (km)	Geology/ rock types	Physiography/ topography	Alignment design	Design standard	Severity and nature of hazards	Specific hazards	Km	Effects on road	Stabilization preventative measures
Dharan-Dhankuta cont./									Debris slide.	25.5	Encroachment of cut slope on to road.	Clearance reconstruction of revetment.
									Flooding/ Erosion.	26.73-26.9 27	Road loss on Leoti Khola floodplain.	Road rebuilt.
										27.15-27.26 27.96 28.2 31.77-31.79 32.3-32.37	Destruction of gabion groynes and falling apron.	
									Rapid fan aggradation.	27.52 29.8 30.2	Bridge inundation by debris fans.	Clearance.
									Two incising gullies and slump block.	40.38-40.6	Damage to channel protection works.	Erosion protection works.
									Gully and mudslide head.	40.94-41.15	No problems to date.	Area drains.
									Two unstable catchments with unstable spur in between.	41.43-41.58	Repeated culvert blockage and scour of erosion protection works. Failure of spur onto road.	Minimal erosion protection. Area drainage and revetment (toe wall) of spur.
									Shallow rock and debris slides.	42.43-42.86	Extensive slope failure.	Minimal area drainage and slope revetment.
									"	43.83-43.9	"	"

TABLE 2.2A Continued.

Road	Date built	Cost (£/km)	Length (km)	Geology/ rock types	Physiography/ topography	Alignment design	Design standard	Severity and nature of hazards	Specific hazards	Km	Effects on road	Stabilization/ preventative measures
Kathmandu-Kodari (Chinese)	1966 Rebuilt in part early 1980's.	30.7x 10^3	114	Gneiss, schist, phyllites, quartzites.	Valley floor and lower valley side slopes of Sun and Bhote Kosi. Long steep slopes with two major quartzite gorges beyond Barabise.	Traverse across lower valley side slopes and floodplain.	High Standard masonry cut slope revetment. Minimal to non-existant slope stabilization works and erosion protection works.	High. Major slope instability on valley sides with eroding gullies and extensive erosion in Sun and Bhote Kosi.	Shallow rock slide on meander bend. Spoil tipping has caused further erosion.	58.83	Road blocked.	Debris clearance.
									Rotational slip in weathered rock.	73.6	Cut slope failure.	"
									"	78	Debris on road.	"
									Rock slide with mudflow lobes on meander bend.	85	Road inundated with debris.	Unsuccessful attempts at realignment.
									Rock slide.	91.92	Failures and washouts in cut slope.	Debris clearance.
									Rock slide with two eroding gullies.	96	"	Groynes in river. Unsuccessful.
									Unstable scree slope.	96.15	Shallow failure on road.	Debris clearance.
									Flooding.	100.9	Road destroyed.	Road rebuilt further up valley side.
									"	100.6	"	"
									Complex deep-seated failure with eroding gullies. Spoil tipping causing further erosion.	103.2-104.2	Road subsidence by 2m in 6 months. Repeated failure of cut slope and erosion below road.	Temporary cut slope stabilization by revetment.
									Rock slide.	107.8-107.95	Road blocked for 150m.	Realignment over slip debris.
									Unstable talluvium with slumps and debris slides. Erosion in gullies enhanced by tipping.	111.1-111.8	Debris on road.	Debris clearance.
									Complex deep rotational and translational failure. Eroding gullies.	112.7-113	Road subsidence, cut slope failure and erosion of road base.	Debris clearance.

TABLE 2.2A Continued.

Road	Date built	Cost (£/km)	Length (km)	Geology/ rock types	Physiography/ topography	Alignment design	Design standard	Severity and nature of hazards	Specific hazards	Km	Effects on road	Stabilization/ preventative measures
Lamusangu-Jiri (Swiss/ Nepalese)	1976-1984	81.8x 10^3	110	Phyllites, schists, mostly gneiss.	Subdued ridge topography. Slope inclinations commonly up to 30°	One hair-pin stack and extensive contouring across side long ground	Low. Occassional dry-stone and gabion revetment and channel protection works. Successful cut slope planting schemes.	Low. Very few examples of naturally occurring instability. Relatively small catchment areas above road.	Erosion caused by concentrated road runoff.	5.25	Erosion below road	Gabion slope revetment.
									shallow rock and debris slides with debris flow.	35.1	Debris on road.	Gabion cascade and revetment.
									Rotational slip.	42.6	Road sub-sided by 2m for 20m	Regrading, gabion cut slope revetment and planting schemes.
									Rock slide and erosion caused by spoil tipping.	73.15	Debris on road with erosion below.	Debris clearance.
									Unstable ravine with erosion caused by spoil tipping.	94	Erosion below road and cut slope failure.	"
									Unstable ravine with deep-seated rotational failure.	102	Sediment accumulation on road.	"
									Two eroding gullies with unstable slope in between	103	Slope displacement towards road	Minor realignment on gabion embankment.
Muglin-Narayanghat (Chinese)	1974-1980	227.3x 10^3	36	Siwalik sediments, quartzites, phyllites,	Lower valley side slope above Narayani R. Frequent engorged sections	Relatively straight alignment with frequent detours into ravines.	Moderate. Masonry cut slope revetment, arch culverts and occassional gabion check dams in eroding channels.	Moderate. Localised toe erosion, slope failure eroding gullies.	Rock slide.	17.5	Cut slope failure,	Debris clearance.
									Rock slide	17.55	"	"
									Eroding gully with slope instability in back scar.	23.15	Debris fan 40-50m wide on road	Gabion checkdams.
									Unstable debris slope	23.7	Bulging of masonry wall. Overspill onto road.	Retaining wall.
									Rock slide and gully.	31.0	Gabion toe wall over-topped and debris on road.	Gabion toe wall.

TABLE 2.2A Continued.

Road	Date built	Cost (£/km)	Length (km)	Geology/ rock types	Physiography/ topography	Alignment design	Design standard	Severity and nature of hazards	Specific hazards	Km	Effects on road	Stabilization/ preventative measures
Dehra-Dun-Mussoorie (British)	1919	—	35	Shales, slates, quartzites	Complex system of ridges and spurs re-entrants and embayments.	Contoured across side long ground and vert-ical and offset hair-pin stacks. Highly sinuous.	Relatively low. Minimal slope stab-ilization and drain-age protect-ion works.	Low. Many examples of relic cut slope inst-ability. The majority of slopes and channels have regained stability.	Kalagarh slip/ flow.	11	Bridge blocked.	Relocation and enlargement to bri dge, fencing and revegetat-ion schemes on catchment slopes.
									Degraded rock slide on ravine flank.	24	Signs of relic instability in cut slope.	Masonry wall.
Mussoorie-Tehri (British)	1920's	—	70	Quartzites, shales, phyllites, Metasst. Dips comm-only out of slope.	Relatively steep(up to 50° slopes below ridge top. High density of incised rav-ines. Short traverse across Bhagirathi floodplain.	Contoured traverse below ridge top. freq-uent detours into ravines	As above.	Moderate. Many degraded and occasion-ally active instability features on incised slope below road. Relatively low runoff rates	Recent rock slide in cut slope. Spoil tipping has led to increased erosion.	1	Road loss.	Road rebuilt on crib retaining wall.
									Degraded slide and erosion scars above and below the road.	8	Undermined masonry embankment.	As above.
									Rock sliding due to bedrock dipp-ing out of slope.	12.3	Slope failure onto and below road.	Debris clearance.
Mussoorie-By-pass (Indian?)	—	—	10	Quartzites, phyllites	Dense net-work of incised gullies.	Contoured traverse, highly sinuous.	As above. -	Moderate. Erosion by spoil tipping.	Unstable ravine. Spoil tipping from access road above.	5	Culvert and road inundat-ion with debris.	Gabion slope revetment.
Siliguri-Darjeeling (British)	Early 1900's	—	81	Shales, phyllites, quartzites, gneisses	Foothill ranges. Complex sys-tem of spurs ridges and re-entrants. Slopes are moderately inclined(up to 50°) but commonly 35-40°.	Contoured with acute detours into valley re-entrants.	Moderate. Stabilizat-ion and protection measures have req-uired mod-ification suggesting element of under-design.	Low-moderate. Shallow inst-ability on ravine flanks localised failure in oversteepened cut slopes.	Walk-over survey of whole road not undertaken due to transport difficulties.			
Ghoom-Bijanbari (Indian?)	—	—	30	Gneiss	Undulating ridge tops with incised channels below.	As above.	Low. Occas-sional cut slope revetment.	Low. Local instability incised lower slopes, mostly relic.	Degraded rock slide flanked by two incised gullies.	4.5	Rock slides and rock fall onto road.	Crib and masonry revetment. Cascades upstream.
Teesta-Rambi (on Siliguri -Kalimpong road) (British)	—	—	12	Slate, phyllite, schist. Dips local-ly out of slope.	Elevated terraces and lower valley side slopes immediately upslope of Teesta River floodplain.	Relatively straight alignment above Teesta with occas -ional detours into re-entrants.	Moderate. Frequent cut slope revetment and drain-age protect-ion works. Groynes and toe protect-ion in river.	Moderate-high. Extensive slope instab-ility, chann-el runoff and sediment transport. Toe erosion by Teesta River.	Rock slide and toe erosion.	2	Road inundated masonry and gabion toe walls destroy-ed.	None.
									Rock slide.	3.2	Road inundated.	Toe protection in Teesta River. Gabion check-walls/revetments and erosion protection in slide back scar.

TABLE 2.2B A Summary of the Design and Stability of Selected Mountain Roads in India.

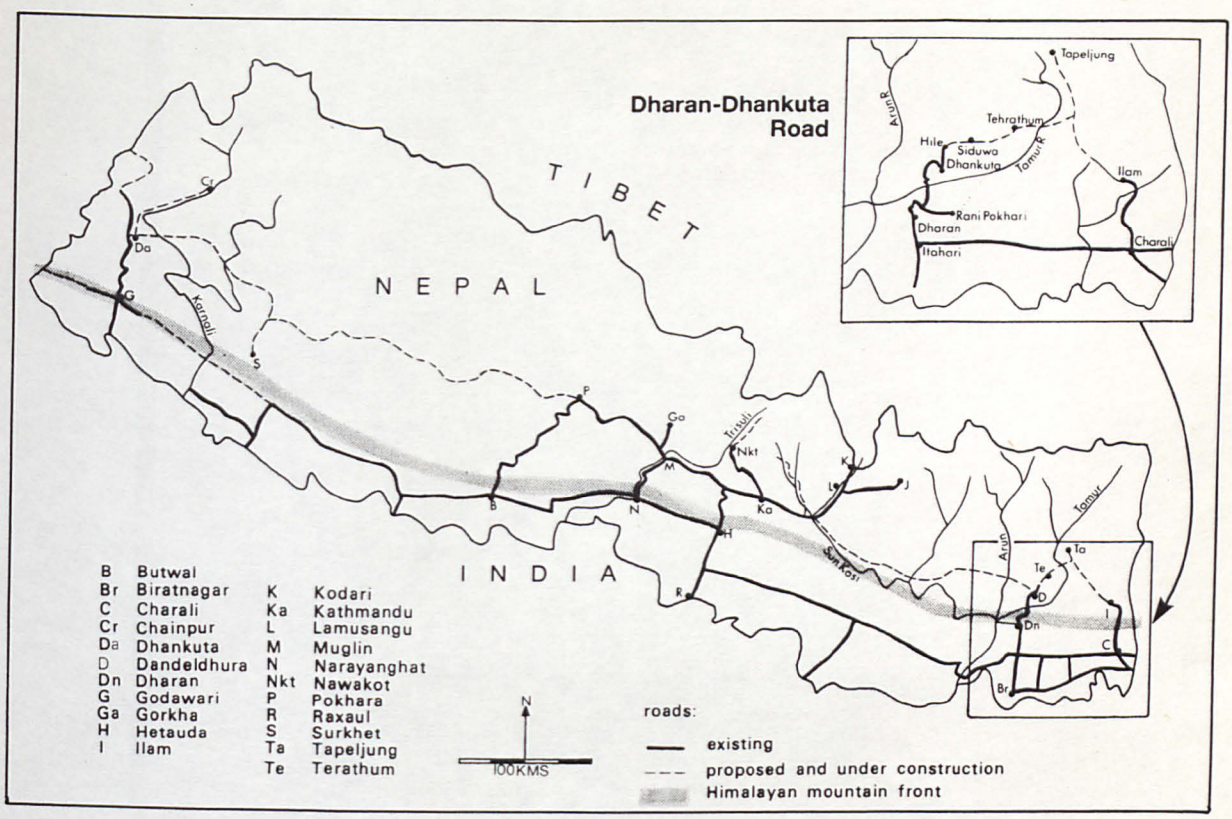

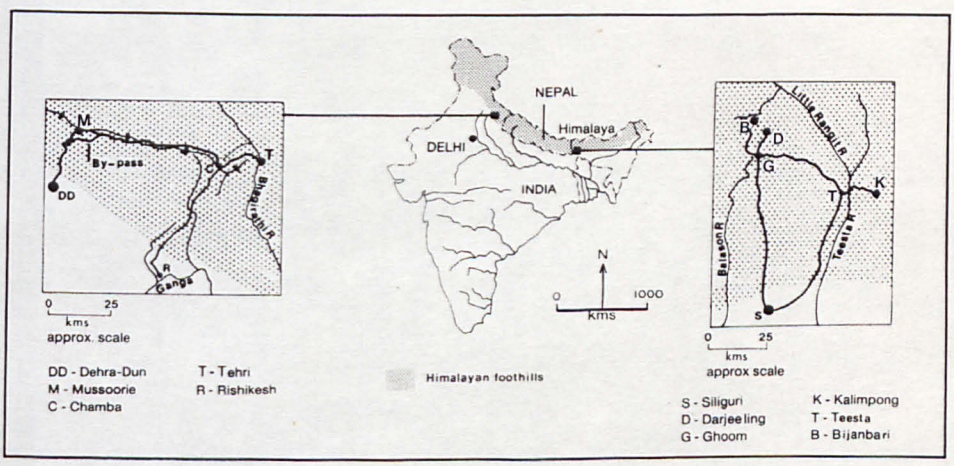

FIGURE 2.2 The Mountain Road Network of Nepal and the Location of Roads Visited in the Nepalese and Indian Himalayas in 1983 and 1984

movements (Sharpe 1938, Eckel 1958, Zaruba and Mencl 1969, Bolt et al 1975, Schuster and Krizek 1978, Varnes 1978, Royster 1979, Brunsden and Prior 1984, Hansen 1984 and Varnes 1984). Most of these classifications recognise principal failure mechanisms of fall, deep-seated and shallow translational and rotational slides, mudflows (fine grained) and debris flows (coarse grained).

Common mechanisms of rock fall include plane, wedge and toppling failure (Hoek 1973, Brunsden 1979, Whalley 1984). Rock falls have been reported in virtually every mountainous region of the world. In the study area they are usually caused by either slope oversteepening due to undercutting, or the development of high cleft water pressures in rock masses that have been rendered discontinuous by weathering and tectonic disturbances.

Compared to other mass movements, rock falls normally have a relatively low impact on mountain road integrity, merely causing temporary blockage, restricted access and minor damage to the road surface. Rock falls have been reported (Table 2.1) along the Gangtok-Sherbathang road (Ayyer 1975), the North Sikkim Highway (Soin 1980) and the Darjeeling-Tista road (Dutta 1966). Rock falls and soil falls commonly occur in road cuts where regoliths are oversteepened and left unprotected. Falls along the Dharan-Dhankuta road, for instance, have resulted in frequent blockage to side drains and often cause single lane access restrictions for up to one hour or so. Road carriageways, excavated into steep rock slopes, may experience loss of support by rock falls from below.

Probably the most common form of slope failure in the Himalayan foothills is the shallow, planar translational debris or rock slide. Regoliths in which debris slides take place are characterised by a rapid increase in shear strength with depth that inhibits deep failure (Brunsden 1979). Shallow rock slides usually occur in weathered rock along discontinuities dipping out of the slope. On steep slopes, composed of granular cohesionless soils, the slip surface is usually coincident with the regolith/bedrock interface. Despite their relatively common occurrence (Tables 2.1 and 2.2), shallow planar translational slides generally have a low impact on Lower Himalayan roads and usually result in cut slope failure and culvert and road blockage. Cut slope failures can either occur where road excavation removes toe support from pre-existing landslides (Plate 2.3) or, more frequently, where slopes are excavated to inclinations greater than the limiting angle for stability of the material concerned (Plate 2.4). Intense precipitation, and the consequent development of high groundwater levels, is often the triggering factor in cut slope failure.

PLATE 2.4 Slope Failure in an Oversteepened Cut Slope in Quartzite Along the Dharan-Dhankuta Road.

These failures were common along the majority of mountain roads visited (Table 2.2). While failures caused by cut-slope oversteepening can usually be rectified by slope drainage, revetment[1] and scaling[2], those that are the result of the reactivation of existing landslides are likely to pose the greatest problems for road maintenance, requiring the implementation of extensive remedial measures.

Mudslides are translational failures that are "relatively slow moving lobate or elongate masses of softened argillaceous debris, which advance chiefly by sliding on discrete boundary shear surfaces" (Hutchinson and Bhandari 1971, p.353). Mudslides are characterised by a source area, a slide track and an accumulation lobe. They are commonly caused by removal of toe support by basal erosion and undrained loading by colluvial deposition. Compared with other forms of mass movements, mudslides result in relatively slow slope displacement rates, and are comparatively infrequent in steeply sloping terrain. At Singla, the Singla-Kalimpong road in Sikkim crosses a lobate mudflow and an elongate mudslide in quick succession (Plate 2.8). These mass movements occur primarily in highly weathered schist, following the removal of toe support by river erosion during floods that overtop the gabion bank protection works. Again, slope displacement here is gradual, thus allowing road access to be maintained. This road has not been described in Table 2.2, as access could not be gained without a permit.

Deep-seated planar slides usually involve plane failure along underlying bedrock discontinuities, and are therefore composed of both bedrock and overlying regolith. These failure mechanisms can also occur in relatively uniform, fine-grained cohesive soils such as clays and weathered shales, where the rate of increase in shear stress with depth exceeds the rate of increase in shear strength.

Deep-seated slope failures, however, often involve some form of rotational movement. In deep cohesive, homogeneous soils, rotational slips may predominate, whereas slope failures in granular soils and underlying bedrock may display a combination of rotational and translational failure modes.

---

1. Revetment is a structural slope protection against erosion and shallow instability and here refers to gabion, masonry and masonry crib walls.

2. Scaling is the removal of loose and potentially unstable material from a slope face.

Common causal factors promoting deep seated instability in the Lower Himalaya can be divided into external and internal categories. External factors lead to increased shear stress along the potential failure surface, and include slope oversteepening, the removal of basal support by lateral erosion and incision along drainage channels and artificial excavation in road cuts. Slope overloading may also be caused by embankment construction, spoil disposal and colluvial deposition. Internal factors promoting instability include the development of high groundwater levels in the slope material during heavy rain or snow melt, the creation of high positive pore water pressures on the potential slip surface, and loss of shear strength through weathering or by the removal of fines in groundwater.

Deep-seated slope instability in the Lower Himalaya tends to result in high magnitude-low frequency slope displacements that occur in response to intense and prolonged precipitation. Table 2.1 gives some examples of recorded rainfall totals that have given rise to high magnitude slope failure with consequent loss or damage to roads in the region. Starkel (1972), for instance, reports a storm rainfall depth of over 1000mm in 4 days in the Darjeeling-Siliguri area of West Bengal (India). During this period more than 200 slides were recorded. Details of this and other storms in the region are given in Chapter 3.

The impact that deep-seated slope failures may have on Lower Himalayan roads depends largely on the configuration and location of the slip surface with respect to the road, and the rate and volume of slope displacement. Deep-seated instability on the slopes above the road, for instance, is not likely to result in road displacement, but instead, may cause extensive blockage and damage to the road surface and associated structures. An example of such an impact is the deep-seated translational failure, involving regolith and underlying bedrock, which occurred on the slopes immediately above the Kathmandu-Kodari road, north of Barabise in the Sun Kosi valley in 1983 (Table 2.2, Plate 2.5). An idea of the scale of this failure can be obtained by comparing its size to that of the truck in the foreground of the photograph and the labourers excavating a new road trace across the slipped debris. The volume of the slip material was so high that removal to expose the buried road surface was not feasible.

Where the slip surface passes through or beneath the road, or where instability occurs on the slopes below the road, extensive road loss or severe deformation

PLATE 2.5 Debris from Large Translational Failure Engulfing Part of the Kathmandu-Kodari Road.

PLATE 2.6 Large Rotational Slide Along the Dharan- Dhankuta Road in 1984.

may result. Rapid, catastrophic slope displacement will usually cause total loss of the section of road affected, while gradual, progressive slope displacement may result in slow but continual road surface deformation and subsidence. In the latter case, the slow rate of movement may allow corrective measures, such as toe protection and slope drainage, to be undertaken and road access to be maintained. Instances of road loss caused by deep-seated instability have been reported (Table 2.1) on the Birehi-Bodrinath road (Krishnaswamy 1980), the Sonauli-Pokhara road (Khaire 1975) and the Dharan-Dhankuta road. Plate 2.6 shows a deep-seated, rotational failure on the Dharan-Dhankuta road that occurred overnight in September 1984, in response to the development of high groundwater levels and channel erosion following intense and prolonged precipitation. The remains of the road can be seen in the photograph, some 100m downslope of its original position. Didwal (1984) has described the impact of the deep-seated rock slide at Nashri on the Kashmir National Highway No. 1A where the road has been blocked on thirteen occasions for a maximum period of thirteen days. Road subsidence and deformation have been reported along the Gangtok-Sherbathang road (Ayyer 1975), the Chakki-Dalhousie road (Krishnaswamy 1980), the Hardwar-Bodrinath road (Krishnaswamy and Jain 1975), the Gangtok-Chungthang and Gangtok-Siliguri roads (Natarajan et al 1980), the North Sikkim Highway (Soin 1980) and the Kathmandu-Kodari road (Table 2.2). In the latter case, road subsidence of 3-5m occurred in 1983 for a distance of 1 km at two locations (Table 2.1 and 2.2, Plate 2.7).

Finally, translational and rotational slide masses may disintegrate downslope to form debris flows. Debris flows often occur when translational failure in regolith and fractured rock takes place on steep slopes, and becomes concentrated into topographic depressions and drainage channels (Johnson and Rodine 1984). In addition, flow may be initiated once debris flow deposits become saturated during heavy rain (Takahashi 1977). The cross-channel profiles of many channelised debris flow deposits are relatively flat and, owing to the often permeable nature of the deposit, storm runoff takes place by flow through the deposit rather than channelised flow across it. During intense precipitation, debris flow may be initiated by undrained loading (Sassa 1984) under conditions of debris saturation and loading, caused by landslide and debris flow accumulations from further upstream.

Debris flows usually consist of a central plug or raft of debris moving at uniform velocity, and a 'dead' peripheral region of cobbles and boulders that

PLATE 2.7 Rotational Slope Failure Causing Gradual Slope Displacement Along the Kathmandu-Kodari Road.

PLATE 2.8 Mudflow and Mudslide Along the Singla-Kalimpong Road.

forms distinct lateral ridges once the core of the debris flow has passed. Plate 2.1 shows a debris flow passing through a road bridge in east Nepal. The lateral dead regions of boulder accumulations, and the characteristic flow mechanism of the central raft are clearly visible. Further upstream, the confined channel immediately below the landslide source area, is characterised by lateral ridges of coarse debris formed entirely in debris flow materials.

Debris flow is often characterised by pulsed movements that reflect the periodic supply and mobilization of debris (Hungr et al 1984). They are commonly composed of angular debris of heterogeneous calibre that may constitute 60-70 per cent of the flow mass by weight (Varnes 1978). Following deposition on debris fan surfaces and in shallowly inclined channels, the majority of fines are removed as the water drains from the deposit.

Jones et al (1983) describe debris flows in the Karakorams where velocities reach 60 km per hour, while Plafker and Ericksen (1978) report debris flow velocities of 170-280 km per hour in the Peruvian Andes. In the Lower Himalaya both relatively slow and rapid debris flows occur in comparatively shallow channels and on steep slopes respectively (see below). In the case of the debris flow shown in Plate 2.1, characteristic of many channelised debris flows in the Lower Himalaya of Nepal, debris is supplied from a rapidly eroding source area, to a less steeply inclined ($11-17^{o}$) main channel through which the debris is transported at comparatively low velocities. Following three intense storms in July 1983, the deposit from this debris flow was resurveyed at consecutive locations between the bridge and the debris source area, to determine the cross-sectional area of flow for velocity and discharge computations using empirical formulae derived for Russian debris flows (Costa 1984). On the basis of the elevation of debris levees and flood deposits bordering the channel, flow depths ranged from 0.25m to 1.35 m. Computed velocities varied between 3m/s and 6 m/s (10-20 km/hr) corresponding to maximum discharges of 20-55 cumecs. Flows tended to last for approximately 10-15 minutes, and consequently the total volume of debris transported amounted to approximately 10,000 - 50,000 m^3 during each event.

On more steeply inclined slopes in the area, debris flows may attain velocities far greater than 20 km/hr, and may cause considerable road and culvert damage and blockage. This may be illustrated by a debris flow along the Dharan-Dhankuta road that has been identified to have been the principal

cause of road and culvert destruction (Plate 2.16, Appendix 1 A.6). Debris flow deposits were observed along many of the Himalayan roads visited, although their impact on these roads and associated structures was not seen to be as severe as that caused by deep-seated mass movements, as the majority occur in relatively large channels that have been either bridged or culverted.

2.2.2 Fluvial Processes

The runoff regime in sub-tropical mountain terrain experiencing monsoonal rainfall, is characterised by moderate to high magnitude flood events (Hewitt 1972, Brunsden et al 1981, Goudie et al 1984), superimposed on ephemeral, seasonally distributed flow. The process by which storm rainfall is converted into channelised runoff, is conditioned by:

i) the often steeply inclined catchment slopes that encourage rapid runoff rates and reduced times to concentration,

ii) the permeability of the catchment slope forming materials,

iii) existing groundwater levels and

iv) catchment physiography and channel network configuration.

Under intense precipitation and/or low soil or rock permeability, overland flow may predominate over much of the catchment in response to an expanded storm flow contributing area. However, slope runoff usually takes the form of saturation overland flow (Hewlett and Hibbert 1967, Dunne 1978) on slopes where the rainfall intensity exceeds hydraulic conductivity, or where existing groundwater levels are at, or close to, the slope surface, as on slopes adjacent to stream channels and in topographic depressions and percolines. Elsewhere, shallow sub-surface flow is likely to be the dominant form of slope drainage.

Channelised storm runoff is capricious, and characterised by a pulsed flow associated with an often multi-peaked hietograph. Channels are often formed in weathered rock and loose, granular fluviatile deposits that are highly susceptible to erosion. Channelised storm runoff may therefore become highly charged with sediment of often large calibre. Conventionally, debris transported in channel flow can be categorised according to whether it is predominantly transported in suspension or as traction load along the channel

bed. In steeply inclined, rocky mountain channels, channel roughness is dominated by an often highly irregular, boulder-strewn channel. Storm runoff is therefore non-uniform and highly turbulent and, consequently, bedload and suspended load are almost inseparable. Sediment is often transported through the channel network in surges or pulses (Gardner 1986), in response to temporally and spatially discrete debris inputs to the channel and unsteady flow. During flood recession much of the transported material becomes deposited in channels, on floodplains and in debris fans at sharp concave breaks of slope in the channel profile, usually on trunk valley floodplains (Plate 2.2) and along the mountain front.

Fluvial hazards encountered by mountain roads include flooding, slope and channel erosion, sediment transport and deposition (Table 2.1). The flood hazard poses a high risk to road stability when the road is located on the floodplain, or when slopes below the road are scoured and undercut by flood-waters. Flooding of the Bhote Kosi in 1981 destroyed much of the Kathmandu-Kodari road (Figure 2.2) upstream of Lamusangu (Table 2.2) by both direct scour and undercutting from below. The Dharan-Dhankuta road was destroyed at four main locations by flooding in the Leoti Khola during the 1984 monsoon (Plate 2.9), as is described in Appendix 1A.7.

Cross-the-road drainage hazards were found to cause considerable problems for road maintenance along the majority of roads visited (Table 2.2, Appendix 1). Common hazards include channel scour, upstream and downstream of culverts and bridges, that may lead to structural damage and rapid sediment accumulation. The latter often causes culvert and bridge inundation (Plate 2.10). Sediment hazards usually have their greatest impact when roads cross highly active fan surfaces located along the mountain front, or on floodplains at the mouths of eroding tributary catchments. The former case can be illustrated by the impact of the Kalagarh debris fan on the Dehra-Dun-Mussoorie road (Plate 2.11), where bridge inundation has taken place on a number of occasions (Table 2.2). The Dharan-Dhankuta road crosses numerous active fans situated on the Leoti Khola floodplain. Rapid aggradation on three of these fans has resulted in frequent bridge blockage and overtopping that has necessitated constant maintenance (Appendix 1 A.7).

During earthworks, the disposal of spoil by tipping onto side-long ground and into gullies had considerably increased short term erosion rates along all

PLATE 2.9 Extensive Damage to the Dharan-Dhankuta Road Caused by Flooding in the Leoti Khola in 1984.

PLATE 2.10 Culvert Blockage Along the Dharan-Dhankuta Road.

PLATE 2.11 Bridge Inundation by Debris Fan Along the Dehra-Dun-Mussoorie Road.

PLATE 2.12 Contoured, Near-Ridge Top Alignment of the Mussoorie-Tehri Road

mountain roads visited. This often creates severe problems for bridge and culvert maintenance, when sections of alignment are directly affected by spoil tipped onto the slopes from above. Slope erosion caused by spoil tipping is most marked along the Bhedetar-Rajarani road in east Nepal (Plate 6.4), where all spoil has been side-tipped at source (see Chapter 6). Kojan (1978) has described the effects of indiscriminate spoil tipping along the Godavari-Dandeldhura road in west Nepal, where extensive erosion and debris sliding has been initiated. Dramatic increases in erosion and instability have been reported in other mountain regions following road construction and associated deforestation by Swanston (1976, 1977) in western United States, O'Loughlin and Pearce (1976) and Selby (1976) in New Zealand and Fujihara (1978) in Japan.

2.3 The Structure of a Highway Project

Conventionally, highway projects, like most other engineering projects, can be conveniently divided into the feasibility, desk study, reconnaissance, site investigation, construction and maintenance stages. The initial phase of project feasibility involves the identification of route corridors and the evaluation of economic and social benefits to be gained by road construction, and the logistical and operational problems likely to be experienced.

During the desk study phase, all available published and unpublished sources of information relating to the geological, geomorphological, hydrological and climatic characteristics of the study area should be collated and reviewed. This usually allows one or a number of potentially suitable route corridors to be chosen. At the reconnaissance stage, route corridors and alignments within the chosen corridor are assessed in respect to their engineering feasibility, the likely cost of road construction and the nature, extent and potential impact of the hazards that are encountered. Rapid ground surveys and air photographs, if available, form the fundamental means of data acquisition at this stage. Once the final alignment has been chosen, detailed reconnaissance ground surveys and ground investigation are undertaken to gain as much information as possible regarding the nature of slope materials, slope stability and drainage conditions, before design and construction begin. During construction and maintenance, observation and design by modified precedent (Deere and Patton 1971), whereby design is modified according to experience gained under similar slope conditions, allow continual evaluation of ground conditions and hazards to be undertaken.

2.4 Design Alternatives and Information Requirements

The most crucial decisions that have to be made at the feasibility stage of a road project relate to its design life and alignment. These decisions require an evaluation of the risks posed by geomorphological hazards, the likely costs that will be incurred by avoiding or accommodating them, and the economic political, social and strategic benefits to be gained by road construction. Feasibility studies are usually undertaken on the larger projects, such as the Dharan-Dhankuta road (Section 4.2) and the proposed Hile-Khandbari road in east Nepal, to examine these considerations. Risk may be defined as a function of hazard magnitude, frequency or probability and total impact or damage potential. Where a number of hazards are identified within the route corridor(s), it may be extremely difficult to evaluate relative risk. In addition, earthworks induced hazards of mass movement and erosion, created by slope oversteepening in excavations and overloading by fill and spoil tipping, are virtually impossible to predict at the feasibility and preliminary design stages. However, experience gained from the construction and maintenance of existing roads in the area, or in areas of similar terrain conditions, might enable this problem to be partly overcome.

Although, ordinarily, the likely benefit to be gained by the construction of the road might determine the amount of money made available for the project, the true benefit is rarely quantifiable in the case of road construction in both the Nepalese and Indian Himalaya, because the benefits are often political. In addition, many of these roads are constructed primarily for strategic and military purposes. Quite often, the design philosophy adopted will be determined by the finance that can be made available. As far as internally funded roads in Nepal are concerned, there is often insufficient finance available to allow anything but low cost design and construction philosophies to be adopted. However, in the case of externally funded roads by the British, Indian and Chinese governments, for instance (Table 2.2), there is often more scope for a greater investment in alignment and construction design, allowing both a greater flexibility in the choice of route corridors and a higher integrity of road construction.

On the basis of the walk-over survey of Lower Himalayan roads (Table 2.2), it is possible to identify two main design philosophies. These are based on the concept of: i) high initial investment during design and construction and low maintenance costs, and ii) low initial investment but relatively high recurring

maintenance costs. The suitability of either philosophy will depend on terrain conditions, hazard severity and funding. A philosophy based upon routine maintenance may be the only option feasible for low-cost roads, and under conditions where hazards cannot be avoided or practically stabilized. High initial investment strategies are more appropriate for important, long-term roads such as the Kathmandu-Kodari, Muglin-Narayanghat and Dharan-Dhankuta roads in Nepal. However, experience has shown (Table 2.2) that high investment roads, often requiring extensive off-site and on-site stabilization and protection works, result in considerable maintenance expenditure, especially when located in particularly hazardous terrain. Consequently, a two-fold categorization of design philosophy is too simplistic.

Essentially, four design options are available to the engineer responsible for location and design, when confronted by geomorphological hazards. The simplest option is to accept that with constraints of limited project finance, the logistical problems dictate that road construction cannot be viable. The project is therefore cancelled or deferred until sufficient finance becomes available. This was the case with the Dharan-Dhankuta road (Section 4.2), in that construction was started ten years after the first trace for the road was cut in the mid 1960s. Alternatively, the option to construct the road and accept the risk posed by these hazards can be taken. The political and strategic necessity to construct mountain roads, and the constraints of extremely low and often uncertain finance, necessitate that this is the option most often taken for internally funded roads in Nepal and India. A prime example of this is the Bhedetar-Rajarani road, currently being financed and constructed by the Nepal Roads Department. The extremely low-cost nature of this road may be illustrated by the fact that only NCRs 1.8 million (approximately £75 000) were made available in 1981/2 for the construction of the first 3.4 kms of the alignment. This figure is only marginally greater than the cost (NCRs 1.6 million (Bofinger and Keith 1985)) of clearing cut slope failure material from the Dharan-Dhankuta road, following a large storm in September 1984. These roads often have contoured and ridge-top alignments in order to reduce earthworks and keep the number and size of structures to a minimum (Plate 2.12). A third option available is to avoid those hazards that pose the greatest risk to road integrity by careful alignment design. The success with which this option can be carried out will depend upon the nature, variety, density and distribution of hazards, and the availability of adequate expertise to properly evaluate their relative risk along each alignment corridor. This option has been chosen for many externally funded roads in India

and Nepal (Table 2.2). The resulting alignments tend to be rather complex in design (Plate 2.13), and are often composed of one or a number of hairpin stacks (Plate 2.14).

Finally, the decision can be taken to avoid the most hazardous slopes and drainage channels, and to attempt to minimise the potential impact of those hazards that are encountered. This option differs from the avoid option, described above, in that preventative and protective measures are undertaken to reduce the risk posed by hazards that have to be crossed, owing to both their sheer number and the locational constraints imposed by horizontal and vertical alignment specifications. These roads are clearly the most costly in terms of initial financial outlay, and therefore the benefit to be gained by creating a long-term road link must be demonstrated at the outset. The Dharan-Dhankuta road provides a good example of this design philosophy (Table 2.2, Appendix 1), and is the most expensive road per kilometre yet constructed in Nepal.

In order to illustrate this final design option, a brief review will be made of the costs incurred in implementing remedial measures at two particularly hazardous sites on the Dharan-Dhankuta road, where road loss has resulted from: a) slope failure in an unstable valley re-entrant, and b) a debris flow that occurred in September 1984 as a result of instability on the slopes above the road. These sites are described in Appendix 1 A.3 and A.6 respectively, and discussed in detail in respect to geomorphological assessment in Chapter 4.

On the northern side of the re-entrant, at km 4.100 from Dharan, deep-seated rotational failure in September 1983 resulted in the loss of approximately 60m of road line (Plate 2.15). Remedial works undertaken consisted, essentially, of site clearance, road excavation, disposal of spoil material, reconstruction of the gabion retained embankment, side drains and erosion protection works. The total costs (materials and labour) incurred in implementing these works are shown in Table 2.3. Measures designed specifically to increase the stability of this slope included the reconstruction of the checkdams in the gully at the base of the slope, and dry stone pitching[1] and contour wattling[2] of the back-

---

1. Stone pitching is the placement of blocks of rock on a slope or channel bed to discourage erosion.

2. Contour wattling is the construction of brushwood (in this case bamboo) fences across a slope to discourage slope erosion.

PLATE 2.13 Sinuous Alignment of the Dehra-Dun-Mossoorie Road.

PLATE 2.14 Hairpin Stack Along the Teesta-Darjeeling Road.

PLATE 2.15 Deep-Seated Rotational Failure at Km 4.100 on the Dharan-Dhankuta Road in September 1983.

PLATE 2.16 Road Loss by Debris Flow at Km 23.400 on the Dharan-Dhankuta Road.

ITEMS OF WORK	QUANTITY	COST (NCRs)
Site clearance	----	745
Earthworks (incl. excavation, disposal and trimming)	----	170 075
Gabions-founding	$210m^3$	2 580
-filling and weaving	$600m^3$	34 950
Side drains, kerbs and confidence blocks	----	14 420
Erosion protection		
a) Excav. of slip material from gully	$500m^3$	2 500
b) Excav. of foundation trench	$192m^3$	1 536
c) Extra hard rock excav. and spreading	----	2 178
d) Filling	----	5 440
e) Checkdams	$240m^3$	14 640
f) terram filter membrane	$50m^2$	50
g) Dry stone slope protection	$360m^3$	20 160
h) Revegetation(25 plants/m^2)	$3000m^2$-75000 plants	6 000
Road sufacing (incl. sub-base, base and surfacing)	----	17 530
Labour and lorry hire	----	19 095
TOTAL		311 899

TABLE 2.3 Breakdown of Costs for Remedial and Associated Works Undertaken Following the Landslide at Km 4.100 Along the Dharan-Dhankuta Road in 1983.

Source : PSA

£=24 NCRs in 1983

scar to prevent erosion. The cost of these works amounted to NCRs 40 800 (£1 700 at 1983 exchange rates), while the total cost of road construction and associated on-site and off-site works, excluding site clearance, plant and labour, road surfacing, base course, sub-base, kerbs and confidence blocks, amounted to NCRs 260 109 (£10 838).

On the opposite, southern, flank of the re-entrant, deep-seated rotational failure in September 1984, involving some 10^5-$10^6 m^3$ of material, destroyed approximately 100m of road line (Plate 2.6). The remedial measures employed on this slope are described in Chapter 4 (Section 4.5). These include surface masonry and subsoil filter drains, dry stone revetments, gabion cut slope retaining wall and erosion protection works (wire meshing of the landslide back-scar together with contour wattling and turfing, to encourage vegetation). Table 2.4 lists the items of work undertaken in connection with road reconstruction (although not surfacing) and slope remedial measures, along with the quantities and costs incurred. The total cost of these works, including contract, labour, materials and miscellaneous items amounted to NCRs 1 047 558 (£43 648 prior to NCR devaluation).

Finally, at km 23.400 on the descent to the Leoti Khola floodplain, the passage of a debris flow through the central drainage channel of an unstable bowl in September 1984, caused road loss and destruction of the gabion retained embankment and erosion protection works below (Plate 2.16). Remedial works employed at this site have included the reconstruction of the road, on gabion retained embankment, pipe culvert and the erosion protection works in the gully below. These works have involved the construction of 6435.5 m^3 of gabion, and the total cost of works at this site amounted to NCRs 2 827 406 (£117 809 prior to NCR devaluation). These figures can be compared with the overall cost of the construction of the Dharan-Dhankuta road (Table 2.5). Items in this table applicable to the works carried out at the sites mentioned above (access and site clearance, earthworks, construction of retaining walls, side drains, area drainage and stability, protection of side slopes and masonry and gabion revetments) amounted to £6 559 311 for the whole road or, on average, £12 978 per 100m.

So far, little mention has been made of the influence that physiography and geology play in the choice of alignment options and the overall cost of the project. The construction costs, per kilometre, of Nepalese hill roads (Table 2.2) serve to illustrate these variations. The highest costs, of the order of £0.2-0.3 million per kilometre, have been incurred along the Dharan-Dhankuta and Muglin-Narayanghat roads, where the terrain of the Mahabharat Lekh

ITEMS OF WORK	QUANTITY	COST (NCRs)
Soft earthworks	1 398.43m^3	14 767.41
Hard earthworks	214.45m^3	3 019.46
Gabion work	701.0 m^3	226 253.18
Boulder breaking	1 537.0 m^3	85.04
Masonry breaking	30.76m^3	1 624.13
Supply of chicken mesh	2 625.0 m^2	160 125.00
Masonry work	1 126.19m^3	316 012.75
Boulder collection and transportation	1 797.0 m^3	89 880.00
Dry stone wall pitching	481.87m^3	35 585.86
Subsurface(French) drains	415.41m^3	77 681.67
Earthworks backfilling	1 033.56m^3	12 464.73
Grass planting	4 369.60m^2	8 739.20
Staff and labour	------	82 943.00
Miscellaneous items	------	18 376.38
TOTAL		1 047 557.81

TABLE 2.4 Breakdown of Costs for Remedial and Associated Works Undertaken Following Slope Failure at Km 3.900 Along the Dharan-Dhankuta Road in 1984.

Source: Roughton and Ptnrs
£=24 NCRs in 1983/4

ITEMS OF WORK	COST(£)	% OF TOTAL
Access and site clearance	139 995	1.19
Earthworks	2 929 728	25.02
Retaining walls	2 261 953	19.32
Sub-base	378 795	3.23
Base course	887 646	7.58
Road surfacing	773 812	6.61
Side drains	379 602	3.24
Culverts	1 035 936	8.85
Bridges	500 532	4.27
Bridge protection	1 242 118	10.61
Site investigation	26 594	0.23
Area drainage and stability	300 038	2.56
River training	304 869	2.60
Side slope protection	207 188	1.77
Masonry and gabion revetment	340 807	2.91
TOTAL	11 709 613	

TABLE 2.5 Breakdown of Costs for the Dharan-Dhankuta Road.

Source: PSA

(Chapter 3) is most steep, and mass movement and flooding hazards are most severe (Table 2.2). The construction cost of the Kathmandu-Kodari road was £0.03 million per kilometre at 1966 prices (Raj 1978). In view of the age of this road, this cost must be regarded as being high. The road has recently (1982-1986) been reconstructed beyond Barabise, following extensive damage caused by flooding in 1981 (Table 2.2), at an estimated cost of approximately £0.25 million per kilometre (Swiss Association for Technical Assistance (to Nepal), pers. comm. 1983). This figure reflects the high risk posed by flooding and mass movement hazards to the road in the engorged Bhote Kosi valley (Plate 2.17), and the relatively high design standard of the road. By contrast, the recently completed (1982-1984) Lamusangu-Jiri, Dhankuta-Hile and Hile-Siduwa roads, that cross relatively stable, shallowly inclined ridge-top topography, underlain by schists and gneisses of the Midland Himalayan zone, have construction costs of less than £0.1 million per kilometre.

The cost figures described above, suggest that the final cost per kilometre of roads constructed in the Lower Himalaya depends upon both their design specifications (dictated by intended function, traffic volumes and design life) and geological and geomorphological setting. It is not possible here to examine the justification for the high design specifications (vertical and horizontal alignments, road width, bend curvature and construction materials) for the Dharan-Dhankuta road, as the necessary cost-benefit data are unavailable. However, it can be concluded that road construction costs in the steep, geomorphologically active terrain of the foothill ranges of the Mahabharat Lekh (Chapter 3) are likely to be higher than elsewhere in the region. On this basis, the relatively high costs of the Dharan-Dhankuta and Muglin-Narayanghat roads may be justified. In addition, both these roads are of high strategic importance; the former being the first and most important stage in the economic development of the Kosi zone, while the latter forms a short, fast route between the Terai Plain and the Kathmandu-Pokhara road and the prosperous Kathmandu valley (Figure 2.2).

Successful road alignment and construction design, based on the philosophy of risk reduction by avoidance, stabilization and protection, requires a sound knowledge of the locations, mechanisms, areal extent and magnitude/frequency of geomorphological hazards. Although prudent alignment design may enable the most severe of these hazards to be avoided, it is inevitable that some unstable and potentially unstable slopes and drainage channels will have to be crossed. Road damage and temporary loss during events of high magnitude are, therefore, likely to be unavoidable within a low-

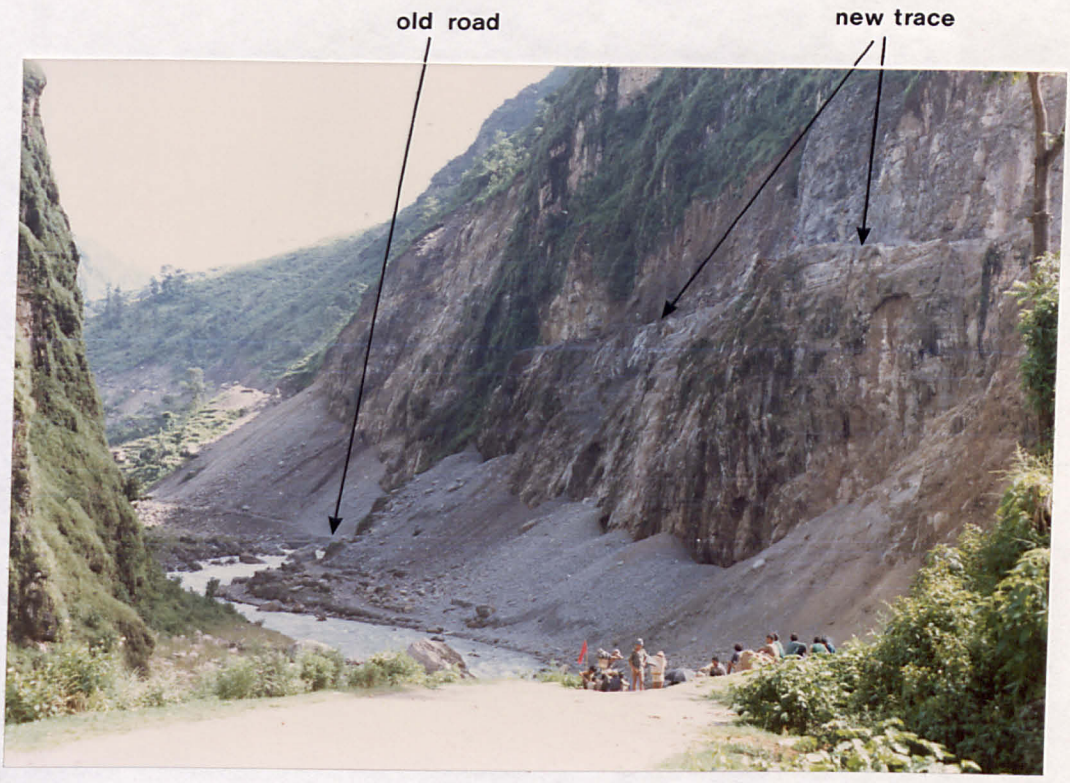

PLATE 2.17 Location of the Kathmandu- Kodari Road in the Engorged Bhote Kosi Valley. (Following Removal of the Road by Flooding, the Alignment has been Relocated Further up the Gorge Flank in Full Cut).

cost design framework, characteristic of roads in unstable mountains. Techniques currently available for terrain and geomorphological hazard evaluation for road feasibility, design and construction will be described and assessed in the remainder of this chapter.

2.5 Geomorphological Hazard Evaluation Techniques for Mountain Highway Design

2.5.1 Mass Movement Hazards

For highway design purposes, the evaluation of mass movements requires the determination of their areal distribution, size, depth, mechanism of failure, present stability, frequency and rate of movement and their likely impact on the proposed road. In addition, effective alignment and earthworks design will require an evaluation of the impact that road construction itself will have on these hazards, through slope oversteepening and overloading. Conventional information sources available at the desk study stage include topographic and geological maps and air photographs, and consequently, with the exception of the distribution, size and possibly mechanism of mass movements, most of this information is unobtainable at this stage. Topographic maps are usually of too small a scale and too generalised to be of any real value to slope stability assessment. Geological maps are usually available in mountain terrain, although they may be too generalised and of too small a scale to be of any practicable value for engineering purposes. However, in certain circumstances, they may allow unstable and potentially unstable slopes to be inferred from bedrock associations and may, in rare instances, actually show landslide deposits.

Air photography, when available, has formed one of the main sources of slope and drainage data at the desk study and reconnaissance stages of highway projects for the last 30 years (Fookes et al 1985). Detailed slope evaluation, including the identification, mapping and classification of individual landslides, may be achieved by stereoscopic analysis of good quality air photographs (Norman 1970, Rib and Liang 1978). However, air photographs may be either unavailable or difficult to obtain for remote mountain terrain, especially in developing countries, or for areas regarded as politically or strategically sensitive. Satellite imagery, while useful for regional terrain and materials assessments is, at present, of too low a resolution to provide any sound basis for the analysis of slope instability, except where this relates to major structural discontinuities (Fookes et al 1985). However, White (1983) maintains

that LANDSAT imagery may be used to identify large, prehistoric landslides in the Nepal Himalaya. It is also apparent that improved landslide identification has been facilitated with imagery obtained from the Thematic Mapper with a ground resolution of 30 m.

Ground reconnaissance geotechnical mapping exercises usually include geomorphological and engineering geological surveys, that are undertaken as a rapid and relatively inexpensive means of assessing the distribution, mechanism and severity of slope and drainage hazards. Geomorphological ground reconnaissance techniques include detailed mapping, slope profiling and the systematic collection of slope and drainage data by the proforma method (Hansen 1984). Geomorphological mapping is a useful technique of terrain assessment for highway design, particularly at the reconnaissance stage, and especially in the absence of air photography. Combined with air photograph interpretation, the technique can be made even more expedient and precise. An account of the development and nature of morphological and geomorphological mapping has been given by Martin (1978).

Engineering geological mapping, as defined by Fookes (1969), Geological Society of London (1972), and Dearman and Fookes (1974), is a mapping technique for recording slope morphology and rock and soil conditions, pertinent to engineering design. These maps often contain a greater emphasis on rock and soil descriptions than geomorphological maps, but usually do not portray the same degree of morphological detail. Engineering geological mapping should ideally follow on from a geomorphological survey, in order to assess the geomorphological findings in terms of engineering design criteria. Engineering geological mapping and geomorphological mapping have been used in connection with road projects in many mountain regions, including the Lower Himalaya (Brunsden et al 1975a and b, Gangopadhyay 1978), the Alps (Fenti et al 1979) and the West Carpathians of Czechoslovakia (Malgot and Mahr 1979).

Slope profiling, using an abney level or clinometer, can be used in conjunction with geomorphological mapping, to provide a third dimension to the interpretation and recording of slope morphology. This technique, first explored at Stonebarrow Hill, Dorset (Brunsden and Jones 1972, 1976), was used as part of the detailed geomorphological reconnaissance survey for the Dharan-Dhankuta road, in conjunction with mapping and slope inventory using proformas (Brunsden and Jones 1975, Martin 1978). Accurate slope profiles are also required for stability analyses following ground investigations (see below).

The inventory technique, using proformas and check lists, allows slope data to be recorded systematically and objectively, on the basis of measured distances along an existing or proposed road, or within grid cells on a map, and was first proposed by Cooke and Doornkamp (1974). The technique has since been used in southern Italy (Carrara et al 1977, 1982), southern Spain (Martin 1978) and on the Dharan-Dhankuta road (Martin 1978). Although the technique can be time consuming, necessary fieldwork can be reduced if suitable air photographs, topographic maps and geological maps are available. However, in complex terrain, the efficiency of the proforma technique may be reduced owing to the difficulty in deriving representative data for each sample length or grid cell (Martin 1978).

In addition to its application at the reconnaissance stage, geomorphological mapping may form the basis for the design of more detailed ground investigations (Chapter 4). This is certainly the case where geomorphological and engineering geological mapping can be used to rapidly identify problematic slopes that will require further investigation. However, the ability of geomorphological mapping to predict sub-surface soil conditions by extrapolating site specific site investigation data across landform units, will depend largely on the complexity of landscape development and the nature of superficial deposits. Martin (1978) found that the coefficients of variation in the Atterberg limits of colluvial slope materials in the vicinity of the Sevenoaks by-pass in Kent, were independent of mapping units, and concluded that geomorphological mapping would have been of little use in predicting sub-surface conditions. However, in mountainous terrain, where slope and drainage processes are far more active, and where discrete landforms are easily distinguishable and relatively fresh, predictions of soil types, by geomorphological mapping, may be more successful.

At the desk study and reconnaissance stage of a highway project, landslide hazard maps can be a useful back-up to air photograph interpretation. These maps may either simply depict the distribution of landslides within an area (direct mapping), or they may attempt to determine the spatial distribution of landslide susceptibility by a systematic evaluation of slope and drainage criteria that determine the location of, and potential for, slope failure (indirect mapping). Techniques and applications of landslide hazard mapping are described in detail in Hansen (1984) and Varnes (1984), and are discussed in Hearn and Fulton (1986) and Chapter 5 of this thesis. While these techniques may be of some value for preliminary hazard assessment at the small scale, they are of little value at the site scale, where detailed geotechnical mapping and ground investigation should be used.

Descriptions of ground investigation techniques and slope stability analyses for soil slopes are given in Clayton et al (1982), Petley (1984) and Bromhead (1986). Methods of investigating and analysing the stability of rock slopes are described in Hoek and Bray (1982). These analyses rely on the availability or derivation from the ground investigation of geotechnical data relating to soil and rock density, structure, strength parameters and groundwater levels. However, owing to problems of inaccessibility and the general low-cost technology characteristic of most mountain highway projects, detailed ground investigation is normally impracticable. Kojan et al (1972, p.125) maintain that "Even if accurate stability assessments of natural slope stability could be performed by intensively applied engineering techniques, it is obvious that an entirely new approach is needed if the essential forecasts of slope stability are to be made at reasonable costs ...". This requirement can be largely fulfilled by detailed geotechnical, and particularly engineering geological mapping together with a limited number of trial pits and benches (Fookes et al 1985) and logging of exposures, both natural and in excavations. Procedures for field description of rock slopes for engineering purposes are described by Piteau (1970). A number of cases have been reported in the literature where trial pitting, sampling and laboratory testing have been used to investigate individual, high risk landslides along Lower Himalayan roads. Hashmi and Haq Izhar (1984), for instance, describe the use of trial pitting to determine the depth of the slip surface and the groundwater table for the new Rara landslide on the Murree-Muzaffarabad road in Pakistan. Block samples were removed for the laboratory determination of plasticity index, density, moisture content and residual shear strength. Similar studies have been undertaken along the Jammu and Kashmir National Highway No 1A (Didwal 1984) and the Dharan-Dhankuta road (Chapter 4).

Monitoring of landslide displacement provides a data base that can be used directly in design, if sufficient time for data collection is available at the beginning of the project. This data may allow engineering designs to be continuously assessed and modified where necessary. There are very few published cases of the use of long-term monitoring for landslide hazard assessment in the Lower Himalaya. Consequently, there appears to be some scope for increasing the use of the technique on future highway projects in the region. The monitoring of slope displacement can be undertaken in a variety of ways, by ground survey, inclinometers and extensometers, repeated air and ground photography (photogrammetry), topographic surveys, morphological mapping and slope profiling. A description of some of these and other monitoring techniques has been given by Hutchinson (1970) and Franklin (1984).

The principal disadvantage of the monitoring technique for slope stability assessment is that it may take some time (of the order of 2-10 years) before meaningful results are obtained.

In conclusion, an optimum procedure for assessing mass movement in mountain terrain for highway design purposes should include the interpretation of available air photographs, followed by detailed geomorphological walk-over surveys, engineering geological mapping, trial pitting and monitoring. Although geomorphological ground survey techniques offer a great potential for the assessment of mass movement, their application and ability to provide useful terrain data for highway design in unstable mountains needs to be examined (Chapter 4).

2.5.2 Flood Hazards

Catchment runoff prediction methods can be categorised into two main approaches (Anderson and Howes 1986), namely those directed towards scientific advancement and research, and those that are developed to solve practical problems for engineering design and watershed management purposes. Progress in the former category depends on the derivation and modelling of within-catchment variability in runoff controlling factors (Beven 1986) such as rainfall intensity and duration, infiltration, antecedent moisture conditions, sub-surface, overland and channel flow rates and hydrograph routing through the channel network. Anderson and Howes (1986, p 161) maintain that "Improvements in hydrological forecasting for ungauged catchments will only be realised by selective application of elements of physically based models of hillslope processes whose parameters relate directly to measurable, physical basin characteristics". Thus, rigorous physical modelling often requires a high integrity data base and lengthy computer programming, and at best may be only applicable to a limited number of instrumented slopes or catchments. These techniques are, therefore, of little use in remote ungauged catchments, where both catchment and hydrological data are often non-existent. Under these conditions, less rigorous ungauged catchment techniques of runoff prediction are likely to be the most appropriate and rapid methodologies to adopt for practical engineering purposes. Anderson and Howes (1986, p164) define an ungauged catchment as one "in which the only available data are those of topographic and soil maps together with precipitation and antecedent moisture conditions". In the Lower

Himalaya, the engineer cannot usually rely on even these data sources being available, and consequently, is forced to adopt oversimplified rainfall-runoff models and universal and regional flood formulae.

Essentially, storm runoff predicting models can be divided into linear and non-linear varieties. The Unit Hydrograph method, first proposed by Sherman (1932) is a very simple, but popular, linear transformation of rainfall data into a runoff hydrograph. The technique incorporates the notion of the 'effective' rainfall that generates storm runoff, and this is estimated from existing rainfall and runoff records. In mountainous terrain, especially in developing countries, few catchments are sufficiently well instrumented for the Unit Hydrograph technique to be practicable, unless synthetic hydrographs are computed by calculating catchment time to concentration and hydrograph base time from catchment area, length and slope (Watkins and Fiddes 1984).

The Rational Method (Kuichling 1889) is probably the simplest and best known rainfall-runoff model for calculating storm runoff from rainfall data. The standard form of this model is

$$Q = CIA \qquad \text{.....2.1}$$

where Q is peak runoff rate (cumecs), C is a runoff coefficient, I is maximum rainfall intensity (mm/hr) and A is catchment area (kms^2). Owing to its simplicity and ease of computation, this linear transformation of rainfall into runoff has been widely applied in civil engineering. However, in large catchments especially, the assumption of uniform rainfall intensity and a runoff coefficient that remains constant, both temporally and spatially, is untenable (Armentrout and Bissell 1970). The application of the model to mountain catchments, where rainfall duration and intensity are highly variable and dominated by intense localised events, is particularly limited. Nevertheless, the lack of available data in these areas, upon which to develop more analytical models, means that the Rational Method may be the only practical way of undertaking preliminary hydraulic design. The Gupta Modified Rational Formula (Gupta 1966, 1973) has been developed to augment the Rational Method by incorporating additional catchment parameters of shape, slope and the concept of effective catchment area, and therefore may allow flood discharge prediction to be more accurate.

Watkins and Fiddes (1984) describe the computation of the Generalised Tropical Flood Model from the ORSTOM and TRRL models. Discharge is

calculated using total storm rainfall, hydrograph base time and a runoff coefficient that combines indices of soil permeability, catchment slope, land-use and catchment wetness, in the following equation,

$$\bar{Q} = F \frac{C_s C_w C_L P A}{360\, T_B} \qquad \text{.....2.2}$$

where

C_s, C_w and C_L are catchment runoff, wetness and land use coefficients,
P is total storm rainfall (mm),
A is catchment area (kms^2),
T_B is hydrograph base time (hours) and
F is a dimensionless peak flow rate conversion factor.

While the inclusion of these physical and hydrological catchment coefficients into the discharge computation may enable the model to become representative of rainfall-runoff conversion, difficulty may be experienced in assigning values to these coefficients. For instance, the categories of the peak flow factor F, derived in West Africa (Watkins and Fiddes 1984), are arid, humid and forest. This differentiation might be inappropriate in humid sub-tropical mountains. Caution should be exercised, therefore, when applying discharge prediction models to areas outside the physio-climatic region for which they were derived.

Regional flood discharge formulae are usually based on the principle that rainfall-runoff response is a simplified input-output system, parameterised for a particular catchment, or suite of catchments, within the same hydrological domain. Within this domain, the catchment runoff response to storm rainfall is considered to be uniform. Both linear and non-linear transformations have been devised. Many of these empirical ungauged catchment equations take the form of envelope curves for maximum flood data for particular regions, and therefore, may tend to overestimate flood discharges. The most simple of these equations is one where storm runoff is computed from catchment area alone. The major disadvantages of these techniques are the exclusion of rainfall data and catchment variables other than area from the computation. More elaborate models incorporate empirical optimisation of additional catchment variables such as slope, drainage length, drainage density, relative relief and indices of land use and soil type. Griffiths (1983) has tested 61 ungauged catchment equations using data obtained from eighteen catchments in the Gila River Basin, U.S.A. He concluded that the majority tend to over-estimate peak discharge, and that storm runoff prediction in semi-arid

catchments could not be satisfactorily achieved using ungauged catchment techniques derived elsewhere. The same must be true for runoff prediction from mountain catchments, such as those in the Lower Himalaya, where monsoonal storm rainfall tends to be areally concentrated, and where slope inclination and soil and rock permeability, and hence runoff response, are highly variable. The problem is further exacerbated by the fact that the rate of runoff per unit area of catchment usually decreases as catchment area increases (Pilgrim et al 1982).

Representative storm runoff hydrographs may be obtained by direct monitoring. V-notch weirs, flumes and stage recorders have been used effectively in a number of different hydrological regions, to obtain a continuous record of stream flow from predetermined stage-discharge relationships (Gregory and Walling 1973, Taylor and Pearce 1982). This enables the determination of runoff parameters pertinent to hydraulic design, namely total storm runoff volume, peak discharge and time to concentration, and forms the basis for direct physical modelling. However, the proportion of catchments that are monitored in this way is small, especially in remote mountain terrain where direct monitoring is both hazardous and fraught with design and operational problems (Chapter 8).

In the event of a complete absence of rainfall and channel discharge data and suitable ungauged catchment equations, it may be necessary to look to field evidence and historical records for an estimate of peak flow rates. Morphological changes, brought about by the passage of a flood, serve as indicators of peak flow stage. Erosional landforms indicative of peak stage include undercut regolith and rock slopes adjoining the channel, and newly created flood channels. Eroded banks and river terraces, above the level of the contemporary floodplain, provide an approximate indication of the lateral extent and peak stage of floodwaters. The accuracy with which peak discharge can be determined from these erosional indicators is likely to be low. In humid sub-tropical mountain terrain with a seasonally distributed, high intensity rainfall regime, the concept of a dominant channel forming discharge, equivalent to bank-full in humid temperate regions (Nixon 1959, Leopold et al 1964, Richards 1982), is inappropriate, as channel morphology tends to be controlled by rare, high magnitude events (Wolman and Gerson 1978).

Depositional evidence of peak flood level consists of stranded flood deposits of silt, sand, boulders and brushwood on river terraces and adjacent slopes. Once

peak flow channel cross-sectional area has been determined, using these stage indicators, it can be combined with the peak velocity from the Manning formula to yield peak discharge by the slope-area method (see Chapter 7). However, flood-level indicators and channel cross-sectional form may relate to a number of peak flows of uncertain date and recurrence interval, while the assumption of a constant channel and flow roughness coefficient for velocity computation, is far from satisfactory. These considerations are discussed in more detail in Chapter 7.

In conclusion, there is a variety of storm runoff predicting formulae that range in complexity according to their data requirements and computation. In many remote mountain regions, and particularly in the Lower Himalaya, rainfall and runoff data are extremely limited, and the degree to which the various flood discharge formulae outlined above can give satisfactory predictions, remains uncertain.

2.5.3 Sediment Hazards

Reliable evaluations of sediment yields from mountain catchments are vital to efficient hydraulic design, and depend upon an understanding of sediment supply, transportation and deposition. While the engineering and geomorphological literature contains many detailed, process-based studies concerning all three aspects of sediment dynamics, the ability to predict, with any certainty, rates of sediment transport and deposition in a given channel reach, remains limited. This is because the identification and measurement of slope and channel characteristics, and the runoff hydraulics that govern sediment supply and transportation, have proved difficult.

In mountain catchments, channel sediment is derived from valley-side mass movement, slope erosion and channel scour (Anderson 1975). Despite a considerable development in geotechnical engineering and geomorphological research, the ability to predict the distribution and magnitude of mass movements and channel scour is still very limited. The problem is exacerbated by the fact that not all eroded material is transported through the catchment immediately; it may be stored for considerable periods of time in terraces, debris fans and braided channel reaches.

Considerable experimental work has been undertaken to determine critical flow velocities for particle entrainment (Brahms 1753, Shields 1936). However, the combination of variable particle size, and the effect of larger particles on

the distribution of flow shear, reduces the applicability of the concept of a single critical flow or entrainment velocity, to the prediction of suspended sediment transport rates. Once entrained, suspended sediment may travel for considerable distances, supported by turbulence, requiring very little additional energy expenditure by channel flow. In addition, a gradual exhaustion of sediment may take place during the wet season or even during individual storms (Gregory and Walling 1973, Renard 1974). For these reasons, the prediction of suspended sediment loads transported during storm runoff, on deterministic grounds, has been largely unsuccessful. Despite the complexity of suspended sediment production and entrainment, attempts have been made to relate concentrations to discharge by way of rating curves (Walling 1977). Regression equations have been derived from such data in order to produce a statistical 'best-fit' relationship between these two variables, for predictive purposes (Richards 1982). At best, these techniques may only provide general approximations of sediment loads for the reasons outlined above, and require the development of a considerable data base for their compilation.

It might be assumed that bedload transport rates are more reliably predictable than suspended sediment rates, owing to the dependence of bedload movement on definite hydraulic parameters of flow. However, major discrepancies have arisen between observed bedload transport rates and those predicted by the various bedload formulae. Flow parameters that determine bedload movement are essentially randomly distributed on the channel bed and they are extremely difficult to quantify, as their relationships with readily measureable hydraulic variables, such as flow velocity and depth, are uncertain. In addition, the majority of predictive formulae assume a uniform flow and an homogeneous bed material size. These assumptions are untenable, particularly in mountain channels where flow dynamics are controlled by channel constrictions, rapid changes in channel gradient and large calibre bed material.

The majority of bedload formulae, with the exception of those proposed by Einstein (1950) and Bagnold (1960), are synonimous with the original duBoys (1879) tractive force formula. A number of computational definitions of the critical tractive force have been proposed. They all refer to a characteristic grain-size of bed material, and therefore, oversimplify boundary conditions (Thornes 1979). In addition, most bedload formulae have been derived for bed material with a diameter of 0.3-7 mm (Kinori and Mevorach 1984) and, consequently, may be largely inappropriate for the gravel, cobble and boulder material found in mountain channels in the Lower Himalaya.

Many investigators have preferred to adopt the concept of available stream power. Stream power represents the amount of energy available for total sediment transport, once the internal flow and channel boundary friction has been overcome (Bagnold 1960, Yang 1972). The notion of stream power provides a conceptual upper limit to the rate at which debris can be transported (Dunne and Leopold 1978). However, while the concept has application to theoretical studies and intensely monitored flume and channel flows, its practical application for engineering purposes is restricted by limited flow data.

Another important method for predicting bedload transport that has received considerable support, is the probabilistic concept of Einstein (1950). Einstein, and subsequent investigators, attempted to incorporate the crucial parameter of flow turbulence into the prediction of bedload transport. The procedure has gained popular support but requires high integrity flow and sediment data in its computation. Kinori and Mevorach (1984, p303) conclude that the Einstein method presents "formidable difficulties" when applied to engineering.

An alternative methodology, to those described above, has been to correlate observed transport rates with measureable discharge parameters, such as peak discharge or velocity. This has the advantage of avoiding the theoretical assumptions and computational difficulties of the deterministic techniques, but nevertheless requires the development of a considerable experimental data base.

In conclusion, although considerable effort has been directed towards the development of bedload transport formulae, there is often a significant difference between predicted and observed bedload rates in natural channels. The bedload transport rate, as predicted by the different formulae available, can vary by up to ten-fold (Muir 1970). This has resulted mainly from the difficulty in accurately monitoring bedload transport, especially in high energy mountain channels, the complexity and essentially random nature of flow parameters, and the heterogeneity of bed material calibre and channel roughness.

Quite often slope and drainage disturbance by earthworks, road drainage and spoil tipping may cause extensive soil erosion, and a higher rate of sediment transport through the channel network than would be expected from natural processes of sediment supply. There appears to have been very little experimental work undertaken to examine the severity and longevity of these

construction-induced hazards. Consequently, at the beginning of a road project, the potential for, and impact of, these hazards may be uncertain.

2.6 Conclusions and Specific Aims of the Thesis

This chapter has described the various geomorphological hazards operating in humid sub-tropical young fold mountains with particular reference to the Lower Himalaya. The exact nature of these hazards depends largely upon physiography, climate and geology. Nevertheless, it is possible to recognise a broad range of mass movements and flood and sediment hazards that tend to be characteristic of this terrain.

The impact of these hazards on mountain roads has been described and illustrated by reference to the Lower Himalaya of Nepal and India. These hazards affect the stability of mountain roads in a variety of ways, depending upon their mechanism, impact severity, magnitude and frequency and location with respect to the road. For instance, the impact of mass movements on a road, can vary from cut slope failures that may recur on an annual basis, to large infrequent slope failures that cause road loss. The impact of flooding may be equally severe, leading to road and culvert inundation by sediment, and damage or removal of long sections of floodplain alignment by erosion.

This chapter has discussed the various techniques available for assessing these hazards for highway design purposes. On the basis of this discussion, it is possible to identify a number of distinct fields of research, that might lead to an improvement in the nature and execution of techniques of slope and drainage hazard evaluation for highway design in general and, more specifically, with reference to roads in young, sub-tropical fold mountains.

The specific aims of the research described in this thesis are therefore to:

i) critically assess the contribution made by geomorphological ground survey to road design in unstable mountain terrain, and make recommendations for the future application of geomorphological reconnaissance techniques (Chapter 4),

ii) identify and evaluate the factors that control the distribution and nature of both naturally occurring and construction-induced slope instability, and develop and test a landslide hazard mapping technique for use at the desk study and reconnaissance stages (Chapter 5),

iii) evaluate the extent of erosion and instability caused by spoil tipping and make recommendations for future practice (Chapter 6),

iv) develop a geomorphological reconnaissance technique for evaluating channel stability and predicting peak storm runoff from field evidence and ungauged catchment techniques (Chapter 7),

v) develop and test suitable monitoring schemes for evaluating hazardous processes along mountain roads, namely erosion rates at spoil disposal sites, storm runoff and sediment transport, in steeply inclined channels, and landslide displacement (Chapter 8),

vi) propose an optimum package of techniques and procedures for evaluating mass movement and drainage hazards for highway design purposes in this terrain (Chapter 9).

The fieldwork for the research has been undertaken in the Himalayan foothills of Nepal and India. The majority of the work has been concerned with a post-construction evaluation of the Dharan-Dhankuta road in eastern Nepal, where the geomorphological and geotechnical input to design has been relatively extensive, in a terrain of immense slope and drainage instability. The physical setting of the Lower Himalaya, and the Dharan-Dhankuta area in particular, is described in the following chapter.

CHAPTER 3

THE PHYSICAL SETTING OF THE LOWER HIMALAYA AND THE DHARAN-DHANKUTA AREA IN EAST NEPAL

3.1 Introduction

This chapter briefly describes the geological, geomorphological and climatological character of the Lower Himalaya and, in particular, the Dharan-Dhankuta area in east Nepal, in order to provide a background to the field research presented in the remainder of this thesis.

3.2 Physical Setting of the Lower Himalaya of Nepal and India

3.2.1 Physiography and Geology

The Himalayas are one of the youngest, and certainly, the most tectonically active of fold mountain chains in the world. The Himalayan Range extends in a northwesterly-southeasterly arc, from where the R. Indus rises in the Karakoram Mountains in the west, to the Bhrahmaputra gorge in the east - a total distance of 2 400 kilometres. The Himalayas are bounded to the south by the Ganges Plain, and to the north by the Tibetan Plateau. They have evolved through a complex prolonged episode of tectonic activity associated with the collision of the Eurasian and Indian continental blocks which began in the Mid-Late Cretaceous period (Gansser 1973, Allegre et al 1984, Yielding et al 1984) and continued into the Tertiary with major crustal deformation during the Miocene. Tectonic activity has continued into the Pliocene and Quaternary, with the majority of disturbance and uplift concentrated along the Main Boundary Thrust/Fault (Allegre et al 1984). Indeed, Low (1968) suggests that parts of the Himalayas have risen by up to 1500m since the Lower Pleistocene.

The present mean rate of uplift has been calculated as approximately 1-1.4 mm per year (Brunsden et al 1981, Windley 1985), while the mean denudation rate is of the order of 1.0 mm per year (Khosla 1953,Menard 1961). Much of this activity is concentrated along the first foothill ranges known as the Mahabharat Lekh, where the presence of the Main Boundary Thrust (MBT) has resulted in continued uplift, while high precipitation (see Section 3.2.2) has

enabled drainage incision to keep pace. Both uplift and denudation rates vary considerably within the region, with uplift rates of up to 4 mm per year reported for the foothill ranges in Pakistan (Windley 1985). Mean denudation rates of up to approximately 5 mm per year have been reported for the Darjeeling area of West Bengal (Starkel 1972) and the Tamur catchment in east Nepal (Ahuja and Rao 1958, Seshadri 1960). The result is a landscape with a physiography that is characterised by extremely high relative relief. Further north, away from the main zone of current tectonic activity, the relative relief becomes less and the topography more subdued. However, uplift along subsidiary thrusts, such as the Main Central Thrust (MCT), and incision along the main rivers such as the Arun, Tamur and the Sun Kosi in east Nepal have created localised zones of high relative relief. Much of the base level lowering in the trunk rivers has been transmitted rapidly upstream, in the respective catchments, to cause local oversteepening of the lower side-slopes of tributary rivers. Therefore, while the rates of uplift and denudation vary temporally and spatially, the Lower Himalaya, and the Mahabharat Lekh in particular, appears to be rising at a rate that is at least equal to that at which it is being denuded under present climatic conditions.

The Himalayas can be divided into five longitudinal, strike oriented, east-west trending, relief units (Brunsden et al 1975a and b, Fookes and Marsh 1981). Four of these units are shown on the geological cross-section in Figure 3.1. The three northern-most units are, from north to south, the Tibetan Marginal Range (6000-7000 m asl), the High Himalaya (6000-8000 m asl), which includes mountain peaks such as Everest and Kanchenjunga, and enclosed intermontane basins. The remaining two relief units are the extensive Middle Himalaya, rising to 4500m, and the narrower Lower Himalaya which rises to 1200 m and often has an abrupt termination at the margin of the Ganges Plain.

Three main geological units can be identified that constitute the Himalayan Range (Figure 3.1): the High Himalayan Unit (granites, gneisses and Tibetan sediments) that underlies the High Himalaya; the Lesser Himalayan Unit (phyllites, schists, gneisses and quartzites) that underlies the Middle and Lower Himalayas and the sedimentary Siwaliks and low grade metamorphics (sandstones and phyllites) of the Border Unit that have been thrust together along the MBT. It is generally agreed (Hagen 1952, Gansser 1964, Stocklin 1980) that the crystalline granitic and gneissic bedrocks underlying the High Himalaya have been overthrust southwards onto the

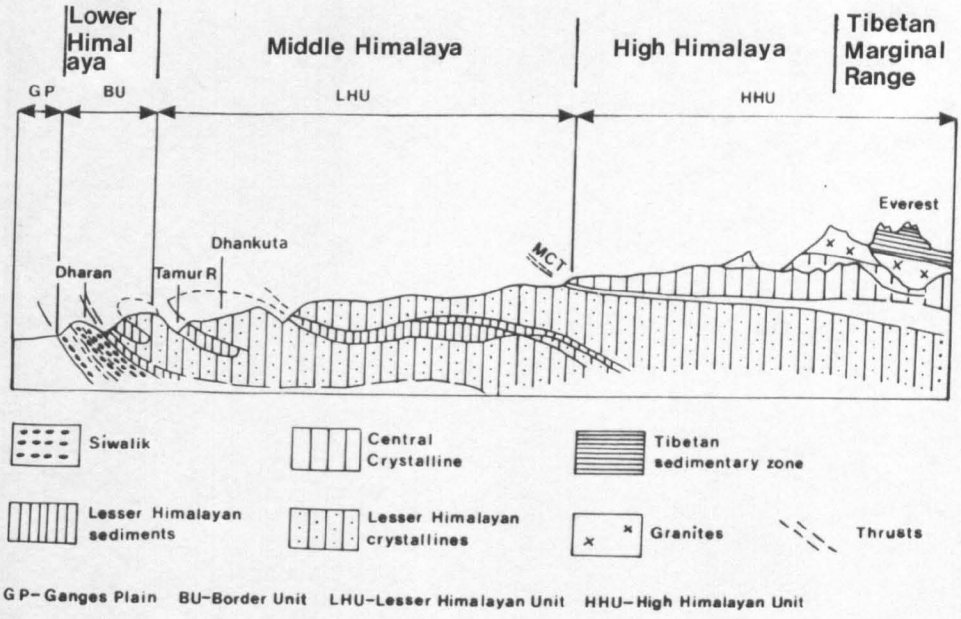

Figure 3.1 Geological Cross-Section of the Himalayas

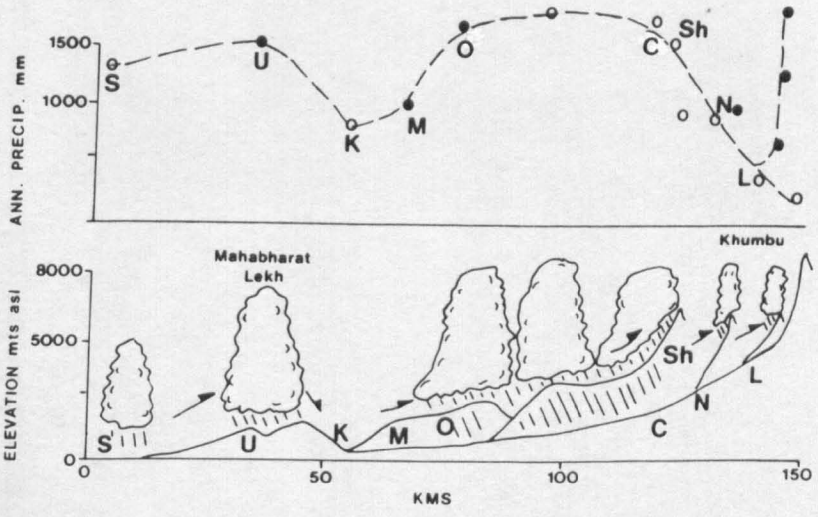

S - Sirawa
U - Udayapur Gadhi
M - Mane Bhanjyang
O - Okhaldhunga
Sh - Shorong
C - Chaurikharka
N - Namche Bazar
L - Lhajung

Figure 3.2 The Distribution of Annual Precipitation with Elevation in the Himalayas between Sirawa and Lhajung, Nepal.
(Black circles denote recording stations around peaks, ridges and plateaux, open circles denote stations located in valley bottoms). (After Higuchi et al 1982).

phyllites, schists and quartzites of the Middle and Lower Himalayan ranges, along the MCT. Similarly, the Lesser Himalayan sediments that now form the Middle and Lower Himalayas, have been thrust onto the rocks of the Border Unit. The MBT separates the Lower Miocene Siwaliks from the overlying metamorphosed rocks at the foot of the Mahabharat Lekh. These rocks are referred to as the Dharan Bazar and Sangure Series, respectively, in the Dharan-Dhankuta area (Section 3.3.3). The two main thrust zones (the MCT and MBT) dominate the structural geology of the Lower and Middle Himalayas, and extend along the entire length of the mountain chain.

The structural geology and stratigraphy of the Lesser Himalayan Unit that underlies the Lower and Middle Himalayas are extremely complex owing to the considerable folding, faulting and thrusting that has occurred. One of the most conspicuous characteristics of the Lesser Himalayan sediments, is the decrease in metamorphic grade with depth in the geological succession. This apparent reversal of metamorphism is accompanied by a younging of sediments with depth. These phenomena have been explained by reference to widespread 'napping' (Hagen 1952, Gansser 1964, Hagen 1969, Stocklin 1980) although other, less probable, interpretations have been suggested, such as recumbent folding and heat metamorphism by granite intrusion (Banerjee and Bisaria 1975, Kumar and Agarwal 1975) and the development of horst and graben structures (Sharma 1977). The main nappe structures postulated are intimately related to the thrust zones described by Bordet (1961) and shown in Figure 3.1.

Along the majority of the foothill ranges, the Siwalik rocks form a narrow range of hills that are separated by the MBT from the Mahabharat Lekh mountain range of the Lower Himalaya, further north. However, in the vicinity of Dharan, in east Nepal, the Siwalik and Sangure Series sediments converge to form the Mahabharat Lekh, but still remain separated by the MBT (Figures 3.1 and 3.4).

The highly disturbed condition of the metamorphosed rocks that form the Lower Himalaya, renders them highly susceptible to the exogenic processes of weathering, erosion and mass movement described below.

3.2.2 Climate and Geomorphology

The present hydrological regime of the Lower Himalaya is controlled, primarily, by the South Asian Monsoon. During the winter months, the upper

tropospheric air-flow is dominated by westerlies, including a pronounced jet stream. This jet steers winter depressions over Pakistan and northern India. By the end of spring (May), the westerly jet has migrated northward and is replaced by a higher level (150 mb) easterly jet over southern Asia at approximately $15^{o}N$. This wind reversal marks the onset of the Asian 'monsoon' (Lockwood 1974, Nayava 1974, Nieuwolt 1977). Depending upon location, the monsoon rains begin in May or June, but are usually preceeded by short, violent and discrete thunderstorms.

Owing to the orientation of the Himalayan chain with respect to the south-easterly low-level monsoonal air flow, rainfall tends to decrease from east to west, and south to north. However, the mountains exert a significant orographic influence on rainfall (Nayava 1974). Figure 3.2 shows the distribution of mean annual precipitation in a north-south direction in central Nepal, between Sirawa on the Ganges Plain and Namche Bazar and Lhajung in the Middle Himalaya. As a general rule, precipitation is highest over the Mahabharat Lekh and the Middle Himalaya (approximately 1500mm per annum in the cases of Udayapur Gadhi and Okhaldhunga (Figure 3.2)). Annual precipitation tends to decrease rapidly on the leeward side of the Mahabharat Lekh (Figure 3.2) to approximately 800 mm and towards the High Himalaya where, at Lhajung for instance, mean annual precipitation is approximately 200 mm. Superimposed on this generalised precipitation distribution, are local variations caused by orography. Nayava (1974) and Dhar and Bhattacharya (1976) have demonstrated that the majority of monsoon rain in the Nepal Himalaya falls on the windward side of the Mahabharat Lekh, and generally increases with altitude. This altitudinal variation has also been demonstrated by Higuchi et al (1982) who describe five-fold increases in annual precipitation with altitude in the High Himalaya (Figure 3.2).

The Mahabharat Lekh, being the first main ridge encountered by the monsoon air flow, usually experiences the highest precipitation totals and intensities. Mean annual rainfall totals for recording stations along the ridge are usually in the range of 2000-4000mm. At Dehra Dun, in the north-west Himalayan state of Uttar Pradesh (India), the average annual rainfall is 2162mm, whereas in the Darjeeling hills of West Bengal, in north-east India, it is 3092mm (Starkel 1972). However, as much as 80-85 percent of this annual total can fall during the four month period between June and September.

Catastrophic downpours can affect large portions of the Lower Himalaya and may last for a number of days. Starkel (1972) quotes the 1968 storm over Darjeeling when 465.1 mm of rainfall were recorded in 24 hours. Soin (1980) reports 72-hour storm rainfall totals of 403 mm and 461 mm in 1968 and 1973 respectively in the Sikkim Himalayas of northeast India. The large storm of September 1984 (Section 3.4) affected large areas of the Lower Himalaya in east Nepal. Okhaldhunga and Dhankuta, for instance, received 132mm and 146mm of rainfall respectively in 24 hours, while 275 mm and 291 mm of rainfall were recorded at Dharan and Mulghat (Section 3.4). Further west, rainfall recorded during this storm was significantly less, with 24-hour totals of 33 mm and 25 mm being received at Pokhara and Kathmandu respectively.

The intense rainfall associated with these downpours, often exceeding 100-200 mm per hour (Starkel 1976, Natarajan et al 1980), causes a rapid rise in groundwater levels leading to widespread mass movement, overland flow (when soil and rock permeabilities are exceeded), headward extension of drainage networks and major flooding.

Rapid uplift and channel incision have combined to produce a landscape characterised by high relative relief. Slope inclinations are usually in the range of 30-40^{o}, but frequently increase to 50^{o} or more wherever channel erosion causes active slope undercutting, or where relatively resistant bedrocks, such as quartzites and hard schists, crop out. During high magnitude storms, considerable volumes of debris are supplied to the drainage networks from mass movement and both channel and slope erosion. This debris accumulates in channels, on active debris fans, or in the contemporary floodplain and elevated terraces of the trunk rivers.

3.3 The Dharan-Dhankuta Area of East Nepal

3.3.1 Introduction

The Dharan-Dhankuta road, constructed over the period 1976 to 1982, represents the first British funded and designed all-hill road in Nepal. The 50km long road joins Dharan Bazar, on the northern edge of the Terai (Ganges) Plain at an altitude of 400 m asl. with Dhankuta at 1,200 m asl, situated on a north-south trending spur of the Mahabharat Lekh, 27 kms to the north (Figure 3.3). The road represents one of a small number of important north-south

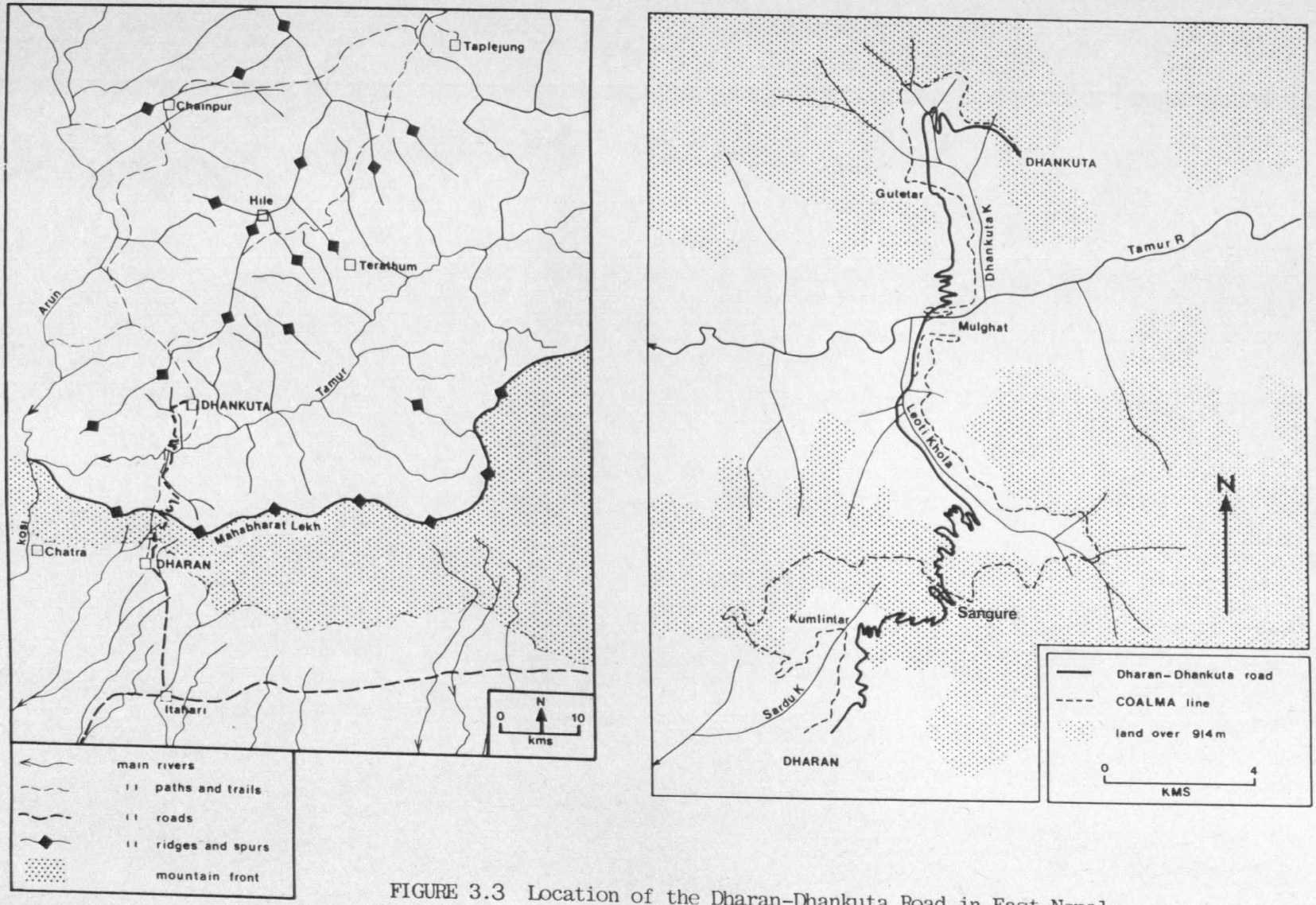

FIGURE 3.3 Location of the Dharan-Dhankuta Road in East Nepal

oriented roads through the Mahabharat Lekh, (Figure 2.2) and has become the first stage in the economic development of the Dharan-Dhankuta area and the Kosi zone in general (Figure 3.3).

The remainder of this chapter describes the physiography, geology, climate and geomorphology of the Dharan-Dhankuta area. Special attention is paid (Section 3.4) to the distribution and geomorphological impact of a high magnitude storm that occurred in September 1984. This storm was the first real test of the road's capability of withstanding a high magnitude event and has provided a good opportunity for examining the hazard assessments and predictions of the geomorphological reconnaissance surveys (Chapter 4).

3.3.2 Physiography and Road Alignment

The physiography of the area is composed of landforms found in zones 2 to 5 of the fold mountain model (Figure 2.1) and is dominated by the east-west oriented Sangure Ridge (Mahabharat Lekh) and the Hile Ridge to the north of Dhankuta, separated by the synclinal valley of the Tamur River (Figure 3.1). Tectonic uplift and rapid incision by the Tamur River and its tributaries, the Leoti and Dhankuta Kholas, have combined to produce a terrain characterised by high relative relief and long, steep slopes. Relative relief is highest on the flanks of the Sangure Ridge and adjoining areas where, in the Leoti Khola catchment for instance, slopes are up to a kilometre long and commonly exceed 40°. The physical constraints on the choice of road alignments are, therefore, immense and consist of an ascent through 1000 m to cross the Sangure Ridge, a descent through 1100 m to the Tamur River, followed by a climb through 900 m to Dhankuta - all within a horizontal distance of 27 kms.

From Dharan (400 m asl), the Dharan-Dhankuta road ascends the Sangure Ridge to a height of 1420 m asl via a series of contour traverses, and vertical and offset hairpin stacks across complex valley re-entrants and side-long ground (Plate 3.1). Crossing the ridge, the road descends into the Leoti Khola valley, again via a complex arrangement of offset hairpin stacks, and traverses across side-long ground (Plate 3.2). Reaching the Leoti Khola floodplain, the road runs along the western bank before crossing the river to follow its eastern bank to the confluence with the Tamur River (Figure 3.3) at approximately 300 m asl. After bridging the Tamur, the road ascends the northern flank of the Tamur valley above Mulghat via a dramatic vertical hairpin stack (Plate 4.2),

PLATE 3.1 Ascent to the Sangure Ridge Via the Kumlintar Hairpins.

PLATE 3.2 Descent from the Sangure Ridge to the Leoti Khola Floodplain.

PLATE 3 .3 Traverse Across Shallowly Inclined Slopes of the Upper Dhankuta Khola.

before traversing northwards across the middle slopes of the Dhankuta Khola valley immediately above its incised gorge. Finally, the alignment crosses the headwaters of the Dhankuta Khola (Plate 3.3) and climbs steadily to Dhankuta. A full description of the alignment is given in Appendix 1.

3.3.3 Geological Setting

The geology of the area (Figure 3.4) conforms with the regional framework for the Lower Himalaya outlined in Section 3.2.1, and has been described in recent geological and geomorphological publications (Brunsden et al 1981, Fookes and Marsh 1981). The main characteristic of the outcrop pattern is the reversal of stratigraphic succession and, in particular, the outcrop of younger strata at low elevations, at the foot of the Sangure Ridge, and older rocks on the high ground of the Dhankuta Ridge to the north. In addition, metamorphic grade also increases in a northerly direction and with elevation. These reversals can be attributed to thrust faulting and superposition (Section 3.2.1).

The stratigraphy of the area, using the Bordet (1961) terminology, can be divided into two main units: the older Lesser Himalayan Unit (LHU), which is locally composed of the Basal Unit and the Mulghat Formation, and the younger Border Unit (Table 3.1). The Basal Unit consists of migmatic gneisses and schists with intercalated quartzites. Bordet (1961) and others have postulated a thrust zone (the Dhankuta Thrust (Figures 3.1 and 3.4)) between this unit and the underlying Mulghat Formation. Although the outcrop of this thrust zone can be found along the Dharan-Dhankuta road, approximately 3km to the north of Mulghat, it is elsewhere difficult to locate and the boundary is probably transitional (Auden 1935, Bordet 1961, Ohta and Akiba 1973, Kayastha 1981).

The Mulghat Formation consists of a complex assemblage of phyllites, slates, schists and quartzites that tend to increase in metamorphic grade from south to north. Inspection of natural and artificial rock exposures in road cuts reveals that folding and faulting have been intense, and that the majority of lithologies display characteristic metamorphic properties of fracture, slaty and schistose cleavage.

A second thrust zone (the Mulghat Thrust (Figures 3.1 and 3.4)) separates the Mulghat Formation of the LHU to the north, from the Border Unit. The latter

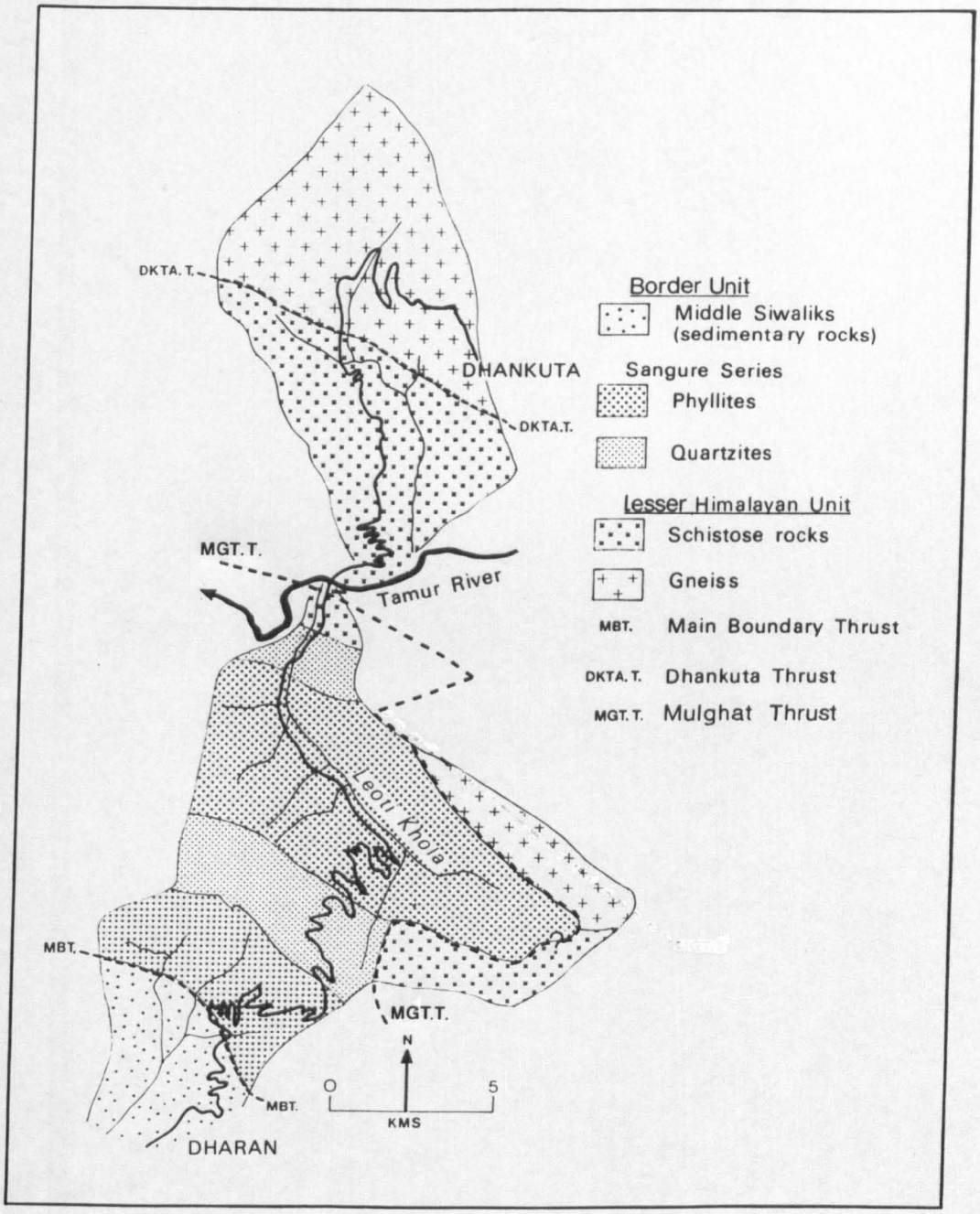

FIGURE 3.4 The Geology of the Dharan- Dhankuta Area.

Unit		Lithology	Age
The Border Unit	Dharan Bazar Series	Sandstones Phyllites	Lower Miocene
	Sangure Series	Quartzites Phyllites	Permo-Triassic
Lesser Himalayan Unit		Upper Phyllites	Devonian-Carboniferous
		Calc-Schists	Devonian
		Upper Quartzites	Silurian-Devonian
		Lower Phyllites	Silurian
		Lower Quartzites	Cambrian-Silurian
		Mica Schists Migmatic Gneiss	Pre-Cambrian

Table 3.1 The Stratigraphy of the Dharan-Dhankuta Area (After Bordet 1961)

consists of Sangure Series quartzites and phyllites and the Siwalik sediments of the Dharan Bazar Series. The Sangure Series underlies the vast majority of the Leoti Khola catchment, and the Sangure Ridge itself is locally developed in highly fractured quartzites. The Sangure and Dharan Bazar Series are separated by the MBT. The southern slopes of the Sangure Ridge are composed of Sangure quartzites and phyllites overlying Middle Siwalik sediments. Continued tectonic activity, centred along the Sangure Ridge in association with the MBT, is demonstrated by the superimposition of Siwalik sediments over Gangetic alluvium at Kherwa to the east of Dharan (Hagen 1969).

3.3.4 Climate

The climate of the area is characterised by a distinct seasonality of rainfall. Dharan receives an average annual precipitation of over 2000mm. Forty percent of this falls during July and August. Rainfall totals are highest over the Sangure Ridge and then decrease northwards, so that the annual figure for Dhankuta is only 950mm. Summer temperatures rise to 35-40^{o}C, and relative humidities frequently exceed 95 percent. This humid sub-tropical climate encourages the growth of tropical deciduous forest below 1000 m asl, and coniferous firs and pine forests above 1000m on the drier slopes below Dhankuta. The distribution of forest types is described in Chapter 5.

Figure 3.5 has been compiled from rainfall data collected over the period 1977 to 1984 from a series of standard raingauges established and recorded at six

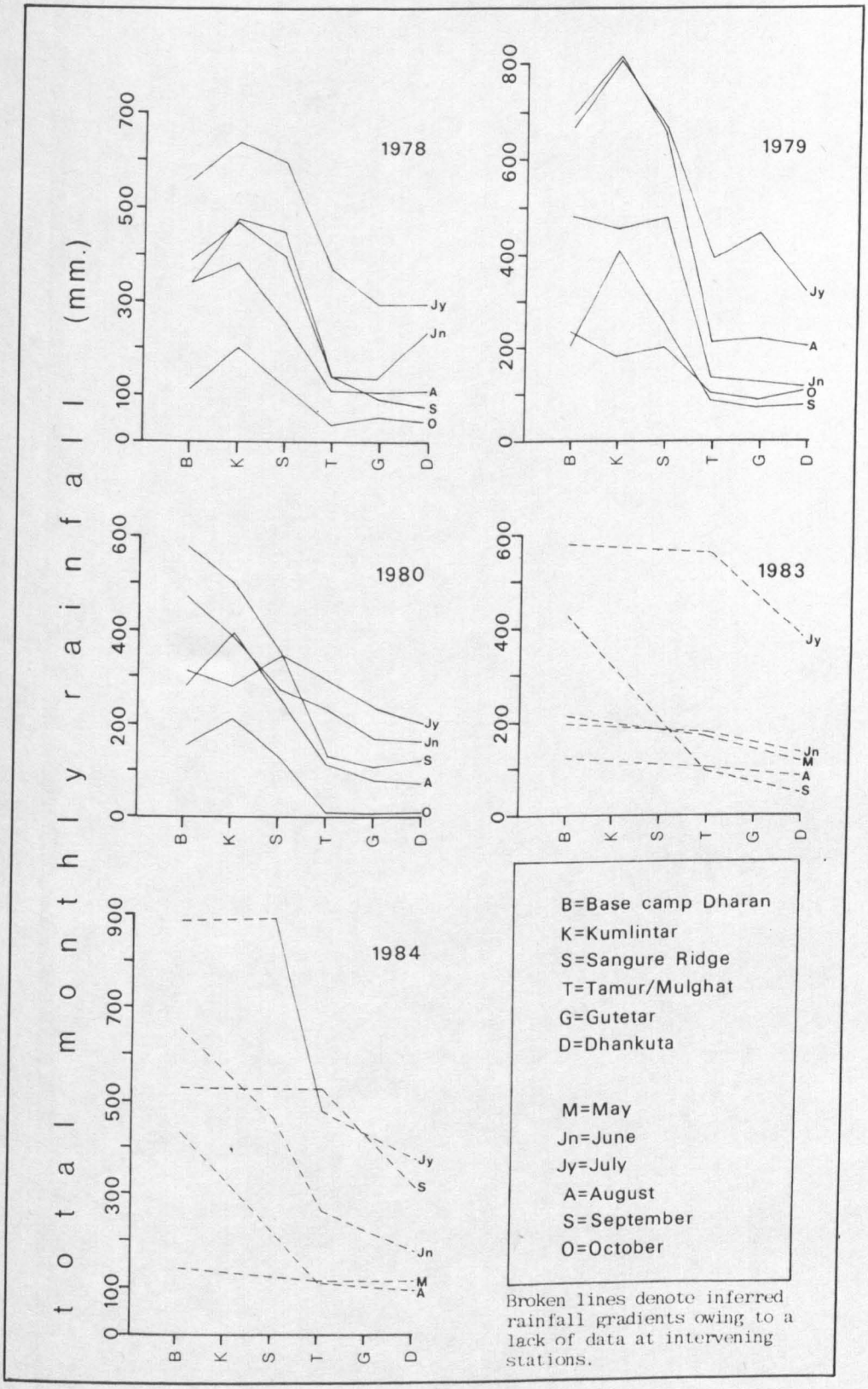

FIGURE 3.5 Summary of Rainfall Records From 24 - Hour Recording Stations Along the Dharan-Dhankuta Road.

locations along the road. The locations of these raingauges are shown on Figure 3.3 as follows: 1 = Dharan (400 m asl); 2 = Kumlintar (900 m asl); 3 = Sangure (1400 m asl); 4 = Mulghat (300 m asl); 5 = Gutetar (750 m asl); 6 = Dhankuta (1 200 m asl). Although these graphs only show monthly trends in rainfall, the overall decrease in a northward direction is evident. During the period 1978-1980, when rainfall data for all recording stations were available, total monthly rainfall depths were greater on the crest of the Sangure Ridge than anywhere else along the road. The wettest month here is July, and the maximum recorded monthly total during the measurement period was 893.1mm in July 1984.

An examination of 24 hour rainfall records from standard raingauges established at Dharan Bazar, Mulghat (Tamur) and Dhankuta since 1947, has enabled recurrence intervals of individual storm events to be determined for each station. The maximum annual 24-hour precipitations for each station were ranked in order of magnitude, and the recurrence interval for each event was calculated from the equation:

$$T \text{ (years)} = \frac{N + 1}{R} \qquad \ldots.3.1$$

where N = number of years
and R = rank of event.

Figure 3.6 shows the recurrence intervals for annual maximum storms recorded at Dharan Bazar, Mulghat and Dhankuta respectively, plotted against 24-hour rainfall depth on semi-logarithmic paper. The relationships show that storms of specified rainfall depth tend to occur more frequently at Dharan Bazar than at Mulghat or Dhankuta. The magnitude of a storm with a recurrence interval of 25 years, for instance (approximately equivalent to the design flood for the Dharan-Dhankuta road on the Leoti Khola floodplain), is approximately 300mm between Dharan and the Sangure Ridge, and 220mm in the lower Leoti Khola and between Mulghat and Dhankuta.

However, diurnal and monthly rainfall totals give very little indication of the maximum rainfall intensities that occur. Although a seasonal build-up of groundwater levels, followed by large storms during September, appear to be responsible for many of the larger slope failures in the area, it is the duration and intensity of storm rainfall, in relation to the permeability of the slope

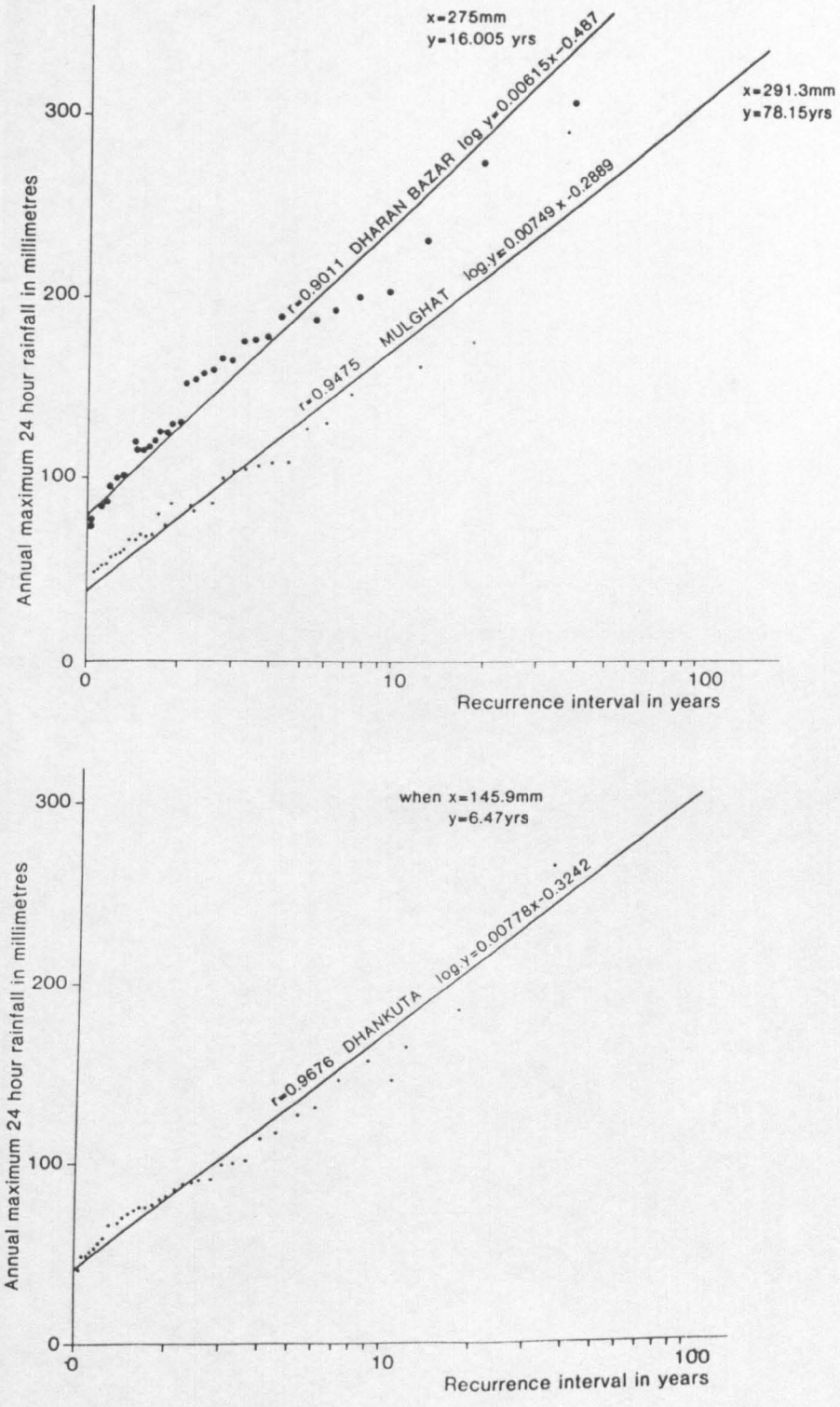

FIGURE 3.6 Graph Plots of 24-Hour Rainfall Depths Versus Recurrence Interval for Annual Storms Occurring in the Dharan-Dhankuta Area.

forming materials, that determine the potential for mass movement on steeply inclined slopes (Chapter 5). A study of available site records of rainfall intensities suggests that instantaneous intensities over the Sangure Ridge exceed 100mm per hour on at least one occasion during a normal monsoon season. Both intensity and duration are likely to decrease northwards from here into the Tamur Valley, but increase again on the higher ground of the Hile Ridge to the north of Dhankuta. This spatial variability of storm rainfall significantly influences the potential for slope instability, flooding and erosion, and is described with reference to the September 1984 storm in Section 3.4.

3.3.5 Geomorphology

The majority of mass movement processes described in Chapter 2 can be identified in the study area, although some are more common than others. The principal mass movement processes found in the study area are listed in Table 3.2 along with their causes, geomorphological significance and the rock type, physiographical and geographical localities in which they occur. The distribution of these mass movements is analysed for landslide hazard mapping purposes in Chapter 5. Rock fall activity is presently confined to cliffs and rock bluffs formed in quartzite and schist. These occur along the Sangure Ridge and on the steep, incised lower slopes below degraded rock fall scars in the Leoti and lower Dhankuta Khola valleys. With the exception of minor rock and debris falls, during heavy rain, most of the rock scars on the middle and upper valley-side slopes are relic features attributable to either seismic activity or periglacial processes, active during the Pleistocene. In fact, road excavation has, in places, exposed boulders many metres in diameter that are more likely to be of ancient rock fall origin, than a product of residual weathering. Planar rock slides occur most frequently on the shales, phyllites and schists, in response to slope oversteepening above incised drainage lines. High densities of rock slides are found on the engorged flanks of the lower Dhankuta Khola valley (Plate 3.4), where the close proximity of the Dhankuta Thrust has caused the underlying schistose rocks to become highly shattered. Rock slides can develop into catastrophic mass movements when discontinuity, bedding and schistosity planes dip out of the slope, as is the case, for instance, in the lower Dhankuta Khola valley.

The most common forms of mass movement in the study area are shallow translational debris slides that occur in soil and weathered rock. Debris slides are usually up to 3m deep and are found on all rock types. By contrast,

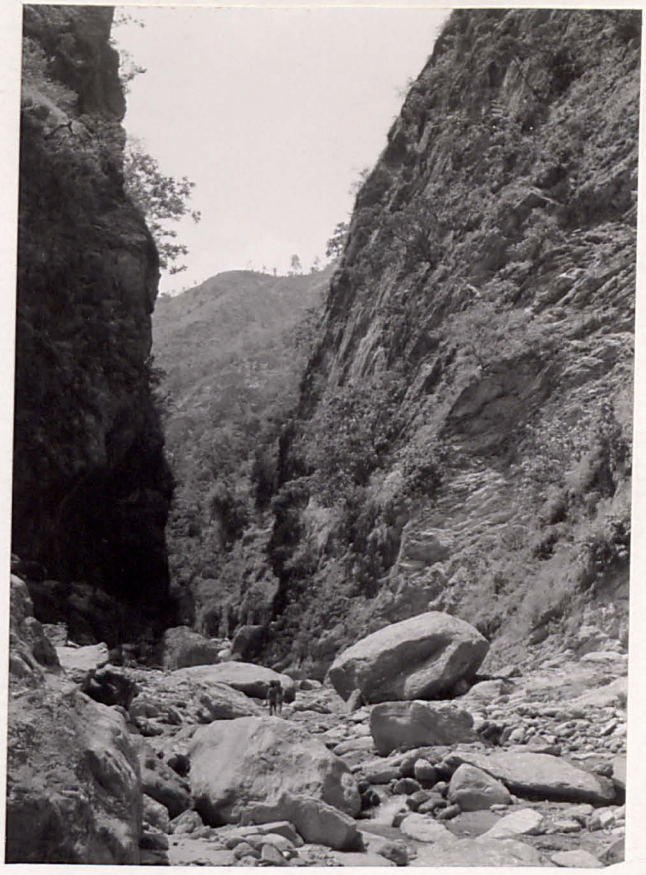

PLATE 3.4 Engorged Lower Dhankuta Khola Valley.

PLATE 3.5 Rotational Failure on the Southern Flank of the Tamur Valley, Reactivated During the September 1984 Storm.

MECHANISM:	ROCK FALLS	ROCK SLIDES	DEBRIS SLIDES	DEBRIS FALLS	MUDSLIDES	ROTATIONAL SLIDES	EROSION/MASS MOVEMENT CATCHMENTS
ROCK TYPES	Quartzites, schists	Phyllites, shales schists, occasional quartzites Siwaliks	All rock types	All rock types except quartzite	Phyllites, schists	Phyllites, shales schists, Siwaliks	Phyllites, schists, Siwaliks
TYPICAL PHYSIOGRAPHICAL GEOGRAPHICAL LOCALITIES	*Quartzite cliffs along Sangure Ridge and in Lower Leoti Khola valley *Incised slopes (cliffs), for example in lower Dhankuta Khola valley.	*Incised valley flanks *Schistose rocks of Lower Dhankuta Khola and Leoti Khola valleys *Steep tributaries of Leoti Khola valley.	*Incised valley flanks *Headwater slopes of Sangure Ridge	*Incised slopes (cliffs) adjacent to drainage lines	*Moderately inclined slopes adjacent to river channels in Lower Dhankuta Khola and upper Leoti Khola valleys	*Incised valley flanks in all three catchments	*Incised valley flanks and steep tributaries of lower Dhankuta and Sardu Kholas and Leoti Khola
OCCURRENCE	Infrequent	Infrequent-common	Common	Infrequent	Rare	Infrequent	Infrequent-common
CAUSES	*Slope undercutting and oversteepening *Highly jointed rock *High groundwater levels *Earthquakes	*Slope undercutting and oversteepening *Adverse dip *Discontinuous and foliated rock *High groundwater levels *Earthquakes	*Slope undercutting and oversteepening *High groundwater and soil moisture levels	*Slope undercutting and oversteepening *High groundwater and soil saturation	*Slope undercutting and oversteepening *High groundwater levels *Undrained loading	*Slope undercutting and oversteepening *High groundwater levels	*Steep slopes *Rapid runoff *Highly jointed rock *Adverse dip
GEOMORPHO-LOGICAL SIGNIFICANCE	*Form boulder fields and scree below cliffs on upper slopes (Figure 5.1)	*Often lead to blockage of tributaries of the Leoti Khola and the lower Dhankuta Khola *Often contribute large volumes of debris to fans on Leoti Khola on floodplain * Important in landscape development.	*Relatively low significance *Often form headward extensions to drainage net *Disintegrate to debris flows.	*Relatively insignificant	*Relatively infrequent and slow moving in comparison to other mass movements.	*Often of high magnitude *Can be catastrophic or gradual in occurrence	*Rapid supply and transport of sediment. *High rates of catchment erosion and fan accretion *Debris flow activity *Result in large-scale erosion bowls

TABLE 3.2 Mechanisms, Occurrences and Causes of Primary Mass Movements in the Study Area

rotational failures and mudslides are the least common forms of mass movements in the area. Both occur primarily in deeply weathered phyllites, shales and schists. Rotational slides take place during, or immediately after, intense precipitation and/or rapid channel erosion. For example, a large (400-500m wide) rotational slide, on the southern flank of the Tamur River at Mulghat (described in Brunsden et al (1981)), became reactivated during the September 1984 storm, in response to heavy rain and extensive bank erosion (Plate 3.5). The largest rotational failure in the study area is approximately 500m wide and has occurred on the western flanks of the lower Sardu Khola in Siwalik sediments (Plate 3.6). Another rotational slip removed approximately 100m of roadline on the Siwalik slopes above Dharan during the September 1984 storm (Plate 2.6, Appendix 1A.3). Mudslides are relatively uncommon in the study area owing to the comparatively steep slopes (most mudslides reported in the literature occur on slopes shallower than 20^0 (Brunsden 1984)) and the predominance of other forms of mass movement. The mudslides that do occur are found on slopes of up to 39^0 (probably the steepest on record (Brunsden et al 1981)). These occur mostly in the Dhankuta Khola valley (Chapter 5) in deeply weathered schist.

Debris flows are common on the lower, southern flanks of the Sangure Ridge and in the steeper tributary catchments of the Leoti Khola. They characteristically occur where large rock and debris slides enter defined gully channels and constitute an important means by which debris is transported through severely eroding catchments. A typical example is shown in Plate 2.1. In the study area, differentiation can be made between debris flows that arise from individual mass movements, and debris flow catchments. In the latter case, widespread catchment erosion gives rise to a 'conveyor belt' of debris on the floor of the main channel. This enables often large calibre sediment to be rapidly transported in pulses through the catchment during heavy rain. Debris flow catchments are found predominantly on the northern flanks of the Leoti Khola valley (Plate 5.5). The causes and mechanisms of debris flows are discussed in Chapter 2.

Earthworks-induced erosion and slope instability is common along the majority of the road, and has been caused primarily by slope oversteepening due to excavation and overloading following spoil bench construction (Appendix 1, Chapter 6).

PLATE 3.6 Large Deep-Seated Failure on the Western Flank of the Sardu Khola, Activated During the September 1984 Storm.

The most conspicuous hydrological and drainage features in the Dharan-Dhankuta area are the seasonally distributed, temporally and spatially discrete storm flows, and the rapid and capricious nature of sediment transport. The maximum flow in the Tamur River at Mulghat, since flow gauging began in 1965, is 5700 cumecs which occurred as a result of the July 1974 storm (Brunsden et al 1981). This flow had a recurrence interval of 21 years (Barker 1976). During the same storm, the peak flow calculated for the Leoti Khola was 511 cumecs with a recurrence interval of only 10-15 years (Barker 1976). These figures illustrate the spatial variability in storm runoff caused by the often localised nature of precipitation. This is discussed further with respect to the distribution of the September 1984 storm in Section 3.4.

Important sources of channel sediment include extensive areas of soil erosion, caused in part by forest clearance and side-tipping of spoil along road lines (Chapter 6), landslides and channel erosion. Much of this sediment, especially that derived from landslide sources, moves through the channel network in a series of pulses in response to rapid variations in rainfall intensity, and hence runoff from the contributing area, and sporadic debris supply.

The localised nature of storm runoff dictates that during storms of low to moderate magnitude, such as those that recur every one to two years on average, the sediment supply and transport system is largely asynchronous and is manifested by the accumulation of often large sediment deposits on slopes, along channel banks, on floodplains and in debris fans. However, during higher magnitude storms, with recurrence intervals greater than one year, the sediment delivery ratio increases considerably and debris may be transported rapidly and for considerable distances through the channel system.

3.4 The September 1984 Storm and its Geomorphological Impact.

The storm of 15/16 September 1984 resulted in 275mm, 291.3mm and 145.9mm of rainfall at Dharan, Mulghat and Dhankuta, which represented 24-hour storm recurrence intervals of 16 years, 78 years and 6.5 years respectively (Figure 3.6). This large spatial variation in recurrence interval for the same storm is normal for orographic stimulated convective storms with relatively restricted spatial extents and locally very intense precipitation. However, the magnitude of the event at Mulghat indicates that the zone of most intense rainfall was not restricted to the highest parts of the Sangure Ridge, as is usually the case,

but extended well to the north to include the high ground on the northern flank of the Tamur valley. Indeed, a comparison of 24-hour rainfall records in an approximately south-north line between Biratnagar on the Terai Plain and Taplejung, 50 kms to the north of Dhankuta (Figure 3.3), reveals that storm rainfall increased from 23 mm at Biratnagar to 275 mm and 291mm at Dharan and Mulghat respectively, and then decreased to 146mm at Dhankuta and finally to 60mm at Taplejung. Thus, the storm may be considered to have been a relatively rare, high-magnitude event over the whole stretch of roadline from the southern flanks of the Sangure Ridge to the top of the Mulghat hairpin stack (km 38.450). Elsewhere along the road, the storm represented an event with return periods of between 6 and 25 years (Hearn and Jones 1985).

The contention that the storm was concentrated between Dharan and Mulghat is further supported by a comparison of the magnitude of the flood flows in the Tamur River and Leoti Khola. The Tamur drains the area to the north and east of Dhankuta, and Barker (1976) has established rating curves relating flow depth, at Mulghat, to discharge and recurrence interval. The storm resulted in a maximum flow depth of 5.58m on 17th September, corresponding to a discharge of 830 cumecs. This discharge approximates to the yearly flood at Mulghat, and hence, the size of the storm north and east of Dhankuta was relatively small. By contrast, as Chapter 7 will show, the flood in the Leoti Khola, generated by this storm, was 910 cumecs with a recurrence interval of approximately 75 years.

Eye-witness accounts of the period of high intensity rainfall, are conflicting and unreliable, but it would appear that the storm followed the usual temporal pattern of rainfall in this area; short periods (approximately 4 hours) of intense rain during the evenings of the 15th and 16th September, with more moderate, prolonged rainfall during the intervening 20 hours. Total rainfall depths for the 48 hours amounted to 392mm, 317.7mm and 157.8mm at Dharan, Mulghat and Dhankuta, respectively. The proportion of these rainfall totals falling on the 16th September is 70 percent for Dharan and 92 percent for both Mulghat and Dhankuta.

The storm had a major impact on slope and drainage processes as a result of both its intensity, duration and areal extent, and the fact that it occurred at the end of a particularly wet monsoon season when groundwater levels must have already been high. On the basis of the 24-hour annual maximum rainfall

series (Figure 3.6), the one-year recurrence interval storms at Dharan Bazar (79 mm) and Mulghat (37 mm) were exceeded on six and five occasions respectively in 1984. Consequently, the storm rainfall in September would have enabled groundwater levels to rise rapidly, hence triggering extensive instability.

Figure 3.7 shows the areal distribution of landslides and linear slope erosion features following the storm, as mapped from terrestrial photography (Chapter 5). The majority of these features are shallow and many form headward extensions to the drainage network and existing landslides. The distribution of this instability is discussed and analysed with respect to the proposed alignments for the Dharan-Dhankuta road in Chapter 4, and for purposes of landslide hazard mapping in Chapter 5. Suffice to note here that much of this shallow instability has occurred on the slopes formed in Siwalik materials in the Sardu Khola catchment (Plates 4.4 and 4.5) and in the Leoti Khola catchment (Plates 5.1 and 5.2). Deeper instability, in the form of rock slides and rotational slides, occurred in the Sardu Khola catchment on the oversteepened lower flanks. At two main sites this instability has led to road loss and severe deformation (Chapter 5, Appendix 1A.3 and A.4). In the Leoti Khola catchment, the majority of instability caused by the storm took the form of shallow landsliding and slope erosion. Plates 3.7 and 3.8 illustrate the extent to which these processes have accelerated in one sub-catchment of the Leoti Khola as a result of the storm. In the Dhankuta Khola catchment, the storm had a relatively low magnitude and no new deep-seated, large-scale instability was detected, although shallow instability and erosion were widespread in the steeper, southern half of the catchment (Chapter 5), which must have experienced higher rainfall totals and intensities.

The storm also caused extensive channel erosion. In Chapter 7 it is demonstrated that the capacity of streams crossed by the Dharan-Dhankuta road, to the south of the Tamur River, increased by a factor of 3.73 following the storm. Widespread erosion in these catchments was accompanied by high rates of sediment transport. Among the most conspicuous aspects of this was the deposition of large volumes of debris on fan surfaces on the Leoti Khola floodplain. This resulted in the blockage and scour of the Dharan-Dhankuta road at some of these fan crossings (Chapter 4, Appendix 1A.7). The impact of the September 1984 storm on the stability of the road and neighbouring slopes and channels is described in Appendix 1, and discussed with respect to the geomorphological reconnaissance surveys for the road in the following chapter.

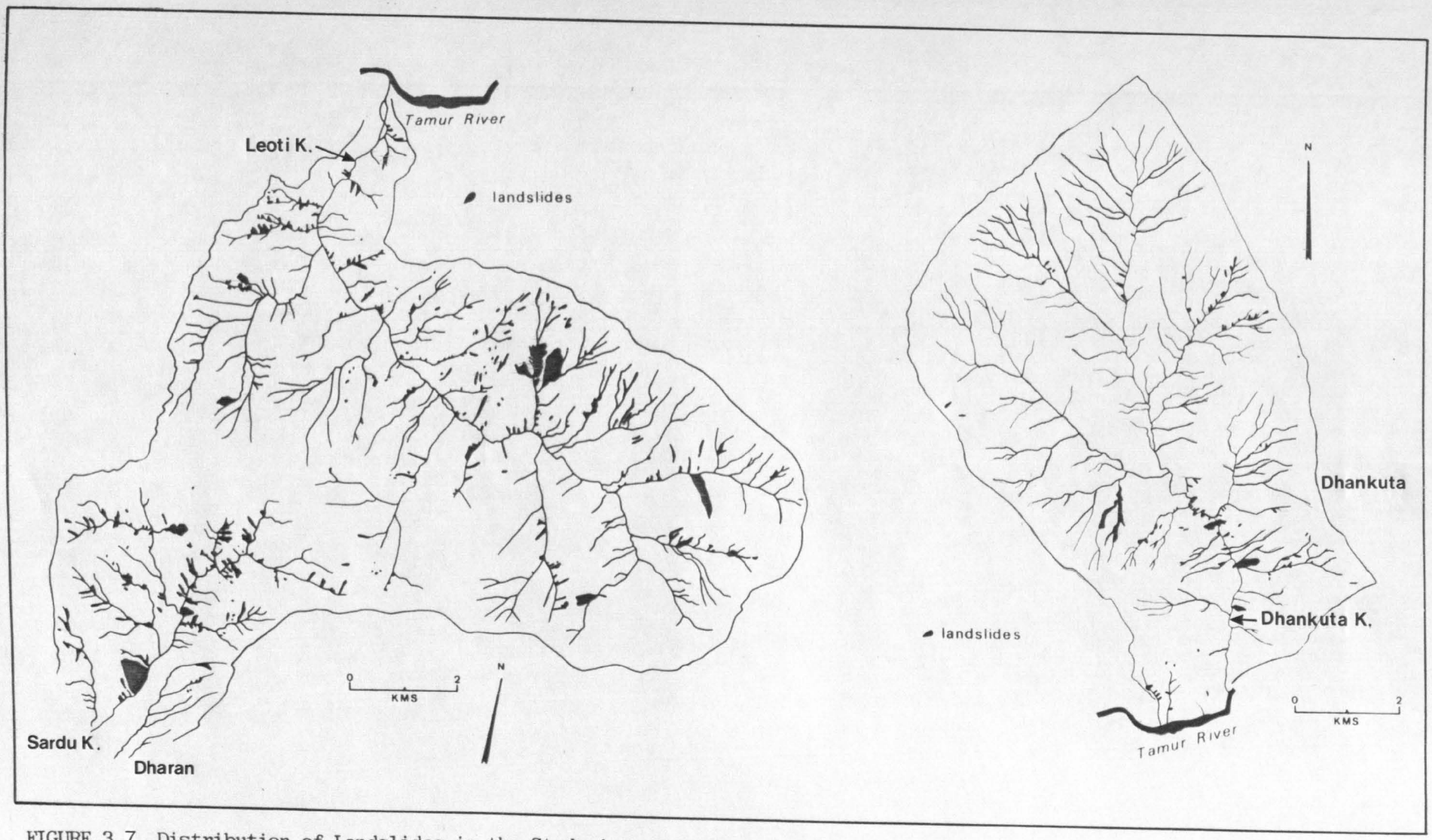

FIGURE 3.7 Distribution of Landslides in the Study Area Following the September 1984 Storm

PLATE 3.7 The Extent of Instability in a Tributary Catchment (Garjuwa K.) of the Leoti Khola Prior to the September 1984 Storm.

PLATE 3.8 The Extent of Instability in the Same Catchment Following the September 1984 Storm.

CHAPTER 4

A CRITICAL ASSESSMENT OF THE RECONNAISSANCE GEOMORPHOLOGICAL SURVEYS OF THE DHARAN-DHANKUTA ROAD

4.1 Introduction

This chapter is principally concerned with critically assessing the contribution made by the geomorphological reconnaissance surveys of 1974 and 1975, and the geomorphological observations made during construction and maintenance, to the design of the Dharan - Dhankuta road. This is undertaken in three parts, as listed below.

i) A comparison is made between the first geomorphological survey of alternative alignments, undertaken in 1974, and a post-construction retrospective walk-over assessment made by the author in 1984.

ii) The later geomorphological survey (1975) is compared with a follow-up engineering geological survey, undertaken in May 1975, and the final design of the road. In addition, the predictions and recommendations made by the geomorphological surveys are examined in the light of the instability caused by the September 1984 storm - an event that put both the geomorphological assessment and the road design to the test.

iii) The application of geomorphological mapping to stability assessment and the design of remedial measures, at a site of continued slope instability during construction and maintenance, is examined.

Before the geomorphological reconnaissance surveys are assessed, a brief summary is given of the development of the road project, including project funding, the choice of alignments and the timing and nature of the reconnaissance surveys.

4.2 Background to the Study

The first proposals for a road between Dharan and Dhankuta were made in the

early 1960s by the Regional Transport Organisation (RTO) of the Indian, U.S. and Nepalese governments. The proposed route (Figure 4.1) climbed from Dharan to the crest of the Sangure Ridge at Ahale (1 070m asl) via the western flanks of the Sardu Khola, and then descended to the Tamur River at Tatopani. Tatopani and Mulghat, approximately 8km to the east, represented the only feasible sites where a road bridge across the Tamur could be constructed. Beyond Tatopani, two possible routes to Dhankuta were proposed. The first turned eastwards to Mulghat along the northern flanks of the Tamur valley, crossing numerous tributary fans, channels and steep, often unstable slopes (Plate 4.1). From Mulghat, the route followed the middle, western flanks of the Dhankuta Khola valley, before crossing the headwaters and ascending the eastern valley flank to Dhankuta (Figure 4.1). The second route ran north and westwards, climbing through nearly 1 000m before turning eastwards to Hile and then south to Dhankuta (Figure 4.1). Although a track was excavated as far as Tatopani, the project was abandoned due to lack of finance and the difficulty of track excavation on the northern flanks of the Tamur valley.

The road project was then revived as a joint venture between the UN and His Majesty's Government (HMG) of Nepal. A group of Italian consultants (Comtec, Alpina, Macchi-COALMA) were employed to undertake a feasibility study for the Dharan-Dhankuta road and a number of other hill roads in Nepal in 1972 (COALMA 1973). On the basis of an examination of enlarged 1:63 360 Survey of India topographic maps, Forestry Department air photographs and walk-over survey, they proposed an alternative route between Dharan and Mulghat that crossed the Sangure Ridge by an alignment that contoured around the western and northern flanks of the Sardu Khola and the southern and lower eastern flanks of the Leoti Khola (Figure 4.1). Crossing the Tamur at Mulghat, the trace gained some elevation on the northern valley side before following a similar route, to Dhankuta, as the proposed RTO line. The length of the COALMA line was approximately 65 kms.

In 1972, the Overseas Development Administration (ODA) of the British Government undertook to finance the project. A preliminary ground survey of both the RTO and COALMA alignments was made by the Transport and Road Research Laboratory (TRRL) in 1972 (Boffinger and Lawrence 1973). While this survey noted a number of slope instability and erosion features along the RTO line, especially between Dharan and Tatopani, the most serious problems were judged to be associated with the traverse along the Tamur valley

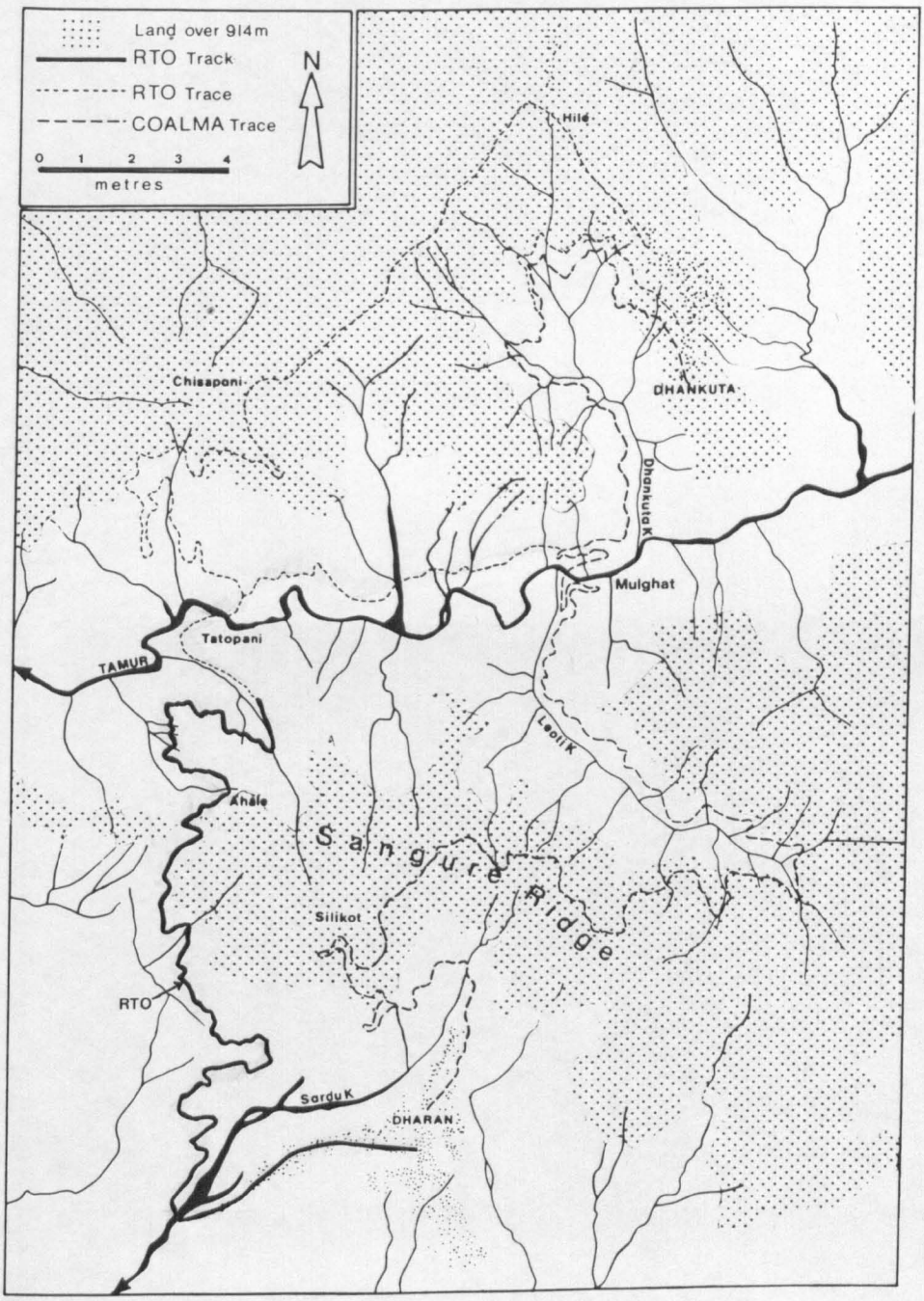

FIGURE 4.1 Proposed Road Alignments Between Dharan and Dhankuta

PLATE 4.1 Unstable Incised Flank of the Tamur Valley, Crossed by the Proposed RTO Line at Mulghat.

PLATE 4.2 Vertical Hairpin Stack at Mulghat.

between Tatopani and Mulghat. The route via Hile, and then south to Dhankuta, was also regarded as being unfavourable due to the steep slopes and unstable ground encountered, and the fact that the road would pass through Hile before Dhankuta; this was unacceptable on political grounds as Dhankuta is the district headquarters of the Kosi zone.

The TRRL survey also identified numerous areas of unstable ground along the COALMA line, but chose this route as the most favourable, and it was subsequently accepted, in principle, by the ODA. However, the consulting engineers (Rendel, Palmer and Tritton, London) were unsatisfied with the alignment, owing to the difficult and unstable terrain encountered. Consequently, an independent geomorphological ground survey (GS1) was commissioned by the consultants, in order to assess ground conditions along the COALMA trace. The survey was undertaken during April/May 1974 by three geomorphologists (Dr. D. Brunsden of King's College London, Dr. J.C. Doornkamp of University of Nottingham and Mr. D.K.C. Jones of the London School of Economics and Political Science).

A critical appraisal of this survey is given in the following section. Suffice to note here that the geomorphologists recognised that the incised and oversteepened lower and middle valley-side slopes, crossed by the majority of the COALMA line, posed the highest potential for instability. Although the eastern flanks of the Leoti Khola and the traverse above the Dhankuta Khola gorge were judged to be the most hazardous and unacceptable sections of the alignment, the geomorphologists confirmed that the whole route should be rejected. As an alternative, GS1 proposed an alignment concept that avoided the unstable lower and middle slopes by gaining elevation in hairpin stacks, located on relatively stable slopes, and distance along ridge-tops or on valley floors. This design philosophy is reflected in the final design of the alignment, of which hairpin stacks form a conspicuous part (Plate 4.2).

Following GS1, a new Rendel Palmer and Tritton (RPT) alignment was designed (1974), and a second geomorphological survey was commissioned to evaluate the terrain hazards encountered by the route, and make recommendations for design. This survey, henceforth referred to as GS2, was

conducted by three geomorphologists (Brunsden, Jones and Dr. R.P. Martin[1]) during a 16 day period in January 1975 and generally approved the alignment, except for detailed criticisms of short sections. This second survey, and its contribution to the design of the road, is assessed in detail in Section 4.4.

In May 1975, an engineering geological, 'construction notes' survey henceforth referred to as EG1, was undertaken by Mr. M. Sweeney[2] to assess and augment the findings of GS2 for highway design purposes, to identify the likely scope of works for the preparation of the Bill of Quantities and to make preliminary proposals for design. Construction of the road began in 1976 and was completed in 1982. Geotechnical assessment during construction was undertaken by reference to the reconnaissance surveys, particularly EG1, supplemented by direct observations during earthworks, trial pitting, trial benching and geomorphological mapping, thus allowing progressive ground and hazard assessment and design by modified precedent.

4.3 A Critical Assessment of the 1974 Geomorphological Survey (GS1) of the COALMA line

A number of factors served to limit the scope of this survey. These included a Brief given to the geomorphologists to concentrate on an evaluation of mass movements at the possible expense of drainage hazards, a relatively short time (4 weeks) to undertake the survey and an almost total lack of background and supporting reference data, such as air photographs of suitable scale and clarity, detailed topographic maps and published literature. The COALMA trace had been plotted onto Survey of India sheets enlarged from 1:63 360 to 1:10 000. Quite often the configuration of the trace on the ground departed significantly from that shown on the maps. Detail was plotted onto these sheets by GS1 and included slope and drainage hazards, rock and soil conditions, slope inclinations and topography. These features were discussed in an accompanying text.

---

1. Then at King's College, London but subsequently with RPT (1977 - 1981) and with the Geotechnical Control Office, Hong Kong (1981 - present).

2. Then with RPT but subsequently with British Petroleum.

The principal findings and recommendations of this survey are listed below.

i) The main hazards encountered by the COALMA line included the following-

a) Phusre (north of Dharan) to Sangure col: debris flow tracks; active rock and debris slides and scree accumulations.

b) Sangure col to Tamur: long steep slopes; rock slide scars; debris flow catchments; unstable scree; a mass movement complex consisting of debris slides, rock slides, a mudslide and two rotational slides; a major active rotational slide and frequent gullying. Most of these features were found on the eastern flanks of the Leoti Khola valley.

c) Tamur to Dhankuta: deeply incised unstable tributaries of the Tamur; a large instability complex on the engorged flanks of the lower Dhankuta Khola valley consisting of a rock slide embayment, an active mudslide and scree; numerous rock slide scars and mudslides.

ii) The most unstable of these sites, namely those on the eastern flanks of the Leoti Khola valley and the engorged flanks of the lower Dhankuta Khola valley, should be avoided by extensive realignment of the trace.

iii) Deeply incised gullies should be crossed ideally at their lower (depositional) or upper (shallowly incised) reaches.

iv) The mid-slope elements of the valley sides and the currently unstable lower slopes should be avoided wherever possible.

v) Elevation should be gained or lost in relatively stable vertical route corridors.

In order to assess the evaluation made by GSI, it was decided to undertake a resurvey of the COALMA line in 1984, in the light of a hindsight knowledge of the design, construction and stability of the final road and other roads visited in the Lower Himalaya. As a reassessment of the whole line would be unnecessary and time consuming, the walk-over resurvey was restricted to the eastern Leoti Khola valley section. The decision to concentrate on this one section is justified by the fact that it was this section of the COALMA

line that was initially rejected by the consulting engineers, although it was not considered to be the most difficult stretch by GSI. A resurvey of the COALMA line in the lower Dhankuta Khola was not attempted, as access on these slopes is extremely difficult. In fact, this prevented GSI from undertaking a detailed walk-over survey in this area.

The resurvey was undertaken in three days during August 1984. Great difficulty was experienced in locating the trace on the ground, as this had been cut over ten years previously, and had become degraded and revegetated. Observations made by both GSI and this hindsight survey, concerning slope and drainage stability, are summarised in Table 4.1, while the principal hazards and ground conditions recorded by the latter, are shown on the strip map in Figure 4.2.

Between the crossing of the main Leoti Khola channel (km 29.0) and km 34.5, six main gully catchments were described by GSI. Three of these gullies (km 29.4, 30.3 and 33.0) were regarded by GSI as being currently active, with unstable gully heads and debris flow deposits. The 1984 reassessment found the catchment crossed at km 33.0 to be particularly unstable, and the observations made by GSI concerning debris flow activity were supported. The remaining five gullies were seen by the resurvey to have stable channels, both upstream and downstream of the intended crossing points, although reactivation of relic slope instability on the channel flanks was regarded as a potential hazard.

Between km 34.5 and km 35.75, GSI observed gentle slopes with few problems for road construction. However, at km 35.6, the trace encountered an unstable tributary valley, containing a rotational slide and a mudslide that, according to GSI, would require expensive stabilization (Table 4.1). The 1984 resurvey recorded the rotational slide and mudslide as largely relic features. Rock sliding below the trace, not identified by GSI, was seen to be particularly hazardous.

At km 35.75, GSI recorded slope inclinations as high as 60° on slopes that had been oversteepened by four incised tributaries. Several shallow debris slides were observed in the sharp re-entrants. The resurvey recorded numerous shallow gullies with unstable heads above the trace, along with an active mudslide and numerous debris slide scars. The resurvey also noted a small re-entrant valley, crossed at km 38.0, that had a relic rotational slide on its

CHAINAGE	GSI ASSESSMENT	CHAINAGE	1984 REASSESSMENT
Km 29–33	Most instability is confined to head areas of tributaries, each of which is a debris flow catchment. Three of these catchments (Km 29.4, Km30.3, Km33) are active. Debris flows, fed by erosion and debris slides, are likely to be turbulent and destructive. These channels should be bridged as near to the Leoti Khola as possible to allow for the passage of flood surges. Three inactive debris flow catchments at Km31, Km32 and Km32.4. The channel crossed at Km32 poses a problem due to the presence of several old rock slides and one active debris slide on the southern flank, slope stabilization and bank protection will be required.	Km 29–30 Km 30–Km30.5 Km30.5–Km33	Trace crosses irregular boulder-strewn colluvial slopes with schist bluffs above. Evidence of unconcentrated surface runoff. Recently active debris flow catchment. Channel at present appears relatively stable. Unstable banks downstream of crossing point. Slopes inclined at 40°, locally up to 50°. Numerous shallow rock and debris slide scars below irregular schist bluffs. Springs and poor drainage in rock embayments. The three main tributaries are largely stable at present. At Km31 recent rock sliding on the southern flank, close to the crossing point was observed. Tributaries at Km32 and Km32.4 have beds composed of up to 4m diam. boulders, indicative of relic instability.
Km33–Km34.5	High, steep slopes on bend of Leoti Khola valley. Patches of schist scree, up to 32°, beneath cliffs. Superficially unstable if disturbed. Steep rock slopes(40–60°) on meander scar.	Km33–Km34.5	At Km33 trace crosses highly active debris flow catchment. On southern flanks there are numerous active and relic mudslides and debris slides and rock bluffs.
Km34.5–Km35.75	Gentle slopes, few instability problems. Unstable tributary at Km35.6. Large area of rotational sliding. On the southern flank is a large active mudslide 25m wide with tension cracks and leaning trees. Stabilization will be expensive.	Km34.5–Km35.75	Slopes are inclined at up to 43°. No active instability. At Km35.6 steep sided re-entrant with a high waterfall upslope and rock sliding downslope was observed.
Km35.75–Km38.5	High, steep slopes, locally up to 60°. Slopes are incised by four tributaries of the Leoti Khola. Several shallow debris slides seen in the sharp re-entrants. Short span bridges will be required.	Km35.75–Km38.5	Locally steep slopes at up to 50° with numerous shallow gullies. Stable channel crossed at Km38 with relic rotational slide on southern flank. Eroding gully head and many old and recent rock slides on the northern flank.

TABLE 4.1 A Comparison Between the Observations and Interpretations Made by the 1974 Geomorphological Survey and the 1984 Reassessmentof the COALMA Line on the Eastern Flanks of the Leoti Khola Valley.

(cont.next page).

CHAINAGE	GSI ASSESSMENT	CHAINAGE	1984 REASSESSMENT
Km38.5– Km39.5	Generally stable slopes with three deep but stable streams.	Km38.5– Km39.5	Trace crosses rocky slopes composed of quartzite bluffs, boulder fields and talluvium inclined at40°.Numerous shallow rock embayments,old slip scars and eroding gully heads were also observed.Two main gully re-entrants with extensive boulder fall and rock sliding on both banks were recorded. The trace has been totally obliterated.
Km39.5– Km41.5	Steep slopes(40–70°).Numerous sharp tributary re-entrants will require Irish crossings. Slopes are composed of foliated and distressed schist. Numerous small debris slides were also observed. At Km39.8 the trace crosses a large embayment with relic and active instability and debris flow activity.Trace crosses a rotational slide on the northern valley flank. High quartzite bluffs have given rise to toppling failure.Unstable scree is inclined at 40°.Slope failure will occur if the area is further disturbed.	Km39.8	Trace crosses a quartzite re-entrant with numerous relic rock slides.Many unstable rock bluffs above the trace were observed. The trace has been obliterated in places.
		Km40– Km40.7	The trace crosses slopes inclined at 42–56° formed in loose contorted schist.Small spurs separate incised gullies with unstable wet landslipped heads. Rock fall and slide scars and bluffs above the trace occur with colluvium and boulder fields below.
		Km40.7– Km41.5	The trace circumscribes a large embayment with elevated fan below. Slopes are steep, up to 52°on re-entrant margins.No major instability problems are envisaged.

TABLE 4.1 cont/.

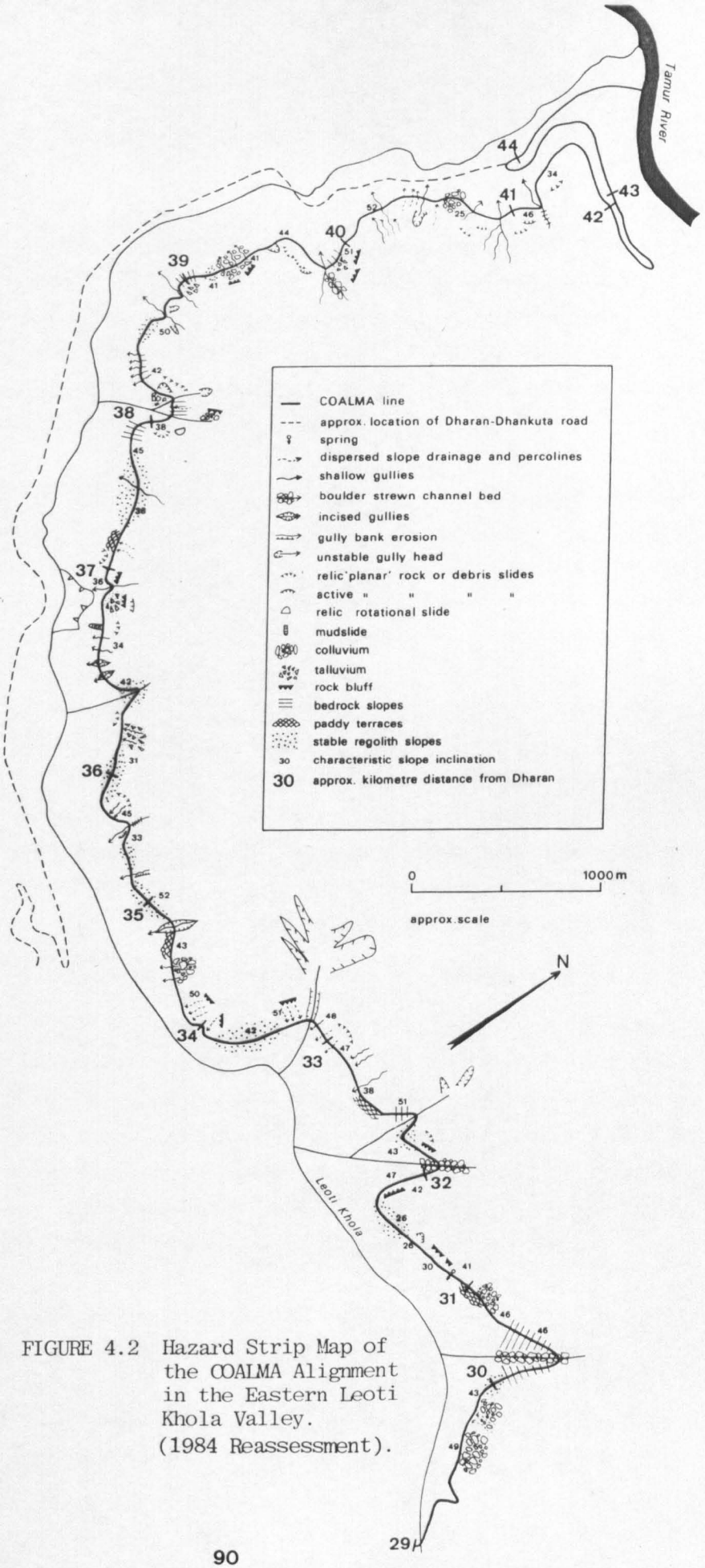

FIGURE 4.2 Hazard Strip Map of the COALMA Alignment in the Eastern Leoti Khola Valley. (1984 Reassessment).

southern flank and an eroding gully head and numerous rock slide scars on the northern flank.

The short section between km 38.5 and km 39.5 was described by GSI as being composed of gentle, stable slopes that were drained by three incised, but stable, streams (Table 4.1). The resurvey recorded a number of old slide scars, quartzite rock bluffs, taluvial deposits and eroding gully heads. The upstream re-entrant, in particular, had developed marked instability since the 1983 monsoon season, in the form of a large rock slide (Plate 4.3).

The final section is located between the present Leoti Khola bridge site (km 39.5) and the point of exit from the Leoti Khola valley onto the southern flanks of the Tamur valley (km 41.5). GSI noted both relic and active instability, including a rotational slide, toppling failure from high quartzite bluffs, and shallow debris sliding in scree. The resurvey observed numerous vegetated rock slide scars, unstable rock bluffs above the trace, the old rotational slip, scree/taluvium and active rock slides on both banks that had obliterated the trace. Between km 40.0 and km 40.7, the resurvey described the slopes as mostly vegetated, and characterised by numerous gullies with unstable, wet landslipped heads that were incised into open-jointed schist. Finally, the trace circumscribes a wide embayment downstream of km 40.7 as far as the southern flank of the Tamur valley. The trace is located above an elevated fan on slopes that, with the exception of localised erosion along incised gullies, are stable.

There are two notable cases where GSI and the 1984 resurvey disagree in their interpretation of terrain conditions. Between km 29.0 and km 33.0, GSI identified three currently active debris flow catchments; the resurvey found only one of these to be significantly unstable. Between km 38.5 and km 39.5 the later survey noted numerous slide scars, unstable rock bluffs and eroding gully heads that would have been potentially hazardous, had a road been constructed along this alignment; GSI made no mention of these features.

It should be emphasised here that, on the basis of a comparison between the two surveys, much of the slope instability that has taken place in the intervening period has been of a shallow nature. This has two important implications for the present study. First, shallow instability has, in many cases, been caused by saturation of soils on steep slopes adjacent to eroding

PLATE 4.3 Rock Slide in Quartzite Along the COALMA Line, Initiated During the 1983 Monsoon.

channels during heavy rainfall, and is therefore unlikely to have been predictable in 1974. Second, while similar hazards have caused problems along the Dharan - Dhankuta road, and other Lower Himalayan roads (Chapter 2), their impact has often been low and only short-term. It is usually the more deep-seated instability that causes the most severe and lasting problems for road construction and maintenance, and GSI appears to have succeeded in identifying most of these.

On the basis of this brief assessment within the Leoti Khola valley, it would appear that GSI identified the majority of terrain hazards along the COALMA line. The resurvey noted a number of instances of both slope and drainage instability that had not been referred to by GSI. However, this might be explained by the fact that the 1984 resurvey was intent on recording all instability, while the 1974 storm, and subsequent storms during later monsoon seasons, may have led to a significant increase in slope and drainage instability since GSI was undertaken.

Generally, GSI made little attempt to interpret ground conditions and hazards in terms of highway design criteria. This is not considered to be a poor reflection on the integrity of the survey because of the nature of the Brief and the limited time available to undertake the survey. As the Brief was to describe and assess slope instability encountered by the COALMA line, it must be concluded that the survey was adequate for route feasibility purposes, and provided an important input to both the decision to reject the whole of the COALMA line and the design of the final RPT alignment. This decision may be supported by a brief examination of the distribution of slope and drainage instability following the September 1984 storm. This storm had a maximum recurrence interval of 75-80 years, although again it should be stressed that much of the instability created has been relatively shallow and short-term (Chapter 5).

The distribution of instability in the Sardu, Leoti and Dhankuta Khola catchments, following this storm, is presented and discussed in Chapter 5, and reflects both the vulnerability of the terrain to erosion and slope failure, and the areal distribution of storm rainfall. However, as the storm appears to have been locally concentrated over the upper Sardu Khola, the Sangure Ridge and the Leoti Khola valley (Chapter 3, Hearn and Jones 1985), general comparisons of the distribution of instability on these slopes are considered to be valid.

The storm produced the greatest concentration of instability on the western flanks of the Sardu Khola valley and the eastern flanks of the Leoti Khola valley. Of the total number of landslide and slope erosion features recorded, 14 percent occurred on the former, while 32 percent occurred on the latter. Combined, these two valley flanks accounted for 46 percent of the total number of landslides recorded in the study area, while occupying only 32 percent of the area of the three catchments. The extent of increased instability on these flanks is shown in the photographs taken before and after the storm (Plates 4.4 and 4.5). By contrast, the slopes crossed by the RPT alignment, in the eastern Sardu Khola and western Leoti Khola catchments, occupy 42.5 percent of the area of the three catchments, but account for only 30 percent of the instability. Therefore, on the basis of these data, the decision to reject the COALMA line in favour of the new RPT alignment is justified. The Dhankuta Khola catchment experienced comparatively little renewed slope instability, owing to the significantly smaller storm rainfall depth received (Chapter 3).

As predicted by GS1, the majority of instability has occurred on the lower and middle valley flanks adjacent to eroding drainage lines. The hairpin stacks at Kumlintar and Mulghat have remained intact, thus supporting the decision to locate vertical route corridors at these sites. However, the alignment on the Leoti Khola floodplain has been considerably damaged (Appendix 1A.7), and this raises the general question as to whether alignments on active floodplains, experiencing high magnitude events, are justifiable.

4.4 The Contribution of the 1975 Geomorphological Survey (GS2) to the Design of the Dharan–Dhankuta Road

4.4.1 Introduction

Most of the remainder of this chapter is concerned with the hindsight assessment of the second (January 1975) geomorphological survey (GS2) of the RPT alignment. This is done by comparing the observations and recommendations made, with those of the subsequent engineering geological 'construction note' survey (EG1), the final design, and the performance of the road during the September 1984 storm. It should be noted that this is not intended to be a direct comparison between a geomorphological and engineering geological survey, but a means of assessing the contribution of the former to the design process. A brief description of the nature and execution of GS2 is given. This is followed by a general overview of the survey with

PLATE 4.4 Slopes Crossed by the COALMA Line on the Western Flanks of the Sardu Khola:Pre-1984 Storm.

PLATE 4.5 Slopes Crossed by the COALMA Line on the Western Flanks of the Sardu Khola:Post-1984 Storm.

regard to the alignment as a whole, and then a detailed appraisal of its findings at particularly problematic sites. This assessment highlights any inadequacies in GS2 and enables recommendations for future surveys to be made. In addition, a brief examination is made of the contribution of continued geomorphological assessments, during road construction and maintenance, to a progressive design approach.

4.4.2 The Nature of the Survey

Essentially, three techniques were adopted by GS2 for recording slope and drainage data along the new alignment: geomorphological mapping, slope profiling and the systematic collection of slope and drainage data by the proforma method. Geomorphological maps and field sketches were the most frequently used of these techniques. The survey consisted of field notes and sketches between Dharan and the Sangure Ridge, strip mapping on 1:1 000 scale topographic maps in the Leoti Khola valley and sketch strip mapping using 1:2 000 scale compass traverses, without other locational detail, between the Sangure Ridge and the Leoti Khola floodplain, and from the northern side of the Tamur River to Dhankuta. Detail plotted onto the maps was usually limited to the slopes immediately adjacent to the trace. However, mapping was frequently extended to encompass slopes several kilometres away, wherever ground conditions along the trace could be explained by reference to geomorphological activity occurring outside the route corridor. The importance of assessing site in respect to its slope situation in this way has been stressed by Cooke and Doornkamp (1974), Brunsden et al (1975 b) and Martin (1978). Reference was made on the maps to relic and active slope and channel instability and erosion, major channel crossings, percolines, springs and wet areas, and the lithological and structural aspects of bedrock exposures. Recommendations were also made, where necessary, for spoil disposal, drainage protection, slope stabilization works and cut slope design.

Wherever problematic sites required a more detailed assessment, purpose designed proformas were completed. These were employed to provide an unbiased, objective and systematic means of recording data. The proforma, shown in Figure 4.3, consisted of five main sections: Geology, Slopes, Fluvial, Vegetation and Design. Owing to the considerable length of time required to complete each proforma, and the difficulty experienced in characterising lengthy sections of the trace by one sheet, their use was discontinued north of

LOG NUMBER	DATE	LOCATION	OPERATOR	LENGTH OF UNIT
XXII	24/1/75	Markers 41 – 44	RPM, DB, DKCJ	40 – 60 m.

GEOLOGY

a) Lithology

Green to grey to yellowish brown, fine to coarse grained, thinly to medium foliated, with discontinuities closely to moderately spaced, moderately to completely weathered MICA SCHIST; moderately permeable

b) Structural features

Extreme small scale contortion in some exposures

Open joints up to 5cm were observed.

Important joint dips are 35° at 290°, 25° at 320°, 28° at 315°

This means these dips are generally favourable on the south facing flanks of gullies but unfavourable elsewhere.

c) Nature and depth of regolith

Light reddish brown to greenish grey, friable, weathered SILT with some SAND and GRAVEL; moderately permeable (pieces of weathered schist become frequent with depth of profile increasing)

Maximum depth = 1·5m but very often less. Rock often exposed at surface.

d) Rock parameters

Dip	—	Strike	—
Rock hardness	R1 – R3	Weathering Grade	III – IV
Fracture spacing index	VL – M	% Rock outcrops within 20m of trace	10% – 20%

SLOPES

a) Angle

Characteristic	
20m upslope	35 – 50
20m downslope	40 – 45
Range	
20m upslope	22 – 50
20m downslope	18 – 45

b) Stability The entire unit, particularly between markers 44 and 43 is very unstable. Many landslide features at different scales both up and downslope from the trace (see sketch map). Two major unstable gullies.

c) Dominant Processes

Soil creep but especially landsliding. Debris slides, rock slides and two rotational slips. The northern flank of gully side between marker 42 and 43 upslope of trace may represent a huge partly degraded rotational slip scar

d) Drainage Character

Some parts of north facing slopes are poorly drained, particularly in gully side between markers 43 and 44

Elsewhere regolith is well drained

e) Erosion Index

H_e = —

FLUVIAL

a) General Two deeply incised unstable gullies cross the trace. Calibre of bed material is not large (generally less than 50 cm maximum diameter) but deep incision has been a major cause of the extensive mass movement

b) Erosion Index

F_e = —

VEGETATION AND HUMAN

a) General

Thin open woodland with much grass covered bare ground

No signs of human influence in this unit

b) Cover Factor: V2

c) Penetrability: P2

DESIGN

1) Recommend careful investigation of whole unit by resident engineering geologist – it is suspected that the widespread instability is associated with the presence of a major thrust plane (Dhankuta thrust)

2) Gullies crossed by strong box culverts with cut-off walls and rock fill. Culverts must be large to carry large volumes of monsoon debris in unstable gullies

3) A slight realignment to the east would minimise dangers slightly but the principle must be to run straight across the gullies on high embankments.

4) Although the major slump block does not represent an immediate hazard it is suggested the southern gully is partially stabilised by bank protection and check dams to reduce rapid erosion of the toe of the slump.

FIGURE 4.3 Proforma used During the Second Geomorphological Reconnaissance Survey for the Dharan-Dhankuta Road (After Brunsden and Jones 1975, Martin 1978).

the Tamur River and replaced by direct annotation onto the sketch strip maps. Slope profiling was used at a limited number of sites, in order to enhance geomorphological interpretation, by allowing complex slopes and bedrock conditions to be evaluated. In addition, slope profiles were produced at sites of proposed hairpin bends or stacks for the purpose of alignment and earthworks design.

4.4.3 Overview of the Survey

This section reviews the assessment made by GS2 of slope and drainage hazards, and briefly compares the recommendations of the survey with the design and stability of the road. However, it must be stressed that the integration of the GS2 findings into the design was more complex than a direct comparison would suggest. There are four main reasons for this. First, the GS2 observations and recommendations were interpreted by EG1 prior to being incorporated or otherwise into the design. Second, the design process was progressive, being based largely on continued observation and re-assessment. Third, the majority of the final design proved to be a compromise between measures to reduce costs and maintain a satisfactory design standard. Finally, road earthworks may have removed many of the shallow instability and erosional features recognised by GS2.

i) Slope Hazards

The principal observations made by GS2 concerning slope hazards are listed in Table 4.2, along with details of the design and stability of the road following the September 1984 storm. A total of sixty cases of slope instability were identified by GS2. Recommendations for avoidance, stabilization or earthworks design were made in thirty-two of these cases. In twenty-one of these, the recommendations were implemented in design (Table 4.2). Of the eleven sites where the recommendations were not implemented, four have been the location of continued instability. These sites are at km 6.430 -7.460, km 16.700 -16.960, km 23.300-23.350 and km 24.375. In the first case, shallow slide scars in the cut slope are indicative of minor slope failure during construction. At the second site, a large rock slide in quartzite led to temporary road and culvert blockage in 1984. In the third case, a debris slide in the cut slope caused blockage of half the carriageway width in 1984. Finally, at km 24.375, shallow mudflow and gully erosion occurred in both

	1975 Geomorph. survey		This thesis	
CHAINAGE	SLOPE INSTABILITY	RECOMMENDATIONS	FINAL DESIGN	STABILITY 1984
2.160	Degraded rock slide scar	None	No allowance	Shallow rilling
2.230–3.000	Potentially unstable slopes	None	Dry-stone revetment	Shallow rilling and sliding
4.200–4.340	Potentially unstable scree	None	No allowance	"
4.340–4.630	Soil creep	Good drainage	No allowance	OK
4.630–4.744	Old shallow slides	Blanket drainage	Cascade in cut	OK
4.820–5.100	Shallow surface and old rotational slides	Full drainage and cut slope protection	Gabion and dry-stone revetment	Extensive slope failure
6.350–6.430	Potentially unstable slope	Protect gully	Gully protected	OK
6.430–7.460	Potentially unstable scree	Stabilize cut slope	Gully revetment	Shallow slide scars in cut slope
7.780, 8.160 8.485	Disintegrating debris slide track	Drain slope or provide culvert	Culvert provided	Debris flow onto road
7.800–8.050 8.500–8.600	Degraded rock slide scar	Drainage, half-cut, half-fill and full-fill	Area drainage and excavation	OK
9.910–10.000	Rock slide scar below road	None	Gabion retained embankment	OK
13.600–14.000	Creep, and shallow slide scars	None	Dentition, gabion and dry-stone revetment	Minor rilling and sliding
15.030–15.175	Potentially unstable scree	Construct retaining wall	Dry-stone walls	Revegetated slip scars
15.175–15.290	Potential rock fall	None	None	Rock fall and slide onto road
16.480	Wedge failures	Stabilize all loose rock	Dentition	Minor rock fall
16.700–16.960	Wet, potentially unstable slopes	Define drainage	No allowance	Culvert blocked by rock slide
16.960–17.100	Shallow debris slide scars in scree	None	No allowance	OK
17.165	Old shallow debris slides	None	Drainage	OK
19.000–19.100	Possible gravity slide scars	Do not load or discharge drainage onto slope	Minimum disturbance, drainage to the south	OK
20.130–20.200 20.540–20.630	Unstable quartzite pinnacle	Realign, clear unstable debris do not cut	As recommended	Debris slide
20.640–20.780	Potentially unstable slope	None	Low cuts, crib wall	OK
21.125	Slide scars	None	No allowance	Rock slides in cut slope
21.640–21.980	Debris slides high groundwater.	None	Low cuts	OK
21.980–22.050	Potentially unstable scree	Full cut	Full cut	OK
23.264–23.285	Debris slide	Drainage	Drainage	OK
23.300–23.350	Boulder tongue	Protect boulders in cut	Full cut, no protection	Large debris slide onto road
23.355–23.370	Debris slide	"	Full-fill	OK
23.430–23.445	Debris fan	"	No cut or fill	OK
23.470–23.525	Rotational slide	Do not cut	"	OK

TABLE 4.2 Observations and Recommendations Made by the 1975 Geomorphological Survey Concerning slope Instability and their Bearing on the Final Design.

	1975 Geomorph. survey		This thesis	
CHAINAGE	SLOPE INSTABILITY	RECOMMENDATIONS	FINAL DESIGN	STABILITY 1984
23.550–23.610	Unstable slopes.	Full cut, remove debris.	Full cut.	Major slope failure.
23.600	Slide scars.	None.	Drainage.	Slope failure.
23.650–23.680	Debris slide.	Drainage.	Drainage and slope revetment.	Sliding.
24.375	Recent slump.	Drainage and remove loose material.	No allowance.	Gully erosion and sliding.
24.480–24.540	Boulder fan.	Full drainage.	Drainage.	Settlement of gabion wall.
24.540	Debris slide track.	None.	No allowance.	OK
24.555–24.580	Old rock slide.	None.	Gabion retaining wall.	Rock slide blocked road.
24.800–24.890	Small debris slide scars.	Retaining structures and drainage.	Drainage and revetment.	Major cut slope failure.
25.000	Recent shallow slide.	None.	No allowance.	OK
25.100–25.140	Active planar slide.	None.	Gabion embankment and channel protection.	Rock slide onto road.
25.160–25.180	Slides.	None.	Gabion embankment and toe protection.	OK
25.290–25.340	Old planar debris slides.	None.	Drainage and revetment.	Debris slides onto road.
25.365	Debris slides.	None.	Full cut area drainage, revetment.	OK
25.500	Active debris slide.	None.	"	Continued failure onto road.
27.180	Rock slide.	Detailed investigation required.	Trimming and catchwall.	OK
28.169–28.400	Rock slide.	Cut slope stabilization.	No allowance.	OK
35.030–35.070	Slide.	None.	No allowance.	Large failure upslope.
35.515	Old rock slide.	None.	Dry-stone revetment.	Minor sliding and fall.
35.810	Large debris slide.	None.	No allowance.	OK
36.480–37.560	Ancient boulder fans.	Lateral drains.	Drainage and revetment.	OK
37.560–38.420	Loose boulders, talus creep.	Drainage.	"	Some cut slope failure.
38.420–38.800	Potentially unstable boulder cones.	Remove loose material apply netting to cuts.	Dry- stone revetment.	Minor cut slope failure.
40.360–40.400	Slides and slumps.	None.	No allowance.	OK
40.450	Debris slide scar.	None.	No allowance.	OK
40.540	Old instability.	None.	No allowance.	OK
40.413–40.575	Potential block glide.	Realign and stabilize gullies.	Realigned, revetment, check-dams in gullies.	Continued instability.
41.080–41.170	Head of active mudslide.	Realign and drain.	As recommended.	OK
41.100–41.170	Landslide embayment above road.	None.	Low cut, area drainage.	Shallow slide onto road.
41.430	Active debris slide scars.	None.	No allowance.	OK
41.430–41.590	Boulder covered spur with slide scars.	Drainage and scaling.	Drainage and revetment.	Rock and debris slides onto road.
42.400	Potentially unstable slopes.	Avoid.	Realigned.	Road OK but slopes unstable.

TABLE 4.2 cont./

1983 and 1984, and had virtually no effect on the road.

It can be concluded, therefore, that where instability has occurred at sites where the GS2 recommendations were not followed through in design, it has been of a shallow nature, and has had only a short-term impact on the road. By contrast, there are four sites in particular, where GS2 failed to recognise the full potential for major deep-seated failure and road loss (km 3.900, km 4.100, km 5.100 and km 8.900). These sites are discussed in Chapters 5 and 6 and Appendix 1 (A.3 and A.4). The full potential for slope failure at km 3.900 was not realised by GS2, despite signs of both relic and active instability mapped during construction (Section 4.4.4.3). At km 4.100 and km 8.900 slope failure, resulting in road loss and deformation was not anticipated by GS2, although it must be noted that, at both sites, slope overloading by spoil disposal (Chapter 6) may have been a significant contributory factor that could not have been foreseen by GS2. Finally, at km 5.100 deep-seated slope failure and road deformation has occurred on the steep, southern flank of a spur above the Khardu Khola. While GS2 noted some instability on this slope, total failure was not anticipated (Section 4.4.4.2).

ii) Drainage Hazards

Drainage channels crossed by the trace were described by GS2 in terms of their general stability and, wherever possible, an estimation was made of bed width, bedload size and maximum depth of flow likely to be conveyed. Excluding the alignment on the Leoti Khola floodplain, twenty-three drainage crossings were referred to specifically as being unstable or potentially unstable (Table 4.3). Eighteen specific recommendations were made for culverts and channel protection works; all of these were adopted in the final design. However, virtually every sizeable channel crossed by the road has been culverted or bridged and provided with erosion protection works, and hence, it is difficult to determine the extent to which the recommendations were applied directly in design.

One of the most conspicuous drainage hazards to occur during construction was associated with accelerating erosion caused by concentrated road runoff and spoil tipping. The distribution and extent of this erosion is difficult to predict prior to construction, primarily because it is dependent on the final design of earthworks and road drainage (Chapters 5 and 6). Nevertheless, it

	1975 Geomorph. survey		This thesis	
CHAINAGE	DRAINAGE PROBLEM	RECOMMENDATIONS	FINAL DESIGN	STABILITY 1984
2.160–2.230	Complex gully head.	None.	Single gully with mattresses and cascades.	Erosion of unprotected bank. Some debris in culvert inlet.
3.000–3.200	Eroding gully.	Checkdams, box culvert.	Cascade, box culvert.	OK
3.920–4.000	Incising gully.	Requires stabilization.	Checkdams.	Continued erosion, inundation by slide.
4.744–4.820	Two large gullies. First-debris flow. Second-stable.	First gully-4-5m guide walls, erosion protection.	First gully-box culvert, guide walls and cascade. Second gully-bridge, guide walls, cascade.	First gully-largely stable. Second gully-debris flow activity, highly unstable with damage to erosion protection.
8.670–8.900	Five gully heads below trace.	Drain and provide checkdams.	Gabion cascades and mattresses.	Erosion alongside structures, unstable channel.
13.600–14.000	Gully erosion.	Checkdams.	Cascade and checkdams.	OK
14.600	Gully erosion.	Box culvert.	Avoided by realignment.	OK
16.070–16.480	Potential for gully erosion.	Define drainage, culverts, checkdams.	As recommended.	Minor erosion.
22.880–23.130	Incised gully in boulder fan.	Stabilize floor with boulders.	Gabion mattresses and boulders.	OK
23.400	Deeply incised gully.	Checkdams and boulders.	"	Erosion upstream.
24.470	Unstable gully.	Embankment.	Embankment with outfall cascade.	Major erosion upstream.
24.540	Incised gully.	None.	"	Culvert blocked.
25.220	Incised gully.	None.	Cascade at inlet mattress below outfall.	OK
25.365	Gully head.	None.	Area drainage.	OK
25.470	Small gully.	Small culvert.	Pipe culvert.	OK
23.200–25.350	Unstable drainage lines and wet areas.	Stabilize with checkdams and boulders.	As recommended.	Incision in main gully.
33.850–35.100	Relic and active gullies and percolines on lower hairpins.	Dig out percolines, install drainage.	As recommended.	Accumulation of debris onto road from unculverted gullies above cut.
33.070,34.650 34.580,34.120 35.800,35.730 35.160	Road crosses particularly unstable gullies.	Stabilize with checkdams.	As recommended.	Localised erosion generally OK.
40.413,40.560	Two eroding gullies with large-scale side-slope instability.	Bank protection checkdams upstream and downstream of large culvert.	"	Checkdams and matresses broken, highly unstable side-slopes.
41.430,41.590	Incising gullies with large-scale instability.	Checkdams and bank protection large culvert.	"	Major erosion in both gullies, culverts blocked, bank protection destroyed.
42.000–Dhankuta	Many incising gullies in weathered gneiss.	Channel protection.	Box and pipe culverts with short cascades below outfall.	Erosion below some outfalls, culverts clear and stable.

TABLE 4.3 Observations and Recommendations Made by the 1975 Geomorphological Survey Concerning Drainage Hazards and their Bearing on the Final Design.

would appear that GS2, and the reconnaissance investigations for the road in general, underestimated the potential for road runoff-induced erosion.

4.4.4 The Contribution of the Survey to Road Design at Specific Problem Sites

4.4.4.1 Introduction

This section is concerned with a more detailed evaluation of GS2 by comparison with the subsequent engineering geological construction notes (EG1), the final design and present stability of the road and adjacent slopes, along particularly problematic sections of the road. The analysis provides the basis for assessing the contribution of GS2 to the final design and, more importantly, enables recommendations to be made for the improvement, where necessary, of reconnaissance survey techniques for highway design in this or similar terrain. Reference is made throughout the discussion to Appendix 1, which contains a detailed description of road design and construction and an assessment of stability following the September 1984 storm.

The road sections chosen for the analysis consist of the hairpin stack at Kumlintar, three areas of unstable ground, displaying both relic and active mass movement, and the alignment on the Leoti Khola floodplain. The Kumlintar hairpin stack has been included because it is an important element in the overall design philosophy of the alignment, and failure of the slope upon which it is constructed would result in considerable road loss. Although the hairpin stack at Mulghat is probably a more important element in the alignment design philosophy than that at Kumlintar, slope instability features are relatively infrequent, and consequently, a detailed examination of GS2 at this site might not be particularly instructive. The three areas of unstable ground cover what are generally considered to be the most hazardous slope sections crossed by the road, and hence, provide an ideal opportunity for testing the predictive ability of GS2. Finally, a road constructed on a floodplain may suffer some form of damage from periodic flooding, and hence, the problems for road stability here are totally different from those experienced elsewhere along the route. An evaluation of the performance of the floodplain route, therefore, forms an important section of this analysis.

This discussion deals with the hairpin stack, the three areas of unstable ground

and the floodplain route separately. For ease of comparison, the observations of both GS2 and EG1, and relevant details of the road design and present stability, have been tabulated for three of the five sections (Tables 4.4-4.6). Comparative tables have not been produced for the unstable valley re-entrant, as this is essentially a site - specific problem, affecting only a short length of road, or the Leoti Khola floodplain, as the GS2 observations and recommendations here were often generalised, and no original contributions were made by EG1 concerning flooding, erosion or sediment hazards. The reader is advised to consult each of the tables and details of the present stability (Appendix 1) whenever necessary, as continual reference to these is not made in the text. As most of the final alignment is a modification of that mapped by GS2, the kilometre marks referred to in the text have not been transferred onto the geomorphological maps. Instead, the sites of main interest are identified on the maps with capital letters.

4.4.4.2 The Kumlintar Hairpins (Km 5.100 - km 8.700)

The Kumlintar hairpins form one of the two vertical hairpin stacks along the road. A full description of slope conditions at this site, the road design and present stability is presented in Appendix 1A.4 . Details of the observations and recommendations made by the reconnaissance surveys, and the design and present stability of the road, are given in Table 4.4. The geomorphological strip map produced by GS2 is reproduced in Figure 4.4.

On the lower half of the hairpin stack, the main features noted by GS2 were steep vegetated scree slopes (A), a spur thinly mantled with debris (B), an ill-defined gully with unstable side-slopes and a 'spring sap hollow' below the trace at km 6.030 (C). The recommendations made by GS2 included full-cut through the spur, and drainage and erosion protection measures in the spring hollow and gully crossings. These suggestions were largely endorsed by EG1 and reflected successfully in the design.

A short re-entrant slope at km 6.360 - 6.440 (D), was described by GS2 as potentially unstable and formed in closely jointed phyllite. Due to the height and steepness of this slope, GS2 suggested full-cut to 60^{o} and protection works in the gully below. In the final design, the cut slope was excavated to 55^{o} and stabilized by gabion revetment, while further undercutting in the gully has been prevented by gabion protection works. At km 6.440, the trace crosses this

			This thesis	
CHAINAGE	GS2 COMMENTS/ RECOMMENDATIONS	CONSTR. NOTE RECOMMENDATIONS	FINAL DESIGN	STABILITY 1984
5.770–5.920	Steep vegetated scree.	Mostly scree.	Low cuts and revetment.	OK
6.300–6.350 5.840–5.900	Thinly mantled spur. Lower trace-full-fill upper trace-full-cut.	Cut to 63°.	As recommended by GS2.	OK
5.950,6.235	Ill-defined gully install checkdams.	None.	Masonry channel.	OK
6.030	Spring sap hollow, horizontal drains.	Spring sap hollow, drain.	As recommended.	OK
6.360–6.440	Re-entrant slope formed in jointed phyllite, highly permeable with scree. No overloading, 60° cut, basal protection	Stability is joint controlled cut to angle of joints.	Full cut 55°, gabion revetment basal protection.	OK
6.440	Gully with small slide scars and debris lobe. Install culvert.	Old slide scars and debris lobe.	Culvert and bank protection.	OK
7.775,8.185 8.460	Debris slide/flow track. Full drainage-culvert.	Debris slide track. Pick up flow in side drain.	As recommended by by constr. notes.	Reactivated 1984.
8.510–8.585	Degraded rock slide of earthquake origin. Lower trace-embank. Middle trace-half-cut, half-fill. Upper trace-full-cut. Herringbone drains and retaining wall.	Degraded rock slide(?). Install area drains.	Road realigned, full-cut herringbone drains, retaining wall.	OK

TABLE 4.4 Details of Comments and Recommendations Made by the 1975 Geomorphological Survey and the Construction Notes, and the Final Design and Stability of the Kumlintar Hairpins.

N.B. GS 2.... Second Geomorphological Reconnaissance Survey(1975).

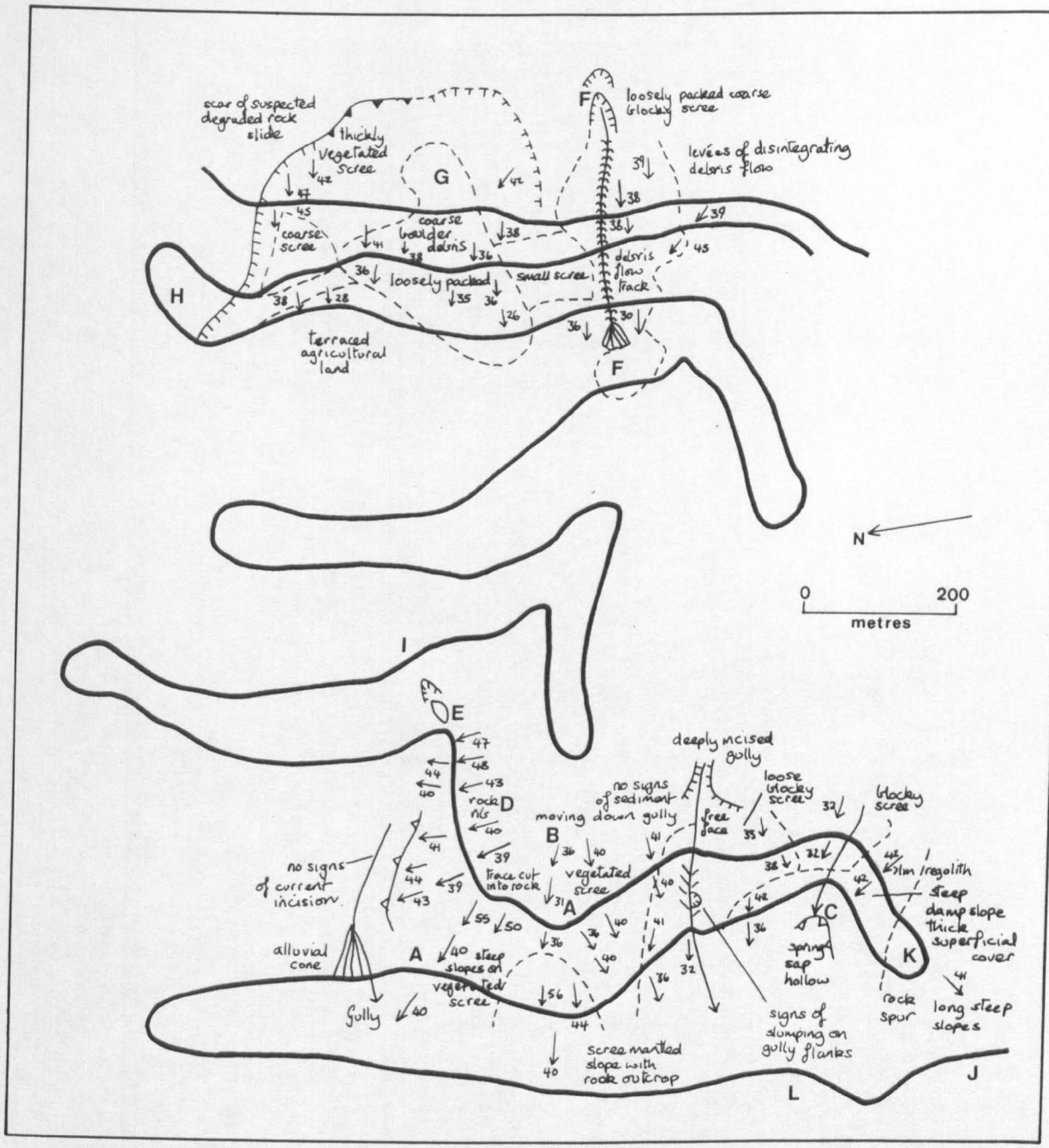

FIGURE 4.4 Geomorphological Map(GS 2) of the Kumlintar Hairpins.

gully immediately below a debris slide (E). GS2 recommended adequate culverting to allow for high runoff rates and sediment loads. These remarks were largely duplicated by EG1, and the final design consisted of a slab culvert with upstream bank protection works and channel lining. The gully has remained stable.

The final area of instability noted by GS2, occurs between km 7.750 and the up-chainage exit from the hairpin stack (km 8.680). This section of the alignment has also been described by Fookes et al (1985). A deep, coarse scree was identified, and it was suggested that the road here would require extensive foundation and cut slope stabilization. EG1 provided a more detailed description of excavation and foundation conditions, based largely on trial pit observations.

On the upper part of the hairpin stack, a debris flow track (F) was identified by GS2, crossing the trace at three locations. The track had two scarps on the slopes above the upper trace, and depositional levees and lobes. The uppermost scar and the track itself were regarded by GS2 as being the result of earlier instability, while the lower scar was possibly formed during the 1974 monsoon season. The feature was, therefore, of recent origin, according to GS2. The survey suggested that this track should be adequately drained and culverted at the crossing points. EG1 mapped this feature also as a debris flow track, but recommended that a cut-off drain be constructed through the head of the back scar, and that any flow within the track itself be directed into the road side drain. Although this feature was re-examined during construction (Martin pers.comm. 1986), no drainage provision had been made in the final design, except into the side-drain as EG1 had suggested. The main reason for this was the lack of a feasible drainage path on the slope (Manby pers. comm. 1985). During the September 1984 storm, shallow instability, gully incision and debris flow on this slope caused inundation of the road lines below (Appendix 1A.4), thus confirming the observations of GS2. However, it is likely that overspill from a contoured surface drain above, may have significantly contributed to the instability at this site.

A large ancient rock slide (G), of possible earthquake origin, was identified by GS2 at the top of the hairpin stack (Figure 4.4). Although the antiquity of this rock slide was recognised, it was recommended that drainage of the slip material, above the trace, be undertaken. In addition, GS2 suggested that the

three uppermost sections of trace be realigned in order to minimise slope disturbance. Although EG1 raised question as to whether this was a rock slide, it endorsed the recommendations for slope drainage and full-cut with a slope retaining wall. In the final design, one of the hairpins (H) has been relocated downslope (km 8.000) so as to reduce the number of traverses across the rock slide from three to one. Slope drainage has been installed and the full-cut has been stabilized with gabion revetment. There has been no evidence of slope movement since construction, and hence the design appears to have been satisfactory. Interestingly, an examination of slope excavations during earthworks (Martin pers. comm. 1986) failed to reveal any conclusive evidence for an ancient rock slide on this slope, thus questioning the validity of the GS2 interpretation.

Instability problems arising during construction were confined to small cut slope failures in oversteepened scree, repeated collapse of the retaining wall at km 6.800 (I), and erosion of the slope on the northern side of the stack. Here, a continuous gabion and masonry cascade discharges runoff from the side drain exits of the hairpins, to the Khardu Khola below (Appendix 1A.4).

During the September 1984 storm, in addition to gully incision on the slopes above the stack, major instability occurred on the slopes below the lowest hairpin (Appendix 1A.4). Extensive cracks have formed in the road at km 5.100 (J) due to deep-seated instability on the flanks of the Nishane and Khardu Kholas. Minor cracks around the hairpin at km 6.100 (K), appear to be associated with the same instability. Spoil tipping at km 5.100 may have been a contributory factor in the initiation of slope failure here, although channel erosion and high groundwater levels are likely to have been the main causes. Gullying and sliding on the flanks of the Khardu Khola at km 5.300 (L) have also placed the road at risk of failure if further erosion takes place. Neither of these developments were foreseen by either of the surveys, although GS2 noted relic debris slide scars and unstable stream banks below the road at km 5.060.

In view of the final design of the Kumlintar hairpin stack, and its current stability, it can be concluded that GS2 provided an extremely useful description and assessment framework of slope and drainage processes and their likely effect on road construction. The majority of recommendations have been adopted in the design, and although EG1 provided a more detailed

assessment of slope materials for foundation and excavation purposes, the comments and recommendations of GS2 were largely reiterated.

GS2 failed to recognise the potential for extensive slope failure and road loss on the flanks of the lower Khardu and Nishane Kholas. This shortcoming is partly due to the fact that instability here has become accelerated in recent years by relatively large storms in 1983 and 1984, and possibly spoil tipping and drainage disturbance in the Khardu Khola catchment during and following earthworks (Chapter 5).

4.4.4.3 Unstable Valley Re-entrant (km 3.825 - km 4.150)

This section of road has been included in the assessment because it has undergone major slope failure during the maintenance period. The re-entrant is located within a system of spurs and incised gully catchments of the first foothill range, composed of Siwalik sediments (Chapter 3), overlooking the Terai Plain. A full description of this re-entrant is given in Appendix 1A.3.

The GS2 geomorphological map of this section is shown in Figure 4.5. GS2 described the underlying bedrock as a micaceous sandstone, moderately to highly permeable, and dipping at 20-25^{o} northwards, into the slope. The re-entrant is drained by two gullies that join immediately downslope of the road at km 4.000 (Figure 4.5). With the exception of scree accumulation on the spur at km 4.200 (A), GS2 noted no signs of instability, but emphasised that basal erosion by either gullies could cause slope movement on re-entrant margins. The recommendations made for design were concerned with adequate culverting, and the prevention of further gully incision by the installation of checkdams in the channel. The survey proposed that the waterfalls at the culvert inlets should be 'laid back' to prevent scour, and discouraged spoil tipping and vegetation clearance.

Details of the final design and stability along this section are given in Appendix 1A.3. On the down-chainage re-entrant margin, the road has been excavated in full-cut, while on the up-chainage side, it has been constructed in half-cut, half-fill on gabion retained embankment. A series of gabion check-dams were installed in the gully below the road. During construction, spoil was tipped onto the spur and adjacent re-entrant margin at km 4.200. Major slope failure and road loss occurred on this re-entrant flank in September 1983 when

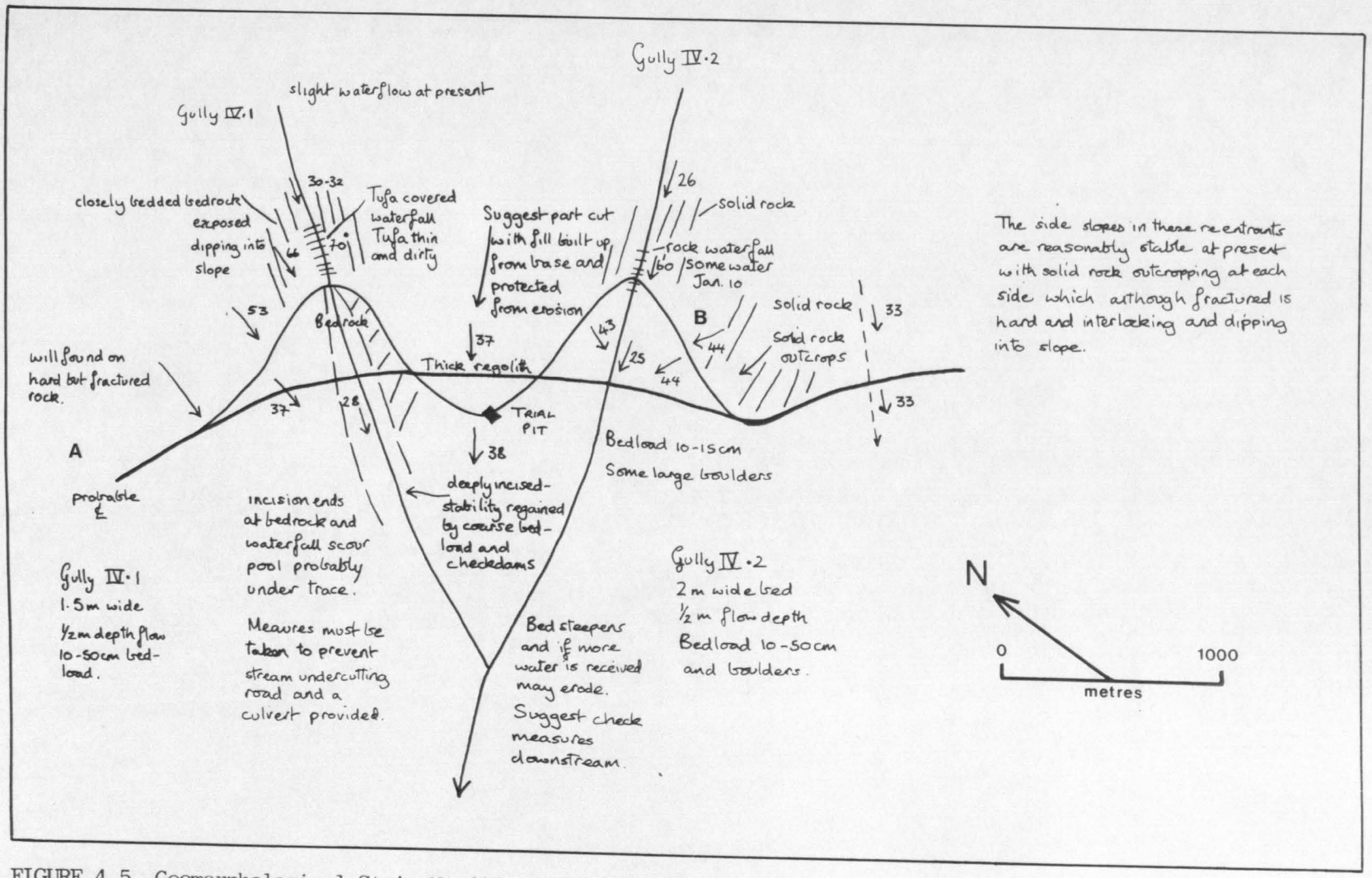

FIGURE 4.5 Geomorphological Strip Map(GS 2) of Valley Re-entrant.

373 mm of rain fell in 72 hours. Failure here, appears to have been caused by the development of high groundwater levels following a particularly wet monsoon season, channel erosion and possibly slope overloading by spoil tipping.

On the opposite re-entrant margin (B), cracks began to develop in the road surface in 1978 between km 3.840 and km 4.000. During the September 1984 storm, extensive rotational failure occurred on this slope (Appendix 1A.3). Approximately 200m of road length was displaced some 100m further downslope (Plate 2.6). Again, failure appears to have been caused by the development of high groundwater levels and basal erosion. The creation of a small spoil bench below the road, during construction and maintenance, may have been a contributory factor. The failure of this slope is discussed further in Section 4.5.

Despite the observations made by GS2 regarding channel incision, and the possibility of slope failure taking place if spoil disposal was undertaken in this re-entrant, there is no indication that GS2 regarded these slopes as being inherently unstable. However, the potential for slope failure was realised by the consulting engineers during reconnaissance, and the road was located as far upslope as possible, in order to keep the length of road at risk to a minimum. The principal causes of instability on both margins appear to have been increased channel erosion during construction and the development of high groundwater levels. The full potential for these developments may have been largely unpredictable at the time of the geomorphological survey.

4.4.4.4 Triple Crossing of an Unstable Bowl (km 23.180-km 25.360)

The final few kilometres of descent to the Leoti Khola floodplain, on the steepened lower valley side slopes (Plate 4.6), involves the triple crossing of a large bowl-shaped catchment that is characterised by mass movements, boulder fan accumulations and a drainage system that has become incised into both colluvium and weathered phyllite and paper shale. A full description of the geomorphological character of this section, along with relevant details of road design and present stability, is given in Appendix 1A.6. The observations and recommendations made by GS2 and EG1, and details of the final design and present stability, are shown in Table 4.5. The geomorphological map produced by GS2 is reproduced in Figure 4.6.

PLATE 4.6 Triple Crossing of an Unstable Bowl Depression on the Lower Flanks of the Leoti Khola Valley.

CHAINAGE	GS 2 COMMENTS/ RECOMMENDATIONS	CONSTR. NOTE COMMENTS RECOMMENDATIONS	This thesis: FINAL DESIGN	This thesis: STABILITY 1984
23.180	Open cut. Protect against debris slides.	Short box cut through spur.	Box cut.	OK
23.230–23.280	Debris slide.	Superficial erosion and slumping. Install retaining wall, counterfort and herringbone drains. Regrade slope.	Counterfort and herringbone.	Minor rilling and slumping.
23.300–23.350	Boulder tongue. Cut into with care, protect against falling boulders.	Spur with boulders, no bent trees or springs. Full-cut to 12m, revet against falling boulders.	Half-cut, half -fill, drainage, no revetment.	Total slope failure in 1984.
23.355–23.370	Debris slide scar, may be old rotational slip.	GS 2 notes slide scar investigate during construction.	No cut, gabion embankment.	OK
23.415	Two streams and springs, drainage.	Springs.	Cut-off drain to direct spring into main gully.	Road lost.
23.420–23.445	Boulder fan, cut into with care. protect against falling boulders	Road on gentle(20°) cultivated terrace.	No cut or fill due to realignment.	OK
23.450	Stream with unstable banks.	Upright trees, no seepage or instability. Lobe of quartzite boulders.	Pipe culvert, no protection.	Major erosion culvert blocked.
23.465–23.535	Rotational slip, F.S.=1. Do not cut.	GS 2 noted slip scars and much recent shallow instability above road. Alignment avoids trouble and loads toe of any possible major instability. Potential for erosion below.	Slip avoided by realignment.	OK
23.545	Stream incised below trace.		No allowance.	OK
23.560	Slide scar, 1.5m deep.		Gabion toe wall.	Rock slide.
23.600	Slide scars.		"	Rilling, slumping below road.
23.640–23.680	Deep debris slide in weathered paper shale at head of eroding gully. Ground below road is unstable. Remove slide, full-cut, horizontal drainage.	Active surface slumps and erosion. Bent trees no seepage. Construct 5m high retaining wall, founded below instability. Checkdams in gully and re-establish vegetation. Drain slope with counterfort and herringbone.	No cut, herringbone and counterfort drains installed. Masonry cascade and checkdams in gully below.	Scour below culvert. Some slumping onto road.
23.690	Slip scars, steep slopes below trace. Full-cut.	Irregular slopes, bent trees. Full-cut into spur, 10m high. Use revetment to prevent shallow instability.	Full-cut, gabion revetment.	Rilling and slumping over wall.

TABLE 4.5 Comments and Recommendations Made by the 1975 Geomorphological Survey and the Construction Notes and the Final Design and Stability in the Bowl.

cont./ next page.

N.B. GS 2....Second Geomorphological Reconnaissance Survey(1975).

CHAINAGE	GS 2 COMMENTS/ RECOMMENDATIONS	CONSTR. NOTES RECOMMENDATIONS	This thesis	
			FINAL DESIGN	STABILITY
24.185–24.235	Shallow debris slide caused by trace cutting. Remove slide and bench slope.	Full-cut up to 20m high. Install two box culverts and revetment.	Full-cut with gabion revetment.	OK
24.300–24.320	Wet slopes with open joints. Open cut and drain.	No trees or springs. Construct 8m high gabion revetment. Trial bench suggests 2/3 :1 cut slope.	Gabion revetment.	Gullying and slumping on tip slope below.
24.400	Deeply incised gully. Debris slides and two gully heads above trace. Stabilize gully using checkdams and boulders. Stabilize slumped area by drainage and retaining walls.	GS 2 notes slip scars. Recent slip below road, 4m deep. Cracked and bulging slope. Construct 12m high retaining wall. Full-cut into spur. Excavate slumped debris and replace with revetment. Protect gully with checkdams and lining.	Full embankment. Gabion cascade and checkdams.	Slump remains incised slopes below. Reactivated debris slides.
24.425–24.440	Shale spur. Careful drainage.	15m cut through spur. 2/3 :1.	Half-cut, half-fill with retaining wall.	OK
24.470–24.530	Boulder fans, small gully and spring line. Full drainage.	High calibre boulder lobe. Trees straight no rock seen, even at 4m. Springs mapped by GS 2 are runoff from abandoned paddy. Full-cut, up to 10m at 45°. Masonry revetment between boulders. Cut-off drain to direct stream into gully.	Generally embankment with some box cut and gabion retaining wall. Herringbone drains.	Wet, seepage, broken side-drain and small slump behind wall.
24.470–24.500	Double gully with unstable slopes.	Small slips in gully.	Gabion cascade and checkdams.	Culvert blocked major scour.
24.535	Incised gully with unstable slopes.	Checkdams and channel lining.	Gabion cascade.	Culvert blocked.
24.540–24.575	Bedding slide. Retaining wall required for cut.	GS 2 notes shallow slide. Investigate during construction.	Road cutting truncates slide.	Rock slide blocked road.
24.600	Old rock slide with stream incision below. Drainage.	GS 2 mapped shallow scars. Bowl of surface erosion and small fresh failure at toe of slope. No bent trees or seepage, ground below trace is irregular.	2m gabion retaining wall. Masonry cascades in cut slope. Area drainage.	Shallow debris sliding. Slide scar extended upslope.

TABLE 4.5 Cont/

			This thesis	
CHAINAGE	GS 2 COMMENTS/ RECOMMENDATIONS	CONSTR. NOTES RECOMMENDATIONS	FINAL DESIGN	STABILITY 1984
24.600–24.725	Thinly mantled and weathered paper shale. Full drainage essential.	Fractured, weathered and eroded paper shale. Half-cut, half-fill. Control stream by lining and checkdams.	Masonry dentition, crib walls.	Major cut slope failure.
24.800–24.890	Debris slide scars.	None.	Minor revetment.	Major failure.
25.115–25.200	Active, deep-seated planar slide, undercut by stream. Fractured, contorted, weathered shale. River training, toe loading. Either : a) Full-cut with gabion retaining wall. b) Clear debris and build up on unweathered shale.	Bowl of superficial erosion, 3–4m deep, caused by stream incision. Excavate slipped mass, rock bolt exposed faces. Control stream by lining and checkdams. Build gabion wall from toe of slope (20m)	Gabion embankment. Mattresses and bank protection in gully.	Rock slide onto road, slip scars below.
25.210	Trace crosses three gullies.	Embankment up to 3m high across gully. Good foundation in stream bed.	8m high embankment. Gabion cascade at culvert inlet.	OK
25.260–25.360	Four old planar debris slides, 2–3m deep with two small streams.	No seepage or exposures. GS 2 mapped small slip scars some distance above the trace. Trace may cross large ancient slump, not mapped as such by GS 2. Shallow cut and fill, small gabion retaining wall.	Full-cut, 4m high gabion and crib retaining wall. Counterfort drains upslope and cascade at culvert inlet.	Shallow rotational and translational debris slides. Road blocked.
25.500	Active slide.	None	Gabion retaining wall, area drains.	Continued slope displacement.

TABLE 4.5 Continued.

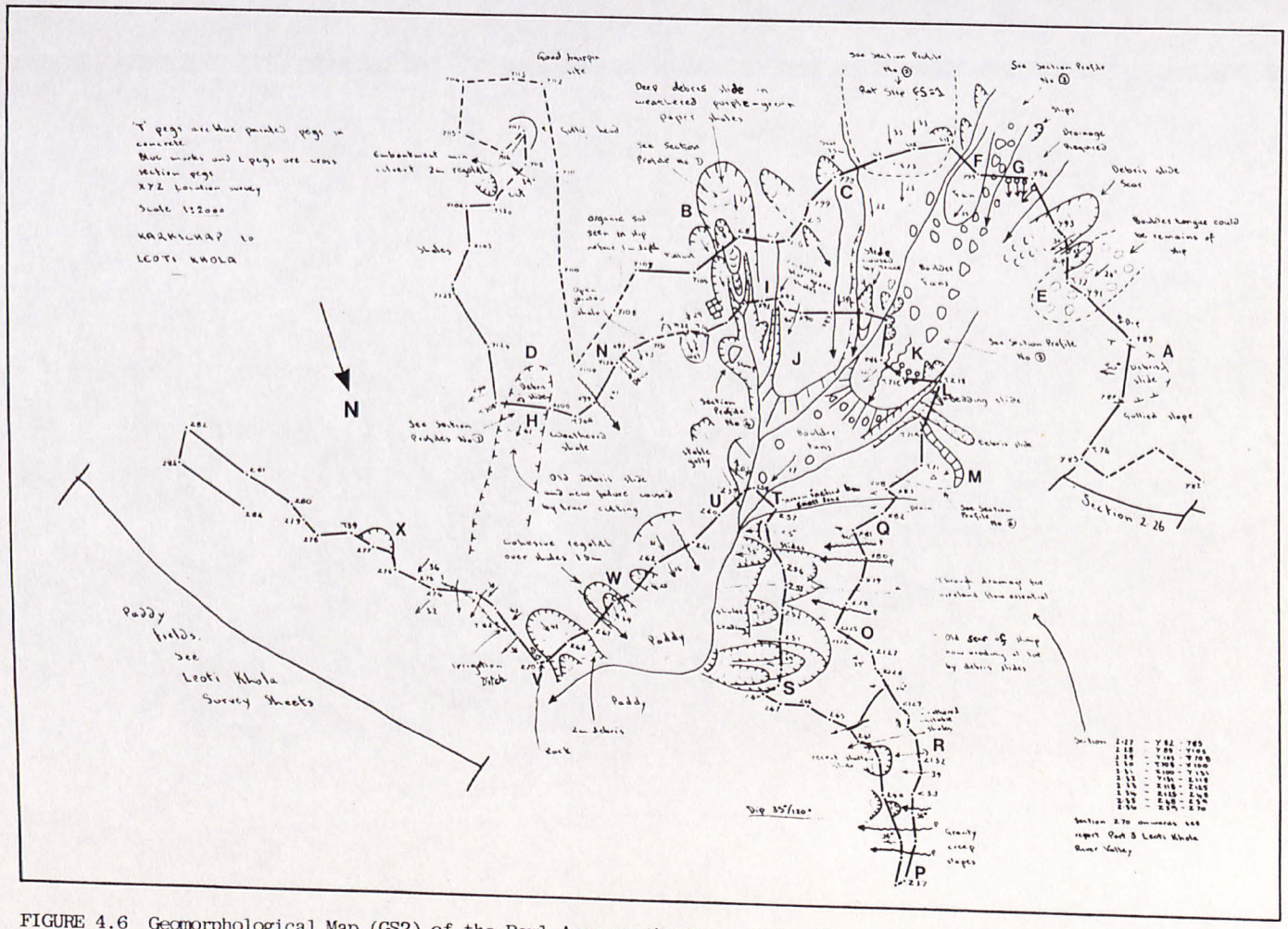

FIGURE 4.6 Geomorphological Map (GS2) of the Bowl Area on the Descent to the Leoti Khola Floodplain.

The discussion is subdivided into the upper, middle and lower crossings of the bowl.

i) Km 23.180-km 23.690 (Upper Trace)

This upper crossing of the bowl was regarded as the most unstable by GS2. The trace crosses, in quick succession, six debris slides, two boulder tongues, one rotational slip and three eroding gullies (Table 4.5, Figure 4.6). Although EG1 recognised all six debris slides, only the most conspicuous and potentially active, at km 23.230-280 (A) and km 23.640-680 (B), were provided with slope drainage in the final design. This has succeeded in stabilizing both of these slides, although minor slumps and mudflows onto the road occur from each of them during heavy storms (Table 4.5). Two of the remaining debris slides have been reveted by 1m gabion breast walls[1] and, although they pose little threat to road stability, they too have suffered minor erosion by small slumps and mudflows.

At approximately km 23.550 (C), GS2 recorded stream incision below the trace and a 1.5m deep slide scar above. During the September 1984 storm, considerable gully erosion took place below the road at this point, along with rock sliding onto the road from above the gabion revetment (Table 4.5). At the point (D), where the road exits from the bowl (km 23.690), GS2 noted slip scars both above and below the trace and recommended that the road be constructed in full-cut to avoid the steep, unstable slopes below. EG1 also suggested full-cut and revetment, and this was adopted in the final design.

GS2 suggested that the two boulder fans at km 23.300-350 (E) and km 23.420-445 (F) be cut into with great care and adequate provision be made for cut slope protection. These recommendations were reiterated by EG1, although by then, the alignment had been modified to avoid cutting into the front of the latter boulder fan. The fan at km 23.300-350 has been crossed in half-cut, half-fill, without cut slope revetment. A large debris slide occurred here during the September 1984 storm, totally blocking the road and extending for

---

1. A breast wall is a low, commonly 1-2m high, revetment at the toe of a slope.

approximately 40m upslope. Finally, the rotational slip described by GS2 as having a factor of safety of approximately one, has shown no signs of movement, although slope disturbance has been avoided, as recommended, by minor realignment to the east.

Stabilization of the incising streams in the bowl, was regarded by both GS2 and EG1 as crucial to road integrity. Culverts with drop-pipe outfalls have been installed at most gully crossings along with gabion cascade channel protection works at km 23.300 and km 23.470. With the exception of culvert inlet blockage during the 1983 monsoon season at km 23.420 (G), these gully crossings remained stable until September 1984. During this event, a debris slide, approximately 50m in slope length and 4m deep, occurred on the slopes above (Appendix 1A.6). This slide appears to have developed downslope into a debris flow as it entered the channel above km 23.420 and caused the total destruction of both the culvert and gabion embankment at this point. Neither GS2 or EG1 gave any indication that this form of instability might take place. All other instances of instability occurring along the upper trace, during the 1984 storm, can be explained by reference to the observations made by GS2.

ii) Km 24.180-km 24.725 (Middle Trace)

At km 24.185-km 24.235, GS2 recorded a recent shallow debris slide (H) that, although associated with older mass movement, had been reactivated by trace cutting. Full-cut was suggested through the spur, and this along with slope revetment was also proposed by EG1, and reflected successfully in the final design.

The debris slide/eroding gully complex, identified by GS2 at km 24.400 (I), is the downslope continuation of that found on the upper trace at km 23.640-km 23.680 (B). Both surveys suggested channel stabilization as the most appropriate method of reducing further instability and this was implemented in the final design. Extensive slope failure has occurred on the slopes above the road, causing temporary road blockage. Renewed instability in the gully below the road, and the development of additional slip scars, also took place during the 1984 storm.

A shale spur (J) and a boulder fan (K) are encountered at km 24.425-km 24.440 and km 24.470-km 24.530, respectively (Figure 4.6). Both were seen as being

potentially unstable by GS2 and full drainage was recommended. The boulder fan has been crossed in full-cut with gabion revetment and slope drainage, but remains very wet during the monsoon season due to either the presence of a spring-line (GS2) or abandoned paddy fields (EG1). Between km 24.540 and km 24.575, GS2 noted an old shallow rock slide (L), and proposed that a cut slope retaining wall be provided (Table 4.5). In the final design, a 1-2m breast wall was constructed. The September 1984 storm caused the reactivation of the rock slide which led to temporary road blockage. Finally an old rock slide, mapped by GS2 at km 24.600 (M), was redefined as a 'bowl of surface erosion' by EG1. The slipped debris was reveted by a 2m breast wall, and until the September 1984 storm, had remained relatively stable. During this storm, however, major failure took place and the road was blocked for 30m.

Instability in the three main gullies at km 24.470, km 24.500 and km 24.535 was referred to by GS2, although it was EG1 that specifically recommended channel protection. In the final design, extensive gabion cascades were installed below the culvert outfalls. Incision and side- slope instability in both the up-chainage and down-chainage gullies during September 1984, resulted in culvert and catch-pit blockage. The central, main channel experienced extensive erosion upstream of the culvert, associated with the passage of the debris flow (described above), while the gabion protection works below were destroyed.

Instability during the September 1984 storm, not anticipated by GS2, occurred at km 24.280-300 (N) and km 24.700-900 (O-P). At the former site, a small debris slide from above a gabion revetment deposited debris onto the road,while gully incision occurred in the compacted spoil below. Although the possibility of debris sliding was not mentioned specifically at this location by GS2, the slopes immediately down-chainage were observed to be unstable. The incised gully is clearly an unpredictable feature - being formed wholly in spoil material. Between km 24.700 and km 24.900, major cut slope failure has taken place (Appendix 1A.6). Instability began in July 1983, when failure at km 24.650 (Q) blocked the road. During the September 1984 storm, cut slope failure blocked the road for a distance of 190m. Inspection of the slopes above the road revealed numerous relic slip scars.These had not been detected by either of the surveys, although GS2 did refer to debris slide scars between km 24.800 (R) and km 24.890 (P). EG1 recommended cut slope revetment and this was implemented in design. GS2 also referred to the section between km

24.600 and km 24.725 (M-O) as being composed of deeply weathered shales requiring full drainage. Unfortunately, the slope drainage and revetment were inadequate to maintain stability, primarily because of an unfinished earthworks contract.

iii) Km 25.110-km 25.700 (Lower Trace)

This section of alignment traverses the more shallowly inclined lower slopes of the bowl. The main tributary gullies join immediately above the road, and hence incision downstream has been concentrated along the main channel draining the bowl. Slope undercutting by stream erosion has been largely confined to the left bank where GS2 mapped an active planar slide complex. This survey proposed the installation of river training works and protection at the toe of the unstable slope. The survey also suggested that the road between km 25.115 (S) and km 25.200 (T) be built either in full-cut with cut slope protection or, preferably, entirely on gabion retained embankment. These views were supported by EG1, and the final design consisted of full-fill with gabion retained embankment. Slope drainage schemes, including counterforts[1], were installed both above and below the road, while gabion protection works were constructed in the gully below. The stabilization of this slope is described in more detail in Fookes et al (1985). The September 1984 storm caused two rock slides above the road and small debris slides below.

On the southern side (U-V) of the bowl (km 25.260-360), GS2 mapped four planar debris slides. EG1 suggested that these features were in fact part of a large ancient slump. These slopes have been excavated mainly in full-cut with gabion and crib wall revetment, and drained with counterforts at the toe of the main slide mass at km 25.300 (W). These measures failed to prevent the development of four cut slope debris slides during September 1984, two of which blocked the road.

---

1 Counterfort drains are trench drains constructed to a depth below the slip surface to provide both slope drainage and a buttressing effect against displacement.

Between the exit from the bowl and the final hairpin onto the floodplain, GS2 mapped a small active slide scar above the road at km 25.500 (X), although no reference was made to this in the accompanying text. A deep-seated translational slide has developed here as a result of slope undercutting by road excavation (Appendix 1A.6). The slope has been partly retained by a gabion wall which has failed repeatedly. Slope drainage and dry-masonry revetment walls have been installed upslope of the road, but these have been dislocated and destroyed by continued slope movement. Although the possibility of instability here was inferred by the slip scar on the GS2 map (Figure 4.6), the extent of failure likely to occur following road construction was not appreciated by either of the two surveys. The monitoring of this slide is described in Chapter 8. With the exception of a debris slide onto the road, from above the cut through the spur at km 25.380 (approximately at V), there are no significant instances where GS2 failed to recognise the potential for instability that occurred during or after road construction along this trace.

iv) Conclusions

GS2 was extremely successful in identifying most areas of natural instability likely to affect the construction and stability of the road. The most notable exceptions to this relate to the debris slide and debris flow along the upper trace, and the highly unstable shale spur between km 24.700 and km 24.900. In the former case, many of the slopes above the road are composed of colluvium with several old slip scars. It is unlikely that GS2 would have been able to determine which of these were most likely to become reactivated. Nevertheless, future reconnaissance surveys should endeavour to recognise conditions where potentially unstable slopes provide the opportunity for channelised debris flow downslope, once failure takes place. In the case of the unstable shale spur, the weathered nature of the underlying rock and the need for slope drainage were recognised by GS2, but the failure of the survey to identify the slip scars above the trace led to the underestimation of the potential for slope instability at this site.

GS2 appears to have contributed significantly to the decision to realign the upper trace, thus neatly avoiding the boulder fan and large rotational slip. Many of the recommendations made by GS2 were repeated by EG1 and incorporated into the final design. In the majority of cases, it is possible to explain the current distribution of instability by reference to GS2; thus

establishing, by hindsight, the good predictive ability of the survey. However, a number of recommendations made by GS2 were found to have been omitted from the final design at no apparent detriment to stability. More importantly, some of the instability features identified by GS2, such as the large rotational slip on the upper trace, appear to be inactive and possibly of little consequence to road design and construction, considering the extent to which some of the slopes have been disturbed by earthworks.

4.4.4.5 Traverse Above the Dhankuta Khola Gorge (km 40.400-km 41.600)

This section of road-line is located immediately above the steep, highly unstable, incised slopes of the Dhankuta Khola gorge. Slope and drainage instability features extend upslope from the gorge and, hence, the road not only crosses a variety of instability features but is also threatened by slope failure from below. A full description of this section, along with road design and present stability, is given in Appendix 1A.9. The GS2 geomorphological maps are shown in Figures 4.7 and 4.8, while the comments and recommendations of this survey and EG1, and details of road design and stability, are given in Table 4.6.

Between km 40.380 and km 40.600, GS2 mapped, in some detail, a large instability complex associated with two incising gullies (A and B), and a suspected major slump block (C, Figure 4.7). A number of large, mostly active, debris slides were noted along the gully side-slopes above and below the trace. GS2 recommended channel protection works in the two gullies, along with minor realignment to the east to avoid the slumped block. EG1 questioned the validity of the GS2 interpretation, especially in respect to the slumped block. Nevertheless, full channel protection works were constructed in both gullies (Table 4.6, Appendix 1A.9), and the trace was realigned as suggested. During the September 1984 storm, both catchments experienced renewed instability, causing extensive damage to channel protection works, although the slumped block does not appear to have moved.

Below the trace, between km 40.940 and km 41.150 (Figure 4.8), a large unstable gully (D), rock slide (E) and expanding mudslide head (F) were mapped by GS2. Above the mudslide head, the trace crosses a shallow landslip embayment (G), composed of small slipped blocks, that GS2 interpreted as the 'feeder zone' for the mudslide below. Both surveys stressed the importance of

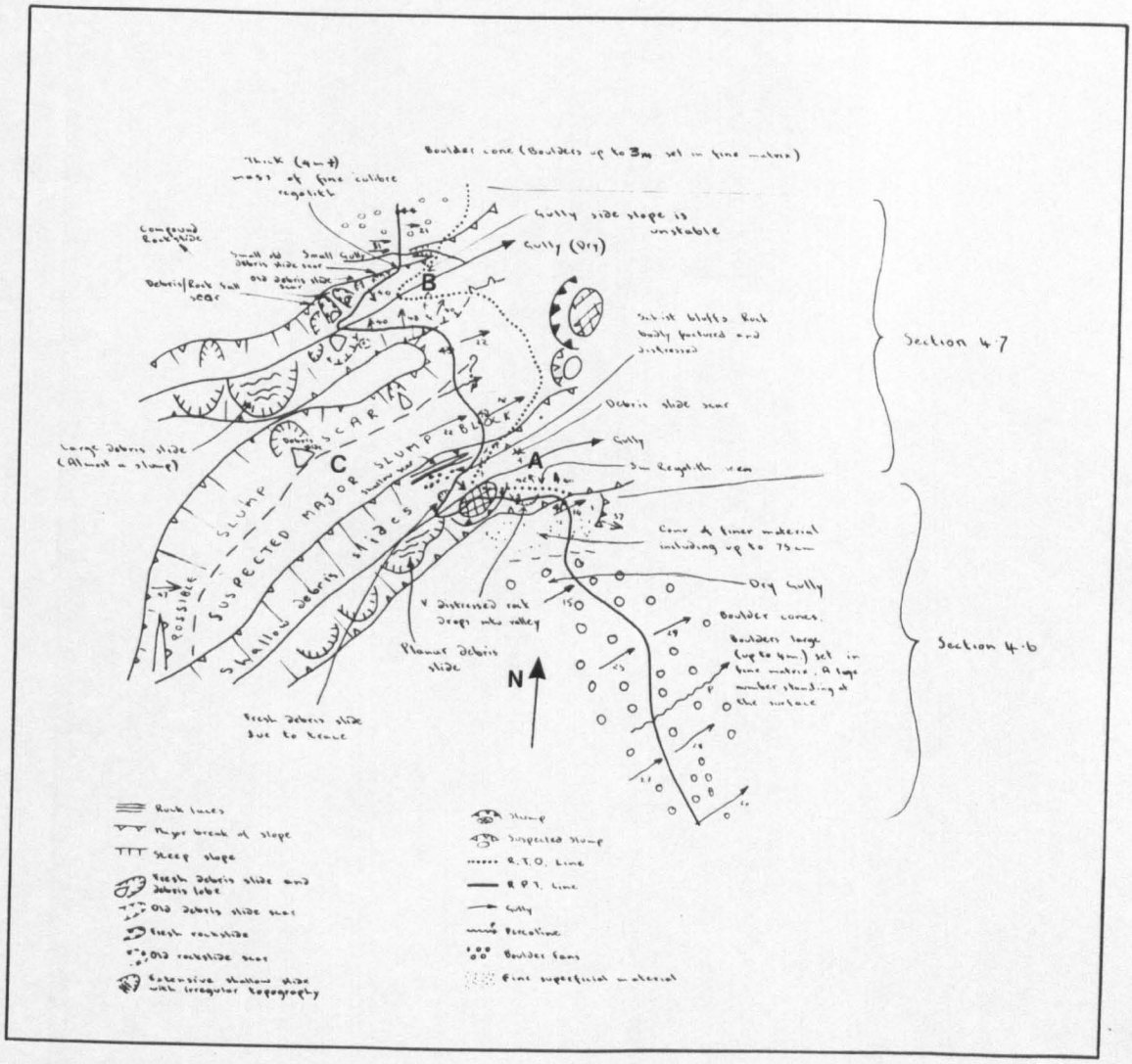

FIGURE 4.7 Geomorphological Map(GS 2) of Suspected Slump Block on the Traverse Above the Dhankuta Khola Gorge.

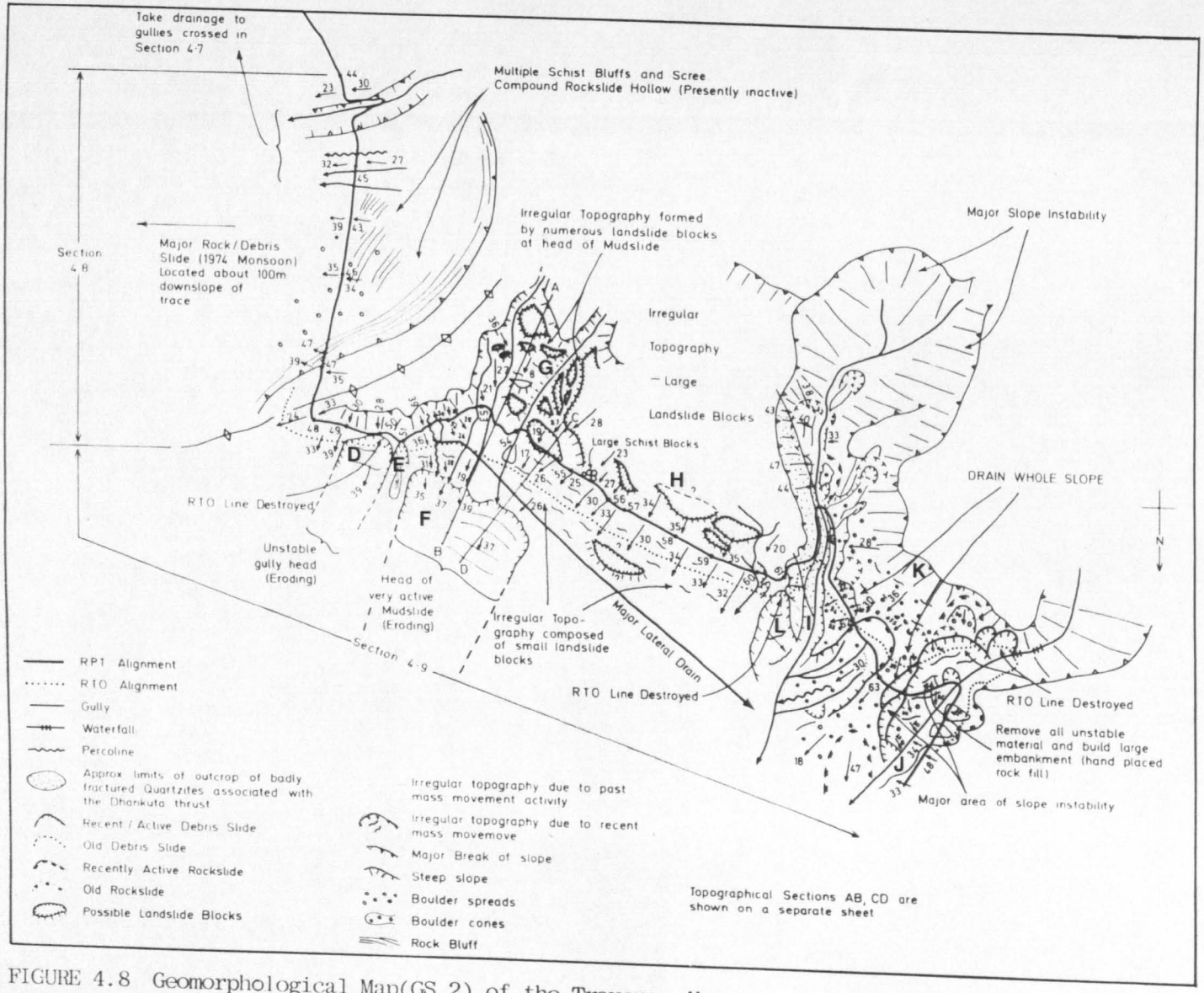

FIGURE 4.8 Geomorphological Map(GS 2) of the Traverse Above the Dhankuta Khola Gorge Showing the Mudslide Head and Unstable Catchments.

CHAINAGE	GS 2 COMMENTS/ RECOMMENDATIONS	CONSTR. NOTES RECOMMENDATIONS	This thesis	
			FINAL DESIGN	STABILITY 1984
40.380	Fresh debris slides in distressed rock.	Recent slump.	Crib wall, full-cut.	Shallow erosion and debris fall.
40.413	Trace crosses unstable gully with three fresh debris slides on north facing bank and an unspecified number on the south-facing bank. Cross using hand-placed rock-fill and large box culverts. Install bank protection and checkdam above and below trace. Slight realignment to the East to avoid instability.	Major slide block on south-facing gully bank.	Gabion checkdams and mattresses. Box culvert and 5m cascade with mattress below outfall. road religned to East.	Major scour along right bank. Protection works damaged. Extensive instability on north-facing bank. Culvert OK.
40.420	Debris slide scar below trace.	Shallow debris slide(?).	No allowance.	OK
40.440–40.560	Suspected major slump block and scar due to undercutting below.	Possible slumps below trace.	No allowance.	Shallow rock slides onto road.
40.565	Old debris slide scar below trace.	None.	Full-cut, 3m gabion retaining wall.	OK below road but large slips onto road.
40.575	Incised gully with large active debris slides. Compound rock and debris slide scars. Hand-placed rock-fill and box culvert. Channel protection and realignment to east.	Many shallow debris slides upslope of crossing.	Three checkdams with mattresses. Mattress below outfall.	Mattresses damaged, scour along right bank. Unstable side-slopes.
40.600	Gully side-slope below trace is unstable.	Two shallow debris slides on left bank, downstream.	No allowance.	Continued instability.
40.630	Boulder cone.	Colluvium.	No allowance.	OK
40.657	Gully with steep side-slopes. Divert drainage into larger gully to south to avoid major rock slide 100m downslope.	Recent debris slides in gully. Divert drainage to south via a cut-off bund to avoid slide below. No tipping, establish slide boundaries by survey, monitor movement. Check that gully to south does not feed instability below.	No allowance, gully has small checkdams and mattresses.	Generally OK but mattress damaged.

TABLE 4.6 Details of Comments and Recommendations Made by the 1975 Geomorphological Survey and the Construction Notes and the Final Design and Stability of the Road in the Lower Dhankuta Khola Valley.

cont./ next page.

N.B. GS 2.... Second Geomorphological Reconnaissance Survey(1975).

			This thesis	
CHAINAGE	GS 2 COMMENTS/ RECOMMENDATIONS	CONSTR. NOTES RECOMMENDATIONS	FINAL DESIGN	STABILITY 1984
40.660–40.930	Multiple schist bluffs. Inactive compound rock slide. Clean all cut faces of loose material.	Massive schist crags. Rock at less than 1m. Irregular, fractured and foliated schist. Clean loose blocks from rock faces.	Full-cut. Dry-walls downslope.	Numerous shallow slides and boulder falls onto road
40.940–41.000	Unstable gully head below trace. RTO line destroyed. Realign road further upslope.	Ancient rock slides below trace. Unstable gully head not found.	Full-cut through spur with gabion revetment.	Highly unstable cut slope. Slump below road.
41.000–41.150	Head of very active mudslide below trace. Drainage should be channelled to west to avoid mudslide. Realign further upslope. Upslope of trace topography is irregular and formed of landslide blocks. Minimal cut and fill.	Divert twin gullies to west, away from mudslide head. Rock slide below trace, do not tip. Establish slide boundaries and monitor movement. Upslope of trace rock is at 2m. Steep scarps, degraded ancient movement.	Twin gullies have been drained below trace by large drain to east. No cut or fill.	No problems to date.
41.150–41.390	Large landslide blocks, irregular topography. Major rotational blocks upslope with tension cracks 3m wide. Slide becomes more planar downslope.	Schist colluvium, slipped blocks(?) Haphazard jumble of steps and scarps. Movement to be expect-ed within life of road. Steep back scarp well above trace is result of ancient movement. Counterfort and herringbone drainage of shallow soil cuts. Construct cut-off bunds 50m upslope and drain into northern gully. Regrade or excavate scarps and monitor movement.	Area drainage with masonry cascade and revetment.	Large tension cracks forming behind cut slope. Extensive slope failure likely at 41.350. Cracks in road at 41.270. Many shallow cut slope failures.
41.432	Unstable gully, active debris slides upslope and downslope of trace. Soil creep, concentrat-ed slope wash, high throughflow. Actively eroding north-facing bank. Debris slides and rock slides could endanger road or block culvert. Slide below road at 41.400 is a hazard. Construct check-dams for 200m upslope and downslope of trace. Protect banks.	Gully bed composed of boulders, gravels and sand. Possible large slipped block and debris slide track upslope. Recent shallow slump below trace. Construct checkdams from gully confluence below trace to 200m above. Install bank protect-ion upstream and downstream. Found embankment on competent material.	Design has evolved from Irish crossing through rock-fill causeway to box culvert. Only one check-dam installed. Mattresses and Cascades constr-ucted below outfall in 1983.	Highly unstable gullies with major rotation-al failure in 1984. Almost all north-facing slopes are unstable. Culvert blocked several times. Mattresses damaged below outfall.

TABLE 4.6 cont./

			This thesis	
CHAINAGE	GS 2 COMMENTS/ RECOMMENDATIONS	CONSTR. NOTES RECOMMENDATIONS	FINAL DESIGN	STABILITY 1984
41.432-41.583	Boulder covered spur with numerous rock slide scars. Major threat to road. Inte - grated drainage required. Remove slip material and grade slope.	Spur is the centre of much small-scale instability. Construct cut-off drains 50m upslope. Allow for stripping of 3m of rock slide debris for foundat- ion. Possibly revet- ment/retaining walls required.	Half-cut, half- fill, gabion toe wall, slope drainage.	Numerous shallow debris slides and one large rock slide onto road.
41.583	Extremely unstable, poorly drained gully head. Rock fall and sliding likely in cuts. Waterfalls above and below trace. Bedload up to 5m diameter. Estim -ated maximum flow depth of 0.5-1m. Major instability on right bank. Remove unstable debris. Install check- dams from upstream waterfall to the Dhankuta Khola.	Active slump on right bank across trace. Many tension cracks and bent trees. Remove slip and repl- ace with rock fill. Seal open joints to minimise infiltration.	Bank protection/ retaining wall on left bank. Mattresses and cascades constr- ucted below outfall.	Bank protection and culvert inlet broken. Culvert const- antly blocked. Erosion below outfall extending to road. Outfall mattresses and cascades broken. Shallow sliding into culvert from right bank.

TABLE 4.6 cont./

diverting slope drainage to the west, away from the mudslide head and the active rock slide below, by means of a large lateral drain. GS2 also proposed minor realignment uphill, with minimal cut and fill. In the final design, slope drainage was diverted to the east via a lateral drain and spillway apron located above the mudslide head. So far, no instability problems have arisen, although the volumes of runoff generated are small. The alignment has been relocated upslope with minimal slope disturbance, as suggested by GS2. Although the slope has generally remained stable, this is probably due to the fact that no large storms have occurred in the area since 1974. It is possible that instability might be reactivated during high magnitude events. Between km 41.150 and km 41.390, GS2 identified slumped blocks immediately upslope of the trace (H) that were interpreted as remnants of large landslide blocks above. This interpretation was supported by EG1, which recommended slope drainage. Minor slope failure has resulted from insufficiently protected cut slopes, while cracks appeared in the road following the September 1984 storm.

The final instability complex along this section is encountered between km 41.432 and km 41.583. It consists of two eroding gullies (I and J), separated by a boulder covered spur (K). Widespread instability in both gullies was seen by GS2 to pose a major threat to road stability. GS2 mapped most of the instability in the smaller down-chainage catchment (I), including a rock slide immediately below the road (L) at km 41.400. Checkdams were proposed upstream of both crossings for a distance of 200m, and for an unspecified distance downstream. Although these recommendations were endorsed by EG1, channel protection works were limited during construction to a single checkdam upstream in the down-chainage gully (I), and bank protection works upstream in the up-chainage gully (J). An early design for the road at these two gully crossings was for the carriageway to be constructed on a rock-fill causeway (Appendix 1A.9). This design was abandoned owing to sedimentation and erosion problems, and was replaced by two slab culverts that, owing to limited finance, were under-designed. The final design of the culvert at km 41.583 (J), for instance, was less than half that originally intended (Martin, pers. comm. 1986). Continued channel erosion and instability in the two catchments caused repeated culvert blockage during 1983 (Appendix 1A9). Following construction, additional channel protection measures were installed below the culvert outfalls, but these were damaged during the 1983 and 1984 monsoon seasons. The rock slide (L) has received no stabilization works, and although the slope has remained stable, cracks developing in the road at km

41.300 may be indicative of the initiation of more widespread slope failure.

The spur in-between these two gullies was regarded as potentially unstable by GS2, due to the presence of numerous slide scars. Both surveys recommended slope drainage and grading[1]. While limited drainage has been carried out, quite extensive slope failure onto the road occurred in 1983 and 1984. During the September 1984 storm, cut slope failure and drainage instability became widespread throughout this section, but in only one case (at km 40.950 (Appendix 1A.9)), where extensive cut slope failure occurred, was this not reflected in the observations made by GS2.

In conclusion, the majority of current instability along this section can be explained by direct reference to GS2. The four unstable gullies were noted by GS2 to be the most important factors in the initiation and distribution of slope instability. With the exception of minor cut slope failures, the majority of road maintenance problems to date have been concerned with erosion in these gullies, and especially the two crossed at km 41.432 and km 41.583. Again, the predictive ability of GS2 is supported by this analysis. However, there are a few instances, as in the case of the slumped block and the expanding mudslide head, where GS2 appears to have over-estimated the hazard posed by ancient mass movement features. These features remained stable during the September 1984 storm, and hence, may be associated with events of large recurrence interval and are, therefore, only periodically active.

4.4.4.6 The Leoti Khola Floodplain (km 25.700 - km 32.800)

The main problems for road stability on the Leoti Khola floodplain relate to the risk of inundation and scour of the road during flooding, the reactivation of

---

1. Slope grading is the process of reducing slope inclination to a design value by cut and fill towards the top and bottom of the slope respectively.

mass movements on the valley sides and the rapid development of debris fans across the road from tributary catchments. Detailed descriptions of the floodplain, the final design of the road, and its present stability are given in Appendix 1A.7. The first recorded major flood of the Leoti Khola occurred in 1974, and had a discharge with an estimated recurrence interval of 10-15 years (Barker 1976). The storm caused renewed instability on slopes and in drainage channels along much of the proposed line, but the most widespread changes took place on the Leoti Khola floodplain. Fortunately, GS2 was able to map, and in some cases, quantify the extent of bank erosion, channel relocation, sediment transport, tributary instability and fan accretion.

The GS2 assessment of the floodplain alignment made a number of general, but highly significant, observations. It was noted that the present course of the river is determined by alternating valley-flank spurs of resistant quartzite, schist and slate, large ancient high level fans, coarse gravel terraces and fan development at the mouths of vigorous mountain tributaries. GS2 suggested that it would be difficult and expensive to relocate the main torrent tract without causing problems of disequilibrium downstream. Erosion was likely to occur in valley constrictions, on the outside of valley meander bends and opposite high angle tributary fans. Field evidence suggested that the 1974 flood caused local bank erosion of up to 15m, and that this should be borne in mind when choosing the road alignment and designing protection works.

The identification of the 1974 flood levels by GS2 was instrumental in determining the recurrence interval for the flood (Barker 1976). The training works and revetments were constructed with a 2m freeboard above this stage. Five active debris fans at the mouths of eroding left bank tributary catchments (A-E, Figure 4.9) are crossed by the alignment, and these were held by GS2 to present major potential hazards to bridges and culverts. GS2 recommended that the alignment be relocated as close to the floodplain edge as possible, in order to bridge these fans at their apices and reduce the likelihood of road inundation by fan accretion. In most cases, the alignment was modified as proposed, and river training and bank protection works were installed upstream and downstream of the fan crossings. However, during the September 1984 storm, three bridges became totally blocked and major bank scour and road loss on the bridge approaches, took place (Appendix 1A.7).

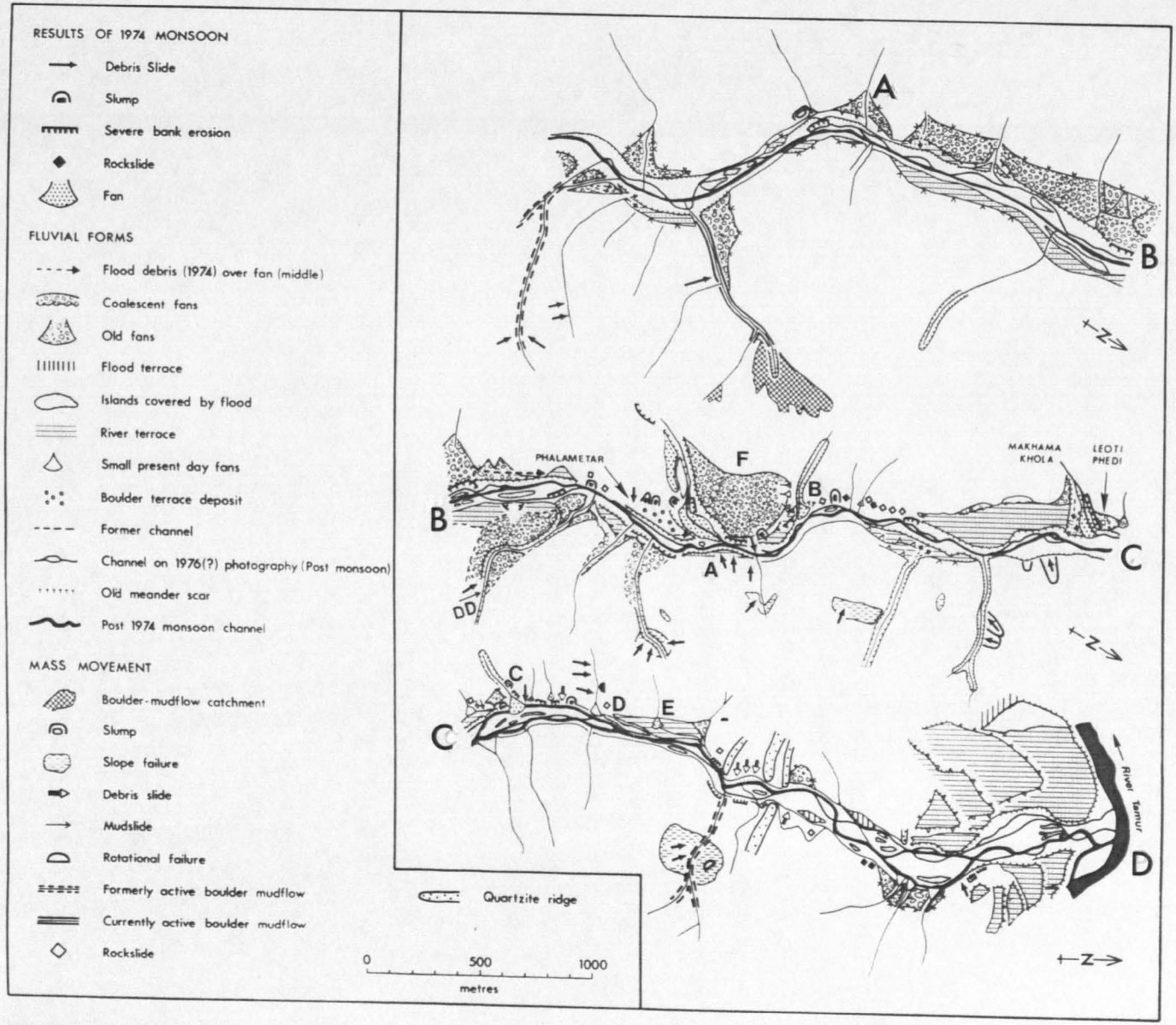

FIGURE 4.9 Geomorphological Map(GS 2) of the Leoti Khola Floodplain Route.

The GS2 geomorphological map (Figure 4.9) of the Leoti Khola floodplain shows clearly the distribution of erosional and depositional landforms, and the location of the main torrent tract following the 1974 storm. As a comparison, the distribution of instability and road damage on the Leoti Khola floodplain and adjacent slopes, following the September 1984 storm, is shown in Figure 4.10. These two maps reveal the extent to which the distribution of instability in 1984 was predictable from GS2. Detail on the 1984 map is confined to the floodplain and immediately adjacent flanks, and shows the location of floodplain erosion, debris slides, rock slides, boulder deposits and fans. Many of these have occurred at sites of similar instability noted on the 1975 map.

The section of floodplain alignment between km 27.200 and km 29.350 (immediately upstream of A and downstream of B, Figure 4.9) is analysed below in greater detail, in order to assess the influence of GS2 on the final design along a particularly problematic section. This section is characterised by active fan development, and erosion and instability of the valley-side slopes and floodplain terrace, and is representative of the floodplain route as a whole. It therefore provides a suitable means for examining GS2 in detail. EG1 was concerned almost exclusively with the description of rock conditions wherever cutting was envisaged, and referred to GS2 for notes on fan crossings and erosion protection works. Consequently, EG1 will be given no further mention here.

Between km 27.200 and km 28.150 (Figure 4.9), the alignment contours around the relatively steep, frontal slope of an elevated fan (F), that is bounded on both sides by two tributary gullies with active debris fans at their mouths (A and B). The largest of these gullies (A), at km 27.520 (Bataha Khola), deposited an extensive fan during the 1974 storm. According to GS2, boulders up to 2.5m in diameter were transported over the fan surface. GS2 identified both a lower active fan surface and a middle, now dissected and partly vegetated, surface below the elevated fan. On morphological evidence, the 1974 maximum flood level was found to be located 2.3m below the middle fan surface. GS2 suggested that, during the design life of the road, the maximum flow depth was likely to exceed this level, and the bridge should have a minimum clearance of 2m above the middle fan level. As this fan was relatively isolated from the main torrent tract, high accretion rates could be expected, and a realignment closer to the fan apex was suggested. Bank protection works, especially along the left bank were considered essential to

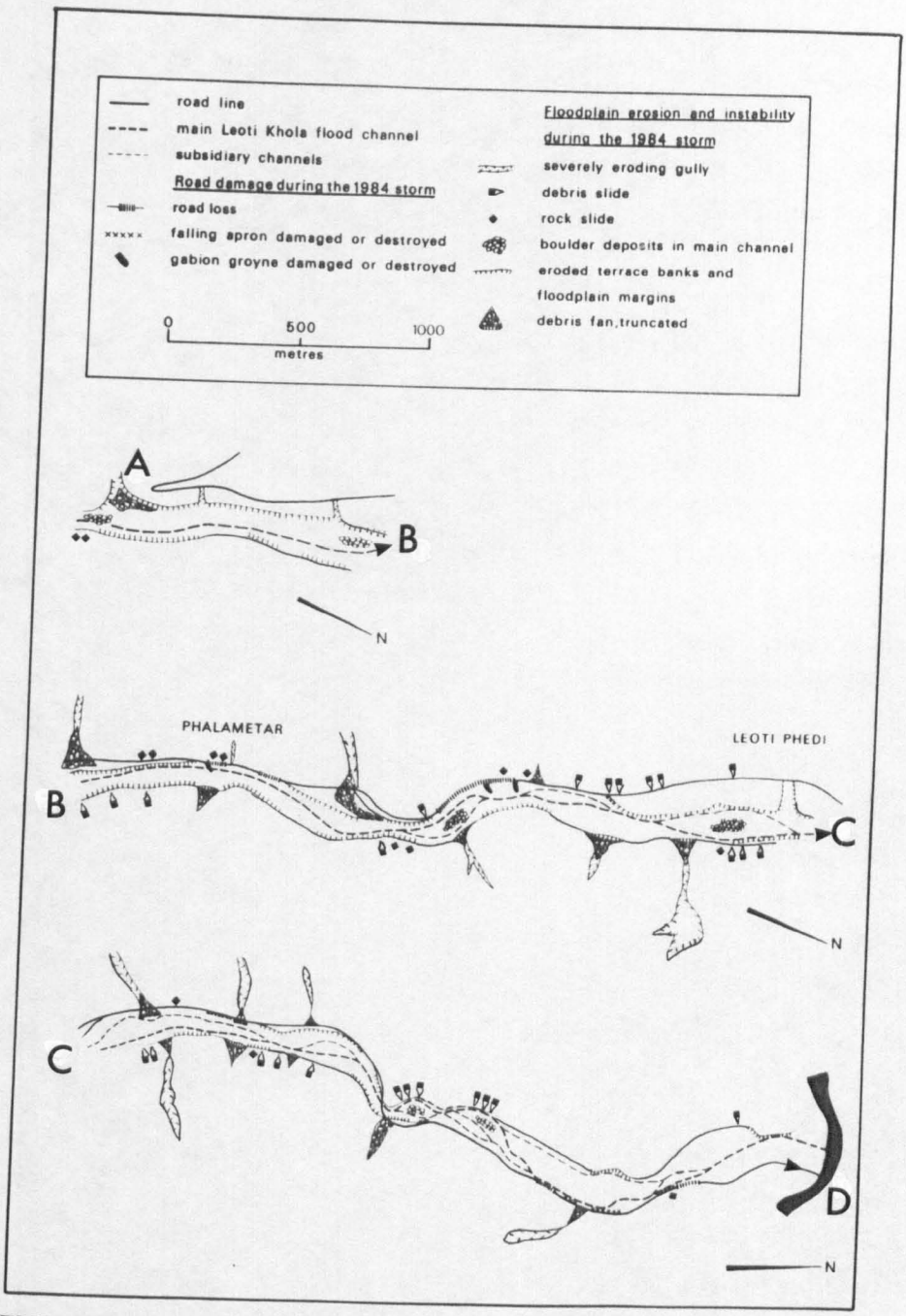

FIGURE 4.10 The Distribution of Instability and Road Damage on the Leoti Khola Floodplain Caused by the September 1984 Storm.

bridge stability. A smaller gully is bridged on the downstream side of the elevated fan (km 28.110 (B)). The sediment load of this gully (Ghante Khola) is far coarser than that of Bataha Khola. The proximity of the Leoti Khola torrent tract to this gully (B) has resulted in fan surface incision. GS2 anticipated that scour rather than accretion would be the principal concern for bridge stability, and recommended extensive bank protection works, a realignment closer to the fan apex and a minimum bridge clearance of 1m above the middle fan level.

Both bridges have been constructed to a level approximately equivalent to that proposed by GS2, and have been located as close to the fan apices as possible. Gabion training and bank protection works were constructed along the right bank upstream, and both banks downstream of the crossing in both gullies, along with channel bed protection in Ghante Khola. During the September 1984 storm, Bataha bridge became blocked with cobbles and boulders, and major scour took place along the right bank of the gully and the bridge approach (Appendix 1A.7). Ghante Khola remained relatively stable during the event, but westward migration of the Leoti Khola channel undermined and destroyed the bridge and bank protection works.

GS2 noted that the elevated fan, bounded by these two gullies, was being eroded by the Leoti Khola. In view of the minor realignments proposed at the fan crossings, GS2 suggested that the road be relocated further into the frontal slope of this fan, in full-cut. This suggestion was adopted in the final design. Shallow slipping on the frontal surface of the fan at km 27.800, during the September 1984 storm, extended to road level, and hence, road loss might have occurred here had the alignment not been modified.

Beyond Ghante Khola (B), the alignment begins a causeway route along the base of high, steep (45-60^{o}) valley-side slopes around the outside of a valley meander. The 1974 flood had, according to GS2, caused the Leoti Khola to become diverted for a distance of up to 65m to the west so that it was impinging directly against the base of these slopes. GS2 considered two alternatives for design here. First, the road might run in half-cut, half-fill around the outside of the meander. This would require both adequate cut slope stabilization and slope drainage, and the construction of a gabion retained embankment. Alternatively, the Leoti Khola might be directed back to its pre-1974 position, and the road constructed on a well protected gabion retained

embankment at the foot of the slope. This latter alternative was favoured by GS2 in view of the expected difficulty and expense in stabilizing any slope excavations.

The final design along this section comprises of an elevated causeway, constructed at the foot of the valley side, with shallow cutting. The gabion embankment retaining wall was protected by a 6m wide falling apron. Two gabion spurs were installed downstream, and one upstream of the Ghante Khola confluence, in order to direct the Leoti Khola away from the gabion embankment, towards the centre of the floodplain (Appendix 1A.7). During the 1983 monsoon season, minor scour of the two upstream spurs took place. However, the September 1984 storm resulted in the total removal of the upstream spur, partial removal of another, and road loss for approximately 80m (Appendix 1A.7), due to the relocation of the Leoti Khola torrent tract against the outside of the meander bend.

In conclusion, the outstanding feature of the GS2 evaluation of the floodplain alignment, has been the extent to which the location and nature of instability caused by the 1974 storm was reproduced in 1984, although at a higher magnitude. The two storms resulted in a similar distribution of erosion, deposition and slope instability, and GS2 was able to predict floodplain hazards and make suitable recommendations for design. However, it must be stressed that the geomorphologists were extremely fortunate to be working so soon after the 1974 storm, and so were able to gauge its effects. Normally an evaluation of this kind would rely on the interpretation of the morphological evidence for a number of events of uncertain age and recurrence interval and would, therefore, tend to be far less precise. Fundamental recommendations were made by GS2, with respect to minor realignment, fan crossings, road protection and training works. Many of these were incorporated into the final design, and it is clear that had this not been the case, more disastrous road loss would have occurred in 1984.

4.4.5 Conclusions

This analysis has demonstrated conclusively, that the geomorphological reconnaissance surveys (GS1 and GS2) had a highly significant input to the design of the Dharan-Dhankuta road. While it is concluded that both surveys paid considerable attention to the description of mass movements, possibly at

the expense of drainage hazards in mountain channels, this was justifiable in view of the Brief given to the geomorphologists. The interpretations and recommendations made by GS1 formed the basis for much of the design of the RPT alignment. Many of the recommendations made by EG1 were found to be based wholly on GS2, especially in respect to the evaluation of mass movement. Understandably, EG1 was more concerned with materials assessment, earthworks and foundation design. GS2 was particularly useful in identifying and assessing drainage hazards on the Leoti Khola floodplain, and contributed significantly to the design of the alignment and erosion protection works.

GS2 succeeded in identifying the majority of mass movement hazards along the proposed alignment. Much of the instability that occurred during the 1984 storm, could be explained by reference to the observations of GS2. However, in a number of instances, GS2 mapped and described relic mass movements that have remained stable and of little consequence to road stability. Notable examples include the rock slide at the top of the Kumlintar hairpin stack, the rotational slide in the bowl and the slumped block, mudslide and adjacent instability in the lower Dhankuta Khola valley. It is difficult to determine whether failure would have occurred at these sites had their existence not been noted by GS2, and avoidance measures not been undertaken. Slope undercutting by road excavation, for instance, may have led to renewed instability on these slopes, with disastrous consequences for road stability. In the case of the instability in the lower Dhankuta Khola valley, storm rainfalls since 1974 have been relatively small, and hence the high groundwater levels and slope erosion required to trigger further instability, may not have arisen. On this basis, the attention paid by GS2 to these relic mass movement features is justifiable.

The analysis has also drawn attention to a number of instances where GS2 failed to recognise the risk posed by slope and drainage hazards. Many of these hazards have been relatively short-lived and associated with disturbance by earthworks, and could not, therefore, have been predicted by GS2. Deep-seated failure and road loss or severe deformation occurred in 1983 and 1984 at at least four sites where the potential for slope failure does not appear to have been fully appreciated by GS2. At three of these sites, failure may have been associated with renewed erosion in the Khardu Khola, caused by large storms in 1979, 1983 and 1984, and possibly slope and drainage disturbance by

earthworks (Chapter 6). At the fourth site (km 3.900), the evidence suggests that GS2 failed to identify the full potential for slope failure, although instability at this site was anticipated by the design team.

In addition to identifying and evaluating mass movement and drainage hazards, GS2 also proposed measures for slope stabilization and erosion protection. Many of these proposals were repeated by EG1 and reflected in the final design. However, in a number of instances, the remedial measures proposed by GS2 (for example in respect to the drainage of the debris flow track on the Kumlintar hairpins and the mudslide in the Dhankuta Khola gorge) were not carried through in the final design due to impracticalities and prohibitive costs during construction. While it is important for reconnaissance surveys to propose stabilization and erosion protection works, the final design of these works will depend on ground conditions revealed during earthworks.

4.5 The Contribution of Geomorphological Assessment During Road Construction and Maintenance

4.5.1 Introduction

As illustrated above, geomorphological evaluation probably has its greatest potential contribution to highway design at the reconnaissance stage, for alignment design purposes. However, there is scope for continued geomorphological assessment, using conventional mapping and observational techniques during construction and maintenance, for both the design of more detailed geotechnical investigations and remedial measures.

This section discusses the geomorphological contribution to the design of remedial measures at Girl Friend Slip (km 3.825-km4.000), where extensive slope failure, leading to eventual road loss, has required continual appraisal. While this discussion focusses attention on this single site, it should be noted that geomorphological assessment during construction has had a significant input to design at a number of sites, including the unstable bowl (km 23.180 - km 25.360) and in the Dhankuta Khola gorge (km 40.400 - km 41.600). In addition, the instability occurring during maintenance, at a number of sites following the September 1984 storm, has been assessed by geomorphological mapping and walk-over surveys undertaken by the author, and discussed with respect to proposals for remedial measures by Hearn and Jones (1985).

4.5.2 Geomorphological Assessment and Design at Girl Friend Slip

A full description of this site is given in Appendix 1A.3, while the contribution that GS2 made to the assessment of stability for highway design purposes is discussed in Section 4.4.4.3. Detailed geomorphological and engineering geological appraisals of this slope were undertaken during construction, following the development of tension cracks in the road surface in 1978, and during maintenance when total slope failure occurred in 1984.

Following the development of localised instability below the road in December 1977, and the appearance of numerous cracks in the road surface in the following year, a site investigation was undertaken in 1978 in order to identify the areal extent, mechanisms and causes of instability and propose measures for stabilization. The investigation comprised of detailed geomorphological mapping supplemented by trial pitting, soil sampling and the laboratory determination of Atterberg limits and moisture content.

The geomorphological map is reproduced in Figure 4.11 from the site drawing (no. RPT/RM/05). The map shows clearly the areal extent and configuration of the unstable slope and its characteristic features, including the main back scar and subsidiary slide scars, springs, seepages, tension cracks, surface erosion features and rotated blocks. Four trial pits were excavated (Figure 4.11) on the slope to depths of up to 6m. The slope materials exposed in these pits consisted of loose to compact silty, sandy gravels that were defined variously as colluvium, talluvium or residual soils. A shear surface was exposed in pit A (Figure 4.11), at a depth of 2-2.5 m below ground level, with a dip of 45° at 216°N. The causes of this instability were seen to be slope undercutting and oversteepening by channel erosion at the base of the slope, and the development of high groundwater levels by the end of the monsoon season (Martin 1980). A number of remedial measures were proposed, including gabion channel protection works, trench drains and slope regrading and revegetation schemes.

The slope remained relatively stable until September 1984 when extensive rotational failure and road loss occurred (Plate 2.6). A geomorphological map of this slip was produced in December 1984 by the author (Figure 4.12), using a series of slope profiles as ground control. In addition, slope profiling was undertaken between the top of the back scar and the debris flow channel at

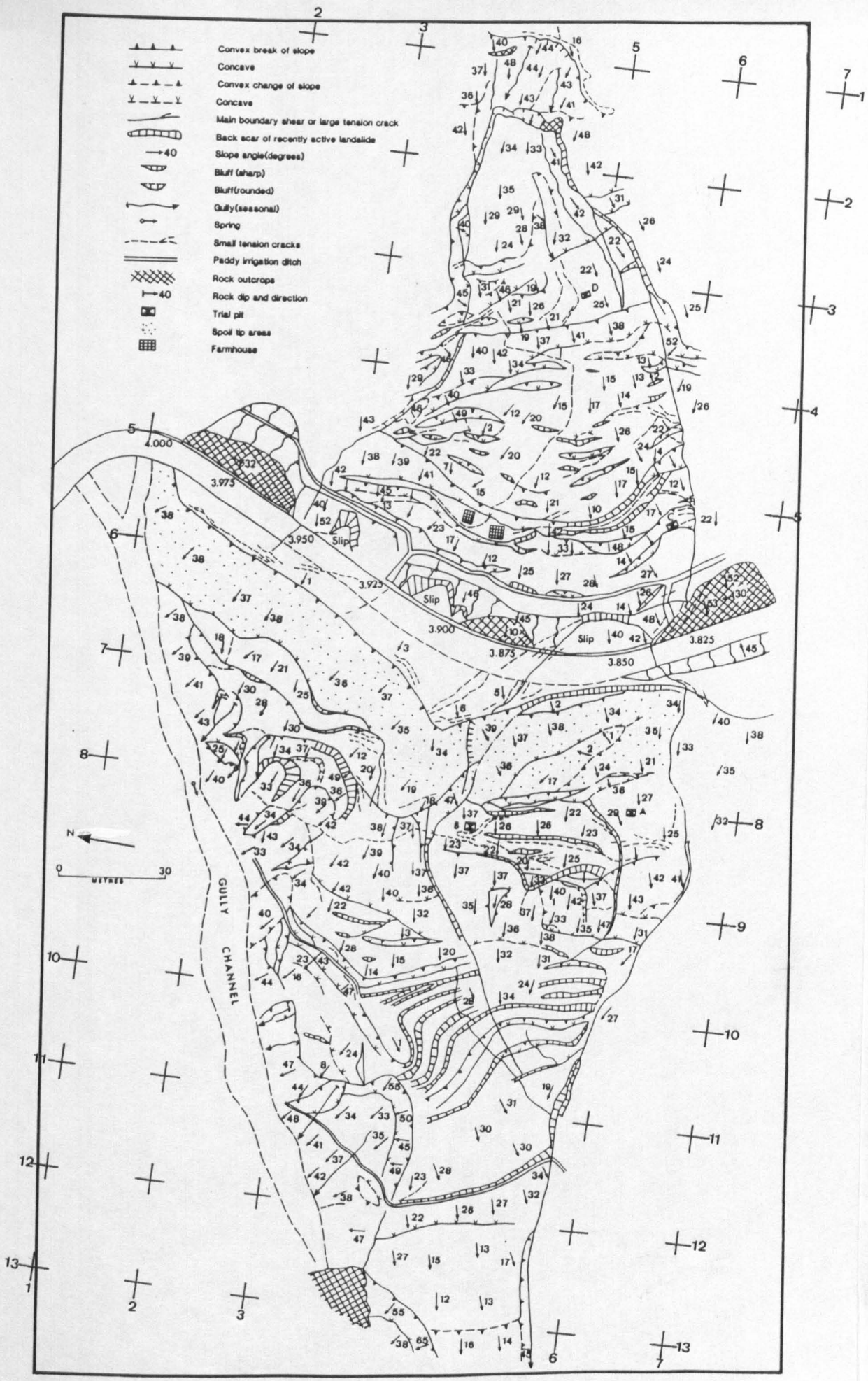

FIGURE 4.11 Detailed Geomorphological Map of Girl Friend Slip (1978). (Redrawn from site drawing No. RPT/RM/05).

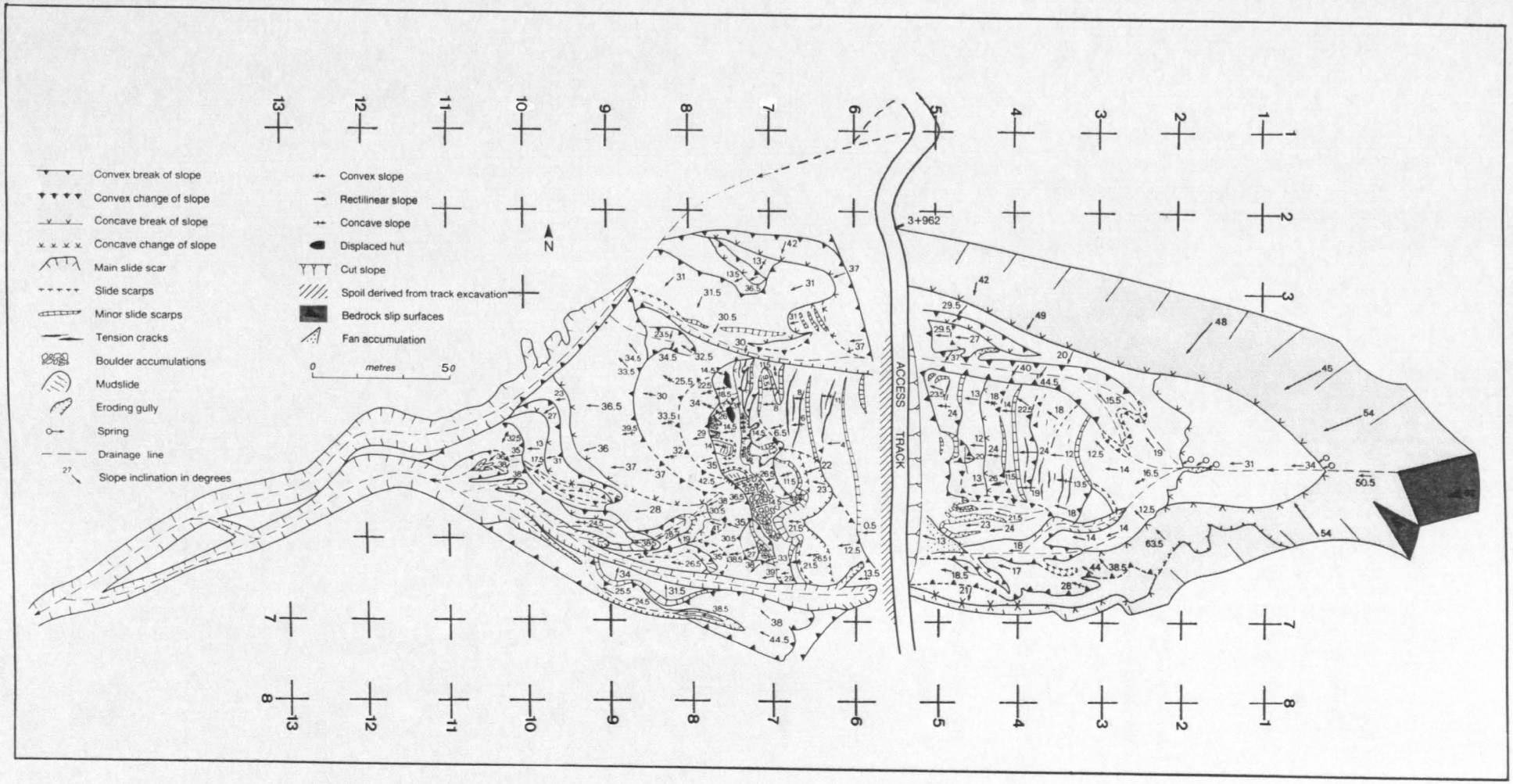

FIGURE 4.12 Detailed Geomorphological Map of Girl Friend Slip (1984).

the base of the failed slope. On the basis of surface evidence, it was concluded (Hearn and Jones 1985) that failure had been rotational, and had probably begun on the lower half of the slope below the road, leading to undercutting and failure of the slope above. The mapping identified numerous tension cracks, subsidiary slip scars, rotated blocks, springs, surface erosion and debris flow channels (Figure 4.12).

From these observations, the following recommendations for remedial measures were made in a report prepared for the Transport and Road Research Laboratory in March 1985 (Hearn and Jones 1985).

i) Construct a series of checkdams and gabion, crib and masonry revetments in the gully culverted at km 4.000.
ii) Install slope drainage (surface masonry and french drains) on the slipped mass above and immediately below the road, and reinstate the cut off drain above the back scar.
iii) Discharge road drainage and slope drainage from above the road into the catchment to the south.
iv) Regrade the slope to remove tension cracks and redistribute the slip material further downslope.

The final design of remedial measures on this slope has been based largely on recommendations made in April 1985 and January 1986 by the Transport and Road Research Laboratory (Brooks and Lawrence 1985, 1986). The principal measures undertaken to date are listed below.

i) Reinstatement of the cut off drain above the back scar.
ii) The installation of wire meshing onto the back scar to prevent erosion.
iii) The installation of french drains and masonry surface drains in the slipped material above the road.
iv) Crib revetment of the cut slope.
v) Revegetation and erosion control by wattle fencing.
vi) The covering of tension cracks with bituminous jute.
vii) The removal of an irrigation ditch above the road.

As far as the author is aware, no remedial measures have been undertaken on the failed slope below the road. The quantities and costs of the remedial measures undertaken between December 1984 and April 1986 are discussed in Chapter 2. It is too early to determine whether these measures have been successful.

4.5.3 Discussion

Geomorphological ground survey appears to have two main potential contributions to engineering design at sites of slope instability: i) as a basis for planning detailed investigation, and ii) for use directly in the design of remedial measures. However, in the first instance, owing to the difficulties and cost constraints on undertaking intensive ground investigations in remote mountain areas (Chapter 2), the scope for using geomorphological maps in this way is, therefore, limited. Nevertheless, these maps may be used in conjunction with engineering geological surveys, as was the case on the Dharan-Dhankuta road, to draw attention to the main areas of instability, and help plan the location of slope monitoring, trial benches and trial pits. At km 41.150, for example, a total of nine trial pits were excavated, logged and sampled in the mudslide head identified by the 1975 geomorphological survey (Section 4.4.4.5).

4.6 Recommendations for Future Practice

The geomorphological reconnaissance surveys examined in this chapter, form useful guidelines for future terrain and hazard assessment for highway design purposes in the study area, and young fold mountains in general. Ideally, these surveys should follow or coincide with a hazard mapping exercise for route corridor selection, using desk study data sources of topographic maps, geological maps and air photographs, if available. Techniques of landslide hazard mapping are developed and discussed in the following chapter. Geomorphological reconnaissance surveys should form the early stages of the geotechnical assessment of the route corridor(s) and should be followed by more detailed mapping, localised ground investigation and monitoring. The main problems likely to be faced by geomorphological reconnaissance surveys undertaken for future road projects include:

i) uncertainty, at the preliminary stages of a project, as to the final design of the alignment and the design philosophy of the road itself,

ii) uncertainty of the extent to which slopes and channels are likely to be disturbed during earthworks and construction,

iii) difficulty in estimating recurrence intervals for slope hazards, and

iv) access problems on highly unstable and precipitous, or densely vegetated, slopes.

The first two constraints are unlikely to be resolved unless a more definite indication can be given by the engineer of the probable location, width, drainage design and earthworks requirements of the intended road. At the preliminary stages of a project, this information is unlikely to be available. This problem was experienced by both the geomorphological survey (Jones pers.comm. 1986) and the engineering geological survey (Sweeney pers.comm. 1986). The third constraint probably represents the most important limitation on geomorphological surveys at present. Unless the recurrence interval of landslides and floods can be estimated by reference to historical accounts, hydrological records or sedimentological evidence (see, for example, Johnson 1986), the geomorphologist is unlikely to be able to indicate the true risk posed by geomorphological hazards to the road during its intended design life. There appears to be considerable scope for developing this aspect of hazard risk assessment for highway design purposes. Until this is done, the geomorphologist must endeavour to provide the most objective and quantitative assessment possible of hazard risk, based on an examination of air photographs, hydrological data and ground survey. This is discussed further in Chapter 9, with respect to engineering requirements of geomorphological data.

Finally, access difficulties may prohibit mapping in some areas. Under these conditions, remote observations from air photographs or from opposite sides of the valley may be necessary. However, ground that is inaccessible on foot, such as the engorged sections of the lower Dhankuta Khola, is unlikely to be suitable for road construction anyway.

On the basis of the findings of this chapter, and particularly the above discussion, the following recommendations for future practice can be made.

i) As well as providing information relating to the location and nature of slope and drainage hazards, estimates of recurrence intervals or rates of activity, and the likely impact of these hazards on the intended road, should be made wherever possible (Chapter 5).

ii) The likely impact of road construction on slope and drainage stability should be discussed, and sites regarded as particularly vulnerable to accelerated instability, caused by excavation, loading, spoil tipping and drainage disturbance, should be identified (Chapter 6).

iii) Greater attention should be paid towards the assessment of drainage hazards (storm runoff, erosion and sediment transport) in mountain channels (Chapters 7 and 8).

iv) Hazard monitoring should be established at the earliest opportunity (Chapter 8).

Despite these suggestions for improving future practice, it must be concluded that the geomorphological reconnaissance surveys for the Dharan-Dhankuta road form landmarks in both the development of applied geomorphology with respect to highway engineering, and the use of detailed terrain and hazard assessment for mountain highway design. Geomorphological surveys should, therefore, form important elements in future road projects in unstable terrain.

CHAPTER 5

LANDSLIDE HAZARD MAPPING FOR HIGHWAY DESIGN

5.1 Introduction

Time and financial constraints at the feasibility, desk study and early reconnaissance stages of highway projects usually prevent the employment of detailed surface mapping, as has been described in Chapter 4. Consequently, there is scope for the development and application of hazard mapping techniques for route corridor identification and evaluation. Chapter 2 has identified three principal hazards along mountain roads, namely mass movement or landsliding, flooding and erosion/sediment transport. This chapter concentrates on landslide hazard assessment; techniques for assessing channel hazards (flooding, erosion and sediment) are discussed and developed in Chapters 7 and 8. In the present chapter the contribution that landslide hazard mapping (at medium scales (ie 1:10 000 - 1 : 50 000)) can make to landslide hazard assessment for route selection is examined. The study concentrates on the Dharan-Dhankuta area of east Nepal (henceforth referred to as the study area), but is broadly applicable to other humid mountain regions.

The chapter has three principal aims. First, to present a brief review of the more common landslide hazard mapping techniques, with respect to their potential to contribute to landslide hazard assessment for highway design purposes in the study area. Second, to examine the geographical distribution of measurable factors that contribute to the development of landslides and associated slope erosion hazards in the study area, using terrestrial and air photographs. This will enable medium-scale landslide hazard mapping techniques, based principally on air photograph interpretation, to be assessed in terms of their ability to provide meaningful data for preliminary highway design purposes. Finally, the effects of road construction on slope stability and erosion will be discussed in respect to their implications for route selection and design in general.

5.2 Review of Landslide Hazard Mapping Techniques for Highway Design

5.2.1 Highway Design Requirements of Landslide Hazard Assessment.

At the route planning and early reconnaissance stages of a highway project,

rapid, effective and low-cost landslide hazard assessment is crucial to the selection of the most appropriate route corridor(s). In Chapter 2, it has been demonstrated that the impact that different forms of landslide hazards have on road stability in the Lower Himalaya depends largely upon their mechanism, size and recurrence interval, or frequency. In the study area, slope instability and channel incision often lead to oversteepening of the slopes above, and the creation of shallow, linear slope erosion features, while, on the steeper slopes, rock and debris slides often develop downslope into debris flows that create shallow, linear erosion tracks. For the purpose of this discussion, landslide hazard mechanisms can, therefore, be usefully categorised into : i) linear slope erosion features, ii) shallow debris slides and rock slides, and iii) more deep-seated mass movements. The causes of these hazards, in the study area, are discussed in Section 5.3, while their impact on the Dharan-Dhankuta road and other roads in the Lower Himalaya is described in Appendix 1 and Chapter 2.

Generally, linear slope erosion hazards, unless perpetuated by continued slope undercutting or disturbance by irrigation, agriculture or road construction, are usually temporary phenomena; requiring only 1-3 years to regain stability. Their impact on road stability is, therefore, usually low and only short-term, and may be easily remedied by appropriate erosion protection works. Shallow, planar rock and debris slides often have a greater impact on road stability and usually require a higher investment in remedial measures. However, unless these features are particularly large, or are likely to remain active for a considerable period of time, for instance, due to continued slope undercutting on incised valley flanks, their impact is also likely to be short-term. Sharma (1974) suggests that these landslides often take 5-7 years to stabilize naturally. Deep-seated, high magnitude and low frequency mass movements, however, often cause extensive slope disturbance and road loss (Chapter 2), unless high investment stabilization treatment is undertaken and should be avoided, wherever possible, by prudent alignment design.

It is important, therefore, at the route planning stage, to identify the location, size, possible mechanisms and degree of hazard posed by these slope processes to the intended road. Rapid, cost-effective medium-scale landslide hazard mapping, using good quality air photographs, may enable this to be achieved. A review is given below of some of the more common landslide hazard mapping techniques developed to date. These techniques are discussed in terms of their applicability to route corridor selection in the study area.

5.2.2 Review of Landslide Hazard Mapping Techniques

Most landslide hazard mapping techniques developed to date have been undertaken at medium (1:10 000 - 1:50 000) and small (1:50 000 - 1:100 000) scales, and therefore have some potential application to route planning. Synoptic scale maps, at scales of 1:100 000 and smaller, have been produced for regional and national landslide inventories in Czechoslovakia (Rybar and Nemcok 1968) and in the West Carpathians (Nemcok et al 1975, Malgot and Mahr 1979). Maps at these scales are likely to be too generalised for route corridor identification and selection. Medium and small scale landslide hazard mapping techniques have been described in recent publications by Brabb (1984), Hansen (1984) and Varnes (1984) and are reviewed in Hearn and Fulton (1986). Two principal categories of landslide hazard mapping, namely direct and indirect mapping, have been proposed by Hansen (1984). Techniques within these categories are listed in Table 5.1.

Mapping Category	Mapping/Hazard Assessment Procedures
Direct Mapping:-	Landslide distribution maps, landslide registers and inventories, maps of regional landslide incidence, geomorphological maps, hazard zoning maps, maps of hazards to linear constructions, ie strip hazard mapping.
Indirect Mapping:-	Land system mapping, landslide isopleth and hazard isoline maps, landslide susceptibility maps, risk maps, hazard forecasting maps.

Table 5.1 Categorisation of Direct and Indirect Mapping Techniques

Direct methods of hazard mapping record the distribution of hazards from ground surveys (including surface mapping and inventories) and air photographs. If air photographs are unavailable or ground detail is obscured by forest or cloud cover, rapid surface mapping and inventory techniques (Cooke and Doornkamp 1974), such as those described by Carrara and Merenda (1976)

in S. Italy and Keinholz (1978) in Switzerland, can be used. However, these techniques require considerable man-time and, consequently, may be largely inappropriate at the route planning stage.

Direct landslide mapping often forms the first stage in a landslide hazard mapping exercise (see below), and may be exemplified by work undertaken by Brabb and Pampeyan (1972) and Roth (1983) in San Mateo County, California, Kojan et al (1972) in the San Rafael Mountains, Wright and Nilsen (1974) and Nilsen and Brabb (1975) in the San Francisco Bay Region, Drennon and Schleining (1975) in S. Dakota, Keinholz (1978) in Switzerland and Malgot and Mahr (1979) in the West Carpathians. A useful review of the development of landslide hazard mapping in the San Francisco Bay Region is given by Nilsen (1986). These maps have been published at a variety of scales, ranging from the 1:10 000 scale geomorphological maps produced by Keinholz (1977, 1978), that allow differentiation between hazard mechanisms, to the 1:125 000 scale maps by Nilsen and Brabb (1975) that depict the regional distribution of landslide deposits only.

Direct landslide hazard maps portray the geographical distribution of active and relic landslides, landslide scars and deposits, and do not usually allow interpretation of hazard potential or susceptibility. The observation that landslides tend to occur on historically unstable slopes (Kojan et al 1972, Palmquist and Bible 1980) is clearly a useful one for landslide prediction. However, in geomorphologically active terrain, such as the Lower Himalaya where the geographical distribution of landslide causal factors such as erosion, high groundwater levels and engineering activity (see Section 5.3) may change rapidly over time, the spatial distribution of landslide susceptibility may also be subject to short-term change.

A number of indirect landslide hazard mapping procedures have been developed to zone relative landslide hazard using the geographical distribution of contributory factors. Essentially, two main forms of indirect landslide mapping can be identified, that differ according to analytical procedure and data requirements. Factor mapping and numerical - cartographic techniques probably represent the most common and simple forms of indirect mapping. Numerical and cartographical comparison is made between landslide distributions, produced by direct mapping, and geographical variations in geological and terrain factors. This leads to the production of landslide hazard

maps that can be used to zone relative hazard both within and outside the area in which they were derived, as long as the underlying processes and factors that promote instability are understood and remain the same. Geological maps and air photographs form the main data sources for these indirect techniques. While these data sources are available in most mountain areas, they may be of inadequate scale and clarity, and consequently, additional mapping and photography may be required.

Some of the more simple factor mapping or zonation methods rely on slope inclination and geological variability to explain landslide distributions. These methods form the most common indirect hazard mapping techniques, and have been developed, for example, by Brabb et al (1972) in San Mateo County, Nilsen and Brabb (1975) in San Francisco Bay Region, Drennon and Schleining (1975) in S.Dakota, Stevenson and Sloane (1980) in Tazmania and by the Los Angeles County Regional Planning Commission (Cooke 1984). Haruyama and Kitamura (1984) have incorporated altitude, slope angle, geology, stream density and slope long profile shape in a landslide susceptibility study in the Sakurajima area of Japan.

The complexity of the mapping procedure is increased when additional factors, such as bedrock structure, slope aspect, rainfall, soil type and vegetation (Roth 1983) are included. Quite often, on a regional scale, primary bedrock structures are oriented in a consistent direction and inclusion of these parameters may, in some cases, increase the representability of the analysis. Studies of this nature have been undertaken by Briggs (1974) in Pennsylvania, Garland (1976) in W.Germany, De Graff and Romesburgh (1980), Pomeroy (1982) in the Pittsburg area, Lessing et al (1983) in W. Virginia and Payne (1985) in South Wales. Crozier (1986), Crozier et al (1980) and Owen (1981) discuss the effects of slope aspect on landslide distribution in the Wairarapa hill country, New Zealand, in respect to soil moisture, the history of instability and regolith depth.

Clearly, the success of a factor mapping exercise will depend on the ability of the investigator to recognise contributory factors in landslide development, and upon the ease and accuracy with which these factors can be evaluated. The relative simplicity of these techniques makes them particularly attractive as means of rapidly assessing the distribution of landslide hazards for route planning purposes in the study area. However, in east Nepal, as is the case

with many remote mountain regions, terrain data is often lacking and consequently the number of quantifiable contributory factors, and the accuracy and resolution with which they can be evaluated, is low. This may seriously reduce the representability of the analysis. In addition, variability within contributory factors, such as weathering grade, rock structure and groundwater levels, that can only be evaluated by detailed site assessment, will obviously reduce the dependability of the technique. This problem of over-simplification of factor variability can be further illustrated by the fact that the linear relationships between slope inclination and susceptibility, claimed by Nilsen and Brabb (1973) and Civita et al (1975), may be too simplistic and invalid (Carrara et al 1977, Stevenson and Sloane 1980), as both upper and lower threshold angles for the development of slope instability have been reported (Ward 1976, Carrara et al 1977, Iida and Okunishi 1983). The possible existence of both minimum and maximum limiting slope inclinations, for the development of instability in the study area, is discussed in Section 5.3.

The second, more analytical technique of statistical hazard mapping often incorporates the use of surface inventory for data collection and computer-assisted approaches to data analysis. Examples of these applications are given by Neuland (1976) in W.Germany, Carrara et al (1977) in S. Italy, Neuman et al (1978) in California, Simons et al (1978) in Oregon, Huma and Radulescu (1978) in Rumania, Martin (1978) in SE Spain and Perkins and Olmstead (1980) in California. While these techniques may offer considerable potential for landslide hazard mapping, their success depends on the collection of a high integrity, high density data base and the use of often long-winded statistical techniques and computer modelling to analyse and interpret the data. Unless developed using detailed ground inventory, they may have relatively little application to route planning in difficult and relatively remote terrain.

An additional problem, with statistically based landslide susceptibility techniques, is that data collection and analysis are usually undertaken on a grid cell basis, and contributory factors are assumed to be constant within each cell (Carrara et al 1977, Martin 1978, Haruyama and Kitamura 1984). Martin (1978), for instance, has used a computer-based multiple regression and principal components analysis to produce a landslide susceptibility map for a 23 km^2 area of SE Spain using 250m x 250m sampling units. Considerable difficulty was experienced in obtaining representative values of slope, geology and soil parameters for these units, and many of these variables had to be excluded from the analysis.

Klugman and Chung (1976) and Poschmann et al (1983) have developed a technique of landslide hazard assessment based on soil strength parameters for clay slopes in eastern Canada, using assumed values of effective cohesion and friction angle. Similar studies, using extensive geotechnical data banks developed by the Norwegian and Swedish geotechnical institutes, have been described by Viberg (1984). Stevenson (1977) has developed a 'risk' assessment technique in Tazmania based on plasticity index (PI), water table, slope angle, slope form and land use. The factors used in this analysis, and their vulnerability scores, are listed in Table 5.2. Ward et al (1981) describe the application of the infinite slope model to landslide susceptibility mapping, using soil cohesion and friction angle, root strength, groundwater weight and depth, slope inclination and loading. The predictive ability of the technique, when applied to forested catchments in Oregon, was better than 80 percent. However, the costs and time involved in deriving suitable data bases for these types of analyses are likely to rule out their use at the preliminary stages of highway projects in the study area.

No matter what technique is used, landslide hazard mapping, based on the principles described above, can only provide an indication of relative hazard in a given area. While this is usually all that is required for route selection purposes, a complete landslide hazard assessment would require an evaluation of the probability of a landslide event occurring within a specified time or, more simply, the size of an event that might be expected to occur during the design life of a road. So far, very little has been achieved in this field, as recurrence intervals of landslides in remote areas are difficult to determine reliably, as very few, are documented.

Probably the greatest contributions to landslide prediction have been made in respect to the magnitude-frequency rating of landslide-generating storm rainfall. Studies of this nature have been undertaken in Hong Kong (So 1971, Lumb 1975), New Zealand (Eyles 1979, Crozier and Eyles 1980, Crozier 1986), the Kathmandu-Kakani area of Nepal (Caine and Mool 1982), La Honda, California (Wieczorek and Sarmiento 1983) and in respect to world-wide reported debris flows (Caine 1980). The most common methodology employed is to compare historical records of landslide occurrence with 24- hour rainfall depths (Eyles et al 1978, Crozier 1986). Landslide incidence may be examined by reference to threshold storm rainfall depth (Eyles 1979, Wieczorek and Sarmiento 1983). The identification of triggering rainfall thresholds, from

daily rainfall records and antecedent soil water status, has been described by Crozier and Eyles (1980), Akutagawa et al (1983) and Crozier (1986). However, the lack of long-term rainfall records in many remote mountainous areas, such as the Lower Himalaya, often precludes the use of hydrological variability, both spatially and temporally, in the examination and prediction of landslide distributions.

Clay factor P (use range of values of PI for appropriate geology)	Score
Low PI (lower third of range)	1
Mid PI (mid third of range)	2
High PI (upper third of range)	3
Water factor W (annual maximum piezometric surface relative to typical failure plane)	Score
Below plane	1
Between plane and half depth	2
Above half depth	3
Slope angle S (use range of values for appropriate geology)	Score
Low (lower third)	1
Medium (mid third)	2
High (upper third)	3
Slope complexity C	Score
Simple slope, no failures	1
Old failure, now runoff eroded	2
New failure, stable but not runoff eroded	3
Land use U	Score
Woodland	1
Cleared or built on under special precautions	1.25
Built on without special precautions	1.5
Risk R = (P + 2W) (S + 2C)/U	

TABLE 5.2 Stevenson's (1977) Landslide Risk Evaluation Scheme

Finally, very little has been published on the prediction of road construction-induced hazards, that may arise from slope overloading by fill embankments, slope undercutting and oversteepening in excavations, drainage disturbance and spoil tipping. A notable exception is the work of Meneroud (1978) who has produced hazard ratings for cut slope failure along Alpine roads in France, based largely on qualitative assessments of geological, slope and engineering conditions. Haigh (1979, 1982) has logged cut slope failures along the Mussoorie-Tehri and Mussoorie By-pass roads in Uttar Pradesh (India) and has regressed failure volumes with scar dimensions. However, the full extent of slope disturbance by highway construction can only be reliably evaluated once earthworks are in progress and the final design of drainage works is known, and consequently these hazards cannot be predicted at the route planning stage.

In the Lower Himalaya, notable examples of landslide hazard mapping undertaken to date include the relatively large-scale (1 : 10 000) hazard strip mapping undertaken by Brunsden et al (1975 b) for the Dharan-Dhankuta road (Chapter 4), and the factor mapping developed by Wagner (1981) in the Walling district of west Nepal. In the latter case, geological, slope inclination and slope aspect factor maps were used to produce maps of landslide and gully erosion potential. It appears that these maps were developed from a qualitative and rather subjective evaluation of contributory factors without reference to an existing distribution of landslides or erosion features. Consequently, the representability of this analysis may be limited. Mayumdar (1980) has reviewed some of the causes of landslides in northeast India and concluded that there is insufficient data with which to undertake a quantitative hazard mapping exercise. Instead, a rather subjective and qualitative hazard zonation map was produced, based on rock type and relief, at an approximate scale of 1 : 5 million. This scale is far too small for any meaningful landslide hazard assessment.

A hazard mapping study, funded by UNESCO and His Majesty's Government (HMG) of Nepal, is currently being undertaken in the Kathmandu-Kakani region of central Nepal (Ives and Messerli 1981). This mapping procedure, based on the superimposition of factor maps depicting geomorphological processes, land use and 'human response' at a scale of 1 : 10 000, may enable effective land use planning to be undertaken and, depending upon the representability of the final maps, may provide a useful tool for route

corridor selection in the area. Road construction projects located outside this area, however, do not benefit from such a data base. At present, land use, land systems and land capability maps are being produced in Nepal from air photographs (Oli 1983), at a scale of 1 : 50 000, by the Topographic Survey Branch. While the maps do not show landslides, as they are primarily a means of land classification, they may provide useful documents for preliminary terrain evaluation.

In conclusion, a wide range of landslide hazard mapping techniques have been developed to suit particular ground conditions, data bases and academic, planning and engineering requirements of landslide hazard assessment. The success of any mapping exercise depends, primarily, on the quality of the data base and the validity of any assumptions and generalisations that are made in its compilation and analysis. In the Lower Himalaya, very little landslide hazard mapping has been attempted, owing to a general lack of terrain data and a relative disinterest, until recently, in hazard assessment for planning and engineering purposes (Ives and Messerli 1981, Wagner 1981).

Unless landslide hazard maps already exist for an area where a highway is planned, medium-scale landslide hazard mapping, for route corridor selection purposes, will have to be organised and paid for by the funding agency of the road project. This may only be undertaken if the mapping exercise can be demonstrated to be rapid, low-cost and effective. There is some scope, therefore, for the development of rapid, cost-effective landslide hazard mapping techniques in the Lower Himalaya, using air photographs, topographic and geological maps, if available, as the primary data sources. Most of the remainder of this chapter is concerned with the development of such techniques.

5.3 Factors Promoting Slope Instability in the Study Area and their Bearing on Landslide Hazard Mapping

5.3.1 Introduction

In the study area, as in most terrains, landslides and slope erosion occur in response to a number of inherent geological, slope and climatic conditions, and dynamic geomorphological and anthropogenic processes. Probably the most important of these factors include: rock strength, weathering grade, discontinuity spacing and orientation; soil strength, depth and permeability;

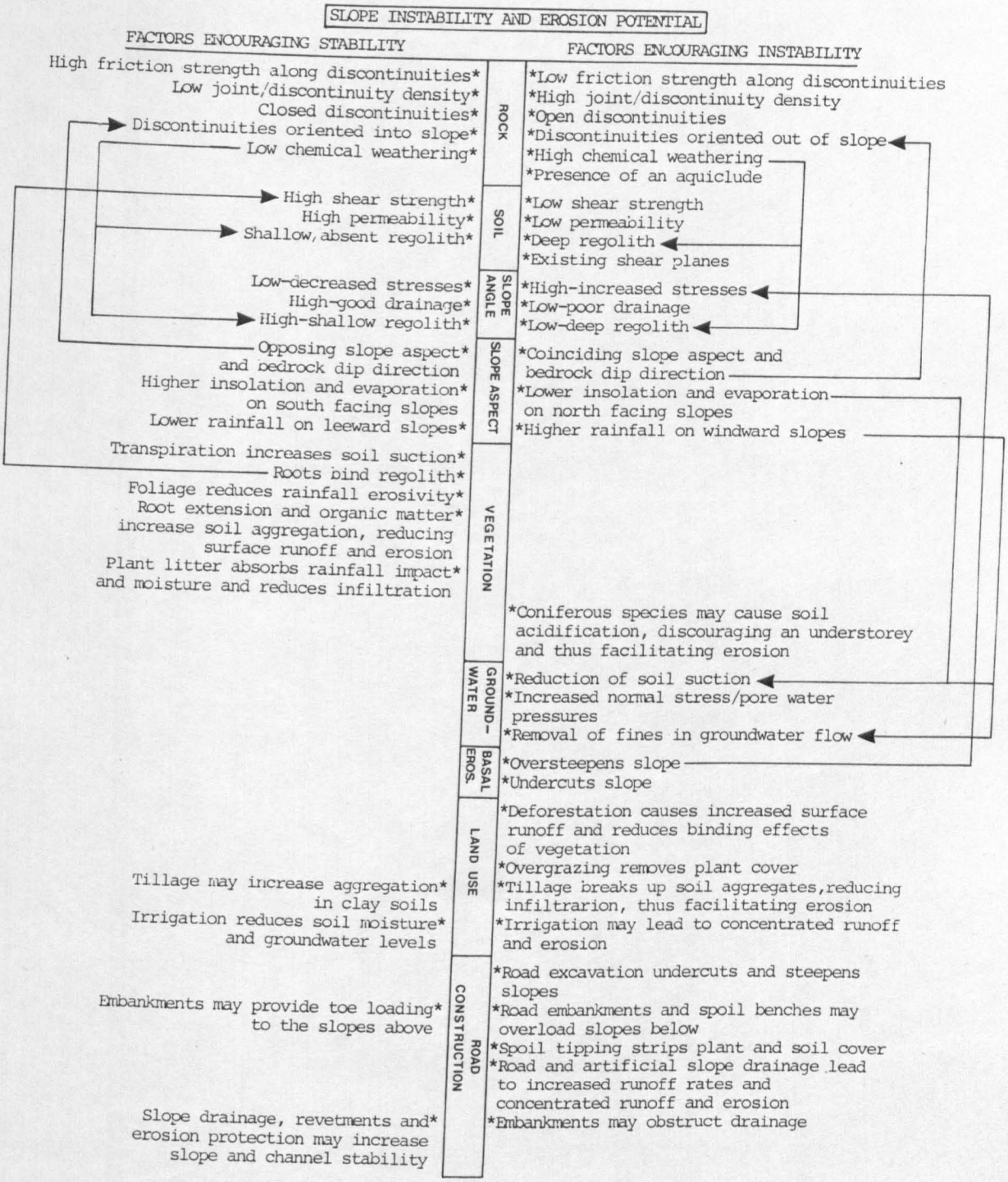

TABLE 5.3 Factors Influencing the Potential for Slope Instability and Erosion in the Study Area

slope inclination and aspect; vegetation; groundwater and soil moisture conditions; basal slope erosion; and anthropogenic disturbance by deforestation, agriculture and road construction. These factors are listed in Table 5.3 where their positive and negative influences on stability are identified. In particular, slope angle and aspect may influence stability in a number of ways, depending on site conditions, and this complicates hazard assessment based on these factors. The factors listed in Table 5.3, and their influence on stability, are discussed in the following section.

At the medium-scale of landslide hazard mapping, it is not possible to analyse all these factors, owing to measurement and computational difficulties. Therefore, for the purpose of this analysis, they have been grouped into four factor categories (Geology, Hydrology (including slope drainage), Physiography and Land use) that can be evaluated from geological maps and air photographs. These categories are listed in Table 5.4.

MEDIUM-SCALE FACTOR CATEGORY	LARGE -SCALE COMPONENT FACTORS
Geology	Rock type or lithology, structure (including fracture, dip, dip direction), weathering grade, permeability.
Hydrology	Precipitation (including intensity and duration), insolation, surface and sub-surface drainage, erosion.
Physiography	Aspect, slope inclination, physiographic zone in landscape model (Figure 5.1).
Land Use	Intense cultivation, overgrazing, drainage disturbance, deforestation, slope overloading and oversteepening/undercutting by road construction, spoil tipping.

TABLE 5.4 Factor Categories for Medium-Scale Landslide Hazard Mapping

This section of the chapter briefly discusses the influence of each factor on the distribution of slope instability in the study area, for the purpose of landslide hazard mapping discussed in Sections 5.4 and 5.5. The factors will be discussed separately in the order presented in Table 5.4.

5.3.2 Geological Factors

The Geology category is composed of rock type, structure, weathering grade and permeability. As far as rock type is concerned, it is possible to identify five different lithologies in the study area, namely Siwalik sedimentary rocks, phyllites, quartzites, schists and gneisses (Chapter 3). Siwalik sediments are probably the most susceptible rock types in the study area to erosion and instability (Chapter 3). By contrast, quartzites are relatively resistant to erosion and form steep, comparatively stable slopes. Quartzites and gneisses tend to be quite massive, while phyllites and schists are characterised by high fissility that often promotes instability. Permeability and weathering grade also display broad variations according to rock type. Phyllites and Siwalik rocks, for instance, weather rapidly to produce clayey regoliths of relatively low permeability. On the other hand, weathering profiles on the gneisses are composed of up to 15m of relatively well drained, sandy soils on shallowly inclined, generally stable slopes. Weathering rates on the quartzites are relatively low, and yield shallow (0 to 20cm deep) granular soils that are usually free draining. Owing to the presence of intact bedrock close to the surface, slope failure is uncommon on the quartzites.

Rock structural orientations also have a significant influence on stability. While the overall original dip of bedrocks is approximately northerly, in association with the west-east structural strike of the region, dip direction and inclination often vary locally as a result of thrusting and fold development. Nevertheless, the regional northward dip may have some bearing on the broad distribution of landslides by causing northward facing slopes, such as those in the southwestern and western Leoti and Dhankuta Khola catchments to be more susceptible to instability. The intensity of rock fracture, caused by tectonic disturbance, is likely to be greatest in the vicinity of the Main Boundary Thrust and the Dhankuta and Mulghat thrusts (Figure 3.4), and this might also have some influence on the distribution of instability.

5.3.3 Hydrological Factors

Precipitation, insolation, drainage and erosion comprise the main components of the Hydrology category. Slope instability in the study area often occurs in response to the development of high groundwater levels, combined with slope undercutting and oversteepening due to channel erosion (Chapter 3). Quite often, maximum rainfall intensities and soil permeability determine the potential for the development of high pore pressures and instability in shallow soils (Okuda et al 1980, Anderson and Howes 1985), rather than the delayed response of the water table at depth. Linear erosion usually occurs under similar conditions, and often forms headward extensions to eroding channels and landslides in unstable catchments, as channel incision and mass movement activity progress upstream as "waves of aggression" (Brunsden et al 1981, p37) during high magnitude storms. Plates 5.1 and 5.2 demonstrate the extent of linear erosion and shallow landsliding on the northeastern flanks of the Leoti Khola valley caused by the storm of September 1984.

South and southeast facing slopes in the study area are likely to receive the greatest precipitation owing to the predominantly south to southeasterly monsoon airflow direction. Consequently, during storm rainfall soil moisture and groundwater levels may be highest on these slopes, although slope inclination and soil and rock permeability will also have an important influence on slope drainage. However, insolation levels are also likely to be highest on these slopes, and hence soil moisture depletion by evaporation may be rapid. Depending upon site conditions, these two climatic factors may work to cancel one-another out. By the same arguement, on north facing slopes, both precipitation and insolation levels may be low, thus having opposing influences on groundwater levels and hence stability.

The intensity of stream erosion, through its effects on slope inclination and loss of basal support, by both channel incision and lateral migration, also appears to be an important factor in the initiation of landslides and linear slope erosion. A general discussion of the influence of toe erosion on the development of slope instability is given by Richards and Lorriman (1986). The extent of channel erosion at the base of a slope will depend largely on the erodibility of the channel material (a function of bedrock) and stream power. While stream power is difficult to evaluate at the medium-scale, stream order may form a useful surrogate.

PLATE 5.1

PLATE 5.2

PLATES 5.1 and 5.2 The Extent of Erosion and Instability on the Northern Flanks of the Leoti Khola Valley Before and After the September 1984 Storm.

5.3.4 Physiographical Factors

The Physiography category includes slope aspect, inclination and the physiographical location (physiographic zone) of a slope within the terrain model described below. The importance of slope aspect has already been discussed with respect to bedrock dip direction, precipitation and insolation, and consequently will not be discussed further here.

The relationship between slope inclination and landslide potential is often complex, as steeper slopes can have both negative and positive effects on stability (Ward 1976, Carrara et al 1977). The existence of minimum threshold slope angles for instability is usually attributable to insufficient effective stresses on slopes shallower than the threshold slope (Carson and Petley 1970, Francis 1986). The presence of a maximum threshold slope angle is more difficult to explain, although possible factors might include:

i) an increase in hydraulic conductivity and consequently lower groundwater levels and pore water pressures on steeper slopes (Freeze 1986), and

ii) a reduced depth of material available for shallow instability on steeper slopes owing to a predominance of non-mass movement, erosional processes (Ward 1976).

Brunsden et al (1981) have proposed a schematic physiographic model for the study area (Figure 5.1), based largely on the broad geographical distribution of slope inclination. Three main facets in the landscape were identified: gentle (less than 35^{o}) convexo-concave upper slopes with level (less than 10^{o}) crestal slopes on the ridge tops and spur divides; steeper middle slopes ($35\text{-}50^{o}$) and extremely steep ($40\text{-}90^{o}$) incised valley flanks adjacent to incising drainage lines. On the upper slopes, mass movements are relatively infrequent, while instability features on the middle slopes are largely relic. The incised lower slopes, however, are frequently unstable (Brunsden et al 1981), owing to the steeper slopes found there and the incidence of slope undercutting by channel erosion. Shallow rock slides and debris slides form the most predominant mass movement mechanisms on these slopes. This terrain model is most applicable to the Dhankuta Khola catchment (Brunsden et al 1981), and requires modification in the Leoti Khola and Sardu Khola valleys. In particular, many of the tributary sub-catchments that flank the Sangure Ridge, are

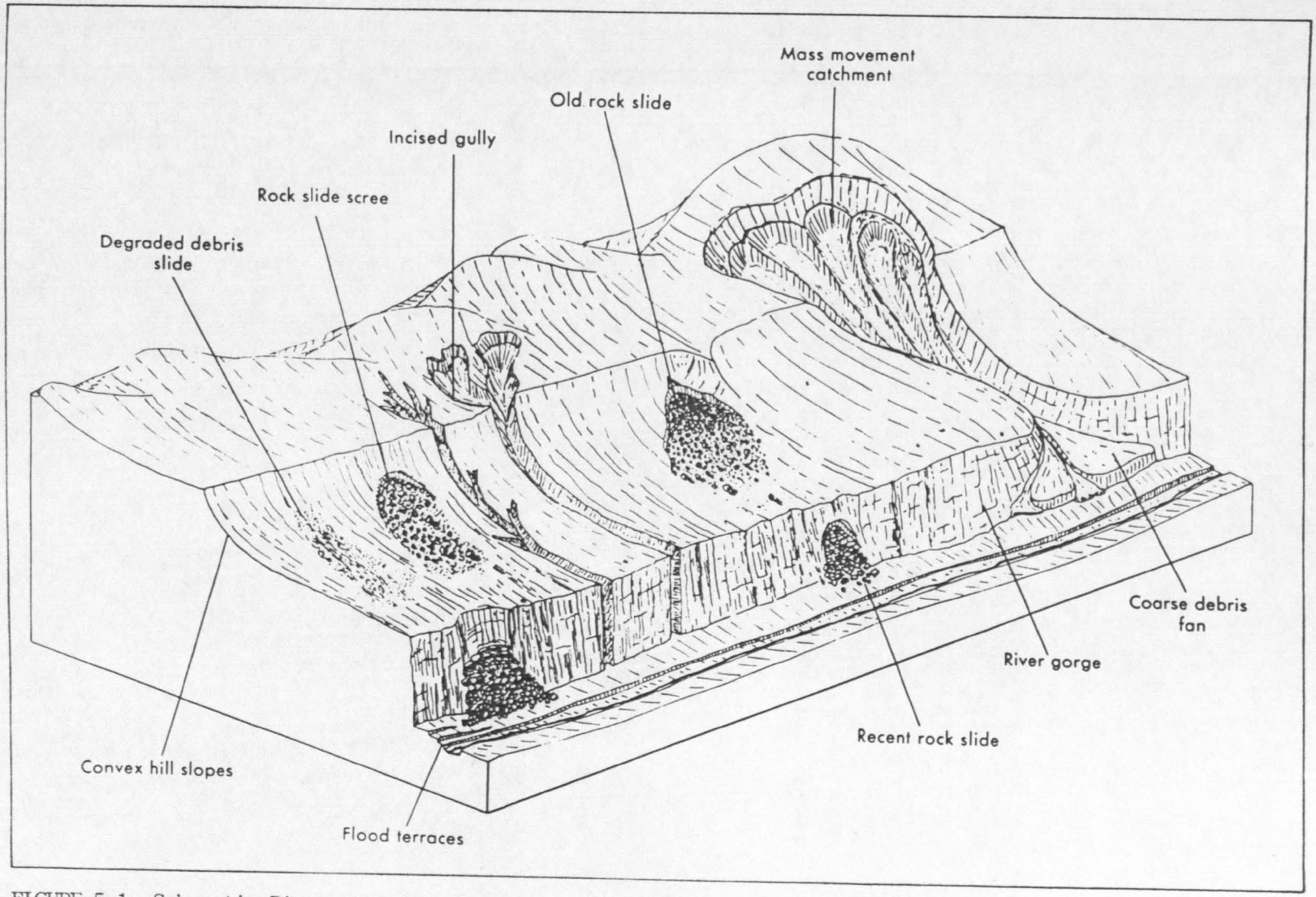

FIGURE 5.1 Schematic Diagram of the Major Slope Elements and Associated Processes of the Dharan-Dhankuta Area. (After Brunsden et al 1981).

characterised by high relative relief and long, steep slopes where both erosion and mass movement tend to develop.

A simple, three-fold physiographic model has been adopted for factor mapping purposes in this chapter. The model is not intended as an improvement to that of Brunsden et al (1981), but rather a means of facilitating broad terrain classification based on air photograph interpretation. The model recognises three main physiographic units that are easily identified on air photographs. These are: i) steep, incised, lower valley flanks that are the location of widespread instability, ii) long, steep tributary valley flanks that, while not occupying locations adjacent to eroding drainage lines, are sufficiently steep to promote instability, and iii) relatively gentle (less than 35^{o}) and stable, 'normal' slopes that frequently occupy middle, upper and crestal slope locations. The distribution of these terrain types in the study area is discussed in Section 5.4.3.2.

5.3.5 Land Use

The fourth category listed in Table 5.4 is that of land use. This relates, essentially, to anthropogenic factors that cause accelerated erosion and instability by slope and drainage disturbance. Generally, deforestation leads to an increased potential for soil erosion. Chakrabarti (1971) suggests that a forest cover of at least 50 percent is desirable along the Mahabharat Lekh for the maintenance of soil stability. In the study area, the development of agriculture has led to the depletion of the forest cover to below this level (see Figure 5.8). Overgrazing, nutrient depletion and erosion often lead to the eventual abandonment of agricultural land, and the creation of bare ground that becomes colonised by short shrubs and Eupatorium (Banmara). The potential for accelerated erosion is often high on these slopes. Deforestation and slope irrigation, for agricultural purposes, often lead to increased and concentrated surface runoff, that may also cause erosion and shallow instability further downslope.

To the south of the Tamur River, the majority of the forest is composed of Shorea robusta (Sal), Lagerstroemia parvifolia (Jarool) and Adina cordifolia (Siamese Kwao) with a dense understorey. In the Dhankuta catchment, however, the distribution of forest types is more complex. On the wetter slopes of the lower Dhankuta Khola, Sal forms the dominant tree species, and

an understorey is relatively well developed. By contrast, the dry, often overgrazed and overcultivated headwater slopes are, with the exception of pioneering Pinus roxburghi (Chir pine), usually quite bare (Plate 5.3). The pine litter is often collected for fuel, and consequently top soils remain relatively shallow and susceptible to erosion. Other tree species found in the catchment include Alnus nepalensis (Alder) and Adina cordifolia in moist valley bottoms, and Acacia catechu (Acacia), Rhus parvifolia (Sumach) and Albizzia (Siris) on dry slopes.

Finally, road construction in the area often increases the potential for mass movement (Chapter 2) and, ideally, this should be included in any landslide hazard assessment for highway design purposes. Slope overloading by embankment and spoil tip/bench construction may be an important contributory factor in the initiation or acceleration of mass movement on the slopes below a road, while slope undercutting in excavations may cause failure of the slopes above. Spoil tipping and artificial slope drainage tend to increase and concentrate slope runoff rates, leading to erosion and sediment hazards on the slopes below. These construction-induced hazards are discussed further in Section 5.5 and Chapter 6, but are difficult to predict prior to earthworks and, as they cannot be sensibly incorporated into a landslide hazard mapping exercise for route planning purposes, shall not be analysed here.

5.4 Development of Medium-Scale Landslide Hazard Mapping in the Study Area for Route Selection Purposes

5.4.1 Introduction

The review of landslide hazard mapping techniques in Section 5.2.2 has concluded that their ability to evaluate the spatial distribution of landslide hazard is dependent upon the quality of the data base and the assumptions made in the analysis. Computer and statistically-based landslide susceptibility mapping techniques may be largely inappropriate and unjustified in the study area owing to the poor quality of terrain data currently available. Alternatively, less rigorous techniques of factor mapping, that do not place such high demands on the data base, may be more appropriate.

In order to test this contention, and examine the contribution that landslide hazard mapping can make to route planning, techniques based on both the

PLATE 5.3 Bare Slopes Below Dhankuta with Occasional Chir Pine.

statistical and factor mapping methodologies are tested for the study area. While the methods of analysis used by each methodology differ considerably, they have both been developed largely from the same data base. The derivation of this data base is described below.

5.4.2 Selection and Measurement of the Dependent and Independent Variables

i) Dependent (Hazard) Variable

The distribution of landslides and slope erosion features in the study area following the September 1984 storm was used as the dependent variable in the analysis. For ease of analysis, slope erosion and landslide mechanisms have been combined to produce one data set. Differentiation between landslide mechanisms was not possible as, in the majority of cases, the actual mechanisms of failure could not be identified from the air and terrestrial photographs (see below). The identification of all failure mechanisms would have required an extensive field survey that was considered to be beyond the scope of the study. Only in the cases of the larger instability features could failure mechanisms be identified, and these are discussed in Section 5.4.5. Henceforth, mass movement and slope erosion features will be referred to, collectively, as slope hazards.

The geographical distribution of slope hazards generated during the 1984 storm was recorded from terrestrial photography taken in November 1984, and this data was transfered onto 1 : 25 000 scale base maps drawn from air photographs. Obviously, this technique was open to some subjectivity when slope hazard boundaries were plotted directly onto the base maps from the photographs, using topographic control only. However, terrestrial photography was the only method available for rapidly recording slope hazards that occurred during the September 1984 storm and during previous monsoon seasons. A sortie of air photographs was flown over the Dharan-Dhankuta road by TRRL in 1985, but unfortunately these were of limited coverage, variable scale and often obscured by dust and ultra-violet reflectance[1], and thus could not be used.

---

1. An example of this photography is shown in Plate A.1 of Appendix 1

The slope hazard distribution obtained by terrestrial photography was supplemented by data from both 1 : 25 000 scale black and white air photographs, flown for the Overseas Development Administration in November - December 1978 over the Kosi-Ilam area, and the maps produced by the 1975 geomorphological reconnaissance survey (Chapter 4). A total of 369 slope hazards were recorded in the Sardu, Leoti and Dhankuta catchments, over an area of 102 km^2. Many of the slope hazards recorded from these additional sources may have been caused by the July 1974 storm that had a local recurrence interval of 10-15 years (Barker 1976).

The slope hazard distributions for the Sardu and Leoti and Dhankuta Khola catchments are shown in Figures 5.2 and 5.3 respectively. Differentiation has been made on these maps, wherever possible, between hazard mechanisms (linear slope erosion, shallow, planar rock slides, debris slides and mudslides, and deep-seated rotational slides and rock slides). It is quite possible that these distributions do not represent the total population of slope hazards in the study area, as the efficiency with which relic, and sometimes active landslides can be identified on medium-scale air photographs is reduced in complex, steep terrain, where they are often obscured by dense vegetation and shade. The quantification of the slope hazard distribution is described in Section 5.4.3.

ii) Independent Variables (Contributory Factors)

Using geological maps published by Bordet (1961), Fookes and Marsh (1981) and Kayastha (1977), the outcrops of the five rock types identified in Section 5.3, were plotted onto the 1 : 25 000 scale base maps to produce a Geology factor map, a reduced version of which is shown in Figure 3.4. To determine whether the slope hazard distribution was controlled in any way by the location of streams of different order, the drainage networks in all three catchments were mapped from the air photographs, and are shown in Figures 5.2 and 5.3. Channel definition became difficult in areas of dense forest, and differentiation between channels and linear clusterings of vegetation along percolines proved difficult in headwater areas. The channel network was ordered according to the Strahler (1952) method; the fifth order stream of the lower Dhankuta Khola being the largest recorded in each of the three catchments.

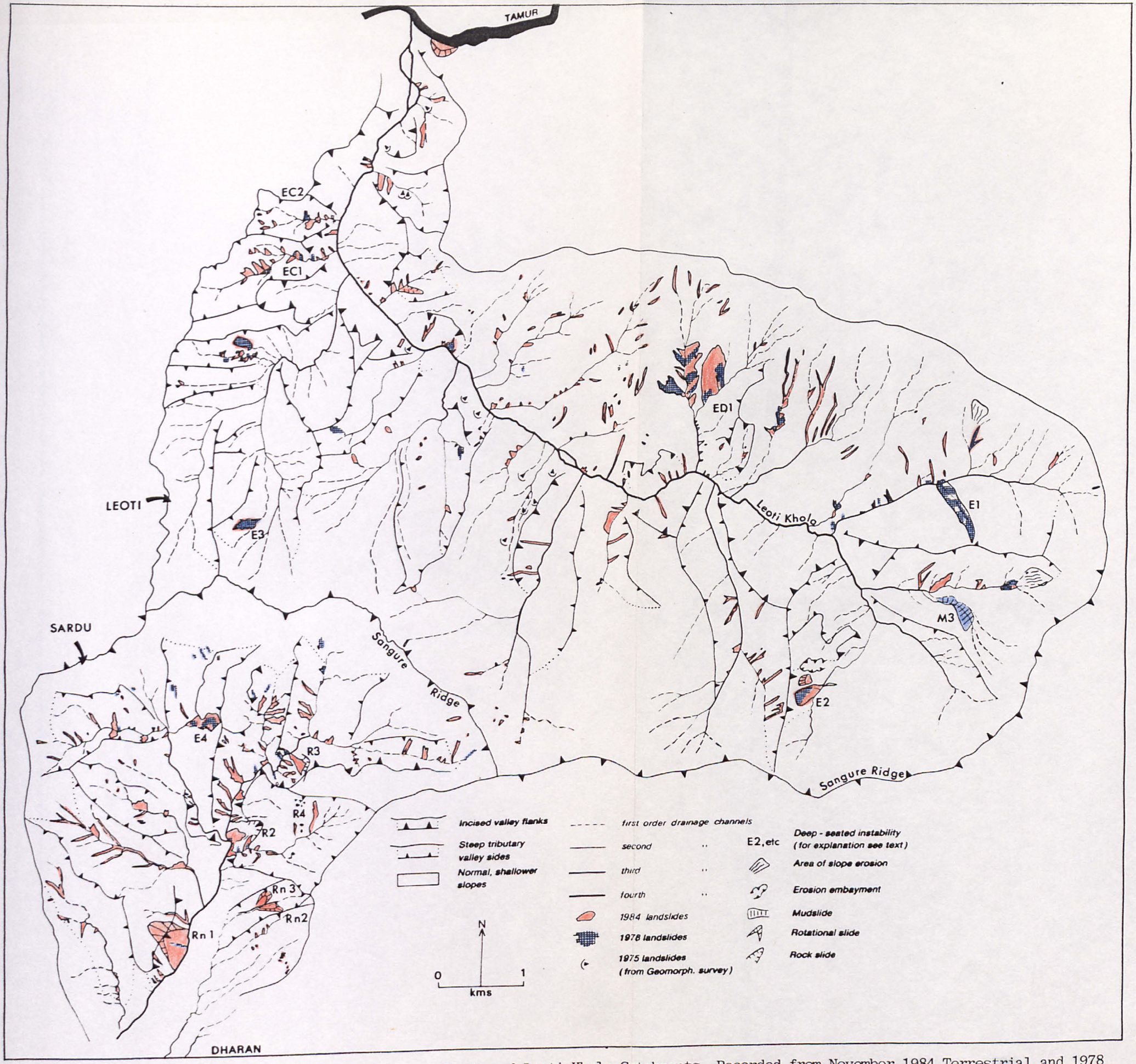

FIGURE 5.2 The Distribution of Slope Hazards in the Sardu and Leoti Khola Catchments, Recorded from November 1984 Terrestrial and 1978 Air Photography and the 1975 Geomorphological Reconnaissance Survey, and its Relationship with the Drainage Network and Catchment Physiography.

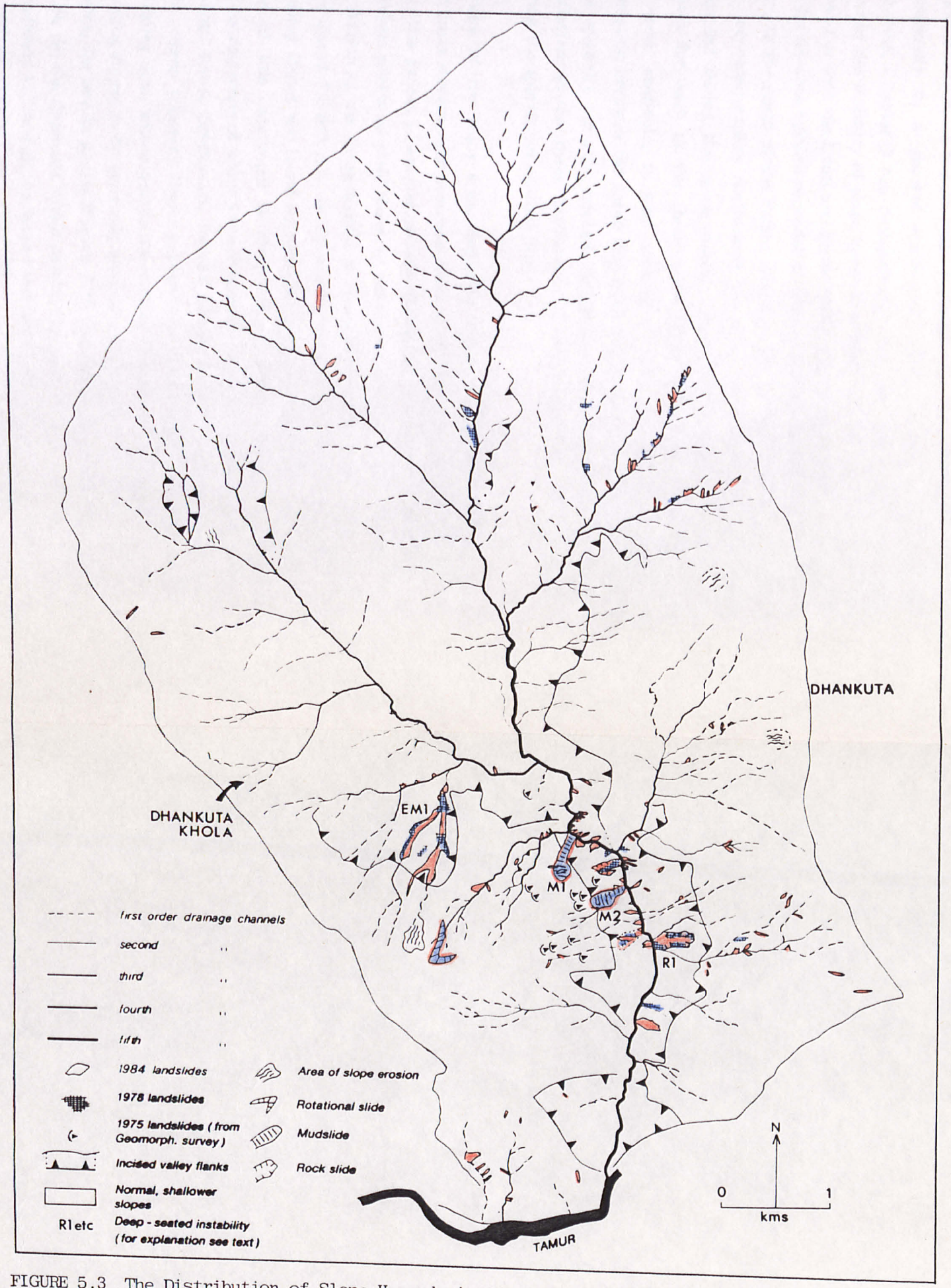

FIGURE 5.3 The Distribution of Slope Hazards in the Dhankuta Khola Catchment, Recorded from November 1984 Terrestrial and 1978 Air Photography and the 1975 Geomorphological Reconnaissance Survey, and its Relationship with the Drainage Network and Catchment Physiography.

Owing to the sparsity of rainfall data in the study area (Chapter 3), variable rainfall depth, and particularly intensity, could not be measured. This limits the representability of the analysis, especially as storm rainfall is known to vary markedly in a general north-south direction and with orography. Nevertheless, Chapter 3 has demonstrated that the September 1984 storm, that caused the majority of slope hazards recorded in the data base, was quite widespread in both the Leoti and Sardu Khola catchments. This is indicated by the similar 24-hour rainfall recorded at Dharan (275mm) and Mulghat (291mm). However, to the north of the Tamur River, in the Dhankuta Khola catchment, rainfall decreased rapidly northwards towards Dhankuta, where only 146mm was recorded during the same storm. Therefore, separate analyses were undertaken for each of the three main catchments. On the basis of the rainfall data available, it was considered that this broad geographical differentiation between the three catchments was the only possible means of taking a spatially variable rainfall distribution into consideration; further differentiation within these catchments would have been wholly arbitrary considering the sparsity of rainfall data.

Topo maps of the study area, depicting the major breaks of slope, were produced from stereoscopic interpretation of the air photographs (Figures 5.2 and 5.3). The aspect of each slope unit identified, was assigned to one of the eight cardinal points to yield slope aspect factor maps (Figures 5.4 and 5.5). The distribution of the three terrain physiographic units in the study area is shown in Figures 5.2 and 5.3. In the Sardu Khola catchment, the majority of incised valley flanks are found adjacent to the trunk river, while most of the remainder of this catchment is composed of slopes categorised as steep tributary flanks, many of which form the southern flanks of the Sangure Ridge. In the Leoti Khola catchment, incised flanks border much of the Leoti floodplain. Steep tributary flanks predominate in the sub-catchments on the southern valley side, where quartzites outcrop (Figure 3.4) along the Sangure Ridge, causing slopes to be generally steeper and longer. Most of the northern valley flanks, formed in gneiss (Figure 3.4), are relatively shallowly inclined (Figure 5.2). In the Dhankuta Khola catchment, only incised valley flanks and normal, shallowly inclined slopes, have been identified (Figure 5.3); the former occupy locations along the Dhankuta Khola gorge, while the latter form most of the remainder of the catchment, and are characteristically subdued and developed predominantly on gneiss.

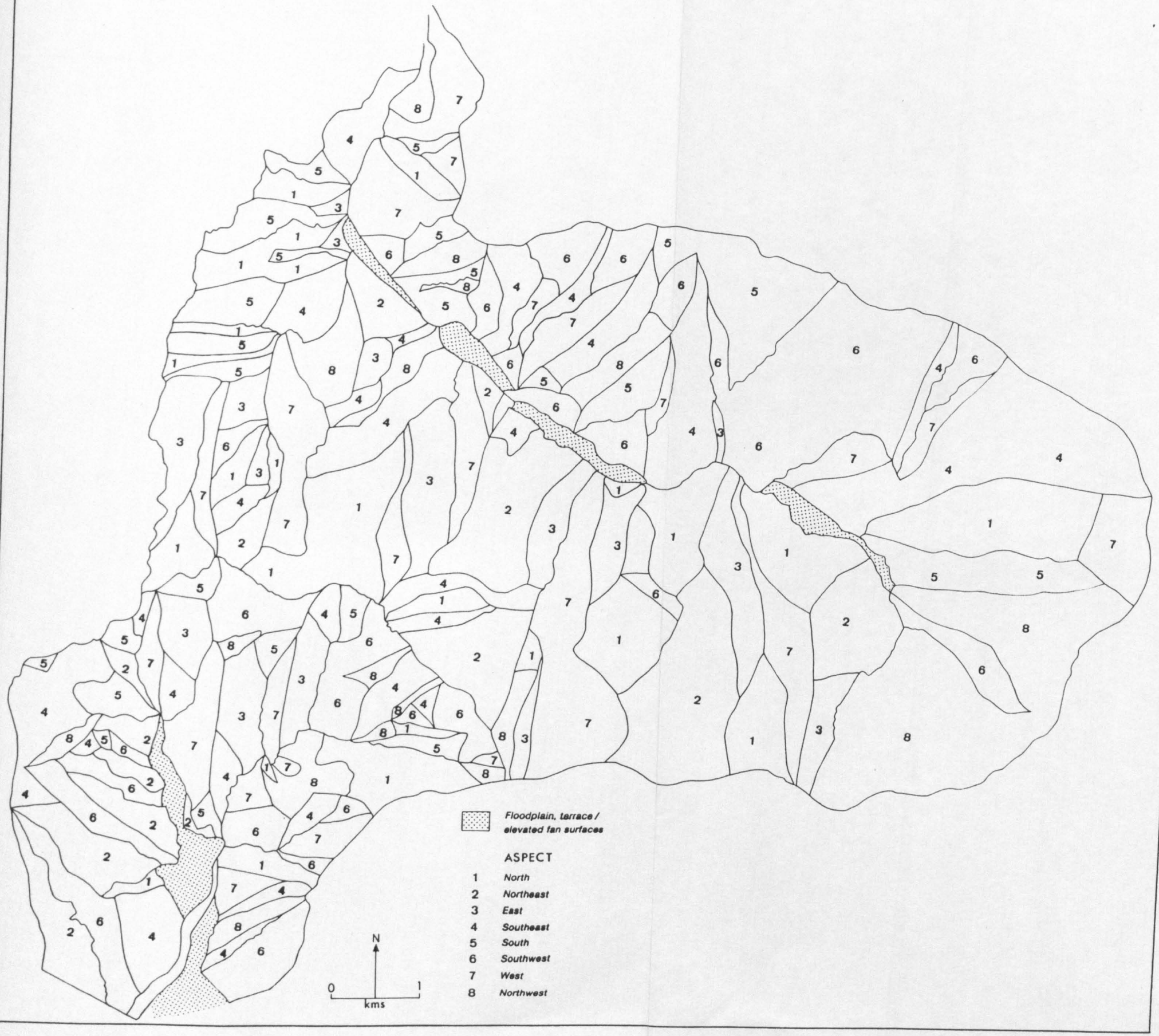

FIGURE 5.4 Slope Aspect Map of the Sardu and Leoti Khola Catchments.

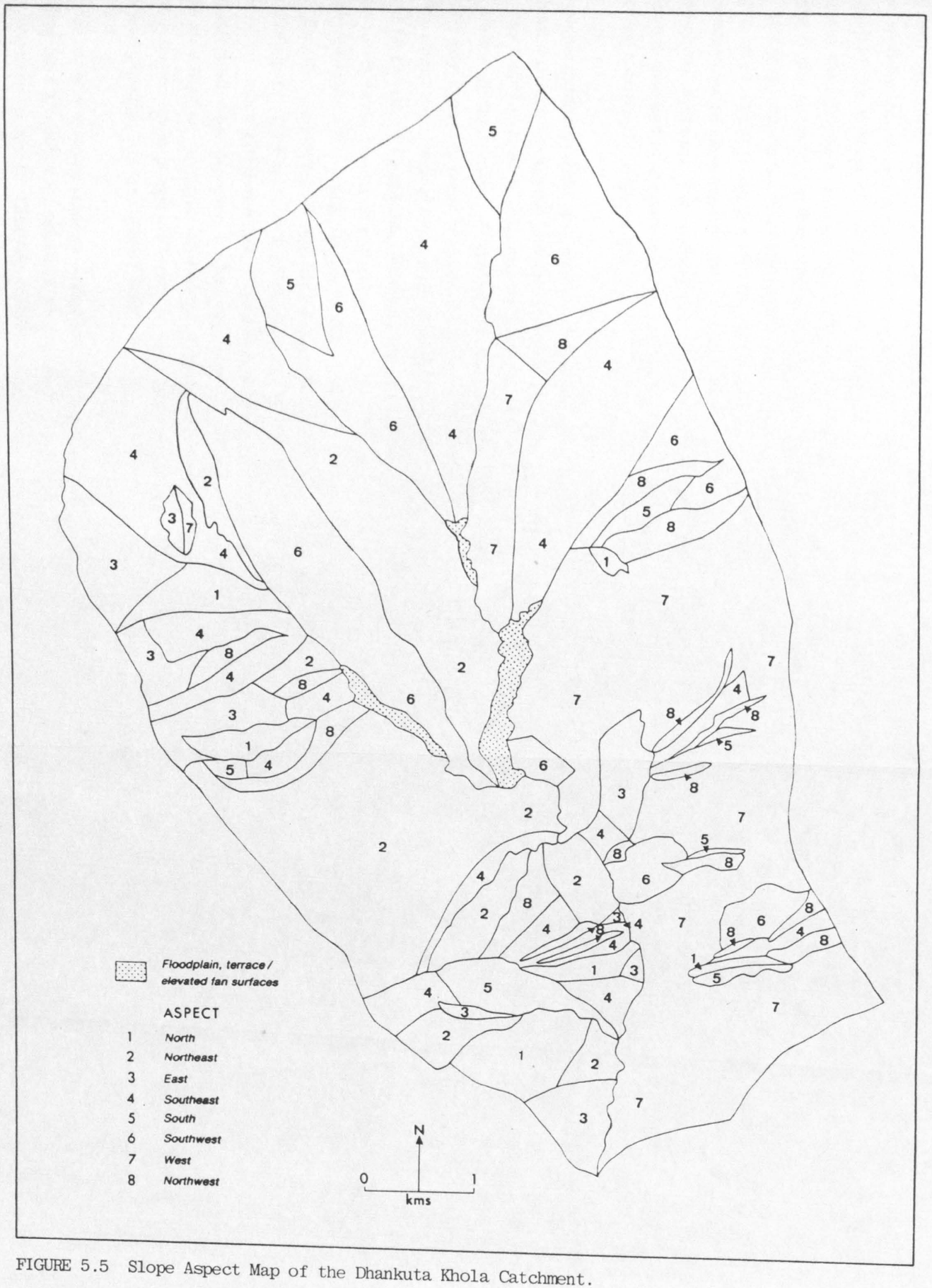

FIGURE 5.5 Slope Aspect Map of the Dhankuta Khola Catchment.

A slope category map was produced for the study area by superimposing a cellular grid onto the base maps and determining the average slope inclination for each cell, using the parallax bar method. The grid cells were 1cm square, corresponding to an average ground resolution of 232m. Relative relief was calculated for a total of 2 229 cells by combining the parallax difference, between the upslope and downslope boundaries of each cell, with the flying height of the aircraft, and the distance between the plotted principal points of the stereo photographs. Relative relief was then combined with the cell length, adjusted for projection into the horizontal plane of the photograph, to determine overall slope inclination (in degrees) for each cell. The accuracy of parallax measurement was reduced on forested slopes, where the ground surface is obscured by the canopy. In a few cases, parallax was determined by assuming a constant canopy height.

The slope category maps are shown in Figures 5.6 and 5.7. While slope inclinations were calculated and recorded on an interval scale, the overall slope inclination in each cell was assigned to one of five classes for the compilation of these maps. A comparison between the slope category maps and the physiographic maps (Figures 5.2 and 5.3), indicates that the former provide a poor reflection of catchment physiography. This may be illustrated by the fact that, on Figure 5.6, shallowly inclined and steeply inclined slopes on the Leoti Khola floodplain and along the Sangure Ridge, respectively, are barely distinguishable, owing to the inclusion of variable slopes within each cell. Smaller grid cells, of 50-100m dimension, would have increased the representability of the slope inclination data, but would have also necessitated considerably more air photograph interpretation and data analysis. In the Dhankuta catchment, however, a clustering of steep slopes (greater than 30^{o}) can be identified on the flanks of the incised gorge, while inclinations tend to decrease on the upper peripheral slopes of the catchment, as indicated by the catchment physiography map (Figure 5.3).

From the air photographs, land use categories of Forest, Agriculture and Scrub (including bare ground) were delimited on the base maps. Land use category maps, recently produced (January 1987) by the Kosi Hills Area Rural Development Programme as far south as the Sangure Ridge, were unavailable at the time of this study and, with 25-30 land use categories in the Dhankuta area alone, are probably far too complex to be readily interpreted for landslide hazard mapping purposes. On the basis of the discussion in Section 5.3, the

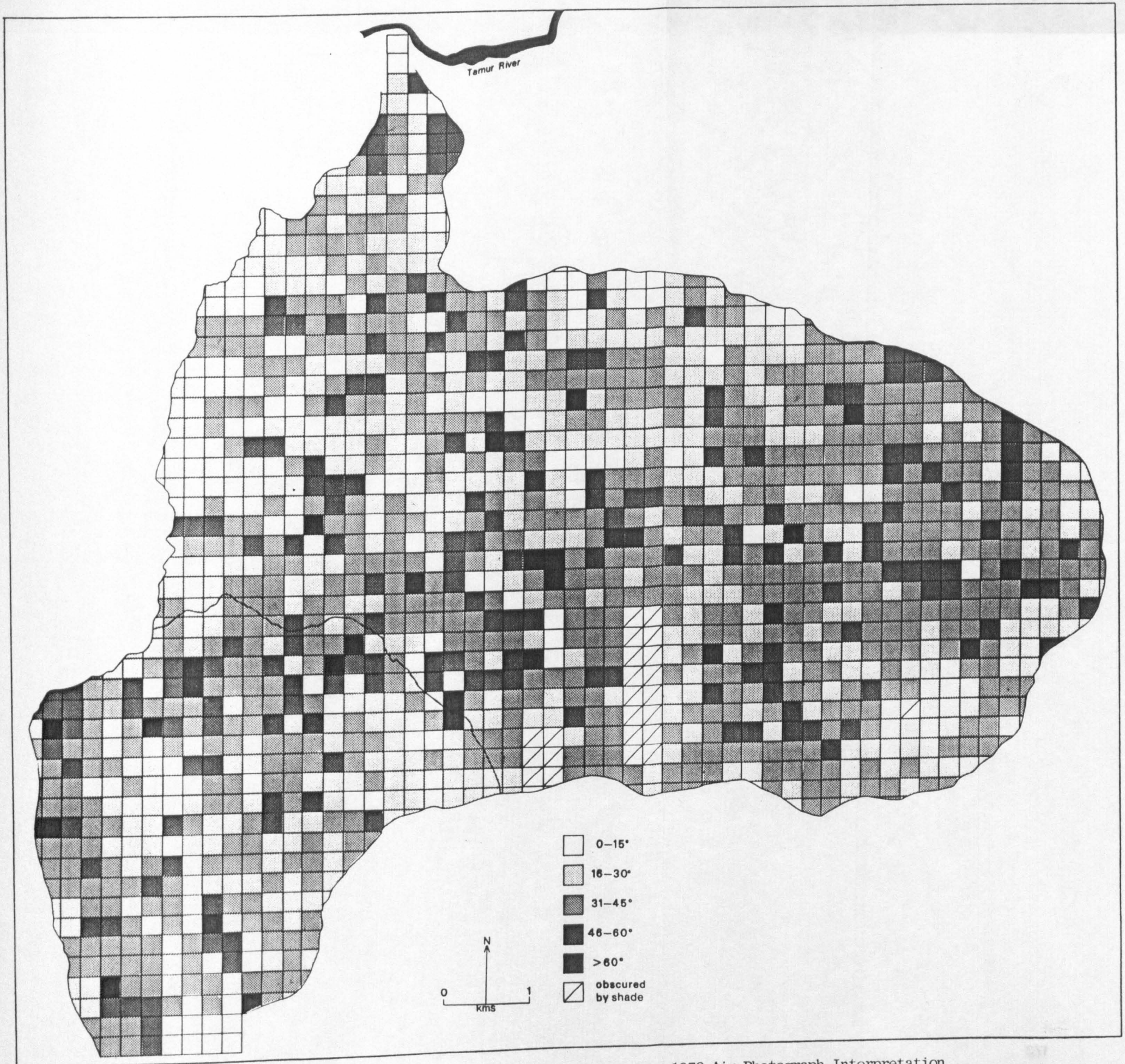

FIGURE 5.6 Slope Category Map of the Sardu and Leoti Khola Catchments Based on 1978 Air Photograph Interpretation.

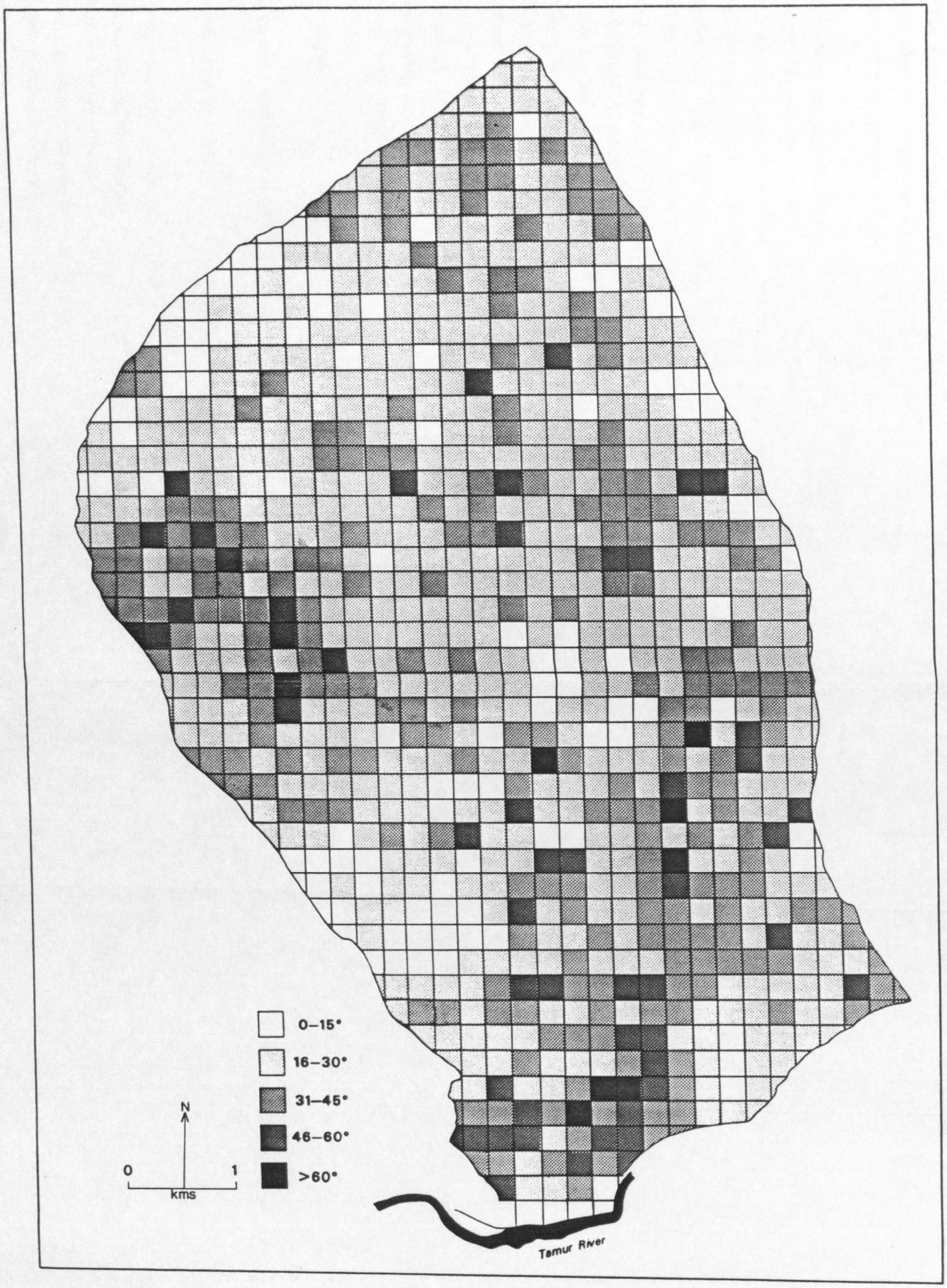

FIGURE 57 Slope Category Map of the Dhankuta Khola Catchment, Based on 1978 Air Photograph Interpretation.

three-fold categorization adopted here is justified. The recognition and mapping of forested areas from the air photographs was relatively straight forward. Agricultural land and scrubland were also easily identified on the air photographs; the former is characterised by terraced fields, plough furrows and goat tracks, while the latter was defined on the basis of high reflectance, patchy vegetation or bare ground, and short grasses and shrubs.

The land use categories are shown on Figures 5.8 and 5.9. In the Leoti catchment, forested slopes are concentrated on the lower, steeper flanks and southern flanks of the valley, where the relative relief is highest and slopes are too steep for agriculture. Patches of scrub occur throughout the catchment, although a large concentration was mapped on the southeastern and eastern valley flanks. Here scrubland is likely to have developed from the degeneration of intensely cultivated agricultural land, associated with the relatively high population densities in the ridge-top settlements of Okhre and Danda Bazar. A similar land use pattern can be identified in the Dhankuta catchment, where forest occupies the incised lower slopes, and agriculture is found on the shallower slopes towards the periphery of the catchment. A large patch of scrubland occurs on the slopes below Dhankuta, caused probably by intense cultivation and overgrazing. In the Sardu catchment, forest again occupies the steeper, incised valley flanks, while agriculture is found on the shallower upper slopes, particularly in the west of the catchment. Scrubland is concentrated to the north, on the steep quartzite slopes of the Sangure Ridge.

5.4.3 Data Analysis

5.4.3.1 The Statistical Method of Analysis

i) Data Collection and Analysis

All slope hazards identified on the 1978 air photography and 1984 terrestrial photography have been defined (Figures 5.2 and 5.3) as the 1978 and 1984 slope hazard distributions respectively. A total of 128 and 425 grid cells were occupied by slope hazards from these distributions. The landslides identified by the 1975 geomorphological reconnaissance survey were not included in this analysis, as reliable values for slope hazard area could not be obtained.

Most of the slope hazards recorded in 1978 and 1984 are likely to have been caused by the July 1974 and September 1984 storms respectively.

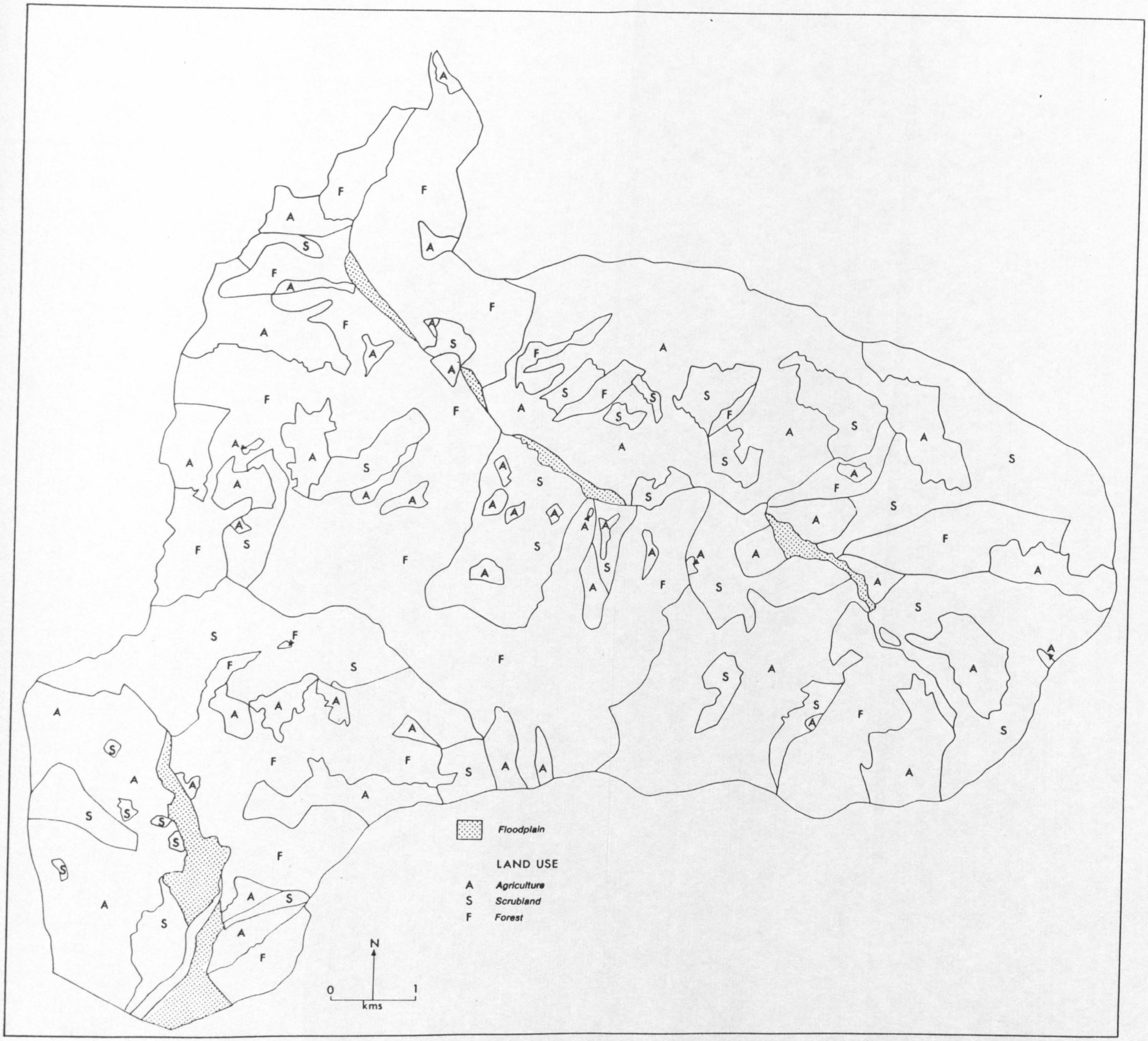

FIGURE 5.8 Land Use Category Map of the Sardu and Leoti Khola Catchments.

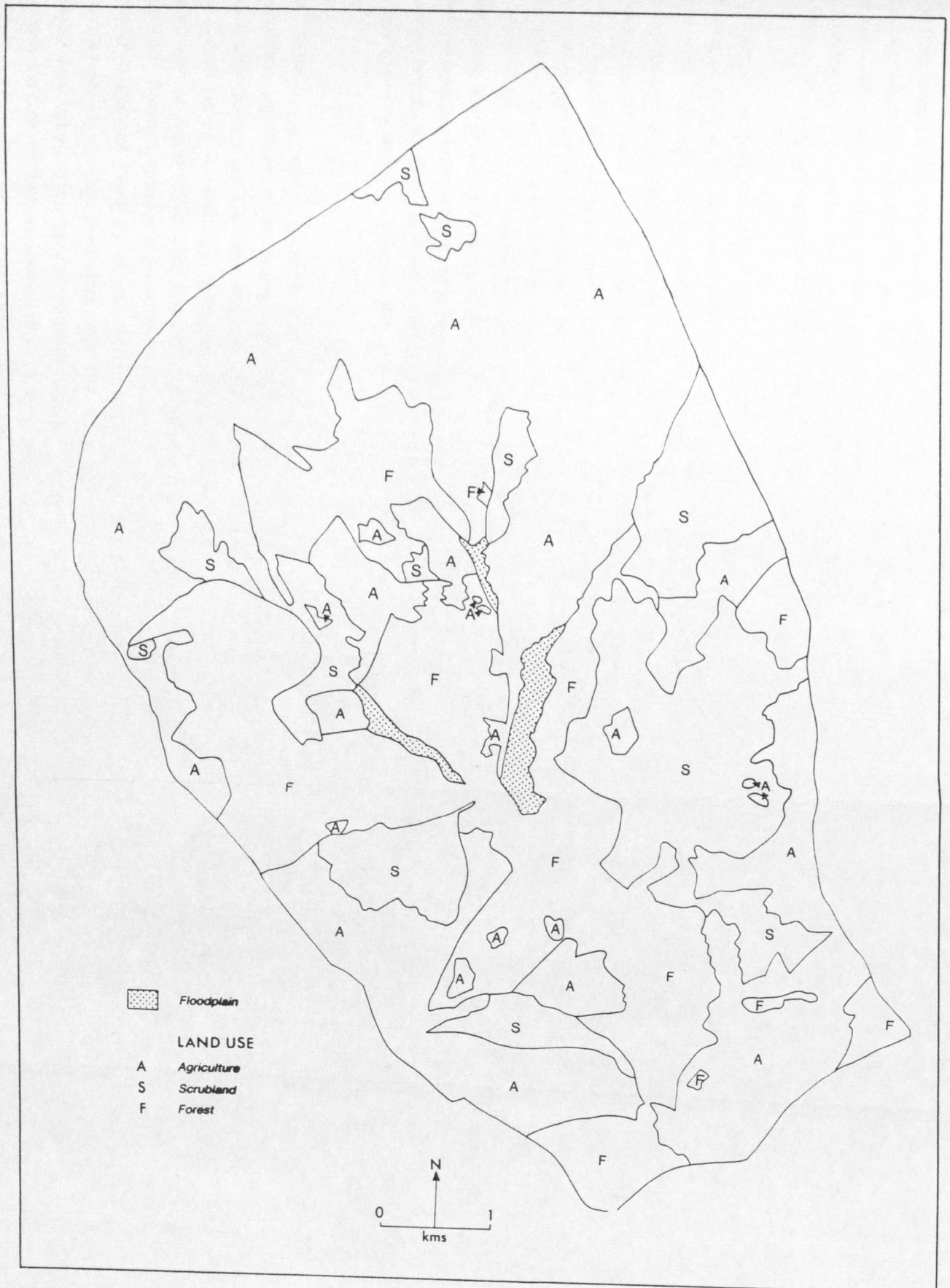

FIGURE 5.9 Land Use Category Map of the Dhankuta Khola Catchment.

Consequently, the two distributions have been examined separately. Separation of the data base in this way also enabled direct comparison between the two data sets to determine whether slope hazards recorded in 1984 occurred on slopes that had become unstable during the 1974 storm. The distributions were quantified by summing the total area of slope hazards found in each cell. As the actual ground surface area covered by each cell varied according to slope angle, the area of each slope hazard was divided by the cosine of the angle of the slope covered by the cell in which it occurred.

In order to compare the spatial distribution of slope hazards with that of the drainage network, the channel length of each stream order was measured in each cell from the factor maps (Figures 5.2 and 5.3). This allowed the identification of stream orders that had the highest association with the distribution of slope hazards. By definition of the ordering system, lower stream orders are more common than higher orders, and are consequently likely to show a higher correlation with a random slope hazard distribution. The stream order channel lengths per cell were, therefore, standardised by dividing each channel length by the proportion of each stream order comprising the drainage network (for the three catchments combined). As most cells on the base maps have zero values for both slope hazard area and channel length, all such cases were excluded from the data file. The overall slope inclination and rock type in each cell were also inputed onto computer file.

The SPSS(X) regression package was used to determine whether any statistically significant relationships exist between the 1984 and 1978 slope hazard distributions and the slope and drainage variables. Regression analysis was chosen as it is relatively quick and simple to perform. The main requirement of the SPSS(X) linear and multiple regression packages, using the parametric Pearson Product Moment correlation test, is that data sets are normally distributed about the mean. When histograms of slope hazard area were plotted, it was apparent that only the slope inclination data were normally distributed. Near-normal distributions were obtained for most data sets when the data were square-rooted (Figure 5.10). However, the population distribution of square-rooted 1984 hazard area (Root A84) remained highly positively skewed (skewness = + 1.985), while the distribution of the fifth order channel length (Root A DD5) was almost rectangular. Square-root transformation decreased the skewness of the 1978 slope hazard area distribution, although the population still remained positively skewed (Figure 5.10B).

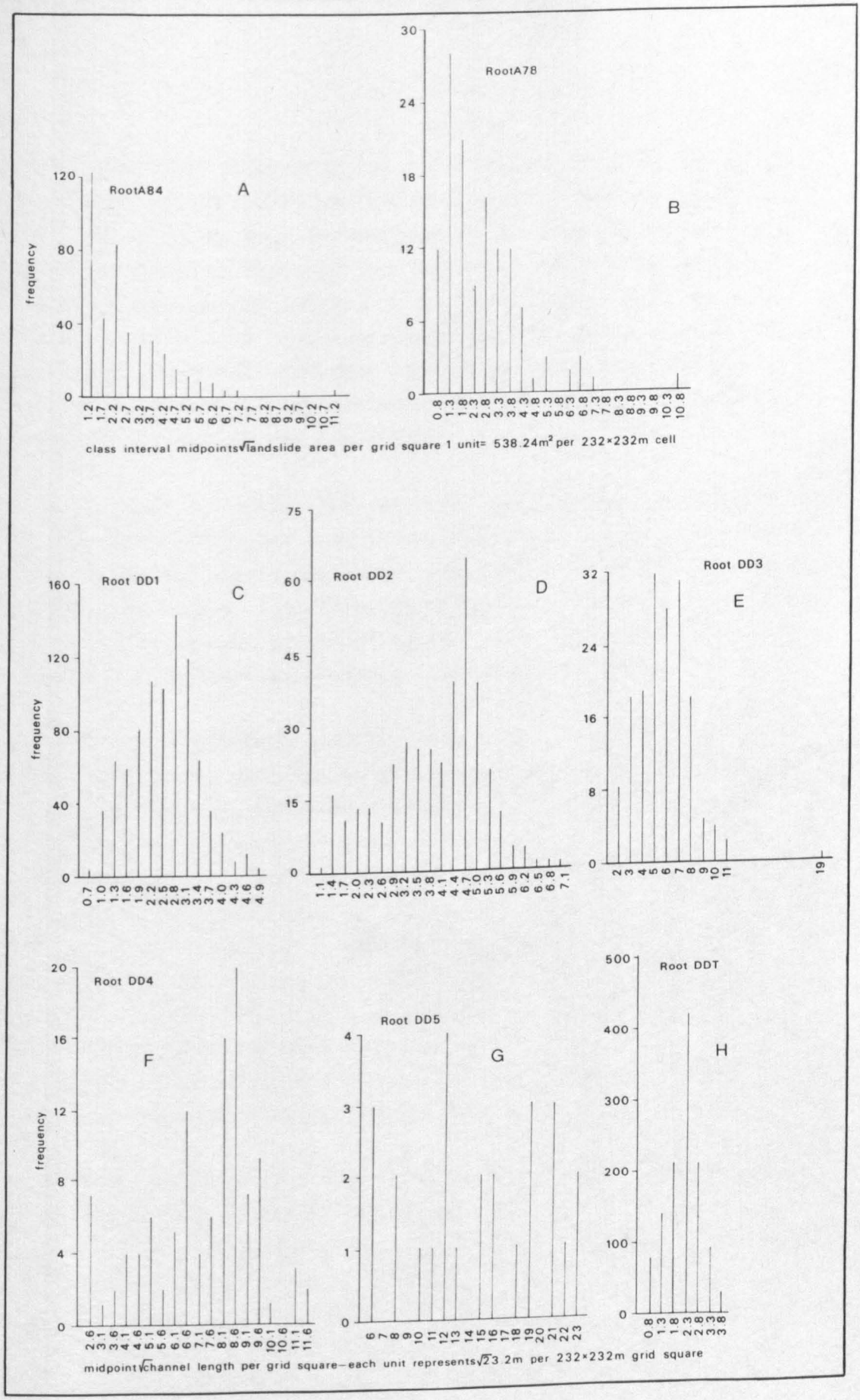

FIGURE 5.10 Frequency Distributions of the Dependent and Independent Variables.
(ROOT A84 - Square root 1984 landslide area per cell; ROOT DD1 - DD5 - Square root of drainage length for each stream order (1-5) per cell; ROOT DDT - Square root of total drainage length per cell).

Further statistical manipulation of these variables, by the fitting of increasingly complex distribution functions, would be time consuming and would, in any case, make interpretation of the final correlations more uncertain. Therefore, Root A78 was regressed with all data sets (slope inclination, drainage order lengths 1 to 5 and total channel length), while the non-parametric Spearman's rank correlation test was used to examine the relationships between the 1984 slope hazard areas (A84) and the independent variables. Each regression and correlation test was run both with and without the data file divided according to rock type.

Tables 5.5 and 5.6 display the regression and correlation coefficients respectively, and the degree of significance between the dependent variables (Root A78 and A84) and the independent variables of slope inclination and the drainage order lengths. Table 5.5 indicates that for all cases, Root A78 was significantly correlated, at the 95 percent level or above, with slope inclination, fifth order drainage length and total drainage length.

When the latter two variables were combined, multiple regression yielded the highest coefficient of determination ($r^2 = 0.210$). With the data files divided according to rock type, the computed coefficients of determination did not appear to be significantly increased. In fact, the small number of slope hazards recorded on quartzites and schists rendered the regression coefficients meaningless. The highest significant coefficient of determination ($r^2 = 0.327$) was obtained for slopes formed in gneiss, when Root A78 was regressed on slope inclination and total channel length. Slope inclination was significantly correlated with Root A78 on all rock types, except Siwaliks, but again the coefficients of determination were particularly low. Figure 5.11 shows the scattergrams between Root A78 and the independent variables. The high degree of scatter reflects the general lack of association.

A regression coefficient of + 0.660, significant at the 99 percent level, between Root A78 and Root A84, suggests that slope hazards tend to occur on slopes that are historically susceptible to instability. The association between the two slope hazard distributions is also shown on the scattergram (Figure 5.11) for each rock type. The slope hazard distribution maps (Figures 5.2 and 5.3) show that many of the 1984 slope hazards were, in fact, enlargements to those recorded in 1978. These observations suggest that once instability has

REGRESSION DATA FOR ROOT A78 ON THE INDEPENDENT VARIABLES

ROCK TYPE	ROOT A84			SLOPE			√DD1			√DD2			√DD3			√DD4			√DD5			√DDT			MR (SLOPE√DDT)		
	R	R^2	SL	R	R^2	SL	R	R^2	SL	R	R^2	SL	R	R^2	SL	R	R^2	SL	R	R^2	SL	R	R^2	SL	R	R^2	SL
GNEISS	0.610	0.373	99.9	0.445	0.198	99.4	0.089	0.008	68.2	0.237	0.056	90.0	-0.150	0.022	78.9	0.291	0.085	94.4	no cases			0.469	0.220	99.6	0.572	0.327	99.6
PHYLLITE	0.644	0.414	99.9	0.387	0.150	99.8	0.290	0.085	70.9	-0.120	0.014	80.8	0.252	0.064	96.8	-0.007	0.000	52.0	no cases			0.256	0.066	97.1	0.441	0.194	99.6
QUARTZITE	0.955	0.913	97.8	0.921	0.849	96.1	0.746	0.556	87.3	-0.282	0.079	64.1	no cases			no cases			no cases			0.650	0.422	82.5	0.960	0.922	72.1
SCHIST	0.804	0.647	99.9	0.344	0.119	97.5	-0.254	0.064	92.3	0.056	0.003	62.2	-0.016	0.000	53.5	-0.191	0.036	85.7	0.551	0.304	99.9	0.208	0.043	87.7	0.377	0.142	89.9
SIWALIK	0.516	0.266	81.3	-0.003	0.000	50.2	0.030	0.001	51.9	0.781	0.610	94.1	-0.648	0.420	88.2	0.869	0.756	97.2	no cases			0.557	0.310	83.5	0.565	0.320	32.0
ALL CASES	0.660	0.436	99.9	0.377	0.142	99.9	0.137	0.019	93.8	0.039	0.001	66.9	0.024	0.001	60.8	0.068	0.005	77.8	0.203	0.041	98.9	0.305	0.093	99.9	0.459	0.210	99.9

TABLE 5.5 Regression Data for the 1978 Slope Hazard Distribution on the Independent Variables.

R - Regression coefficient
R^2 - Coefficient of determination
SL - Significance level (%)
MR - Multiple regression data for slope and total drainage length combined

DD1 - First order drainage length
DD2 - Second "
DD3 - Third "
DD4 - Forth "
DD5 - Fifth "

DDT - Total drainage length
ROOT A78 - Square root 1978 landslide area per cell
ROOT A84 - " 1984 "
SLOPE - Slope angle in each cell

CORRELATION DATA FOR A84 ON INDEPENDENT VARIABLES

ROCK TYPE	SLOPE			√DD1			√DD2			√DD3			√DD4			√DD5			√DDT		
	R	R^2	SL	R	R^2	SL	R	R^2	SL	R	R^2	SL	R	R^2	SL	R	R^2	SL	R	R^2	SL
GNEISS	0.184	0.034	89.2	0.069	0.005	45.2	0.203	0.412	92.3	0.024	0.001	16.5	0.009	0.000	6.0	no cases			0.239	0.057	96.5
PHYLLITE	0.190	0.036	98.6	0.141	0.020	93.1	0.171	0.029	97.3	0.103	0.011	81.8	-0.100	0.010	79.9	no cases			0.311	0.096	99.9
QUARTZITE	0.457	0.209	94.4	0.367	0.135	86.6	-0.101	0.010	30.9	no cases			-0.030	0.001	9.5	no cases			0.378	0.143	87.8
SCHIST	0.123	0.015	77.0	0.047	0.002	35.4	0.293	0.086	99.6	0.107	0.011	70.3	0.008	0.000	6.4	0.321	0.103	99.9	0.434	0.188	99.9
SIWALIK	-0.050	0.002	31.0	-0.055	0.003	33.5	0.226	0.051	93.0	-0.128	0.016	68.9	0.259	0.067	96.3	no cases			0.059	0.003	36.1
ALL CASES	0.179	0.032	99.9	0.088	0.008	93.1	0.203	0.041	99.9	0.050	0.002	70.0	0.029	0.001	44.5	0.103	0.011	96.7	0.304	0.092	99.9

TABLE 5.6 Spearman Rank Correlation Data for the 1984 Slope Hazard Distribution on the Independent Variables.

R_s - Spearmans rank correlation coefficient
R^2 - Coefficient of determination
SL - Significance level (%)
A84 - 1984 landslide area per cell.

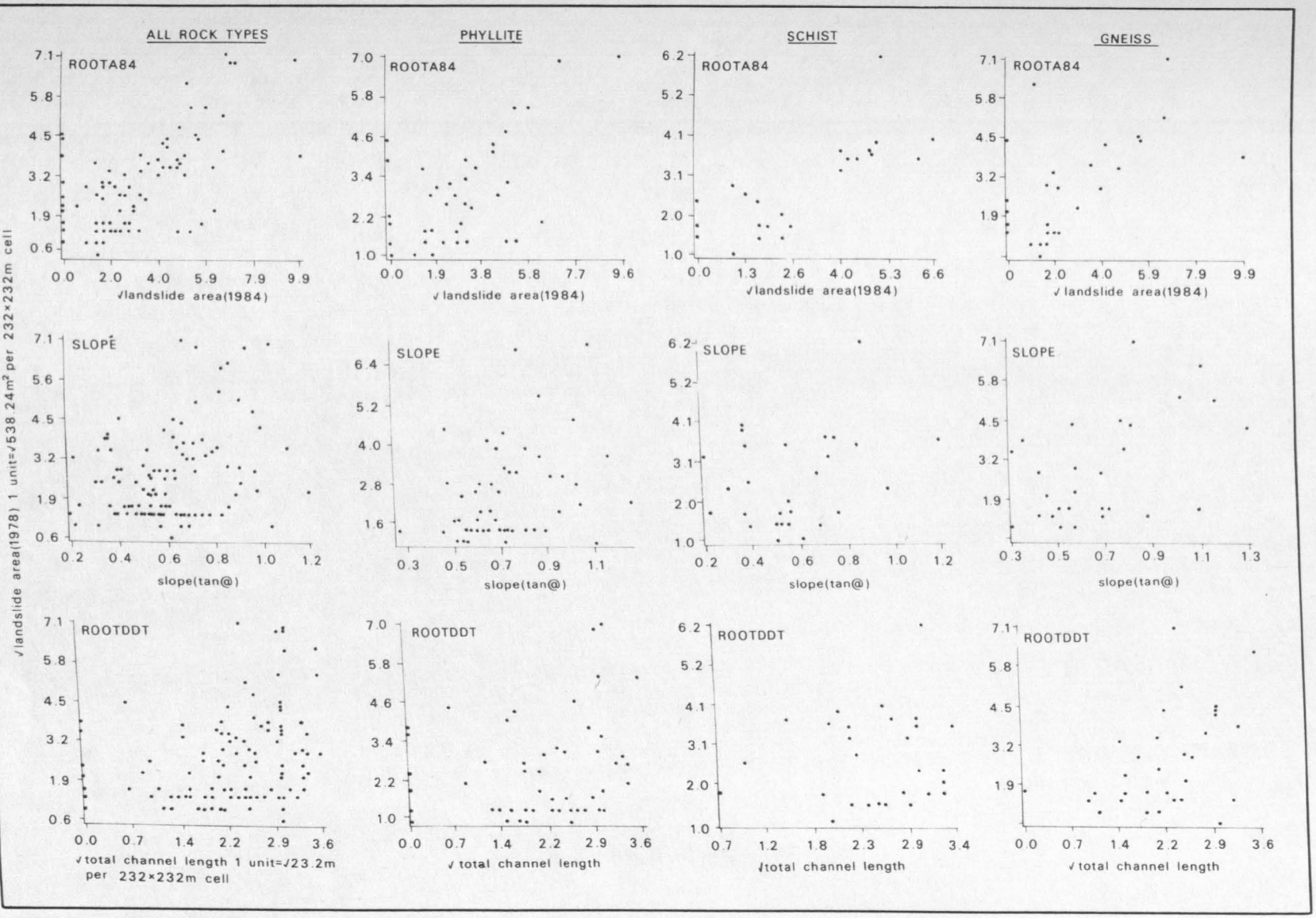

FIGURE 5.11 Scattergrams for the Dependent Versus the Independent Variables
(ROOT A84 - Square root 1984 landslide area per cell; Slope - Overall slope angle in each cell;
ROOT DDT - Square root of total drainage length per cell)

been initiated on a slope, that slope tends to be the site of further instability during subsequent storms, either by reactivation of the slip mass or enlargement of the slip by headward erosion and progressive failure.

The results of the correlation tests (Table 5.6) on the 1984 data, were even less encouraging. Although slope inclination, second and fifth order and total channel length were all positively correlated with A84, at the 95 percent significance level, the coefficients of determination were extremely low. These coefficients were not improved when the file was divided according to rock type. Again, total drainage channel length and slope inclination were the variables most associated with slope hazard area.

ii) Discussion of Results

While slope inclination and total channel length, on a grid square basis, were significantly correlated with both slope hazard distributions, the low coefficients of determination obtained do not allow the production of a valid slope hazard susceptibility map from the data. Consequently, no further analysis or interpretation of the results have been made. It must be concluded, therefore, that this attempt to develop a landslide susceptibility mapping exercise, using grid cell sampling units and computer analysis, has been largely unsuccessful. This is attributable to two main facts. First, owing to the lack of terrain and geotechnical data, the choice of variables was restricted to those that could be measured on an interval scale from air photographs and the geological map. Second, the assumption made in the analysis, that the dependent and independent variables remained constant within each grid cell, is not valid. This problem might have been overcome by concentrating on a smaller area and decreasing the size of the grid cells. This, however, would have led to a geographically incomplete analysis that would not have allowed overall comparison of route corridors within the study area, had the analysis been successful. Bearing in mind the data constraints, this form of landslide hazard mapping, from air photographs alone, is unlikely to be productive for highway engineering purposes.

5.4.3.2 Factor Map Analysis

The methodology adopted here is similar to that used by Brabb et al (1972) in San Mateo County, California and Drennon and Schleining (1975) in S. Dakota

(Section 5.2.2), whereby a numerical rating is assigned to factor categories, according to the frequency or density of slope hazards in each category. By overlaying the factor maps a final hazard map is produced, that depicts the distribution of summed hazard scores or zones of differing levels of hazard.

i) Determination of Factor Ratings

The class categories for all six factors (rock type, slope aspect, slope physiography, land use, slope angle and drainage density (by channel order)) are listed in Table 5.7. The derivation of the hazard scores shown on this table is discussed below.

Using the factor maps (Figures 5.2 to 5.9) and the slope hazard distribution (Figures 5.2 and 5.3), the total number of slope hazards occurring in each factor category was determined for each of the three catchments (Sardu, Leoti and Dhankuta Kholas). The total area occupied by each of the factor categories was determined from the factor maps and expressed as a proportion of the total area of each of the three catchments. Using the chi-squared test (described in Hammond and McCullagh 1978), it was possible to determine whether, at the 95 percent significance level, the hazard frequencies on each factor category were significantly different from those expected had the slope hazard distribution been random. Where significant chi-squared (χ^2) values were obtained, the ratios of the observed to expected frequencies (O/E) were used to assign a numerical score to each of the factor categories. Hazard scores of 1 to 3 were found to be the most convenient (Table 5.7). Highest hazard scores were allocated to factor categories with the greatest O/E values. Where more or less than three categories were identified for each factor, as was the case with slope aspect in all three catchments and physiography in the Dhankuta catchment, the hazard scores were adjusted to ensure that the maximum value for each factor was 3. This allowed for equal representation among factors in the hazard score summation (Section 5.4.4); a condition that had to be assumed, given the unavailability of sufficient data to suggest or confirm otherwise.

ii) Rock Type

Table 5.8 shows the observed and expected frequencies and χ^2 values for slope hazards recorded on each of the five rock types in the three catchments. In the Sardu catchment, only Siwalik, phyllite and quartzite rocks crop out. A χ^2

FACTOR	CATEGORY	HAZARD RANK SCORES		
		SARDU K	LEOTI K	DHANKUTA K
ROCK	Siwalik	3	-	-
	Phyllite	2	3	-
	Quartzite	1	1	-
	Schist	-	0.5	3
	Gneiss	-	3	0
ASPECT	North	1	0	0
	South	2.5	2	3
	East	3	1.5	2.5
	West	1	1	0
	Northwest	0	0.5	1.5
	Northeast	2	0.5	1
	Southeast	2	3	0.5
	Southwest	0	2.5	2
PHYSIOGRAPHY	Incised Flank	3	3	3
	Steep Tributary	2	3	-
	Normal	1	1	1
LAND USE	Scrub	Not significant	3	3
	Agriculture	"	2	1
	Forest	"	1	2
SLOPE ANGLE	$0-15^{o}$ $16-30^{o}$ $31-45^{o}$ $46-60^{o}$ $>60^{o}$	Not significant (see text)		
DRAINAGE ORDER	First Second Third Fourth Fifth	Hazard scores not computed (see text)		

TABLE 5.7 Summary of Hazard Rank Scores Assigned to the Significant Factor Categories

value of 6.5 (χ^2 critical = 6.0) indicates that there is a significant difference between the susceptibility of these rock types to instability. The O/E values suggest that slopes developed on Siwalik rocks and quartzite, in this catchment, are the most and least susceptible, respectively. Consequently, hazard rating scores of 3, 2 and 1 have been assigned to slopes underlain by Siwaliks, phyllites and quartzites respectively (Table 5.7).

	SIWALIK	PHYLLITE	QUARTZITE	SCHIST	GNEISS	χ^2	χ^2 Crit
SARDU KHOLA O	50.0	35.0	3.0	-	-		
E	42.3	41.7	9.0	-	-		
$(O-E)^2/E$	1.4	1.1	4.0	-	-	6.5	6.0
O/E	1.2	0.8	0.3	-	-		
LEOTI KHOLA O	-	123.0	12.0	13.0	34.0		
E	-	90.4	25.3	43.3	22.9		
$(O-E)^2/E$	-	11.8	7.0	21.2	5.4	45.4	7.8
O/E	-	1.4	0.5	0.3	1.5		
DHANKUTA KHOLA O	-	-	-	67.0	26.0		
E	-	-	-	40.4	52.6		
$(O-E)^2/E$	-	-	-	17.5	13.5	31.0	3.8
O/E	-	-	-	1.7	0.5		

Table 5.8 Chi Squared Statistics for Slope Hazard Frequencies on Rock Types

In the Leoti catchment, a χ^2 value of 45.4 (χ^2 critical = 7.8) indicated that the outcropping phyllites, quartzites, schists and gneisses differ significantly in their susceptibility to slope hazards. On the basis of the O/E values, gneisses and phyllites appear to be the most susceptible rock types to instability, with approximately equal ratio values, while quartzites and schists are the least susceptible. Slopes underlain by gneisses and phyllites were assigned hazard scores of 3, while quartzite and schist slopes were given values of 1 and 0.5 respectively.

In the Dhankuta catchment, slopes are underlain by either schistose or gneissic rocks. Again, a χ^2 value of 31 (χ^2 critical = 3.8) indicates that there is a significant difference between the slope hazard susceptibility of these rocks. O/E values for schist (1.7) and gneiss (0.5) suggest that slopes underlain by the former are far more susceptible to instability than those underlain by the latter and, consequently, hazard rating scores of 3 and 0 were assigned to each rock type, respectively. The difference between the hazard rating for gneiss in the Dhankuta and Leoti catchments probably reflects the marked decrease in the September 1984 storm rainfall in a northerly direction (from the schist to the gneiss slopes) in the former catchment, and the fact that the gneiss in this catchment outcrops, generally, on more shallowly inclined slopes that tend to be more stable.

iii) Channel Proximity

Of the total number of slope hazards recorded in the Sardu (94), Leoti (182) and Dhankuta (93) catchments, 96, 79 and 85 percent, respectively, occurred on slopes immediately adjacent to a stream channel. These figures probably reflect the importance of slope oversteepening and undercutting by channel erosion in the initiation of slope erosion and instability. This is supported by the work of Martin (1978), who has found undercut slopes to be more susceptible to instability than others. By overlaying the drainage network factor maps (Figures 5.2 and 5.3) onto the cellular grid (Figures 5.6 and 5.7), the frequency of stream orders occupying grid cells with slope hazards was determined. This yielded the observed frequency of slope hazards in proximity to channel orders.

Table 5.9 displays the observed and expected frequencies and χ^2 values for the channel order factor for each catchment. Separate analyses have also been undertaken with the slope hazard data base divided according to rock type (Table 5.9). The data in this table indicate that the distribution of slope hazards in the Sardu Khola catchment is not significantly associated with the distribution of the four stream orders. However, in the Leoti and Dhankuta Khola catchments, the χ^2 values are higher than the critical values at the 95 percent significance level. In the former catchment, the O/E ratios suggest that slopes flanking second and fourth order channels are more prone to

	DRAINAGE ORDER						
	FIRST	SECOND	THIRD	FOURTH	FIFTH	χ^2	χ^2_{crit}
SARDU K							
SIWALIKS O	43	18	14	9	---		
E	48.2	17.6	8.5	9.8	---		
$(O-E)^2/E$	0.6	0.0	3.6	0.1	---	4.5	7.8
PHYLLITE O	26	25	10	---	---		
E	31.2	22.0	7.8	---	---		
$(O-E)^2/E$	0.7	0.4	0.6	---	---		
QUARTZITE O	---	---	---	---	---		
ALL ROCK							
TYPES O	69	43	24	9	---		
E	79.4	39.6	16.3	9.8	---		
$(O-E)^2/E$	1.4	0.3	3.6	0.1	---	5.4	7.8
O/E	---	---	---	---	---		
LEOTI K							
PHYLLITE O	53	54	18	21	---		
E	69.0	38.3	19.3	19.3	---		
$(O-E)^2/E$	3.7	6.4	0.1	0.1	---	10.3	7.8
O/E	0.8	1.4	0.9	1.1			
QUARTZITE O	10	4	0	4	---		
E	11.9	4.5	0.3	1.3	---		
$(O-E)^2/E$	NA	NA	NA	NA	---	NA	NA
SCHIST O	9	6	1	1	---		
E	10.6	4.5	1.4	0.4	---		
$(O-E)^2/E$	NA	NA	NA	NA	---	NA	NA
GNEISS O	32	23	10	1	---		
E	37.5	18.5	9.5	0.5	---		
$(O-E)^2/E$	NA	NA	NA	NA	---	NA	NA
ALL ROCK							
TYPES O	104	87	29	27	---		
E	129	65.8	30.5	21.5	---		
$(O-E)^2/E$	4.8	6.8	0.1	1.4	---	13.1	7.8
O/E	0.8	1.3	0.9	1.2	---		
DHANKUTA K							
SCHIST O	38	26	9	3	15		
E	50.7	21.7	8.0	2.7	8.0		
$(O-E)^2/E$	3.2	0.8	0.1	0.0	6.1	10.2	9.5
O/E	0.7	1.2	1.1	1.1	1.9		
GNEISS O	11	13	6	6	0		
E	22.9	6.9	6.9	2.6	0.1		
$(O-E)^2/E$	NA	NA	NA	NA	NA	NA	NA
ALL ROCK							
TYPES O	49	39	15	9	15		
E	73.6	28.6	14.9	5.3	8.1		
$(O-E)^2/E$	8.2	3.8	0.0	2.6	5.9	20.5	9.5
O/E	0.7	1.4	1.0	1.7	1.8		

TABLE 5.9 Chi-Squared Statistics for Slope Hazard Frequencies on Slopes Drained by the Five Stream Orders Identified in the Study Area.

instability than others, while in the latter catchment, slopes adjacent to fifth, fourth and second order channels are the most susceptible. While the significance of second order streams is difficult to explain, the tendency for slope hazards to occur in proximity to streams of higher order, may be explained by the fact that these larger streams are usually flanked by steep incised lower valley side slopes, that are often the locations of instability (see (vi) below). When the slope hazard data base was divided according to rock type (Table 5.9), the χ^2 values obtained were generally less than the critical values. Only in the cases of phyllite and schist slopes in the Leoti and Dhankuta Khola catchments, respectively, was the slope hazard distribution significantly associated with stream order. In both cases, the χ^2 values were only marginally significant at the 95 percent level. In the Dhankuta Khola catchment, the highest value of O/E (1.9), for fifth order channels underlain by schist, may be due to the fact that the lower Dhankuta Khola is the only fifth order channel in the catchment, and is flanked by oversteepened and unstable lower valley side slopes.

It would seem then, that while there is a significant association between the distribution of slope hazards and stream orders, this association may be indirect and dependent upon the relationship between catchment physiography and the slope hazard distribution (discussed below). Therefore, so as not to duplicate the physiographic variable in the analysis, stream order has not been used in the compilation of the hazard zonation maps.

iv) Slope Aspect

Table 5.10 shows that the χ^2 values for this factor were considerably greater than the critical values at the 95 percent significance level, in all three catchments, indicating that slope aspect plays an important role in the distribution of slope hazards. However, the slope aspects most susceptible to instability show some variation between catchments. Those most susceptible are the easterly and southerly aspects in the Sardu Khola, southeasterly, southwesterly and southerly aspects in the Leoti Khola and southerly, easterly and southwesterly aspects in the Dhankuta Khola. Hazard rating scores (Table 5.7) have been assigned to each category in the three catchments, according to the O/E values shown on Table 5.10.

		SLOPE ASPECT									
		NORTH	NORTH EAST	EAST	SOUTH EAST	SOUTH	SOUTH WEST	WEST	NORTH WEST	χ^2	χ^2_{crit}
SARDU K	O	6	8	22	20	17	9	8	4		
	E	8	9.1	10	21.8	8.3	17.6	11.8	7		
	$(O-E)^2/E$	0.5	0.1	14.4	0.2	10.1	4.5	1.3	1.3	32.4	14.1
	O/E	0.7	0.9	2.2	0.9	2.0	0.5	0.7	0.6		
LEOTI K	O	10	14	18	35	36	38	19	12		
	E	32.6	23.1	14.2	15.6	24.7	21.8	28.9	20.6		
	$(O-E)^2/E$	15.7	3.6	1.0	24.1	5.2	12.0	3.4	3.6	68.6	14.1
	O/E	0.3	0.6	1.3	2.2	1.5	1.7	0.7	0.6		
DHANKUTA K	O	1	17	12	16	14	20	9	4		
	E	3.5	17.3	5	23.7	3.3	14.7	21.8	3.5		
	$(O-E)^2/E$	1.3	0.0	9.8	2.7	40.3	1.7	7.7	0.3	63.8	14.1
	O/E	0.3	1.0	2.4	0.7	4.3	1.4	0.4	1.1		
TOTAL	O	17	39	52	71	67	67	36	20		
	E	41.3	53.9	26.6	60.9	33.6	55.0	68.3	29.1		
	$(O-E)^2/E$	14.3	4.1	24.2	1.7	33.2	2.6	15.3	2.8	98.2	14.1
	O/E	0.4	0.7	1.9	1.2	2.0	1.2	0.5	0.7		

TABLE 5.10 Chi-Squared Statistics for Slope Hazard Frequencies According to Slope Aspect.

The concentration of hazards on southerly (including southwesterly and southeasterly) facing slopes is probably due to their exposure to the dominant rain direction, as discussed in Section 5.3. It would appear that the regional northerly dip has relatively little influence on the distribution of these slope hazards. This may be explained by the often highly disturbed and weathered nature of most rocks at outcrop, causing local variations in dip direction and, more importantly, rendering slope materials so potentially unstable that they fail if oversteepened and/or subjected to rapid rises in groundwater or increases in soil moisture. However, dip direction may become significant in the location of more deep-seated instability (Section 5.4.5).

v) Slope Inclination

The slope steepness category maps (Figures 5.6 and 5.7) depict five categories of slope inclination (0 - 15°, 16-30°, 31-45°, 46-60° and over 60°). Using these slope category maps, the frequency of slope hazards occurring in each slope steepness category was determined on a grid cell basis. The expected frequencies were calculated by multiplying the total number of slope hazards in each catchment, by the proportion of the catchment area occupied by each slope steepness category. Without exception, the χ^2 values obtained were less than the critical values (Table 5.11), and consequently, the distribution of slope hazards is not significantly associated with the slope category of the grid cells. The χ^2 values were not significantly increased when the data file was divided according to rock type (Table 5.11). This almost certainly reflects the high variability of slope steepness likely to occur within each cell, as already discussed in Section 5.4.3.1, and the arbitrary choice of slope category classes. This problem might be overcome by reducing the size of the slope angle sampling units (grid cells) or by designing the sampling strategy to be more representative of slope morphology. Had average slope inclination been determined for slope elements identified by morphological mapping from air photographs, the relationship between slope inclination and slope hazard distribution might have been more meaningful.

vi) Physiography

The χ^2 data in Table 5.12 indicate that, for all three catchments, there is a significant tendency for slope hazards to occur on incised valley flanks. In the Sardu catchment, O/E values decrease from 2.9 for incised flanks, through 1.1,

	SLOPE CATEGORY (DEGREES)						
SARDU K	0-15	16-30	31-45	46-60	>60	χ^2	χ^2_{crit}
PHYLLITE O	3	17	24	8	1		
E	2.5	17.2	20.8	10.3	2.1		
$(O-E)^2/E$	0.1	0.0	0.5	0.5	0.6	1.7	9.5
QUARTZITE O	0	0	2	0	1		
E	NA	NA	NA	NA	NA		
$(O-E)^2/E$	NA	NA	NA	NA	NA	NA	
SIWALIK O	1	19	38	6	0		
E	5.6	19.6	28.8	7.6	2.4		
$(O-E)^2/E$	3.8	0.0	2.9	0.3	2.4	9.4	9.5
ALL ROCK TYPES O	4	36	64	14	2		
E	5.7	36.8	49.6	17.3	4.5		
$(O-E)^2/E$	0.5	0.0	4.2	0.6	1.4	6.7	9.5
LEOTI K							
PHYLLITE O	7	37	52	18	4		
E	8.8	38.7	50.9	16.6	2.8		
$(O-E)^2/E$	0.4	0.1	0.0	0.1	0.5	1.1	9.5
SCHIST O	1	2	8	3	0		
E	0.6	4.9	6.9	1.6	0.1		
$(O-E)^2/E$	NA	NA	NA	NA	NA	NA	
QUARTZITE O	2	5	5	5	0		
E	1.9	4.3	7.0	1.8	0.6		
$(O-E)^2/E$	NA	NA	NA	NA	NA	NA	
GNEISS O	1	20	27	11	0		
E	0.7	15.5	33.9	8.5	0.4		
$(O-E)^2/E$	0.1	1.3	1.4	0.7	0.4	3.9	9.5
ALL ROCK TYPES O	11	64	92	37	4		
E	12	63.4	98.7	28.5	3.9		
$(O-E)^2/E$	0.1	0.0	0.4	2.5	0.0	3.1	9.5
DHANKUTA K							
SCHIST O	8	31	20	12	3		
E	9.3	33.0	21.8	7.8	1.5		
$(O-E)^2/E$	0.2	0.1	0.1	2.3	1.5	4.2	9.5
GNEISS O	0	10	9	2	0		
E	1.8	13.3	4.7	1.1	0.1		
$(O-E)^2/E$	1.8	0.8	3.9	0.7	0.1	7.3	9.5
ALL ROCK TYPES O	8	41	29	14	3		
E	11.1	46.3	26.5	8.9	1.6		
$(O-E)^2/E$	0.9	0.6	0.2	2.9	1.2	5.8	9.5

TABLE 5.11 Chi-Squared Statistics for Slope Hazard Frequencies According to Slope Inclination Category.

		NORMAL	INCISED	STEEP TRIBUTARY FLANK	χ^2	χ^2_{crit}
SARDU K	O	11	27	56		
	E	32.5	9.3	52.2		
	$(O-E)^2/E$	14.2	33.7	0.2	48.1	6.0
	O/E	0.3	2.9	1.1		
LEOTI K	O	69	28	81		
	E	115	16.4	46.6		
	$(O-E)^2/E$	18.4	7.3	26.4	52.1	6.0
	O/E	0.6	1.7	1.7		
DHANKUTA K	O	68	25	----		
	E	81.2	11.7	----		
	$(O-E)^2/E$	2.1	15.1	----	17.2	3.8
	O/E	0.8	2.1	----		

TABLE 5.12 Chi-Squared Statistics for Slope Hazard Frequencies According to Slope Physiography.

		AGRICULTURE	SCRUB	FOREST	χ^2	χ^2_{crit}
SARDU K	O	37	26	29		
	E	34.6	26.4	30.9		
	$(O-E)^2/E$	0.2	0.0	0.1	0.3	6.0
LEOTI K	O	58	70	54		
	E	59.9	47.5	74.4		
	$(O-E)^2/E$	0.1	10.6	5.6	16.3	6.0
	O/E	1.0	1.5	0.7		
DHANKUTA K	O	31	30	32		
	E	45	18.2	28.3		
	$(O-E)^2/E$	4.3	7.6	0.5	12.4	6.0
	O/E	0.7	1.6	1.1		

TABLE 5.13 Chi-Squared Statistics for Slope Hazard Frequencies According to Land Use.

for steep tributary valley sides, to 0.3 for 'normal', shallowly inclined slopes. Hazard rating scores of 3, 2 and 1 have been assigned to these three categories respectively. In the Leoti catchment, both incised flanks and steep tributary valley sides have O/E values of 1.7, and consequently these categories have been given hazard rating scores of 3. 'Normal', upper slopes, with an O/E value of 0.6 have been given scores of 1. In the Dhankuta catchment, where steep tributary valley-side slopes (as defined in Section 5.4.2) are absent, incised lower valley flanks and 'normal' slopes have O/E values of 2.1 and 0.8, respectively. These categories were assigned hazard rating scores of 3 and 1 on the basis of the large difference between the O/E values.

vii) Land Use

The observed and expected frequencies and χ^2 values for land use, the final contributory factor considered in this analysis, are shown in Table 5.13. The χ^2 values were significant only in the Leoti and Dhankuta catchments. In the former, slope hazards appear to be most common on scrubland (O/E = 1.5) and least common in forested areas (O/E = 0.7). In the Dhankuta catchment, however, while slope hazard vulnerability appears to be highest for scrubland (O/E = 1.6), it is lowest for agricultural land (O/E = 0.7). In the Dhankuta catchment, the seemingly greater susceptibility of forested areas to slope hazards, may reflect the fact (discussed in Section 5.4.2) that Chir pine tends to be a pioneering tree species on bare ground, and is consequently associated with a poorly developed understorey and a potential for slope erosion.

On the whole, agricultural land is no more susceptible to slope hazards than is forest or scrubland. In fact, in the Sardu catchment, these three land uses have approximately equal O/E values. However, much of the scrubland identified in the study area, is likely to be abandoned, overcultivated or overgrazed farmland. In addition, the majority of the agricultural land occupies shallowly inclined ground on terraces, elevated fan surfaces and interfluve slopes, where the potential for slope hazards is relatively low. The hazard rating scores assigned to each of the land use categories in the Leoti and Dhankuta catchments, are shown on Table 5.7.

A final point worthy of mention, is that while land currently being cultivated is relatively stable, irrigation and overgrazing of land adjacent to farm holdings may initiate and accelerate instability on the slopes below. In order

to test this contention, the land use immediately upslope of each slope hazard was recorded. In all three catchments, agriculture formed the most common land use upslope of these hazards, accounting for 64, 45 and 55 percent of cases in the Sardu, Leoti and Dhankuta Khola catchments, respectively.

5.4.4 Compilation of the Slope Hazard Zonation Maps

By superimposing the boundaries of the four significant factor maps (rock type, slope aspect, physiography and land use) and summing the hazard rating scores for each overlapping factor category, hazard zonation maps were produced for the three catchments (Figures 5.12, 5.13 and 5.14). The factor categories were given equal weighting in the summation procedure. The summed hazard indices were renumbered from 1 to a maximum of 20 in order to remove half-numbered indices. The hazard indices, derived for the three catchments, are expressed below as functions of the significant contributory factors.

Catchment	Hazard Function
Sardu Khola	H = RAPh
Leoti Khola	H = RAPh L
Dhankuta Khola	H = RAPh L

where H is compound hazard index
R is rock type
A is slope aspect
Ph is physiography
and L is land use

The hazard zonation maps comprise a total of twenty hazard indices in both the Leoti and Dhankuta catchments and ten in the Sardu catchment. These maps enable visual interpretation of the distribution of hazard index, although comparisons between catchments are not possible as the hazard ratings were derived from different data sets. In the Sardu catchment, the distribution of hazard zones appears to be random, although two of the highest zones (hazard zone 10) occur along the steepened eastern bank of the Sardu Khola, while all cases of hazard zone 1, and most of hazard zone 2, occur along the Sangure

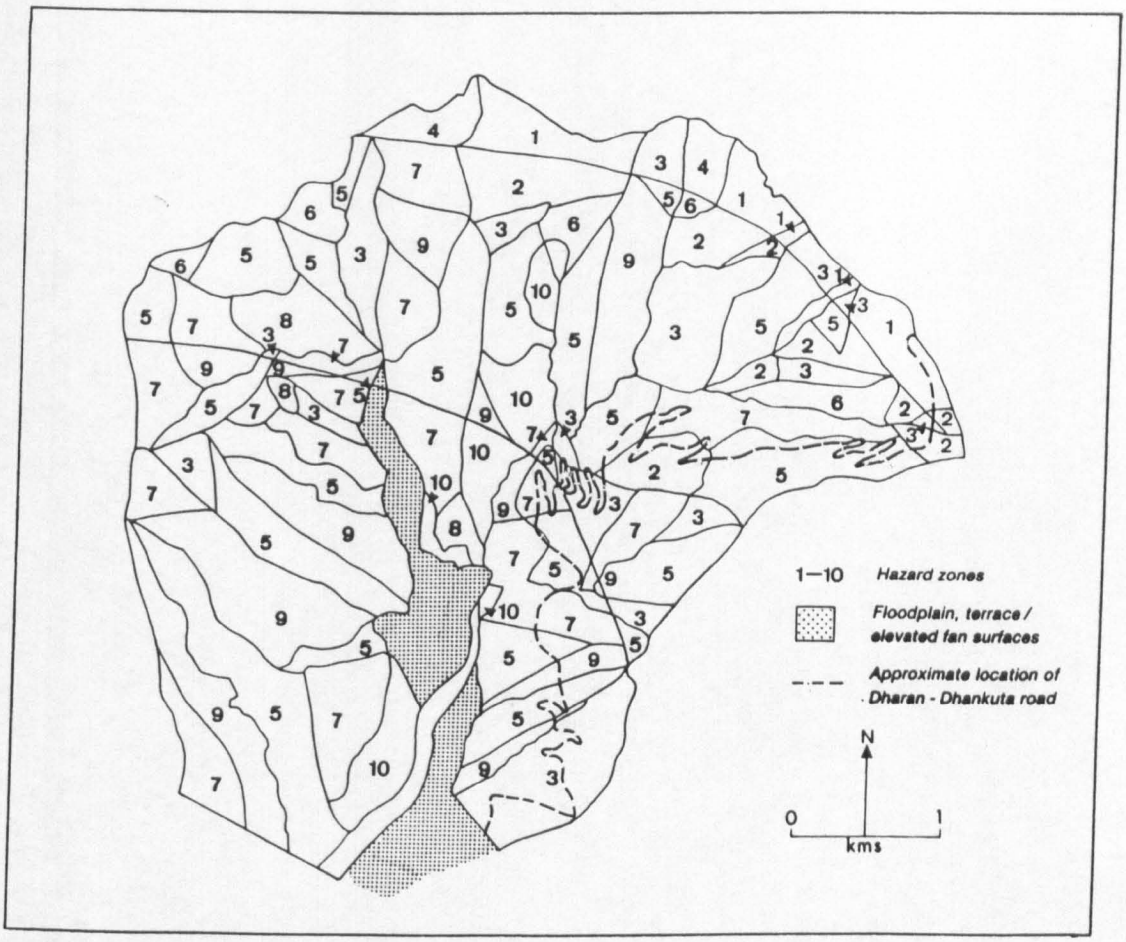

FIGURE 5.12 Slope Hazard Zonation Map for the Sardu Khola Catchment.

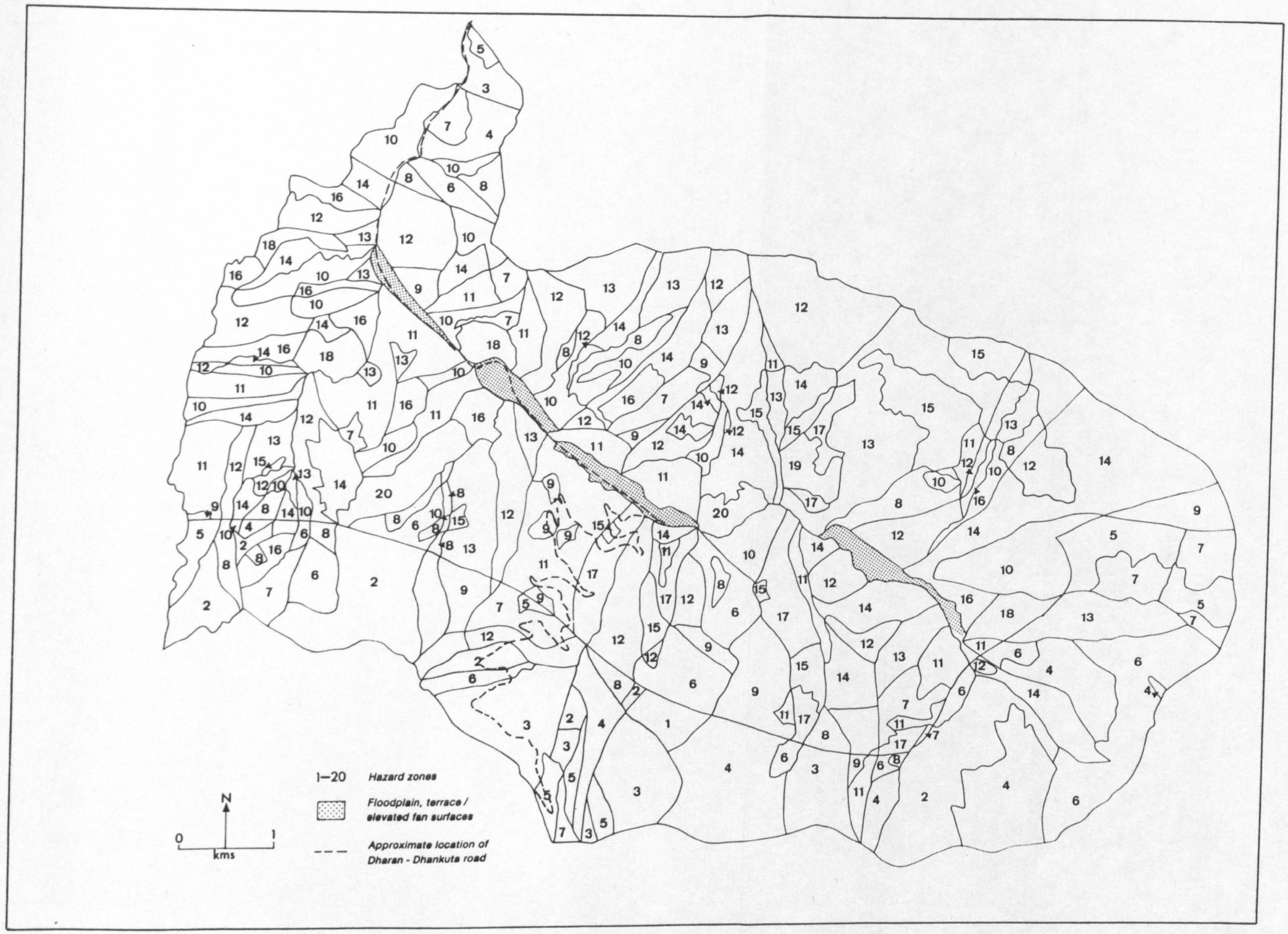

FIGURE 5.13 Slope Hazard Zonation Map for the Leoti Khola Catchment.

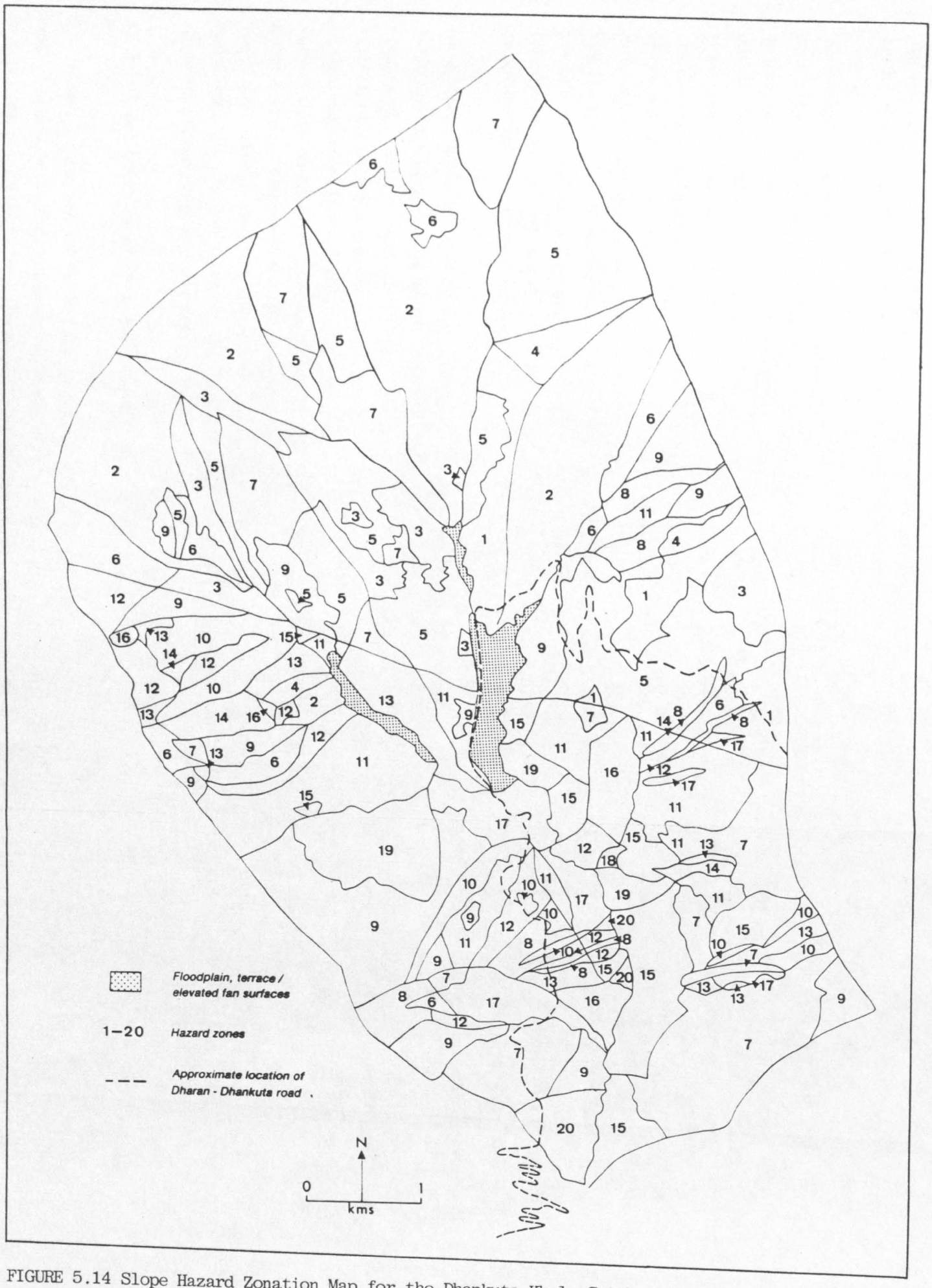

FIGURE 5.14 Slope Hazard Zonation Map for the Dhankuta Khola Catchment.

Ridge. In the Leoti Khola catchment, the distribution of hazard index is, again, relatively random. However, the southern and eastern slopes of the catchment, that form the northern flanks of the Sangure Ridge, are mostly low hazard zones. Most of the highest hazard zones in the Dhankuta catchment, occur on the incised flanks of the lower Dhankuta Khola, developed in schist.

Interestingly, most of the terrain crossed by the hill section of the Dharan-Dhankuta road (Figures 5.12, 5.13 and 5.14) is of relatively low hazard index. In the Sardu catchment, the majority of the road crosses hazard zones 3 to 7; in only two cases is hazard zone 9 encountered, and one of these is where the road failed in 1984 at km 3.900. On its descent to the Leoti Khola floodplain, the road crosses hazard zones ranging between 2 and 17, although the majority of its length is constructed in hazard zones 3 and 11. Figure 5.14 demonstrates the manner in which the road traverses the less hazardous slopes (hazard zones 7 to 13) above the unstable Dhankuta Khola gorge (hazard zones 9 to 20). These observations lend support to the success of the reconnaissance surveys in identifying slopes most prone to instability in the area, for alignment design purposes (Chapter 4).

By contrast, in the Sardu catchment the COALMA line (see Chapter 4) crosses relatively high hazard zones (hazard zones 7 to 9) on the western flanks of the catchment. In the Leoti catchment, the COALMA line crosses slopes of moderate hazard (hazard zones 3 to 17) on its descent from the Sangure Ridge to the headwaters of the Leoti Khola, while the remainder of the route to the Tamur River confluence is across slopes of generally higher hazard (hazard zones 7 to 20). Finally, in the Dhankuta catchment, the COALMA line crosses the higher hazard zones on the slopes immediately above the gorge. In conclusion, the decision to reject the COALMA line, in favour of the final alignment, is supported by these data.

5.4.5 Representability of the Slope Hazard Zonation Maps

The hazard indices derived above have no absolute value, and can be used in only comparative terms within each of the three catchments. While the hazard zonation developed here probably represents the most feasible method that could have been used in the study area, given the unavailability of more detailed geological, geotechnical and hydrological data, it nevertheless suffers from two main limitations. First, rainfall intensity and duration are likely to

have varied spatially within the three catchments, and this could not be taken into account in the analysis. Second, spatial covariance between contributory factors, such as between land use and physiography and rock type and physiography, may have led to spurious and duplicated associations between the dependent and some of the independent (factor) variables. For this reason, stream order was not used in the hazard map compilation. Interdependency among some of the factors means that the true influence of any one factor, on the distribution of slope hazards, is difficult to gauge. Owing to the limited data available, it is not possible to examine the influence of each factor separately, by keeping all other factors constant, and therefore this problem cannot be resolved here.

In order to test the representability of the hazard indices (Figures 5.12, 5.13 and 5.14), in explaining the distribution of slope hazards, the hazard densities (number of occurrences per km^2) in each hazard zone were computed and compared statistically with the hazard index rating, using the Spearman's rank correlation test. The results of this test are shown in Table 5.14. In all three catchments, the correlation coefficients obtained were significant at the 99 percent level, indicating that the null hypothesis, that there is no significant correlation between hazard density and hazard index, can be rejected. Interestingly, the lowest correlation coefficient ($r = +0.658$) was obtained for the Dhankuta catchment, where the concentration of storm rainfall in the southern portion of the catchment is likely to have had a significant influence on the distribution of instability. Although the high significance levels obtained partly reflect the fact that the hazard zone scores are based on slope hazard density, the correlation test supports the factor mapping method adopted.

While the hazard zonation maps are likely to be representative of the distribution of slope hazards in the study area, the success of the technique must depend ultimately on its ability to predict the distribution of slope hazards outside the study area. As there are no data available concerning the distribution of slope hazards in adjacent catchments, following the September 1984 storm, this assessment could not be undertaken. Nevertheless, it is contended here that the technique of slope hazard zonation developed in this chapter should be broadly applicable to similar catchments in the Lower Himalaya. Slope hazard zonation, undertaken in steep catchments flanking the Sangure Ridge, might profitably adopt a strategy similar to that developed for

LEOTI CATCHMENT				DHANKUTA CATCHMENT				SARDU CATCHMENT			
HAZARD RANK	ZONE AREA(km²)	No OF SLOPE HAZARDS	HAZARD DENSITY/km²	HAZARD RANK	ZONE AREA(km²)	No OF SLOPE HAZARDS	HAZARD DENSITY/km²	HAZARD RANK	ZONE AREA(km²)	No OF SLOPE HAZARDS	HAZARD DENSITY/km²
1	0.25	0	0.00	1	1.66	1	0.60	1	0.68	0	0.00
2	3.19	10	3.13	2	7.65	8	1.04	2	0.86	1	1.17
3	2.37	5	2.10	3	1.80	0	0.00	3	1.86	7	3.77
4	3.84	4	1.04	4	0.60	0	0.00	4	0.14	0	0.00
5	1.40	2	1.43	5	6.09	3	0.49	5	4.29	17	3.96
6	3.25	4	1.23	6	1.53	7	4.58	6	0.40	4	9.93
7	2.13	6	2.81	7	5.82	6	1.03	7	2.60	22	8.44
8	1.64	7	4.27	8	0.58	5	8.57	8	0.38	6	15.83
9	1.74	4	2.30	9	3.78	5	1.58	9	2.33	46	19.74
10	3.34	13	3.88	10	1.11	7	6.29	10	0.77	16	20.76
11	4.10	12	2.92	11	2.90	9	3.10				
12	5.94	26	4.33	12	1.34	9	6.70				
13	4.81	27	5.61	13	1.01	6	5.99				
14	5.89	35	5.94	14	0.39	1	2.57				
15	1.66	12	7.20	15	1.90	12	6.30				
16	1.62	9	5.57	16	0.67	1	1.48				
17	1.30	9	6.69	17	1.13	11	9.75				
18	0.82	9	10.97	18	0.05	1	21.11				
19	0.28	6	21.40	19	1.18	8	6.78				
20	0.78	9	12.29	20	0.44	1	2.29				

r =+0.916, rcrit=0.534

r =+0.658, rcrit=0.534

r =+0.940, rcrit=0.746

TABLE 5.14 Number and Density of Slope Hazards in Each Hazard Zone.

the Sardu and Leoti catchments, while the method used in the Dhankuta catchment is most applicable to relatively subdued topography, underlain by gneissic bedrocks. This topography is characteristic of much of the gneissic terrain of east Nepal. Catchment-based studies are probably the most convenient for undertaking the analysis as they form self-contained and manageable units. The success of the technique, when applied to other areas, will depend on the availability of geological maps and air photographs of sufficient scale and quality. In Nepal, these data sources exist for most areas, while in India, however, air photographs are usually restricted in border regions.

The data analysis, presented in this chapter, has made no differentiation between slope hazard mechanisms. As discussed in Section 5.2.1, slope erosion and shallow instability features are usually only short-term phenomena and have a relatively low to moderate impact on roads in the area (Chapter 2). Most of the slope hazards in the data base are of this type. Large, deep-seated, but usually low frequency mass movements often have the highest, most lasting and costly impact on road stability. Consequently, these mass movements deserve special consideration.

The locations of the more deep-seated, high magnitude slope hazards, namely deep-seated rock slides, rotational slides, mudslides and eroding catchments, as mapped from 1 : 25 000 air photographs, are shown on Figures 5.2 and 5.3. Unfortunately, they are too few in number to allow any statistical analysis of their distribution. In the Dhankuta Khola catchment (Figure 5.3), two mudslides (M1 and M2) are located on the western, northeast facing, flanks of the Dhankuta Khola gorge, formed in schist. A deep-seated rock slide (R1) is also located on the engorged lower valley flanks of the catchment, and this has a northwesterly aspect. A large slope erosion/mudslide complex (EM1) occurs on the north facing slopes in the centre-west of the catchment (Plate 5.4), also formed in schist. These features occur on steep slopes in proximity to the Dhankuta Thrust (Figure 3.4), and where bedrocks are likely to be dipping predominantly out of the slope.

In the Leoti Khola catchment (Figure 5.2), large-scale instability features identified comprise of a slope erosion/debris flow complex (ED1) on the northern valley flanks (Plate 5.5), a large, linear erosion feature (E1) on the northerly facing headwater slopes, a possible mudslide (M3) on relatively

PLATE 5.4 Eroding Mudslide Sub-Catchment on the North Facing Slopes of the Dhankuta Khola.

PLATE 5.5 Highly Unstable Debris Flow Catchment on the Northeast Flanks of the Leoti Khola.

PLATE 5.6 Large Eroding Catchment on the West Facing Slopes of the Sardu Khola.

shallowly inclined headwater slopes, two large slope erosion features (E2 and E3) on the southern flanks and two mass movement/slope erosion catchments (EC1 and EC2) on the western flanks (Plate 3.8), close to the R.Tamur confluence. Much of this instability occurs on slopes with a northerly aspect, similar to that of the regional bedrock dip, and in proximity (in the cases of ED1, E1, EC1 and EC2) to the Mulghat Thrust (Figure 3.4).

In the Sardu Khola catchment, three rotational slides (Rn1, Rn2 and Rn 3), one large slope erosion feature (E4, Plate 5.6) and three deep-seated rock slides (R2, R3 and R4) have been identified (Figure 5.2). All but R4, a relic feature identified by the 1975 geomorphological reconnaissance survey (Chapter 4), are active. With the exception of R3, all features occur in Siwalik rocks, that are often highly weathered, and are close to the Main Boundary Thrust. Rn2, Rn3, R2 and R3 are located along the Dharan-Dhankuta road, and may have been initiated or accentuated, in part, by road construction (Chapter 6).

In conclusion, while the initiation of shallow instability may be controlled largely by rainfall intensity, soil and rock permeability, slope angle and degree of undercutting, deeper-seated instability in the study area may, on the whole, be more dependent on bedrock structure in relation to slope aspect and inclination. This would suggest that slopes with northerly aspects may be more prone to deeper instability, while southerly facing slopes appear to be the locations of shallow instability. Clearly, while more data is required to substantiate this observation, it has important implications for landslide hazard mapping and road alignment design in the study area. An additional consideration, that should be borne in mind when undertaking a landslide hazard mapping exercise for route alignment purposes, is the likely impact that road construction will have on hazard severity. This is discussed below.

5.5 Impact of Road Construction on Terrain Hazards: Implications for Hazard Mapping and Preliminary Design

5.5.1 Introduction

In steep terrain, slope disturbance by road construction may initiate or accelerate slope instability and erosion (Hearn 1987). The impact of this disturbance can be subdivided into on-road and off-road categories. These

hazards are reviewed and illustrated in Chapter 2. It is proposed to analyse these hazards in this section of the chapter, and discuss their implications for hazard assessment at the reconnaissance stage of road projects and for design in general.

5.5.2 On-Road Hazards

i) Cut Slope Failure

Factors that control cut slope stability include the shear strength, porosity and permeability of the slope material, the dip, orientation and frictional strength of structural discontinuities, groundwater conditions, cut slope inclination and height, and the success of any stabilization works employed. In addition, the stability of a cut slope, if oversteepened to failure, will tend to increase with time as it degrades through mass movement and erosion to the limiting angle of stability for the slope material. Cut slope design and slope stability assessment can only be satisfactorily achieved during earthworks when the engineering characteristics of slope materials at depth can be examined. There would appear to be little scope, therefore, for the prediction of cut slope failures prior to earthworks, except where excavations are planned in areas of known instability, or on slopes formed in deep, relatively uniform, soils that are likely to fail if oversteepened.

This section briefly examines the impact that cut slope failures have had on the Dharan-Dhankuta road. This is illustrated by reference to the distribution and volume of cut slope failures recorded along the road during May to August 1983, some 3 to 7 years after earthworks. Cut slope failure during earthworks often caused problems for vehicle access along the road and created large volumes of spoil material. In addition, failure often led to short-term progressive instability on the slopes above. By 1983, 5 to 7 years after the commencement of earthworks from Dharan, the majority of cut slopes along the Dharan to Sangure Ridge section of the road had become vegetated and apparently stable. To the north of the Sangure Ridge, cut slope failures have occurred during storm rainfall, but these have had very little impact on the road (the largest resulted in road closure for only half a day).

During the 1983 monsoon season, the distribution and volume of cut slope failures along the Dharan-Dhankuta road were determined in order to examine

the influence of rock type and age of cutting on stability. The width, depth and slope length of each failure were measured following each storm event in 1983. The total volume of cut slope failures occurring on each rock type was divided by the cut slope area to give a mean depth of failure (Table 5.15). Total slip volumes per storm event, occurring on each rock type, are also shown on this table. The three storms of July resulted in a total volume of 20 697 m^3 of slip material. The greatest total volume of cut slope failure occurred during the storm of 15 July, in cut slopes formed in schist, when a total volume of 8 441 m^3, with a mean rate of 675 m^3 per kilometre of cut slope length, was recorded. For the 1983 monsoon season as a whole, the failure rate for schist slopes amounted to 1 275 m^3/km.

To determine whether the observed distribution of cut slope failures was significantly influenced by rock type, a chi-squared (χ^2) test was used. With a null hypothesis that rock type plays no significant role in the distribution of cut slope failure, expected frequencies were calculated by multiplying the total number of failures recorded, by the proportion of the total road length of outcrop of the five rock types. The slope failure frequency data, for the three storms occurring in July 1983, satisfy the criteria of the test, and computed values of χ^2 are shown in Table 5.16. The χ^2 critical value, at the 95 percent significance level, is 9.49, and consequently the null hypothesis can be rejected for all three storms. Rock type would, therefore, appear to be a significant controlling factor in the distribution of cut slope failures along the road.

The O/E ratios, for these storms (Table 5.15), reveal that cut slopes formed in schist material were by far the most unstable. The maximum O/E value of 3.10, for the storm of the 24 July, suggests that during this event, schist cut slopes were more than three times as unstable as would have been expected had failures been evenly distributed amongst rock types. On the basis of the O/E values, cut slope failure susceptibility decreases from slopes formed in schists, through gneisses, Siwaliks/phyllites, to quartzites.

As a general rule, earthworks began at the Dharan end of the road, where Siwalik and phyllite rocks outcrop, and finished towards Dhankuta, in schists and gneisses. Consequently, cut slopes formed in the latter rock types are relatively young, and therefore may still be degrading, through mass movement and erosion, towards their threshold angle of stability. Cut slopes in Siwaliks and phyllites, on the other hand, would have had a far greater

DATE	SIWALIK				PHYLLITE				QUARTZITE				SCHIST				GNEISS				TOTAL SLIP VOL(m^3)
	O*	E*	O/E	V/A*	O	E	O/E	V/A	O	E	O/E	V/A	O	E	O/E	V/A	O	E	O/E	V/A	
12.5.83	618.9	71.5	8.7	21.7	9.7	165.0	0.1	0.1	0.0	119.5	0.0	0.0	0.0	190.5	0.0	0.0	0.0	85.6	0.0	0.0	632.4
23.6.83	11.0	1.5	7.4	0.4	0.0	3.4	0.0	0.0	2.1	2.5	0.8	0.0	0.0	3.9	0.0	0.0	0.0	1.8	0.0	0.0	13.1
3.7.83	78.4	510.7	0.1	2.7	393.5	1179.6	0.3	6.0	0.9	854.2	0.0	0.0	3424.2	1361.2	2.5	45.2	622.3	611.9	1.0	18.3	4519.4
15.7.83	86.8	1335.1	0.1	3.0	2015.0	3083.8	0.6	30.7	0.0	2233.1	0.0	0.0	8441.0	3558.8	2.4	111.3	1234.2	1599.8	0.8	36.2	11815.5
24.7.83	0.0	492.9	0.0	0.0	0.0	1138.5	0.0	0.0	0.0	824.4	0.0	0.0	4078.9	1313.8	3.1	53.8	283.1	590.6	0.5	8.3	4362.0
9.8.83	7.8	1.3	5.9	0.3	0.0	3.1	0.0	0.0	4.0	2.2	1.8	0.1	0.0	3.5	0.0	0.0	0.0	1.6	0.0	0.0	11.7
Cut area	28 512.57m^2				65 708.57m^2				47 581.44m^2				75 816.86m^2				34 078.63m^2				251630.1

TABLE 5.15 Observed Versus Expected Cut Slope Failure Volumes According to Underlying Rock Type.

* O - Observed failure volume(m^3)

E - Expected failure volume(m^3) from Null Hypothesis

V/A- Failure volume/cut slope area($x10^{-3}$)

DATE	SIWALIK			PHYLLITE			QUARTZITE			SCHIST			GNEISS			TOTAL
	O	E	χ^2	O	E	χ^2	O	E	χ^2	O	E	χ^2	O	E	χ^2	χ^2
3.7.83	5	7.6	0.89	10	31.9	15.04	1	9.8	7.86	45	20.7	28.45	29	9.9	36.69	88.96
15.7.83	2	9.2	5.64	10	38.7	21.28	3	11.8	6.59	61	25.1	51.25	21	12.0	6.69	91.45
24.7.83	0	5.5	5.51	0	23.1	23.14	0	7.1	7.08	33	15.0	21.52	15	7.2	8.48	65.73

TABLE 5.16 Chi-Squared Statistics for Cut Slope Failure Frequencies According to Rock Type.

* χ^2-Chi-squared statistic.

period (up to seven years) to adjust to slope oversteepening and therefore may have regained stability by the time the 1983, survey was undertaken. The first heavy storms to follow the excavation of the schist and gneiss cut slopes occurred in 1983, and it is not surprising that large slip volumes were recorded during this period.

ii) Slope Failure from Below

Since the construction of the Dharan-Dhankuta road, slope failure causing road loss, or severe deformation, has occurred at four principal sites (Appendix 1). All four sites are located between Dharan and the Sangure Ridge, in slope materials developed in weathered Siwalik sediments and phyllite. At three of these sites, the creation of large spoil benches during earthworks could have contributed to slope failure in 1983 and 1984, when heavy rain may have given rise to exceptionally high groundwater levels and channel erosion below. Slope failure at these sites is discussed in Chapter 6, where a review is given of spoil disposal along Lower Himalayan roads, and the Dharan-Dhankuta road in particular. This form of construction-induced instability is, therefore, not discussed further here.

5.5.3 Off-Road Hazards

Construction-induced erosion and sediment hazards, caused by artificial slope drainage and spoil tipping, can often cause problems for land uses downslope, and may lead to culvert blockage and slope erosion on hairpin stacks (Chapter 6). The construction of the Godavari-Dandeldhura road in west Nepal, for instance, has resulted in an estimated 10 to 100 fold increase in the annual sediment load in some of the catchments crossed by the road (Kojan 1978). These off-road, construction-induced hazards, are discussed in Chapters 2 and 6 and Appendix 1, with illustrations from Lower Himalayan roads.

It is difficult to quantify the impact that road construction can have on the severity of erosion, sediment and mass movement hazards, as there are insufficient data available to allow differentiation between those hazards that are construction-induced and those that would have occurred naturally. As far as landslide hazard mapping at the route planning stage is concerned, the potential for off-road hazards can only be assessed by assuming that either the potential will increase with slope inclination, slope length or degree of

disturbance by road construction, or that these hazards are likely to be more common on slopes and in channels that are already unstable. Again, the final design of earthworks and slope and road drainage will ultimately control the location and severity of these hazards.

In order to identify whether slopes and drainage channels located below the Dharan-Dhankuta road, are more susceptible to instability than others in the area, the total numbers of slope hazards found in each of the sub-catchments of the Sardu and Leoti Kholas were calculated from the slope hazard data base, and expressed as densities per sub-catchment area. A comparison between the slope hazard densities of sub-catchments that are crossed by the road with those that are not, provides an indication of the impact of the road on stability. However, the results from such an analysis cannot be conclusive, as variations in slope hazard density are likely to reflect variable geology, slope inclination, soil conditions and rainfall, as much as the effects of road construction.

Table 5.17 lists the slope hazard densities (expressed as areal percentages) and the extent of road line (km/km^2) within each of the sub-catchments. Figure 5.15 shows a scattergram of these two variables. Sub-catchments 1 to 9 are located on the western and northern flanks of the Sardu Khola catchment (Table 5.17), and are not crossed by the Dharan-Dhankuta road. The remaining sub-catchments (10-15) occur on the eastern flanks of the Sardu catchment and, with the exception of sub-catchment 12, are crossed by the road. These sub-catchments have road lengths per unit area ranging up to 12.40 km/km^2 (Table 5.17). The four sub-catchments with the highest slope hazard percentages (15 (13.6%), 14 (6.7%), 11 (5.8%) and 13 (5.2%)) are all crossed by the road. In contrast, the three sub-catchments (25, 26 and 27) crossed by the Dharan-Dhankuta road on its descent from the Sangure Ridge to the Leoti Khola floodplain, have slope hazard percentages of only 1.08, 0.33 and 1.52, respectively (Table 5.17). These figures are less than the mean percentage of 1.8 for the seventeen sub-catchments located on the southern flanks of the Leoti Khola.

The contoured alignment of the Bhedetar-Rajarani road (BR on Table 5.17) crosses the headwater slopes of sub-catchments 29, and 31 to 34 on the southern and northeastern flanks of the Leoti catchment. The slope hazard percentages in these sub-catchments are 0.33, 1.32, 0.96, 1.97 and 3.00,

SUB CATCHMENT	MAIN CATCHMENT	AREA (km^2)	% AREA OCCUPIED BY SLOPE HAZARDS	ROAD LENGTH PER km^2 CATCHMENT AREA
1	W.Sardu	1.49	0.00	0.00
2	"	0.69	3.30	0.00
3	"	0.41	1.20	0.00
4	"	1.50	4.20	0.00
5	N.Sardu	0.60	0.00	0.00
6	"	1.89	3.10	0.00
7	"	0.98	4.10	0.00
8	"	1.48	1.90	0.00
9	"	0.96	0.50	0.00
10	E.Sardu	1.06	2.40	2.80
11	"	0.75	5.80	3.10
12	"	0.59	3.90	0.00
13	"	0.29	5.20	12.40
14	"	1.18	6.70	0.70
15	"	0.28	13.60	1.40
16	S.Leoti	0.41	7.40	0.00
17	"	0.95	6.42	0.00
18	"	0.56	5.00	0.00
19	"	0.35	0.73	0.00
20	"	1.17	0.00	0.00
21	"	1.82	0.00	0.00
22	"	2.80	0.82	0.00
23	"	2.28	0.89	0.00
24	"	2.10	0.00	0.00
25	"	1.64	1.08	4.69
26	"	1.53	0.33	1.57
27	"	0.67	1.52	1.49
28	"	1.62	1.57	0.00 *
29	"	1.52	0.33	1.15(BR)
30	"	1.81	2.38	0.00
31	"	4.24	1.32	0.53(BR)
32	"	5.30	0.96	0.10(BR)
33	N.Leoti	2.83	1.97	0.26(BR)
34	"	5.80	3.00	0.22(BR)
35	"	0.93	1.36	0.00
36	"	2.27	3.80	0.00
37	"	0.83	6.12	0.00
38	"	3.41	9.83	0.00
39	"	1.49	3.41	0.00
40	"	1.07	1.42	0.00
41	"	1.02	1.49	0.00
42	"	0.53	6.23	0.00
43	"	0.55	3.69	0.00
44	"	0.41	5.58	0.00

TABLE 5.17 Percentage Area of Slope Hazards and Road Line Density in Sub-Catchments of the Sardu and Leoti Kholas.

* BR denotes Bhedetar-Rajarani Road; remaining road line densities are for Dharan-Dhankuta Road.

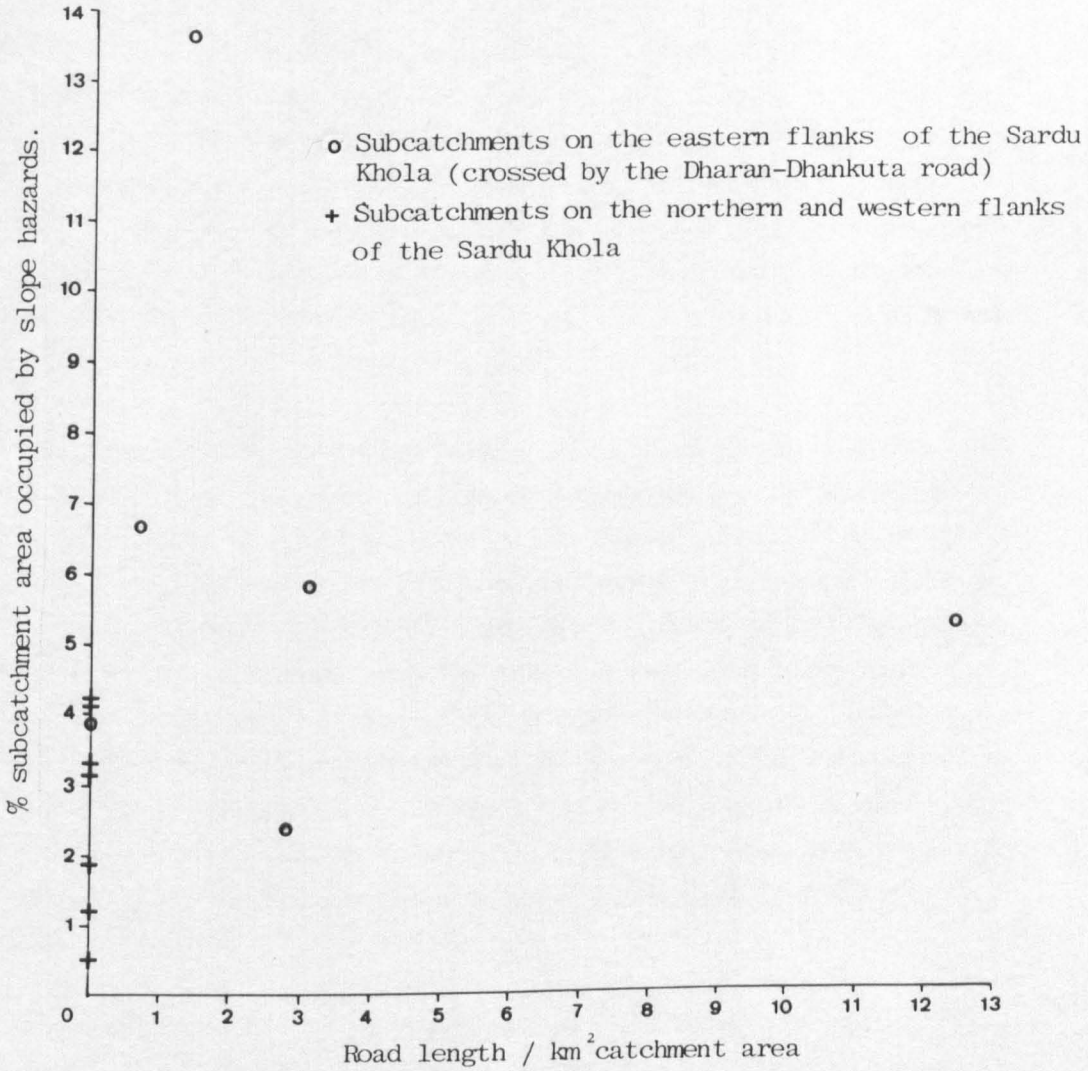

Figure 5.15 Slope Hazard Density Versus Road Length in Subcatchments of the Sardu Khola.

respectively. With the exception of sub-catchment 34, these percentages are less than the mean of 2.71 for all 29 sub-catchments of the Leoti Khola.

On the basis of these limited data, it appears that sub-catchments of the Sardu Khola that are crossed by the Dharan-Dhankuta road, have higher slope hazard percentages than those that have not been affected by road construction. The slopes crossed by the road in the Sardu Khola catchment are steep, and are composed of often weathered and highly erodible materials that have been susceptible to disturbance by road construction. Instability is also encouraged by the high rainfall on these slopes. Obviously,a much larger data base is required, enabling catchment variables of rock type and structure, slope inclination, rainfall intensity and soil erodibility to be held constant, in order to substantiate and quantify the impact of road construction on catchment stability.

In contrast, most of the sub-catchments of the Leoti Khola crossed by the Dharan-Dhankuta road on its descent to the floodplain, have comparatively low slope hazard percentages. Most of the descent to the floodplain is on moderately inclined and stable slopes, where rainfall tends to be lower than in the Sardu catchment (Chapter 3). Consequently, the impact of the Dharan-Dhankuta road on catchment stability may have been lower in the Leoti than the Sardu catchment. In the sub-catchments traversed by the Bhedetar-Rajarani road, the slope hazard percentages are slightly higher than those for sub-catchments crossed by the Dharan-Dhankuta road on its descent to the floodplain. This may reflect the greater degree of slope disturbance by spoil tipping along the former road (Chapter 6) and the generally steeper catchment slopes encountered.

A final point, worthy of mention here, is the positive effect that road construction may sometimes have on slope stability. Extensive slope drainage and erosion protection works may actually lead to increased stability. This may have been the case in the unstable bowl (Appendix 1 A.6) on the descent to the Leoti Khola floodplain, where the apparent continued stability of many of the relic landslides and colluvial deposits may be due, in part, to successful remedial measures (Chapter 4).

5.6 Landslide Hazard Mapping for Highway Design

In this chapter, medium-scale landslide hazard assessment has been examined using two different approaches. First, statistically-based techniques, that

compare observed slope hazard distributions with measurable terrain variables on a grid cell basis, have been found to be largely unsuccessful. This methodology requires data collected on an interval scale, and of a quality that cannot be easily attained from air photograph, topographical and geological map interpretation alone. This technique is, therefore, only appropriate when a sufficiently high resolution data base (perhaps collected by surface mapping and inventory) is available, and when the relative importance of factors that influence the development of instability in the study area is known, and can be effectively taken into consideration in the analysis. This is unlikely to be the case at the route planning stage of a highway project in the Lower Himalaya. In fact, given a general absence of terrain data, it is difficult to envisage how this technique can be of significant use to design at any stage of a highway project. Once the route corridor is chosen, by less intense and rapid assessment techniques (including walk-over survey, factor mapping and air photograph interpretation), then more intensive geotechnical mapping (Chapter 4) can be undertaken. Only when the development of road networks are being planned, involving the construction of a number of roads, are the rigorous data collection and analysis of the statistical approach likely to be justified.

The second methodology examined in this chapter, that of factor mapping, is far less demanding, both in terms of the data base and the analysis. The technique has compared an observed slope hazard distribution with that expected had this distribution been random. Six contributory factors, quantifiable from geological maps and air photographs, have been examined in terms of their spatial covariation with the slope hazard distribution. The significant factor categories have been assigned hazard rating scores for final summation on the composite factor map. This mapping exercise has been undertaken relatively rapidly (in approximately sixteen man-days compared to one man-month for the statistical method) and proved to be successful in explaining the distribution of slope hazards.

If good quality air photography of sufficiently large scale (ideally larger than 1: 20 000) is available at the desk study stage of the highway project, then it may be possible to rapidly and cheaply produce a landslide hazard map of the area under study that either shows the distribution of landslides themselves or zones relative hazard. Route corridor selection can then proceed with the aid of rapid reconnaissance surveys. If, however, suitable air

photography is not available, then the compilation of a landslide hazard map may require specially commissioned aerial photography. This may not be feasible for low-cost road projects and consequently walk-over survey will be necessary. Ground survey maps may allow the spatial distribution of landslide density to be determined, and used in conjunction with topographic maps to zone relative hazard.

It is important that landslide hazard mapping, for route corridor identification and selection purposes, differentiates between slope hazard mechanisms in order to assess their likely impact on road stability. A simple two-fold classification into: i) erosion and shallow instability, and ii) deep-seated, large-scale mass movement would be of value. However, only in the first category is their likely to be a sufficiently large number of slope hazards, occurring in a given study area, to allow any form of statistical assessment. Deep-seated mass movements may occur in response to different geological and slope conditions and, owing to their relative infrequency, may require assessment in qualitative terms using air photograph interpretation and site inspection.

Construction-induced, on-road and off-road hazards often have a high, short-term impact on mountain roads. Very little can be achieved in the prediction of these hazards prior to earthworks, and their potential should be assessed by detailed site appraisal.

On the basis of the analysis and discussion presented in this chapter, it is possible to suggest broad guidelines and recommendations (listed below) for medium-scale landslide hazard mapping for future road projects in the Lower Himalaya, both for highway engineering and research purposes.

i) The analyses presented in this chapter have been undertaken using a relatively low quality data base, and are largely experimental. The representability of the analyses and resultant hazard maps might be increased if the quality of the data base is improved.

ii) The hazard zonation developed in this chapter should be tested to assess its ability to predict the location of slope hazards in similar catchments outside the study area. The production of hazard maps for other areas in the region, that are targetted for economic development, would be of considerable benefit for both engineering and land capability assessment.

iii) Variability within factor categories should be examined in order to determine whether the methods of factor mapping and hazard score allocation adopted here can be made more representative of terrain conditions. In particular, the relative importance of each factor in the development of instability, should be examined in order to avoid the problems of covariation amongst contributory factors.

iv) Landslide hazard mapping exercises, undertaken for future road alignments in the Lower Himalaya, would benefit from a more representative rainfall data base than is currently available, and consequently a higher density of rainfall recording stations would be desirable.

v) Given the poor quality of terrain data available in the study area, there is insufficient grounds for the development of statistically-based landslide susceptibility mapping techniques, unless extensive ground survey is carried out. This is not feasible at the route planning stage of a highway project, and therefore, such an exercise is likely to be of academic interest only.

vi) While time and data constraints have served to limit the scope and quality of the landslide hazard mapping technique developed in this chapter, the factor mapping approach nevertheless forms a useful model for future road projects in the region, if the necessary air photography and geological maps are available.

CHAPTER 6

AN EVALUATION OF EROSION AND SLOPE INSTABILITY CAUSED BY SPOIL DISPOSAL WITH RECOMMENDATIONS FOR FUTURE POLICY.

6.1 Introduction

Spoil is created when the volume of excavated material exceeds the local requirements for fill, road sub-base and base course, and aggregate materials. Spoil disposal can take place either indiscriminately at source, with little or no regard for any potential increase in erosion on the affected slopes, or discriminately within a framework of designated safe and unsafe disposal sites. The philosophy adopted depends on the potential for spoil-induced erosion or instability, the engineer's awareness of the hazard posed by ill-conceived spoil disposal and the finance available for, and the practicalities of, spoil haulage to safe disposal sites (Hearn 1987).

Spoil disposal can pose a considerable hazard to road integrity. The stability of the slopes and drainage channels below roadlines can be affected in two principal ways. First, spoil tipping can lead to the removal of the vegetation cover and top-soil, thus facilitating concentrated slope erosion. Second, the creation of large spoil tips or benches may lead to failure of the slope below by overloading. Verstappen (1983) quotes several examples in South America and southern Italy where spoil tipping and the creation of large spoil 'dumps' have led to erosion and slope failure, requiring the installation of often extensive remedial measures. He maintains that "the tendency often exists for engineers to dump the material (spoil) from cuts in the immediate surroundings of the excavation, without much thought of the effect this may have on the morphodynamics." (Verstappen 1983, p182). Despite these observations, very little analytical work has been published concerning the effects of spoil related hazards on road stability and neighbouring land uses.

Verstappen's statement appears to be true for the majority of roads constructed in the Lower Himalaya of Nepal and India (Table 2.2). Here, steep slopes, often weathered slope materials and heavy rain combine to make indiscriminate spoil disposal an often particularly hazardous aspect of earthworks. Unfortunately, indiscriminate spoil tipping is usually the only feasible option for low-cost road construction in mountainous terrain, such as

the Lower Himalaya, because earthworks costs escalate when large-scale haulage of spoil is undertaken. In fact, of the roads visited by the author in the Lower Himalaya (Table 2.2), only in the case of the Dharan-Dhankuta road was it apparent that a philosophy of discriminate spoil disposal had been adopted and generally adhered to.

The first effect of spoil tipping onto the slopes below a road is to remove or flatten the vegetation cover. Depending on slope angle, much of this early spoil may become caught in slope vegetation or remain, temporarily, as a small bench on the side of the road. However, further tipping usually strips the vegetation cover and forms a shallow layer of loose debris over the top-soil. Runoff on these slopes removes the spoil material and exposes the unprotected soil to erosion. By this process, the zone of soil erosion extends further downslope as tipping proceeds. Eventually, a linear erosion track or channel is formed which tends to concentrate runoff and perpetuate the erosion process. The potential hazard of spoil-induced erosion was emphasised by the 1975 geomorphological reconnaissance survey, partly as a result of the unsightly effects of spoil tipping. A post-construction examination of the impact of spoil disposal is presented in this chapter and permits the geomorphologists' concern over spoil tipping to be assessed.

This chapter assesses the impact that different spoil disposal policies have on the short and long-term stability of roads and adjacent slopes and channels in the Lower Himalaya. This is undertaken in order to determine: a) whether the caution exercised in spoil disposal along the Dharan-Dhankuta road was justified, and b) if discriminate spoil disposal policies are cost-effective for low-cost mountain roads in general.

The principal aims of the chapter are four fold:-

i) To review the factors that determine the volume of spoil material generated during earthworks and the manner in which it is disposed.

ii) To assess the impact that indiscriminate spoil disposal has had on both road and adjacent slope and channel stability along selected Lower Himalayan roads.

iii) To assess the extent of erosion and instability caused by discriminate and indiscriminate spoil disposal along the Dharan-Dhankuta road and the Bhedetar-Rajarani road respectively, in east Nepal.

iv) On the basis of the conclusions drawn from these assessments, to make recommendations for future disposal policies.

6.2 Factors that Determine the Volume and Disposal of Spoil Created During Earthworks

The earthworks quantities (volumes of excavation and requirements for road fill and construction materials) for many low-cost roads in steep terrain are characterised by an excess of excavated material over road fill requirements (Verstappen 1983). This is due to the fact that fill embankments, greater than say 2-3m in height, are usually avoided because they require some form of retaining structure, and these may be time consuming, costly and difficult to construct on steep ground. On the other hand, while full-cut solutions may result in progressive failure and ravelling of the slope above (Chapter 2), this is usually considered to be an acceptable outcome in view of the ease with which excavations can be made in often highly weathered rocks.

Two main methods of spoil disposal can be identified. The term side-casting, or tipping, refers to the tipping of spoil onto the slopes below the point of excavation. Side-casting is typical of the majority of the Lower Himalayan roads visited (Table 2.2). Conversely, spoil benching refers to the discriminate disposal of spoil in large tips or benches, located at selected sites on less steeply inclined ground. Spoil benches along the Dharan-Dhankuta road were often constructed on spurs and at the end of hairpin loops as 'end tips'.

The choice of disposal sites is usually limited by the economic feasibility of spoil haulage, and the problems of access for haulage vehicles. In the case of contoured alignments, across gently sloping side-long ground, vehicle access may be relatively easy to achieve. However, where complicated alignments are designed across difficult terrain characterised by high relative relief, as was the case with the Dharan-Dhankuta road, the provision of access may prove problematic, resulting in delays and escalating construction costs. Fookes et al (1985) suggest that the maximum practical carrying distance for labour intensive haulage techniques of head pan, basket and barrow, is 500m.

Where vehicle access is prohibited, this figure becomes the maximum distance over which spoil material can be realistically hauled.

Ideally, excess spoil material should be disposed of as cheaply as possible and at locations where it will not encourage erosion or slope failure. Listed below are several important questions, that should be addressed during the earthworks design phase, concerning erosion rates likely to be caused by discriminate side-casting.

i) Which slopes are likely to prove the most susceptible to erosion, following side-casting?

ii) How much material can be side-cast at any one site, before accelerated erosion takes place?

iii) During which seasons of the year, and at what rate, should side-casting be undertaken?

iv) How much erosion is likely to take place, and to what extent will this effect the stability of the road, and what will be its impact on surrounding land uses?

v) Approximately how much time will be required for stability to be regained?

vi) What erosion protection measures, if any, should be adopted?

In addition, the following questions should be addressed during construction concerning the location and stability of spoil benches or large tips.

i) Which slopes, in the vicinity of the intended route, appear to be unstable or, given their slope situation, may become unstable following increased geomorphological activity due to either natural causes or the effects of road construction?

ii) On the basis of physiography, alignment design and road cross-sections, where are the major sources of spoil likely to occur?

iii) How much material may be benched at each site?

iv) If instability does take place, how frequently and with what magnitude will it recur, and what short and long-term effects will it have on road stability and neighbouring land uses?

v) What measures should be taken to ensure spoil bench stability and road integrity?

Most of these questions are usually unanswered, due to a lack of information during preliminary earthworks, or unasked by the engineer because of an unawareness of the hazards posed by side-casting and benching. Even if these questions can be answered there may be insufficient finance for the appropriate action to be taken. A short overview of past and present practice and the consequences of spoil disposal along Lower Himalayan roads, is given below. This will allow both the short and long-term effects of spoil disposal to be assessed.

6.3 The Effects of Spoil Disposal Along Some Lower Himalayan Roads

Information drawn from the itinery of Lower Himalayan roads (summarized in Table 2.2) serves to illustrate some of the consequences of ill-considered spoil disposal. Considering that most roads visited in the Indian Himalayas, and the Tribhuvan Raj Path in Nepal, are comparatively old (Table 2.2) it is difficult to assess the criteria that were used to design the respective spoil disposal policies, and the extent and longevity of consequent erosion and slope instability.

There are frequent examples along many of these roads where side-casting has caused short-term erosion problems that have lasted for a few years only; stability has been regained at most sites without severe, adverse long-term consequences. Quite often, slope erosion scars and the presence of dry-masonry and gabion slope and channel erosion protection works are indicative of extensive spoil-induced erosion along some of the older roads. Notable examples occur along the Mussoorie-Dehra Dun, Mussoorie-Tehri and Siliguri-Darjeeling roads, in particular. Plate 2.12, for example, shows numerous erosion scars on the slopes below the Mussoorie-Tehri road, where extensive side-casting occurred during construction.

With the exception of the Dharan-Dhankuta road, recently constructed roads in the Nepal Himalayas are characterised by widespread spoil tipping. This has often led to the removal of the vegetation and soil cover, and the creation of large areas of unsightly bare ground below roadlines (Plate 6.4). However, as discussed in Section 6.2, the volume of excess spoil created, and the potential for widespread tipping is dependent largely on physiography. For instance, relatively low spoil volumes are characteristic of roads aligned along ridge tops or shallowly inclined side-long ground such as the Dhankuta-Hile, Hile-Siduwa (Plate 6.1) and Lamusangu-Jiri roads (Table 2.2), while the earthworks quantities for the Dharan-Dhankuta, Bhedetar-Rajarani and Kathmandu-Kodari roads, where the terrain is particularly steep, are characterised by excessive volumes of spoil material.

Along the Bhedetar-Rajarani and Kathmandu-Kodari roads widespread side-casting has destroyed the vegetation cover for considerable distances and created ideal conditions for gullying, slope erosion and shallow instability (Table 2.2, Plate 6.2). In addition to these direct effects, side-casting has, in many instances, led to increased runoff rates and problems of channel erosion and sediment transport further downstream. This may be illustrated, in the case of the Bhedetar-Rajarani road, by the extensive channel erosion, landsliding and sediment transport that has taken place in the Sinsua Khola and on the Leoti Khola floodplain below (Section 6.5). Along the Mussoorie By-Pass and the Dharan-Dhankuta road, channel erosion and culvert blockage have been caused by side-casting from sections of alignment further upslope. Spoil tipping on the hairpin section of the Lamusangu-Jiri road, in the Sun Kosi valley, has led to problems of erosion and culvert blockage on the lower hairpins. These problems have been rectified by erosion protection works, within less than five years of construction.

This brief review of spoil tipping along selected Lower Himalayan roads has indicated that while spoil tipping can cause erosion, instability and sediment hazards, most of these hazards are quite localised and relatively short-term (in the order of a few years duration). With the exception of the Dharan-Dhankuta road, most of the roads visited had been constructed using indiscriminate spoil disposal policies that have had no apparent detrimental effect on their long-term stability.

PLATE 6.1 Ridge-Top Alignment of the Hile-Siduwa Road.

PLATE 6.2 Gullying on the Tip Slopes Below the Bhedetar-Rajarani Road.

During the construction of the Dharan-Dhankuta road, considerable restrictions were placed on the location of spoil disposal sites, as it was considered by both the consulting engineers and the second geomorphological reconnaissance survey, that spoil related hazards were likely to have a high impact on road stability. In fact, the geomorphological survey (p7) stressed that "The dumping of spoil should be restricted to land which has already been cleared of vegetation for agricultural purposes". This survey also emphasised that "The consequences of ill advised tipping ... in terms of accelerated gully erosion and surface instability are likely to have a profound effect on the life and maintenance cost of the road". However, during construction, the large volumes of spoil created and problems of haulage along the road, served to restrict the choice of spoil disposal sites. Factors affecting the location of these sites are described below. Ensuing erosion rates and slope instability are evaluated and used to critically assess the policy of spoil disposal adopted, and the validity of the geomorphologists' concern over the potential for spoil related hazards.

6.4 Spoil Disposal Along the Dharan-Dhankuta Road

6.4.1 Criteria Used in the Choice of Spoil Disposal Sites

Recommendations regarding spoil disposal were first made by the 1975 geomorphological reconnaissance survey. These recommendations were based on the identification of unstable and potentially unstable slopes and eroding channels. In all, only six sites were identified as being suitable for spoil disposal. These sites commonly occupied gently sloping and relatively stable ground. Spoil tipping was specifically discouraged at twelve locations between Dharan and the Leoti Khola floodplain. During construction, five of these sites were the locations of limited tipping, and three developed accelerated erosion.

While these recommendations appear to have been accepted by the design team, the actual choice of spoil disposal sites was determined by three main factors. First, the construction of a two-lane carriageway across steep, complex terrain generated large earthworks volumes and a correspondingly large volume of excess spoil material. Second, severe access problems along much of the alignment and especially on the ascent to the Sangure Ridge and the alignment in the lower Dhankuta Khola valley, restricted access by haulage vehicles. Finally, in similarity to other low-cost roads in the region

(Shombrot and Hinch 1980), earthworks and construction techniques were labour intensive and hence, there was a limit to the practical distance over which spoil could be carried.

Despite these constraints, extensive spoil disposal was confined, whenever possible, to specific sites for side-casting and benching, where the potential for erosion and instability was considered to be acceptably low by the design team. Spoil benches were constructed on the more shallowly inclined ground, such as on spurs, where the spoil material was less likely to be washed away. Tipping, where allowed, took place on the steeper slopes where it was not practical to construct benches. As a result of this policy of discriminate spoil disposal, the earthworks costs for the road amounted to a total of almost £3 million. While, in absolute terms, this figure is quite high, its proportion of the total construction cost (approximately 25%, Table 2.5) is comparable to other low-cost roads in the region, such as the Lamusangu-Jiri and Dhankuta-Hile roads, where the costs of both earthworks and construction were proportionally much lower.

6.4.2. The Impact of Spoil Disposal on Erosion and Stability

The immediate effect of side-casting along the Dharan-Dhankuta road was to remove the vegetation cover and create large areas of bare ground. The area of slope laid bare is thus a reasonable indicator of the areal extent of erosion and slope disturbance caused by side-casting. By comparing at each site, the maximum area of bare ground caused by side-casting during earthworks with the same slope in 1984, 3-7 years after earthworks, it is possible to assess the extent of erosion and the time required for stability to be regained and slope revegetation to commence. Clearly, this methodology does not allow the depth of erosion to be determined or compared, as this would require detailed site measurement.

In order to map the extent of bare tip slopes during earthworks, site photographs of the hill section between Dharan and Gutetar (Figure 3.3), taken during construction, were obtained from members of the design team. From these, the extent of bare ground caused by side-casting was plotted directly onto 1:2 500 scale alignment drawings. The procedure was repeated using photographs taken systematically of the whole alignment in 1984. Three sections of the alignment were excluded from the study (Dharan to km 3.900,

the Leoti Khola floodplain and Gutetar (km 40.000) to Dhankuta (km 50.300)). In the first case, above Dharan, the alignment is composed of a series of irregular and complex hairpin bends located on predominantly south facing slopes overlooking the Terai Plain. Photography of these slopes is therefore difficult. Spoil disposal on the Leoti Khola floodplain, apart from increasing the sediment load of the Leoti Khola, has had no adverse affect on the stability of the road. Finally, between Gutetar and Dhankuta there is a general lack of suitable site photographs taken during earthworks and, owing to the combined effects of a dry climate and deforestation, most of these slopes are devoid of vegetation.

Figure 6.1A-C shows the distribution and maximum extent of bare ground caused by both controlled and unauthorised spoil tipping, as mapped from both sets of photographs. Inspection of these distributions reveals that unauthorised side-casting took place along a large proportion of the road, albeit to a limited extent in many places. Spoil was tipped onto slopes of up to 40^0 inclination with runout lengths of as much as 300m. The calibre of this spoil material varied according to lithology. The quartzites yielded coarse, angular material that is relatively resistant to erosion, while spoil derived from excavations in phyllitic, shaly and schistose materials, for instance, was more fine grained and susceptible to erosion. This influence of grain size and lithology on tip slope erosion rates, is discussed further in Chapter 8. With the exception of the quartzite re-entrants (km 15.500-17.500, Figure 6.1B) and two slopes (see below) on the Mulghat hairpins (Figure 6.1C), all slopes originally stripped of vegetation by side-casting during earthworks, have regained stability and have either partly or completely revegetated. This has taken place despite the heavy storms of 1983 and 1984 and is counter to the views of the 1975 geomorphological survey. However, it should be pointed out that the recolonisation of tip slopes has been achieved by quick growing grasses and Eupatorium that provide protection against surface erosion, but may be unable to prevent deeper instability during intense precipitation.

The tip slopes that have remained devoid of vegetation are largely confined to the quartzite outcrops on the northern flanks of the Sangure Ridge. Here, revegetation has been impeded, owing to both the relatively coarse nature of the spoil and underlying soil, the proximity of bedrock to the slope surface and the preponderance of slope wash caused by relatively low bedrock permeability. Elsewhere, as at km 35.150 and km 38.770 (Figure 6.1C),

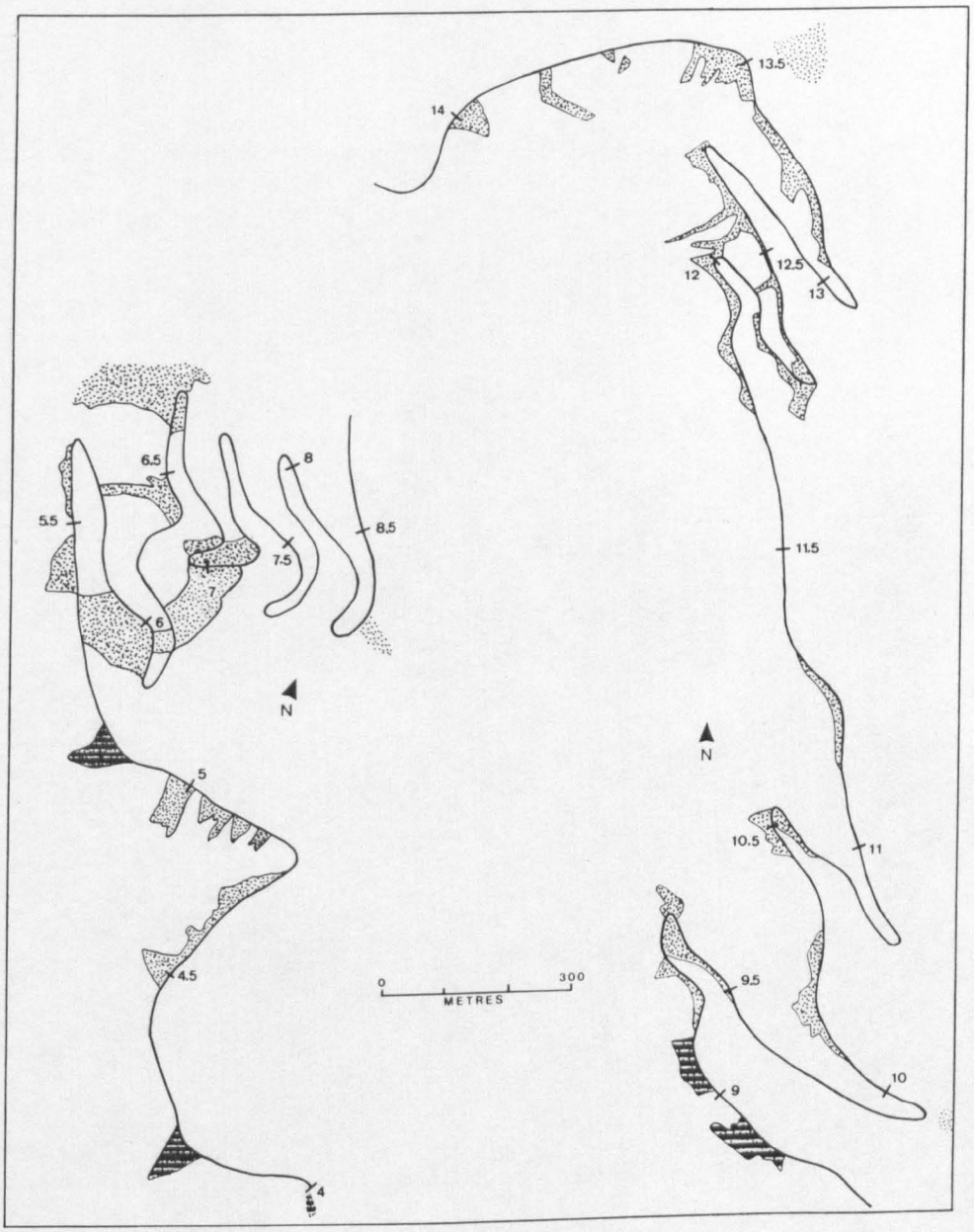

FIGURE 6.1A Extent of Bare Ground Caused by Tipping Along the Dharan-Dhankuta Road (Km 4.000-14.000).(For explanation see Figure 6.1C).

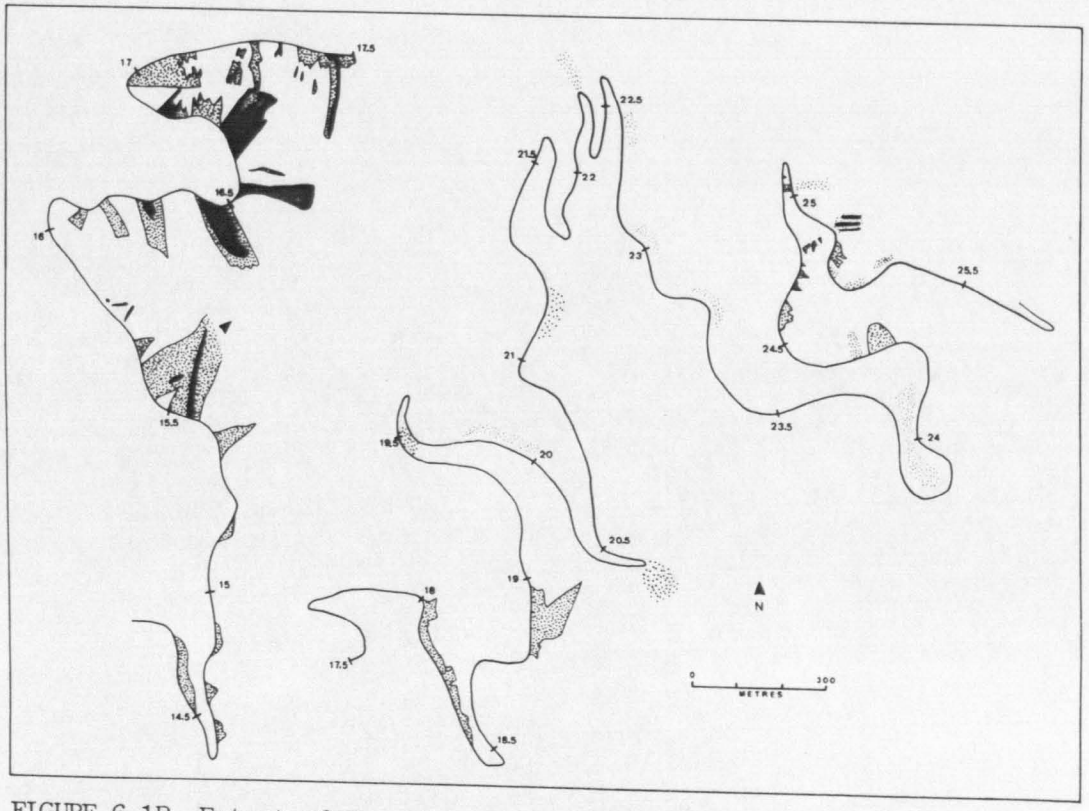

FIGURE 6.1B Extent of Bare Ground Caused by Tipping Along the Dharan-Dhankuta Road (Km 14.000-25.500).(For explanation see Figure 6.1C).

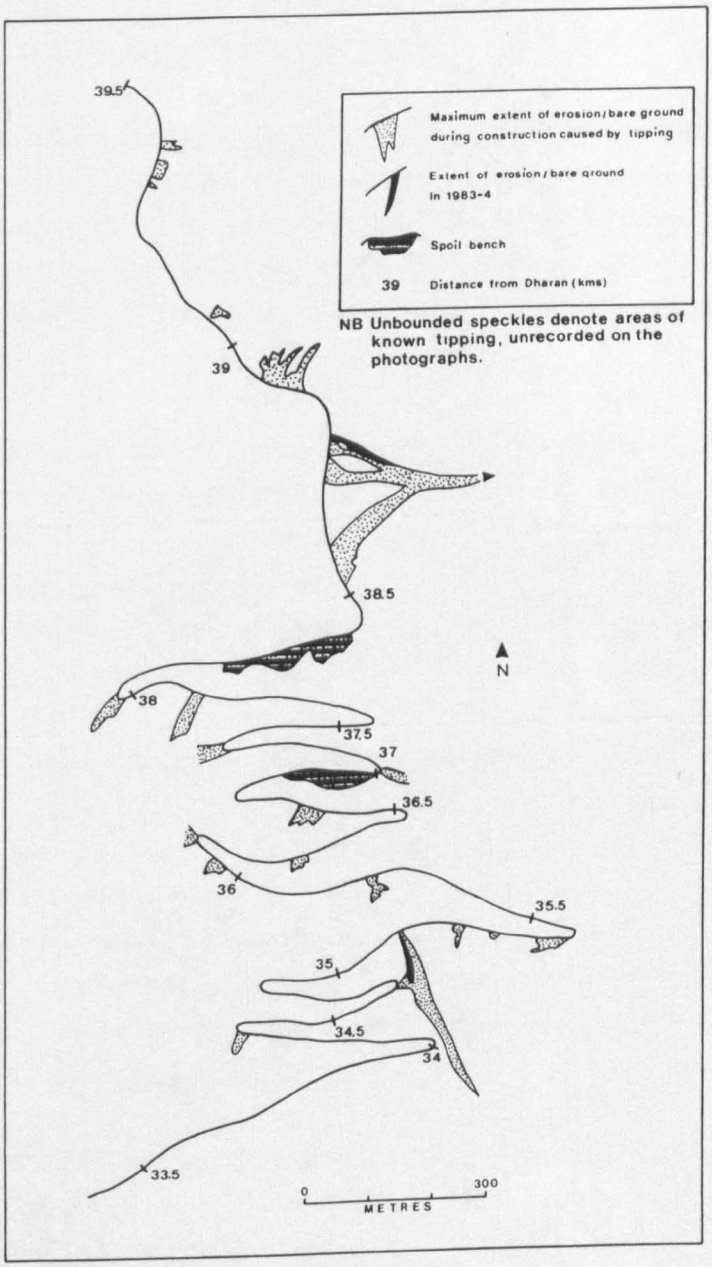

FIGURE 6.1C Extent of Bare Ground Caused by Tipping Along the Dharan-Dhankuta Road (Km33.500 -39.500).

localised patches of bare ground remain on particularly steep slopes (greater than 45^{o}) and slopes adjacent to eroding channels below culvert outfalls.

During construction however, considerable volumes of spoil material were washed from the tip slopes into the channels below, causing blockage to culverts along the roadlines at lower elevations. This was particularly prevalent on the hairpin sections at Kumlintar and Mulghat. In addition, tipping from the road on the ascent from Dharan to the Sangure Ridge may have led to increased runoff rates, erosion and sediment transport in the Khardu (Sardu) Khola (Chapter 5). Following the storms in 1983 and 1984, the Nepal Roads Department maintenance unit undertook localised side-casting of material derived from cut slope failures. While the majority of the slopes affected by this small scale tipping have remained stable, tipping in the bowl area at km 24.600-700 led to short-term channel erosion, culvert blockage and road inundation below.

In conclusion, although side-casting has given rise to problems of erosion and sediment transport during construction, on the whole, these have been relatively short-term; most tipping slopes have become revegetated and apparently stable over a maximum period of 5 to 7 years. However, this may be due to only a relatively small amount of spoil being tipped at each site. Greater depths of spoil material on the slopes below the road, might have led to deeper instability during heavy rain, and the eventual undermining of the road. Nevertheless, the possibility remains that side-casting, except at sites of slope instability and gully erosion, might in fact have a lower overall impact on slope and drainage stability than concentrated tipping and benching (see below). Clearly, this could only be possible where roads are constructed on side-long ground, and not on hairpin stacks, where spoil would almost certainly lead to problems of erosion and sediment below. This may be illustrated by the abandonment of a hairpin stack on the Bhedetar-Rajarani road, due to the effects of widespread spoil tipping (Section 6.5.2).

Figure 6.1 A-C also shows the locations of the main spoil benches and large tips along the road. Between km 3.800 and Gutetar, a total of eight areas of sizeable benching have been identified. While most of these benches are stable it would appear that at three and possibly five sites, extensive slope failure and road loss may have been aided by slope overloading due to spoil bench construction on often highly weathered slope materials. These failures are

discussed in Chapter 4 and described in Appendix 1. At km 4.100, extensive rotational slope failure immediately below the road occurred in September 1983, removing part of the road at this point. The failure appears to have been caused by the combined effects of the development of high groundwater levels following a wet monsoon season, slope overloading by the construction of a large spoil bench on the spur immediately below the road, and channel erosion at the base of the slope. Renewed instability and severe road deformation occurred at km 8.900 during the September 1984 storm, and may have been caused by both erosion in the Khardu Khola and slope overloading by the construction of a large spoil bench below the road (Appendix 1). A third spoil bench (Figure 6.1B), located on a small spur below the road at km 25.070, began to show signs of rotational failure in 1983, following channel erosion at the toe of the slope. Fortunately, the road is not directly at risk from this instability. Finally, at km 3.825-4.000 and km 5.100, major slope failure causing road loss and deformation, took place during the September 1984 storm. While a limited amount of spoil was benched on these slopes (Figure 6.1A), the principal causes of failure, from surface evidence, appear to have been high groundwater levels and basal erosion.

With the exception of the failure below the road at km 25.070, all of the spoil bench-related failures described above have occurred along the first 10kms of the alignment, where the road is underlain by often highly weathered Siwalik sediments (Chapter 3). The incoherent nature of these rocks is likely to have been an important factor in the instability at these sites. The remainder of the sizeable spoil benches appear to be presently stable. However, during earthworks many of the spoil disposal sites, and especially those on the lower hairpins at Kumlintar, became unstable. In the slope embayment below km 6.000, for instance, mudflow in spoil material gave rise to culvert blockage below.

The conclusion drawn from this review is that in highly unstable terrain, discriminate spoil disposal is the most appropriate philosophy to adopt for engineered roads, although considerable care must be taken in the choice of spoil benching sites. A more flexible, less costly approach to that adopted for the Dharan-Dhankuta road might be achieved by relaxing, in appropriate cases, the often stringent restrictions placed on limited side-casting, and increasing the number of spoil benching and tipping sites. This may be justified by the fact that almost everywhere else along the road, erosion caused by normal

side-casting has been relatively short-lived. In order to test this assertion further, a brief overview of the effects of large-scale side-casting on the slopes below the Bhedetar-Rajarani road is given in the following section.

6.5 The Effects of Spoil Disposal Along the Bhedetar-Rajarani Road

6.5.1 Introduction

The Bhedetar-Rajarani road links Bhedetar, located on the Dharan-Dhankuta road at the crest of the Sangure Ridge, with Rajarani (Rani Pokhari), 22 kms to the east (Figure 2.2). The road, for the most part, traverses the north facing slopes of the Sangure Ridge, crossing often highly disturbed quartzites, phyllites and schists. Spoil tipping has taken place indiscriminately along almost the entire length of the road, regardless of slope conditions below. The road has a low design standard (Table 2.2), an unsurfaced and only 3-4m wide carriageway, and minimal erosion protection works.

The largest excavation volumes, and most widespread tipping, have occurred along the first 3.4 kms of alignment, between Bhedetar and Namje Bazar. This section of the alignment, therefore, provides a good opportunity for assessing the effects of widespread spoil tipping along a low-cost road in steep terrain formed in often weathered and erodible slope materials. Earthworks for this section began in 1981/82 and, with one or two exceptions, were completed in 1983. The Nepal Roads Department initially made NCRs 1.8 million (approximately £75 000) available for the construction of this section of the alignment. The average cost of earthworks along the Dharan-Dhankuta road amounted to almost NCRs 1.4 million (approximately £58,000) per kilometre, and hence, by comparison, the design philosophy for the Bhedetar-Rajarani road must be regarded as extremely low-cost and in keeping with its low design specifications.

The aims of this brief study are essentially two-fold: i) to evaluate whether discriminate spoil disposal would have been economically feasible along the road, and ii) to determine the extent to which the indiscriminate spoil disposal policy adopted has reduced the stability of both the road and the neighbouring slopes. To achieve the first aim, the volume of excavation at 20m intervals along the entire 3.4 km length of study alignment was computed. These volumes were summed and combined with the rate paid to contractors for excavation to yield an estimated total cost of earthworks for this section.

The second part of the study involved the use of terrestrial photography, taken in 1983 and 1984, to establish the extent of slope erosion caused by indiscriminate spoil tipping. These two erosion distributions were mapped and compared in order to determine whether slopes have shown signs of either continued erosion or revegetation over the relatively short intervening period. These trends will be compared graphically with slope inclination.

6.5.2 Field Data Collection and Analysis of Results

In respect to the first objective, the volumes of excavation were calculated geometrically, at 20m intervals along the alignment, by field measurement of road width, cut slope and natural slope inclination, and the inclination from the edge of the road to the top of the cut slope. The excavated cross-sections at both ends of each 20m length were averaged and multiplied by 20m to determine the total excavation volume. These values were then summed for the 3.4 km length. As the road is constructed almost entirely in full-cut along the study length (Plate 6.3), it can be assumed that the vast majority of this material was side-cast at source.

Using a scheduled rate of NCRs 8 (approximately £0.33) for excavating $1m^3$ of soft rock (Taylor 1982) and a computed excavation volume of 319 $321m^3$ for the 3.4 kms, a total cost of NCRs 2.55 million (approximately £0.11 million) is obtained. As only NCRs 1.8 million were made available at the beginning of the earthworks stage, it is apparent that there has been very little additional finance available, if any, with which to undertake spoil haulage, road surfacing, slope stabilization or drainage protection. Due to the extremely low-cost nature of this road, indiscriminate spoil disposal was the only feasible option. The effects that this has had on erosion and slope stability are assessed below.

By 1983, extensive erosion had occurred on the slopes below the Bhedetar-Rajarani road (Plate 6.4). However, photographs taken in 1984 (Plate 6.5) reveal that many of these slopes had regained stability and were showing signs of revegetation. The extent of bare ground, recorded from each set of terrestrial photographs, was plotted onto separate 1:1 333 scale alignment drawings surveyed by the author using compass traverse. These maps have been reproduced here, at a reduced scale, in Figure 6.2. The lengths of slope erosion, in a downslope direction normal to the roadline, were measured from

PLATE 6.3 The Bhedetar-Rajarani Road Along the Study Section, Showing the Full Cut Excavation and Side Casting of Spoil.

PLATE 6.4 Extent of Bare Ground Caused by Side Casting Along the Bhedetar-Rajarani Road in 1983.

PLATE 6.5 Extent of Bare Ground Caused by Side Casting Along the Bhedetar-Rajarani Road in 1984.

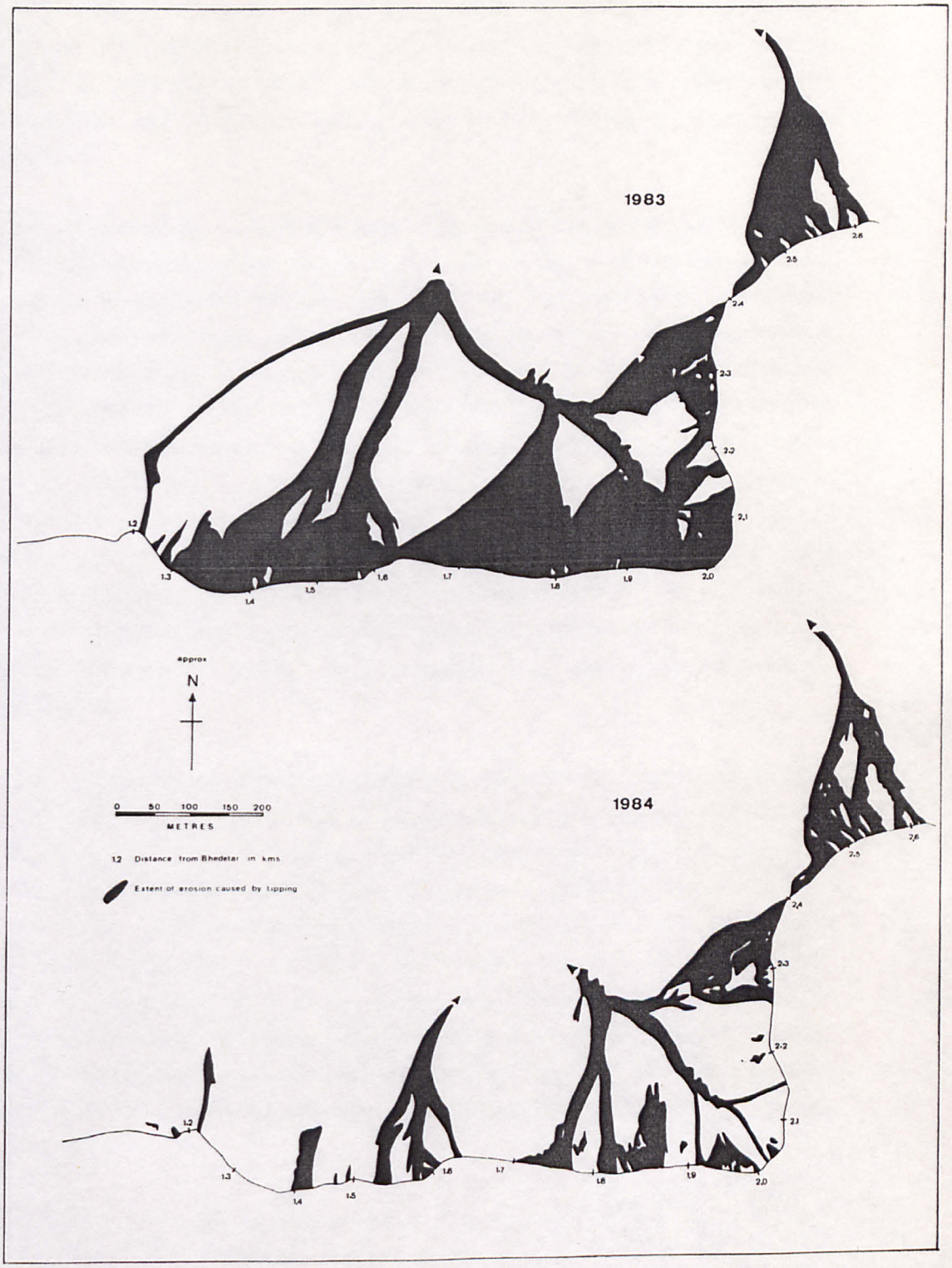

FIGURE 6.2 The Extent of Bare Ground Caused by Side Casting of Spoil Along the Bhedetar-Rajarani Road.

both alignment drawings at 20m intervals. In most cases, these measurements represented the line of maximum slope. Initially, in order to determine the approximate volume of erosion along each length, the depths of channel erosion were measured in the field by stretching a 30m tape across the slope and measuring vertical distances from the tape to the eroded ground surface. However, these measurements had to be discontinued when slopes became precipitous and unstable, making access both difficult and extremely hazardous.

A comparison of the extent of erosion on the slopes below the road in 1983 and 1984 was, therefore, made on the basis of the change in the length of eroded slope below the road, at 20m intervals along the alignment. This method suffers from two main limitations. First, slope erosion below the road is largely channelised. Owing to the fact that some of these channels are not oriented normally to the road alignment, measurement of erosion length along a single dimension does not allow an entirely representative value of slope erosion length to be obtained. Second, the length of slope erosion is conditioned ultimately by the total length of slope below the road. This was allowed for by subtracting the 1984 erosion lengths from those of 1983, and dividing the result by the 1983 length. This factor was then used to directly assess the trend in erosion along each 20m length; positive and negative factor values indicated a trend towards revegetation and continued erosion, respectively.

Figure 6.3 shows the graphical relationship between the erosion factor and slope inclination at each site. A general decrease in factor values with increasing slope inclination can be identified indicating, as would be expected, that revegetation has predominated on the more shallowly inclined slopes. Only one case of increased erosion length was recorded, and this corresponds to a slope inclination of 57.5°. Clearly, factors other than slope inclination also need to be considered in any assessment of the distribution of erosion caused by spoil tipping, including the erodibility of the underlying soil and the spoil material itself, and the intensity and duration of following rainfall. These factors are discussed with respect to erosion monitoring of tip slopes in Chapter 8.

Nevertheless, it is significant to note that slope revegetation has begun to occur on all but the steepest slopes, within 2 years of spoil tipping. This

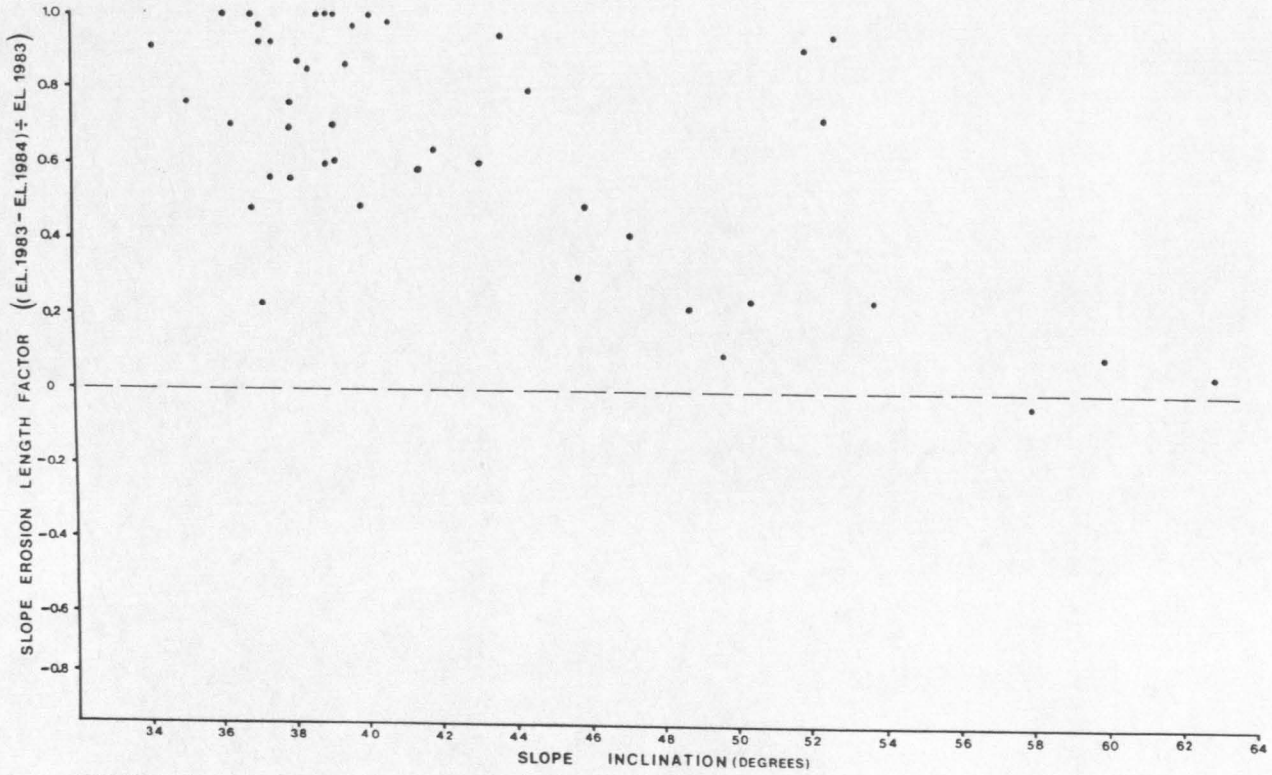

FIGURE 6.3 Graphical Relationship Between Slope Erosion Factor and Inclination.

supports the contention made in Section 6.4.2, that under most slope conditions, where stable slopes are moderately inclined and are not being actively undercut or oversteepened from below, slope erosion consequent to side-casting is only a temporary phenomenon. It must be pointed out, however, that increased runoff rates and erosion on the slopes below the Bhedetar-Rajarani road, have caused severe problems of instability and sedimentation on the Leoti Khola floodplain during the storms in 1983 and 1984. In 1983, for instance, a large debris fan was deposited at the confluence between the Sinsua Khola, that drains the headwater slopes crossed by the Bhedetar-Rajarani road, and the Leoti Khola trunk river, forcing the latter to erode extensive areas of paddy terrace along its right bank. Following the September 1984 storm, the bed level of the lower Leoti Khola was raised significantly, by up to 3m in places. Erosion below the Bhedetar-Rajarani road appears to have contributed significantly to this sediment load.

Finally, brief mention should be given to the abandonment in 1980, of an earlier hairpin stack (consisting of approximately 300m of roadline) along the Bhedetar-Rajarani road, due to hazards caused by tipping. Construction began at the base of the stack, and spoil was side-cast as excavation proceeded. This resulted in the progressive inundation, and eventual obliteration, of the lower roadlines (Plate 6.6). The stack was finally abandoned at a cost of NCRs 0.8 million (approximately £33 000). The cost of repairing the stack, had this been attempted, was estimated to be NCRs 0.6 million. These figures are quite high in comparison to the total money made available in 1981/2 (NCRs 1.8 million) for the construction of the first 3.4 kms of the new alignment.

6.6 Discussion and Conclusions

This chapter has reviewed the factors that determine the volume and disposal of spoil material generated during earthworks, and has examined the impact of spoil hazards on road integrity and slope and drainage stability. Roads constructed in the Lower Himalaya of Nepal and India have had particularly low-cost design philosophies and therefore, in most cases, very little attempt has been made to adopt discriminate spoil disposal policies. While this has led to often severe cases of erosion and sediment transport, these have usually been short-term. In the case of the Dharan-Dhankuta road, the maximum time required for stability to be regained has been 5-7 years, while tip slopes along the Bhedetar-Rajarani road are showing signs of revegetation after only 2-3

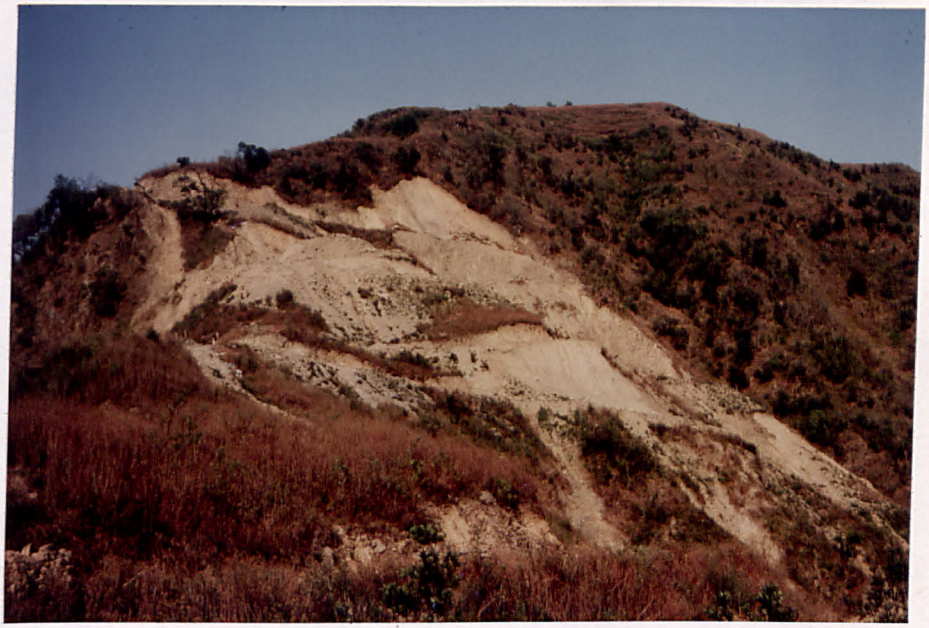

PLATE 6.6 The Obliteration of a Hairpin Stack Along the Original Alignment for the Bhedetar-Rajarani Road Following Extensive Spoil Tipping.

years. Only where slopes are being actively undercut, or where they are inherently unstable, is side-casting of spoil likely to have any lasting effect. Therefore, the main conclusion to be drawn is that, while the immediate effects of spoil tipping along mountain roads are rather unsightly, they are usually of only short-term significance to road maintenance. Consequently, the importance attached by the geomorphological reconnaissance survey of the Dharan-Dhankuta road to the disposal of spoil on shallowly inclined agricultural land, can be shown to be largely unfounded. The evidence suggests that the geomorphologists over-estimated the hazard posed by spoil tipping. Accordingly, it could be argued that the spoil disposal policy adopted along the Dharan-Dhankuta road was, in many cases, over-cautious.

Nevertheless, spoil tipping can have major short-term consequences for both road stability and the stability of neighbouring slopes and channels, and the integrity of other land uses, such as high value agricultural land, village settlements and road alignments below. If the short-term impact of spoil-related hazards is to be reduced, then some form of discriminate disposal policy should be adopted. At comparatively little extra cost, these hazards may be reduced by discouraging tipping in areas particularly vulnerable to erosion or instability, such as eroding gullies, unstable slopes and hairpin stacks. The practicalities of this will depend on the finance available to undertake spoil haulage, accessibility along the alignment and the volume of spoil created. In particularly steep, complex terrain, such as that crossed by the Dharan-Dhankuta road, both high excavation volumes and access problems combine to make discriminate spoil disposal extremely difficult. In addition, it is in this terrain that the potential for erosion on spoil tips is likely to be greatest, and the availability of suitable spoil disposal sites, lowest.

A conspicuous feature of discriminate spoil disposal policies is the creation of often large spoil benches. These are characteristic of spoil disposal along the Dharan-Dhankuta road. The failure of three benches along this road, due primarily to channel erosion, unusually high groundwater levels, and the possible effect of overloading by the bench itself, has caused the most severe problems along the hill section of the road to date. These failures have occurred on slopes underlain by weathered Siwalik rocks that are among the most susceptible to instability along the whole route (Chapter 5). Nevertheless, while slope failure at spoil benching sites may be the result of a number of geomorphological and geological factors, slope overloading by spoil

benching appears to have had a significant impact on the stability of some of the slopes below the road. Rather ironically, therefore, under conditions where suitable benching sites are limited, the adoption of a discriminate spoil disposal policy that incorporates the construction of large benches, may actually cause an acceleration of slope instability and road loss.

A number of general recommendations can be made concerning future spoil disposal policy along low-cost roads in the Lower Himalaya. Differentiation must be made between roads constructed across relatively shallowly inclined ridge-top topography, such as east-west oriented alignments to the north of the Mahabharat Lekh, and those road alignments that cross transverse to the foothill ranges, in a north-south direction, across terrain characterised by high relative relief. In the former case, earthworks volumes are likely to be quite low, and hence, the need for extensive spoil disposal is reduced. Side-casting, avoiding actively eroding or unstable slopes and gullies, should create few long-term problems for road stability and have a relatively low impact on surrounding land uses. However, if the road is to be constructed upslope of a relatively high risk land use, then even the short-term spoil-related hazards may prove disastrous. Under these conditions the risk posed to the land use should be weighed against the cost and practicalities of adopting a discriminate spoil disposal policy.

Roads located in areas of high relative relief (eg. the Mahabharat Lekh), and especially those that run normal to the physiographic lineaments, are the most likely to generate severe erosion and instability problems. While side-casting onto side-long ground is unlikely to have any adverse long-term effects on these roads, tipping should be discouraged on hairpin stacks and on unstable slopes. Unstable and potentially unstable slopes, in terms of both mass movement and erosion, should be identified prior to earthworks, and preferably during the reconnaissance surveys, and declared as unsafe tipping sites. These sites should be identified, primarily, on the basis of their present stability and by reference to slope inclination, the presence or absence of active or degraded erosional landforms and mass movement features, slope materials and groundwater conditions.

Regular monitoring of tip slopes should be undertaken, perhaps along the lines described in Chapter 8, in order to assess their stability and provide forewarning of possible imminent failure or erosion. Future research should be

directed towards the objective assessment of slope parameters (inclination, soil type and depth, rock type and weathering grade, groundwater conditions, slope vegetation and erosion) for examining the potential for spoil-induced erosion and instability. This may be achieved by a proforma method of data collection, such as that described in Chapter 9, combined with a programme of tip slope instrumentation.

CHAPTER 7

A FIELD RECONNAISSANCE TECHNIQUE FOR PREDICTING STORM RUNOFF USING CHANNEL SURVEY AND UNGAUGED CATCHMENT MODELS

7.1 Introduction

The impact of flooding and sediment hazards on road stability in mountainous terrain, and the limitations of existing predictive formulae were outlined in Chapter 2. Problems of storm runoff prediction become acute when there are no rainfall and runoff data or locally derived ungauged catchment models available. These problems are amplified in humid sub-tropical mountain catchments, where both rainfall and catchment response are highly variable over relatively short distances. Frequently, there may be no indication as to which models are likely to be the most suitable for predicting storm runoff from the catchments to be crossed by the intended road.

There is no set procedure for the choice of design flood for culvert and bridge specifications. The philosophy commonly adopted for low-cost roads, is to weigh the costs of designing for storms of various recurrence intervals with the likely impact of these storms on culvert or bridge stability, and the consequences of any temporary loss of road access. With the exception of major bridges, it is often assumed that routine maintenance of hydraulic structures will enable design storms to be chosen with recurrence intervals lower than the intended design life of the road, as occasional culvert inundation, or temporary loss of access, is normally tolerable. The choice of the design storm is usually based on the accepted probability of the culvert design being surcharged by an event of equal or greater magnitude during its design life (Wilson 1985). On the Dharan - Dhankuta road, for instance, a 50 percent probability was accepted that the culverts would not be surcharged once in 10 years, while for bridges, the same probability was accepted for overtopping in 20 years (Cross 1982).

In order to identify the most appropriate design storm, three main criteria need to be assessed:

i) the magnitude - frequency rating of storms in the area,

ii) the impact of these storms on underdesigned culverts and bridges, both in terms of repair costs, maintenance and temporary loss of road access,

iii) the economic, political and strategic importance of the road and the importance placed on maintaining good drainage and road access.

Probably the most important of these criteria is the need to gain an adequate knowledge of storm runoff magnitude and frequency in the channels to be crossed by the intended road. Unfortunately, in remote mountain terrain such as the Lower Himalaya, there is frequently an inadequate hydrological data base to achieve this. Ordinarily, this problem might be solved by the adoption of a suitable flood prediction model, derived from similar catchments elsewhere. However, the designer may be unaware of the applicability of the various discharge prediction models (discussed in Chapter 2) to flood prediction in the catchments encountered. Consequently, it may be necessary to turn to field evidence (Chapter 2) in order to provide the basis for hydraulic design. This chapter examines the contribution that low-cost, rapid reconnaissance surveys can make to flood estimation for hydraulic design purposes in small to medium-sized channels in the Lower Himalaya.

The principal objectives of this chapter are therefore to:

i) formulate a rapid technique of channel assessment, applicable at the reconnaissance stage, for evaluating storm runoff, channel stability and sediment transport,

ii) test selected existing rainfall-runoff and empirical ungauged catchment models that have potential application to storm runoff prediction in small humid sub-tropical mountain catchments in Nepal, and

iii) derive empirical relationships between storm discharge and catchment variables for small watersheds in the Dharan-Dhankuta area.

The fieldwork and analysis described in this chapter is divided into five main components. In Sections 7.2 and 7.3, a method for field evaluation of flood potential and channel stability in small channels, using a purpose-designed

proforma, is described and assessed with respect to hydraulic design criteria. Information derived from this study is used in Section 7.4 to estimate peak flow velocities and discharges that occurred during the large storms in July 1974 and September 1984. In Section 7.5, 24-hour rainfall depths recorded during these two storms, and catchment characteristics determined from air photographs, are used to compute peak flow rates from eight selected discharge prediction models of the rainfall-runoff and empirical ungauged catchment varieties (Chapter 2). These predicted discharges are then compared with the discharge rates derived from field evidence, in order to test the applicability of the models. In Section 7.6, the field derived discharge rates for the 1984 storm are compared statistically with a number of selected catchment variables, in order to establish the basis for the development of a regional empirical ungauged catchment model from locally derived discharge data. Finally, also in Section 7.6, the computation of the 1984 peak flow in the Leoti Khola is described and compared with the most successful rainfall-runoff and empirical models identified in Sections 7.5 and 7.6, in order to test their ability to predict this discharge from a comparatively large catchment.

7.2 Philosophy of the Field Data Collection

In the Dharan-Dhankuta area, two large storms have taken place since the first geomorphological reconnaissance survey of 1974. In July 1974, a storm with a recurrence interval of 10 years (Barker 1976) occurred, and caused considerable morphological change in the Leoti Khola and its tributaries (Brunsden et al 1981). Between this date and the final completion of the road in 1982 and the Tamur Bridge in 1983, relatively little widespread storm-induced geomorphological activity took place, and hence, it can be assumed that many of the erosional and depositional effects of the 1974 storm would have remained visible and largely unaltered during this period, unless locally obliterated by road construction and the impacts of localised storms. Therefore, while local modifications to the 1974 flood channels by subsequent erosion and deposition, may have removed some of the evidence of this storm, the only way of estimating the peak discharges generated during this event was to assume that, on the whole, channel capacities prior to the 1984 storm (see below) had remained unchanged. The validity of this assumption is discussed further in Section 7.4.

In September 1984, an exceptionally large storm occurred over the Himalayan foothills of central and eastern Nepal. This was locally concentrated in the Leoti Khola catchment and adjoining Sangure Ridge (Chapter 3), causing a 75-80 year recurrence interval flood in the Leoti Khola (Section 7.6). Clearly, a storm of this size would have caused widespread destruction of the evidence of the earlier (1974) storm and created its own suite of channel forms and flood deposits. These new fluvial landforms were used to determine the peak flow channel capacities generated by the 1984 storm. The field methodology adopted is described below.

Channel data were collected by proformas prior to and after the September 1984 storm. The principal aim of the fieldwork was to collect channel data for purposes of discharge computation. However, the channel proforma also included reference to channel morphology and sediment, and the nature and stability of banks and side-slopes, for purposes of assessing channel stability and sediment supply. The design and execution of the proforma survey are described in the following section.

7.3 Proforma Design and Field Use

7.3.1 Introduction

In order to be an effective technique of drainage assessment, during geomorphological reconnaissance surveys for road projects, a proforma needs to be flexible enough to be able to take account of varying channel conditions and be of a form that will allow rapid and objective data collection and channel evaluation. In addition, the technique should also allow continued channel assessment during site investigation, construction and maintenance.

A completed proforma, designed with these aims in mind, is shown in Figure 7.1. It can be seen that the proforma is composed of four main components (channel cross sectional area and slope, bedload calibre, general channel and side-slope morphology and composition, and the proportion of channel banks and side-slopes occupied by landslides). These require numerical data inputs, wherever possible, to minimise the level of subjectivity. Each component is independently assessed at successive intervals upstream from the proposed or existing culvert or bridge site. During fieldwork, sampling in the smaller gullies extended from the channel crossing to the headwaters, while, in the

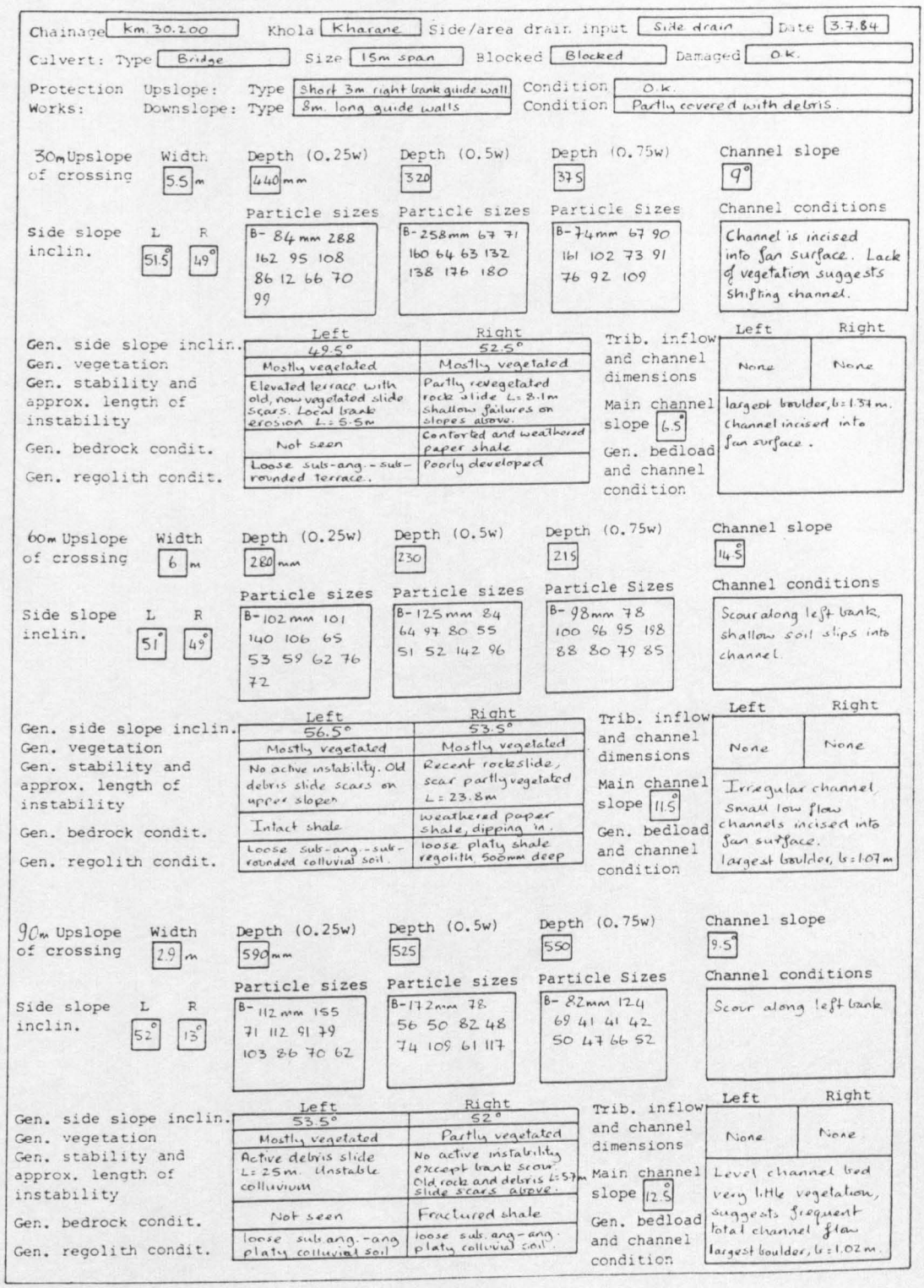

FIGURE 7.1 Completed Channel Proforma.

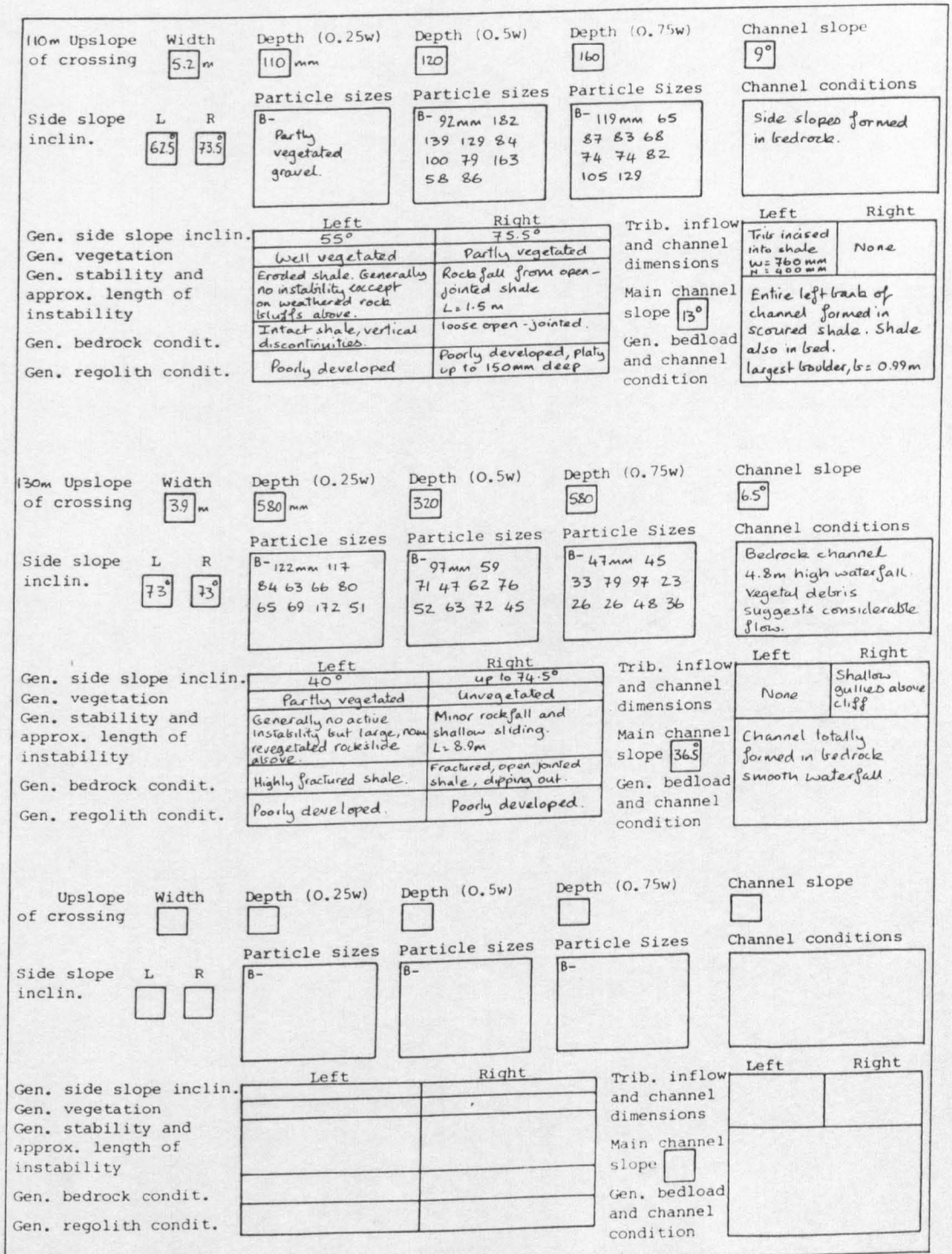

FIGURE 7.1 Cont. Reverse Side of Completed Channel Proforma.

larger gullies, channel lengths of up to 974m upstream of the channel crossing were sampled. This was the case in Garjuwa Khola (bridged at km 29.830), where a total of four proformas were used. This repetition of data collection, every 20-50m upstream, depending upon the overall size of the gully, is designed to allow the variability in channel morphology, stability and flow conditions to be evaluated and placed within a framework for the gully as a whole.

The fieldwork was undertaken, first in July and August 1984, and then repeated in November 1984, following the heavy rainfall in September. The Leoti Khola and the Tamur River were excluded from the survey, as these catchments are clearly too large and varied to be surveyed in this manner. With four exceptions (see Section 7.4), proformas were completed for each of the 42 mountain channels culverted or bridged by the Dharan-Dhankuta road. The catchments of these channels are shown in Figure (7.2 A and B).

Logistical problems experienced in the completion of the proformas were associated, primarily, with access along the channels. Many of the steeper tributaries of the Leoti Khola are characterised by up to 20m high, vertical waterfalls, boulder ruckles composed of boulders of up to 5m diameter, and landslide deposits that totally fill the channel. Where landslides had occurred in the 24 hours prior to the surveys, mudflows continued to issue from the slide material, inhibiting access. These obstructions combined to reduce the accuracy with which channel distances could be measured from the culvert. However, this is not considered to be a serious limitation as distance from the culvert was not incorporated into any of the later analyses.

7.3.2 The Determination of Channel Capacity (peak flow cross-sectional area)

The determination of peak flow cross-sectional area relied on the recognition of peak flow depth indicators along the channel side-slopes. In the case of the 1984 event, stranded vegetation, including grass, twigs and logs, was probably the most dependable evidence of flow depth. This was often left as a distinct marker on more shallowly inclined bedrock side-slopes, terrace banks and on bushes and trees growing in the channel. In the same way, stranded gravel, sand and silt, from flows highly charged with sediment, remained in recognizable form, unless washed away by overland flow on bare rock slopes.

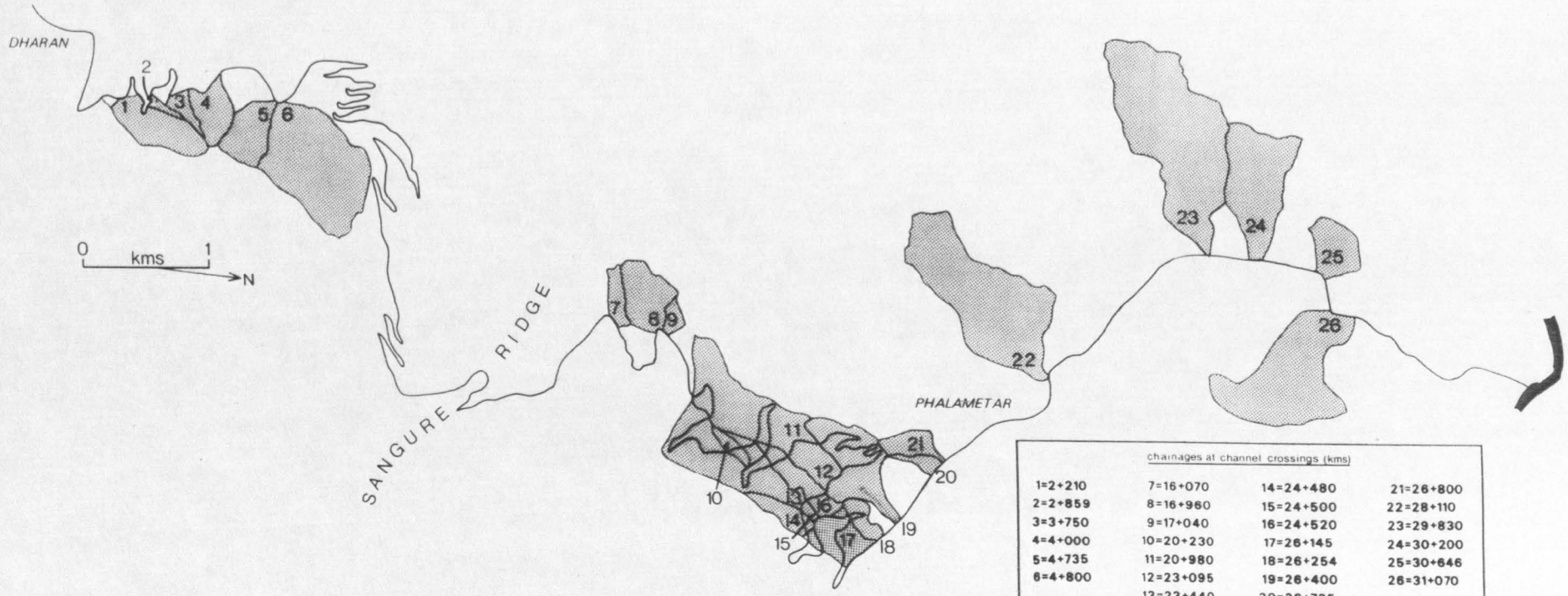

FIGURE 7.2A Surveyed Catchments Between Dharan and Tamur.

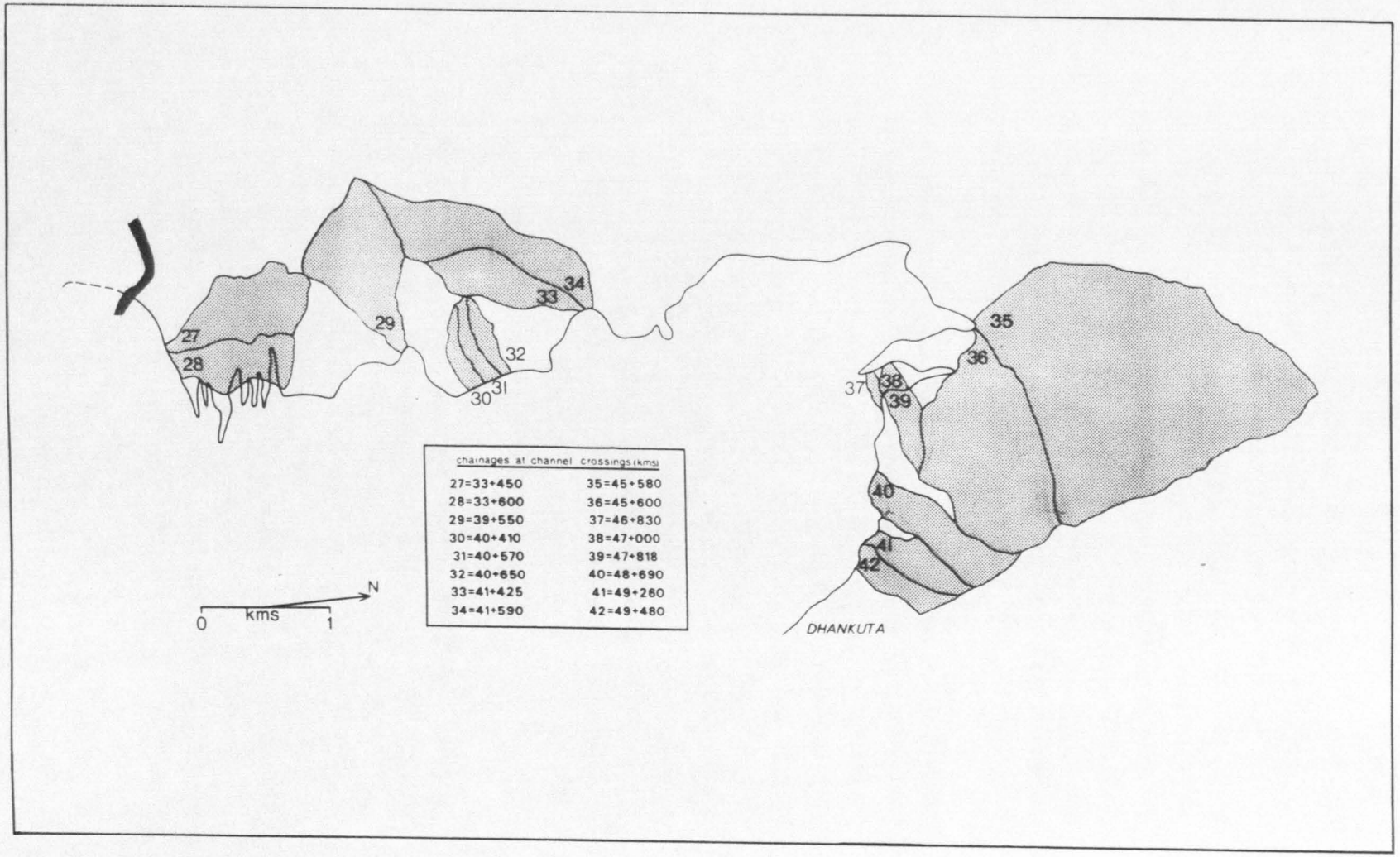

FIGURE 7.2B Surveyed Catchments Between Tamur and Dhankuta.

Finally, owing to the generally highly fractured nature of the rock exposed in the channel, storm runoff often scours the channel banks or side-slopes to the height of the peak stage, thus creating erosion undercuts that can act as subsidiary indicators of maximum flow depth. Much of the depositional evidence of the 1974 storm, however, is likely to have been removed during subsequent monsoon storms. Therefore, peak flow depth determination for this event was based on the recognition of the more long-term morphological indicators. For these reasons, the accuracy and dependability of the surveyed 1974 peak flow cross-sectional areas and computed discharges (Section 7.4) are likely to have been less than those for 1984.

Once a reliable flood level was identified, a 30m tape was stretched horizontally across the channel, from bank to bank at this level. Depth to bed surface was measured vertically at a quarter, half and three-quarter widths of the channel (Figure 7.1). The total cross-sectional area of the peak flow channel was then determined by summing the areas of the measured vertical sections at each surveyed station. While the accuracy of the proforma survey would have been improved had a greater number of channel depth measurements been undertaken in each cross-section, many of the surveyed channels were sufficiently narrow, of the order of 1-3m in width, to make a larger number of depth measurements unnecessary. Clearly, the number of depth measurements taken in any survey should depend upon channel width, variability in bed elevation and the time available.

The accurate determination of maximum flow depth was hampered by a number of problems, and these are described with respect to flow monitoring, in Chapter 8. The most serious error that can arise in the determination of maximum flow depth is that caused by channel aggradation on the falling limb of the flood hydrograph. During flood recession, in the larger catchments especially, silt, sand and gravel are usually deposited in the main channel. This process of channel aggradation is particularly notable in channels composed of highly comminuted shale and phyllite debris. Garjuwa Khola is a prime example of this, where bed levels at the fan apex, are often raised by up to a metre by mudflow accumulations in the channel during the 48 hours following large storms. Further upstream, aggradation becomes more localised, and sample cross-sections were chosen at points of least aggradation wherever possible. Flood level indicators were not present along the entire length of the channels, and this restricted the choice of sampling locations. As a result,

stations were not always located at equal intervals along the channel (see Figure 7.1). However, the surveys undertaken after the September 1984 storm, endeavoured to locate stations as close as possible to those employed during the previous survey, in order to enable direct comparison. The choice of the representative cross-sectional area and flow rate at the culvert or bridge, was made by an objective comparison of the flow estimates obtained for each surveyed cross-section and the justifiable assumption that discharge increases downstream.

7.3.3 Channel Gradient, Side-Slope and Channel Morphology

Channel gradient was determined at each cross-section, and between successive cross-sections, using a clinometer and ranging rod. Channel gradient was employed as a surrogate for water surface slope (energy-grade line) in the calculation of velocity using the Manning equation (Section 7.4). While the assumption of equivalent gradients may, in some instances, be untenable due to highly irregular channel beds and non-uniform flow conditions, there was insufficient hydraulic data to allow more rigorous modelling to be undertaken. The stability and general morphology of the channel and side-slopes were described qualitatively on the proformas in order to gain an overall impression of stability, sediment supply and flow conditions.

7.3.4 The Calibre of the Channel Bed Material

At each station cross-section, samples of bed material were taken at the centre and quarter distances across the channel. The intermediate axes of the ten largest particles in each sample were measured. These data were collected for the purposes of computing the Manning's roughness coefficient (Section 7.4), and to provide an indication of the likely size of bedload transported during storm runoff.

7.3.5 Landslide Density

The determination of the proportion of channel side-slopes that are unstable was considered important for two reasons. First, as checkdams are most effectively located at relatively strong points in the channel, the recognition of reaches prone to landsliding is an important factor in channel stabilization. Second, landsliding is seen as the major source of channel sediment in the

study area (Hearn and Jones 1985), and hence, an assessment of channel side-slope stability is fundamental to the evaluation of sediment supply. The total channel length of all landslides occurring between successive stations was measured and expressed as a percentage of between-station channel length. While the measurement of landslide volume rather than length would have been more meaningful in the evaluation of sediment input to the channel, this would have been very time consuming and subject to the errors that might have arisen in estimating landslide depth.

7.4 The Computation of Peak Flow Velocity and Discharge

Conventionally, computations of flow velocity in the absence of flow data, usually rely on one of three main velocity formulae (Manning, Cezy and D'Arcy Weisbach) that equate velocity (v) with channel hydraulic radius (R), water surface slope (S) and channel roughness (n). Probably the most commonly employed formula is that proposed by Manning (1891),

$$v = R^{2/3}S^{1/2}n^{-1} \text{ measured in S.I. units.} \qquad \text{.....7.1}$$

The main limitation of this method of calculating flow velocity is the difficulty in obtaining a representative value of flow roughness. Total resistance to flow is composed of grain/particulate resistance, form resistance of the channel bed, internal distortion resistance caused by flow turbulence, and spill resistance associated with accelerating and decelerating flow (Richards 1982). In addition, the transport of sediment load, especially in traction along the channel bed, may in some instances, lead to reduced velocities through a reduction in stream power, although Coleman (1986) has demonstrated that this is restricted to the 'wake' zone close to the channel boundary. An evaluation of the effect of transported sediment on stream velocity requires considerable experimental data and rigorous modelling, and cannot be undertaken here.

Most velocity formulae, such as that proposed by Manning, are based on the assumption of uniform flow resistance; a condition that is rarely found in nature, especially during high magnitude flows when the computation of peak velocity is crucial. Using data on gravel bed streams in Switzerland, Strickler (1923) produced an empirical relationship between the Manning's roughness coefficient (n) and the median particle diameter (D_{50}) measured in mm:

$$n = 0.0151\ D_{50}^{1/6} \qquad .....7.2$$

This assumption that flow resistance is dependent only on grain roughness is untenable in steep mountain channels (Chapter 2). The character of these channels indicates that internal resistance and form resistance, caused by irregularly distributed boulders and cobbles, and morphological irregularities in the channel itself, should ideally be given adequate representation in the determination of roughness and velocity computations. The concept of large-scale roughness, where the median dimension of individual cobbles or boulders is expressed as a proportion of total flow depth, has been used to compute velocity (Bathurst et al 1981, Bathurst 1982). A review of presently available models has led Bathurst (1982) to conclude that further research is required to produce a reliable, process based, flow resistance equation for mountain rivers.

An alternative method is to determine the dimensions of particles entrained during peak flow and calculate velocity from an entrainment function, such as that proposed by Bradley and Mears (1980):

$$V_b = \sqrt{\frac{2(\gamma_s - \gamma_f)}{C_d \gamma_f} \cdot \frac{(a.b.c)}{a.c.} \cdot g \cdot (\mu\cos\theta - \sin\theta)} \qquad ....7.3$$

Where C_d is the drag coefficient,
μ is a particle friction coefficient,
γ_s and γ_f are the densities of solids and fluids respectively,
a, b and c are the axial dimensions of the median particle entrained at the channel bed during peak flow,
g is the acceleration due to gravity, and
θ is the water surface slope.

Peak flow velocity, for each channel during the 1984 storm, was computed in three separate ways: a) by the entrainment function (equation 7.3), using values of C_d and μ as 0.79 and 0.75 respectively (Caine and Mool 1981), and the Manning formula (equation 7.1) with both b) a variable, and c) a constant roughness coefficient (Table 7.1). The variable roughness coefficient was calculated from the Strickler formula (equation 7.2), using the median grain diameter determined from the measurements of bed particles recorded on the proforma sheets. The adoption of a constant, assumed value for the Manning

Road Chainage at Crossing	Catchment Area(km^2)	Catchment Slope(%)	Total Channel Length (m)	Channel Density (km/km^2)	Channel Capacity 1974(m^2)	Channel Capacity 1984(m^2)	Pptn.al Increase Channel Capacity	Peak Velocity Constant n (m/s)	Peak Velocity Variable n (m/s)	Peak Velocity Entrain. f (m/s)	Peak Discharge 1984(m^3/s)	Peak area Adjusted Discharge 1984(m^3/s)	Peak Discharge 1974(m^3/s)
2.210	0.1975	26.91	800.16	4.051	0.909	2.880	3.168	5.63	7.08	1.88	16.23	82.17	3.49
2.859	0.0150	28.07	300.06	20.004	0.762	1.837	2.411	5.93	7.83	1.48	10.89	726.33	3.51
3.750	0.0337	30.43	475.09	14.098	0.283	0.367	1.297	4.29	5.66	1.16	1.57	46.74	1.04
4.000	0.0975	31.12	425.08	4.360	0.347	0.984	2.836	6.84	8.72	1.21	5.18	53.09	1.38
4.735	0.1525	27.08	625.12	4.098	0.440	2.471	5.616	5.07	6.26	1.42	12.54	82.23	1.43
4.800	0.6350	26.64	3800.76	5.985	—	—	—	—	—	—	—	—	—
16.070	0.0600	22.67	437.58	7.293	0.180	0.746	4.133	5.21	4.68	1.72	3.89	64.83	0.35
16.960	0.1725	26.22	612.62	3.551	—	—	—	—	—	—	—	—	—
17.040	0.0342	46.08	212.54	6.215	—	—	—	—	—	—	—	—	—
20.230	0.0360	34.98	275.05	7.640	0.753	1.516	2.013	6.34	8.50	0.95	9.61	266.97	2.23
20.980	0.3875	26.08	975.19	2.517	0.390	0.976	2.504	5.18	7.03	1.27	5.05	13.04	1.65
23.095	0.4650	22.36	1337.77	2.877	0.575	2.150	3.739	6.86	8.96	1.39	14.75	31.72	1.46
23.440	0.3975	24.69	1112.72	2.799	0.987	4.133	4.187	8.11	10.95	1.39	33.51	84.31	4.74
24.480	0.0625	25.09	625.12	10.002	0.360	3.546	9.850	6.01	11.96	1.29	20.43	326.88	0.77
24.500	0.4125	24.66	1275.25	3.091	0.527	2.672	5.070	6.67	11.17	1.51	17.82	43.20	1.76
24.520	0.0525	24.18	412.58	7.859	0.371	1.693	4.563	6.95	9.20	1.19	11.76	224.02	1.59
26.145	0.6450	21.92	2500.50	3.877	1.548	0.640	0.413	5.50	7.89	1.37	20.52	31.81	3.58
26.254	0.0850	25.21	412.48	4.853	0.398	2.107	5.294	2.89	3.99	1.59	6.09	71.60	0.67
26.400	0.7275	22.71	2000.40	2.750	—	—	—	—	—	—	—	—	—
26.725	0.0225	42.46	325.06	14.450	1.046	1.112	1.063	6.23	17.25	0.38	6.93	308.10	7.00
26.800	0.0775	35.88	500.10	6.453	0.607	4.557	7.507	10.47	14.54	1.01	47.71	615.61	2.55
28.110	0.8125	2.89	1900.38	2.339	1.429	6.814	4.768	5.56	6.98	1.89	37.91	46.66	5.75
29.830	0.9500	13.73	3450.69	3.630	2.028	9.390	4.630	5.65	7.07	2.13	53.09	55.88	7.83
30.200	0.4150	12.67	1800.36	4.338	1.560	9.204	5.901	4.93	6.69	1.61	45.43	109.47	3.96
30.646	0.1450	4.68	525.10	3.621	1.111	0.399	0.359	2.82	3.63	0.64	1.13	7.76	4.60
31.070	0.6225	21.41	1525.30	2.450	2.156	5.842	2.709	6.45	8.22	1.77	37.66	60.50	7.79
33.450	0.5200	31.28	775.15	1.490	2.223	7.362	3.312	5.03	6.75	1.70	37.05	71.25	4.06
33.600	0.3250	33.07	1050.21	3.231	1.379	2.893	2.098	4.99	4.27	1.86	14.45	44.46	4.23
39.550	0.6625	25.76	2375.47	3.586	2.38	1.29	0.54	4.92	6.40	1.63	6.34	9.57	8.22
40.410	0.0825	22.23	787.66	9.547	0.89	1.70	1.91	8.04	7.54	1.03	13.67	165.70	3.28
40.570	0.0800	24.52	312.56	3.907	1.27	1.49	1.17	4.75	4.40	1.29	7.08	88.50	6.11
40.650	0.0825	23.80	450.09	5.456	0.57	1.02	1.79	5.35	5.92	1.84	5.32	64.48	3.00
41.425	0.3225	21.12	1825.36	5.660	1.35	4.43	3.27	6.68	8.95	1.48	29.62	91.84	4.93
41.590	0.4800	20.26	2425.48	5.053	3.10	6.03	1.94	7.14	9.41	1.67	43.05	89.69	14.00
45.580	3.1625	21.80	15128.03	4.783	1.96	5.00	2.55	4.31	5.87	1.49	21.55	6.81	4.47
45.600	1.3350	24.40	6501.30	4.87	3.57	2.17	0.61	4.43	5.90	1.57	9.61	7.20	12.53
46.830	0.0275	24.53	325.06	11.82	1.24	1.25	1.01	5.51	7.84	1.48	6.91	251.31	6.94
47.000	0.1650	19.37	1000.20	6.06	1.25	1.12	0.90	4.55	6.34	1.25	5.11	30.97	5.12
47.818	0.1300	18.65	750.15	5.77	0.46	0.36	0.78	2.67	3.52	1.76	0.95	7.31	0.85
48.690	0.4075	9.45	1500.30	3.68	1.39	2.83	2.03	6.33	9.48	1.28	17.94	44.02	5.39
49.260	0.2100	19.35	625.12	2.98	0.80	1.10	1.37	2.85	3.85	1.65	3.13	14.90	2.47
49.480	0.1525	20.59	1075.21	7.05	0.34	0.44	1.27	3.15	4.21	1.62	1.37	8.98	1.36

TABLE 7.1 Catchment, Channel and Flow Data Determined From Air Photographs and Proformas.

roughness coefficient is open to some criticism because of the subjectivity in its choice and the variability in channel roughness. However, it enables velocity computation to be made using an all-encompassing grain, flow and form roughness coefficient obtained by reference to proven standards. A roughness coefficient of 0.045 is recommended (Gregory and Walling 1973) for mountain channels composed of cobbles and boulders, and this value was adopted in the present study.

Table 7.1 displays the three sets of peak velocity computations for each channel at the cross-sections where the computed discharge is considered to be representative of the gully at the culvert or bridge. These data reveal that peak velocities estimated using a variable value of 'n', calculated from the Strickler formula, are on average 1.36 times greater than those calculated using a constant 'n', and 6.45 times greater than those derived from the entrainment function. The variable roughness coefficient, based on grain roughness alone, leads to an underestimation of flow resistance and a consequent overestimation of peak velocity. In the case of the entrainment function, particle size measurements taken of the bed material after the passage of a flood are likely to be considerably smaller than the sediment load entrained during peak flow, due to post-peak deposition of finer material. As a result, peak flow velocities are grossly underestimated. On the basis of these findings, a constant value of the Manning's roughness coefficient has been used in the computation of peak discharge, as this is considered to be the only feasible means of representing total channel and flow roughness, without detailed hydraulic experimentation.

Table 7.1 also shows the computed velocities for the 1974 storm. These velocities have been calculated on the assumption of a constant roughness coefficient and a channel configuration that has remained largely unchanged during the intervening 10 years. Although a relatively small number of sizeable storms have occurred during this period, they have been quite localised and their effect on overall channel capacity could be considered likely to have been minimal. This contention is based on a review of rainfall records obtained from the Meteorological Department in Dhankuta. Between 1974 and 1983, the largest storms recorded at Dharan Bazar, Mulghat and Dhankuta were 218mm (14.6.1979), 108mm (19.7.1980) and 112mm (24.7.1979), respectively. These maximum storm depths are considerably less than those of the July 1974 storm at Dharan Bazar (282mm) and Mulghat (162mm).

Therefore, channel capacities in catchments between the start of the Dharan-Dhankuta road, above Dharan Bazar, and the lower Dhankuta Khola, may have remained largely unchanged between 1974 and when the first channel survey was undertaken in July/August 1984. It is, recognised, however, that the spatial variability in rainfall intensity, which cannot be quantified owing to a lack of rainfall data, may limit the validity of this argument. The July 1974 storm depth recorded at Dhankuta (48mm) has been exceeded on at least one occasion during each of most of the intervening years. Therefore, channel capacities surveyed prior to the 1984 storm in the Dhankuta Khola catchment (to the north of the Tamur valley), are unlikely to be representative of discharges generated by the 1974 storm. Consequently, the following comparisons between the 1974 and 1984 flow data, will concentrate on those channels surveyed to the south of the Dhankuta Khola valley.

The computed velocities for the 1984 storm, in surveyed channels to the south of the Dhankuta Khola catchment (km2.210-33.600), were on average 1.82 times greater than those for the 1974 storm. The extent to which the surveyed channel capacities were increased during the 1984 storm is also shown in Table 7.1. Channel capacities increased by an average factor of 3.73. Some of the variation in the magnitude of increase between individual channels (Table 7.1) is attributable to the spatially variable resistance to scour of the channel forming materials. When these channels are divided according to predominant bedrock type, the mean rate of increase in channel capacity varies between factors of 4.41 for phyllites and shales, 2.95 for quartzites and 2.43 for Siwalik rocks. Although no firm conclusions can be drawn from these results, owing to the small number of channels surveyed in Siwalik (4) and quartzite (5) materials and the spatial variability in rainfall intensity, the general trend is for the greatest increase in channel capacity to occur in channels formed predominantly in phyllitic and shaly materials. These are often highly weathered and susceptible to erosion when exposed in channel banks and side-slopes.

For each channel surveyed, peak flow cross-sectional area was combined with computed flow velocity, using the constant Manning's roughness coefficient, to yield peak flow rate at each station for the 1974 and 1984 storms. A representative peak flow rate for each channel was chosen by an assessment of between-station variability in computed discharge. In most cases a sensible progression of increasing discharge downstream emerged, and the discharge

chosen was that for the cross-section closest to the culvert. However, peak flow rates were undeterminable in the cases of the four channels crossed by the road at km 4.800, 16.960, 17.040, and 26.400. In the gully crossed at km 17.040, almost 40 percent of the identifiable channel length above the culvert had been engulfed by a rock slide, making sensible discharge computation impossible. In the other three cases, peak flow was dominated by debris flow activity, and hence, a peak runoff rate is less applicable and difficult to compute (Hungr et al 1984). The computed peak discharges for each of the other channels surveyed, are shown in Table (7.1).

Having substantiated that the majority of the pre-September 1984 channel capacities to the south of the Dhankuta Khola catchment (km 2.210 - 33.600) were essentially those created during the 1974 storm, the data in Table 7.1 indicate that peak 1974 flood discharges varied between 0.35 and 7.83 cumecs. By contrast, peak discharges occurring during the September 1984 storm, in all of the surveyed channels, varied between 0.95 and 53.09 cumecs. In the cases of the channels crossed at km 26.725 and km 30.646, the computed 1974 discharges were greater than those discharges for 1984 (Table 7.1). This may reflect spatial variations in storm rainfall or, more likely, unreliability of the 1974 discharges.

A one-tailed Spearman's Rank Correlation test was used to determine whether the discharge computations for these storms displayed the same variation between channels to the south of the Dhankuta Khola catchment. A positive correlation coefficient, significant at the 95 percent level, led to the rejection of the null hypothesis that there is no significant association between the two data sets. Therefore, in terms of peak flow rate, the channels surveyed responded in the same manner to both storms. This supports the validity of the computed discharges, although, as discussed above, the 1974 discharge data should be treated with caution.

7.5 An Assessment of Selected Ungauged Catchment Models in Terms of their Ability to Predict High Magnitude Storm Discharge in the Dharan-Dhankuta Area.

A brief discussion of rainfall-runoff and ungauged catchment models was given in Chapter 2. A number of models were identified that have potential application to the prediction of storm runoff in the Lower Himalaya. A total

of eight of these models are tested in this section with regard to their ability in predicting the 1984 peak storm discharges, derived from the field survey described in Section 7.4. The models were chosen on the basis of the runoff data that they yield, the catchment variables that are required to be evaluated for their computation, and the climatic-physiographic similarity between the catchments for which they were derived and those in the Dharan-Dhankuta area. These eight models are listed in Table 7.2, and it can be seen that six of them have been derived in either Nepal or India. While the author is aware of a number of other models that could have been tested, their data requirements and the climatic and physiographic conditions under which they have been developed, were considered inappropriate for the present analysis.

Three of the chosen models (Rational, Gupta Modified Rational and the Generalised Tropical Flood Model) are variants of the rainfall-runoff method of storm discharge prediction, while the remainder are regionally derived ungauged catchment models, based on catchment area alone. These latter models rely on the concept of the Probable Maximum Discharge (PMD). In steep, sub-tropical mountain catchments that experience high intensity monsoon rainfall of long duration, the PMD is a useful concept in catchment studies, especially as the return period of high magnitude floods is extremely difficult to evaluate with any precision. The PMD has been defined as the "flood that may be expected from the most severe combination of critical meteorologic and hydrologic conditions that are normally possible in the region" (Wang and Revell 1983, p400). Chapter 3 has shown that the September 1984 storm had an estimated maximum recurrence interval of 75 to 80 years between the southern flanks of the Sangure Ridge and the Tamur valley. Consequently, peak discharges in channels crossed by the road in this area, may have corresponded approximately to the PMD. The computation of peak discharge from these channels using models based on the PMD may, therefore, be valid. This is supported by the fact that the magnitude-frequency rating for events of larger recurrence interval is uncertain owing to a lack of hydrological data.

Peak rainfall intensity, for use in the Gupta and Rational methods, was derived by a method devised by Gupta and adopted by Barker (1976) for the flood assessment in the Tamur River using the following equation:

MODEL	EXPLANATION	ORIGIN
GUPTA (1973): $Q=640PRAe^{x}$	Q=Peak discharge(cusecs) P=Average area rainfall(ins/hr) R=Runoff coefficient Ae=Effective catchment area($miles^2$) x=0.92+1/42logAe	INDIA
RATIONAL/Kuichling (1889): $Q=0.277CAI$	Q=Peak discharge(cumecs) C=Runoff coefficient A=Catchment area(km^2) I=Rainfall intensity(mm/hr)	UNIVERSAL
GENERALISED TROPICAL FLOOD MODEL (1984): $Q=FCaPA/360Tb$	Q=Peak discharge(cumecs) F=Peak flow factor Ca=Runoff coefficient P=Storm Rainfall(mm) A=Catchment area(km^2) Tb=Base time(hr)	TROPICS
CRAIG *1 (1884): $Q=440CW\,Loge(\frac{8L^2}{W})$	Q=Peak discharge(cusecs) C=Runoff coefficient L=Basin length(miles) W=Basin mean width(miles)	INDIA
DICKENS *1 (1865): $Q=CD^{0.75}$	Q=Peak discharge(cusecs) C=Runoff coefficient D=Catchment area($miles^2$)	INDIA
INGLIS (1949): $Q=7000D/(D+4)^{0.5}$	Q=Peak discharge(cusecs) D=Catchment area($miles^2$)	INDIA
GOSWAMI: *2 $Q100=28.78A^{0.75}$	Q100=100 year peak discharge(cumecs) A=Catchment area(km^2)	INDIA
COALMA(1973) $Q50=100.52A^{0.49}$	Q50=50 year peak discharge (cumecs) A=Catchment area(km^2)	NEPAL

TABLE 7.2 The Discharge Prediction Models Tested in the Dharan Dhankuta Area.

*1 Referenced in Chow(1962)
*2 Undated reference in Barker(1976)

$$P = \frac{C}{T_c + 2} \qquad .....7.4$$

where, P is peak rainfall intensity in mm/hr,

C is a constant for each rainfall return period, and

T_c is the time to concentration in hours.

Using the return periods of the 24-hour storm rainfalls recorded at Dharan, Tamur (Mulghat) and Dhankuta (Figure 3.6) during the 1974 and 1984 storms, the recurrence intervals of storm rainfall, occurring at the centre-point of each catchment, were calculated on the assumption of a linear, progressive change in recurrence interval in a straight line between the three recording stations. Although a number of models have been developed for the computation of catchment time to concentration (T_c) (Natural Environmental Research Council 1975), it is the Bransby-Williams technique, adopted by Barker (1976), which has been used in the present analysis, owing to its simplicity and ease of computation (equation 7.5):

$$T_c = \frac{L}{D}^{5} \frac{A}{F}^{2} \qquad .....7.5$$

where, T_c is time to concentration in hours,

L is catchment length in miles,

D is the diameter of a circle with the same area as the catchment,

A is catchment area in square miles, and

F is catchment slope in percent, from the highest point of the catchment to the culvert.

The combination of C and T_c in equation 7.4, yielded a value of P in mm/hr for each catchment. Clearly, a more accurate determination of rainfall intensity would have been achieved using continuously recording raingauges, had these been available. Unfortunately, one standard raingauge installed on the Sangure Ridge was removed prior to the September 1984 storm by the Road Remedial Works Unit, while another, at Phalametar on the Leoti Khola floodplain, became buried in sediment. Consequently, only three raingauges were in operation along the road during the 1984 storm, namely at Base Camp Dharan, Mulghat and Dhankuta.

The Generalised Tropical Flood Model was used to compute peak discharge by the method described by Watkins and Fiddes (1984). This model (Table 7.2) relies on the determination of catchment area, total hydrograph base time, a peak flow factor and a runoff coefficient. The runoff coefficient is determined by reference to standard matrix tables of indices for catchment wetness, soil permeability, catchment slope and land use. As the 1984 storm occurred at the end of the monsoon season, a catchment wetness index of 1.00 was adopted, corresponding to a soil moisture recharge value greater than 75mm in a humid zone climate. As soil permeability is likely to vary considerably within each catchment, discharge was computed twice using soil indices of 3 and 4, corresponding to soil of low and fair permeability, respectively. The majority of the catchment slope values fell into the greater than 20 percent category. Catchments between km 2.210 and 41.590 inclusive are characterised by dense vegetation on the steepened slopes adjacent to drainage channels, and intense cultivation on the interfluves; a land use category of 1.00 (according to the scheme of Watkins and Fiddes 1984) was, therefore, chosen for these catchments. The remaining catchments, on the slopes below Dhankuta, are characterised by a relatively dry climate and 'large patches of bare soil' (Watkins and Fiddes 1984), and these were assigned a land use category of 1.5. Peak flow rate was computed using a conversion factor (F) of 2.5 for humid zone catchments.

The determination of catchment variables (area, length, width and slope) was achieved by photogrammetric means. Stereoscopic analysis of black and white 1:25 000 scale air photographs taken in 1978, enabled the watersheds of the gullies crossed by the road (Figure 7.2) to be delimited with sufficient accuracy. Catchment relative relief, defined as the vertical distance from the highest point of the watershed to the road culvert or bridge, was calculated by the parallax method. Catchment slope was computed by dividing this value by the basin length, measured directly on the air photographs, and adjusted for horizontal projection. Total channel length and drainage density were more difficult to determine as drainage channels were occasionally obscured by vegetation and shade. The heads of the drainage channels were taken as the points where a distinct channel and associated vegetation terminated. In the upper reaches of the drier catchments, especially those located on the slopes below Dhankuta, the precise point where runoff becomes channelised was often difficult to determine.

The catchment data is shown in Table 7.1. Catchment areas vary between 0.015 km^2 and 3.1625 km^2. Overall catchment slope varies between 2.89 and 46.08 percent, and hence, runoff rate per unit area is likely to vary considerably. Table 7.3 shows the predicted peak discharge for each surveyed channel during the 1984 storm, using the eight models. A comparison between these values and those that are field derived, or 'observed' from the proforma data (Section 7.4), demonstrates the extent to which each of the models can be used to predict the 75-80 year recurrence interval, or high magnitude, discharge from small catchments in the Dharan-Dhankuta area. With the exception of the COALMA method, all models provided a reasonable correspondence with the field derived discharges. To the south of the Dhankuta Khola catchment (km2.210 - 33.600) all models, with the exception of the COALMA method, tended to underestimate the field derived discharges. The Gupta model produced the best predictions, producing a mean underestimation of only 19.7 percent. For the 14 surveyed channels in the Dhankuta Khola catchment, seven of the models tended to overestimate the field derived discharges, as expected.

A two-tailed, two-sample Kolmogorov-Smirnov test (Norcliffe 1977) was used to determine the significance of the predictions. This test determines the significance of the maximum cumulative difference between two data sets grouped by frequencies. The test has the advantage of being non-parametric and simple to apply. Its main disadvantage is that it fails to compare directly corresponding values from the two populations. With a null hypothesis that there is no significant difference between the predicted and field derived discharges, the data sets for all 38 channels were grouped into class intervals of 5 cumecs. The total number or frequency of discharges falling into each class was determined. Each class frequency was then expressed as a cumulative proportion of the total. The maximum difference in corresponding cumulative proportions between the two distributions was calculated for each model, with the exception of COALMA. This model grossly overestimated discharges and has been disregarded for the purposes of further analysis. The maximum differences (D max) are shown in Table 7.4. There is no significant difference between the predicted and field derived 1984 distributions for all seven models at the 95 percent significance level, and hence, the null hypothesis is accepted in all cases. Smaller values of Dmax correspond to greater associations between the distributions, and it can be concluded from Table 7.4 that the Gupta and Dickens techniques are the most applicable.

Road Chainage at Crossing	1974 Field Derived Discharge (cumecs)	1984 Field Derived Discharge (cumecs)	Gupta 1974	Gupta 1984	Rational 1974	Rational 1984	Tropical Flood Model 1974	Tropical Flood Model 1984	Craig 1984	Dickens 1984	Inglis 1984	Goswami 1984	COALMA 1984
2.210	3.49	16.23	6.54	10.19	4.89	7.61	4.89	9.41	10.41	9.92	7.56	8.51	45.40
2.859	3.51	10.89	0.82	1.28	0.40	0.62	0.40	0.81	1.88	1.46	0.59	1.23	12.84
3.750	1.04	1.57	0.85	1.35	3.34	1.53	6.75	1.77	3.28	2.62	3.76	2.26	19.09
4.000	1.38	5.18	2.21	3.53	9.77	4.18	0.58	4.88	5.83	5.84	11.81	5.01	32.13
4.735	1.43	12.54	4.94	8.04	4.05	6.49	0.60	7.44	8.59	8.18	17.53	7.01	39.99
16.070	0.35	3.89	2.59	4.60	1.66	2.92	3.47	3.13	4.33	4.01	2.27	3.48	25.32
20.230	2.23	9.61	1.64	2.81	1.02	1.86	5.25	1.93	2.88	2.76	1.38	2.37	19.72
20.980	1.65	5.05	13.86	22.05	10.17	17.89	2.07	17.81	16.25	16.43	14.69	14.11	63.17
23.095	1.46	14.75	14.61	24.77	11.60	20.45	1.25	20.98	18.01	18.90	17.64	16.18	69.07
23.440	4.74	33.51	12.00	22.09	10.22	17.99	11.49	18.23	16.44	16.76	15.07	14.38	63.96
24.480	0.77	20.43	2.53	4.81	1.84	3.07	13.48	3.28	4.68	4.14	2.37	3.59	25.84
24.500	1.76	17.82	12.65	22.35	10.40	18.26	11.73	18.84	16.77	17.24	15.65	14.79	65.13
24.520	1.59	11.76	2.40	4.24	1.50	2.65	2.10	2.77	3.99	3.61	1.98	3.15	23.72
26.145	3.58	20.52	17.74	31.34	15.15	26.24	12.13	27.99	21.74	24.13	24.22	20.68	81.08
26.254	0.67	6.09	3.64	6.65	2.42	4.42	1.78	4.41	5.02	5.25	3.26	4.52	30.04
26.725	7.00	6.93	0.68	1.24	0.69	1.25	18.02	1.23	2.80	1.95	0.87	1.67	15.66
26.800	2.55	47.71	2.52	4.62	2.10	4.10	2.77	4.03	5.87	35.21	2.98	4.22	28.71
28.110	5.75	37.91	19.66	35.67	17.20	31.42	0.77	10.30	24.29	28.69	30.28	24.59	90.79
29.830	7.83	53.09	24.83	46.16	18.36	41.29	2.57	29.86	27.64	32.25	35.17	27.64	98.02
30.200	3.96	45.43	13.10	24.56	9.72	20.07	6.39	14.94	16.18	17.32	15.74	14.85	65.33
30.646	4.60	1.13	5.36	9.87	4.33	7.98	17.96	4.40	6.77	7.91	5.61	6.75	39.02
31.070	7.79	37.66	17.91	33.12	17.05	32.15	8.90	27.69	21.87	23.48	23.38	20.13	79.68
33.450	4.06	37.05	17.38	32.95	16.36	27.63	2.56	22.51	18.45	20.52	19.63	17.59	72.96
33.600	4.23	14.45	10.91	20.68	9.19	16.46	16.15	14.69	15.11	14.43	12.39	12.37	52.96
39.550	8.22	6.34	17.09	32.29	16.79	31.52	13.18	25.31	23.17	24.63	24.88	21.10	82.15
40.410	3.28	13.67	2.94	6.00	2.08	3.87	1.77	3.53	5.79	5.13	3.16	4.42	29.60
40.570	6.11	7.08	3.19	6.43	2.20	4.13	1.72	3.43	3.26	5.01	3.06	4.32	29.16
40.650	3.00	5.32	3.19	6.44	2.21	4.15	1.77	3.53	5.23	5.13	3.16	4.42	29.60
41.425	4.93	29.62	9.00	18.16	7.65	14.41	6.16	12.36	10.33	14.35	12.29	12.29	57.73
41.590	14.00	43.05	11.70	23.93	9.92	19.94	9.00	17.90	16.79	19.29	18.11	16.57	70.15
45.580	4.47	21.55	9.24	25.15	34.22	47.38	18.16	59.80	61.77	79.48	107.00	68.13	176.71
45.600	12.53	9.61	11.82	37.40	19.23	39.28	11.88	33.33	36.41	41.60	48.57	35.68	115.81
46.830	6.94	6.91	0.80	2.06	0.68	1.11	0.41	1.04	2.62	2.30	1.09	1.94	17.28
47.000	5.12	5.11	3.14	8.11	3.67	5.93	1.80	4.57	8.83	8.63	6.29	7.44	41.57
47.818	0.85	0.95	2.68	6.95	3.01	4.86	1.45	3.68	7.65	7.28	5.02	6.22	36.99
48.690	5.39	17.94	5.62	15.01	8.17	12.25	2.73	7.06	15.69	17.08	15.45	14.65	64.75
49.260	2.47	3.13	3.95	9.20	4.98	24.94	2.15	5.56	9.57	10.40	8.04	8.91	46.79
49.480	1.36	1.37	2.83	7.42	3.34	5.34	2.02	5.22	8.51	8.18	5.88	7.01	39.99

TABLE 7.3 The Field-Derived and Predicted Discharges for the 1974 and 1984 Storms.

MODEL	All Channels		Channels South of the Tamur	
	Dmax	Dcrit	Dmax	Dcrit
GUPTA 1974	0.436	0.312	---	---
GUPTA 1984	0.132	0.312	0.208	0.390
RATIONAL 1974	0.463	0.312	---	---
RATIONAL 1984	0.210	0.312	0.250	0.390
TROPICAL 1974	0.436	0.312	---	---
TROPICAL 1984	0.263	0.312	0.292	0.390
CRAIG 1984	0.158	0.312	0.292	0.390
DICKENS 1984	0.132	0.312	0.250	0.390
INGLIS 1984	0.184	0.312	0.250	0.390
GOSWAMI 1984	0.158	0.312	0.250	0.390

TABLE 7.4 Dmax Versus Dcrit Values for the Discharge-Predicting Models Using the K-S Test.

Down-stream Direction	Station (approx. road chainage)	Peak Flow CSA (m^2)	Peak Velocity (m/s)	Peak Discharge (cumecs)	Rec.Int (years)
↓	SINSUA	175.75	2.86	503.52	unknown
	25.800	137.50	3.11	428.17	77.5
	27.100	154.37	3.34	515.59	78.7
	26.260	167.00	2.86	477.95	89.0
	28.250	203.75	2.85	581.09	64.2
	29.800	218.37	3.01	674.33	61.7
	30.050	225.85	3.14	708.49	76.6

TABLE 7.5 Flow Data for the 1984 Flood in the Leoti Khola.

While the former technique is the more comprehensive of the two, it requires considerably more data on catchment parameters and rainfall in its computation. Therefore, under conditions of limited or non-existent data, the Dickens method may be the most appropriate. Insufficient hydrological data is available in the study area to enable either of the two techniques to be improved.

Considering the fact that the Generalised Tropical Flood Model includes reference to catchment soil permeability, wetness, land use and slope indices, it is disappointing that the degree of peak discharge underestimation by this model is greater than for all other models tested, apart from COALMA. The inclusion of arbitrary catchment indices into this model will, therefore, only increase its predictive ability if they can be adequately evaluated and adjusted to take account of within-catchment heterogeneity in runoff controlling factors. The land use, physiographic and climatic classifications for choosing representative values of the catchment indices used in the model, such as the runoff coefficient and the peak flow factor, are in some cases inappropriate for catchments in the Lower Himalaya.

When the Kolmogorov-Smirnov test was restricted to those catchments south of the Tamur valley, the Gupta equation, with a Dmax value of 0.208 (Table 7.4), provided the best fit discharge estimate. Again, only the COALMA predicted discharges were significantly different from the 'observed' values at the 95 percent significance level.

As the Gupta, Rational and Tropical Flood models all include reference to either total storm rainfall depth or peak intensity in their computation, it was possible to test these models in terms of their ability to predict peak discharges generated by the July 1974 storm. Using storm depths of 282 mm, 162mm and 48mm for Dharan, Mulghat and Dhankuta, respectively, and the storm magnitude recurrence interval rating curves shown on Figure 3.6, the peak rainfall intensity was calculated for each catchment for this storm. The predicted discharges using the three models are shown in Table 7.3, and these can be compared with the 'observed' discharges obtained by field survey. Table 7.4 shows that, using the Kolmogorov-Smirnov test, Dmax values of 0.436, 0.436 and 0.463 were obtained for the Gupta, Tropical Flood and Rational models, respectively. As these values are greater than the critical value at the 95 percent significance level, it can be concluded that either none

of these models are reliable as predictors of peak runoff from storms of relatively low recurrence interval, or that the data regarding the 1974 storm is suspect. The latter explanation is the most probable.

7.6 The Development of an Empirical Technique for Predicting High Magnitude Storm Discharge from Small Catchments In the Lower Himalaya

This section correlates and regresses the field derived discharges with measured catchment variables in order to develop an empirical technique for predicting peak discharges associated with high magnitude storms. Linear regression was chosen as the most suitable technique for determining whether peak discharge and catchment area - adjusted peak discharge are statistically associated with independent catchment variables. This choice of analysis is justified on the grounds that the method is probably the most applicable under conditions of limited available rainfall, runoff and catchment data, and that it avoids the uncertain assumptions of more rigorous models.

The dependent variables (peak discharge and area-adjusted peak discharge) and the independent catchment variables have been evaluated for each of the thirty-eight catchments (Table 7.1). The area-adjusted peak discharge enables the association between discharge and catchment variables to be assessed independently of catchment area. Data relating to sub-catchments of the Dhankuta Khola have been excluded from the regression analysis because the magnitude of the 1984 storm was significantly lower in this area, making high magnitude discharge prediction, based on catchment variables alone, largely inappropriate.

Linear regression, using the Pearson Product Moment Correlation test, should only be undertaken when the population distributions of the dependent and independent variables are approximately normally distributed, and when there is no significant correlation between the independent variable and the regression residuals of the dependent variable. The first stage in this analysis, therefore, was to test the normality of the dependent variables of peak discharge (Q) and area adjusted peak discharge (Q/A). Approximate frequency distributions for these variables are shown in Figures 7.3A and C. These population distributions are positively skewed. Before any regression analysis could be undertaken, it was necessary to logarithmically (base 10) transform

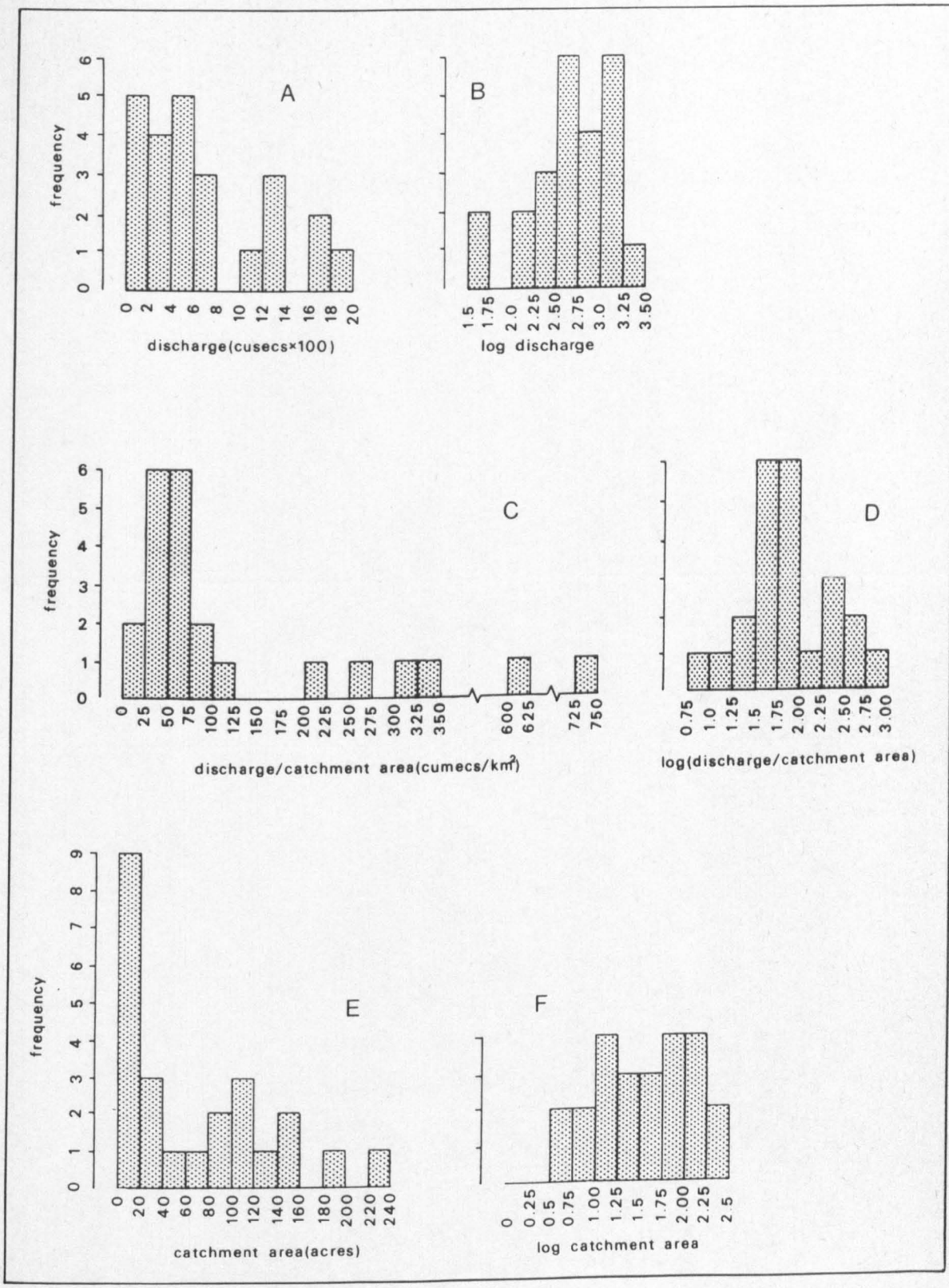

FIGURE 7.3 Frequency Distributions of Dependent (Discharge) and Independent (Catchment) Variables

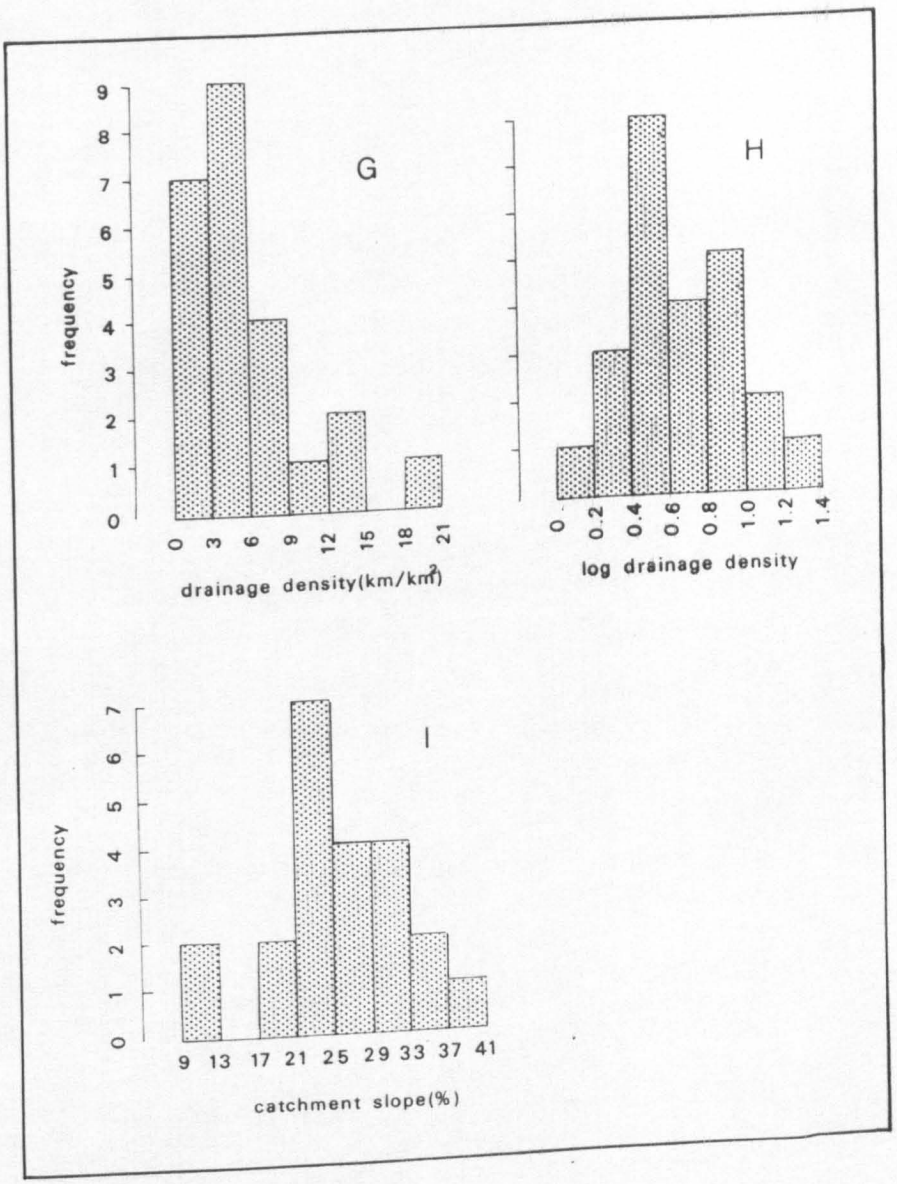

FIGURE 7.3 - continued

the data in order to normalise the data sets (Figures 7.3B and D). This transformation yielded skewness values of -0.135 and +0.441 for the peak discharge (Q) and area-adjusted discharge (Q/A) populations respectively, which are within the arbitrary range of $\pm$1.00, suggested by Champion (1981) to be the acceptable limits for a normal distribution. The population distribution of catchment areas in acres is shown in Figure 7.3E. Log-transformation of this positively skewed distribution yielded an approximately normal distribution (skewness = -0.127, Figure 7.3F).

A Pearson Product Moment correlation coefficient of r= +0.563, significant at the 99 percent level and corresponding to a coefficient of determination of 0.316, was obtained between log discharge (Y) and log catchment area (X). Linear regression yielded the following relationship:

$$Y = 0.479X + 1.888 \pm 0.732 \text{ (2 S.E.s Y on X)} \qquad .....7.6$$

The regression line for this equation has been drawn through a scattergram of points in Figure 7.4A. Assuming that the populations are normally distributed, 95 percent of observations of Y on X lie within two standard errors (X = 0.366) either side of the regression line. In order to test the validity of this regression analysis, the Spearman's Rank correlation test was used to determine whether the regression residuals and the independent variable (catchment area) were correlated. A correlation coefficient of r = -0.338 indicates that no significant correlation exists, and hence, the regression equation (7.6) remains valid.

When log (Q/A) (Y) was regressed against log catchment area (X) the following relationship was obtained:

$$Y = -0.515X + 2.729 \pm 0.763 \text{ (2 S.E.s Y on X)} \qquad .....7.7$$

A correlation coefficient of r = -0.574, significant at the 99 percent level, led to a coefficient of determination of 0.329. The scattergram and regression line for the equation are shown in Figure 7.4C.

These results suggest that, while peak discharge is positively correlated with catchment area as would be expected, there is a strong tendency for peak discharge per unit area to decrease with increasing catchment area (although

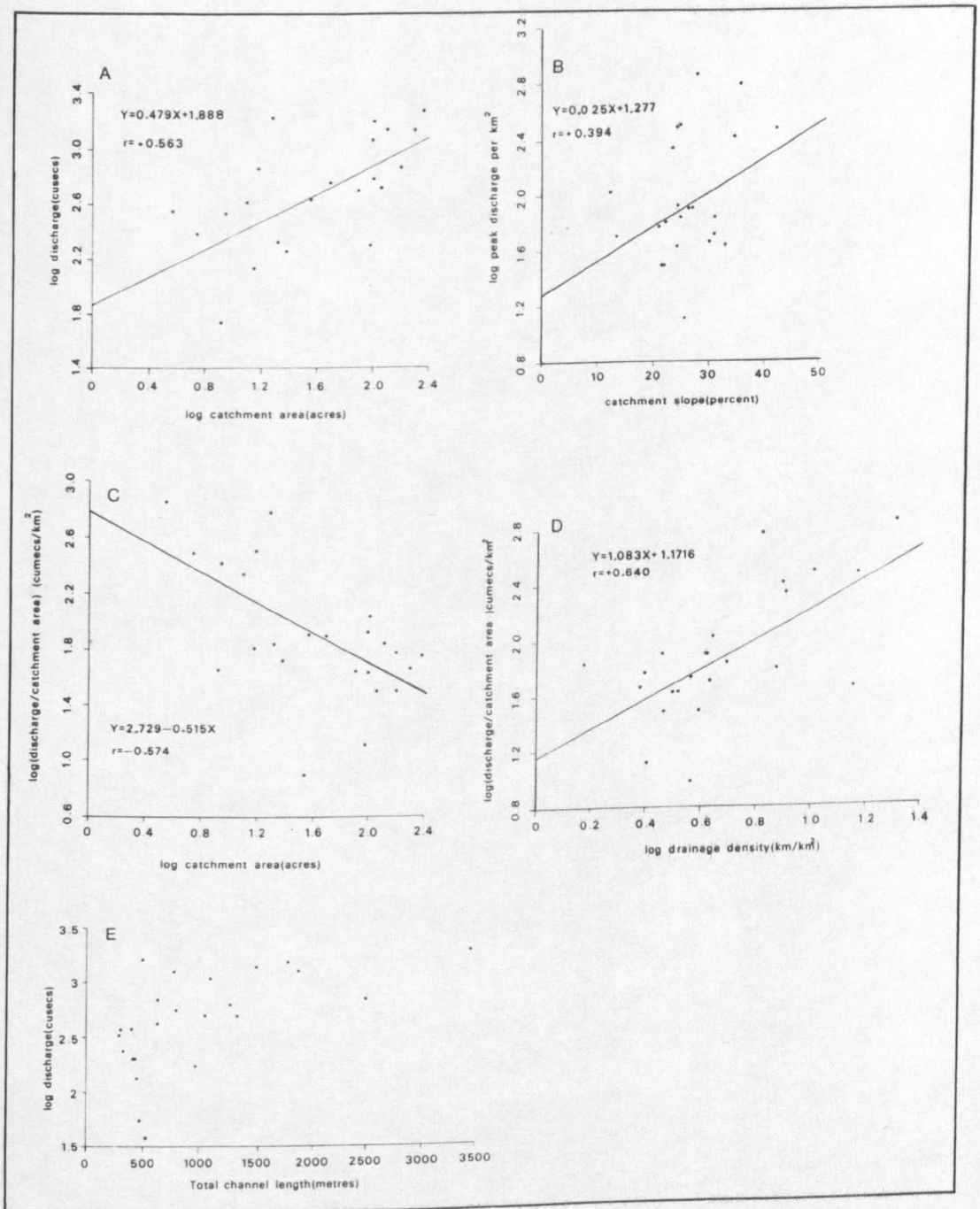

FIGURE 7.4 Scattergrams and Regression Lines for the Dependent and Independent Variables.

by dividing peak discharge by catchment area a degree of autocorrelation may have been introduced). This negative correlation reflects the possible asynchronisation of tributary inflow to the main channel, caused by within-catchment variability in rainfall intensity and duration, slope runoff response and channel hydraulic efficiency in larger catchments, and the fact that drainage density tends to decrease with increasing catchment area (see below). This underlines the deficiency of discharge computation from catchment area alone.

The population distributions of the remaining catchment variables (drainage density and overall catchment slope) were plotted to determine whether they were, or could be made, normally distributed for the purpose of linear regression with log (Q/A). The population distributions of these two independent catchment variables are shown in Figures 7.3G and 7.3I. While the frequency distribution for catchment slope was acceptably normal, with a skewness value of +0.652, the distribution for catchment drainage density was positively skewed. Logarithmic transformation increased the normality of the distribution (Figure 7.3H) to yield a skewness value of +0.534.

Regression of log (Q/A) on catchment slope yielded the following regression equation:

$$Y = 0.025X + 1.277 \pm 0.857 \text{ (2S.E.sY on X)} \qquad .....7.8$$

The correlation coefficient of r = +0.394 (coefficient of determination = 0.155) is marginally significant at the 95 percent level. The scattergram and regression line for this relationship are shown in Figure 7.4B. A positive association between these two variables indicates, as would be expected, that steeper catchments generate higher runoff rates per unit catchment area, as rainfall is more efficiently and rapidly converted into runoff. However, the low coefficient of determination suggests that catchment slope alone is a relatively poor indicator of peak discharge per unit area, owing to the complexity of catchment response.

A correlation coefficient of r = +0.640, significant at the 99 percent level, was obtained when log (Q/A) was regressed on drainage density. The scattergram of data points (Figure 7.4D) can be described by the following regression equation:

$$Y = 1.083X + 1.172 \pm 0.716 \text{ (2 S.E.s Y on X)} \quad .....7.9$$

A Spearman's Rank correlation coefficient of r = +0.056 suggests that there is no significant correlation between regression residuals of Y on X and the independent variable, and hence, the regression equation remains valid.

The regression analysis presented above has demonstrated that while absolute peak discharge (Q) is significantly positively correlated with catchment area, catchment area-adjusted peak discharge (Q/A) is both inversely correlated with catchment area and positively correlated with drainage density. It would seem, therefore, that peak discharge might be best correlated with total channel length. It was not possible to normalise the catchment total channel length data for purposes of linear regression, and hence, the association between this variable and peak discharge had to be tested by non-parametric means. The Spearman's Rank test was chosen with a null hypothesis that there is no correlation between the variables. A correlation coefficient of +0.676 (r^2 = 0.457) was obtained, and the null hypothesis was rejected at the 99 percent level. This coefficient is considerably greater than that obtained by regression of peak discharge (Q) on catchment area.

Total channel length would appear, therefore, to offer the greatest potential for the prediction of high magnitude storm discharge from small ungauged catchments in this terrain. Drainage density was found to be negatively correlated at the 99 percent significance level (r = - 0.854) with catchment area, suggesting that as catchment area increases, the rate of increase in total channel length decreases. Therefore, total channel length may be used more effectively than drainage area in discharge prediction, and reflects the progressive decrease in area-adjusted discharge as catchment area increases.

In order to test the applicability of the Gupta and Dickens models and the regression equation (7.6) to larger catchments, the peak September 1984 discharge in the Leoti Khola was determined from field evidence. A number of discharge computations, from a range of cross-sections, were made in November 1984, using field survey techniques described in Section 7.3.2. The search for peak flow stage indicators was confined to the lower Leoti Khola floodplain, below the point where the Dharan-Dhankuta road hairpins onto the floodplain (Figure 8.1). Wherever possible, survey sites were chosen where reliable flood stage indicators were found on opposite floodplain margins.

Stage indicators consisted of stranded brushwood and silt found on terrace banks bordering the floodplain, in the gabion wire of the road embankment and in within-channel vegetation and boulder deposits.

Seven floodplain cross-sections, with evidence of peak flow stage, were identified. The locations of these cross-sections are shown in Figure 8.1. The cross-sections were surveyed using an engineers level and graduated staff at 10m intervals across the floodplain. The cross-channel bed profiles obtained were combined with the elevation of the peak flow stage indicators to compute peak flow cross-sectional area. The cross-profiles are shown in Figure 7.5. These profiles terminate abruptly along the left bank owing to the presence of the vertical road embankment on the floodplain.

Samples of the bed material were taken following the passage of the flood, in order to compute a value for Manning's 'n', based on the Strikler formula (equation 7.2). Owing to the difficulties in transporting these samples from the site to the laboratory in Dharan, only a limited number of samples could be taken. Therefore, the rigorous sampling techniques necessary for the assurance of sample representability, described by Moseley and Tindale (1985), could not be adhered to. Instead, 30kgs samples were taken at 30m intervals across the floodplain at each cross-section. Figure 7.6 displays the grain-size distribution curves for the three samples collected in cross-section 7 (Figure 8.1). Using the Strickler formula (equation 7.2), the Manning's roughness coefficient was computed using the median particle diameter determined from each of these curves. Without exception, the computed Manning's roughness coefficients were within the range of 0.02-0.03. This is considerably smaller than the value of 0.1 proposed and adopted by Barker (1976) and quoted by Brunsden et al (1981) for the Leoti Khola. This inconsistency may be explained by both the deposition of finer-grained material on the channel bed during flow recession, and the inability of the Strickler formula to compute total roughness in steep, irregular channels with coarse bed material. For these reasons, a Manning's roughness coefficient of 0.1 has been adopted in the present analysis.

The peak flow cross-sectional areas for each survey station have been tabulated (Table 7.5) along with computed velocity, using a roughness coefficient of 0.1, and peak discharge. Barker (1976) has calculated the peak discharge for the 10, 25, 50 and 100 year floods for ten floodplain cross-

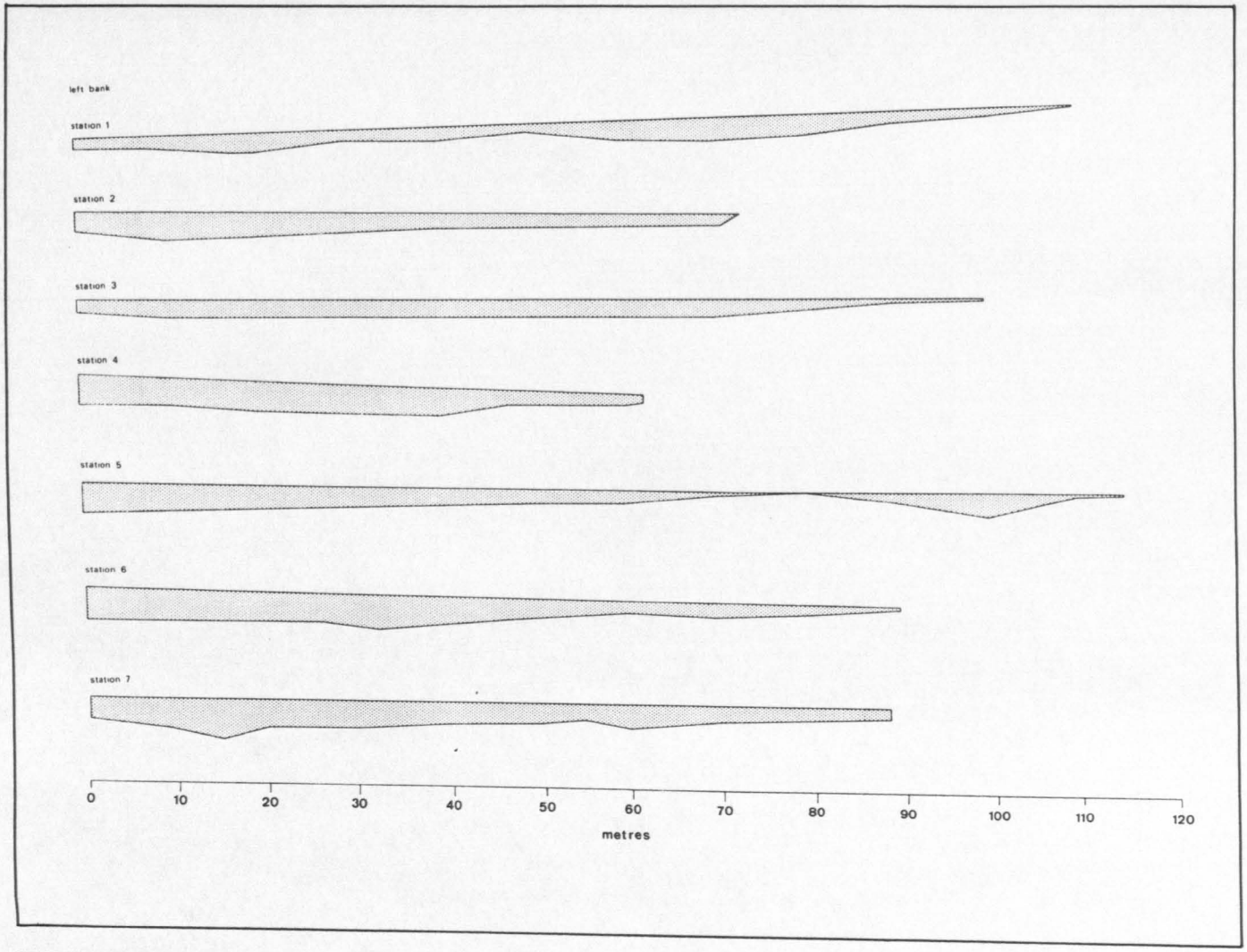

FIGURE 7.5 Surveyed Cross-Profiles Used to Determine Peak Flow Cross-Sectional Area in the Leoti Khola in 1984 (for Location of Stations see Figure 8.1).

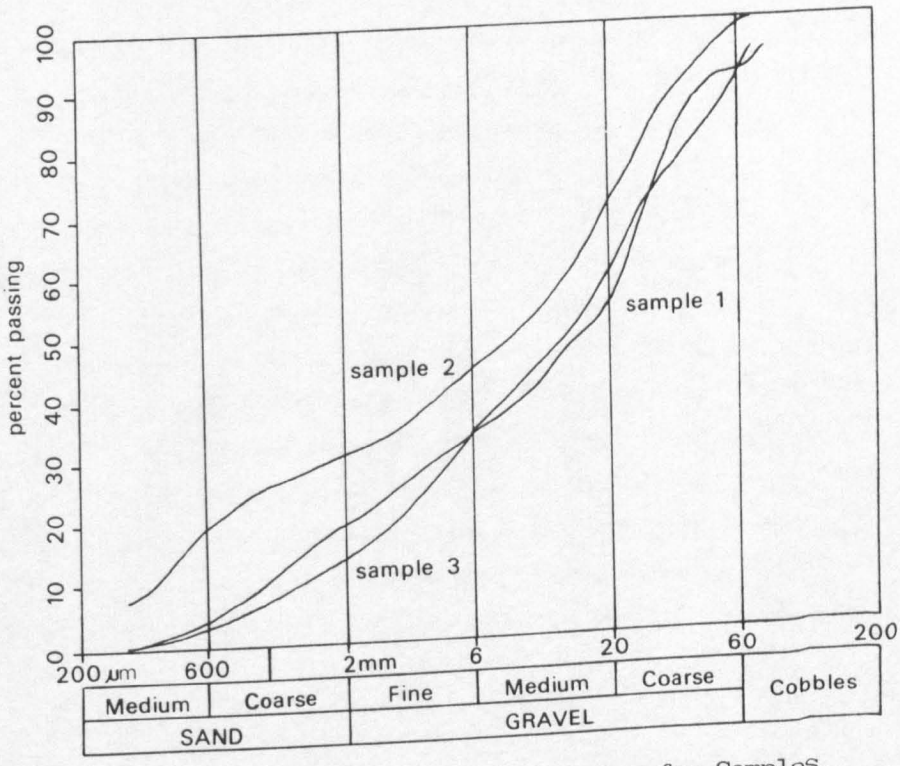

FIGURE 7.6 Grain-Size Distribution Curves for Samples Collected from the Ìeoti Khola Floodplain in November 1984.

sections located between the Sinsua Khola and the Tamur confluences. Using these data (reproduced in Brunsden et al (1981)), the recurrence intervals for each of the computed discharges for the September 1984 storm were calculated and are listed in Table 7.5. A progressive increase in peak discharge in a downstream direction can be identified between stations 1 and 7. Recurrence intervals fall within the range of 62 to 89 years with a mean of 75 years.

The Gupta Modified Rational formula was used in the same manner as described in Section 7.5, to compute a peak discharge of 924.7 cumecs for the Leoti Khola with a catchment area of 49 km^2. Using the progressive downstream increase in discharge calculated for the September 1984 flood (Table 7.5), the peak discharge in the Leoti Khola at the Tamur confluence was computed. A value of approximately 910 cumecs corresponds extremely well with that predicted by the Gupta formula. The Gupta formula would, therefore, appear to offer considerable potential for the prediction of flood discharges of large recurrence interval in humid sub-tropical mountain catchments, irrespective of catchment size. From the Dickens formula, a predicted value of 620 cumecs was obtained for the Leoti Khola, which is significantly lower than that indicated by field evidence. Using equation 7.6, the predicted peak discharge for the Leoti Khola, is 198 cumecs. This is considerably less than the observed (field derived) discharge value. Therefore, from this evidence, the regression equation developed for small catchments, considerably underestimates the runoff response of larger catchments.

7.7 Conclusions

7.7.1 Summary

A proforma technique has been described in this chapter for the systematic collection of data pertinent to the assessment of channel stability and hydraulic design at the reconnaissance stage of a highway project. Proformas were completed prior to and following the September 1984 storm, an event with a local maximum recurrence interval of 75-80 years. Data extracted from these proformas enabled an assessment of the effects of the storm on channel capacity to be undertaken, and allowed the computation of peak flow velocity and peak discharge for each of the surveyed channels.

Velocities calculated using the entrainment function, were found to be considerably less than those computed from the Manning formula, with both a constant and variable roughness coefficient. This was explained by the fact that particles found on the channel bed after the passage of a storm flow, are significantly smaller than those entrained during peak flow as a result of channel aggradation by fine grained material on the recession limb of the hydrograph. It would appear that the Manning formula, with an assumed roughness coefficient of 0.045, is the most feasible method presently available, of computing velocity in irregular, ungauged mountain channels with coarse bedload.

Eight discharge predicting models, mostly derived in India or Nepal, were used to compute the peak storm discharges likely to have occurred during the September 1984 storm. Three of these models incorporated reference to rainfall intensity or total storm depth, while the remainder had been empirically derived on the basis of catchment area alone. These latter models are based on the concept of the maximum recorded discharge or probable maximum discharge. The peak discharges predicted by these models were compared statistically with the observed discharges, determined by field survey, and it was found that the Gupta Modified Rational method was the most effective. However, this method requires considerable computation, and consequently, the Dickens method may be a useful alternative when catchment physiographic and rainfall data are unavailable.

The Gupta, Rational and Tropical Flood rainfall-runoff models were also tested in their ability to predict the discharges generated by the 1974 storm, of relatively low recurrence interval. The discharges predicted by these models were significantly different from those derived by field survey, and it was concluded that their ability to predict peak storm discharge may decrease with decreasing storm recurrence interval. However, it must be emphasised that the validity of the 1974 discharge data is uncertain.

Observed peak and catchment area-adjusted discharges, occurring during the 1984 storm, were regressed against catchment area and other catchment variables, determined from air photographs. Catchment area was found to be significantly positively correlated with peak discharge. The highest correlation was obtained between catchment area-adjusted peak discharge and drainage density, suggesting that this independent variable is an important indicator of

the efficiency with which storm runoff is conveyed through the catchment. Finally, the association between unadjusted peak discharge and total channel length yielded a considerably higher correlation than that obtained for catchment area. Total channel length would, therefore, appear to offer the greatest potential for high magnitude discharge computation, using the linear regression method.

The peak discharge in the Leoti Khola was calculated using flood stage indicators and channel survey. A progressive increase in discharge downstream enabled a peak flow rate to be computed for the whole catchment. The regression equation, based on catchment area, predicted a peak discharge for the Leoti Khola that was considerably less than that inferred from field evidence. This was explained by the fact that the regression equation was developed using data from catchments that were significantly smaller (up to 3 km^2) than the Leoti Khola (49km^2). On the other hand, the Gupta model was able to predict the Leoti Khola discharge with remarkable precision.

7.7.2 Discussion

The fieldwork and data analysis summarised above have proved that, by using specially designed proformas, valuable data can be collected during highway reconnaissance surveys for storm runoff assessment for hydraulic design purposes. The proforma offers a rapid and objective technique for gathering data for the assessment of channel runoff, stability, sediment supply and transport. The data collected on stability and sediment is examined in the following chapter. The analysis of proforma flow data, presented in this chapter, has been successful in that it has enabled existing flood prediction models to be tested, and has allowed the basis of an empirical regression model to be developed for small catchments. This success, however, has been partly dependent on the fact that a high magnitude storm occurred over most of the study area during the period of field research. Reconnaissance surveys for other mountain road projects are unlikely to be as fortunate, and consequently, channel data will have to be collected and interpreted carefully, with respect to rainfall records and river gauging data, if available. Nevertheless, the proforma used in the present study might be beneficially employed during reconnaissance surveys for other road projects.

There is considerable scope for the refinement and development of empirically based discharge predicting equations based on the method described in this chapter. Future research might profitably be directed towards the development of a storm discharge prediction model that takes account of rainfall intensity, catchment area, or preferably total channel length, catchment slope, variation in storm runoff contributing area and channel flow synchroneity within the drainage network. This could be undertaken using air photograph interpretation, channel proforma surveys and an analysis of river gauging and rainfall records to establish return periods for flood events.

Another important area for future research, that can be suggested on the basis of this analysis, is the determination of flow roughness for velocity computation. Accurate estimates of roughness are crucial to the computation of flow velocity. At present, the Manning formula is probably the most viable option. By flow monitoring and back analysis of the Manning formula, it might be possible to produce a series of roughness standards for mountain streams of varying bedload and channel configuration. Low-cost, experimental methods of monitoring channel flow are discussed in the following chapter.

CHAPTER 8

THE DEVELOPMENT OF PROCESS MONITORING TECHNIQUES FOR HIGHWAY DESIGN

8.1 Introduction

Many mountain road schemes undertaken within a low-cost framework have not had the facility to adopt costly, sophisticated, high technologically based monitoring programmes. One argument for this is the fact that the monitoring of slope and drainage hazards that have a low, 'nuisance' impact on the intended road is not cost-effective, as these hazards can normally be catered for in routine maintenance. However, this must not be seen to diminish the possible value of low-cost monitoring schemes. Considering the high rate and severity with which slope and drainage processes operate in mountains and the hazards that they pose to road stability, the operation of low-cost monitoring and observational programmes must be viewed as a possible means of providing the improved appreciation of these processes that is so essential for good design. It is argued in this chapter that field monitoring data can be rapidly and effectively integrated into the framework of terrain and geomorphological process assessment for highway design purposes at relatively low cost. Indeed, monitoring of geomorphological processes, and design performance with respect to these processes, is crucial to the concept of 'design by modified precedent' (Deere and Patton 1971). The representability of the monitoring data will almost certainly increase with time so that towards the end of the construction period, an extensive data base may be developed.

Where the road design and construction period is likely to last for several years (in the case of the Dharan-Dhankuta road, the consulting engineers were on site for 9-10 years), monitoring established during reconnaissance may begin to contribute valuable data by the time construction begins. During the construction of the Dharan-Dhankuta road, it became quickly apparent that the hazards posed by channel processes of storm flow, erosion and sediment transport had been underestimated, especially following drainage disturbance by earthworks and the installation of road drainage schemes. Although a degree of monitoring was attempted during construction, such as: a) the

monitoring of trial benches and tips[1], b) the observation of marked boulders on the Leoti Khola floodplain, and c) repeated measurement of slope displacement on high risk landslides, such practices were undertaken in a piecemeal fashion. It is now clear, with hindsight, that the geotechnical and geomorphological assessments would have benefited from the introduction and development of a co-ordinated, long-term monitoring programme at the start of the road project.

In order to evaluate the extent to which short-term, low-cost, largely improvised monitoring can provide useful process data for highway design purposes, a series of monitoring programmes were developed by the author along the Dharan-Dhankuta road. These programmes were designed specifically to monitor storm discharge and sediment transport from small channels, slope displacement and erosion. The results and conclusions drawn from the analyses are applicable not only elsewhere in the Lower Himalaya, but also in humid sub-tropical young fold mountains in general. The monitoring data obtained will be interpreted to the fullest extent possible in order to gain a better understanding of the scale and nature of slope and drainage processes in this terrain.

8.2 Process Monitoring for Highway Design in the Lower Himalaya

The principal aims of the field monitoring programmes described below are to determine whether low-cost, low technologically based monitoring schemes can, in the first place, be practically established in geomorphologically highly active mountain environments, and secondly, produce data that is of direct use to highway design.

Considerable research has been undertaken in Semi Arid and Humid Temperate environments in the field of process monitoring. The majority of those techniques designed to monitor fluvial processes, for instance, have been developed as components of instrumented catchment studies (Gregory and Walling 1971, 1973) or, in the case of slope monitoring, as part of geotechnical assessments of slope stability. Accordingly, many of these techniques are high

---

1. Interestingly, as far as the author is aware, the monitoring data from the tip benches were never properly analysed.

technology based, costly and their establishment and operation require considerable logistical support.

The potential for establishing high technology based monitoring systems in the Lower Himalaya, for highway design purposes, is restricted for two main reasons. First, the sheer magnitude and severity of storm discharge and erosion, for instance, dictates that channel instrumentation, such as stilling basins for autographic level recorders (see below), can only be sensibly constructed along the most stable channel reaches where flow is less capricious. Gauging stations have been established, therefore, on the major rivers only, such as the Arun at Tribeni (Seshadri 1960) and the Jog Mai Khola below Ilam in east Nepal. Shanker (1983) reports 50 regular stream - gauging stations in Nepal, 25 of which have autographic stage recorders. Elsewhere, such as on the Tamur River at Mulghat, river gauging is undertaken by reference to a stage board or dip stick only, while in steep mountain gullies, with small catchments, monitoring of any kind has been precluded by the often hazardous and destructive nature of channel processes. Flow monitoring in these channels would be of considerable benefit to preliminary hydraulic design for road projects.

As far as slope monitoring is concerned, slope failure in the Lower Himalaya often tends to be catastrophic, in that there is often little forewarning of imminent failure. High investment monitoring under these conditions is largely inappropriate and expensive, considering that any instrumentation would have to be sacrificial. Alternatively, where slope failure is gradual, conventional ground survey monitoring techniques should prove successful. Second, the low-cost design philosophies of many mountain roads, and the uncertainty during the early stages of a project as to the location and design of the final road, are likely to rule out the possibility of using high investment instrumentation at the reconnaissance stage.

Despite these operational and cost restrictions, simple river and slope monitoring systems may prove useful for highway design purposes (Fookes et al 1985). The present study has sought to establish crude and, in comparison with conventional instrumentation used elsewhere, relatively inaccurate schemes for monitoring processes in the Dharan-Dhankuta area. Field assessment has identified four main areas where the development of simple monitoring schemes may be of considerable benefit to highway design. These schemes relate to: a) the monitoring of peak storm runoff and sediment transport, b)

slope displacement, and c) erosion on tip slopes, and are described and discussed separately with respect to highway design requirements of hazard assessment. A brief appraisal of relevant techniques presently available for monitoring these processes is given at the beginning of each section. This is followed by a description of the fieldwork undertaken, and an analysis and discussion of the results obtained. It is important to recognise that these investigations are experimental and that the choice and nature of the techniques were conditioned largely by the equipment and materials that could be transported from the UK or purchased in Dharan Bazar, and the fact that installation and monitoring were undertaken by a single man in the field.

The fieldwork spanned the monsoon seasons of 1983 and 1984. Clearly the representability of such short-term monitoring data is uncertain and requires verification. Networks of standard raingauges were established in order to provide 24-hour rainfall data. The locations of these gauges, and all monitoring sites, are shown on Figure 8.1. The total (24-hour) storm rainfall data recorded in 1983 and 1984 are shown in Tables 8.1 and 8.4, respectively.

8.3 Monitoring Storm Runoff

8.3.1 Introduction

The design of hydraulic structures, such as bridges and culverts, is based primarily on computed design peak velocities and discharges using techniques similar to those discussed and developed in Chapter 7. These procedures, at best, only yield approximate values and should be augmented by monitoring data if successful hydraulic design is to be achieved.

The conventional method of directly monitoring storm discharge is the velocity - area method, whereby representative values of flow velocity are obtained, usually by current metering, and multiplied by channel cross-sectional area to yield discharge (Kinori and Mevorach 1984). Maximum flow depth is usually determined by reference to a stage board, crest-stage or autographic level recorder, including rising float and bubble gauge varieties (Gregory and Walling 1971, 1973). In stable channel reaches, the production of a stage (depth)-discharge relationship provides the opportunity for determining discharge from flow depth alone. Other less common methods of discharge determination include salt or dye injections (Bauwens et al 1982), radioactive tracers (Clayton and Smith 1964, Ellis 1967) and rising float and

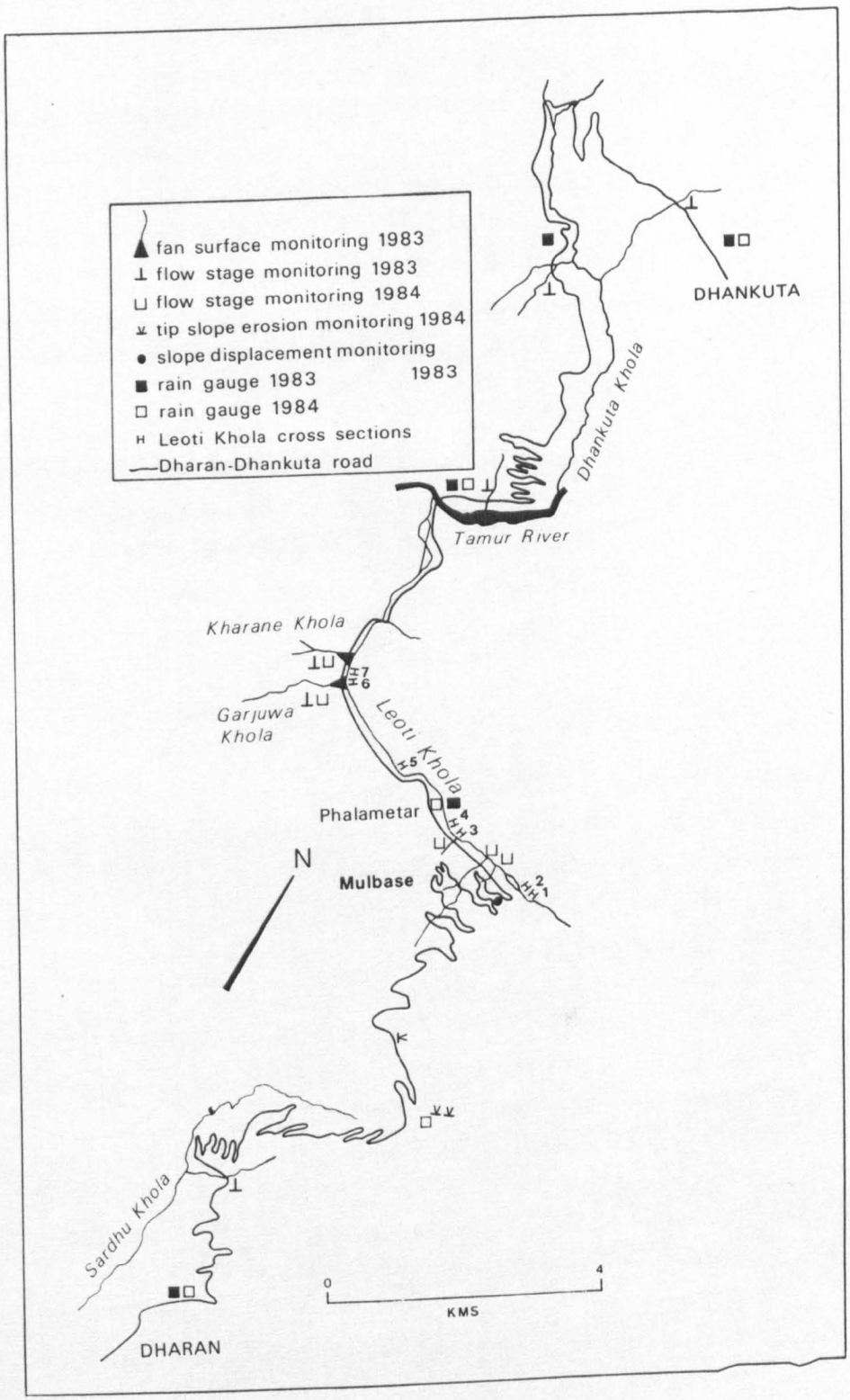

FIGURE 8.1 Location of Monitoring Sites.

electromagnetic techniques (John et al 1982, Sargent 1982). These more elaborate techniques require considerable site calibration and have very little or no application to flow monitoring in steep, rocky channels characterised by capricious flow, high turbulence and rapid changes in channel cross-section over time. Bathurst (1982, p 63) maintains that "Direct methods of gauging discharge are often precluded from use in steep rivers with coarse bed material by the hydraulic conditions typical of such rivers". This statement is particularly pertinent to storm runoff monitoring in the study area.

A description and evaluation of the fieldwork undertaken to determine whether direct and indirect monitoring of stream discharge from small mountain gullies, using low-cost techniques, are practicable in the study area, is given below. Ideally, it would have been appropriate to locate the monitoring sites in instrumented catchments to facilitate comparison between the experimental data yielded and that obtained by established river gauging techniques. However, as there are no gauging sites in the study area, with the exception of the Mulghat stage records on the Tamur River, this was not possible.

8.3.2 Direct Monitoring

Direct monitoring of storm discharge was undertaken during the monsoon season of 1983, using the velocity-area method of current metering and direct measurement of flow depth and width. As most storms in the study area occur at night, it was important that the stream chosen for the field monitoring was accessible by road and sufficiently close to the living quarters to allow rapid access, thus enabling flow measurements to be taken on the rising limb of the storm hydrograph. Kharane Khola, a relatively small left bank tributary of the Leoti Khola, was chosen for this purpose (Figure 8.1); access could be gained, on foot, in under thirty minutes. The initial intention had been to ascend the channel from the road bridge, to a suitable reach where flow width, depth and velocity would be monitored using a 30m tape, a 3m steel tape and a portable Mini Ott current meter. Unfortunately, access upstream from the fan surface was, in practice, found to be impossible owing to the highly turbulent and variable nature of storm flow. Instead, for safety and logistical reasons, all monitoring was confined to the apex of the fan surface. Even then, high calibre bedload and a rapidly shifting channel presented major problems and posed considerable hazard.

The flow velocities and computed discharge rates obtained are shown in Table 8.2. Due to problems of equipment operation, flow velocities were not recorded during the first storm (4.6. 1983). While flow velocities recorded on fan surfaces are likely to be lower than for the upstream channel as a whole, these values are considered to be representative of storm flow across small fans in the study area. Direct monitoring of storm runoff was discontinued following the storm of 14/15 July, as conditions had become unacceptably hazardous owing to the rapid, boulder-charged nature of the storm flow and the loss of the bedload sampler on 14.7.1983 (see Section 8.4.2). Effort was then concentrated towards the development of indirect techniques of flow monitoring.

8.3.3 Indirect Monitoring

The estimation of peak storm discharges for the 1974 and 1984 events in streams crossed by the Dharan-Dhankuta road, using the slope-area method, has been presented in Chapter 7. This indirect technique relies on the determination of peak flow cross-sectional area and peak velocity, calculated from the Manning formula, that equates velocity with water surface slope, hydraulic radius and channel roughness.

This indirect technique suffers from a number of disadvantages when compared with direct monitoring methods. The most serious of these, concerns the problems associated with the evaluation of flow roughness in highly turbulent, unsteady flow, characteristic of mountain gullies (see Chapter 7). Another major problem concerns the determination of maximum flow depth in channels that display considerable within-storm variability in bed level. However, these disadvantages may be weighed against the rapid, low-cost nature of the technique and the fact that the number of channels that can be assessed by the method is virtually unlimited. Indirect methods of storm flow monitoring undertaken in 1983 and 1984 are described separately below.

i) Indirect Flow Monitoring in 1983

Six small mountain channels that cross the Dharan-Dhankuta road were chosen for an investigation of the possibility of developing a post-storm, slope-area methodology of peak discharge determination. The choice of these sites was based on the desire to obtain a representative range of flow conditions. This range included a channel characterised by intermittent debris flow activity,

24 HOUR RAINFALL (mm)					
Date	Base Camp	Phalametar	Tamur	Gutetar	Dhankuta
13.5.1983	139.4	118.2	82.5	52.7	34.8
3.7.1983	85.8	98.5	69.1	81.1	73.1
4.7.1983	57.6		70.1	62.5	54.1
14.7.1983	171.1	208.1	75.5	63.6	55.3
15.7.1983			84.2	77.1	62.7
24.7.1983	121.6	65.1	91.6	85.2	69.4

TABLE 8.1 Storm Rainfall Depths Recorded Along the Dharan-Dhankuta Road in 1983.

Date	Time	Bedload Conc.(gm/l)	Susp.load Conc.(gm/l)	Velocity (m/s)
4.6.1983	2130	—	267.13	—
	2140	—	241.96	—
	2150	—	264.33	—
	2205	—	131.75	—
4.7.1983	0340	238.12	—	0.7
	0353	61.64	53.47	1.1
	0405	77.41	—	1.5
	0420	—	—	1.6
14.7.1983	2135	677.13	609.09	—
	2150	243.36	116.30	0.9
	2205	101.62	16.82	1.1

TABLE 8.2 Discharge Data Recorded on the Kharane Khola Fan in 1983.

two channel reaches tributary to the Leoti Khola and characterised by relatively low flow velocities but rapid sediment accumulation rates, one channel entrenched into an elevated fan surface forming the northern bank of the Tamur River, and two typical mountain channels draining catchments underlain by schist and gneiss in the relatively dry Dhankuta Khola catchment. The locations of these six instrumented channels are shown in Figure 8.1.

A relatively stable reach was chosen upstream of the bridge or culvert in each channel. The cross-section was surveyed using a 30m tape to measure channel width combined with vertical depth-to-channel bed measurements. A crest-stage recorder was installed in each channel at the measured station to determine peak flow depth. The recorder (Plate 8.1, Figure 8.2) consisted of a 2m length of bamboo, approximately 5 cm in diameter with an equivalent length of transparent, flexible plastic pipe strapped to it. The bamboo was concreted into the channel bed, in an upright position. A piece of stocking was stretched over the lower orifice of the pipe and secured to it with string, wire and masking tape. Powdered cork was sprinkled into the pipe, and made to rest on the stocking gauze, to a depth of approximately 5mm. The top of the pipe was then covered with tape (though not made airtight) to prevent the ingress of rainwater. A gap of approximately 100mm was left between the base of the pipe and the stream bed to discourage the siltation and blocking of the gauze during low flow. The philosophy behind the design of the instrument was that a ring of cork would remain around the inside of the pipe as channel flow receded from peak stage.

At each site, particles forming the channel bed material were painted with 'dayglo' paint. Measuring the size of recovered particles moved during storm flow, would provide the basis for the determination of peak velocity using an entrainment function. These velocities could then be compared with those computed from the Manning formula with an assumed channel roughness.

Results

Unfortunately, the crest-stage recorders were ineffective in recording peak stage levels. In Nishane Khola (the gully characterised by debris flow activity) and Kharane Khola, the instruments and their foundations were removed during the storms of 12 May and 14/15 July, respectively. The crest-stage recorder in Garjuwa Khola, was almost covered by channel aggradation during the 12 May storm and subsequently removed by scour during the following storm.

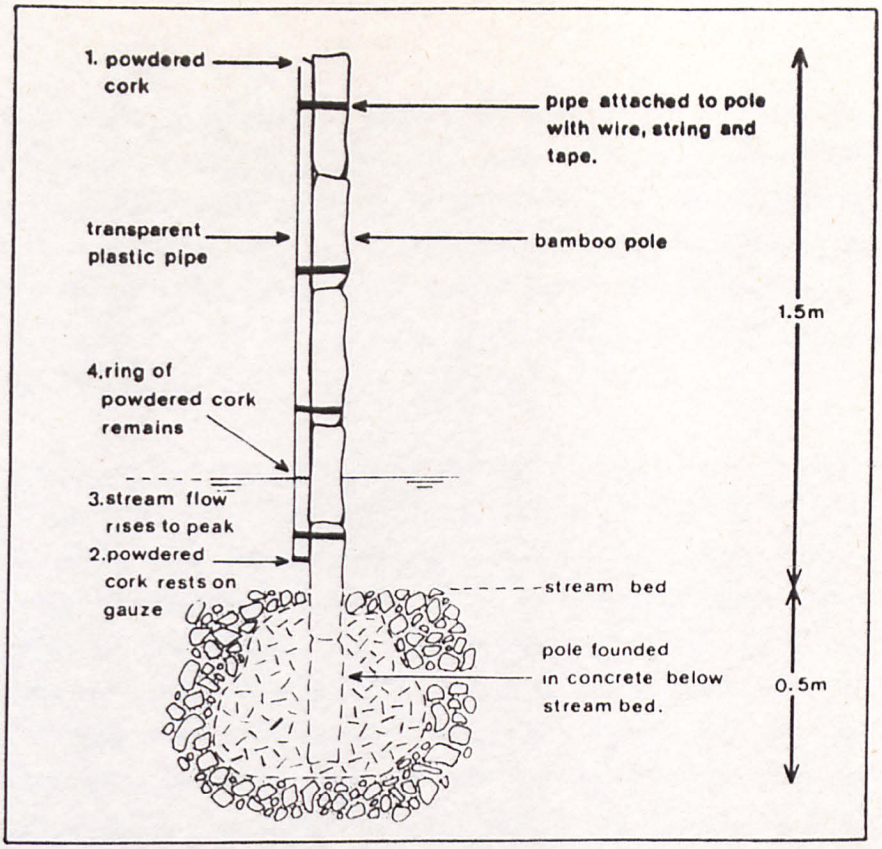

FIGURE 8.2 and PLATE 8.1 The Crest-Stage Recorder

Although the recorders in the other three channels remained intact (except for vandalism), only one registered a flow during the whole monsoon season. Storm runoff in the two northern-most channels, in the Dhankuta Khola catchment, was of insufficient depth to cause any appreciable rise of the powdered cork. This was partly due to the fact that the instruments had been installed towards the slightly elevated margins of the channels to reduce the likelihood of damage during storm flow.

The use of marked pebbles also proved of limited practical value as their recovery rate was quite low. This was primarily because much of the bed sediment was transported for considerable distances, or became buried temporarily in the channel bed. Similar problems of sediment retrieval have been described by Gardner (1986) in the Canadian Rockies. After each storm the bed material was repainted using a different colour or symbol in order to differentiate between material transported by each successive storm. Had this not been done, then it would not have been possible to determine whether pebbles recovered were moved during the most recent storm or were reworked or uncovered sediment load of previous storms. The lengths of the intermediate axes (b) of, and the distances (d) travelled by, all recovered pebbles are shown in Table 8.3. The largest recorded particle to have moved was 66cm (4.7.1983) in Nishane Khola, while the greatest distance travelled by any marked and recovered particle was 930m (12.5. 1983) in the gully at Gutetar. During the first three storms of the monitoring period, none of the marked pebbles in Garjuwa Khola were recovered. This was because, even during moderately sized storms, the vast majority of material supplied to the main channel of this khola, by erosion and slope instability, is conveyed across the fan surface and incorporated into the sediment load of the Leoti Khola. A brief inspection of the bed material in the trunk river, following these three storms, failed to recover any pebbles from Garjuwa Khola. Attempts to recover pebbles in this khola were discontinued after 5 June 1983.

The recovery rate of marked pebbles in the remaining channels was also quite poor. In the two instrumented channels at Gutetar and below Dhankuta, in the Dhankuta Khola catchment, discharges were insufficiently high during the monitoring period to move much of the bed material. Owing to the limited data obtained, there is clearly insufficient basis for determining peak velocity from the entrainment function. Consequently, no analysis has been made of the recorded data.

	NISHANE KHOLA		GARJUWA KHOLA		KHARANE KHOLA		MULGHAT KHOLA		GUTETAR		DHANKUTA	
	INTERMEDIATE AXES OF, AND DISTANCE TRAVELLED BY, RECOVERED PEBBLES											
Date	b(cm)	d(m)	b(cm)	d(m)	b(cm)	d(m)	b(cm)	d(m)	b(cm)	d(m)	b(cm)	d(m)
12.5.1983	14.7	76.0	X	X	36.8	18.8	—	—	5.2	930.0	17.5	14.0
	X	X			11.4	143.8			9.1	3.8	11.2	16.0
					22.5	67.0			8.2	4.9	11.4	19.9
					27.5	5.1			14.0	23.1	10.2	11.2
					38.0	16.0			13.1	50.0	9.8	8.6
					—	—			—	—	10.0	22.1
22.5.1983	35.8	278.7	X	X	23.6	1.5	6.4	63.1	8.1	4.4	—	—
	8.8	270.5			18.2	5.3	8.9	51.6	—	—		
	37.3	379.7			20.2	18.6	11.7	49.4				
	8.7	415.0			13.2	92.6	10.9	49.4				
	X	X					21.4	47.8				
							13.5	47.2				
5.6.1983	X	X	X	X	44.0	12.0	12.9	442.0	5.8	19.0	11.6	4.8
					30.6	5.8	6.0	28.3	—	—	13.6	18.7
					45.4	12.8	15.6	25.7			16.5	33.0
			discontinued		26.2	16.0	17.9	20.0			—	—
					22.5	16.0	13.5	33.8				
					—	—	12.5	74.0				
23.6.1983	59.0	48.0			—	—	—	—	—	—	—	—
	21.0	30.0										
	18.6	34.2										
	11.6	55.0										
	34.5	55.7										
	19.9	48.0										
	14.0	36.0										
	20.0	37.0										
	19.2	65.0										
4.7.1983	66.0	125.0			—	—	22.7	6.0	—	—	25.0	94.2
	25.0	19.5					7.2	37.3			15.0	13.3
	13.4	28.4					13.8	52.0			—	—
	X	X					28.5	49.4				
							17.7	52.3				
							28.0	19.5				
							31.7	9.0				
							12.0	33.2				
							17.0	53.1				
16.7.1983	40.3	350.0			X	X	15.5	60.0	21.0	5.3	51.0	4.9
	12.2	22.5									13.4	107.8
	23.0	256.6									—	—
24.7.1983	16.3	175.0			32.0	17.9	—	—	20.5	19.3	47.0	5.3
	18.3	115.0			X	X			—	—	12.3	12.4
	X	X									28.0	20.3
											—	—

TABLE 8.3 Intermediate Axes of, and Distances Travelled by Recovered Pebbles.

N.B. X .... all pebbles removed, none recovered
—.... all or rest of pebbles remaining.

The determination of peak discharge, therefore, has to rely on both a more effective means of recording peak flow depth and a more reliable method of determining flow velocity. Experience gained during the aborted flow monitoring experiments undertaken in 1983, revealed that cheap and non-robust in-channel instruments for recording peak flow stage, such as stage boards and crest-stage recorders, are likely to be destroyed during storm runoff or become vandalised. The ideal method of recording peak stage should, therefore, be able to withstand the flow that it is designed to record and be of little or no use to the local population. Indirect flow monitoring was continued during the monsoon season of 1984 with these aims in mind.

ii) Indirect Flow Monitoring in 1984

Five channels, tributary to the Leoti Khola, were chosen for the storm flow instrumentation in 1984 (Figure 8.1). In four of these channels, a relatively stable cross-section, composed of bedrock, was chosen. Ledges were excavated into each vertical, or near vertical, bedrock side-slope at intervals of approximately 100-200mm from the channel bed. The floor of each ledge (approximately 30mm wide) was painted with bright red paint and a minimum of five medium gravel-sized particles, painted in the same colour, were placed on each ledge. These particles (10-20mm diameter) were sufficiently small to become entrained by storm flow but also large enough to resist removal by overland flow. In addition, each channel side-slope was painted with two vertical lines, approximately 60mm wide, of white concentrated 'Coolglass' greenhouse shading (Plate 8.2). Greenhouse shading was found to be resistant to overland flow on the bedrock side-slopes, but susceptible to erosion by the abrasive action of entrained debris in storm flow. These techniques, therefore, provided two independent methods of recording peak flow stage on each channel side-slope. Although the accuracy of the excavated ledge method is dependent upon the ledge spacings, the scoured Coolglass strips should, in theory, register the exact peak stage, and is potentially the more accurate. Erosion chains were secured vertically into the channel bed, to allow the determination of bed scour, at two sites where the bed material was sufficiently deep to permit this. Unfortunately, these chains were removed during the first storm and were not replaced.

In the fifth channel, a crest-stage recorder of the type described earlier, was installed. The channel was small (approximately 3m wide), stable and of shallow inclination, and therefore offered acceptable flow conditions for the

PLATE 8.2 Indirect Flow Monitoring in 1984.

survival of an in-channel instrument. The instrument was installed in the centre of the channel.

At each site, the intermediate axes of twenty bed pebbles of varying size, but usually considerably less than 2m, were measured. These pebbles were numbered with bright red paint. Examination of the bed material after the passage of each storm indicated which of these pebbles had been removed during the event. This methodology might prove more successful than the one described above, as the development of the data base is not dependent on the recovery of marked pebbles but rather the identification of those pebbles removed from a known sample.

Results

The success of the two techniques (greenhouse shading and gravel levels), in the identification of peak flow depth, is revealed by data in Table 8.4. Table 8.4 enables a comparison to be made between the total number of cases where the flow depth estimated by the two techniques coincided with the total number of cases where they indicated different flow depths. The highest correspondence occurred at the stations in Mulbase and Garjuwa Khola, where respectively, 8 out of 14 and 10 out of 18 cases of flow recorded, on both banks, were approximately coincidental. The relatively close correspondence in these two channels, between the peak flow depths estimated by the two techniques, is probably due to the fact that the cross-sections chosen were particularly stable and were located in comparatively straight and shallowly inclined channel reaches, characterised by relatively uniform flow. However, there were four cases in Mulbase Khola when quite sizeable flows, of greater than 60cm depth, were registered by one of the techniques, while the other failed to record any flow. In Garjuwa Khola, there were five cases when operational problems did not allow the measurement of flow depth by the greenhouse shading method (Table 8.4). In all of these cases, the failure of the technique can be explained by either the use of too low a concentration of shading or its application to a wet bedrock surface that prevented the paint from drying.

Unpredictable regolith sliding from above the gauging station in Kharane Khola (Figure 8.1) frequently engulfed the side-slope in debris and removed the gravel from the rock ledges. Hence, little meaningful flow data were recorded in this channel. Finally, in four cases of seven recorded flows on the left bank

Rainfall (mm)	Date	Khola	PEAK FLOW DEPTH(CM) LEFT BANK Gravel level	LEFT BANK Cool-glass	RIGHT BANK Gravel level	RIGHT BANK Cool-glass	Peak Velocity (m/s)	Peak Discharge (cumecs)	b-Axis Dimension(cm) Largest Removed	Largest Remaining	Smallest Remaining
26.1	13.6.84	Mulbase	51-71	61	70-►	109	----	----	21.2	75.0	10.4
38.6	19.6."	"	10-43	47	37-60	55	4.36	5.99	24.8	75.0	8.5
63.5	20.6."	"	---	60	64-78	86	4.77	8.45	36.0	33.8	8.5
18.3	3.7."	"	nfr	nfr	nfr	nfr	nfr	nfr	none	none	none
40.4	8.7."	"	0-18	11	64-78	nfr	4.67	7.15	25.0	33.8	16.4
62.3	15.7."	"	0-32	61.5	78-►	nfr	6.43	19.23	33.8	43.0	19.2
27.9	16.7."	"	nfr	nfr	nfr	nfr	nfr	nfr	none	none	none
60.1	25.7."	"	0-32	64	68-►	64	5.60	11.26	26.8	68.5	13.2
15.8	5.8."	"	0-32	13.25	68-►	nfr	6.33	16.21	25.2	68.5	13.2
26.1	13.6."	P.metar	0-24	nfr	nfr	nfr	2.48	0.25	none	none	none
38.6	19.6."	"	0-24	13	nfr	nfr	3.70	1.00	none	none	none
63.5	20.6."	"	60-75	nfr	nfr	nfr	3.90	1.19	18.6	22.2	8.1
18.3	3.7."	"	---	---	nfr	nfr	nfr	nfr	none	none	none
40.4	8.7."	"	0-24	11	nfr	nfr	3.52	0.88	20.6	46.2	10.4
62.3	15.7."	"	51-60	11	nfr	nfr	3.52	0.88	21.3	46.2	9.1
27.9	16.7."	"	0-24	10	nfr	nfr	---	----	none	none	none
60.1	25.7."	"	24-36	21	nfr	nfr	3.88	1.13	none	none	none
15.8	5.8."	"	---	---	nfr	nfr	----	----	none	none	none
26.1	13.6."	Garjuwa	15-33	10	31-50	nfr	2.36	2.25	28.0	28.8	20.6
38.6	19.6."	"	15-33	13	0-11	21	2.41	2.36	32.1	40.4	11.0
63.5	20.6."	"	55-67	55	76-104	43	3.51	7.02	40.4	72.5	18.3
18.3	3.7."	"	44-55	45	0-11	0	2.57	3.08	30.3	72.5	20.6
40.4	8.7."	"	15-33	15	11-31	---	2.50	2.68	28.0	72.5	9.7
62.3	15.7."	"	55-67	55.5	50-76	---	4.07	11.00	31.1	72.5	12.7
27.9	16.7."	"	15-33	20.0	9-23	---	2.12	1.91	34.1	72.5	16.5
60.1	25.7."	"	44-55	47.5	37-70	---	3.25	5.78	29.8	72.5	13.2
15.8	5.8."	"	33-44	42.5	37-70	---	2.33	2.45	24.8	72.5	21.7
26.1	13.6."	Kharane	---	---	nfr	nfr	----	----	none	none	none
38.6	19.6."	"	---	---	nfr	nfr	----	----	none	none	none
63.5	20.6."	"	---	---	9-19	nfr	1.57	0.26	20.0	30.2	4.0
18.3	3.7."	"	---	---	nfr	nfr	----	----	none	none	none
40.4	8.7."	"	---	---	nfr	nfr	----	----	none	none	none
62.3	15.7."	"	28-43	---	9-19	nfr	2.43	0.95	16.6	30.6	4.0
27.9	16.7."	"	---	---	nfr	nfr	----	----	none	none	none
60.1	25.7."	"	28-43	---	nfr	nfr	2.30	0.80	15.6	30.6	9.3

TABLE 8.4 Flow Stage and Discharge Computations by the Gravel-Level and "Coolglass" Greenhouse Shading Techniques.

NB. 70-►....peak flow level is above highest gravel level
--- ....operational difficulties
nfr ....no flow recorded
P.metar ....Phalametar

in Phalametar Khola, there was approximate coincidence between the two techniques. This gully is composed of an extremely steep and narrow bedrock channel, with a 3m high vertical step in the channel bed, upstream of the gauging station. Storm flow in this channel is highly turbulent, and this reduces the effectiveness of the gauging techniques. As a result, there were no flows recorded on the right bank in this channel, during the monitoring period, despite quite substantial flows being registered on the opposite bank.

Following the September 1984 storm, the instrumented gully channels were unrecognizable owing to the extensive channel erosion that took place (see Chapter 7), and without exception, the ledges and shading strips were completely obliterated. It must be concluded, therefore, that low-cost techniques designed to monitor peak storm flow depth are not capable of withstanding flooding and erosion caused by high magnitude - low frequency events. Nevertheless, on the whole, the Coolglass greenhouse shading performed quite well in recording flow depth and should be used in preference to the less accurate and less reliable gravel level method. However, it is important to ensure a relatively high concentration of the shading and an application to a dry and clean bedrock surface. The success of the technique is also dependent on the choice of a stable and uniform channel reach for monitoring.

The crest-stage recorder, installed in the fifth gully, performed quite well in registering peak flow stage. This was primarily due to the stable, shallowly inclined (less than 10^0) nature of the channel and the low flows recorded.

Table 8.4 also shows the values of the maximum and minimum intermediate axes of marked bed particles both removed by, and remaining after, the passage of each flood. In 21 of 22 cases when marked bed material was entrained, the largest particle size removed was less than the largest remaining. However, there were no instances when the largest particle removed was smaller than the smallest remaining which would, in theory, be the case if particle entrainment was dependent upon a uniformly distributed flow velocity at the channel bed alone. This probably reflects a significant variation in flow shear across the channel bed, and illustrates the problems of calculating velocity using the entrainment function without rigorous monitoring of particle entrainment. Flow velocities were, therefore, computed using the Manning formula and a constant roughness coefficient of 0.045 (Chapter 7), with a water surface slope assumed coincident with that of

the channel bed. Peak velocities and discharges computed, using this method, are shown in Table 8.4.

An examination of the discharge data in Table 8.4 shows that while there is a general increase in discharge with increasing rainfall depths in each monitored gully, there is considerable scatter in the data, and a number of seemingly anomalous discharges are apparent. This may be explained by the relative inaccuracy of the monitoring technique, and the fact that peak discharge is more a function of peak rainfall intensity rather than total rainfall depth.

8.4 Monitoring Sediment Transport

8.4.1 Introduction

The abrasive action of entrained debris and the rapid accumulation of sediment in relatively shallowly inclined channel reaches and on fan surfaces has, in many cases, caused greater problems for the construction and maintenance of culverts and bridges along the Dharan-Dhankuta road than storm runoff itself (see Appendix 1). The monitoring of sediment transport and accumulation rates, especially on fan surfaces, would therefore provide invaluable data at the preliminary design stage, and might enable channel stabilization and erosion protection measures to be assessed during construction. Again, techniques for monitoring sediment transport can be divided into direct and indirect methods.

8.4.2 Direct Monitoring

Sediment transport monitoring in mountain streams during high magnitude runoff, although vital to an understanding of channel processes, is an extremely difficult task, in practice. In fact, Newson and Leeks (1985, p.413) maintain that "A compelling reason for the absence of data from mountain streams is the practical problem of establishing measurement procedures capable of coping with the possibility of high and variable bedload yields".

In the active mountain gullies found in the study area, highly concentrated, large calibre bedload yields are quite normal and direct monitoring thus becomes extremely hazardous and often impracticable. Direct monitoring methods can be subdivided into those devised to monitor bedload and suspended load respectively, and have been described by Gregory and Walling (1971, 1973).

Suspended load is probably the easiest to monitor. The conventional method involves the collection of a representative sample of stream flow, using dip bottles or hydrodynamic suspended samplers and the calculation of suspended sediment concentration upon filtration. Automatic pumping installations extract samples from the flow at regular intervals and can be activated by a rise in stage above a specified level (Walling and Teed 1971). An alternative technique is the photoelectric turbidity cell, usually mounted on the stream bank (Fleming 1969).

Bedload transport rates may be gauged by direct sampling, using collector trays, wire mesh baskets or slotted and open basins excavated in the channel bed (Gregory and Walling 1973, Carling 1983). During moderate to high magnitude flows, bedload traps and wire baskets may be rendered inoperable due to the sheer size and volume of the bedload moved.

i) Field Monitoring

Direct monitoring of sediment transport was undertaken in Kharane Khola (Figure 8.1) in conjunction with current metering, as described in Section 8.3.2. While suspended sediment samples could be collected relatively easily using hand-held dip bottles, it became immediately apparent that the only feasible means of determining coarse sediment concentration would be to use an immersed wire mesh basket. The basket could not be expected to remain stationary on the stream bed during storm runoff, and hence, a hand-held wire mesh drum (500 mm diameter x 1000 mm length) was constructed. The mesh spacing was 7.5mm, and hence, water and all entrained debris with an intermediate axis less than this would pass through the collector, keeping flow disturbance to a minimum. In theory, the drum could only collect sediment with an intermediate axis in the range of 7.5mm to 500mm.

At 15 minute intervals, the drum sampler was plunged into the storm flow and held with the orifice oriented upstream in the same position for ten seconds. The sediment load collected was then emptied into cement bags and left at the side of the bridge for later collection by bus or lorry. Immediately after each sample was taken, flow velocity was measured and this was combined with the area of the drum orifice to determine the volume of water passing through the drum in ten seconds, for the computation of sediment concentration. The drum often became at least half full during the period of immersion, and this caused considerable flow disturbance and severe handling problems. Sampling

was discontinued during the storm of 14/15 July 1983, when the drum was carried away during rapid channel flow.

Suspended load and bedload concentrations of samples recovered during field monitoring are shown in Table 8.2. With one exception, these load concentrations appear to be approximately similar and in the range of 50-300 gm/litre at the time of peak runoff. Maximum concentrations of bedload and suspended load were 677.13 and 609.09 gm/litre respectively, and these were derived from samples taken at approximately the same time during the storm of 14 July. Typical particle size distribution curves for suspended and bedload samples are shown in Figure 8.3.

Clearly, bedload sampling is particularly hazardous and problematic in this terrain, and is virtually impossible under conditions of rapid storm flow in small, steep gullies. Conventional bedload traps and sampling mesh baskets are ineffective under these conditions, and the technique described above can only provide approximate values of sediment concentration and cannot include reference to coarse debris. The largest particle recovered in the samples had an intermediate axis of 42.1mm, and this is considerably smaller than the typical cobbles and boulders that constitute many channel beds. Preliminary hydraulic design for highway projects in this type of terrain would benefit, therefore, more from indirect methods of assessing sediment transport than direct monitoring of sediment concentrations during storm flow, although a combination of the two techniques would, ideally, be the most appropriate.

8.4.3. Indirect Monitoring

Total storm sediment transport can be calculated by the re-survey of sediment deposited in discrete accumulation areas, such as gravel banks and debris fans. This indirect method of estimating sediment transport rates may be the only feasible technique when direct monitoring is impracticable (Schick and Lekach 1981).

An alternative, less precise method is to measure changes taking place at the sediment source in order to determine sediment supply rates. In mountain catchments, much of the channel sediment load originates from landslides, and hence, if these can be mapped accurately, total potential sediment yields may be assessed. Moseley (1980), for instance, has mapped sediment sources in the Harper-Avoca mountain watershed in New Zealand from air photographs. A

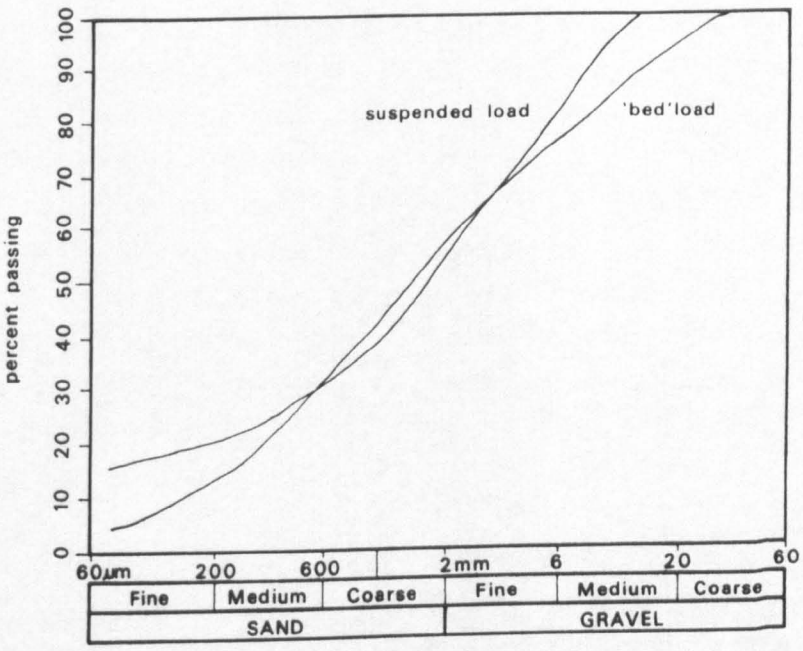

FIGURE 8.3 Typical Grain-Size Distribution Curves for Bedload and Suspended Load Samples Taken From Kharane Khola During Storm Runoff.

similar technique was applied by Grant (1982) in the Ruahine Range, New Zealand.

Indirect monitoring of sediment supply and deposition, in channels crossed by the Dharan-Dhankuta road, was undertaken by determining fan surface elevational change, and both channel bank and catchment landslide density. These investigations are described separately below.

i) Fan Surface Aggradation

As there are no sizeable, discrete and active fan surfaces accessible from the road, monitoring was confined to fans on the Leoti Khola floodplain that are being actively eroded by the trunk river. While this monitoring does not provide absolute data on sediment transport rates, it nevertheless allows typical fan accretion rates to be determined and establishes a basis for future monitoring. Repeated long profiling was undertaken on the active fans of Garjuwa and Kharane Khola following each storm in 1983, using an abney level, 30m tape and ranging rod. Long profiles were surveyed at 10, 15 and 20m intervals along the fan centre-line, from the bridge to the fan apex, using a marker on the upstream side of the bridge soffit for both vertical and horizontal control.

On one and two occasions respectively, on the Kharane Khola and Garjuwa Khola fans, an artificial channel was cleared below the bridge by the maintenance unit. This not only totally altered the fan long profile but also significantly increased the rate of storm flow beneath the bridge. In addition, the presence of the bridge itself influences the rate and distribution of sediment accumulation by both concentrating storm flow beneath it, and by presenting a physical barrier to runoff and sediment transport across the fan when blocked. While the results of the long profile surveys must be interpreted with regard to these considerations, the aggradation rates measured can be regarded as typical of those occurring on active fan surfaces elsewhere in the area.

Results and Discussion

The progressive adjustments of the long profiles of the Garjuwa and Kharane Khola fans, following each storm in 1983, are shown in Figure 8.4. Tables 8.5 and 8.6 respectively, display the incremental change in fan surface elevation,

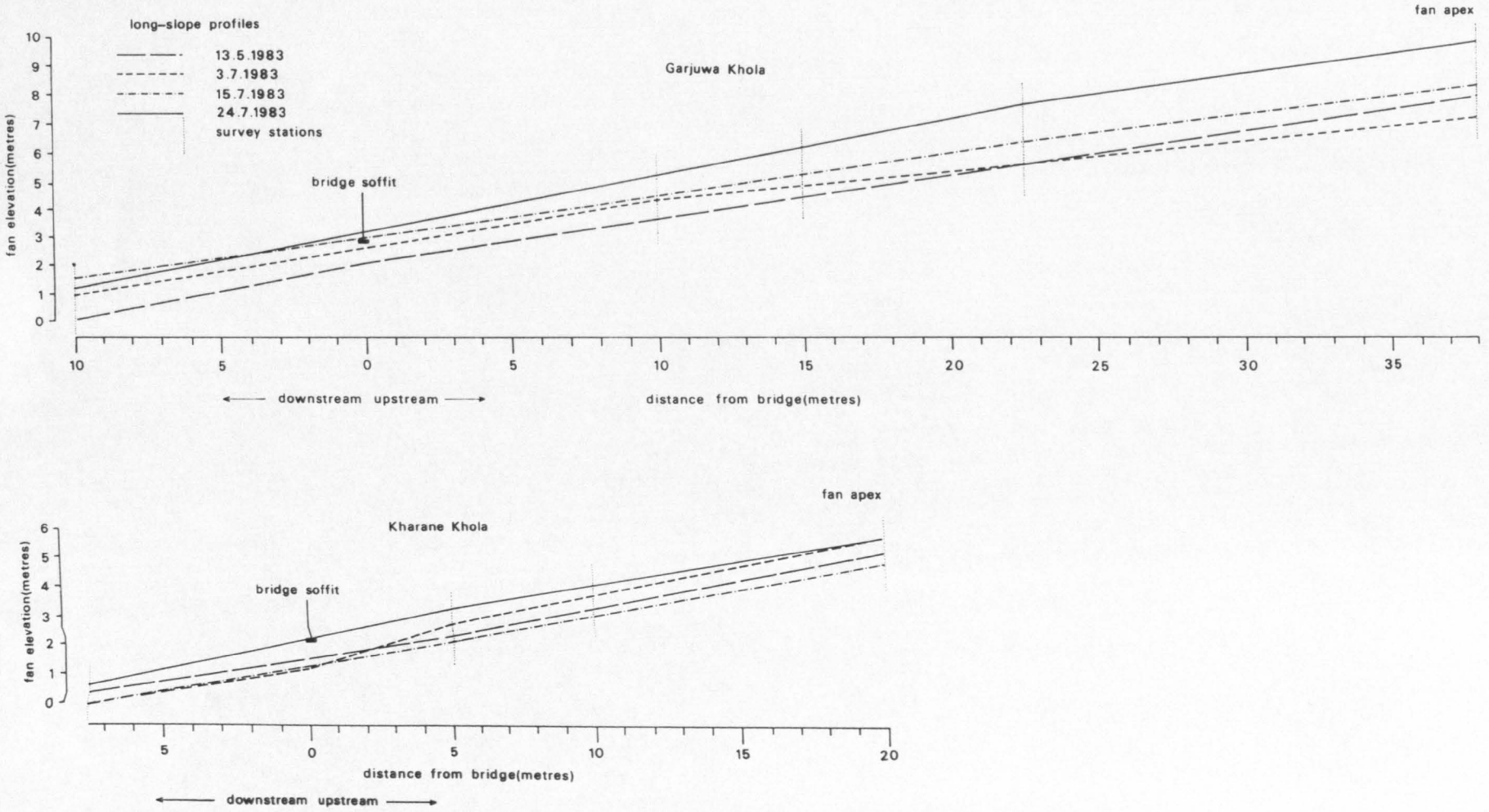

FIGURE 8.4 Progressive Fan Surface Adjustment to Storm Runoff in the Garjuwa and Kharane Kholas in 1983.

GARJUWA KHOLA		INCREMENTAL CHANGE IN LONG PROFILE AREA (DIST.X ELEVATION(m^2))BETWEEN SURVEY STATIONS(DIST. FROM BRIDGE IN METRES).						TOTAL LONG PROFILE AREA (m^2) INCREMENT	INCREMENT OF LONG PROFILE AREA PER METRE (m^2/m)
RAINFALL (mm)	DATE	0-20	20-30	30-45	45-60	60-75	0-(-20)*		
82.5	13.5.1983	-29.60	14.75	18.75	15.37	18.00	42.60	79.87	0.84
27.6	2.7** "	-14.50	-11.60	-30.90	-42.00	-54.00	-13.60	-166.60	-1.75
69.1	3.7. "	7.30	3.25	5.25	6.22	7.35	9.30	38.67	0.41
70.1	4.7. "	11.30	3.25	4.27	7.87	13.87	14.62	55.18	0.58
75.5	14.7** "	-7.00	-5.40	-1.35	0.75	0.75	11.50	-0.75	-0.01
84.2	15.7. "	6.00	7.00	14.25	16.50	15.37	-11.50	47.62	0.50
32.8	17.7. "	8.50	7.25	5.25	0.75	0.00	-8.00	13.50	0.14
91.6	25.7. "	8.00	9.00	28.35	39.60	42.75	3.00	130.70	1.38
Fan incremental volume (m^3) on 25.7.1983		190.40	211.50	637.85	625.70	363.37	71.40	2100.22	

TABLE 8.5

KHARANE KHOLA		INCREMENTAL CHANGE IN LONG PROFILE AREA (DIST.X ELEVATION(m^2)) BETWEEN SURVEY STATIONS (DIST. FROM BRIDGE IN METRES).					TOTAL LONG PROFILE AREA (m^2) INCREMENT	INCREMENT OF LONG PROFILE AREA PER METRE (m^2/m)
RAINFALL (mm)	DATE	0-10	10-20	20-30	30-40	0-(-15)*		
82.5	13.5.1983	8.40	10.10	5.70	-5.25	11.62	30.57	0.56
47.5	22.5. "	2.25	2.75	1.25	1.90	4.12	12.27	0.22
69.1	3.7. "	6.60	6.10	6.50	7.50	5.40	32.10	0.58
70.1	4.7** "	0.00	-3.00	-4.00	-4.25	-5.25	-16.50	-0.30
75.5	14.7. "	-0.20	-9.20	-9.40	-7.50	15.00	-11.30	-0.20
84.2	16.7. "	-4.60	-3.10	6.00	9.00	15.75	23.05	0.42
91.6	25.7. "	20.50	21.00	19.10	18.35	23.25	102.20	1.86

TABLE 8.6

TABLES 8.5 and 8.6 Incremental Change in Fan Surface Elevation on the Garjuwa and Kharane Khola Fans in 1983

NB All survey stations, with the exception of * are upstream of bridge. Survey stations are represented by their distance from the bridge soffit along the fan long profile.

* Downstream of bridge.
** Following artificial bridge clearance during maintenance.

multiplied by the corresponding distance between profiling stations, following each storm flow across the Garjuwa and Kharane fans. These values have been summed and divided by the total fan length to obtain a mean value of incremental change in elevation along the fan centre-line.

In the case of the Garjuwa fan, overall fan degradation, or lowering, took place during the storm flows of 2 July and 14 July with mean lowering rates of 1.75 and 0.01 metres respectively along the long profile. Both of these events followed artificial channel clearance below the bridge, and hence, the lowering of the fan surface in these cases was probably due to a temporary oversteepening of the frontal slope of the fan. The remainder of the long profile increments correspond to fan aggradation, although a progressive reduction with time in accumulation rates, with the exception of those occurring during the storm of 24/25 July, is evident. This trend is not a function of variable storm magnitude, as storm rainfall depths tended to increase through the monsoon season (Tables 8.5 and 8.6). Instead, this trend of decreasing aggradation rate with time may be due, either to a progressive exhaustion of available sediment, or the increasing height of the fan surface itself. There is no evidence to support the former contention as extensive landsliding along the upstream channel occurred during every storm, and especially those of the 14/15 and 24th July. Alternatively, as the elevation of the fan surface increases, sedimentation extends further upstream into the mountain channel. Subsequent storm flows, in the confined channel reach immediately upstream of the fan apex, are able to erode into the loose fan material, and may emerge on the fan surface in deeply entrenched channels. Although these channels aggrade with fine grained sediment during storm recession, very little debris may be available to accumulate on the fan surface itself. Therefore, as fan surface elevation increases, progressively larger storm flows are required before widespread fan surface flow and deposition take place. The storm of the 24 July was the largest to occur during the survey period, and resulted in a mean accumulation rate of approximately $1.38m^2/m$ along the fan long profile, and an incremental volume of $2100m^3$ of debris over the whole fan surface. The majority of transported debris was removed from the fan by the Leoti Khola, and hence, accumulation rates on discrete fan surfaces at the mouths of similar catchments can be expected to be much higher.

Table 8.6 displays the aggradation and degradation rates monitored on the Kharane fan. Fan surface lowering took place during the rainfalls occurring on

the 4 and 14 July, following artificial channel clearance below the bridge. This fan surface took longer to adjust to artificial slope oversteepening than the Garjuwa fan due to the lower rate of sediment supply in Kharane Khola. This lower availability of sediment is reflected in the relatively small fan aggradation rates (generally less than $0.6m^2/m$ per storm event). However, the storm of the 24/25 July caused major slope instability and channel erosion in this catchment, and this is reflected in a particularly high mean rate of long profile aggradation of $1.86m^2/m$ (Table 8.6).

Both the data shown in Tables 8.5 and 8.6 and the monitoring technique employed, are insufficient to allow a rigorous study of fan surface processes or the determination of both instantaneous and total storm sediment transport rates. Nevertheless, an interpretation of the data obtained has enabled some general conclusions concerning fan processes to be made, and has provided useful information relating to the rate of fan accretion. Continued monitoring would allow the success of catchment and channel erosion protection measures to be assessed.

ii) Mapping Sediment Sources

The determination of the areal and channel bank density of landslides in each catchment should enable channels to be assessed in terms of their potential for high sediment yield, and the likelihood of culvert and bridge blockage during storm runoff. However, the potential for culvert blockage will depend upon the design of the culvert and the rate of sediment transport through the catchment. The latter is conditioned by the rate of sediment supply and the continuity of sediment transport along the channel itself. Nevertheless, most landslides in the study area occur adjacent to eroding stream channels (Chapter 5), and consequently, much landslide debris may be rapidly incorporated, into channel flow. Large volumes of sediment may remain in channel storage for considerable periods of time before being transported further downstream during moderate to high magnitude storm flow. Under these conditions, reliable prediction of sediment yields becomes impaired and assessments of sediment potential can only be made, realistically, in very approximate terms.

Landslide mapping, from 1:25 000 scale air photographs and terrestrial photography taken throughout the Dharan-Dhankuta area, was described in Chapter 5. From these maps, total identified landslide area in each catchment

crossed by the road, has been determined and expressed as a landslide density (Table 8.7). Clearly, these landslide densities may be significantly less than the true values because many small landslides that occur along, and immediately upslope of the channel, may not be visible on the photographs owing to problems of scale and shade.

In order to evaluate the smaller channel bank landslides that contribute sediment directly to storm runoff, the proportion of the total channel banks and side-slopes affected by mass movement, as recorded on the channel proformas (Chapter 7), was used as an indicator of channel bank stability. This technique does not take into account landslide volume, but enables rapid comparisons to be made between the relative stability of different channels and channel reaches. This data can be compared with the distribution of blocked bridges and culverts following the September 1984 storm (Table 8.7). Culvert inlet and bridge clearance cross-sectional areas have been calculated and, using flow data derived in Chapter 7, divided by the cross-sectional area of the peak storm flow during the September 1984 storm (Table 8.7).

Results and Discussion

The data in Table 8.7 indicates that catchments with high areal landslide densities did not necessarily have blocked culverts or bridges, following the 1984 storm. In fact, 6 cases of blocked or damaged crossing structures, out of a total of 15, corresponded to catchments in which no active landslides were identified. However, of the 5 catchments with the highest landslide densities, 4 were associated with blocked or damaged culverts or bridges. The proportions of the channel lengths occupied by landslides (Table 8.7) show no relationship with culvert or bridge blockage or damage. For the total channel population, the 22 channels (50%) with the highest channel landslide percentage accounted for only 10 of the 16 cases of blockage or damage. The ratios of culvert inlet area to peak flow cross-sectional area (Table 8.7) display a more definite relationship with culvert or bridge blockage. If the two active fan surfaces on the Leoti Khola floodplain (Garjuwa Khola (km 29.830) and Kharane Khola (km 30.200)) are excluded from the analysis, 8 of the remaining 13 cases of culvert or bridge blockage and damage were associated with peak flow cross-sectional areas that were greater than the culvert area; that is, a ratio value of less than unity.

Culvert Chainage (km)	Catchment Landslide Density (m^2/km^2)	Percentage Channel Length Unstable	Culvert Area/Peak Flow Area	Culvert Blocked or Damaged
2.210	177.59	25.6	1.04	D
2.859	0.00	7.3	0.82	B
3.750	0.00	0.0	5.75	OK
4.000	166.03	5.3	3.59	OK
4.735	0.00	14.8	1.13	OK
4.800	225.19	27.5	8.03	OK
16.070	224.83	46.1	2.05	OK
16.960	0.00	29.7	0.63	B
17.040	631.11	11.6	2.32	B
20.230	0.00	6.1	0.00	B
20.980	0.00	27.6	0.66	OK
23.095	0.00	22.8	0.48	OK
23.440	61.09	33.1	0.56	R
24.480	0.00	40.3	0.32	B
24.500	58.86	51.7	0.85	D
24.520	0.00	32.9	1.34	B
26.145	0.00	0.0	0.89	OK
26.254	0.00	10.9	0.37	OK
26.400	103.84	27.2	0.38	B
26.725	0.00	3.6	3.60	B
26.800	313.32	41.9	0.39	B
28.110	33.21	0.0	6.60	OK
29.830	445.88	32.3	6.39	B
30.200	533.10	28.6	4.89	B
30.646	0.00	5.0	10.02	OK
31.070	242.71	14.0	2.44	OK
33.450	228.29	32.1	4.10	OK
33.600	116.21	47.6	3.89	OK
34.550	0.00	9.6	6.05	OK
40.410	359.73	7.5	3.53	OK
40.570	0.00	13.7	3.62	OK
40.650	163.51	10.3	3.93	OK
41.425	0.00	9.5	0.85	OK
41.590	146.14	10.6	1.18	D
45.580	54.16	11.2	>1	OK
45.600	84.88	9.7	5.54	OK
46.830	0.00	12.6	1.28	OK
47.000	0.00	10.6	1.80	OK
47.818	0.00	12.9	6.30	OK
48.690	0.00	10.7	4.23	OK
49.260	0.00	11.7	3.65	OK
49.480	0.00	9.7	10.07	OK

TABLE 8.7 Culvert Integrity and Catchment and Channel Landslide Density Following the September 1984 Storm.

N.B. B....culvert/bridge blocked
D.... " " damaged
R.... " " removed
OK.... " " intact and clear of debris

These results lead to the conclusion that the processes of sediment supply, transport and deposition are too complex and locally variable to allow sediment yield to be evaluated reliably with respect to catchment landslide density or channel bank stability alone. In addition, the efficiency of a culvert design, in transmitting sediment load, is not only a function of its cross-sectional area, but also its slope, the design of the inlet or outlet control and the slope and configuration of the upstream channel. Nevertheless, culvert blockage often occurs in response to a sudden increase in sediment load caused by intense channel scour or a landslide upstream. Consequently, the mapping of sediment sources and deposits, and an assessment of channel stability during reconnaissance surveys, may enable qualitative evaluation of these hazards for preliminary design of culverts and the siting of erosion protection works.

8.5 Monitoring Slope Displacement

8.5.1 Introduction

"Precise monitoring of the rate and extent of movements in various parts of the landslide complex is most valuable, partly because it helps in the elucidation of the mechanisms of failure and partly because it can give warning of any worsening conditions" (Hutchinson et al 1985 p.12). This statement expresses the great advantages that slope monitoring can have for slope stability assessment and failure prediction. However, this presupposes that potentially unstable slopes can be identified before failure takes place. Quite frequently, in unstable mountain terrain, factors that promote slope instability, such as rapid channel downcutting or a rise in groundwater levels during high intensity rainfall, may occur during an individual storm. Monitoring slope displacement may, therefore, be only applicable to those slopes that either have a history of recurrent instability, or are failing at a slow but perceptable rate.

Techniques for monitoring slope displacement are well developed and documented, and range in sophistication from simple survey monitoring, repeated surface mapping and slope profiling, to the employment of slope instrumentation, such as inclinometers and tiltmeters, surface and borehole extensometers, time-lapse photography and photogrammetry. These monitoring techniques are quite common in both research and engineering based landslide studies, and usually form part of an integrated ground investigation programme of geotechnical assessment. Monitoring techniques

commonly employed have been described with respect to slope instability in the UK, by Hutchinson (1970) and Chandler and Hutchinson (1984).

Photogrammetry provides a useful alternative to conventional ground survey monitoring in steep terrain in that it relies on remote methods of resurvey and allows complete coverage of the monitored slope, within the resolution of the photography. Terrestrial photogrammetric survey networks have been established by City University (Cooper, pers.comm. 1985) on slopes along the Dharan-Dhankuta road and on the hill section of the East-West Highway (Nepal). However, the development of the technique and its application to the monitoring of individual landslides is still in its infancy and is undergoing research. While it offers the advantage of being versatile, its dependence on quite sophisticated computing facilities may limit its application to low-cost road projects.

Using conventional ground survey techniques, the most cost-effective methodology is to establish a low density framework of survey control points on suspected unstable or potentially unstable slopes, at the early reconnaissance stage of the project, in order to allow preliminary assessments to be made prior to the start of construction. These networks could then be supplemented and modified as more information becomes available. Simple resurvey techniques have been used in the present study to determine whether low-cost slope displacement monitoring is practicable and able to yield useful information for design purposes in a relatively short time.

8.5.2 Field Monitoring

This section describes the use of relatively rapid, low-cost slope monitoring techniques to an active, deep-seated planar slide at km 25.500 (Figure 8.1) along the Dharan-Dhankuta road during the monsoon season of 1983. A geomorphological map of this slide is shown in Figure 8.5. The slide is approximately 100m long and 100m wide, and is developed in highly weathered phyllite. The road has cut into the slide and has reactivated instability. There are no signs of deformation to the road surface, and hence, it can be assumed that present instability is confined to the slopes above. The continual encroachment of the cut slope onto the road has caused considerable problems for road maintenance. It was decided, therefore, that this slope would be ideal for testing the application of low-cost, rapid monitoring.

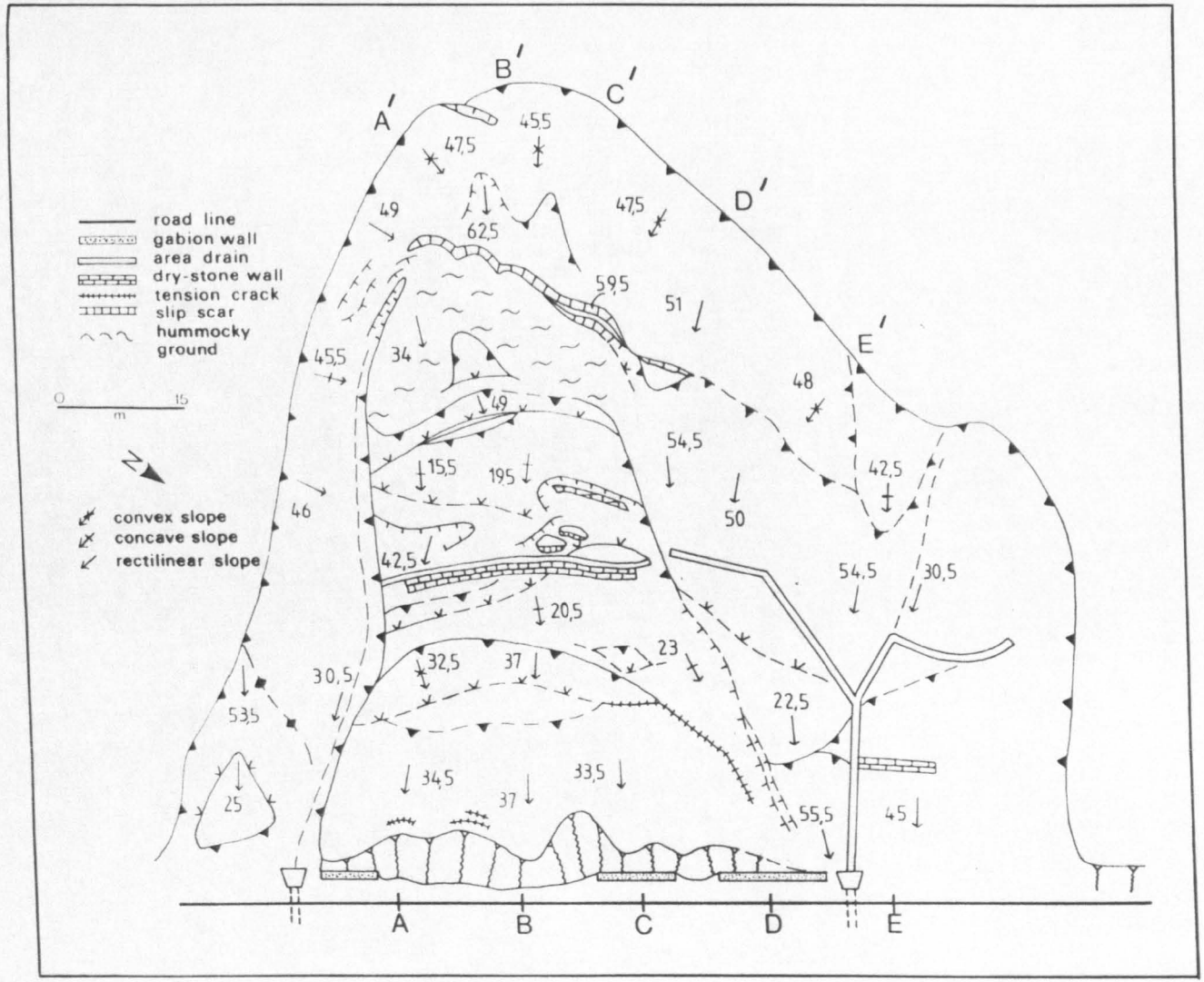

FIGURE 8.5 Geomorphological Map of Monitored Landslide

The monitoring programme consisted of: i) repeated slope profiling, undertaken on 9 May and 15 August, along five slope traverse lines (AA'-EE', Figure 8.5) at approximately 15m cross-slope intervals, and ii) the weekly measurement, with a theodolite, of the displacement of four pegs driven into the slope surface, approximately 10m upslope of the road cutting along profile lines AA'-DD'. The slope profiles were measured in approximately 45 minutes while the resurvey of the pegs took approximately 25-30 minutes. The method used was therefore quite rapid. A standard raingauge installed nearby at Phalametar (Figure 8.1), enabled recorded movements to be examined with respect to 24-hour rainfall. Clearly, rainfall intensity data would have been more desirable had continuous recording raingauges been available.

Results

The surveyed long profiles are shown in Figure 8.6. Slope profile AA' experienced considerable displacement during the measurement period; the cut slope encroached onto the road surface by approximately 3m. The cut slope at profile BB' advanced by approximately 4m, while a dry-masonry revetment wall and an area drain further upslope were displaced downslope by over 5m (Figure 8.6). The surface elevation of this slope profile was lowered along most of its length and the profile change suggested translational sliding. Although the position of the cut slope at profile CC', surveyed on 15 August, appears coincident with that surveyed on 9 May, this is due to the fact that displaced slope material on the road had been cleared, and the slope regraded, by the maintenance unit. A dry-masonry wall and area drain located towards the top of this profile, were displaced downslope by a distance of approximately 5m. The remaining set of slope profiles at DD' shows similar trends of slope displacement.

The geomorphological map of the slide shows numerous active and degraded slip scars that are not immediately apparent on the slope profiles. This is not surprising considering their small size and the low resolution of slope inclination measurements (3m). Clearly, the slope profile should be divided into measuring units of less than 3m length (1.5 or 2m) before these slip scars become detectable. Alternatively, slope profiling, using recognised breaks and changes of slope, would have enabled these features to have been recorded on the profiles, but might have introduced a degree of subjectivity into the survey. However, the locations of these scars were noted during the slope profiling exercise and from this information, the slip surfaces have been tentatively inferred (Figure 8.6).

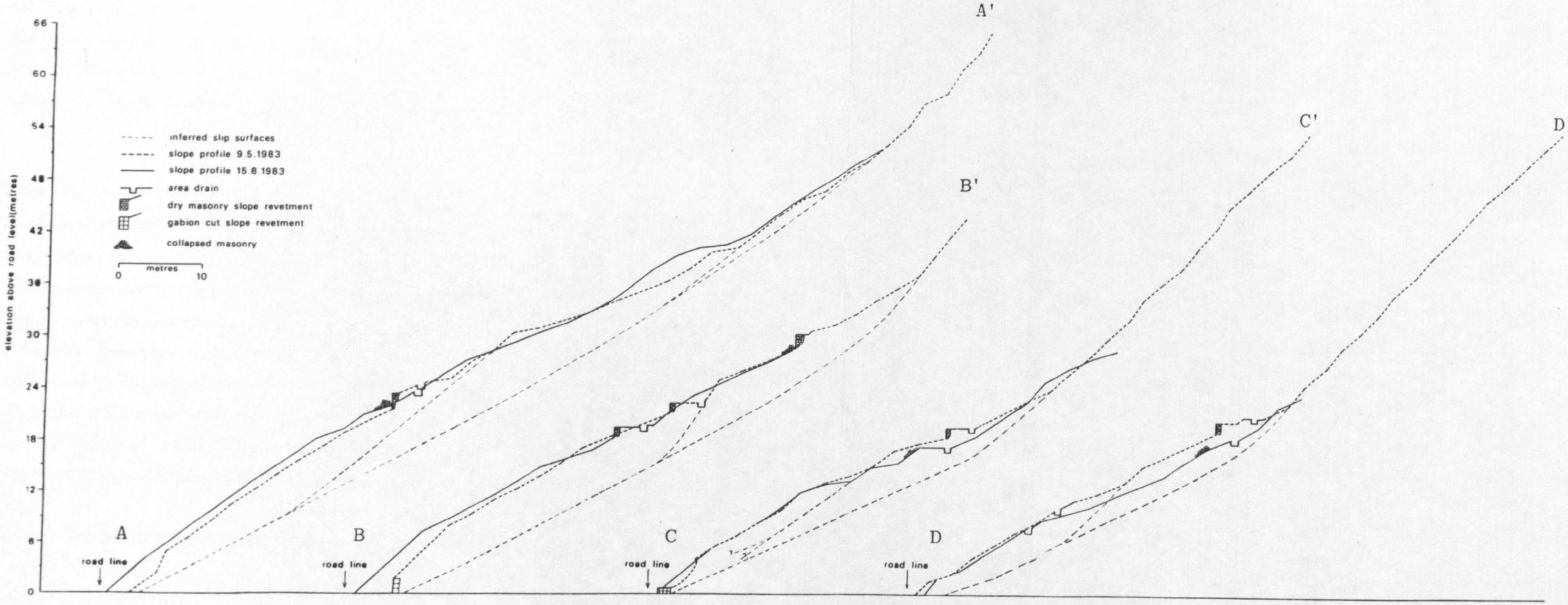

FIGURE 8.6 Slope Profiles of Monitored Landslide.

The displacements of each of the surveyed pegs with time, are plotted in Figure 8.7. The vertical and horizontal positions of these four pegs, as surveyed over fourteen consecutive weeks, are shown on A,B,C and D of this figure, respectively. Beginning with the storm of 12 May (1 on Figure 8.7), the trajectory of peg A increased in elevation until 31 May (4) when the total increase in height reached a maximum of 0.79m in the vertical plane. Thereafter, the co-ordinates of the peg remained approximately the same until the seven days prior to the 5 July (9) when the peg had moved a distance of 2.15m in a downslope direction. This was followed by a further displacement of 2.1m over a period of two weeks. These two downslope movements coincided with the storms of 3 July and 14/15 July respectively, and were followed by very minor slope adjustments (Figure 8.7). It would appear then that, prior to 31 May, movement of the cut slope was characterised by minor adjustments to moderate rainfall, and this was followed by rapid translational sliding towards the road centre-line, following heavy rain. This pattern was repeated for all peg trajectories, although the displacement of peg D was less well marked, with a maximum weekly downhill displacement of 1.4m prior to the 5 July (9).

This relatively short period of monitoring, spanning one monsoon season and incorporating both the direct monitoring of the displacement of survey pegs and indirect monitoring by repeated slope profiling, has provided useful information concerning the rate of slope movement and the nature of the failure, and has confirmed that rapid, low-cost ground survey can provide an adequate means of assessing slope stability. Preliminary monitoring schemes such as this, established at the reconnaissance stage, can be valuable in the assessment of slope movements. In addition, they can provide a basis for the development of more accurate monitoring schemes, once initial data concerning slope displacement rates become available.

8.6 Tip Slope Erosion Monitoring

8.6.1 Introduction

Where spoil material is side-cast, the vegetation cover may be rapidly removed, and under conditions of relatively steep slopes, deep regolith and well jointed, weathered rock, this can give rise to accelerated erosion (Chapter 6). Although this erosion is likely to cease after two or three monsoon seasons (Fookes et al 1985, Hearn 1987), direct monitoring may

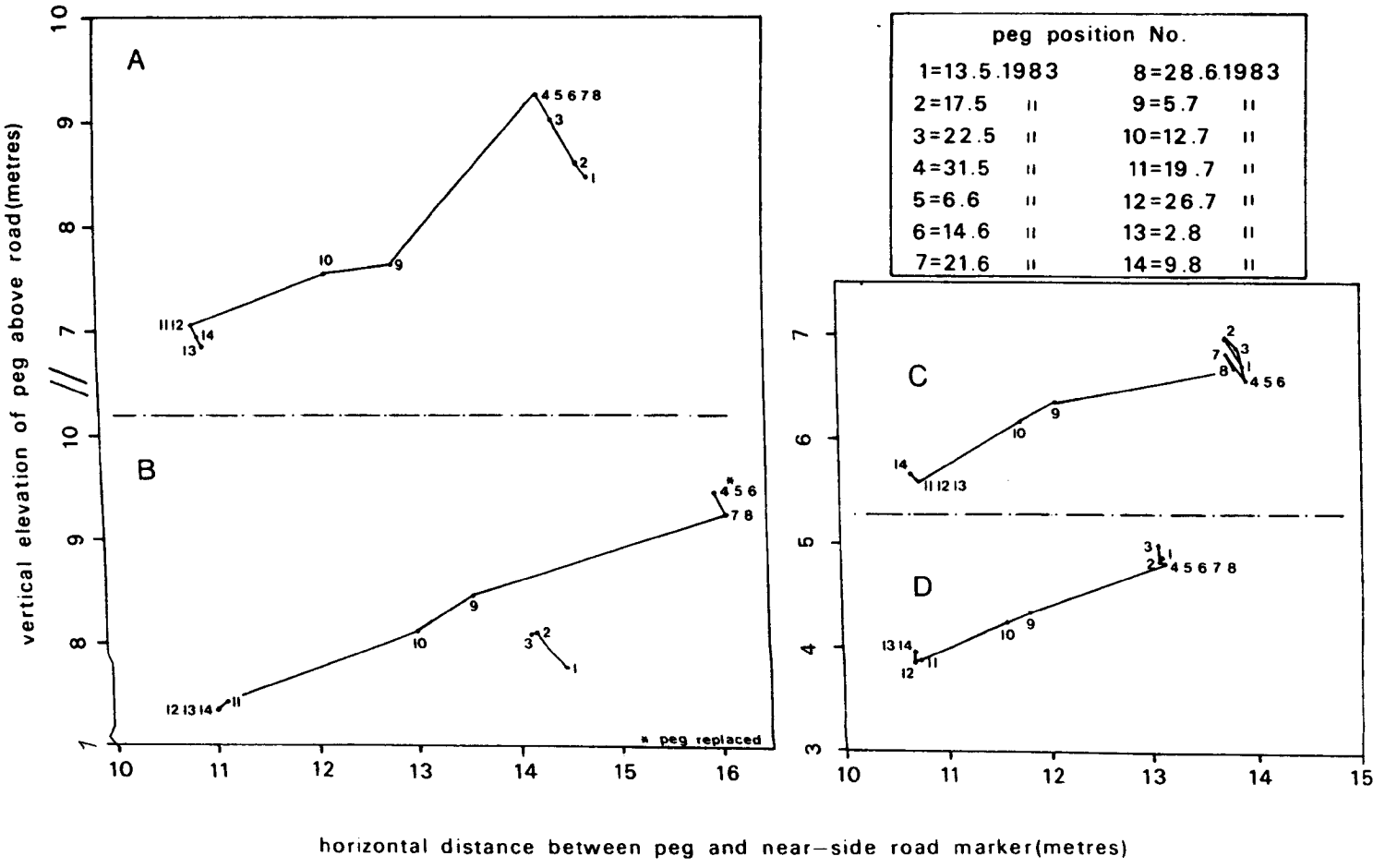

FIGURE 8.7 Peg Displacement Trajectories on the Monitored Landslide.

forewarn of pending accelerated erosion and, more importantly, may allow the prediction of erosion rates that are likely to occur when tipping further along the alignment takes place. A discussion of the factors that influence the rate of erosion on tip slopes is given in Chapter 6.

An understanding of the manner in which different slopes react to spoil tipping is required before any predictive technique or spoil disposal policy can be developed, and this would require considerable field monitoring. Owing to the constraints of time and limited resources, this was not possible in this study. Instead, attention was concentrated towards the monitoring of erosion on three tip slopes in order to determine the extent to which short-term monitoring can be used as a basis for both preliminary planning of spoil disposal, and the design of more comprehensive long-term monitoring schemes.

8.6.2 Field Monitoring

Field monitoring was undertaken during the monsoon season of 1984. In order to minimise the influence of variable rainfall intensity and depth, three monitoring sites were chosen in close proximity to one another, on the northern flanks of the crest of the Sangure Ridge (Figure 8.1). One of these slopes is formed in quartzite, while the other two are composed of phyllite. The quartzite slope (Plate 8.3) has an inclination of $36^{o}50'$ and an aspect of 080^{o}N. Bedrock exposed in the cut slope is relatively massive white quartzite and is overlain by a thin, up to 20 cm deep, sandy, gravelly soil. The two phyllite slopes, hereafter referred to as Phyllite 1 (Plate 8.4) and Phyllite 2 (Plate 8.5), are inclined at $39^{o}40'$ and $37^{o}10'$ respectively, and both are oriented due north. In both cases, regolith is composed of a loose, silty clay with weathered phyllite gravel and cobbles, 30-60cm deep, overlying jointed phyllite, dipping obliquely out of the slope. Phyllite 1 has only been partially affected by spoil disposal from the Bhedetar-Rajarani road and displays a discontinuous vegetation cover, while Phyllite 2 had been totally laid bare by spoil disposal.

Particle size distribution curves of samples taken from the three slopes are shown in Figure 8.8. These samples are composed of both spoil material derived from adjacent cut slope excavation and underlying soil. The curves demonstrate that the quartzite soil sample is dominated by the coarse fraction; sixty percent of the sample being composed of particles larger than 6mm, while the grain size distributions of the two phyllite soil samples are

PLATE 8.3 The Monitored Tip Slope in Quartzite.

PHYLLITE 1

PHYLLITE 2

PLATES 8.4 and 8.5 The Two Monitored Tip Slopes in Phyllite.

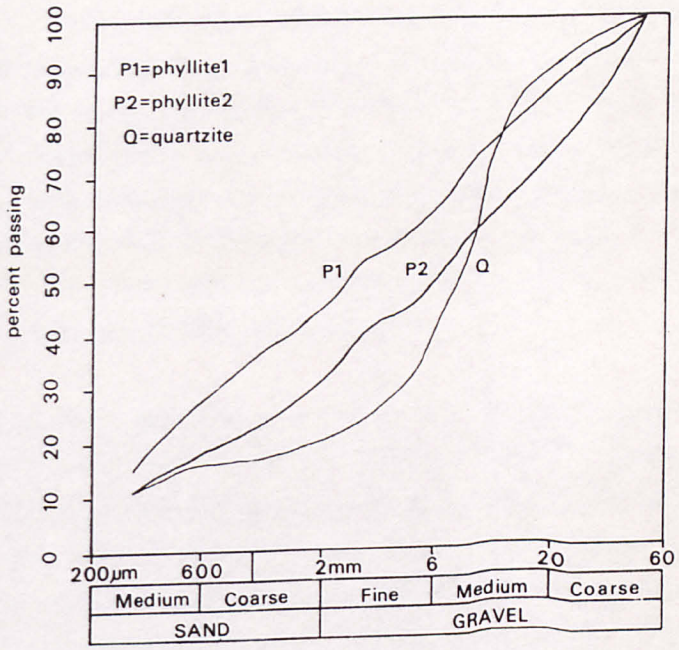

FIGURE 8.8 Grain-Size Distribution Curves for Samples Taken from the Monitored Tip Slope.

more uniform. Sixty percent of the Phyllite 1 and Phyllite 2 samples are composed of particles larger than 1.5mm and 3mm, respectively. Clearly, the marked difference in the particle size distributions of the samples may significantly influence the rate of erosion through its effect on permeability and erodibility of the soil.

A 6m wide x 9m long erosion monitoring grid, composed of twelve reference pegs spaced at 3m cross slope and downslope intervals, was constructed on the quartzite slope. The reference grids on the Phyllite 1 and Phyllite 2 slopes were 6m x 6m and 6m x 10m in size respectively, and were composed of nine and twelve equally spaced pegs. The pegs were 600mm long and were driven vertically into the slope until approximately 200mm remained above the surface. These pegs were then levelled using an engineer's level borrowed from the Road Remedial Works Unit in Dharan. A 30m tape was secured between adjacent pegs across the slope, and the vertical depth to the ground surface below the tape was measured at 200mm intervals.

A standard raingauge was established close to the two phyllite slopes and this was read daily. Following each of the ten storms, arbitrarily greater than 35mm in total depth, and an additional storm on the 5 August when 19.6mm of rain was recorded, the depth to ground surface below the suspended tape was re-measured on each slope, in order to determine the extent of erosion that had taken place. No additional spoil tipping took place during the measurement period. The pegs on the Phyllite 1 slope remained intact during the September 1984 storm, and hence, upon a return visit to the site, it was possible to determine the elevation of the three cross-slope profiles relative to the survey pegs, following this event. Pegs on the other two slopes had been removed by the local inhabitants and erosion.

The configuration and elevation of the cross-slope profiles for each of the three slopes, as surveyed on the 8 June and the 9 August, are shown in Figure 8.9. The intermediate cross-slope profiles have been omitted from this figure to preserve clarity. The depth to ground surface below the suspended tape was determined for each cross profile from measurements taken after each storm. From this data the mean ground elevational change, due to erosion or deposition, was calculated for each cross-slope profile. This data is shown in Table 8.8 along with the mean change in slope elevation over the total area of each grid.

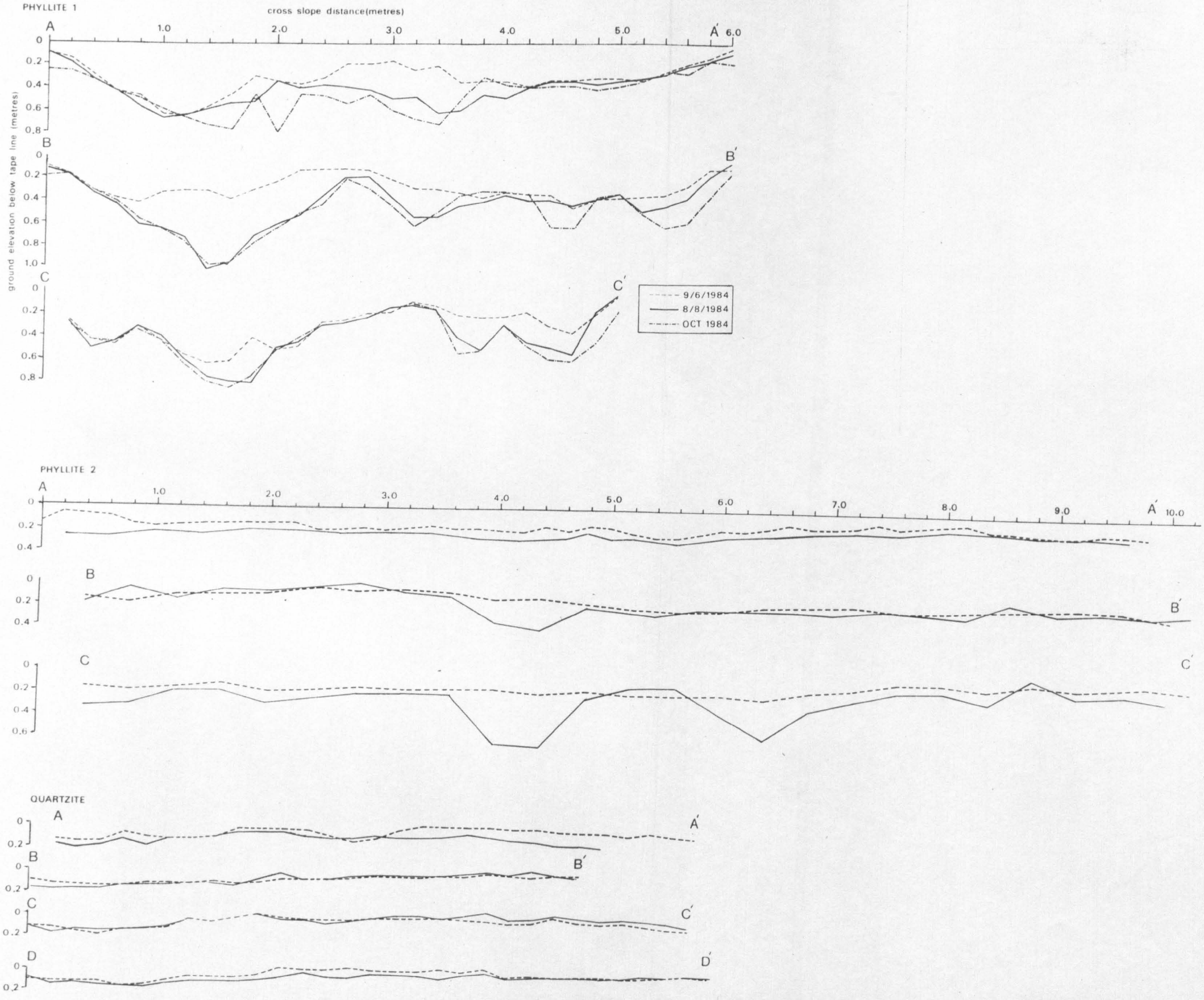

FIGURE 8.9 Cross-Slope Profiles of the Monitored Tip Slopes.

Tip Slope Profile	Between-Station Mean Cross-Profile Elevational Change(cm) Following Each Storm											
	19/6	20/6	23/6	25/6	7/7	13/7	23/7	24/7	5/8	8/8	9/8	Total
Q A-A′	—	0.38	-0.11	0.82	0.06	0.68	—	-0.30	1.81	-1.17	-0.07	2.10
B-B′	—	-3.09	1.86	0.82	1.38	0.19	2.91	-0.39	0.31	0.42	0.17	4.58
C-C′	—	-1.85	0.09	0.30	0.12	0.88	—	-0.15	0.24	0.31	0.40	0.34
D-D′	—	-0.98	-0.29	2.86	-0.09	-0.26	-0.22	-0.41	1.77	0.42	-1.15	2.77
Mean	—	-1.38	0.39	1.20	0.37	0.37	1.34	-0.31	1.03	0.00	-0.16	2.84
P_1 A-A′	0.72	5.68	-0.17	-5.13	2.92	2.28	1.51	2.07	-3.41	2.38	3.94	12.79
B-B′	4.06	9.15	0.57	-3.71	3.48	-2.16	4.41	2.45	-3.27	6.71	0.88	22.57
C-C′	-0.50	9.15	1.19	-1.52	-0.26	2.33	1.83	-0.57	0.53	2.50	-3.83	10.85
Mean	1.43	7.41	0.53	-3.45	2.05	0.82	2.58	1.32	2.05	3.70	0.33	14.66
P_2 A-A′	0.55	1.67	1.21	0.46	0.82	-0.93	0.17	-0.23	—	—	—	3.72
B-B′	0.05	2.26	-0.16	0.16	1.19	2.80	3.45	0.74	0.64	2.00	-0.27	12.86
C-C′	0.75	3.03	0.80	-0.09	-1.86	-1.40	0.58	-0.02	4.14	1.78	-0.04	7.67
Mean	0.45	2.32	0.62	0.18	0.05	0.16	1.40	0.16	2.39	1.89	-0.15	9.45
Rainfall (mm)	45.9	85.9	35.9	42.2	69.2	57.8	106.2	80.5	19.6	51.1	44.6	

TABLE 8.8 Mean Incremental Change of Surface Elevation on Monitored Tip Slopes During Eleven Storms in 1984.

N.B. A negative incremental value denotes slope aggradation, ie deposition.

Results

A visual comparison of the profiles in Figure 8.9 shows the variability in the extent to which erosion has taken place, both between slopes and between cross-profiles on the same slope. The cross-profiles of Phyllite 1 display the tendency for storm runoff to become concentrated into shallow gullies. This is illustrated by the fact that the degree of channelisation increases markedly downslope. The extent of surface lowering that has taken place over the monitoring period increases dramatically between profiles P1AA' and P1BB', but rather less between P1BB' and P1CC'. Total mean erosion depth over the whole grid for the monitoring period, prior to the September 1984 storm, was 146.6mm. Very little additional surface lowering took place as a result of the September 1984 storm (Figure 8.9) and this suggests that the maximum possible erosion depth, approximately coincident with the bedrock/regolith interface, had been reached by August 1984.

The total slope mean erosion depth on the Phyllite 2 tip slope amounted to 94.5mm. While the uppermost cross-profile (P2AA') was lowered approximately equally over its entire length (Figure 8.9), concentrated runoff downslope resulted in the erosion of well defined channels in profiles P2BB' and P2CC'.

During eight of the eleven storms, total slope erosion on Phyllite 1 was greater than on Phyllite 2. Although the overall inclination of the former slope is $2^{\circ}30'$ greater than that of the latter, this factor alone is not considered to be sufficient to account for the large difference in erosion. Instead, the particle size distribution curves indicate that the sample taken from the Phyllite 1 slope is finer-grained than that from the Phyllite 2 slopes. Consequently, the former slope material might be more prone to removal by surface runoff, and this might account for the greater erosion depths found there. In addition, the presence of a discontinuous vegetation cover on Phyllite 1 may increase the potential for erosion by confining surface runoff to bare slope sections between the vegetation, hence facilitating rapid erosion. This is reflected in the marked channelization of the Phylite 1 slope.

In comparison to the phyllite cross-profiles, erosion depths on the quartzite slope were low; the mean depth of erosion over the whole grid during the measurement period amounted to only 28.4mm. Slope lowering was distributed relatively evenly across the slope profile lengths (Figure 8.9), suggesting that concentrated surface runoff does not have a significant effect on the

distribution of erosion. Storm runoff and rainsplash are likely to result in the rapid suspension of silt and fine sand from the surface, leaving a surface armour of gravel-sized material that is sufficiently coarse to resist removal. Concentrated surface runoff and erosion do not, therefore, have the opportunity to develop.

Total slope mean elevational change on all slopes is plotted for each storm event against rainfall depth in Figure 8.10. A positive relationship between rainfall depth and mean slope erosion for the Phyllite 1 slope, where most erosion took place, is evident. With a null hypothesis that there is no significant relationship between rainfall depth and erosion depth, a Spearman's Rank correlation test was performed on the Phyllite 1 data, with the exception of the two cases of slope accretion with negative values. With a correlation coefficient of r_s = +0.667, the null hypothesis can be rejected at the 95 percent significance level, suggesting, as would be expected, that erosion depth is positively correlated with total storm rainfall depth for this slope.

In conclusion, the tip slope erosion monitoring, although restricted in its scope, yielded useful information concerning the rates of erosion on slopes underlain by two dissimilar bedrocks, and may provide the basis for more elaborate erosion monitoring in the future. The grain size of the slope material, and the distribution of slope vegetation, appear to be particularly important in the development of erosion on tip slopes. The study supports the contention that short-term monitoring, using low-cost and rapid measurement techniques, can be usefully incorporated into preliminary earthworks design. In particular, the establishment of monitored trial tips at the reconnaissance stage, may yield vital information on the likely distribution and magnitude of erosion rates, and may contribute to the more effective planning of spoil disposal.

8.7 Conclusions

8.7.1 Introduction

Faced with the problems described in this chapter, it is not surprising that process monitoring has had relatively little application to road projects in geomorphologically active mountain terrain. Among the more important reasons for this are:

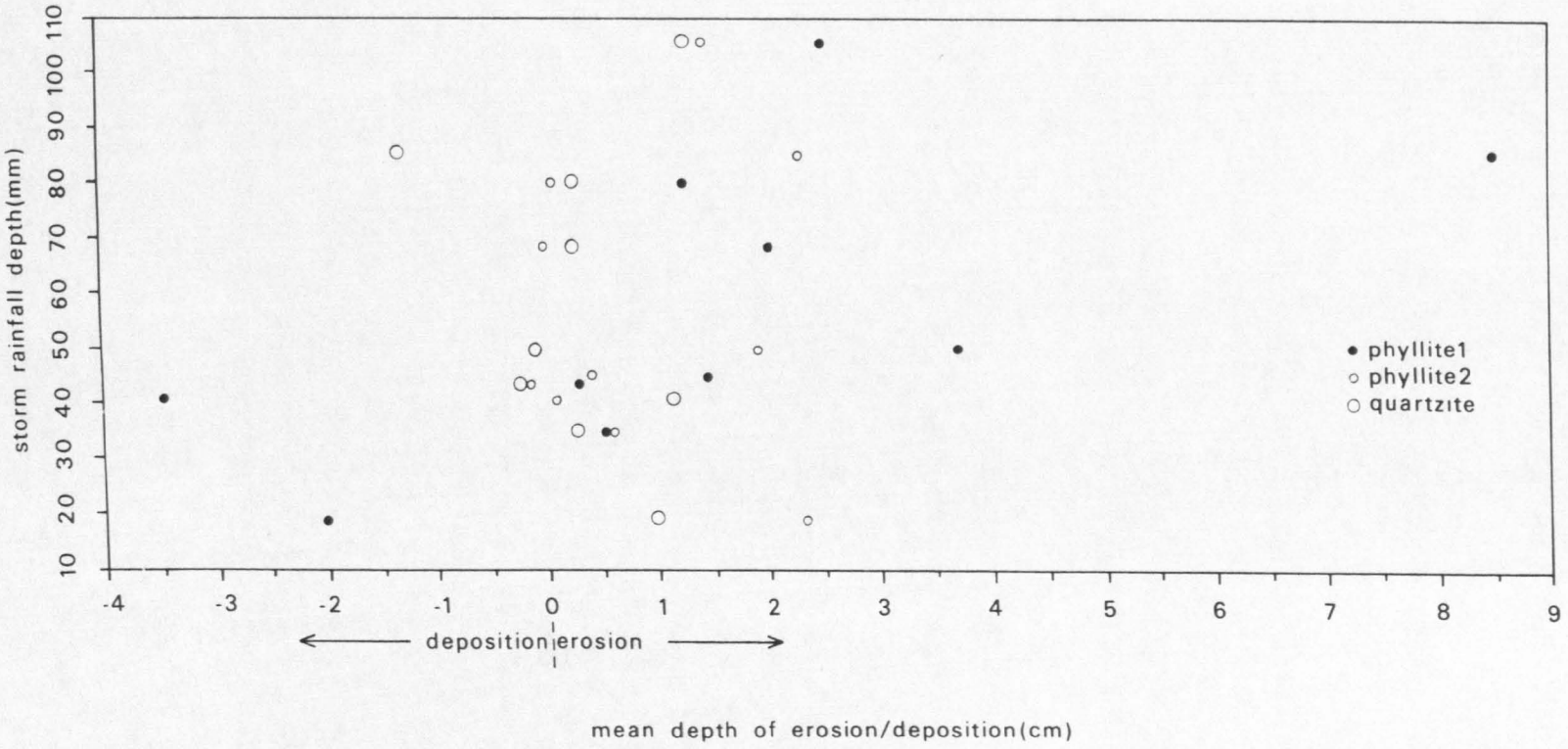

FIGURE 8.10 Mean Depth of Erosion Versus Rainfall Depth on the Three Monitored Tip Slopes During Storms Occurring in 1984.

i) a general lack of awareness amongst engineers of the useful information that can be gained from a properly designed low-cost, low-technology based monitoring scheme for hazard assessment and design purposes, when no other data sources on surface processes are available,

ii) problems of transporting expensive and robust monitoring equipment to the site,

iii) a lack of finance and/or suitably trained personnel to carry out the design and operation of process monitoring schemes,

iv) the prevailing belief amongst many engineers that monitoring will not be able to provide valid and meaningful data soon enough to be of any real benefit to design, and

v) the widely held view that process monitoring is often too hazardous and may prove impracticable in geomorphologically active mountain terrain.

This chapter has examined, by field experimentation, the potential for developing low-cost monitoring techniques that provide 'order of magnitude' data for hazard assessment and preliminary design purposes. Despite the failure of some of the techniques used, some useful results have emerged from the study, and it can be concluded that most of the problems listed above can be overcome. However, owing to time, cost and logistical constraints imposed by research funding, the techniques described in this chapter are only experimental and require further modification and development if they are to be used successfully in the future. On the basis of the field research presented here, the following recommendations can be made for applying and improving the techniques. These are discussed under the headings of storm runoff, sediment transport and slope erosion. Techniques of slope displacement monitoring are considered to be sufficiently well established, for most highway design requirements, and therefore, recommendations for future research and practice are not made.

8.7.2 *Storm Runoff Monitoring*

This research has demonstrated that attempts to directly monitor storm runoff are fraught with operational problems and, in view of the rapid flows

characteristic of steep channels in the Lower Himalaya, are often unacceptably hazardous to personnel. Conventional, robust instrumentation, such as autographic stage recorders, may have some potential application under these conditions, although they would have to be carefully located and extremely well founded to survive. During high magnitude storm runoff, in steep mountain channels, even these instruments are likely to be removed or severely damaged.

There is some potential, therefore, for developing indirect flow monitoring, along the lines discussed in this chapter, although the limitations of the techniques should be recognised. The use of Coolglass greenhouse shading may prove of value in determining peak flow stage at little cost, if properly applied. Clearly, the accuracy of estimates using this, and other methods, needs to be tested in gauged channels against other, more precise, flow monitoring techniques. However, river gauging stations in the Lower Himalaya are located mostly on the larger rivers, and consequently, unless new gauging stations are established, it may not be possible to test these low-cost, experimental monitoring techniques in the small mountain channels for which they were designed. Alternatively, the monitoring techniques discussed in this chapter could be tested in other environments where flow data from small, steep catchments are available.

The indirect flow monitoring techniques tested in this chapter are most appropriate to gauging storm flows of low to moderate magnitude. High magnitude runoff can be determined by the slope-area method, described in Chapter 7, using morphological and sedimentological indicators of peak stage.

At present, the Manning roughness equation, with an assumed roughness coefficient, is probably the most appropriate indirect method of determining velocity. Nonetheless, as concluded in Chapter 7, there is scope for developing a series of roughness standards for highly irregular mountain channels, such as those found in the Lower Himalaya. However, the ability to achieve this will depend on the success with which flow velocities can be measured in the field.

8.7.3 Sediment Transport Monitoring

As with storm runoff monitoring, direct monitoring of sediment transport is extremely problematic and dangerous. Again, indirect methods are likely to

prove the most successful and beneficial to the assessment of sediment loads for culvert design, and the evaluation of erosion protection and sediment control measures. On the Dharan-Dhankuta road, fan aggradation problems at bridge crossings have resulted in high road maintenance costs, and it appears that, although this hazard was anticipated in design (Chapter 4), its scale may have been underestimated. Consequently, repeated survey of fan surfaces, from the reconnaissance stage onwards, might enable the relative hazard posed by different fans to be identified and quantified at an early stage, thereby facilitating the design of erosion and sediment control measures and suitable clearances for bridges. The techniques described in this chapter form a suitable basis for such an approach.

In addition to the monitoring of sediment accumulation rates, the mapping of sediment sources, such as landslides and in-channel deposits, should enable preliminary assessment of channel sediment to be undertaken. The analysis on this theme presented in this chapter was too generalised and small scale to yield any meaningful results. Nevertheless, there would appear to be some scope for experimenting with these methods of channel mapping, in conjunction with the use of proformas (Chapter 7), for the assessment of channel stability and sediment supply.

8.7.4 Tip slope Erosion Monitoring

Finally, it has been demonstrated that short-term monitoring of tip slopes can provide useful information concerning erosion rates and their distribution with respect to underlying rock type, slope materials, slope inclination and vegetation. While the study described in this chapter has proved quite successful in yielding valid data, its scope has been rather limited and could have been improved, had there been more available time and resources, by extending the investigation to cover a wider range of slope types. Future research might, therefore, be beneficially directed towards identifying the impact that spoil tipping has on the range of slope types encountered in an area, using the site monitoring described in this chapter in combination with the photographic and photogrammetric techniques discussed in Chapter 6.

8.7.5 Conclusions

In conclusion, cheap, experimental monitoring established at the reconnaissance stage of a road project would appear to offer some potential

for channel and slope hazard assessment for design purposes. It is difficult to determine what the benefits to design would have been had more planned, integrated and long-term monitoring schemes been adopted during the reconnaissance, investigation, design and construction stages of the Dharan-Dhankuta road. It is interesting to note that during the reconnaissance stage of this road, concern over erosion on spoil tips led to the establishment and monitoring of trial tip benches. While it appears that this quantitative data was not properly analysed, and certainly not used in any interpretation for design purposes, visual assessment of the erosion on, and stability of, these trial benches was undertaken by the design team during earthworks. It would seem then, that engineers are willing to undertake monitoring programmes when they perceive that the hazards endanger the integrity of the project. Had the full extent of slope drainage hazards, for instance, been realised at the start of the Dharan-Dhankuta road project, then it is possible that these too, might have been monitored in a similar way.

It has been demonstrated in this chapter that it is worthwhile making serious attempts at process monitoring during and after the reconnaissance stage of a project, as the data yielded may provide a useful input to hazard assessment in a relatively short period of time. When compared to high technology based techniques, the methods described in this chapter are relatively inaccurate and can only provide approximations to the magnitude of the processes being recorded. However, the logistical problems associated with field monitoring in this terrain and the uncertainty, at the reconnaissance stage, of both the magnitude of slope and drainage processes and the final design of the road, dictate that low-cost techniques, such as those developed here, are the most appropriate.

CHAPTER 9

A STRATEGY OF TERRAIN AND HAZARD EVALUATION FOR HIGHWAY DESIGN IN THE LOWER HIMALAYA

9.1 Introduction

The principal aims of this chapter are essentially two-fold. The first is to discuss the present constraints on the application of geomorphological techniques and expertise of terrain and hazard assessment to highway design in unstable mountains. The second is to establish a strategy of terrain and geomorphological hazard evaluation for highway design purposes, from the initial desk study to the post-construction evaluation and maintenance stages of a project. This incorporates the techniques discussed in this thesis. While the framework is particularly relevant to the Lower Himalaya, it may also be applicable to other unstable sub-tropical fold mountain terrains with similar geomorphological characteristics.

9.2 Factors Constraining the Application of Geomorphological Techniques and Expertise to Mountain Highway Design

9.2.1 Introduction

Historically, road construction in the Lower Himalaya has been accomplished by a combination of engineering design and modified precedent. This was true of British Army practice and has been continued by the Indian Border Roads Unit in India and Nepal, the Nepal Roads Department, the Chinese and recently North American and particularly British consulting engineers. Present constraints on the application of geomorphological techniques and expertise relate mostly to the fact that under the majority of terrain conditions, well established engineering, geotechnical and engineering geological methods of assessment are adequate for construction purposes. Engineers, in general, have not felt it necessary to employ geomorphological techniques, except in the most problematic cases where mass movement and other terrain hazards pose unacceptable risk to proposed roads, and where other forms of assessment, such as engineering geological surveys, are not adequate. This of course, presupposes that the engineer is able to recognise the potential risk posed by these hazards. In the Lower Himalaya this is often

not the case. For example, Sharma (1974) has noted that considerable savings in maintenance and remedial works along mountain roads in Nepal could be achieved by more effective alignment design to avoid slope hazards. In addition, until quite recently, geomorphologists have shown comparatively little interest in applied studies, and especially engineering projects, in mountain terrain. Interestingly, while the present constraint on the application of geomorphological techniques to highway design is primarily due to a lack of appreciation on the part of the engineer, the first application of British geomorphological expertise to mountain highway design (in 1974 and 1975 for the Dharan-Dhankuta road) was due to both the recognition of the potential geomorphological contribution by an engineering geologist (Professor P.G. Fookes) consulting to the design engineers, and the infancy of engineering geological mapping at that time.

The potential for the future involvement of geomorphological expertise in highway design in the Lower Himalaya, depends largely on the constructing nation. Road construction by Indian and Chinese engineers, for instance, is unlikely to involve geomorphological expertise, as design is normally undertaken by the military or public works departments, using standard procedures that are often rigid and not amenable to outside influence. The greatest potential for an increased use of geomorphological techniques and expertise would appear to lie in road design and construction by North American, European and particularly British engineers. For instance, British engineers are likely to be more familiar with the growing field of applied geomorphology, and especially with the technique of detailed mapping which is becoming increasingly used by both geomorphologists and engineering geologists as part of landslide investigations in Great Britain.

In order to ascertain the British engineer's perception of geomorphological techniques and expertise, a postal questionnaire survey, addressed to UK-based engineering consultants, was instigated.

9.2.2 Questionnaire Survey

The specific aims of the questionnaire survey, undertaken in February 1983, were to:

i) gather locational and design details relating to road construction in

mountain or steep slope terrain,

ii) determine which type of specialist each respondent would prefer to consult for the evaluation of listed slope and drainage problems,

iii) determine, where appropriate, why the respondent preferred, or would prefer not, to employ the services of a geomorphologist.

A total of twenty-nine UK-based consulting engineers, as listed in the 'Consulting Engineers Who's Who and Yearbook', were contacted in the survey. Preference was given to those with noted experience of highway design in mountainous or steep slope terrain. The questionnaire was addressed to the Senior Civil Engineer or Highway Engineer of each organisation, and was accompanied by a letter of introduction explaining the purpose of the survey and its concern with road design in mountainous or steep slope terrain.

The questionnaire is reproduced in Figure 9.1. Question 1 was designed to determine which geomorphological hazards were most detrimental to road stability, while Question 2 sought to identify the type of specialist who undertook their evaluation. Question 3 was devised to determine the respondent's order of preference given to various specialists, including the engineering geologist and the geomorphologist, for the evaluation of six specified hazards. Because these hazards are often dealt with by in-house specialists, the question was made hypothetical and stipulated that recourse would have to be made to external consultants. Respondents giving low priority to the services of an engineering geomorphologist were asked to give reasons for their decision in Question 4. Question 5 was again hypothetical, and asked the respondent's opinion of the usefulness of different techniques of slope and drainage evaluation at the reconnaissance, site investigation and construction stages of a project.

As flooding and sediment transport have been found to pose major problems for road design, construction and maintenance in the Lower Himalaya (Chapter 2), Questions 6 and 7 asked the respondent to comment on the use of various forms of channel protection works, and on the methods used to determine design flood discharge and sediment transport for the highway project under consideration.

LONDON SCHOOL OF ECONOMICS AND POLITICAL SCIENCE

DEPARTMENT OF GEOGRAPHY(GEOMORPHOLOGY)

Questionnaire For Highway Engineers

NOTE: All Questions Refer To Highway Construction In Mountainous Or Very Steep Ground.
If You Have Not Been Involved In Highway Design In Mountainous Or Steep Ground
Please Pass This Questionnaire To Someone In Your Company Who Has.
Replies Will Be Treated In Confidence.

Title of respondent (Profession and position) _____

Location of project (Please be specific) _____

1. Please rank, i.e. 1st, 2nd, 3rd etc., in order of importance the following environmental hazards encountered.

A) Gully erosion and undermining of structures [26]
B) Flood discharge [28]
C) Debris transport through gullies and culverts [29]
D) Deep seated rotational slides and subsidence [20]
E) Rock slides and rockfalls [22]
F) Mud slides [46]
G) Debris flows [47]
H) Other (Please specify)_____ [ ]

2. Were these hazards dealt with by (Please tick)

A specialist on permanent staff of your organisation ? [8] Type of specialist _____
And/Or
An external consultant ? [3] Type of specialist _____

3. Imagine that you encounter problems that require the advice of a consultant external to your organisation. Please assign a rank to each of the following specialists according to the potential contribution that they might offer, with regard to the environmental hazards listed.

A) Gully erosion	Engineering Geologist [11], Engineering Geomorphologist [10],	Hydraulic Engineer [16], Other ☐ Please specify _____	Sedimentologist [23],	
B) Flood discharge and debris transport	Engineering Geologist [18], Engineering Geomorphologist [17],	Hydraulic Engineer [17], Other ☐ Please specify _____	Hydrologist [13],	
C) Rockfalls and rock slides	Engineering Geologist [13], Engineering Geomorphologist [21],	Rock Mechanics Engineer [19], Other ☐ Please specify _____		
D) Deep seated rotational slides	Engineering Geologist [12], Engineering Geomorphologist [17],	Soils Engineer [8], Other ☐ Please specify _____		
E) Mudslides	Engineering Geologist [13], Engineering Geomorphologist [14],	Soils Engineer [11], Other ☐ Please specify _____		
F) Debris flows	Engineering Geologist [11], Engineering Geomorphologist [11],	Soils Engineer [17], Other ☐ Please specify _____		

4. Please answer this question only if your answers to Question 3 were generally anything other than 'Engineering Geomorphologist' Why would you not seek the advice of an 'Engineering Geomorphologist' ? (You may tick more than one box)

A) I am unfamiliar with the work of an 'Engineering Geomorphologist' [2]
B) Compared with other techniques Geomorphology is of little value in mountain highway design [2]
C) Geomorphology is generally of value at the reconnaissance stage only [2]
D) Constraint of cost ☐
E) Constraint of time ☐
F) Other, please specify _____ ☐

5. Please indicate the potential use of the following forms of information at the reconnaissance, site investigation and design, and construction stages of the highway project.

Reconnaissance stage	NOT USEFUL	USEFUL	VERY USEFUL
Air photographs	☐	[1]	[7]
Geomorphological strip (route) map with proformas	☐	[2]	[6]
Hazard index map (magnitude and frequency of hazard)	☐	[4]	[4]
Site investigation and design			
Air photographs	[1]	[1]	[6]
Geomorphological strip (route) map with proformas	[1]	☐	[7]
Hazard index map (magnitude) and frequency of hazard)	☐	[5]	[3]
Construction stage			
Air photographs	[4]	[4]	☐
Geomorphological strip (route) map with proformas	[4]	[3]	[2]
Continued observation (e.g. of flood volumes, debris transport and slope stability)	[1]	[3]	[5]

6.A If your contract involved the stabilization and/or crossing of eroding gullies, how useful did you find the following protection methods ? (Please tick)

	NOT USEFUL	USEFUL	VERY USEFUL
A. Concrete/Masonry lining along banks	[2]	[2]	[4]
B. Gabion boxes/reno mattresses along banks	[1]	[3]	[4]
C. Checkdams	☐	[3]	[1]
D. Concrete masonry cascades	[2]	[2]	[2]
E. Gabion cascades	[1]	[3]	[1]
F. Channel armouring/rip rap	☐	[4]	[3]

B Briefly describe the types of culvert that you found most effective and how scour and/or blockage at the inlet and outlet was avoided.

7. Please describe briefly the methods that you found most useful in predicting:-

A. Peak water discharge for a given design flood

B. Bed and suspended sediment transport during this event

8. Have you ever had any professional contact, i.e. contract work, with an 'Engineering Geomorphologist' ? (Please tick)

Yes [2] No [6]

9. Can you think of any other particular circumstances when an 'Engineering Geomorphologist' might be of use to the project ? (Please tick)

Yes [4] No [5]

If yes please give a brief description.

FIGURE 9.1 Questionnaire for Highway Engineers.

Question 8 was included as a cross check of the information supplied on the questionnaire, and particularly the answers given to Questions 3 and 4. Finally, Question 9 allowed for any additional information that the respondent cared to provide concerning his views of the geomorphologist's potential role in mountain highway design.

In order to maximise the return rate, the questionnaire was kept non-technical, and easy to comprehend and complete. Questions requiring lengthy written answers were avoided as these tend to reduce the respondents' willingness to complete the questionnaire and lead to difficulty and subjectivity in its interpretation. In the interest of objectivity and legibility, a draft of the questionnaire was examined by a leading statistician at the London School of Economics and Political Science (Professor O'Muircheartaigh) and modified in the light of his comments.

Unfortunately, of the twenty-nine questionnaires dispatched, only nine positive returns were obtained. A further nine respondents maintained that they had no highway design experience in mountainous or steep ground relevant to the questionnaire. The remainder gave no reply. Clearly, such a low return rate does not provide adequate grounds for statistical analysis as the returned data may not be representative of the total population of consulting engineers in the UK. Nevertheless, the results are of some interest to the present investigation.

Table 9.1 lists the geographical locations of highway projects referred to by the nine respondents. The data for Questions 1-6A, 8 and 9 have been summed as rank scores, or number of ticks, to provide a composite response, representing all nine questionnaires (Figure 9.1). Therefore, lower and higher cumulative ranks or scores reflect, respectively, a greater and lower use or preference.

Questionnaire respondents consisted of five Senior Civil Engineers, two Senior Geotechnical Engineers and two Senior Soils Engineers. Thus, it would appear, that the questionnaires returned were completed by senior staff capable of deciding which techniques and personnel should be used in hazard evaluation for highway projects.

ROAD	LOCATION
Amman - Dead Sea	Jordan
A470 (T)	South Wales
Dharan-Dhankuta	Nepal
Jebel Qara	South Oman
Unspecified	North Wales coast
Unspecified	East Midlands
Various	Austria, Switzerland
Various	NE England, Scottish Highlands
Wamis/Gharian area	NW Libya

TABLE 9.1 Roads Detailed on the Questionnaires

From the combined data, the most important perceived hazards, in rank order, were deep-seated rotational slides, followed by rock slides and falls, gully erosion and flooding. Mudslides and debris flows were considered to be the least important. In all nine cases these hazards were evaluated, in part, by in-house personnel. In six of these cases, an engineering geologist was employed, while an in-house geomorphologist was used on only two occasions, and by the same firm.

The answers given to Question 3 (Figure 9.1) reveal that in respect to all six hazardous processes listed, not once was the engineering geomorphologist regarded as the most appropriate specialist to undertake the evaluation. The engineering geologist and soils engineer appear to be the most favoured in the range of specialists listed. Reasons for rejecting the skills of the geomorphologist are equally divided between 'unfamiliarity', 'general unsuitability' and 'suitability at the reconnaissance stage only'.

The most useful reconnaissance techniques for geomorphological hazard assessment were regarded as being air photograph interpretation, followed by geomorphological mapping. In most cases, geomorphological mapping, followed by air photograph interpretation, was regarded as 'very useful' at the site investigation and design stages while, not surprisingly, these techniques were mainly assigned to the 'not useful' category at the construction stage. Seven of the nine respondents regarded continual observation at the construction stage as being either 'useful' or 'very useful'.

Of the four positive replies to Question 9, two respondents suggested that the geomorphologist was of use at the feasibility and planning stages of the project, while the third was of the opinion that the geomorphologist had a significant role to play in post-construction evaluation and maintenance.

9.2.3 Discussion of the Questionnaire Results and Implications for Applied Geomorphology in Highway Engineering

The questionnaire survey was undertaken towards the beginning of the author's research, and some of the concepts and terminology used are now considered to be less appropriate. For instance, it is difficult to differentiate between the activities of the various specialists listed in Question 3. In addition, the approaches and techniques themselves are equally, if not more important than the background of the specialist employed. Nevertheless, it is contended here, that geomorphologists can contribute significantly to hazard and ground assessment for engineering design in most terrains, not only those found in the Lower Himalaya. Consequently, an examination of the geomorphologist's potential role is considered important to this discussion.

From this limited sample, it appears that the UK engineers sampled, have a low opinion or appreciation of geomorphological expertise, when applied to highway design and construction in mountainous or steep terrain. It is the engineering geologist who is seen as the most capable specialist to undertake a wide range of tasks. However, with the exception of the reply concerning the Dharan-Dhankuta road, for which both consultant and in-house geomorphologists were used, the highway projects quoted may not have been exposed to the same high degree of risk from geomorphological hazards, as roads constructed through the Lower Himalaya. In conclusion, the questionnaire results are not likely to be representative of the engineering response to hazards encountered in the Lower Himalaya, and consequently a more pertinent questionnaire survey might have been directed towards British, European, Chinese, Indian, Nepalese and American engineers who have had experience of road construction in this region. Such a survey was considered to be outside the scope of this study.

This thesis has shown that the greatest potential for the application of geomorphological expertise to mountain highway design in the Lower Himalaya, and similarly unstable mountain terrain, appears to be during the

initial stages of project feasibility, route planning and field reconnaissance (Chapters 4 and 5), when hazard assessment is most crucial to alignment design. However, during construction and maintenance, hazards are likely to continue to pose a threat to road stability, and continued geomorphological assessment will be necessary.

While there is, therefore, considerable potential for the further application of geomorphological expertise to mountain highway design, its realisation is currently constrained by three main factors:-

i) Due to unfamiliarity and convention, engineers may be reluctant to employ geomorphologists, especially as they are often seen to be specialists with a limited knowledge of practical aspects of engineering design.

ii) Geomorphologists who have had very little contact with engineers, regardless of whether they would class themselves as pure or applied, may be unaware of the engineering design requirements of ground and hazard assessment, and may be incapable of translating their data, expertise and often jargonistic language into a format that can be readily digested by engineers and assimilated into the design process. Obviously there is some scope for the engineer to meet the geomorphologist half-way, by increasing his knowledge and understanding of geomorphological concepts and analytical methods in order to improve his interpretation of geomorphological data for design purposes. However, as it is the geomorphologist who is providing the expertise and techniques, he should attempt to become more aware of engineering design requirements of terrain and hazard data. Geomorphologists employed on a long-term basis by consulting engineers may be able to become sufficiently au-fait with engineering procedures and data requirements for design purposes. They may also encourage engineers to become more familiar with the field of geomorphology.

iii) Applied geomorphologists in the UK are becoming increasingly aware of their potential contribution to environmental management, planning, insurance and litigation (Hart 1986), following developments in these fields by earth scientists in the United States. Consequently,

highway engineering applications have been largely demoted in the applied hierarchy since the pioneering work of Brunsden, Doornkamp and Jones (Brunsden et al 1975 a and b). Unlike most of the other applied fields, the gap between engineering and geomorphology is technical, and so far this has been the most difficult to bridge.

In conclusion, the further application of geomorphological expertise to highway design ultimately depends on:

i) the engineer's perception of both the nature of hazardous processes and the potential contribution that geomorphological assessment can make to successful design,

ii) the ability of more conventional engineering specialists, such as geotechnical engineers and engineering geologists, to interpret landforms and processes in terms of their potential impact on road stability, and

iii) the ability of geomorphologists to recognise their potential contribution and provide data, analyses and interpretations that are directly usable by the engineer.

In respect to iii) above, it is possible to identify four main criteria that should be fulfilled by geomorphologists or geotechnical engineers when presenting their findings to the engineer:

i) clear and succinct observations and recommendations in non-jargonistic language, using terms recognizable by the engineer,

ii) a quantification of data wherever possible,

iii) presentation of information in map or plan form,

iv) classifications and impact evaluations of ground conditions and hazards using conventional engineering geological terminology.

The term 'engineering geomorphology' has been purposefully avoided in this discussion as it should form one component of an interdisciplinery field of

geotechnical engineering. Ideally, a multi-disciplinery approach, integrating geotechnical, engineering geological and geomorphological expertise, is the most appropriate methodology for highway design in unstable mountains. This approach is discussed below.

9.3 Strategy for Slope and Drainage Hazard Assessment for Highway Design Purposes

9.3.1. Introduction

This section presents and discusses a strategy of terrain and hazard assessment for highway design purposes that has emerged from the study of the Dharan-Dhankuta highway described in Chapters 4 to 8. It must be stated here that this strategy is comprehensive and ideal, and consequently may be inappropriate for many low-cost road projects, where suitable funds and expertise are unavailable. Under these conditions, an alternative strategy is necessary, and this is discussed in Section 9.4.

The strategy, shown schematically in Figure 9.2, has been designed to suit the requirements of the design of all-weather, high investment roads, that are intended to form principal road links within the region. The strategy is based largely on the design philosophy of the Dharan-Dhankuta road, but has been modified in the light of the techniques developed and discussed in this thesis, a post-construction hindsight evaluation of the road and discussion with project engineering geologists. Many of these techniques, and their application, are also reviewed in Fookes et al (1985).

In the left hand column of Figure 9.2 are listed data sources and evaluation techniques, according to the stage of the highway project. In the top row, the various design aspects are identified. These range from initial route corridor selection through earthworks design, slope stability and drainage assessment, to stabilization and erosion protection measures. This listing does not cover all aspects of design, but instead concentrates on those aspects that relate to geomorphological hazards and their reduction, prevention or avoidance.

The nature and form of the information that can be obtained from each applicable data source, or evaluation technique, are listed for each design aspect in the respective boxes. Thus, a design theme such as alignment design

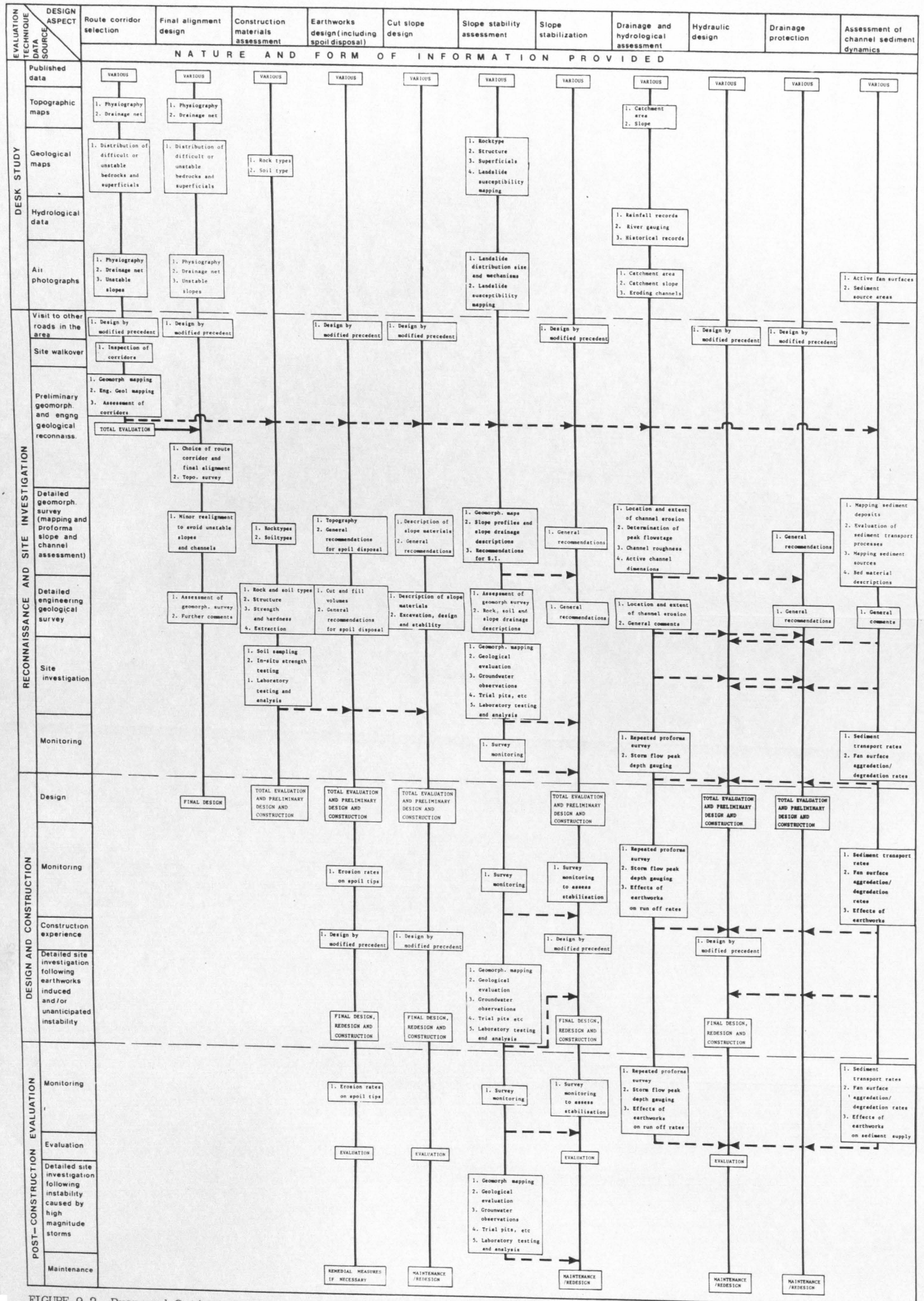

FIGURE 9.2 Proposed Optimum Strategy of Terrain and Hazard Evaluation for Highway Design Purposes in the Study Area.

or slope stability evaluation, can be traced vertically (from top to bottom) on the figure, from the desk study to the post-construction evaluation stage of the project. The vertical arrows between boxes represent progressive design as the project develops, while those that extend horizontally, identify linkages or inputs of information derived from one design aspect to another. Understandably, the greatest number of linkages occur between slope stability assessment and slope stabilization, and between drainage assessment and hydraulic design. The scheme allows flexibility and optimisation of the design approach and encourages the philosophy of an evolving design, based on continued observation, reassessment and modified precedent. It should be stressed, however, that in the case of many mountain road projects, a general lack of data sources, such as aerial photographs or geological maps, may not allow such a comprehensive design framework to be adopted.

The framework is best described and discussed by reference to slope and drainage hazard evaluation.

9.3.2 Evaluation of Mass Movement and Design of Stabilization Works

Geological maps and air photographs, supplemented by ground checking, are the principal sources of mass movement data at the desk study stage (Figure 9.2). From these, landslide distributions, mechanisms and relative age may be identified, along with the locations of potentially unstable slopes, for purposes of route corridor selection. Medium-scale landslide hazard mapping (1:10 000 - 1:50 000), similar to that developed in Chapter 5, may also be undertaken at the desk study stage, using these data sources. While geological map and air photograph interpretation are often used as a matter of course on most highway projects in unstable terrain, hazard mapping has received little attention. It would appear, from the conclusions to Chapter 5, that factor mapping is likely to offer the greatest potential for rapid landslide hazard assessment and the identification of route corridors at the desk study stage. Clearly, these techniques can only be used if adequate scale and sufficient quality air photographs and geological maps are available. If unavailable, hazard assessment will have to be undertaken on the basis of rapid ground survey, as described below.

At the route corridor selection stage, rapid walk-over engineering geological and geomorphological mapping will enable the broad distribution of mass

movements, and their apparent magnitude and severity, to be defined. Later, once the approximate location of the final alignment has been chosen, large-scale surface mapping (greater than 1:10 000 scale and preferably larger than 1:2 000), slope profiling and proforma completion should be undertaken. The latter two techniques are not commonly employed during reconnaissance surveys for highway projects, but have been demonstrated (Chapter 4) to have been useful for recording and interpreting slope and drainage conditions along the Dharan-Dhankuta road.

The proforma used by the 1975 geomorphological reconnaissance survey for the Dharan-Dhankuta road is shown in Figure 4.3. It was found that completion of the proforma proved very time consuming, required subjective judgement and could often not be made representative of all slope conditions found within each sampled unit length. On the basis of discussion with project engineers, Martin (1978) concluded that the proforma data was not easily interpreted for design purposes, required more data on rock structure and weathering grade, and could not be easily applied to slopes other than the type-slope unit. As a result of these observations, a slightly modified slope proforma is proposed in Figure 9.3. Wherever possible, this proforma and the landslide - specific proforma (described below) have been kept relatively simple, objective and quantitative, in order to comply with the recommendations listed (i-iv) in Section 9.2.3, above. The slope proforma (Figure 9.3) retains much of the structure of the 1975 design, but enables specific recommendations to be made for slope drainage and earthworks design. In particular, the proforma includes greater reference to channel conditions, and is more specific in terms of proposals for design.

A comparison of Figures 4.3 and 9.3 reveals that the proforma section on 'Geology' is largely unchanged. In the section entitled 'Slopes', the original sub-section of 'Stability' has been replaced by 'Slope design' on the modified proforma. This sub-section is to include preliminary recommendations for slope stabilization and drainage. In the 'Fluvial' section, the modified proforma includes a sub-section on channel parameters (channel dimensions, maximum flow depth, bedload calibre and stability) for preliminary assessment of storm flow and sediment transport. Additional sub-sections of erosion protection and culvert/bridge design have been included on the modified proforma, although at the reconnaissance stage, these recommendations can only be general and preliminary. Nevertheless, as they are likely to be based

log No.	DATE	LOCATION	LENGTH OF UNIT	OPERATOR	
1 GEOLOGY		**2** SLOPES		**3** FLUVIAL	**4** EARTHWORKS
a) Lithology:		a) Angle: Characteristic 20m upslope ☐☐☐☐☐☐ 20m downslope ☐☐☐☐☐☐ Range 20m upslope ☐☐☐☐☐☐ 20m downslope ☐☐☐☐☐☐		a) General:	a)Cut slope design: ☐ i) Max.angle for stability ii) Retaining/revetment and drainage works:
b) Structure:		b) Dominant processes:		b) Channel parameters: ☐ mean channel width ☐ estim. max. flow depth ☐ channel gradient ☐ bedload calibre ☐ pptn. of channel side slopes unstable	b)Spoil disposal: ☐ benching possible ☐ limited tipping possible ☐ considerable tipping possible ☐ benching discouraged ☐ tipping discouraged
c) Rock parameters: rock hardness ☐ weathering grade ☐ dip ☐ strike ☐ fracture spacing ☐		c) Drainage character and vegetation:		c) Suggestedchannel protection works:	**5** GENERAL
d) Nature and depth of regolith:		d) Slope design:		d) Culvert/bridge design:	

FIGURE 9.3 Modified Proforma for Geomorphological Reconnaissance Surveys.

on an examination of channel morphology, and processes of channel flow, erosion, sediment transport and deposition, they may allow broad design guidelines to be made. A fourth section entitled 'Earthworks' has been included on the modified proforma to enable recommendations to be made for cut slope design and spoil disposal. The former should include maximum cutting angles and stabilization works, from an assessment of slope materials and the inclination and stability of natural slopes in the area. Recommendations for spoil disposal at the reconnaissance stage, are important for the preliminary design of earthworks, and are discussed further with respect to a purpose designed proforma below. Finally, a 'General' category has been included for any additional notes relevant to road design in the area.

In the case of particularly large or unstable mass movements, the landslide-specific proforma (Figure 9.4) might be preferable, with modifications to suit local ground conditions. This proforma has been developed from that used by Geomorphological Services Limited in 1985 to record landslide data in Great Britain for the Department of the Environment. The proforma allows geomorphological, topographical and geological data to be recorded in detail, along with proposals for site investigation and remedial measures. The first two columns (sections 1 to 6) of the proforma enable routine information concerning landslide mechanism, slope drainage, topography, rock type, structure and weathering grade, soil type and depth and causes of instability to be recorded. The identification of landslide causes is obviously important in the choice and design of remedial measures (section 10). Common causes of slope instability include slope undercutting and oversteepening by river or stream erosion, and the development of high groundwater levels. Such details should be listed in section 4. In the third column (sections 7 to 11), the factual information noted in sections 1 to 6 is interpreted for design purposes. Sections 7 and 8 refer to the stability of the landslide in terms of its likely frequency of movement and the potential risk that it would pose to a road. The assessment of stability is likely to be open to some subjectivity, while the evaluation of hazard risk to road integrity is largely conjectural, as this will depend, in part, on the final design of the road at each site. Nevertheless, indications of stability and risk will be of considerable benefit to preliminary design (Chapter 4).

Sections 9 and 10, of the proforma, enable proposals to be made for further ground investigation and remedial measures. Owing to cost restrictions and

LANDSLIDE REF.NO	LANDSLIDE LOCATION	LANDSLIDE SIZE (m^2,km^2)	LANDSLIDE DEPTH(m) approx.	DATE	OPERATOR

1 LANDSLIDE TYPE:

	rock	debris	soil
TRANSLATIONAL			
planar	☐	☐	☐
deep-seated non rotation	☐	☐	☐
ROTATIONAL			
single	☐	☐	☐
multiple	☐	☐	☐
successive	☐	☐	☐
FLOW	☐	☐	☐
COMPLEX	☐	☐	☐

2 TOPOGRAPHY:

a) Slope profile

straight ☐ concave ☐

convex ☐ complex ☐

b) Slope angle

average original ☐ average repose ☐

c) Morphology

3 SLOPE DRAINAGE:

4 CAUSAL FACTORS:

5 GEOLOGY:

a) Lithology

b) Structure

dip ☐ strike ☐

fracture spacing ☐ weathering grade ☐

6 NATURE & DEPTH OF REGOLITH:

7 STABILITY:

seasonally active ☐ >10year movement ☐

1–10year movement ☐ stable at present ☐

8 RISK TO ROAD INTEGRITY:

loss ☐ seasonal ☐

blockage ☐ 2–10 years ☐

damage to structures ☐ >10 years ☐

9 SITE INVESTIGATION PROPOSALS:

10 PROPOSED REMEDIAL MEASURES:

a) Measure		b) Description
avoid	☐	
slope redesign	☐	
slope support	☐	
slope drainage	☐	
other	☐	

11 GENERAL:

FIGURE 9.4 Landslide-Specific Proforma for Geomorphological Reconnaissance Survey.

logistical difficulties, ground investigations of landslides along mountain roads are, at best, usually limited to surface mapping, trial pits, sampling and laboratory soil classification tests (Chapter 2). There is, therefore, only limited scope for the use of this proforma in the design of an investigation. Quite often, remedial measures have to be designed on the basis of surface observations and soil classification data. Consequently, if the proforma is combined with detailed geomorphological and geological mapping, along the lines discussed in Chapter 4, then the recommendations for remedial measures are likely to be valid, and of benefit to design. Therefore, while the proforma is primarily intended as a reconnaissance technique, it may be used during further investigation and construction with the aid of detailed mapping.

The reconnaissance surveys should be able to evaluate the suitability of slopes crossed by the intended road for spoil benching and tipping (Chapter 6). For this purpose, a proforma has been designed, on the basis of the findings of Chapters 6 and 8, to allow rapid and objective date collection. The proforma (Figure 9.5) is divided into eight sections (Topography, Geology, Soil, Drainage, Vegetation, Stability, Land use and General). In the Topography section, space is provided for recording slope profile information, inclination, morphology and length. Slope inclination is considered to be particularly important, especially as it will determine how much spoil can be feasibly benched at a site, and the rate of surface runoff, and hence, scour potential. Section 2 (Geology) includes rock type and rock structural aspects, such as joint spacing, weathering grade, dip and strike. These parameters are likely to influence the potential for scour of the underlying rock once the top-soil has been removed. Soil type (including grain size) and depth are important factors that need to be considered in section 3. An assessment of slope drainage (section 4) is important in determining whether runoff occurs as concentrated or unconcentrated surface or sub-surface flow. Surface runoff may promote erosion, while the latter may result in high groundwater levels, thus leading to slope and spoil bench failure. Section 5 enables information regarding slope vegetation to be recorded, as this is an important factor in soil stability. In section 6, any active or relic instability and erosion, on or at the base of the slope, is recorded. The importance of these factors in the impact of spoil tipping has been stressed in Chapter 6. In section 7, space is provided for recording the land use at risk from spoil tipping, while section 8 allows for any general comments and recommendations to be made. Systematic and qualitative assessment of all the factors detailed on the proforma may enable

SLOPE REF. NO.	SLOPE LOCATION	DATE	ORIENTATION	PHYSIOG/GEOGR. LOCATION	OPERATOR

1 TOPOGRAPHY

i) Slope profile

straight ☐ complex ☐

convex ☐ concave ☐

ii) Slope angle

max ☐ ave. ☐

iii) Slope length

iv) Morphology

2 GEOLOGY

i) Lithology

ii) Structure

dip ☐ strike ☐

fracture spacing ☐ weath. grade ☐

3 SOILS

i) Depth

ii) Grain size %

fines ☐

sand ☐

gravel ☐

cobbles ☐

iii) Angularity of coarse fraction

rounded ☐

sub rounded ☐

sub angular ☐

angular ☐

4 DRAINAGE

i) dry ☐ moist ☐ wet ☐

ii) Surface runoff:

concentrated (gullying) ☐

unconcentrated (wash) ☐

iii) Sub surface runoff:

concentrated (piping) ☐

unconcentrated (throughflow) ☐

5 VEGETATION

i) Type:

forest ☐

bush/shrubs ☐

grass ☐

mixed ☐

ii) % Coverage

6 STABILITY

stable ☐

relic instability ☐

active instability ☐

Description-

relic erosion on slope ☐

active erosion on slope ☐

relic erosion at base of slope ☐

active erosion at base of slope ☐

Description-

7 LAND USE

i) Land use on slope-

ii) Land use below slope-

8 GENERAL (incl. recommendations)

FIGURE 9.5 A Proforma for the Assessment of Slope Suitability for Spoil Disposal

objective evaluation to be achieved. The feasibility of such an exercise should be given consideration, either during reconnaissance or just prior to earthworks, when the location of the road is known, and the earthworks quantities can be estimated.

Chosen tipping sites should be monitored closely during and after earthworks, by both visual inspection and erosion monitoring (Chapter 8), and suitable stabilization measures adopted if failure or accelerated erosion appears likely. In fact, monitoring of all unstable slopes, directly affecting the stability of the road, should be continued through and after construction (Figure 9.2), as a means of evaluating short and long-term slope stability, detecting imminent failure by accelerating creep, and assessing the success of the stabilization measures employed. During the construction of the Dharan-Dhankuta road, discontinuous slope monitoring was undertaken at a number of sites of particularly severe instability, while during the maintenance period experimental monitoring has been undertaken by the author (Chapter 8) and by TRRL/City University using computer-based photogrammetric techniques. While conventional ground survey monitoring is used on most road projects in the region, photogrammetry would appear to offer some potential for future stability assessments, providing it can be readily applied at low cost.

Detailed engineering geological mapping (at scales of 1:500 - 1:2 000) and trial pitting should enable slope stability assessments to be made at problematic sites. Trial pitting and direct observations in trial benches (Fookes et al 1985) and excavations, formed the principal sources of sub-surface data during the construction of the Dharan-Dhankuta road. These techniques should also be employed throughout construction and maintenance to investigate unforeseen ground conditions and reactivated instability.

9.3.3 Evaluation of Drainage Hazards for Hydraulic Design and Erosion Protection Works

Desk study techniques of hydrological assessment usually form an important preliminary stage of hydraulic design. Meteorological records can provide valuable information concerning the intensity, duration and recurrence interval of storm rainfall, although these are frequently unavailable in remote mountain terrain (Chapter 2) and have to be substituted by less reliable historical records and field evidence (Chapter 7).

In the absence of stream gauging records, discharge computation for catchments crossed by a proposed road may be undertaken using rainfall-runoff or ungauged catchment formulae. Catchment area and occasionally catchment slope are usually required to be determined for the computation of these formulae. This data may be obtained from topographic maps or, more precisely, air photographs if available (Figure 9.2). It was concluded in Chapter 7, that the Gupta Modified Rational equation is the most appropriate technique for predicting high magnitude floods in the Dharan-Dhankuta area and consequently, if 24-hour rainfall data are available, this model should be used in preference to ungauged catchment methods based on catchment area alone. Both the Rational and Modified Rational models were used for hydraulic design along the Dharan-Dhankuta road, and proved relatively successful.

A representative network of continuously recording or standard raingauges should be established at the beginning of the project, along with flow gauging stations on principal rivers and streams. During the geomorphological reconnaissance surveys (Figure 9.2), the proforma technique of channel assessment, described in Chapter 7, should be used to determine likely peak flow rates. Flow monitoring schemes, similar to those described in Chapter 8, can be established at the reconnaissance stage, in order to enlarge the data base for hydraulic design. The ability of these monitoring procedures to gauge discharge, will depend on whether they are sufficiently robust and versatile to withstand and record the often capricious nature of storm flow, the extent to which they are likely to be vandalised, and the stability of the channels in which they are installed. The low-cost techniques described in Chapter 8 may be applicable, with some modification, to low to moderate discharge monitoring, in relatively small channels. However, under conditions of high magnitude runoff, they may become inoperable and recourse will have to be made to less accurate, indirect methods of discharge measurement. Clearly, site conditions and the limitations of the techniques to be employed, need to be critically assessed before any monitoring schemes are designed.

Erosion and sediment transport rates are particularly difficult to evaluate, as they are controlled by storm intensity and discharge, slope runoff and channel hydraulics and sediment availability. Sediment sources, such as eroding channels and areas of catchment instability, can be identified on air photographs (Chapter 8) and by ground survey, using mapping and channel

proformas (Figure 9.2). While the latter may allow general statements to be made concerning the likely sediment regime of channels crossed by the intended road, the prediction of sediment transport rates remains problematic. The most practicable method currently available for assessing sediment transport in mountainous terrain, appears to be a combination of geomorphological and sedimentological survey and monitoring, both during and after construction. During the construction of the Dharan-Dhankuta road, a conserted attempt at channel monitoring was not undertaken. Had channel monitoring been established at the reconnaissance stage, a more complete evaluation of discharge, and particularly sediment supply in small gullies, might have been obtained for design purposes. While the engineer may regard channel monitoring studies as largely academic, they allow useful data to be collected over a relatively short period of time. It is recognised that the monitoring schemes developed in Chapter 8 are crude, experimental and extremely low-cost, but nevertheless, they may form a useful basis for further research and engineering application in the future.

9.4 Strategy for Low-Cost Roads

Some of the lowest cost hill roads in the region include the Dhankuta-Hile, Hile-Siduwa, Bhedetar-Rajarani and Char ali-Ilam roads in east Nepal, the Lamusangu-Jiri road in central Nepal and many of the hill roads visited in the Darjeeling and Garhwal Himalayas in India (Chapter 2). Interestingly, in nearly all cases the terrain encountered by these roads is far less severe than that crossed by the more costly principal roads, such as the Dharan-Dhankuta, Muglin-Narayanghat and Kathmandu-Kodari roads (Chapter 2). Clearly, the design philosophy adopted on many of these very low-cost roads cannot be based on rigorous and comprehensive desk studies, ground surveys, ground investigation and field monitoring, undertaken by qualified personnel and consultants.

Probably the greatest constraint to design on these roads is the lack of sufficient funds to undertake remedial and especially preventative works, so as to reduce the risk posed by both naturally occurring and construction-induced hazards. Limited funds usually dictate that discriminate spoil tipping and drainage protection works are not economically feasible (Chapter 6). Nevertheless, relatively low-cost desk study and reconnaissance techniques of air photograph interpretation and rapid engineering geological and

geomorphological ground survey, may allow trouble spots to be identified, and the most stable route alignments to be chosen, at comparatively little cost. In fact, Chandra and Shri (1973) and Sharma (1974) maintain that the cost of the design and construction of more stable alignments, with adequate protection and stabilization measures, is often far less than the maintenance costs incurred from faulty and inadequate alignment and construction design. In the case of the Dharan-Dhankuta road, the cost of the site investigation amounted to less than £30 000, or 0.2 percent of the total cost of the road, while the total cost of the geomorphological reconnaissance surveys was less than one percent of the investigation and design cost (Fookes et al 1985). In addition, it would appear that during construction, common sense and an awareness on the part of the engineer as to the hazard likely to be caused by undue slope and drainage disturbance, might considerably increase the stability of a road at relatively little extra cost. Faulty construction practices, such as inadequate filter material behind retaining structures, have been suggested by Kojan (1978) to be among the principal reasons for some of the instability along the Godavari-Dandeldhura road in west Nepal.

In conclusion, the design requirements of hazard assessment, and the likely extent and costs of stabilization and protection measures, will depend largely on the severity of the terrain encountered, and the importance attached to the establishment of a long-term, stable road. Many of the techniques discussed in Section 9.3 can be applied at comparatively little cost. Engineering geological and geomorphological ground surveys, design by modified precedent and common sense are likely to go a long way towards ensuring a relatively stable alignment for these roads.

9.5 Conclusions

This chapter has provided an overview of the application of geomorphological expertise and techniques to the design of highways in unstable mountains, and has proposed an optimum strategy for hazard assessment and design. Factors restricting the application of geomorphological techniques and expertise were discussed by reference to the results of a questionnaire survey addressed to UK-based consulting engineers.

The results of the questionnaire survey, although inadequate for statistical appraisal, indicated that, in general, the engineering geologist is currently

regarded as the most appropriate specialist for assessing slope and channel hazards. However, with the exception of the Dharan-Dhankuta road, the examples quoted by the respondents were in environments where these hazards are less severe than those encountered in the Lower Himalaya. In the case of the Dharan-Dhankuta road, where these hazards pose considerable risk to road stability, geomorphologists were used throughout the project. In particularly active mountain terrain, therefore, the trained geomorphologist is likely to be one of the most suitable specialists to identify and evaluate hazards. Nevertheless, a multi-disciplinery approach has been advocated, where geotechnical, engineering geological and geomorphological expertise are combined.

The remainder of the chapter was concerned with the proposal of an optimum strategy of terrain and hazard assessment for highway design. This scheme has relied heavily on the geomorphological techniques discussed and developed in Chapters 4 to 8 of this thesis, together with a hindsight appraisal of the design and stability of the Dharan-Dhankuta road. Considerable importance was attached to a flexible approach to design, based on continual observation and modified precedent. Clearly, this scheme will require modification to suit particular site conditions and, in fact, may be too comprehensive for many low-cost road projects that may be constrained by unavailable desk study data sources, insufficient finance and a lack of suitably trained and experienced personnel. For these cases, an alternative, shorter procedure has been proposed, based on air photograph interpretation, rapid ground survey, design by modified precedent and an awareness of the impact that faulty road construction practices may have on slope hazards.

CHAPTER 10

CONCLUSIONS

10.1 Introduction

This thesis has been concerned with the assessment and development of geomorphological techniques of hazard evaluation for highway design purposes in humid, sub-tropical fold mountains, with special reference to the Lower Himalaya.

The principal aims of this thesis, as outlined in Chapter 1, were to:

i) identify the geomorphological hazards that operate in unstable mountains, particularly the Lower Himalaya, and to assess their impact on road stability,

ii) review the techniques presently utilized for assessing these hazards and to identify any deficiencies that may exist in current practice,

iii) critically review the contributions made by the geomorphological reconnaissance surveys of the Dharan-Dhankuta road to hazard assessment for design purposes,

iv) develop and test additional techniques of hazard assessment for highway design purposes.

In Chapter 2 the geomorphological hazards operating in the Lower Himalaya were described and discussed in respect to their impact on road stability. Mass movement, flooding, erosion and sediment transport were seen to be the most significant hazards. This discussion was illustrated by reference to walk-over surveys of hill roads in India and Nepal. A brief examination of the costs of road construction in the region was given, along with a review of stabilization costs at particularly problematic sites on the Dharan-Dhankuta road.

Techniques currently available for evaluating these hazards were also reviewed in this chapter. Air photograph interpretation and geomorphological and engineering geological ground survey were concluded to be particularly

useful at the desk study and reconnaissance stages, especially as geotechnical and hydrological data sources are often lacking in remote mountain terrain. Landslide hazard mapping was regarded as a potentially useful technique, although it was concluded that its application under conditions of limited geotechnical and geomorphological data needs to be tested. Predictive models for storm runoff were found to be quite varied in their input data requirements and the reliability of their predictions. It was concluded that further research was required to test and develop techiques for assessing channel stability, storm discharge and sediment transport. Finally, it was suggested that research might also be profitably directed towards the identification and evaluation of factors that control earthworks-induced instability, namely cut slope failure and erosion and failure of slopes disturbed by spoil disposal. The identification of these research requirements formed the basis for the specific aims of the thesis. These were listed in the conclusions to Chapter 2.

The Dharan-Dhankuta road in eastern Nepal was chosen as a suitable field site for undertaking the research in view of both the high risk posed to the road by slope and channel hazards, and the relatively extensive geomorphological and geotechnical input to the design of the road. Conclusions drawn from investigations undertaken along this road were considered to be generally applicable to other low-cost roads in the Lower Himalaya and unstable young fold mountains in general.

Chapter 3 described the geological, geomorphological and climatalogical setting of the Lower Himalaya and the Dharan-Dhankuta area in particular, and provided an introduction to the study area for the analytical chapters that followed. The analyses and discussions given in these chapters are summarised below.

10.2 The Critical Assessment of the Geomorphological Reconnaissance Surveys

This assessment, presented in Chapter 4, was based on a desk study comparison between the two geomorphological reconnaissance surveys (1974, 1975) undertaken for the Dharan-Dhankuta road, the following engineering geological survey, and the final design and stability of the road. The observations and predictions made by the geomorphological surveys were assessed by field survey, in respect to the stability of the road following the storm in September 1984 that had a maximum recurrence interval of 75-80 years.

The first reconnaissance survey was assessed in terms of its influence on both the decision to abandon the COALMA alignment and the design of the final alignment. A walk-over survey was undertaken of part of the original COALMA line in order to directly assess the hazard evaluations and recommendations made in 1974, with the benefit of a hindsight knowledge of the design and stability of the final road. The second geomorphological reconnaissance survey (1975) was assessed by detailed examination at five particularly problematic sites, together with a general overview of the whole road.

The main conclusions drawn from these investigations are listed below.

i) The first geomorphological survey was found to be instrumental in the decision to realign the proposed road,[1] and the design philosophy of the final alignment was influenced considerably by the recommendations made by this survey.

ii) The second geomorphological survey formed the basis for much of the following engineering geological survey, especially in respect to the evaluation of mass movement.

iii) Many of the recommendations made by the survey formed the basis for the final design.

iv) The distribution of instability occurring within the route corridor during the September 1984 storm was largely predictable from the information provided by the survey.

v) The observations and predictions made by the survey with respect to hazards on the Leoti Khola floodplain, were reflected in the distribution of erosion and deposition that occurred during the September 1984 storm.

vi) At four locations, where road loss or serious deformation have been caused by slope failure from below, the survey failed to predict any instability. However, at three of these sites, slope overloading by spoil benching may have been a contributory factor.

---

1 It should be noted that this survey was commissioned primarily because the consulting engineers were unhappy with the COALMA line. The decision to reject this alignment was confirmed by the geomorphologists.

vii) The survey paid considerable attention to the identification of both relic and active mass movement, almost at the expense of drainage hazards. More attention could have been paid towards the evaluation of drainage hazards, especially as these have caused major problems for road stability. A number of the relic mass movements identified, have had little or no impact on road stability to date.

Despite these limitations, the geomorphological surveys were concluded to be landmarks in engineering geomorphology, and the techniques and methodology used should serve as a model for future reconnaissance surveys for highway projects in similar terrain.

The technique of detailed geomorphological mapping was tested further in terms of its ability to contribute to design during both construction and maintenance. At one site along the Dharan-Dhankuta road, detailed mapping allowed proposals for emergency remedial measures to be made that were, on the whole, implemented. Therefore, while the greatest potential for geomorphological mapping lies during the reconnaissance stage of a road project, there is some scope for its application at individual problematic sites during later stages.

10.3 The Development of Additional Geomorphological Techniques

Although the analysis presented in Chapter 4 required considerable desk study, field interpretation and comparative assessment, the major contributions of this thesis to mountain highway design lie in the development of modified and additional geomorphological techniques of hazard evaluation. These were described and discussed in Chapters 5 to 9, and are summarised below.

10.3.1 Slope Hazard Assessment

Methods of landslide hazard mapping were reviewed in Chapter 5 and discussed in terms of their applicability to route corridor selection in the study area. Factors that contribute to the development of slope instability and slope erosion in the study area were identified and discussed in terms of their evaluation for purposes of medium-scale landslide hazard mapping.

In order to assess the potential application of medium - scale landslide hazard mapping to route corridor selection in the study area, two different methodologies were developed and examined: a statistical technique using regression and correlation, and a numerical - cartographic technique based on factor mapping. The landslide and slope erosion (slope hazard) distribution was mapped from terrestrial and air photography (taken in November 1984 (following the storm in September) and 1978, respectively) and the 1975 geomorphological reconnaissance survey maps (Chapter 4). The independent variables or contributory factors included in the analysis were those that could be determined from geological maps and air photographs, namely rock type, slope inclination, aspect, physiographic zone, drainage density or channel length, and land use.

In the case of the first methodology, statistical comparison was made between the landslide distribution and the independent variables, measurable on an interval scale, namely slope inclination and drainage channel length by stream order, on a grid cell basis. The study area was divided into 2229 grid cells and the slope hazard area, overall slope inclination, drainage channel length (by stream order) and the underlying rock type were determined for each cell. While regression and correlation analyses yielded significant associations, at the 95 percent level, between the slope hazard distribution and slope inclination and total channel length, the coefficients of determination were particularly low, even when the data file was divided according to rock type. The principal conclusions drawn from this analysis were:

i) the disappointingly low coefficients of determination were probably due to the large variability in slope inclination within each cell, and

ii) statistically based landslide susceptibility mapping is largely inappropriate without a sufficiently high quality geological, geomorphological and hydrological data base, and a knowledge of the relative importance of the independent variables in the initiation of slope instability.

Following this relatively unsuccessful analysis, a factor mapping exercise was undertaken by superimposing a series of factor maps to yield a final hazard zonation map. The associations between the geographical distributions of each of the contributory factors and the slope hazards, recorded from the

photography and geomorphological maps, were assessed using the chi-squared test. Separate analyses were undertaken for the Sardu, Leoti and Dhankuta Khola catchments in order to reduce the effects of an unquantifiable rainfall distribution.

On the whole, rock type, slope aspect, physiographic zone and land use were found to be significant factors in the distribution of slope hazards. Siwalik sediments, phyllites and schists were found to be the most susceptible rock types to instability in the Sardu, Leoti and Dhankuta Khola catchments, respectively. Southerly aspects, incised valley flanks and scrubland tended to be the most susceptible categories of the other contributory factors. Slopes with southerly aspects, located on steep incised valley flanks, tend to be the locations of shallow instability initiated during heavy rain.

The final composite factor map (hazard zonation map) was found to be particularly effective in defining the distributions of mainly shallow slope hazards in each of the three catchments. The location of more deep-seated instability, that often poses the greatest threat to road stability, might be influenced more by river undercutting and geological structural orientations. The distribution of these less frequent hazards is best analysed in qualitative terms, from air photographs and ground survey.

Finally, an examination of road construction-induced hazards, namely cut slope failure, slope overloading by spoil benches and erosion and sediment problems caused by drainage disturbance and spoil tipping, concluded that these hazards could not be sensibly predicted prior to earthworks. Nevertheless, sites likely to be most vulnerable to these hazards could be identified by the reconnaissance survey. The distribution of cut slope failures was examined in terms of slope materials and age of the excavations, and it was concluded that at the time of the survey, cut slopes in schist and gneiss, owing to their relative youth, were the most prone to instability, while those in Siwalik rocks and phyllites had taken between 5 and 7 years to regain stability. Slope overloading by spoil benching may have contributed to slope failure and road loss or deformation at three main sites. These sites were discussed further in Chapter 6 (see below).

An examination of the density of slope hazards in the sub-catchments of the Sardu and Leoti Kholas led to the conclusion that, in the former catchment,

construction of the Dharan-Dhankuta road may have significantly increased the number of slope hazards encountered. However, in the Leoti Khola catchment, where the road is concentrated onto a relatively narrow vertical corridor on its descent to the floodplain, no such increase in sub-catchment slope hazard density was observed. This difference may reflect the fact that the slopes crossed by the road in the Sardu catchment are underlain by weathered Siwaliks and phyllites, and are generally steeper than those on the descent to the Leoti Khola floodplain. Clearly, a more comprehensive data base is required before the effects of road construction on on-site and off-site hazards can be properly evaluated.

The analysis presented in Chapter 5 has enabled the following conclusions and recommendations to be made.

i) Landslide hazard mapping based on the statistical approach, has very little application to route corridor selection in the study area, unless a sufficiently high quality data base becomes available. There is usually insufficient time or funding at the beginning of a road project to undertake detailed ground inventories, when all that is required at this stage is a broad but representative overview.

ii) Factor mapping appears to offer some potential for rapid, cost-effective landslide hazard assessment for route planning purposes, although the interpretations must be treated as provisional and followed by more detailed ground survey.

iii) The technique of factor mapping developed in the chapter is only experimental and will require further refinement and verification by ground checking and application to similar catchments outside the study area.

In Chapter 6, the distribution and extent of erosion and instability on slopes affected by spoil disposal along the Dharan-Dhankuta and Bhedetar-Rajarani roads, were discussed. A brief overview was also given of spoil related hazards along a number of roads in the Lower Himalaya. Terrestrial photography of the Dharan-Dhankuta road, taken during earthworks and again in 1984, allowed the extent of erosion caused by spoil tipping to be mapped. Similarly, the extent of slope erosion caused by spoil tipping along the first 3.4 kms of the

Bhedetar-Rajarani road was mapped from photographs taken in 1983, and again in 1984. The two areal distributions of erosion below this road were compared in order to determine whether or not the slopes were continuing to erode. Erosion depth measurements were attempted, but had to be discontinued as access on the slopes below the road became particularly difficult and extremely dangerous. The cost of earthworks was calculated and compared with the finance made available for the construction of the road as a whole. It was concluded that discriminate spoil disposal, along the lines adopted for the Dharan-Dhankuta road, was financially impracticable.

This analysis led to the following conclusions:

i) Spoil tipping along Lower Himalayan roads often leads to extensive slope erosion, although the evidence indicates that in the majority of cases this is not a long-term hazard. Stability is usually regained within less than 5 years. The erosion hazard posed by spoil tipping appears to have been over-estimated during the geomorphological reconnaissance survey for the Dharan-Dhankuta road.

ii) Along the Dharan-Dhankuta road, spoil disposal was undertaken in a discriminate fashion by concentrating spoil at a limited number of tip and benching sites on the more stable slopes. Inevitably, both controlled and unauthorized tipping did take place along the majority of the road, and with two exceptions, where slopes below the road are particularly steep, stability has been regained, and the slopes have revegetated.

iii) The most serious slope failures to affect the road have occurred at four sites; at least three of these were the locations of spoil benching during construction and/or maintenance. Highly weathered slope materials, intense and prolonged precipitation and loss of basal support by toe erosion, appear to have been the principal factors promoting failure at these sites. Nevertheless, it would appear that slope overloading, by spoil bench construction, may have contributed to the initiation of instability.

iv) From the evidence of the Bhedetar-Rajarani road, the majority of low-cost roads cannot afford to adopt discriminate spoil tipping

philosophies similar to that applied to the Dharan-Dhankuta road. Consequently, with the exception of unstable gullies and slopes, an indiscriminate disposal policy is probably most appropriate.

v) While a more flexible spoil disposal policy to that adopted for the Dharan-Dhankuta road may prove cost-effective, tipping should be discouraged on particularly steep slopes (greater than say 45-50°), in gullies, on hairpin stacks and where active or relic instability and erosion are identified on the slopes below. Large spoil benches should be discouraged where the risk of slope failure is high. A geomorphological reconnaissance survey should be able to identify which slopes are likely to be the most vulnerable to instability.

Slope erosion and displacement monitoring techniques were described in Chapter 8. Owing to the limited availability of conventional survey equipment, the techniques used were essentially low-cost improvisations. Nevertheless, the monitoring yielded interesting results and allowed some degree of interpretation to be made.

In respect to the erosion monitoring on tip slopes the following conclusions were made:-

i) Direct monitoring of erosion rates on slopes affected by spoil tipping during earthworks is essential. Data may be rapidly and effectively incorporated into the evaluation of slope erosion hazards and the design of the spoil disposal programme.

ii) Underlying rock type, rainfall depth, slope material and spoil particle size distribution, slope inclination and the nature of the vegetation cover are important factors in determining erosion rates, and should be systematically assessed in future monitoring.

iii) The framework established in Chapter 8 can serve as a useful guideline for the development of a more integrated and systematic approach in future research and engineering practice.

A proforma technique for assessing slope suitability for spoil disposal was presented and discussed in Chapter 9, as part of the overall recommendations for hazard assessment strategies.

10.3.2 Channel Hazard Assessment

In Chapter 7, a method of channel survey using proformas was designed and tested in its ability to allow rapid and objective assessment of channel stability and sediment dynamics, and enable peak runoff rate to be computed. The proforma technique has potential application at both the reconnaissance and site investigation stages of road projects.

Proformas were completed before and after the September 1984 storm. The resultant increases in channel capacities were evaluated in terms of rainfall distribution and the erodibility of channel forming materials. Peak flow velocities were computed using the Manning formula, with both a constant and a variable roughness coefficient and an entrainment function. Peak discharges calculated from the product of flow cross-sectional area and velocity, using a constant roughness coefficient, were compared statistically with expected discharges computed from seven ungauged catchment equations.

The principal conclusions of this analysis were as follows:-

i) The proforma technique could form a rapid means of assessing channel stability for the design of protection works and the qualitative assessment of sediment supply.

ii) Although the Manning formula, with a constant roughness coefficient, probably represents the most realistic method of estimating peak velocity in mountain channels, the technique is far from satisfactory. Further research should be directed towards the development of a more rigorous technique that allows a greater consideration of flow and channel roughness.

iii) The Gupta Modified Rational and the Dickens models are likely to be the most effective means of estimating the peak discharge resulting from high magnitude events, under conditions of limited or non-existent hydrological data.

iv) The regression of peak storm discharge on independent catchment variables indicated that high magnitude storm runoff prediction from small catchments in the area would benefit from the development of a regression model, based on catchment area, slope and, more importantly, total channel length.

Direct monitoring of storm runoff and sediment transport was described in Chapter 8. Using the velocity-area method, channel flow monitoring was attempted with relatively little success. Instead, a method was developed for recording the peak stage of low to moderate magnitude runoff events, using a combination of crest stage recorders, marked pebbles mounted on ledges excavated in the channel side-slopes, and 'Coolglass' greenhouse shading strips painted on bedrock outcrops in the channel banks. The peak flow cross-sectional area was combined with flow velocity, computed from the Manning formula, to yield peak discharge. Unfortunately, with the exception of the Tamur River there are no gauging stations in the study area to test the validity of the discharge data. It would be useful for future research to apply low-cost monitoring techniques, similar to those developed in Chapter 8, to catchments where discharge data are available.

Direct monitoring of sediment transport in mountain gullies, during storm runoff, was found to be both difficult and extremely hazardous (Chapter 8). Instead, the recovery of marked bed material and the monitoring of the erosion of previously measured bed material, was undertaken to enable an approximation to be made of the maximum size of sediment transported. Unfortunately, the recovery rate of the bed material was quite low. A more effective method of monitoring particle entrainment is required, for both assessing sediment supply and calculating flow velocity. However, given the capricious nature of channel flow and sediment transport, there would appear to be little scope for achieving this. Nevertheless, repeated long profiling on two active fan surfaces allowed accumulation rates to be determined and fan aggradation to be examined in respect to storm magnitude and sediment supply.

The monitoring of storm runoff, sediment transport and deposition, described in Chapter 8, allows the following conclusions to be made:-

i) Direct flow monitoring is extremely hazardous and fraught with logistical problems, and can only be feasibly undertaken on the more quiescent fan surfaces.

ii) Indirect monitoring of storm runoff is best achieved using low-cost, low technology based techniques that are able to withstand the erosional forces imposed by storm runoff of moderate magnitude, and that use materials of little value to the local population. The

techniques developed in this thesis may form useful guidelines for future monitoring.

iii) The evaluation of channel sediment supply, transport and deposition is most likely to be best achieved using a combination of the proforma method of channel stability assessment, and repeated survey of sediment accumulations within the channel and on fan surfaces.

iv) Process monitoring can yield valuable hazard assessment data for use in preliminary design.

10.4 Implications for Highway Design in Unstable Mountain Terrain

This thesis has assessed and developed a number of geomorphological techniques for evaluating slope, channel and earthworks-induced hazards for highway design purposes. These techniques are generally applicable to future highway projects in similar terrain to that encountered in the Lower Himalaya and along the Dharan-Dhankuta road in particular.

Rather than concentrate attention on one or a small number of hazards, the research has critically assessed and developed a number of techniques for evaluating a range of hazards. This was considered to be justified, as the engineer is often confronted by a range of hazards, rather than just one or two. The research has, therefore, allowed an optimum strategy or framework for hazard evaluation and highway design to be proposed (Chapter 9), based largely on the design and stability of the Dharan-Dhankuta road. This framework stresses the importance of an integrated geotechnical approach, continued geomorphological evaluation, monitoring and design by modified precedent. Further research will be required to refine the individual techniques discussed in this thesis, and to adapt them to suit particular terrain conditions and design requirements. Proposals for further research have been given, where necessary, in the conclusions to the relevant chapters.

The role of geomorphology in highway design projects has been discussed in Chapter 9, with reference to a questionnaire survey addressed to UK consulting engineers. It would appear that the future role of geomorphology depends largely on the attitude of the engineer and the ability of the geomorphologist to demonstrate that his expertise and, more importantly, the geomorphological techniques themselves are cost-effective if not crucial to geotechnical assessment for highway design in unstable mountains. This thesis has made considerable progress in achieving this goal.

REFERENCES

AHUJA,P.R. and RAO, P.S. 1958. Hydrological aspects of floods. Proceedings of the Symposium on Meteorological and Hydrological Aspects of Floods and Droughts in India, New Delhi.

AKUTAGAWA, S., KAZAMA, H. and NAKAJIMA, K. 1983. Relationship between failures on sandy slopes and rainfall characteristics. Annual Proceedings of the Japanese Society of Civil Engineers, 3, 150, 299-300 (in Japanese).

ALLEGRE, C.J., COURTILLOT, V., TAPPONNIER, P., HIRN, A., MATTAUER, M., COULON, C., JAEGER, J.J., ACHACHE, J., SCHARER, U., TINDONG, L., XUCHANG, X., CHENFA, C., GUANGQIN, L., BAOYU, L., JIWEN, T., NAIWEN, W., GUOMING, C., TONGLIN, H., XIBIN, W., WANMING, D., HUAIBIN, S., YOUGONG, C., JI, Z., HONGRONG, Q., PEISHENG, B., SONGCHAN, W., BIXIANG, W., YAOXIU, Z. and XU,R. 1984. Structure and evolution of the Himalaya-Tibet orogenic belt. Nature. 307, 17-22.

ANDERSON, H.W. 1975. Relative contributions of sediment from source areas and transport processes. In: Present and Prospective Technology for Predicting Sediment Yields and Sources. Agricultural Research Service. United States Department of Agriculture. ARS-S-40.

ANDERSON, M.G. and HOWES, S. 1985. Development and application of a combined soil water-slope stability model. Quarterly Journal of Engineering Geology. 18, 3,225-236.

ANDERSON, M.G. and HOWES, S. 1986. Hillslope hydrology models for forecasting in ungauged watersheds. In: Hillslope Processes. Abrahams, A. (Ed.). The Binghampton Symposia in Geomorphology. International Series, No 16, Allen and Unwin, Boston, 161-186.

ARMENTROUT, C.L. and BISSELL, R.B. 1970. Channel slope effects on peak discharge of natural streams. American Society of Civil Engineers. Journal of the Hydraulics Division. HY2, 96, 307-315.

AUDEN, J.B. 1935. Traverses in the Himalaya. Record Geological Survey of India. 69, 2, 123-167.

AYYER, D.S.N. 1975. Milestones in landslide correction - a case study. Proceedings of the Seminar on Landslides and Toe Erosion Problems with Special Reference to the Himalayan Region. Gangtok, Sikkim, 263-272.

BAGNOLD, R.A. 1960. Sediment Discharge and Stream Power: A Preliminary Announcement. Circular United States Geological Survey. 421.

BANERJEE, D.M. and BISARIA, P.C. 1975. Stratigraphy of the Bageshwar area - a reinterpretation. Himalayan Geology, 5, 245-260.

BARKER, B.H. 1976. River Training and Bank Protection: Tamar River Crossing and Road Location in Leoti Khola Valley. Unpubl. report to Messrs. Rendel, Palmer and Tritton 48pp.

BATHURST, J.C. 1982. Equations for estimating discharge in steep channels with coarse bed material. Advances in Hydrometry, Proceedings of the Exeter Symposium, International Association of Hydrological Sciences. J.A. Cole (Ed). 134, 63-71.

BATHURST, J.C., LI, R.M. and SIMONS, D.B. 1981. Resistance equation for large-scale roughness. Journal of the Hydraulics Division, American Society of Civil Engineers, 107, HY2, 1593–1613.

BAUWENS, W., BELLON, J. and VAN DER BEKEN, A. 1982. Tracer measurements in lowland rivers. Advances in Hydrometry. Proceedings of the Exeter Symposium. International Association of Hydrological Sciences. Cole, J.A. (Ed). 134, 129-140.

BAYAZIT, M. 1978. Scour of bed materials in very rough channels. American Society of Civil Engineers. Journal of the Hydraulics Division. HY9, 104, 1345-1349.

BEAVAN, P.J. and LAWRENCE, C.J. 1982. Terrain evaluation for highway planning and design. Transport and Road Research Laboratory. Supplementary Report. 725, 24pp.

BEVEN, K. 1986. Hillslope runoff processes and flood frequency characteristics. In : Hillslope Processes. Abrahams, A. (Ed). The Binghampton Symposia in Geomorphology. International Series, No 16, Allen and Unwin, Boston, 187-202.

BOFFINGER, H.E. and KEITH, D.S. 1985. The management of remedial works for erosion and landslides in Nepal. Proceedings of the Seminar on Road Maintenance in Developing Countries, Planning and Transport Research and Computation (International) Co., Ltd. 109-116.

BOFFINGER, H.E. and LAWRENCE, C.J. 1973. Report on a Visit to Nepal. Transport and Road Research Laboratory. 33pp.

BOLT, B.A., HORN, W.L., MACDONALD, G.A. and SCOTT, R.F. 1975. Geological Hazards. Springer-Verlag. 328 pp.

BONNARD, C. and NOVERRAZ, F. 1984. Instability risk maps : from the detection to the administration of landslide prone areas. IV International Symposium on Landslides, 2, Toronto, 511-516.

BORDET, P. 1961. Recherches geologiques dans l'Himalaya du Nepal, region du Makalu. Centre National de la Recherche Scientifique (Paris).

BORDET, P. and LATREILLE, M. 1955. La geologie de l'Himalaya de l'Arun. Societe Geologique de France, 529-542.

BRABB, E.E. 1984. Innovative approaches to landslide hazard and risk mapping. IV International Symposium on Landslides, Toronto, 307-323.

BRABB, E.E. and PAMPEYAN E.H. 1972. Preliminary map of landslide deposits in San Mateo County, California. United States Geological Survey Miscellaneous Field Studies Map MF344, scale 1:62,500.

BRABB, E.E., PAMPEYAN, E.H. and BONILLA, M.G. 1972. Landslide susceptibility in San Mateo County, California. United States Geological Survey Miscellaneous Field Studies Map. MF360, scale 1:62,500.

BRADLEY, W.C. and MEARS, A.I. 1980. Calculation of flows needed to transport coarse fraction of Boulder Creek alluvium at Boulder, Colorado. Geological Society of America, Bulletin. 91, 1, 135-138.

BRAHMS, A. 1753. Elements of dam and hydraulic engineering. Aurich, Germany, 1, 105pp.

BRIGGS, R.P. 1974. Map of overdip slopes that can affect landsliding in Allegheny County, Pennsylvania. United States Geological Survey Miscellaneous Field Studies Map MF-543, Scale 1:125,000.

BROMHEAD, E.N. 1986. The Stability of Slopes. Surrey University Press, 366 pp.

BROOKS, D.M. and LAWRENCE, C.J. 1985. Proposals for TRRL/RRWU experiments in slope rehabilitation on two roads in Nepal. Overseas Unit, Transport and Road Research Laboratory.

BROOKS, D.M. and LAWRENCE, C.J. 1986. Proposals for TRRL/RRWU experiments in slope rehabilitation on two roads in Nepal. Report 2: specifications for experimental remedial works to be implemented February - May 1986. Overseas Unit, Transport and Road Research Laboratory.

BRUNSDEN, D. 1979. Mass movements. In: Process in Geomorphology. Embleton, C. and Thornes, J.B. (Eds). Edward Arnold, London, 130-186.

BRUNSDEN, D. 1984. Mudslides. In: Slope Instability, Brunsden, D. and Prior, D.B. (Eds). John Wiley, Chichester, 363-418.

BRUNSDEN, D., DOORNKAMP, J.C., FOOKES, P.G., JONES, D.K.C. and KELLY, J.M.H. 1975a. Geomorphological mapping techniques in highway engineering. Journal of the Institution of Highway Engineers, 12, 34-41.

BRUNSDEN, D., DOORNKAMP, J.C., FOOKES, P.G., JONES, D.K.C. and KELLY, J.M.H. 1975b. Large scale geomorphological mapping and highway engineering design. Quarterly Journal of Engineering Geology, 8, 227-253.

BRUNSDEN, D., DOORNKAMP, J.C., HINCH, L.W. and JONES, D.K.C. 1975c. Geomorphological mapping and highway investigation. Proceedings of the Sixth African Conference on Soil Mechanics and Foundation Engineering, 1, 3-9.

BRUNSDEN, D., DOORNKAMP, J.C. and JONES, D.K.C. 1974. Dharan-Dhankuta Highway Project: Geomorphological Assessment. Unpubl. Report to Messrs. Rendel Palmer and Tritton.

BRUNSDEN, D. and JONES, D.K.C. 1972. The morphology of degraded landslides in south west Dorset. Quarterly Journal of Engineering Geology, 5, 202-222.

BRUNSDEN, D. and JONES, D.K.C. 1975. Dharan-Dhankuta Highway Project: Rendel Palmer and Tritton Alignment. Geomorphological Assessment. Unpubl. Report to Messrs. Rendel Palmer and Tritton. 77 pp.

BRUNSDEN, D. and JONES, D.K.C. 1976. The evolution of landslide slopes in Dorset. Philosophical Transactions of the Royal Society, London, A, 283, 605-631.

BRUNSDEN, D., JONES, D.K.C., MARTIN, R.P. and DOORNKAMP, J.C. 1981. The geomorphological character of part of the low Himalaya of eastern Nepal. Zeitschrift fur Geomorphologie, NF, Suppl Bd-27, 25-72.

BRUNSDEN, D. and PRIOR, D.B. (Eds). 1984. Slope Instability. John Wiley and Sons. 620 pp.

CAINE, N. 1980. The rainfall intensity - duration control of shallow landslides and debris flows. Geografisker Annaler. 62, A, 23-27.

CAINE, N. and MOOL, P.K. 1981. Channel geometry and flow estimates for two small mountain streams in the middle hills, Nepal. Mountain Research and Development. 1, 3-4, 231-243.

CAINE, N. and MOOL, P.K. 1982. Landslides in the Kolpu Khola drainage, middle mountains, Nepal. Mountain Research and Development. 2, 2, 157-173.

CAMPBELL, R.H. 1974. Debris flows originating from soil slips during rainstorms in southern California. Quarterly Journal of Engineering Geology. 7, 339-349.

CARLING, P.A. 1983. Threshold of coarse sediment transport in broad and narrow natural streams. Earth Surface Processes and Landforms, 8, 1, 1-18.

CARRARA, A., CARRATELLI, E.P. and MERENDA, L. 1977. Computer-based data bank and statistical analysis of slope instability phenomena. Zeitschrift fur Geomorphologie, N.F., 21, 2, 187-222.

CARRARA, A., CATALANO, E., SORRISO VALVO, M., REALLI, C. and OSSI, I. 1978. Digital terrain analysis for land evaluation. Geologia Applicata e Idrogeologia. 13, 69-127.

CARRARA, A. and MERENDA, L. 1974. Metodologia per un censimento degli eventi franosi in Calabria. Geologia Applicata e Idrogeologia, 9, 237-255.

CARRARA, A. and MERENDA, L. 1976. Landslide inventory in northern Calabria, southern Italy. Geological Society of America, Bulletin, 87, 1153-1162.

CARRARA, A., REALI, C. and SORRISO VALVO, M. 1982. Analysis of landslide form and incidence by statistical techniques, southern Italy. Catena, 9, 35-62.

CARSON, M.A. and PETLEY, D.J. 1970. The existence of threshold hillslopes in the denudation of the landscape. Transactions of the Institute of British Geographers. 49, 71-95.

CHAKRABARTI, D.C. 1971. Investigation on erodibility and water stable aggregates of certain soils in eastern Nepal. Journal of the Indian Society of Soil Science. 19, 4, 441-446.

CHAMPION, D.J. 1981. Basic Statistics For Social Research. Macmillan Publishing Co. Inc. New York. 452pp.

CHANDLER, M.P. and HUTCHINSON, J.N. 1984. Assessment of relative slide hazard within a large, pre-existing coastal landslide at Ventnor, Isle of Wight. IV International Symposium on Landslides, Toronto, 2, 517-522.

CHANDLER, R.J. 1979. Stability of a structure constructed in a landslide: selection of soil strength parameters. Design Parameters in Geotechnical Engineering. British Geotechnical Society, 3. 175-182, Brighton.

CHANDRA, H. and SHRI, P. 1973. Problems of highway engineers in the Himalayas. Journal of Indian Roads Congress, 35, 2, 363-386.

CHATTERJEE, B. 1975. Role of geological structures in the landslide problems with reference to the north eastern Himalayas. Proceedings of the Seminar on Landslides and Toe Erosion Problems with Special Reference to the Himalayan Region, Gangtok, Sikkim, 89-97.

CHOPRA, B.R. 1977. Landslides and other mass movements along roads in Sikkim and North Bengal. International Association of Engineering Geology, Bulletin, 16, 162-166.

CIVITA, M., DE RISO, R., LUCINI, P. and NOTA D'ELOGIO, E. 1975. Studio delle condizioni di stabilita dei terreni della penisola Sorrentina (Campania). Geologia Applicata e Idrogeologia, 10, 129-188.

CLAGUE, J.J. 1981. Landslides at the south end of Kluane Lake, Yukon Territory. Canadian Journal of Earth Science, 18, 959-971.

CLAYTON, C.G. and SMITH, D.B. 1964. A comparison of radioactive methods for river flow measurements. Radioactive Isotopes in Hydrology, Tokyo.

CLAYTON, C.R.I., SIMONS, N.E. and MATTHEWS, M.C. 1982. Site Investigation : a Handbook for Engineers. Granada.

COALMA. 1973. United Nations - His Majesties Government of Nepal. Road Feasibility Study : Part A Engineering - Project 3, 118pp, Part B Engineering - General Report, 241 pp. Comtec Alpina and Macchi.

COLEMAN, N.L. 1986. Effects of suspended sediment on the open-channel velocity distribution. Water Resources Research, 22, 10, 1377-1384.

COOKE, R.U. 1982. The assessment of geomorphological problems in dryland urban areas. Zeitschrift fur Geomorphologie, N.F. Suppl-Bd. 44, 119-128.

COOKE, R.U. 1984. Geomorphological Hazards in Los Angeles. The London Research Series in Geography, 7, George Allen and Unwin, 206pp.

COOKE, R.U., BRUNSDEN, D., DOORNKAMP, J.C. and JONES D.K.C. 1979. Assessment of Geomorphological Problems of Urban Areas of Drylands. The United Nations University.

COOKE, R.U. and DOORNKAMP, J.C. 1974. Geomorphology in Environmental Management. Clarendon, Oxford, 413pp.

COSTA, J.E. 1984. Physical geomorphology of debris flows. In: Developments and Applications of Geomorphology. Costa, J.E. and Fleisher, P.J. (Eds). Springer-Verlag, Berlin, 268-317.

CROSS, W.K. 1982. Location and design of the Dharan-Dhankuta low-cost road in eastern Nepal. Proceedings of the Institution of Civil Engineers, Part 1, 72, 27-46.

CROZIER, M.J. 1986. Landslides : Causes, Consequences and Environment. Croom Helm, Kent, 252pp.

CROZIER, M.J. and EYLES, R.J. 1980. Assessing the probability of rapid mass movement. Third Australian-New Zealand Conference on Geomechanics. Proceedings of the Technical Group, New Zealand Institution of Engineers, Wellington, 61G, 2.47-2.53.

CROZIER, M.J., EYLES, R.J., MARX, S.L., McCONCHIE, J.A. and OWEN, R.C. 1980. Distribution of landslips in the Wairarapa hill country. New Zealand Journal of Geology and Geophysics. 23, 575-586.

DA COSTA NUNES, A.J. 1969. Landslides in soils of decomposed rock due to intense rainstorms. Proceedings of the Seventh International Conference on Soil Mechanics and Foundation Engineering, Mexico, 2, 547-554.

DAUKSA, L. and KOTARBA, A. 1973. An analysis of the influence of fluvial erosion in the development of a landslide slope (using the application of the queueing theory). Studia Geomorphologica Carpatho-Balcanica, 7, 91-104.

DAY, T.J. 1977. Aspects of flow resistance in steep channels having coarse particulate beds. In: Research in Fluvial Systems. Proceedings of the Fifth Guelph Symposium on Geomorphology. 45-58.

DEARMAN, W.R. and FOOKES, P.G. 1974. Engineering geological mapping for civil engineering practice in the United Kingdom. Quarterly Journal of Engineering Geology, 7, 223-257.

DEERE, D.U. and PATTON, F.D. 1971. Slope stability in residual soils. Fourth Panamerican Conference on Soil Mechanics and Foundation Engineering. Puerto Rico, 1, 87-170.

DE GRAFF, J.V. and ROMESBURG, H.C. 1980. Regional landslide susceptibility assessment for wildland management : a matrix approach. In: Thresholds in Geomorphology. Coates, D.R. and Vitek, J.D. (Eds). George Allen and Unwin.

DENNESS, B. 1973. Colombia Landslip studies in relation to roads and route planning. Institute of Geological Sciences, Engineering Geology Unit Report, 70pp.

DHAR, O.N. and BHATTACHARYA, B.K. 1976. Variation of rainfall with elevation in the Himalayas - a pilot study. Indian Journal of Power and River Valley Development, 26,6, 179-185.

DIDWAL, R.S. 1984. Expanding phases of Nashri landslide of Jammu in India. IV International Symposium on Landslides, 2, 45-50.

DOORNKAMP, J.C., BRUNSDEN, D., JONES, D.K.C., COOKE, R.U. and BUSH, P.R. 1979. Rapid geomorphological assessments for engineering. Quarterly Journal of Engineering Geology, 12, 189-204.

DOWLING, J.W.F. and BEAVAN, P.J. 1969. Terrain evaluation for road engineers in developing countries. Journal of the Institution of Highway Engineers, 14, 6, 5-15.

DRENNON, C.B. and SCHLEINING, W.G. 1975. Landslide hazard mapping on a shoe-string. Proceedings of the American Society of Civil Engineers, Journal of the Survey and Mapping Division, SU1, 107-114.

DU BOYS, M.P. 1879. Etudes du regime et l'action exercee par les eaux sur un lit a fond de graviers indefinement affouilable. Annals des Pont et Chaussees, Series 5, 18, 141-195.

DUNNE, T. 1978. Field studies of hillslope flow processes. In: Hillslope Hydrology. Kirkby, M.J. (Ed). Wiley-Interscience, 227-293.

DUNNE, T. and LEOPOLD, L.B. 1978. Water in environmental planning. W.H. Freeman. San Francisco.

DUTTA, K. 1966. Landslips in Darjeeling and neighbouring hill slopes. Bulletin of the Geological Survey of India, Series B, 15, 7-30.

ECKEL, E.B. (Ed). 1958. Landslides and Engineering Practice. Highway Research Board, Washington. Special Report, 29, NAS-NRC, publication No 544, 323 pp.

EINSTEIN, H.A. 1950. The bedload function for sediment transportation in open channel flows. Technical Bulletin, United States Department of Agriculture, 1026.

ELLIS, W.R. 1967. A review of radioisotope methods of stream gauging. Journal of Hydrology, 5, 233-243.

EYLES, R.J. 1979. Slip-triggering rainfalls in Wellington City, New Zealand. New Zealand Journal of Science, 22, 117-121.

EYLES, R.J., CROZIER, M.J. and WHEELER, R.H. 1978. Landslips in Wellington City. New Zealand Geographer, 34, 2, 58-74.

FALKOWSKI, E. and LOZINSKA - STEPIEN, H. 1979. Some problems connected with engineering geological surveys for road building. Bulletin of the International Association of Engineering Geology, 19, 72-75.

FENTI, V., SILVANO, S. and SPAGNA, V. 1979. Methodological proposal for an engineering geomorphological map. Forecasting rockfalls in the Alps. Bulletin of the International Association of Engineering Geology, 19, 134-138.

FLEMMING, G. 1969. Suspended solids monitoring : a comparison between three instruments. Water and Water Engineering, 377-382.

FOOKES, P.G. 1969. Geotechnical mapping of soils and sedimentary rock for engineering purposes with examples of practice from the Mangla Dam project. Geotechnique, 19, 52-74.

FOOKES, P.G. 1986. Address to the Geological Society of London upon receipt of William Smith Award. Journal of the Geological Society, 143, 2, 374 and 375.

FOOKES, P.G. and MARSH, A.H. 1981. Some characteristics of construction materials in the low to moderate metamorphic grade rocks of the Lower Himalayas of east Nepal. 1: occurrence and geological features. Proceedings of the Institution of Civil Engineers. Part 1, 70, 123-138, paper 8380.

FOOKES, P.G., SWEENEY, M., MANBY, C.N.D. and MARTIN, R.P. 1985. Geological and geotechnical engineering aspects of low cost roads in mountainous terrain. Engineering Geology, 21, 1-152.

FOOKES, P.G. and VAUGHAN, P.R. (Eds). 1986. A Handbook of Engineering Geomorphology. University of Surrey Press. 352 pp.

FRANCIS, S.C. 1986. Slope development through the threshold slope concept. In : Slope Stability. Geotechnical Engineering and Geomorphology. Anderson, M.G. and Richards, K.S. (Eds). John Wiley and Sons, Chichester, 601–624.

FRANKLIN, A. 1984. Slope instrumentation and monitoring. In: Slope Instability. Brunsden, D. and Prior, D.B. (Eds). J. Wiley and Sons, 143-170.

FREEZE, R.A. 1986. Modelling interrelationships between climate, hydrology, and hydrogeology and the development of slopes. In : Slope Stability. Geotechnical Engineering and Geomorphology. Anderson, M.G. and Richards, K.S. (Eds). J. Wiley and Sons, Chichester, 381–403.

FUJIHARA, K. 1978. A study of landslides by aerial photographs. Hokkaido University Agricultural Department Experimental Plantation Research Report, 27, 2.

GANGOPADHYAY, S. 1978. Geotechnical evaluation for planning of land-use in Sikkim Himalayas. Proceedings of the Third International Conference of the International Association of Engineering Geology, 1, 56-63.

GANSSER, A. 1964. Geology of the Himalayas. Interscience Publishers, London. 289pp.

GANSSER, A. 1973. Ideas and problems on Himalayan geology. International Council of Scientific Unions. Inter-Union Commission on Geodynamics. National Geophysics Research Institute, Hyderbad, India. Seminar on Geodynamics of the Himalayan Region.

GARDNER, J. 1970. Rockfall - a geomorphic process in mountain terrain. Albertan Geographer, 6, 15-20.

GARDNER, J. 1986. Sediment movement in ephemeral streams on mountain slopes, Canadian Rocky Mountains. In: Hillslope Processes. Abrahams, A. (Ed). The Binghampton Symposia in Geomorphology. International series, No 16, Allen and Unwin, Boston, 97-113.

GARLAND, G.G. 1976. A note on two different methods of engineering geomorphological mapping. South African Geographical Journal, 58, 2, 134-140.

GEOLOGICAL SOCIETY OF LONDON. 1972. The preparation of maps and plans in terms of engineering geology. Quarterly Journal of Engineering Geology, 5, 293-382.

GEOLOGICAL SOCIETY OF LONDON. 1983. Land surface evaluation for engineering purposes. Quarterly Journal of Engineering Geology, 15, 265-316.

GOUDIE, A.S., BRUNSDEN, D., COLLINS, D.N., DERBYSHIRE, E., FERGUSON, R.I., HASHMETT, Z., JONES, D.K.C., PERROTT, F.A., SAID, M., WATERS, R.S. and WHALLEY, W.B. 1984. The geomorphology of the Hunza Valley, Karakoram Mountains, Pakistan. The International Karakoram Project, 2. Miller, K.J. (Ed). 359-410.

GRANT, P.J. 1982. Coarse sediment yields from Upper Waipawa River Basin, Rauhine Range. Journal of Hydrology, New Zealand, 21, 2, 81-97.

GRAY, D.H. and LEISER, A.T. 1982. Biotechnical slope protection and erosion control. Van Nostrand Reinhold Co., 271 pp.

GREGORY, K.J. and WALLING, D.E. 1971. Field measurements in the drainage basin. Geography, 56, 277-292.

GREGORY, K.J. and WALLING, D.E. 1973. Drainage Basin Form and Process. Arnold, London. 458 pp.

GRIFFITHS, J.S. 1983. A geomorphological approach to flood estimation in drylands for highway engineering purposes. Unpubl. Ph.D. thesis, University of London.

GUPTA, R.L. 1966. An empirical formula for determination of peak flood. Sixth Congress on Irrigation and Drainage, International Commission on Irrigation and Drainage.

GUPTA, R.L. 1973. A general formula for determination of peak flood. International Symposium on River Mechanics, International Association for Hydraulic Research.

HAGEN, T. 1952. Preliminary note on the geological structure of central Nepal. Verh. Schweiz. naturforsch. Luzen.

HAGEN, T. 1969. Report on the geological survey of Nepal. Preliminary reconnaissance. Denkschriften der Schweizerischen Naturforschenden Gesellschaft. 86, 185 pp.

HAIGH, M.J. 1979. Landslide sediment accumulations on the Mussoorie-Tehri road, Garhwal Lesser Himalaya. Indian Journal of Soil Conservation, 7, 1, 1-14.

HAIGH, M.J. 1982. Prediction and morphology of road-induced landslides in the lesser Himalaya: towards a guide for the Sarvodaya. In: Rural Development in the Himalaya. Joshi, S.C. (Ed). Nainital, India.

HAMMOND, R. and McCULLAGH, P.S. 1978. Quantitative Techniques in Geography: An Introduction. Clarendon Press, Oxford, 364 pp.

HANSEN, A. 1984. Landslide hazard analysis. In: Slope Instability. Brunsden, D. and Prior, D.B. (Eds). J. Wiley and Sons, 523-602.

HANSEN, M.J. 1984. Strategies for classification of landslides. In: Slope Instability. Brunsden, D. and Prior, D.B. (Eds). J. Wiley and Sons, 1-25.

HART, M.G. 1986. Geomorphology : Pure and Applied. George Allen and Unwin, London, 228pp.

HARUYAMA, M. and KITAMURA, R. 1984. An evaluation method by the quantification theory for the risk degree of landslides caused by rainfall in active volcanic area. IV International Symposium on Landslides, 2, Toronto, 435-440.

HASHMI, F.A.S. and HAQ IZHAR, U. 1984. Landslides on Murree-Kohala - Muzaffarabad road, Pakistan. IV International Symposium on Landslides, 2, Toronto, 91-96.

HEARN, G.J. 1987. Effects of road construction on geomorphological processes in active mountain terrain and implications for design. Geomorphology and Public Policies. Annual Conference of the Institute of British Geographers, Portsmouth, 6-9 January 1987.

HEARN, G.J. and FULTON, A. 1986. Landslide hazard assessment techniques for planning purposes : a review. Proceedings of the Twenty-Second Annual Conference of the Engineering Group of the Geological Society, Planning and Engineering Geology, Plymouth, 351-365.

HEARN, G.J. and JONES, D.K.C. 1985. An appraisal of slope and drainage instability along the Dharan-Dhankuta road in east Nepal caused by the storm of 15-16 September 1984 and proposals for road remedial and associated stabilization works. Unpubl. report to Transport and Road Research Laboratory. 86pp.

HEARN, G.J. and JONES, D.K.C. 1986. Geomorphology and highway design in the Himalayas : some lessons from the Dharan-Dhankuta highway, east Nepal. Proceedings of the First International Conference on Geomorphology, Manchester, Gardiner, V. (Ed), 203-219.

HEIM, A. 1932. Bergsturz und menschenleben. Vjschr. Naturforschenden Gesellschaft. Zurich, 77pp.

HEWITT, K. 1972. The mountain environment and geomorphic processes. In: Mountain Geomorphology. Vancouver, 17-34.

HEWLETT, J.D. and HIBBERT, A.R. 1967. Factors affecting the response of small watersheds to precipitation in humid areas. In: Forest Hydrology. Sopper, W.E. and Lull, H.W. (Eds). Pergamon, 275-290.

HEY, R.D. and THORNE, C.R. 1981. Flow processes and river channel morphology. In: Catchment Experiments in Fluvial Geomorphology. Burt, T.P. and Walling, D.E. (Eds). Geobooks, Norwich, 489-514.

HIGUCHI, K., AGETA, Y., YASUNARI, T. and INOUE, J. 1982. Characteristics of precipitation during the monsoon season in high-mountain areas of the Nepal Himalaya. In : Hydrological Aspects of Alpine and High Mountain Areas. Glen, J.W. (Ed). International Association of Hydrological Sciences, No. 138, Exeter, 21-30.

HOEK, E. 1973. Methods for the rapid assessment of the stability of three-dimensional rock slopes. Quarterly Journal of Engineering Geology, 6,4, 243-255.

HOEK, E. and BRAY, J.W. 1982. Rock Slope Engineering. Institution of Mining and Metallurgy, London, 402pp.

HUMA, I. and RADULESCU, D. 1978. Automatic production of thematic maps of slope stability. Bulletin of the International Association of Engineering Geology, 17, 95-99.

HUNGR, O., MORGAN, G.C. and KELLERHALS, R. 1984. Quantitative analysis of debris torrent hazards for design of remedial measures. Canadian Geotechnical Journal, 21, 663-677.

HUTCHINSON, J.N. 1968. Mass movement. In: Encyclopedia of Geomorphology. Fairbridge, R.W. (Ed). Reinhold Book Corporation, 688-696.

HUTCHINSON, J.N. 1970. A coastal mudflow on the London Clay cliffs at Beltinge, north Kent. Geotechnique, 20, 412-438.

HUTCHINSON, J.N. 1984. An influence line approach to the stabilization of slopes by cuts and fills. Canadian Geotechnical Journal, 21, 362-370.

HUTCHINSON, J.N. and BHANDARI, R.K. 1971. Undrained loading, a fundamental mechanism of mudflows and other mass movements. Geotechnique, 21, 353-358.

HUTCHINSON, J.N., CHANDLER, M.P. and BROMHEAD, E.N. 1985. A review of current research on the coastal landslides forming the Undercliff of the Isle of Wight, with some practical implications. Problems Associated with the Coastline, Isle of Wight County Council, 1-16.

IIDA, T. and OKUNISHI, K. 1983. Development of hillslopes due to landslides. Zeitschrift fur Geomorphologie, 46, 67-77.

IVES, J.D. and MESSERLI, B. 1981. Mountain hazards mapping in Nepal. Introduction to an applied mountain research project. Mountain Research and Development, 1, 3-4, 223-230.

JOHN, P.H., JOHNSON, F.A. and SUTCLIFFE, P. 1982. Two less conventional methods of flow gauging. In: Advances in Hydrometry. Proceedings of the Exeter Symposium of the International Associaton of Hydrological Sciences, publ. 134, 141-152.

JOHNSON, A.M. and RODINE, J.R. 1984. Debris flow. In: Slope Instability. Brunsden, D. and Prior, D.B. (Eds). J. Wiley and Sons, 257-362.

JOHNSON, R.H. 1986. Dating of ancient landslides in temperate regions. In : Slope Stability. Geotechnical Engineering and Geomorphology. Anderson, M.G. and Richards, K.S. (Eds). J. Wiley and Sons, Chichester, 561-594.

JONES, D.K.C. 1980. British applied geomorphology : an appraisal. Zeitschrift fur Geomorphologie, N.F. Suppl. Bd - 36, 48-73.

JONES, D.K.C. 1983. Environments of concern. Transactions of the Institute of British Geographers, N.S.S., 429-457.

JONES, D.K.C., BRUNSDEN, D. and GOUDIE, A.S. 1983. A preliminary geomorphological assessment of part of the Karakoram Highway. Quarterly Journal of Engineering Geology, 16, 331-355.

KAYASTHA, N.B. 1977. A report on preliminary geological investigation of Dhankuta area in eastern Nepal with reference to the town development project. Department of Mines and Geology, Kathmandu, 19pp.

KAYASTHA, N.B. 1981. Geology and soil of Dhankuta area eastern Nepal. Journal of the Nepal Geological Society, 1, 1, 53-60.

KEINHOLZ, H. 1977. Kombinierte Geomorphologische Gefahrenkarte 1:10 000 von Grindelwald. Catena, 3, 265-294.

KEINHOLZ, H. 1978. Maps of geomorphology and natural hazards of Grindelwald, Switzerland, scale 1:10 000. Arctic and Alpine Research, 10, 2, 169-184.

KENT, P. 1966. The transport mechanism of catastrophic rockfalls. Journal of Geology, 74, 79-83.

KHAIRE, V.A. 1975. SPR Project in Nepal. Journal of Indian Roads Congress, 35, 4, 725-851.

KHOSLA, A.N. 1953. Silting of reservoirs. Central Board of Irrigation and Power (India), Publ. 51, 203 pp.

KINORI, B.Z. 1970. Manual of Surface Drainage Engineering, 1, Elsevier, Amsterdam, 224 pp.

KINORI, B.Z. and MEVORACH, J. 1984. Manual of Surface Drainage Engineering, 2, Stream flow engineering and flood protection. Elsevier, Amsterdam, 523 pp.

KLUGMAN, M.A. and CHUNG, P. 1976. Slope stability of the regional municipality of Ottawa - Carleton, Ontario, Canada. Ontario Geological Survey, Miscellaneous Paper MP68.

KOJAN, E. 1978. Engineering geological evaluation of landslide problems, Western Hills Road Project : Godavari to Dandeldhura Nepal. Department of State Agency for International Development, Washington D.C.

KOJAN, E., FOGGIN, G.T. and RICE, R.M. 1972. Prediction and analysis of debris slide incidence by photogrammetry, Santa Ynez-San Rafael Mountains, California. Proceedings of the Twenty-fourth International Geological Congress. Section 13 (Engineering Geology), 124-131.

KRISHNASWAMY, V.S. 1980. Geological aspects of landslides with particular reference to the Himalayan Region. Proceedings of the International Symposium on Landslides, 2, 171-185, New Delhi.

KRISHNASWAMY, V.S. and JAIN, M.S. 1975. A review of major landslides in north and northwestern Himalayas. Proceedings of the Seminar on Landslides and Toe Erosion Problems with Special Reference to the Himalayan Region. Gangtok, Sikkim, 207-226.

KUICHLING, E. 1889. The relation between the rainfall and the discharge of sewers in populated districts. American Society of Civil Engineers, Transactions, 20, 1-60.

KUMAR and AGARWAL, N.C. 1975. Geology of the Srinagar-Nandprayang area (Alaknanda Valley), Chamoli, Garhwal and Tehri Garhwal Districts, Kumaun Himalaya, Uttar Pradesh. Himalayan Geology, 5, 29-59.

LAKHERA, R.C. 1982. Hydrological aspects of erosion on mountainous terrain - an example from the Himalayan region, India, based on photo-interpretation. In : Hydrological Aspects of Alpine and High Mountain Areas. Glen, J.W. (Ed). International Association of Hydrological Sciences, Publ. 138, Exeter, 343-350.

LEOPOLD, L.B., WOLMAN, M.G. and MILLER, J.P. 1964. Fluvial Processes in Geomorphology. Freeman, San Francisco, 535pp.

LESSING, P., MESSINA, C.P. and FONNER, R.F. 1983. Landslide risk assessment. Environmental Geology. 5, 2, 93-99.

LOAGUE, K.M. and FREEZE, R.A. 1985. A comparison of rainfall-runoff modelling techniques on small upland catchments. Water Resources Research, 21, 2, 229-248.

LOCKWOOD, J.G. 1974. World Climatology. Edward Arnold, London, 330 pp.

LOW, B.L. (Ed). 1968. Mountains and Rivers of India. Prepared for 21st International Geographical Congress of India.

LUMB, P. 1975. Slope failures in Hong Kong. Quarterly Journal of Engineering Geology, 8, 31-65.

McCONNELL, R.G. and BROCK, R.W. 1904. Report on the Great Landslide at Frank, Alberta, 1903. Department of the Interior, Ottawa, Dominion of Canada, government printer.

MAJUMDAR, N. 1980. Distribution and intensity of landslide processes in north-eastern India - a zonation map thereof. Proceedings of the International Symposium on Landslides, 1, 3-8, New Delhi.

MALGOT, J. and MAHR, T. 1979. Engineering geological mapping of the West Carpathian landslide areas. Bulletin of the International Association of Engineering Geology, 19, 116-121.

MANNING, R. 1891. On the flow of water in open channels and pipes. Transactions of the Institution of Civil Engineers, Ireland, 20, 161-207.

MARTIN, R.P. 1978. The application of some low-cost geomorphological techniques to highway engineering, with special reference to mass movement. Unpubl. Ph.D. thesis, University of London, 494pp.

MARTIN, R.P. 1980. Dharan-Dhankuta road project, Nepal: Geotechnical report. Unpubl. site document, Rendel Palmer and Tritton, 77pp.

MENARD, H.W. 1961. Some rates of regional erosion. Journal of Geology, 69, 154-161.

MENEROUD, J.P. 1978. Cartographie des risques des les Alpes-Maritimes (France). Proceedings of the 3rd International Conference of the International Association of Engineering Geology, 1, 2, 98-107.

MENEROUD, J.P. and CALVINO, A. 1976. Carte ZERMOS, zones exposees a des risques lies aux movement du sol et du sous - sol a 1:25 000, Region de la Moyenne Vesubie (Alpes Maritimes). Bureau de Recherches Geologiques et Minieres, Orleans, 11 pp.

MOSELEY, M.P. 1980. Mapping sediment sources in a New Zealand mountain watershed. Environmental Geology, 3, 85-95.

MOSELEY, M.P. and TINDALE, D.S. 1985. Sediment variability and bed material sampling in gravel-bed rivers. Earth Surface Processes and Landforms, 10, 5, 465-482.

MUIR, T.C. 1970. Bedload discharge of River Tyne, England. Bulletin of the International Association of Hydrological Sciences, 15, 35-39.

NANSON, G.C. 1974. Bedload and suspended load transport in a small steep mountain stream. American Journal of Science, 2, 471-486.

NATARAJAN, T.K., BHANDARI, R.K., TOLIA, D.S. and MURTY, A.V.S.R. 1980. Some case records of landslides in Sikkim. Proceedings of the International Symposium on Landslides, New Delhi, 1, 455-460.

NATURAL ENVIRONMENTAL RESEARCH COUNCIL. 1975. Flood Studies Report, 1 - Hydrological Studies, 550pp.

NAYAVA, J.L. 1974. Heavy monsoon rainfall in Nepal. Weather, 29, 12, 443-450.

NEMCOK, A., BALIAK, F., MAHR, T. and MALGOT, J. 1975. Systematicky vyskum svahovych deformacii na Slovensky. Manuscript, Geofond, Bratislava, 181pp.

NEULAND, H. 1976. A prediction model for landslips. Catena, 3, 215-230.

NEUMAN, E.B., PARADIS, A.R. and BRABB, E.E. 1978. Feasibility and cost using a computer to prepare landslide susceptibility maps of the San Francisco Bay region, California. United States Geological Survey, Bulletin, 1443, 27pp.

NEWSON, M.D. and LEEKS, G.J. 1985. Mountain bedload yields in the United Kingdom: further information from undisturbed fluvial environments. Earth Surface Processes and Landforms, 10, 4, 413-416.

NIEUWOLT, S. 1977. Tropical Climatology.

NILSEN, T.H. 1986. Relative slope-stability mapping and land-use planning in the San Francisco Bay Region, California. In : Hillslope Processes. Abrahams, A.D. (Ed). The Binghampton Symposia in Geomorphology. International Series, No. 16, Allen and Unwin, Boston, 390-413.

NILSEN, T.H. and BRABB, E.E. 1973. Current slope stability studies by the United States Geological Survey in the San Francisco Bay region, California. Landslides, 1, 2-10.

NILSEN, T.H. and BRABB, E.E. 1975. Landslides. In: Studies for seismic zonation of the San Francisco Bay region. A75-87, United States Geological Survey Professional Paper, 941-A.

NIXON, M. 1959. A study of bank-full discharges of rivers in England and Wales. Proceedings of the Institution of Civil Engineers, Paper 6322, 157-174.

NORCLIFFE, G.B. 1977. Inferential Statistics for Geographers. Hutchinson and Co. Ltd., London, 263 pp.

NORMAN, J.W. 1970. The photogeological detection of unstable ground. Journal of the Institution of Highway Engineers, 17, 2, 19-22.

NOSSIN, J.J. 1967. Comparative study of the Kalagarh landslip, southern Himalayas. Zeitschrift fur Geomorphologie, 11, 3, 356-367.

OBONI, F., BOURDEAU, P.L. and BONNARD, C. 1984. Probabilistic analysis of Swiss landslides. IV International Symposium on Landslides, 2, Toronto, 473-478.

OHTA, Y. and AKIBA, C. (Eds). 1973. Geology of the Nepal Himalayas. Himalayan Committee of Hokkaido University, Sapporo, Japan.

OKUDA, S., SUWA, H., OKUNISHI, K., YOKOYAMA, K. and NAKANO, M. 1980. Observations on motion of a debris flow and its geomorphological effects. Zeitschrift fur Geomorphologie, NF, Supplement Bd, 35, 142-163.

OLI, P.P. 1983. Land resources mapping in Nepal. Proceedings of Seminar/Training on Application of Remote Sensing Technology to Agriculture, Forestry, Geology and Hydrology. National Remote Sensing Center, Kathmandu, Nepal, 37-39.

O'LOUGHLIN, C.L. and PEARCE, A.J. 1976. Influence of Cenozoic geology on mass movement and sediment yield response to forest removal, North Westland, New Zealand. Bulletin of the International Association of Engineering Geology, 14, 41-46.

OWEN, R.C. 1981. Soil strength and microclimate in the distribution of shallow landslides. Journal of Hydrology, New Zealand, 20, 1, 17-26.

PALMQUIST, R.C. and BIBLE, G. 1980. Conceptual modelling of landslide distribution in time and space. Bulletin of the International Association of Engineering Geology, 21, 178-186.

PAYNE, H.R. 1985. Hazard assessment and rating methods. Proceedings of the Symposium on Landslides in the South Wales Coalfield. Polytechnic of Wales, 59-71.

PERKINS, J. and OLMSTEAD, D. 1980. A guide to ABAG's earthquake hazard mapping capability. Association of Bay Area Governments, Berkeley, California.

PETLEY, D.J. 1984. Ground investigation, sampling and testing for studies of slope instability. In : Slope Instability. Brunsden, D. and Prior, D.B. (Eds)., J. Wiley and Sons, Chichester, 67-101.

PIERSON, T.C. 1986. Flow behaviour of channelised debris flows, Mount St Helens, Washington. In: Hillslope Processes. Abrahams, A. (Ed). The Binghampton Symposia in Geomorphology. International Series, No 16, Allen and Unwin, Boston, 268-296.

PILGRIM, D.H., CORDERY, I. and BARON, B.C. 1982. Effects of catchment size on runoff relationships. Journal of Hydrology, 58, 205-221.

PITEAU, D.R. 1970. Geological factors significant to the stability of slopes cut in rock. In: Planning Open Pit Mines. Van Rensburg, P.W.J. (Ed). South African Institution of Mining and Metallurgy, 33-53.

PLAFKER, G. and ERICKSEN, G.E. 1978. Nevados Huascaran avalanches, Peru. In: Rockslides and Avalanches, 1 : Natural Phenomena. Voight, B. (Ed). Elsevier, Amsterdam, 277-314.

POMEROY, J.S. 1982. Landslides in the greater Pittsburgh region, Pennsylvania. United States Geological Survey Professional Paper, 1229, 48pp.

POSCHMANN, A.S., KLASSEN, K.E., KLUGMAN, M.A. and GOODINGS, D. 1983. Slope stability study of the South Nation River and portions of the Ottawa River. Ontario Geological Survey, Miscellaneous Paper. 112.

RACKSHIT, K.S. 1982. Various causes which affect the stability of hill roads and the measures to be adopted for their improvement. Indian Roads Congress, New Delhi, 10, 5, 54-68.

RAJ, P.A. 1978. Road to the Chinese border. Foreign Affairs Journal Publication, Kathmandu, 77pp.

RENARD, K.G. 1974. Bed material size changes and sediment transport. Transactions of the American Society of Agricultural Engineers, 17, 6, 1001-5 and 1010.

RIB, H.T. and LIANG, T. 1978. Recognition and identification. In: Landslides - Analysis and Control. Schuster, R.L. and Krizek, R.J. (Eds). Washington D.C. National Academy of Science, Transport Research Board, Special Report, 176, 34-80.

RICHARDS, K.S. 1982. Rivers. Form and Process in Alluvial Channels. Methuen, London. 358pp.

RICHARDS, K.S. and LORRIMAN, N.R. 1986. Basal erosion and mass movement. In : Slope Stability. Geotechnical Engineering and Geomorphology. Anderson, M.G. and Richards, K.S. (Eds). John Wiley and Sons, Chichester, 331-357.

RICO, A., SPRINGALL, G. and MENDOZA, A. 1976. Investigations of instability and remedial works on the Tijuana-Ensenada highway, Mexico. Geotechnique, 26, 4, 577-590.

ROTH, R.A. 1983. Factors affecting landslide-susceptibility in San Mateo County, California. Bulletin of the Association of Engineering Geologists, 20, 353-372.

ROYSTER, D.L. 1979. Landslide remedial measures. Bulletin of the International Association of Engineering Geologists, 16, 2, 301-352.

RUNNER, G.S. 1980. Runoff studies on small drainage areas. Techniques for estimating magnitude and frequency of floods in W. Virginia. United States Geological Survey Open File Report, OFR-80-1218.

RYBAR, J. and NEMCOK, A. 1968. Landslide investigations in Czechoslovakia. Proceedings of the 23rd International Geological Congress, Prague, 1, 183-198.

SARGENT, D.M. 1982. The rising air float technique for the measurement of stream discharge. In : Advances in Hydrometry, Proceedings of the Exeter Symposium, International Association of Hydrological Sciences. Cole, J.A. (Ed). 134, 153-164.

SARGENT, R.J. 1979. Variations of Manning's n roughness coefficient with flow in open river channels. Journal of the Institution of Water Engineers and Scientists, 33, 3, 290-294.

SASSA, K. 1984. The mechanism starting liquefied landslides and debris flows. IV International Symposium on Landslides, 2, Toronto, 349-354.

SAUNDERS, I. and YOUNG, A. 1983. Rates of surface processes on slopes, slope retreat and denudation. Earth Surface Processes and Landforms, 8, 5, 473-501.

SCHICK, A.P. and LEKACH, J. 1981. High bedload transport rates in relation to stream power, Wadi Mikeimin, Sinai. Catena, 8, 43-47.

SCHUSTER, R.C. and KRIZEK, R.J. (Eds). 1978. Landslides - Analysis and Control. Transportation Research Board, National Academy of Sciences, Special Report, 176, 234pp.

SELBY, M.J. 1976. Slope erosion due to extreme rainfall: a case study from New Zealand. Geografisker Annaler, 3(A), 131-138.

SESHADRI, T.N. 1960. Report on Kosi River and its behaviour, investigation and research. Dn. Kosi Project, Birpur.

SHANKER, K. 1983. Hydrology requirements in Nepal. Proceedings of Seminar/Training on Application of Remote Sensing Technology to Agriculture, Forestry, Geology and Hydrology. National Remote Sensing Center, Kathmandu, Nepal, 71-78.

SHARMA, C.K. 1974. Landslides and Soil Erosion in Nepal. Sangeeta Sharma, Kathmandu. 91pp.

SHARMA, C.K. 1977. Geology of Nepal. Educational Enterprises, Kathmandu.

SHARPE, C.F.S. 1938. Landslides and Related Phenomena: A Study of Mass Movements of Soil and Rock. Columbia University Press, New York, 137pp.

SHIELDS, A. 1936. Anwendung der aehnlichkeitsmechanik und der turbulenzforschung auf die geschiebebewegung. Mitteilung der Preussischen versuchsanstalt fuer Wasserbau und Schiffbau. Heft 26, Berlin.

SHERMAN, L.K. 1932. Stream flow from rainfall by the unit-graph method. Engineering News Record, 108, 501-505.

SHOMBROT, J. and HINCH, L.W. 1980. Highway construction in Nepal. Proceedings of the Conference on Alternative Technology in Civil Engineering. Institution of Civil Engineers, London, 30-32.

SHREVE, R.L. 1968. The Blackhawk landslide. Geological Society of America, Memoir. 108, 47pp.

SIMONS, D.B., LI, R.M. and WARD, T.J. 1978. Mapping of potential landslide areas in terms of slope stability. Colorado State University Civil Engineering Report prepared for Rocky Mountain Forest and Range Experimental Station, Flagstaff, Arizona.

SO, C.L. 1971. Mass movements associated with the rainstorm of June 1966 in Hong Kong. Transactions of the Institute of British Geographers, 53, 55-65.

SOIN, J.S. 1980. Landslide problems on roads in Sikkim and North Bengal and measures adopted to control them. Proceedings of the International Symposium on Landslides, New Delhi, 69-77.

STARKEL, L. 1972. The role of catastrophic rainfall in the shaping of the relief of the Lower Himalaya (Darjeeling Hills). Geographica Polonica, 21, 103-147.

STARKEL, L. 1976. The role of extreme (catastrophic) meteorological events in contemporary evolution of slopes. In : Geomorphology and Climate. Derbyshire, E. (Ed). Wiley, New York, 203-246.

STEVENSON, P.C. 1977. An empirical method for the evaluation of relative landslide risk. Proceedings of the Symposium of the International Association of Engineering Geology, 16, 69-72.

STEVENSON, P.C. and SLOANE, D.J. 1980. The evolution of a risk-zoning system for landslide areas in Tasmania, Australia. Proceedings of the Third Australia and New Zealand Geomechanics Conference, Wellington.

STOCKLIN, J. 1980. Geology of Nepal and its Regional Frame. Thirty-third William Smith Lecture, Geological Society, London.

STRAHLER, A.N. 1952. Dynamic basis of geomorphology. Geological Society of America, Bulletin, 63, 923-938.

STRICKLER, A. 1923. Beitrage zur frage der geschwindigheits-formel und der rauhigkeitszahlen fur strome, kanale und geschlossene leitungen. Mitteilungen des Eidgenossischer Amtes fur Wasserwirtschaft, Bern, Switzerland.

SWANSTON, D.N. 1976. Erosion processes and control methods in North America. The 16th International Union of Forest Research Organisations World Congress Proceedings, 1, 251-275.

SWANSTON, D.N. 1977. Prediction, prevention and control of landslides on mountainous forest lands. Proceedings of the Seminar on Watershed Management, Peshawar, Pakistan, 226-249.

TAKAHASHI, T. 1977. A mechanism of occurrence of mud-debris flow and their characteristics in motion. Annual Disaster Prevention Research Institute, Kyoto University, 20B-2, 405-435 (in Japanese).

TAYLOR, C.H. and PEARCE, A.J. 1982. Storm runoff processes and subcatchment characteristics in a New Zealand hill country catchment. Earth Surface Processes and Landforms, 7, 5, 439-448.

TAYLOR, D.W. 1948. Fundamentals of Soil Mechanics. John Wiley, Toronto.

TAYLOR, G.A. 1982. An examination of the cost of the Dhankuta-Hile road. Kosi Hills Area Development Programme, KHARDEP Report, 36, 22pp.

TEMPLE, P.H. 1979. Landslide damage in mountain areas and its control. In: International Geography, 1, Adams, W.P. and Helleiner (Eds). University of Toronto Press.

TER-STAPHANIAN, G. 1965. Uber der mechanismus des hackenwerfens. Felsmechanik und Ingenieurgeologie, 3, 43-49.

THORNES, J.B. 1979. Fluvial processes. In: Process in Geomorphology. Embleton, C. and Thornes, J.B. (Eds). Edward Arnold, 213-271.

UNESCO. 1976. Engineering Geological Maps. A Guide to their Preparation. The UNESCO Press, Paris, 79pp.

VARNES, D.J. 1978. Slope movement types and processes. In: Landslides - Analysis and Control. Schuster, R.L. and Krizek, R.J. (Eds). Transportation Research Board, National Academy of Sciences, Special Report 176, 12-33.

VARNES, D.J. 1984. Landslide Hazard Zonation : A Review of Principles and Practice. Natural Hazards, 3. UNESCO. International Association of Engineering Geology, Commission on Landslides and other Mass Movements on Slopes, 63pp.

VERSTAPPEN, H. Th.1983. Applied Geomorphology, Elsevier, 437pp.

VIBERG, L. 1984. Landslide risk mapping in soft clays in Scandinavia and Canada. IV International Symposium on Landslides, Toronto, 1, 325-348.

WAGNER, A. 1981. Rock structure and slope stability study of Walling area, central west Nepal. Journal of the Nepal Geological Society, 1, 2, 37-43.

WALLING, D.E. 1977. Limitations of the rating curve technique for estimating suspended sediment loads, with particular reference to British rivers. Publication of the International Association of Scientific Hydrology, 122, 34-48.

WALLING, D.E. 1979. The hydrological impact of building activity: a study near Exeter. In: Man's Impact on the Hydrological Cycle in the United Kingdom. Hollis, G.E. (Ed). Geobooks, Norwich, 135-151.

WALLING, D.E. and TEED, A. 1971. A simple pumping sampler for research into suspended sediment transport in small catchments. Journal of Hydrology, 13, 325-337.

WANG, B.H. and REVELL, R.W. 1983. Conservatism of probable maximum flood estimates. Journal of Hydraulic Engineering, American Society of Civil Engineers, 109, 3, 400-408.

WARD, J. 1976. Factor of safety approach to landslide potential delineation. Unpubl. Ph.D. thesis, Colorado State University.

WARD, M.J., LI, R.M. and SIMMONS, D.B. 1981. Use of a mathematical model for estimating potential landslide sites in steep forested drainage basins. In: Erosion and Sediment Transport in Pacific Rim Steeplands, Symposium. International Association of Hydrological Sciences, 21-35.

WATKINS, L.H. and FIDDES, D. 1984. Highway and Urban Hydrology. Pentech Press, 206pp.

WHALLEY, B. 1984. Rockfalls. In: Slope Instability. Brunsden, D. and Prior, D.B. (Eds). J. Wiley and Sons, 217-256.

WHITE, P.G. 1983. Remote sensing and geomorphology in Nepal. Proceedings of the Seminar/Training on Application of Remote Sensing Technology to Agriculture, Forestry, Geology and Hydrology. National Remote Sensing Center, Kathmandu, Nepal, 49-50.

WIECZOREK, G.F. and SARMIENTO, J. 1983. Significance of storm intensity - duration for triggering debris flows near La Honda, California. Geological Society of America, Abstracts with Programs, 15, 5, 289.

WILSON, E.M. 1985. Engineering Hydrology. Macmillan, London, 309 pp.

WINDLEY, B.F. 1985. The Himalayas. Geology Today, 169-173.

WISCHMEIER, W.H. and SMITH, D.D. 1958. Rainfall energy and its relationship to soil loss. Transactions of the American Geophysical Union, 39, 285-291.

WOLMAN, M.G. and GERSON, R. 1978. Relative scales of time and effectiveness of climate in watershed geomorphology. Earth Surface Processes, 3, 189-208.

WRIGHT, R.H. and NILSEN, T.H. 1974. Isopleth map of landslide deposits southern San Francisco Bay region, California. United States Geological Survey Miscellaneous Field Studies Map, MF 550, scale 1:125 000.

YANG, C.T. 1972. Unit stream power and sediment transport. Journal of the Hydraulics Division, American Society of Civil Engineers, 98, 1805-1826.

YIELDING, G., AHMAD, S., DAVISON, I., JACKSON, J., KHATTAK, R., KHURSHID, A., KING, G.C.P. and ZUO, L.B. 1984. A micro earthquake survey of the Karakoram. In: The International Karakoram Project, 2, Miller, K.J. (Ed).

ZARUBA, Q. and MENCL, V. 1969. Landslides and their Control. Academia and Elsevier, Prague. 205pp.

Additional References

CHOW, V.T. 1962. Hydrological determination of waterway areas for design of drainage structures in small basins. University of Illinois, Engineering Station Bulletin, 462.

INGLIS, C.C. 1949. The behaviour and control of rivers and canals. Central Waterpower, Irrigation and Research Station, Research Publication, 13.

APPENDIX 1

THE DESIGN AND CONSTRUCTION OF THE DHARAN-DHANKUTA ROAD AND ITS STABILITY FOLLOWING THE SEPTEMBER 1984 STORM

A.1 Introduction

This appendix describes the final design and construction of the Dharan-Dhankuta road, as a background to the critical assessment of the 1975 geomorphological reconnaissance survey (Chapter 4). For convenience, the alignment is separated, physiographically, into a number of distinct sections. For each section, a description and assessment is given of the final design, the terrain and geomorphological hazards encountered, the slope and drainage instability occurring during the September 1984 storm and its effect on road integrity. Much of this appendix is derived from a report prepared for the Transport and Road Research Laboratory (Hearn and Jones 1985).

A.2 Design and Construction Overview

Although the overall design philosophy for the road has been one of low cost, inevitably considerable expenditure has been necessary on slope stabilization and drainage protection works. These costs are briefly reviewed in Chapter 2. Earthworks often resulted in extensive slope and drainage disturbance by slope oversteepening in excavations, and overloading and erosion by benching and side-casting of spoil. Road construction, therefore, created a suite of instability problems additional to those occurring naturally. Consequently, in order to maintain road stability, in the short-term at least, extensive slope drainage, revetment and retaining structures and channel protection works have been necessary.

The road alignment was designed to avoid much of the naturally occurring slope instability. Nevertheless, it was inevitable that some landslides and potentially unstable ground had to be crossed. The majority of landslides encountered or initiated by earthworks are shallow, usually 3-4m in depth, and have been successfully stabilized by trench and counterfort drainage and gabion and masonry revetment. Other techniques of stabilization commonly adopted, have included slope regrading, revegetation and erosion control measures.

Rapidly eroding gully channels, below culvert outfalls and side-drain exits, have caused considerable problems during both construction and maintenance. Channel incision has led to side-slope oversteepening and eventual instability, that has caused culvert damage and blockage and, in some cases, the undermining and deformation of the road itself. Extensive channel protection works, in the form of gabion cascades, channel lining and checkdams, have been necessary.

The September 1984 storm resulted in widespread slope instability and channel erosion that caused considerable road damage. The effects of this storm will be described separately for each section of the road, and reference will be made to alignment drawings that show the distribution and nature of road damage. The figure numbers of these drawings will be given at the beginning of each section. For convenience, the September 1984 storm will be referred to as the storm in the remainder of this appendix.

A.3 Km 1.800-Km 5.100 (Figure A.1)

A.3.1 Introduction

This section of the alignment crosses a complex assemblage of spurs and valley re-entrants between the Dharan fan and the eastern flanks of the Sardu Khola. The alignment consists of a series of hairpins and traverses around spurs and across side-long ground, inclined at up to 40^0, until the more gentle slopes above the Khardu Khola gorge are reached.

The road has been constructed predominantly in full-cut with cut slope inclinations in the range of $50\text{-}60^0$. In many cases, slope oversteepening by road cutting has given rise to surface instability and slope ravelling. Concentrated sub-surface flow, and rapid road runoff during storm events, have necessitated the installation of large-scale gabion channel protection works downstream of the main drainage crossings. In the majority of cases, these have been successful and many channels have remained stable. Slab culverts have formed the main drainage crossing structures employed and these have, on the whole, remained clear of debris.

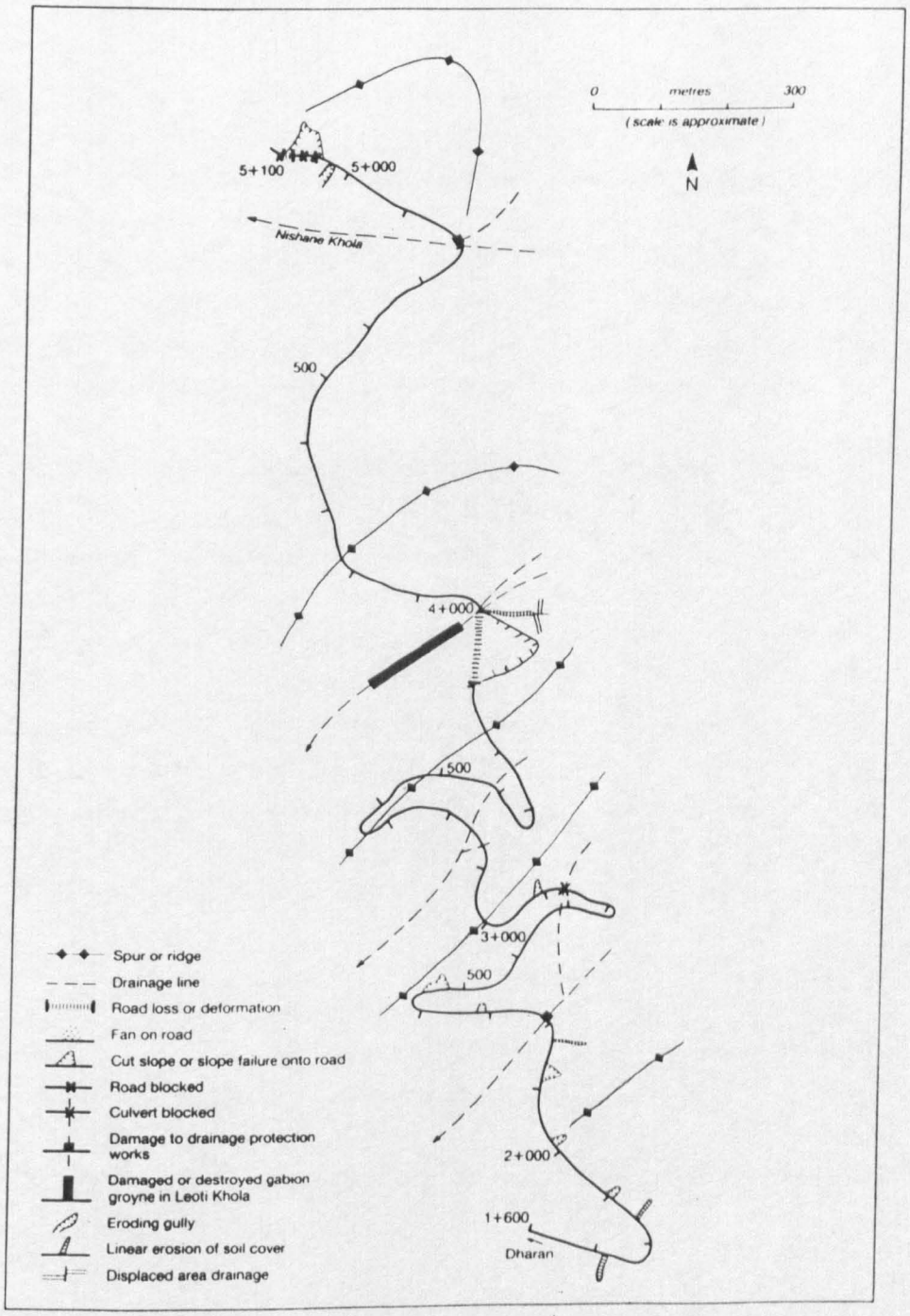

FIGURE A.1 Instability Occurring Along the Dharan-Dhankuta Road in September 1984 (Km 1.800-5.100).

A.3.2 Specific Instability Problems

i) Km 3.840-Km 4.200

The first major instability problem encountered north of Dharan is associated with the crossing of a re-entrant tributary of the Sardu Khola. The re-entrant is formed in highly jointed, moderately weathered and micaceous green meta-sandstone that dips northwards at up to 50°, thereby favouring stability. Common fracture spacing is approximately 5cm, while joints are open to widths of up to 2cm. The 1975 geomorphological reconnaissance survey identified a possible fault along the axis of the main gully channel, and this would account for the extremely distressed nature of the rock in this area.

Slope drainage above the road is dominated by two gully channels that are incised into weathered rock and shallow silty soils, and characterised by frequent waterfalls and small-scale bank instability. These two gullies combine to form the main re-entrant channel immediately downstream of the road. This area is particularly wet, especially during the monsoon season, when sub-surface flow emerges along a faint spring-line immediately above the road. Slope inclinations range from 30-40° but increase to 50-55° on the incised slopes of the main gully below the road. Despite the favourable primary joint orientation, secondary joint sets occasionally dip out of the slope, and this factor, together with steep slopes and a potential for renewed gully instability, combine to make this short section of alignment extremely hazardous for road stability.

The road was constructed mostly in full-cut across the southern (down-chainage) flank of the re-entrant, and half-cut, half gabion retained embankment on the northern flank. Cut slopes were excavated on the southern flank to 67°, and on the northern flank to 55°, and left unprotected. Spoil benching was carried out on the northern spur and later, during maintenance, on the southern flank of the re-entrant.

The slope below the road, on the southern flank, began to move in December 1977, and this was followed by further creep during the August/September periods of both 1978 and 1979. Movement in the late monsoon season of 1979, followed 517mm of rain between 21st and 31st of August. This failure has been attributed (Hearn and Jones 1985) to a combination of the gradual build-up of

groundwater levels over the monsoon period and gully erosion below. The slope was temporarily stabilized, during construction, with a series of gabion cascades in the gully and gabion and dry-masonry revetment walls on the lower portions of the slope. Surface drains were installed immediately upslope of the back-scar of the slide to prevent further ingress of slope runoff into the slip material.

On the opposite, northern flank of the re-entrant, a rotational slope failure, removing approximately 40-60m of road (km 4.080-4.140), occurred in September 1983, following 373mm of rainfall in three days at the end of a wet monsoon season. Slope failure took place immediately below the road on the spur flank, in the direction of the main gully. Approximately half of the road width was removed, including the gabion embankment retaining wall, leading to the creation of an extensive back-scar in weathered rock at road level. The cause of this failure was probably the development of high groundwater in the spoil bench and the natural slope forming materials (scree and meta-sandstone). The road across this slope was re-excavated in full-cut to 60^{o} with masonry crib revetment in early 1984, while the back-scar below the road was reveted with dry-masonry. The checkdams in the gully below were reinstated.

The storm caused major renewed slope failure between km3.840 and km3.950. Again, the development of high groundwater levels in the slope mass appears to have been the main causal factor. Extensive road cracking and side drain dislocation had taken place during the period preceeding the storm, suggesting that gradual creep displacement had occurred. The principal failure mechanism was rotational and resulted in downslope displacements of the order of 100m, involving approximately 100m of road-line (Plate 2.6).

ii) Km 4.800

An unstable ravine is crossed at km 4.800. Prior to construction, the large catchment drained by Nishane Khola was relatively stable and the khola itself took the form of a boulder-strewn mountain gully. However, the discharge of a side drain exit from a hairpin bend at km 9.900, onto the slopes of the upper catchment, has resulted in concentrated slope erosion, and rock and debris sliding (A on Plate A.1). The contour drain was originally discharged over a gabion cascade and mattress, but dislocation of the drain itself caused storm water to erode the unprotected slope below. During heavy rain, high rates of

runoff, sediment transport and instability on this slope, create conditions conducive to debris flow activity downstream. Following the storm, the channel immediately upslope of the bridge was incised by up to 1-2m, and the gabion cascade protection works below the bridge were destroyed.

iii) Km 4.800-Km 5.150

Incision and erosion in Nishane Khola, downstream of the bridge, has resulted in the development of numerous slope instability and erosion features on the northern flank of the valley re-entrant. The slope is formed in micaceous meta sandstone and phyllite beneath colluvial and residual soils. Numerous bedrock exposures occur on oversteepened spurs and in slide scars, and display a highly jointed and fissured structure with a principal dip of 15-20° in a direction 015°N. This orientation is into the slope and is therefore favourable to stability. Slope inclinations are in the range 30-38°, but increase to 45° on erosion and slide scars, and on the oversteepened slopes below the road.

Slope drainage is dominated by unconcentrated surface and sub-surface flow, and hence, drainage channels are relatively undeveloped. The 1975 geomorphological reconnaissance survey (GS2) identified tension cracks, a small rotational slip above the proposed road line, debris slides and a debris slide/flow track. The road was excavated in mostly full-cut with gabion retained embankments across the shallow gullies. Cut slopes have been excavated to 55-60° with little slope revetment. Culverts were installed in the small gullies but some of these were later sealed to prevent concentrated erosion on the slopes below.

During the storm, major slope instability took place along this section. Erosion in Nishane Khola, below the road between km 5.000 and km 5.150, resulted in the extension of the shallow rock and debris slides towards the road-line. Movement of the whole slope caused extensive deformation of the road surface, including the creation of up to 30cm wide tension cracks at km 5.100.

Slope failure above the road, between km 5.030 and km 5.100, completely blocked the carriageway for a distance of approximately 20m. The cut slope had previously been reveted with a 5m gabion wall, but continued slope ravelling, and shallow sliding in both soil and weathered rock, necessitated the construction of small dry-masonry revetments across the slope. On the down-

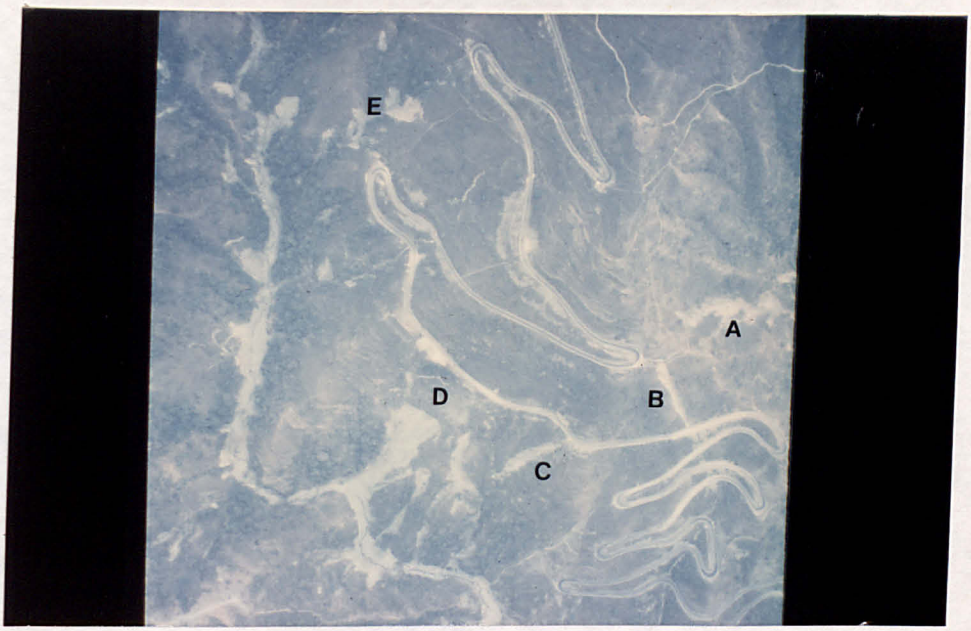

PLATE A.1 Aerial View of Part of Ascent to the Sangure Ridge Showing Areas of Instability in 1984.

PLATE A.2 Debris Flow Deposits on the Kumlintar Hairpins.

chainage side of this unstable slope at km 5.030-40, slope failure above the head of a shallow gully developed into a debris flow upon entry into the channel, and caused considerable incision of the slope below the culvert. This led to undermining and deformation of the gabion embankment. This feature has occurred in approximately the same position as the debris slide/flow track identified in 1975 by GS2. The back-scar of the slide extends virtually to the top of the main spur, where a high density of tension cracks were found. These cracks could be traced, in a direction approximately parallel to the line of Nishane Khola, to the hairpin above Kumlintar at km 6.100. Between here and the road line at km 5.230, a number of small, active and degraded slip scars and tension cracks were identified in spoil material with an orientation, again, approximately parallel to the line of the khola below.

A.4 Km 5.100-Km 14.200 (Figure A.2)

This long section of alignment involves the ascent, from the lower, eastern slopes of the Khardu Khola (Plate A.1), to Bhedetar, situated on the crest of the Sangure Ridge (1420m). The slope above Kumlintar (a terrace immediately adjacent to the incised lower slopes of the Khardu Khola) represents probably the only opportunity from Dharan, of gaining altitude via a hairpin corridor, towards the less steep and relatively stable, middle slopes below the Sangure Ridge. The bedrock underlying this flank is composed of green-grey phyllite and meta-sediment that has been highly fractured and weathered. Rock exposures were rare on the original slope due to an almost ubiquitous veneer of loose phyllite scree. Slope inclinations commonly range from 30-39^{o}, but are locally steeper (up to 50^{o}) on oversteepened gully side-slopes. Owing to the presence of this scree material, slope drainage takes the form of rapid sub-surface flow and some concentrated overland flow in small gullies and percolines in topographic depressions.

Plate 3.1. shows the Kumlintar hairpin stack after completion. The instability that arose during the construction of these hairpins was mainly shallow slipping in temporarily oversteepened scree exposed in road cuts, and localised erosion below side drain exits and around culverts. Erosion in the central drainage channel during the 1979 monsoon season, led to culvert blockage and embankment retaining wall failure at km 6.000.

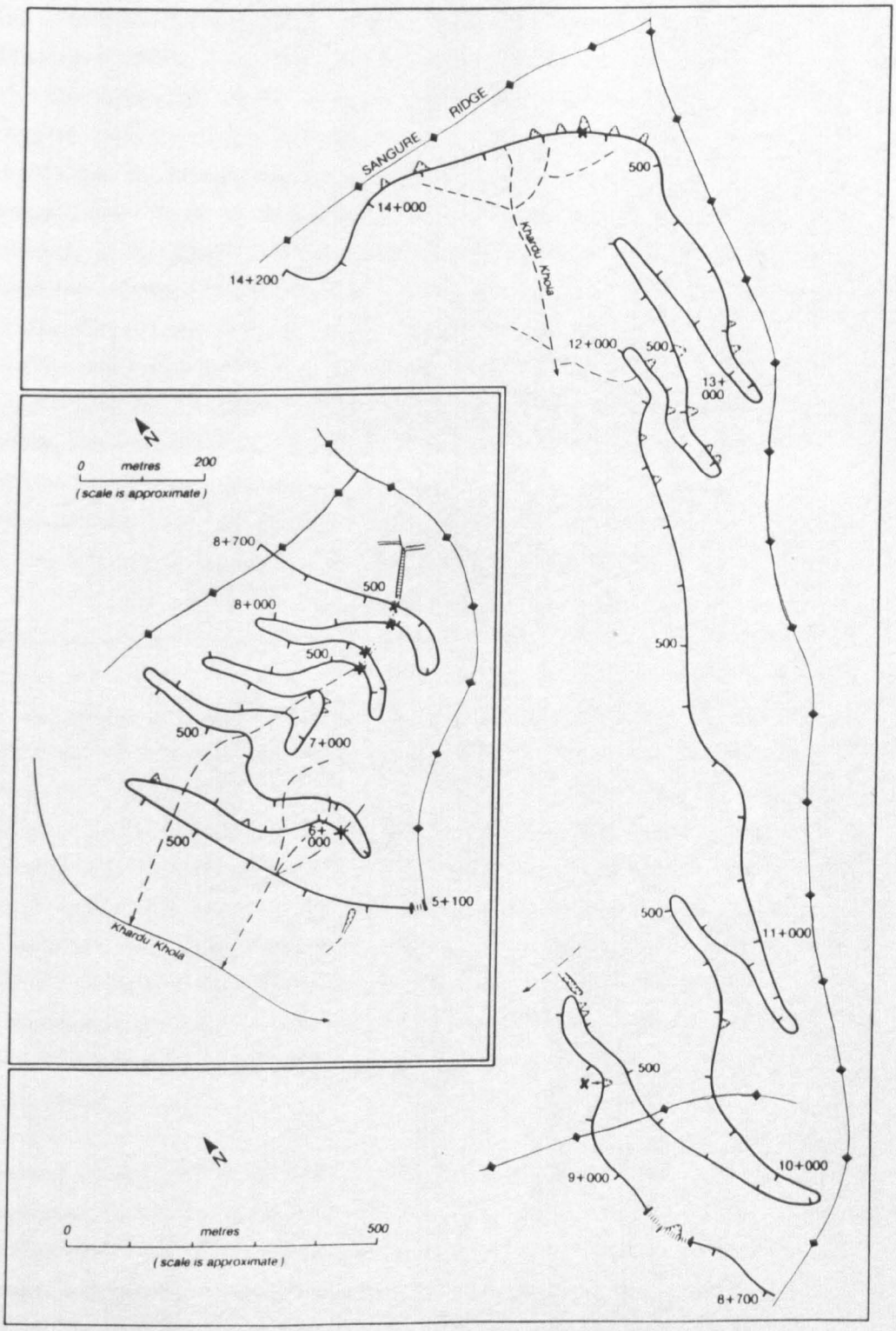

FIGURE A.2 Instability Occurring Along the Dharan-Dhankuta Road in September 1984 (Km 5.100-14.200).(For Legend see A.1)

The construction of a relatively long length of road-line (3.4 kms) within a narrow vertical route corridor, necessitated a greater expenditure on maintaining stability. The most conspicuous feature of this is the almost completely artificial slope drainage network, consisting of cut slope interceptor drains, extensive road drainage and gabion channel protection works. Making the whole slope water-tight prevents erosion, but if dislocation or overspill were to occur at any point, the consequences could be disastrous. At present, there appears to be little chance of this happening, as most channels have been well protected. However, during construction, erosion below side drain exits created severe problems on the northern side of the stack. This was compounded by bank erosion in the Khardu Khola below. Here, stone quarrying for the road was also partly responsible for the initiation of instability. As instability here might eventually lead to the partial loss of the hairpins, a continuous cascade with side-walls and seven cross-slope gabion revetments were constructed from a gabion toe protection structure (Plate 3.1), in the Khardu Khola, to the top of the hairpin stack.

Instability occurring during the storm is shown in Figure A.2, and comprised, essentially, of damage to the cascade toe protection structure in the Khardu Khola, and the headward extension of eroding gullies and shallow slides from the left bank of the incised Khardu Khola, towards the lowest hairpin. At km 5.280, rock sliding and gully-head extension have undermined the slopes immediately below the road. A third instance of instability arising from the storm, has been the creation of a deeply incised gully in loose scree and colluvium above the road at km 8.440 (B on Plate A.1). Debris flow accumulations were deposited onto three road levels below (Plate A.2), although no structural damage was done. This feature may have occurred as a result of either a debris slide that developed downslope to form a debris flow or, more likely, blockage and overspill from a contoured side drain exit at km 9.900, above.

Between the top of the hairpin stack at km 8.700 and the Sangure Ridge, the road traverses the more gentle, middle to upper slopes located above the incised Khardu Khola. Slope inclinations range from 20-30^{o} on the middle slopes, where phyllites, shales and interbedded sandstones form the underlying bedrock, and are covered by a veneer of residual and colluvial soils. However, immediately below the Sangure Ridge, slope inclinations increase to 43^{o} and highly weathered phyllites are found. This section of the alignment can be seen

in Plate A.1. Although the majority of the road between km 8.700 and km 9.000 is located on relatively stable ground, it is endangered by a number of instability problems. At km 8.750, the road crosses a coarse phyllite scree with, according to GS2, a possible rock slide scar above. The cut slope through this scree has been retained by an extensive gabion structure that has failed on a number of occasions during construction and is presently undergoing deformation. The oversteepened slopes below the road, display active instability in the form of rock sliding and gullying below the culvert (C on Plate A.1). During the 1979 monsoon season, instability in the Khardu Khola extended upslope almost to road level at km 8.700-8.900 (D on Plate A.1). Further instability here could eventually lead to road loss. The site immediately downslope of the road, between km 8.860 and km 9.300, was used for spoil disposal between 1977 and 1979. The combination of slope overloading from spoil benching and slope undercutting in the Khardu Khola below, may have contributed to the extension of the valley-side instability towards the road line. During construction, the slope below the road was reveted with a crib and masonry wall, but by the end of 1983 the slide scar had advanced to within a few metres of the road. Following the storm, approximately half of the road width, for a distance of 60m, slipped vertically by up to 2m. There is danger of significant road loss here if this instability is allowed to go unchecked. With the exception of shallow erosion and instability in the gully below the hairpin at km 12.000 (E on Plate A.1), the remainder of the section to the Sangure Ridge is quite stable.

A.5 Km 14.200-Km 23.200 (Figure A.3)

This section comprises the majority of the descent from the Sangure Ridge to the Leoti Khola floodplain. The terrain crossed by the road is composed, essentially, of steep upper slopes (quartzite re-entrant valley flanks located below the Sangure Ridge), and more gently inclined middle slopes formed in phyllite, shale and colluvium. Neither of these two slope units suffer from any significant slope or drainage instability at present (Figure A.3).

Between km 14.200 and km 17.500, the road is excavated mainly in full-cut, through quartzite (Plate A.3). The quartzite structure is dominated by joint planes that dip at up to 50^{o} in a direction that is approximately to the north, and frequently out of the cut slope. Despite these often adverse structural conditions, cut slopes have been excavated successfully to 70^{o} or more.

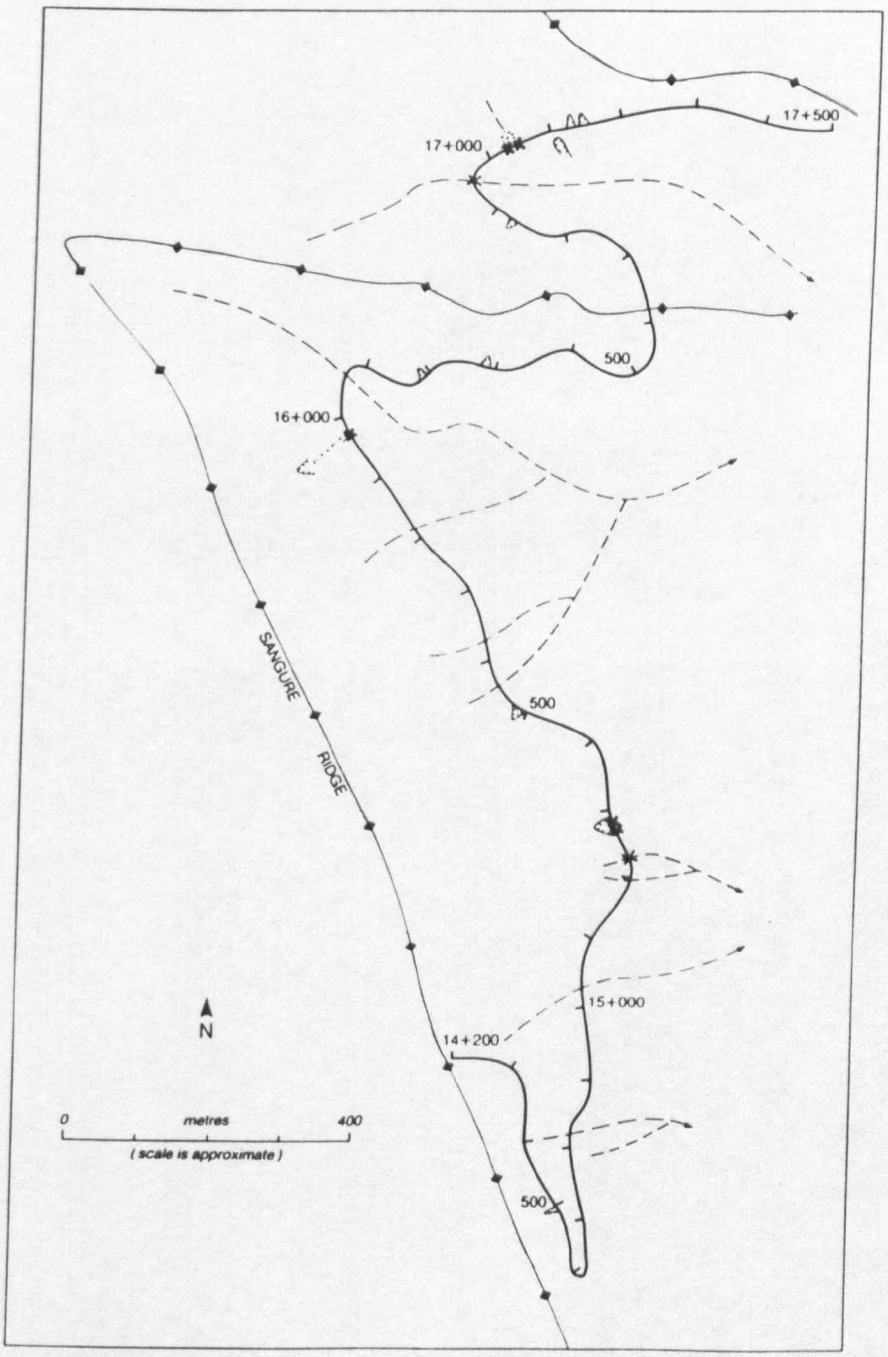

FIGURE A.3 Instability Occurring Along the Dharan-Dhankuta Road in September 1984 (Km14.200-23.200). (For Legend see A.1).

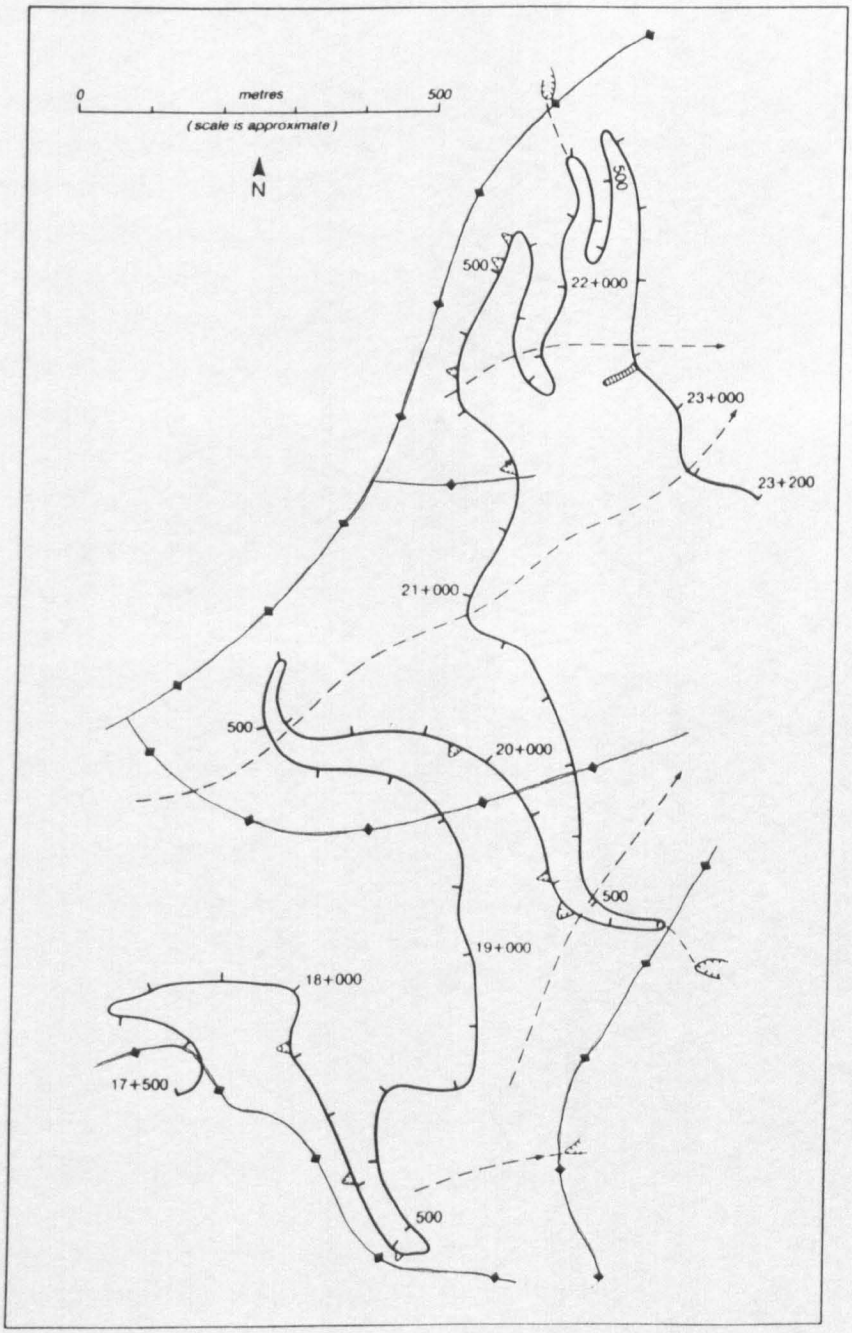

FIGURE A.3 Cont.

Following the storm, only two cases of slope instability have caused problems for road maintenance. First, at km 15.280, rock sliding along joint planes oriented out of the slope, took place in a cut slope excavated to 60°. Second, a rock slide, located well above the road at km 15.970, deposited a fan of coarse angular quartzite debris onto the road.

Channel erosion is negligible along this section of alignment, owing to the small catchment areas above the road, and the proximity of resistant quartzite to the slope surface. One exception has occurred at km 16.970, where the culvert inlet has been blocked by a debris fan originating from channel erosion and rock sliding immediately upslope of the road. Spoil tipping has been widespread throughout the area (Plate A.3), but owing to the relatively large calibre of the quartzite spoil and the stability of the underlying slopes, erosion has been minimal.

From km 17.500 to km 23.200, the road is located on gently undulating, middle slopes of the western Leoti Khola valley. The terrain is characterised by rugged quartzite outcrops, occasional phyllite and shale exposures, and colluvial soils containing quartzite boulders. Slope inclinations are generally in the range of 10-40°. The alignment is irregular in design, consisting of a series of traverses across side-long ground and one short offset hairpin stack. The alignment and terrain encountered are shown in Plate 3.2.

Naturally occurring instability is relatively infrequent, and confined to minor rock and debris falls and slides from quartzite bluffs and bank erosion along incising drainage lines. The quartzite bluff immediately above the road at km 20.190, in particular, has caused problems of debris accumulation on the road surface. Ancient rock falls from these and other quartzite cliffs may have been earthquake generated (Brunsden et al 1981), although extensive undermining by soil erosion could eventually lead to further instability and severe damage to the road below.

Cut slopes excavated in weathered phyllite, shale and colluvium, pose a potential hazard from shallow sliding onto the road. However, in most cases, cut slopes are of insufficient height, or have been successfully reveted to prevent this. Only two cut slope failures have occurred as a result of the storm, and these have been sufficiently small to pose little problem for maintenance.

PLATE A.3 Road Alignment Across the Quartzite Slopes Below the Sangure Ridge, Showing the Extent of Spoil Tipping.

PLATE A.4 Erosion Below Side Drain Exit on the Descent to the Leoti Khola Floodplain.

Probably the most outstanding feature of contemporary slope erosion along this section is the instability taking place below side drain exits. At these locations, concentrated storm runoff from the road surface is discharged onto the slopes below, and extensive erosion has resulted. Slope protection works, in the form of masonry and gabion cascades and mattresses, have been severely damaged (Plate A.4). Although this poses no direct threat to the road itself, it has caused localised slope and drainage instability in the catchments below.

A.6 Km 23.200-Km 25.700 (Figure A.4)

A.6.1 Introduction

This triple crossing of an unstable bowl-shaped depression, located on the steepened lower valley-side flanks immediately above the Leoti Khola floodplain, has always been regarded as one of the most unstable sections of the road (Chapter 4). The bowl is composed of essentially relic mass movements comprising rotational slips, translational rock and debris slides and boulder accumulations originating from rock fall from the quartzite bluffs above.

The bowl is underlain by highly weathered phyllites and paper shales that dip at 25-40^{o} in a northeasterly direction, unfavourable to stability on the southern flank of the bowl. With the exception of exposures in road cuts and slide scars, bedrock outcrops are relatively rare, due to widespread colluvial soils. Numerous springs give rise to waterlogged ground during monsoon periods, especially on the north facing slopes, where insolation levels are low. The drainage system is composed of a single trunk gully and numerous tributary drainage lines that have incised into both colluvial materials and weathered phyllite and shale. The stability of this drainage system determines, in part, the potential for reactivation of mass movement. Natural slope inclinations range from 14^{o} to 40^{o} but are locally higher (up to 55^{o}) on gully side-slopes.

Plate 4.6 shows the road alignment in the bowl. An important aspect of the alignment design has been the manner in which cut and fill have been minimised to reduce disturbance of potentially unstable slopes identified by GS2. Where necessary, cut slopes have been reveted with low gabion walls. Drainage of potentially unstable slopes, especially on recently active debris slides and boulder fans, has been quite extensive.

Channel protection works were initially constructed in dry-masonry, but following widespread erosion during the 1979 monsoon season, these were replaced by more substantial gabion structures. Gabion mattresses and cascades form characteristic protection works below culvert outfalls. Until the storm, these structures had remained relatively intact.

Instability problems arising during construction were mainly associated with shallow failures in oversteepened and unprotected road cuts and scour around culverts. These problems were rectified by additional protection works, mainly gabion cascades and checkdams. During the period between construction and the storm, slope instability consisted of shallow slides in road cuts and one major slip that occurred at km 24.650 in July 1983. This failure took place in weathered paper shale on the northern spur of the bowl, and resulted in road blockage for approximately 50m. Inspection of the slope above the slide revealed a number of old slip scars, suggesting that failure had occurred through the reactivation of older instability. The road is in full-cut at this point with insufficient cut slope revetment due to an unfinished earthworks contract. Cut-off drains behind the cut slope were broken in a number of places. As a remedial measure, the cut slope was regraded and new cut-off drainage installed. The storm caused extensive renewed slope and drainage instability in the bowl (Figure A.4), the most important examples of which are described below.

A.6.2. Specific Instability Problems

i) Km 23.420

The most conspicuous instability resulting from the storm was the destruction of the road at km 23.420 (Plate 2.16). Here a translational debris slide, approximately 3-4m deep, occurred on the colluvial slopes 100m or so above the road, and developed into a debris flow as it entered the central gully channel. The double-pipe culvert was completely destroyed, probably as a result of undermining and removal of both the channel protection works downstream and the gabion embankment retaining wall. A well defined spring-line, located immediately above the road, may have created additional drainage problems in the form of seepage and ground saturation below the embankment.

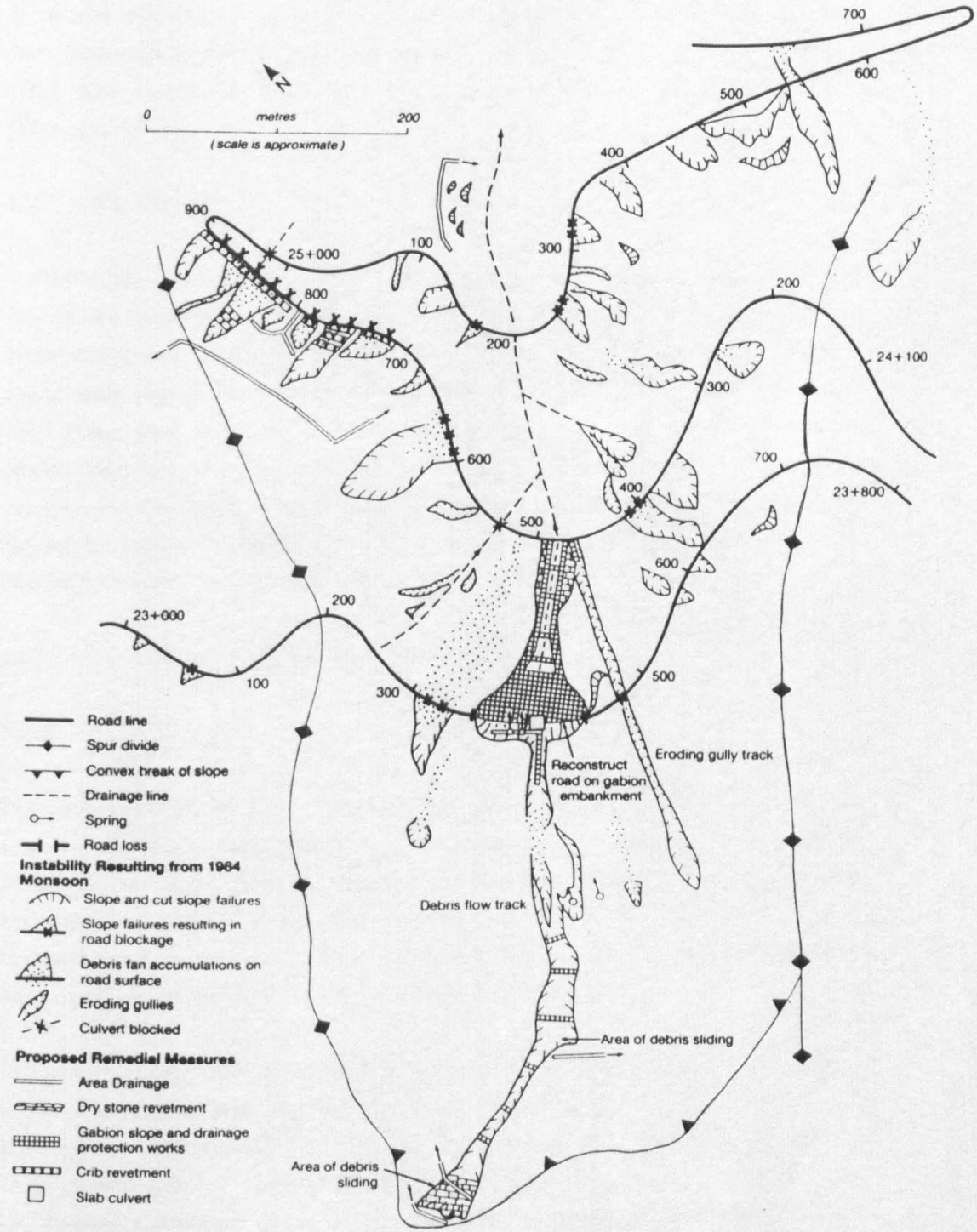

FIGURE A.4 Instability Occurring Along the Dharan-Dhankuta Road in September 1984 (Km 23.200-26.000).

ii) Km 24.560-Km 24.870

Extensive cut slope failure occurred in weathered paper shale between these two chainages around a spur that became unstable, first in 1979 and again in 1983 (see above). A total of eight, coalescent slope failures caused road blockage.

iii) Km 25.500

Immediately up-chainage of the bowl, on the final hairpin onto the Leoti Khola floodplain, an active debris slide has caused repeated failure of the gabion cut slope revetment wall. The slide occupies a shallow embayment developed in paper shale and phyllite that forms the original, now degraded back-scar. Since the slope was undercut during construction, two new slide scars have developed in the slip material. An active gully has formed along the southern margin of the slide, and erosion here has led to further undercutting. Repeated slope displacement following heavy rain (Chapter 8), has necessitated continual maintenance.

A.7. Km 25.700 - Km 32.800 (Figure A.5)

A.7.1 Introduction

The alignment on the Leoti Khola floodplain makes great use of elevated terraces and fan surfaces and extensive cut and fill, in order to minimise the potential for road loss by flooding. However, the road is particularly vulnerable to erosion where the floodplain is constricted, or wherever the topography of the valley-floor concentrates flood torrents against the valley-side, as on valley meander bends and in gorge constrictions.

The storm of July 1974 resulted in a Leoti Khola flood discharge of estimated 10-15 years recurrence interval (Barker 1976). This estimate was based on flood levels identified by GS2. Gabion groynes with protective falling aprons were constructed to deflect flood-waters away from the road line at particularly vulnerable sites, as at km 28.000 - km 28.700 and km 29.450 - km 30.200. Terrace bank protection works were installed immediately upstream of Phalametar at km 27.040 - km 27.260 and km 28.680 - km 28.750.

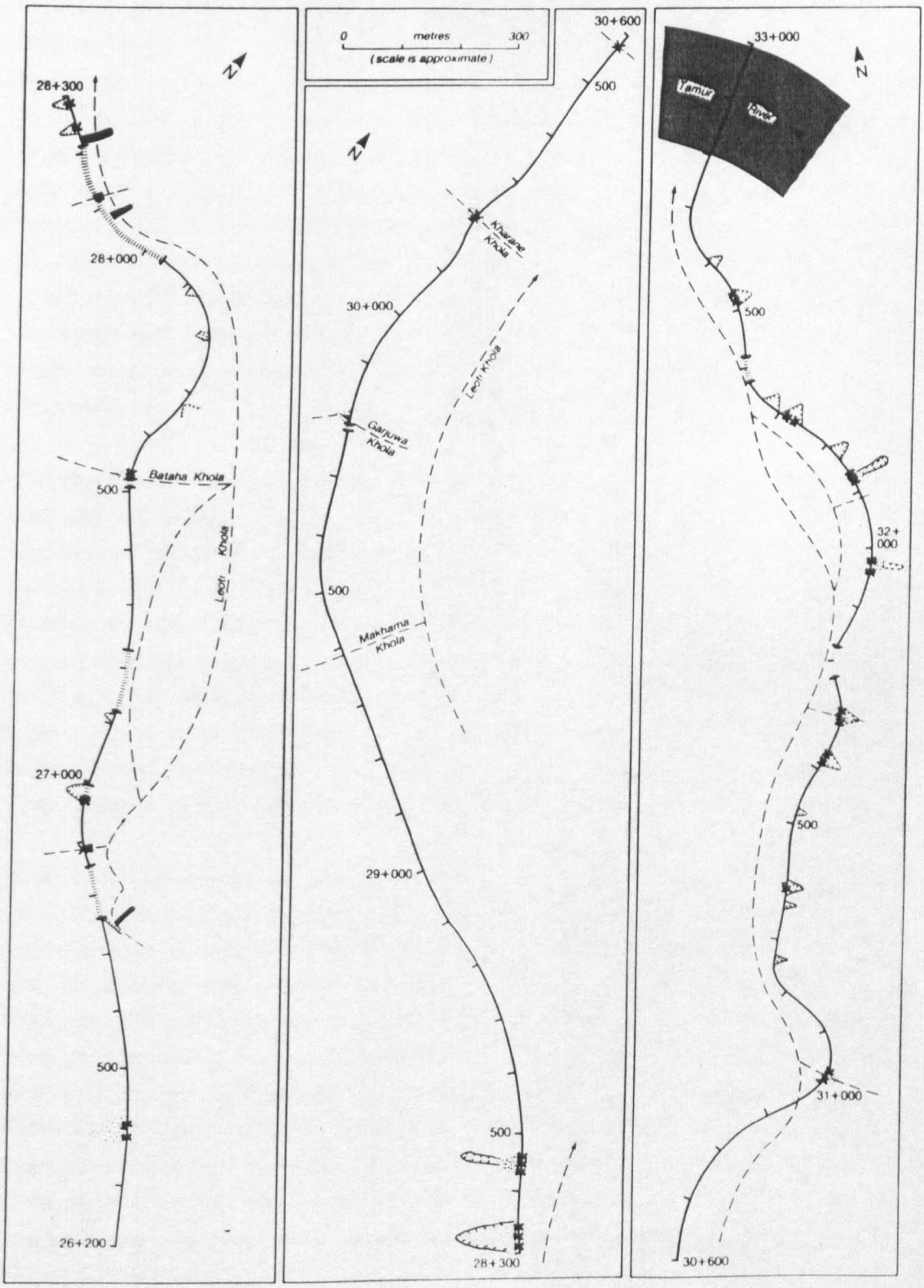

FIGURE A.5 Instability Occurring Along the Dharan-Dhankuta Road in September 1984 (Km 26.200-32.800).(For Legend see A.1).

Five main left bank tributary kholas are crossed by the road with single span bridges. During the 1974 monsoon season, extensive fans accumulated at the mouths of these kholas, where channel gradients decrease from an average of 10-20° to 7-9° on the fan surfaces. The catchments of Garjuwa and Kharane Kholas are particularly unstable and the bridge crossing the former khola has been blocked repeatedly following rainfall depths of as little as 30mm overnight. All of the tributary crossings have been provided with gabion training walls upstream and downstream of their bridges in order to channelise runoff more efficiently across the fan surface, and to provide some protection for bridge abutments and embankment approaches. Additional bed protection works were installed below Ghante Khola bridge to reduce scour of the abutments.

The storm caused extensive flooding in the Leoti Khola, resulting in major road loss and damage to protection works and fan crossings. Major road loss occurred at six main localities (Figure A.5): km 26.730 - 900, km 27.000, km 27.150 - 260, km 27.960 - km 28.200, km 31.770 - 790 and km 32.300 -370. In addition, the falling apron was damaged or removed along a significant proportion of the embanked sections. A gabion groyne, constructed in 1983 in the Phalametar gorge, was totally destroyed along with another at km 28.100. A third groyne at km 28.220, was severely damaged. Terrace bank protection works, immediately upstream of Phalametar, were removed, while the road camp constructed on the floodplain was buried in sediment (Plate A.5).

In view of the distribution of erosion resulting from this flood, it can be concluded that road loss occurred in predictable areas, and that the remaining gabion groynes were instrumental in preventing a much greater degree of road loss. The groynes were designed to withstand a 25 year design flood (Barker 1976) and it is understandable that they were damaged or destroyed during a flood of this magnitude (approximately 75 years recurrence interval). The road, with a designed freeboard of 1.5m above the 25 year flood level, was overtopped in the vicinity of Phalametar. This was probably due to rapid floodplain accretion at this point, caused by channel obstruction by the Bataha Khola debris fan and the sudden release of sediment as the Leoti Khola emerged from the Phalametar gorge. With the possible exception of this section of road, there appears to be no reason to suggest that the highway freeboard is inadequate. This is supported by the fact that road loss in nearly every case was the result of scour of the gabion embankment, rather than road inundation.

PLATE A.5 Partial Burial by Sediment of the Road Camp at Phalametar, on the Leoti Khola Floodplain.

PLATE A.6 Road Loss at Km 28.100 on the Leoti Khola Floodplain.

A.7.2 Particular Instability Problems

i) Km 27.960 - Km 28.230

Greatest damage to the road and associated protection structures occurred between these two chainages. The road along this section is located around the concave bank of a valley meander bend. The natural tendency is for flood flows to become concentrated against this outside bank. This has led to slope oversteepening and subsequent rock and debris sliding on the valley-side slope between km 28.120 and km 28.230. This slope is formed in jointed phyllite and schist with intercallated quartzite. Secondary jointing dips up to 45° at 120°N - a direction unfavourable to slope stability. Upstream (on the Leoti Khola floodplain) of Ghante Khola bridge, the road was built on full-fill on a floodplain terrace, while downstream of the bridge, the road has been constructed using a combination of rock cut and gabion-retained fill.

During the storm, the flood channel of the Leoti Khola became displaced so as to abut against the outside bank and erode the floodplain terrace, the road above and the gabion-retained embankment (Plate A.6). The gabion groyne at km 28.100 was totally removed, and the bridge crossing Ghante Khola became undermined and collapsed into the torrent tract. Downstream of the apex of this bend, the torrent tract crossed to the centre of the channel, and hence, road damage was contained within the chainages given above.

ii) Km 27.520, Km 29.800 and Km 30.200.

Fan accretion from left bank tributaries caused the inundation of three bridges and erosion of embankment fill on the bridge approaches (Figure A.5). The most dramatic of these accumulations took place in Bataha Khola (km 27.520), where bridge blockage occurred to the height of the handrail. Subsequent flow over the fan surface was deflected along the down-chainage side of the fan to scour the road on the bridge approach. The down-chainage approach to Garjuwa Khola bridge was destroyed in a similar way.

A.8 **Km 33.000-Km 38.450 (Figure A.6)**

On the northern flank of the Tamur River valley, above Mulghat, the alignment gains elevation via a thirteen-bend hairpin stack (Plate 4.2). The

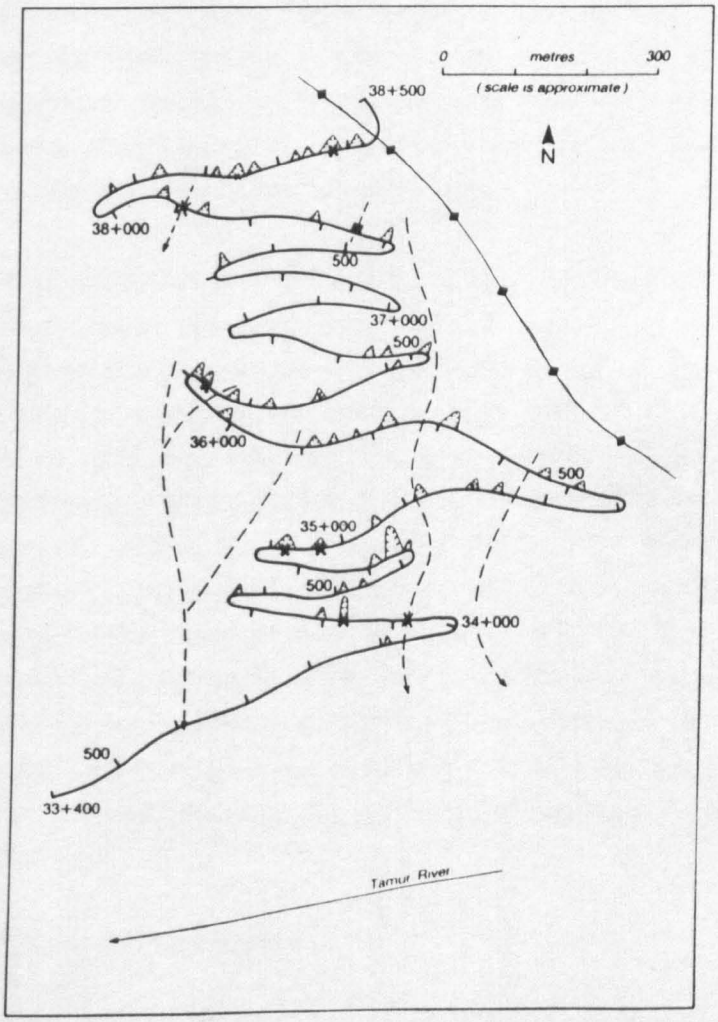

FIGURE A.6 Instability Occurring Along the Dharan-Dhankuta Road in September 1984 (Km 33.400-38.450).(For Legend see A.1).

hairpin section is located on a relatively stable slope formed in boulder cones, fans and colluvium overlying rarely exposed, often highly jointed and weathered, micaceous and graphitic schists, with subordinate shales, siltstones and phyllites. Slope inclinations vary between 21° and 39° but decrease to 10-15° on the elevated terrace and fan slopes adjacent to the Tamur River. The most characteristic feature of this slope is the high density drainage network, which is often incised. Both overland and sub-surface flow during storm rainfall are the dominant slope processes; the latter being especially evident in the loose, coarse-grained boulder spreads. The result is a system of percolines, abandoned channels and active gullies that pose considerable drainage problems. Mass movement features are confined to incising gully banks, and alone, do not pose a threat to road stability.

Throughout both construction and maintenance to date, this hairpin stack has remained relatively stable. However, spoil material washed from the frontal slopes of tip benches often caused sediment problems in neighbouring gullies. Maintenance problems have been concerned largely with cut slope failures. The distribution of instability following the storm is shown in Figure A.6. Cracks have developed in the road surface between km 33.570 and km 33.620, and at km 33.800, km 34.580, km 34.770, km 35.960 and km 36.050. These have probably formed as a result of settlement of poorly compacted road fill. Again, numerous cut slope failures occurred during the storm (Figure A.6). These failures have been confined to the upper portions of the cut slopes, where rapid runoff and sub-surface flow cause gullying, sliding and washouts in the loose regoliths, colluvium and weathered rock. Small scale instability in the main drainage channels was not sufficient to cause any major concern for road maintenance.

A.9 Km 38.450-Km 42.000 (Figure A.7)

This whole section of alignment, across the middle slopes of the lower Dhankuta Khola valley, traverses side-long ground composed of tributary re-entrants and intervening spurs with slopes that steepen rapidly downslope below the road to the Dhankuta Khola gorge.

The major slope and drainage instability features are located along and below the road between km 40.300 and km 42.000. Here, the extent of slope oversteepening is greatest and underlying rocks become far more disturbed due

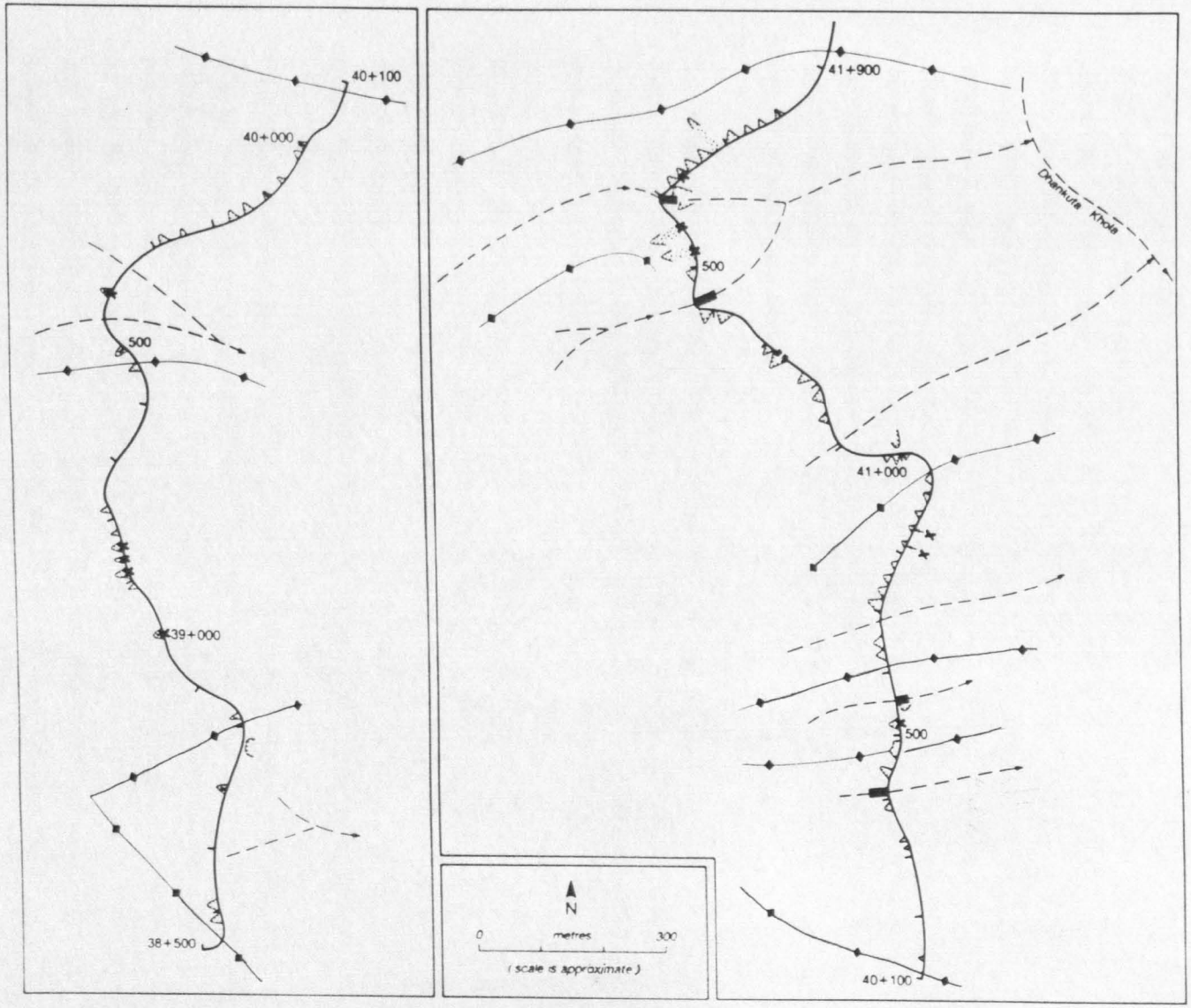

FIGURE A.7 Instability Occurring Along the Dharan-Dhankuta Road in September 1984 (Km 38.450-42.000).(For Legend see A.1).

to the proximity of the Dhankuta Thrust. The whole road section can, therefore, be conveniently subdivided into two sub-units, down-chainage and up-chainage of km 40.300.

Slopes down-chainage of km 40.300 are relatively stable due, primarily, to shallow slope inclinations above the gorge. Slopes crossed by the road are generally in the range of 20^{o} to 35^{o}, but are up to 49^{o} in the gorge immediately upstream of the Tamur River confluence (km 38.450-800). Underlying bedrock consists predominantly of quartz-mica schist, and is exposed as rock bluffs, and occasionally on spurs. However, the majority of slopes, above the road especially, are formed in deep soils and often highly weathered schist, boulder spreads and colluvium, derived from ancient instability of the rock bluffs above. Slope drainage is concentrated into a small number of gullies that, with the exception of localised bank instability, have remained relatively stable.

Cut slope protection works consist mostly of 2-3m high gabion revetments, but these are limited in extent. With one or two exceptions, cut-off and slope drainage have not been employed. Drainage protection works are confined, in most cases, to short gabion mattresses and cascades below culvert outfalls.

In view of the comparative stability of slopes and drainage channels in this sub-section, it is not surprising that the lack of protection works has had very little effect on road integrity. Probably the most notable problem that occurred during construction was that of shallow sliding and erosion on the tip slopes below the road in the Dhankuta Khola gorge (km 38.450-38.800).

Figure A.7 shows the distribution of instability occurring along this sub-section arising from the storm. Most slope failures consisted of small slips of weathered schist and colluvium, in cut slopes that have been oversteepened and insufficiently protected. Two large cut slope failures occurred at km 39.000 and between km 39.100 and km 39.200. In the latter case, three rock slides combined to block the road for a total distance of approximately 90m. At both locations, the cut slope is formed in highly weathered schist.

The second sub-section between km 40.300 and km 42.000 at Gutetar, has often been regarded as one of the most potentially hazardous lengths of the whole alignment (Chapter 4). The topography along this section is dominated

by four eroding gully catchments characterised by localised incision, side-slope instability and high runoff and sediment transport rates. These catchments are separated by boulder covered spurs with inclinations up to 30^{o}, but locally steeper in back-scars and on frontal slopes of slipped blocks. Below the road, an eroding mudslide and a network of gullies have undercut the slopes crossed by the road. The slopes are underlain by highly fractured green mica schist. The Dhankuta Thrust here has a dip of 24^{o} oriented 010^{o}N, and the majority of local bedrock discontinuities conform with this inclination and orientation. Conditions for instability are, therefore, inherent on the predominantly north facing slopes. Fractured quartzite outcrops along the thrust zone, as intercallations within the schist.

Due to the widespread distribution of instability along this length of road, the alignment, by necessity, has had to cross some unstable and potentially unstable slopes, in order to reach the more stable ground beyond Gutetar. Between km 40.380 and km 40.600, is a large instability complex associated with two incising unstable gullies, and a suspected major slumped block. Channel protection works have been constructed in both gullies, and consist of gabion checkdams and mattresses. Prior to the storm, these gullies had remained generally stable, although slight deformation to cascades and mattresses had occurred in the northern gully, where bank scour and shallow side-slope instability has continued.

Almost immediately after leaving this instability complex, the road makes a long traverse across side-long ground formed in schist between km 40.657 and km 40.930. Weathered schist and colluvium are exposed in the road cuts and have been excavated to inclinations of up to 57^{o}, without protection measures. Falls have occurred frequently from the cut slopes and slopes immediately above the road. Below the road, spoil disposal during earthworks gave rise to slope erosion, but this has been rectified by the construction of masonry revetments.

A large unstable gully head and expanding mudslide below the road at approximately between km 40.940 and km41.150, caused concern for road stability among the reconnaissance surveys. Above the mudslide head, the road crosses a shallow landslipped embayment that was interpreted as a feeder zone for the instability below. The road crosses this embayment with negligible cut or fill, and hence, slope disturbance has been minimal. A large masonry drain,

located above the mudslide head, collects slope and gully drainage and discharges onto the spur flank immediately to the south. Shallow slides onto the road occurred during 1983 from the irregular colluvial slopes above. The most noteworthy instability to occur during the maintenance period has been the development of a relatively deep rock slide in the cut slope around the spur at km 40.950.

The final instability complex along this sub-section is encountered between km 41.432 and km 41.583. It consists of two highly unstable gullies separated by a potentially unstable boulder covered spur. Both gullies have landslipped and eroding catchments, and sediment transport rates become particularly high during storm runoff.

In an original design (1978), the road across these gullies was to be built on rock-fill[1] causeways. The causeways were intended to act as large checkdams that would encourage sediment deposition and, at the same time, allow storm runoff to percolate through the fabric. However, before this structure was completed, a single storm caused the area behind the dam to become filled with debris, and runoff consequently overtopped the causeway. The final design at these crossings consists of two slab culverts and a gabion retained embankment. The culverts (2m x 2m and 2m x 3m) have been underdesigned due to financial constraints. A single checkdam has been constructed in the down-chainage gully, upstream of the road. Since construction, problems of instability and sediment transport in both gullies have continued, and consequently, both culverts remained almost continually blocked during the 1983 monsoon season (Plate 2.10). The problem has been exacerbated by erosion of the original rock-fill and spoil slopes around the culvert outfalls.

Instability resulting from the storm is shown in Figure A.7. Considering the inherent instability of the slopes in the area, it is surprising that very little major road damage took place. The gabion channel protection works upstream and downstream of the culverts at km 40.410 and km 40.570, have been damaged and both catchments demonstrate major renewed instability. This is

---

1. In this instance, rock-fill is hand-placed embankment fill composed of granular rock material.

especially evident in the down-chainage catchment, where a large rotational slide on the right bank has filled the channel for a distance of 70m upstream of the culvert.

Cut slope failures have occurred along almost the entire length of this stretch of road (Figure A.7). A total of thirty-nine individual slips were recorded. The most conspicuous sections of failed cut slope are around the unstable spur at km 40.950, and between km 40.450 and km 40.570. Slope failure has developed below the road at km 41.000, and further headward extension might endanger the road. Cracks have appeared in the road surface at km 41.270, and these are probably due to side-slope instability in the gully at km 41.430, downstream of the culvert.

A.10 Km 42.000-Km 45.600 (Figure A.8)

This section of alignment forms the traverse around the upper Dhankuta Khola floodplain between Gutetar and the ascent of the eastern valley slopes to Dhankuta.

Owing to the location of the road on elevated floodplain terrace, between km 42.000 and km 44.770, instability problems are minimal. Slope failure is confined to two main locations where the road has been excavated into adjoining valley-side slopes (Figure A.8). Between km 42.430 and km 42.860, the alignment descends from Gutetar and crosses the Raduwa Khola. Cut slope failures have been numerous along this section, especially during the storm (Figure A.8). The largest of these occurred at km 42.650, where the road became blocked for 50m. Surface drainage above the cut slope was dislocated, and this accelerated the instability by concentrating runoff over the cut slope.

The other main area of cut slope failure, between km 43.830 and km 43.900, became active during the 1983 monsoon season. Here, the road is generally in full-cut through a steep-fronted spur formed in schist. Renewed failure took place during the storm and the road became blocked for a distance of 76m.

From km 44.770 to the Bakhre Khola crossing, the road traverses gentle slopes inclined at 17-30^{o} that form the northern margin of the Dhankuta Khola floodplain. The road is mostly in full-cut through weathered schist and gneiss, and despite a general lack of slope revetment structures, the cut slopes have

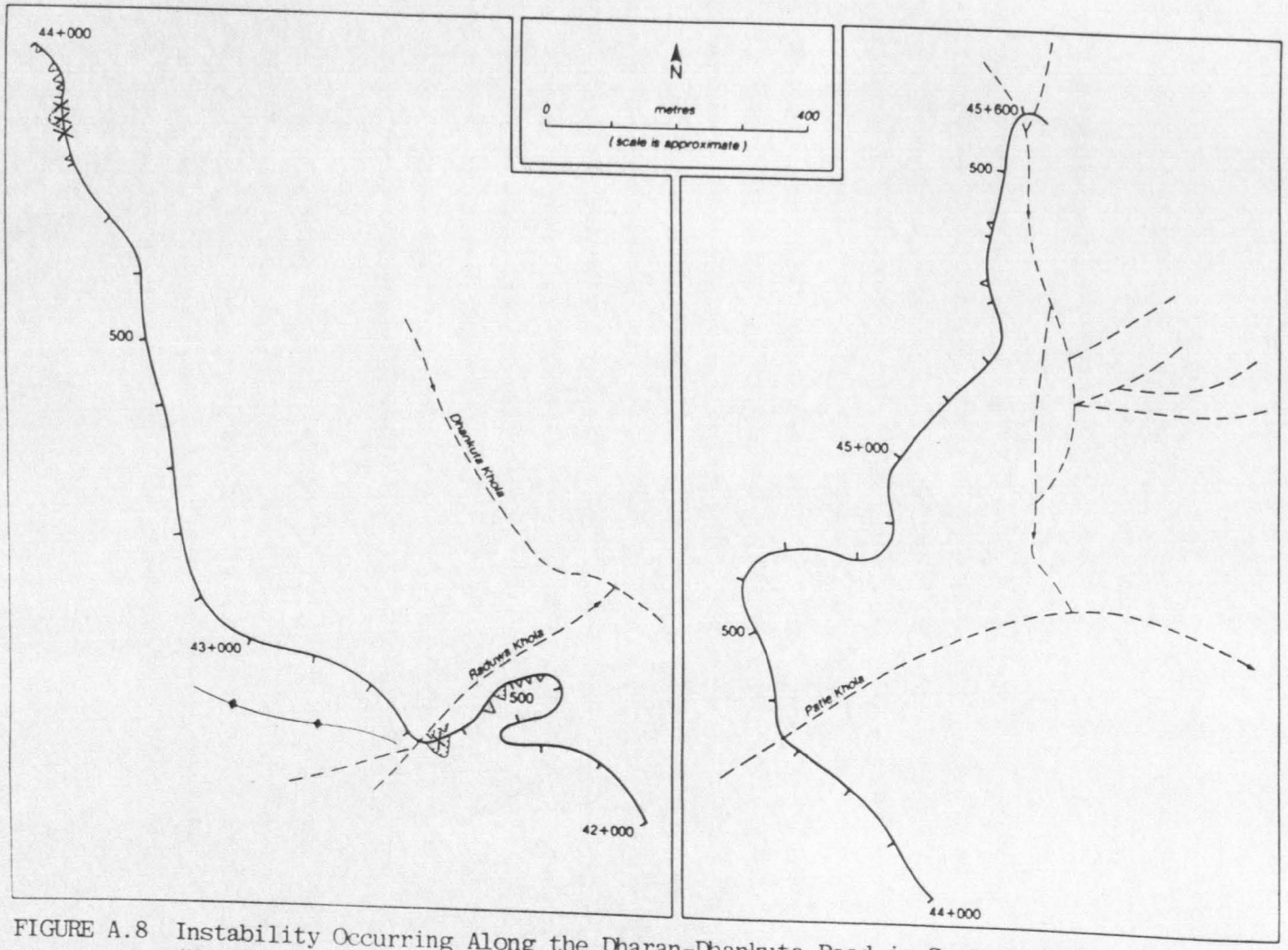

FIGURE A.8 Instability Occurring Along the Dharan-Dhankuta Road in September 1984 (Km 42.000-45.600).(For Legend see A.1).

remained relatively stable. Although there are no serious problems of drainage instability along this section, some of the bridge protection works at the Patle and Bakhre Khola crossings were damaged in 1983 by channel scour around the bridge abutments.

Cracks in the road surface, apparently due to settlement of fill, have developed at km 44.040 and km 44.980.

A.11 Km 45.600 - Km 50.300 (Figure A.9)

The ascent to Dhankuta from Bakhre Khola, consists of a double hairpin section followed by a traverse across side-long ground. Slopes along the entire section are composed of gneiss that varies from intact, relatively sound rock, to weathered soil, up to 15m deep. The characteristic feature of these slopes is the deeply incised drainage network. Gullies are incised to depths of 12m and commonly have oversteepened side-slopes with inclinations of the order of 50-60°. Instability in the drainage network is confined to localised shallow failures in soils and weathered rock bordering the channels.

Problems for road stability along this section relate to rapid sub-surface flow in the loose sandy regolith and shallow translational (rock) and rotational (soil) slope failures in road cuts. Extensive filter and cut-off drains have been installed behind the cut slopes to intercept both shallow sub-surface and overland flow, in order to prevent cut slope failure and erosion. However, many of the surface drains have been undermined (Plate A.7) and, in general, have had very little stabilizing influence.

Instability resulting from the storm is shown in Figure (A.9). The frequency of cut slope failures is evident, and in six instances the road became temporarily blocked or damaged. These failures pose little problem for long-term road stability. Drainage instability has been minimal, and damage to hydraulic structures is confined to the occasional scour and deformation of short culvert outfall mattresses and cascades.

PLATE A.7 Undermining of Area Drainage by Erosion on the Gneiss Slopes Below Dhankuta.

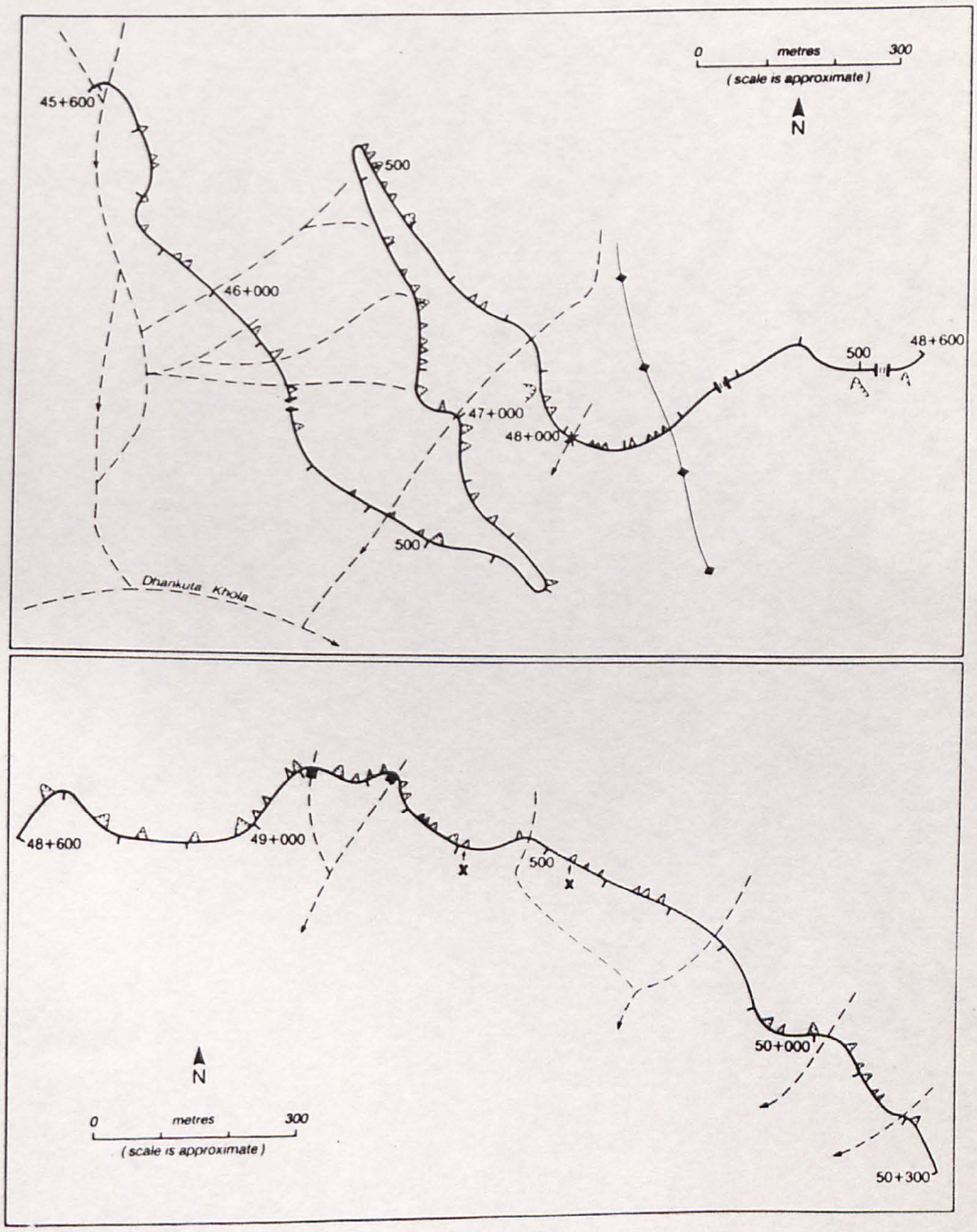

FIGURE A.9 Instability Occurring Along the Dharan-Dhankuta Road in September 1984 (Km 45.600-50.300).(For Legend see A.1).